

THE UNIVERSITY OF CHICAGO

RHODIUM-CATALYZED C–C BOND ACTIVATION OF FOUR-MEMBERED RING  
KETONES

A DISSERTATION SUBMITTED TO  
THE FACULTY OF THE DIVISION OF THE PHYSICAL SCIENCES  
IN CANDIDACY FOR THE DEGREE OF  
DOCTOR OF PHILOSOPHY

DEPARTMENT OF CHEMISTRY

BY  
LIN DENG

CHICAGO, ILLINOIS

JUNE 2019

Copyright © 2019 by Lin Deng

All rights reserved



To my family

## TABLE OF CONTENTS

<b>LIST OF SCHEMES</b> .....	ix
<b>LIST OF TABLES</b> .....	xiv
<b>LIST OF FIGURES</b> .....	xvi
<b>LIST OF ABBREVIATIONS</b> .....	xxv
<b>ACKNOWLEDGEMENT</b> .....	xxxix
<b>PREFACE</b> .....	xxxiii
<b>CHAPTER 1</b> .....	1
<b>1.1 Introduction</b> .....	1
<b>1.2 C–C Bond Activation of Cyclopropenones</b> .....	3
<i>1.2.1 Reactions with stoichiometric metals</i> .....	3
<i>1.2.2 Catalytic reactions with different metals</i> .....	7
<b>1.3 C–C Bond Activation of Cyclobutenediones and Cyclobutenones</b> .....	12
<i>1.3.1 Reactions with stoichiometric metals</i> .....	12
<i>1.3.2 Catalytic reactions with different metals</i> .....	17
<b>1.4 C–C Bond Activation of Cyclobutanones</b> .....	28
<i>1.4.1 Reactions with stoichiometric metals</i> .....	29
<i>1.4.2 Catalytic reactions with different metals</i> .....	30
<b>1.5 Conclusions and Outlook</b> .....	42
<b>1.6 References</b> .....	43

<b>CHAPTER 2</b> .....	48
<b>2.1 Introduction</b> .....	48
<b>2.2 Results and Discussion</b> .....	51
2.2.1 <i>Condition optimization for rhodium-catalyzed carboacylation of C=N bonds</i> .....	51
2.2.2 <i>Substrate scope for rhodium-catalyzed carboacylation of C=N bonds</i> .....	57
2.2.3 <i>Synthetic applications for rhodium-catalyzed carboacylation of C=N bonds</i> .....	61
<b>2.3 Conclusion</b> .....	63
<b>2.4 Experimental</b> .....	63
2.4.1 <i>General information</i> .....	63
2.4.2 <i>Synthetic routes for substrate synthesis</i> .....	64
2.4.3 <i>Synthesis of precursors</i> .....	65
2.4.4 <b>Route I</b> <i>synthesis of substrates <b>1b</b> to <b>1f</b></i> .....	70
2.4.5 <b>Route II</b> <i>synthesis of substrates <b>1a</b> and <b>1g</b> to <b>1m</b></i> .....	73
2.4.6 <i>Synthesis of substrates <b>1n</b></i> .....	78
2.4.7 <i>General procedure for C–C activation reactions</i> .....	79
2.4.8 <i>Synthetic applications</i> .....	99
2.4.9 <i>X-ray data</i> .....	106
<b>2.5 References</b> .....	114
<b>2.6 NMR Spectra</b> .....	117
<b>CHAPTER 3</b> .....	169

<b>3.1 Introduction</b>	169
<b>3.2 Results and Discussion</b>	172
3.2.1 <i>Rh-catalyzed enantioselective “cut-and-sew” reactions to construct fused indolines</i>	172
3.2.2 <i>Substrate scope for the Rh-catalyzed synthesis of tricyclic indolines via C–C activation</i>	176
3.2.3 <i>Rh-catalyzed diastereoselective cyclopropanation</i>	178
3.2.4 <i>End game</i>	182
<b>3.3 Conclusion</b>	184
<b>3.4 Experimental</b>	185
3.4.1 <i>General information</i>	185
3.4.2 <i>Synthetic routes for substrate synthesis</i>	186
3.4.3 <i>Procedure for C–C bond activation and characterization of compounds 8 to 8l</i>	199
3.4.4 <i>Procedure and characterization data for the total synthesis of (–)-cycloclavine</i>	223
3.4.5 <i>Procedure and characterization data of total synthesis of (–)-5-epi-cycloclavine</i>	230
3.4.6 <i>X-ray data</i>	233
<b>3.5 References</b>	235
<b>3.6 NMR Spectra</b>	238
<b>CHAPTER 4</b>	281
<b>4.1 Introduction</b>	281

<b>4.2 Results and Discussion</b> .....	284
4.2.1 Condition optimization for “cut-and-sew” reactions between cyclobutanones and alkynes.....	284
4.2.2 Substrate scope for “cut-and-sew” reactions between cyclobutanones and alkynes	287
4.2.3 Mechanistic study for “cut-and-sew” reactions between cyclobutanones and alkynes .....	290
4.2.4 Synthetic applications for “cut-and-sew” reactions between cyclobutanones and alkynes.....	295
<b>4.3 Conclusion</b> .....	295
<b>4.4 Experimental</b> .....	296
4.4.1 General information.....	296
4.4.2 General information about substrate synthesis .....	297
4.4.3 Synthesis of precursors .....	298
4.4.4. Synthesis of substrates .....	301
4.4.5 Rh-catalyzed intramolecular coupling between cyclobutanones and alkynes.....	317
4.4.6 Procedures and data for synthetic applications.....	330
4.4.7 Mechanistic study.....	337
4.4.8 X-ray data .....	353
<b>4.5 References</b> .....	358
<b>4.6 NMR Spectra</b> .....	361

CHAPTER 5 .....	425
<b>5.1 Introduction</b> .....	425
<b>5.2 Results and Discussion</b> .....	428
<i>5.2.1 Condition optimization for kinetic resolution of cyclobutanones</i> .....	428
<i>5.2.2 Substrate scope for kinetic resolution of cyclobutanones</i> .....	434
<b>5.3 Conclusion and Outlook</b> .....	437
<b>5.4 Experimental</b> .....	438
<i>5.4.1 General information</i> .....	438
<i>5.4.2 Substrate synthesis</i> .....	439
<i>5.4.3 Rh-catalyzed kinetic resolutions between cyclobutanones and alkynes</i> .....	449
<i>5.4.4 X-ray data</i> .....	474
<b>5.5 References</b> .....	475
<b>5.6 NMR Spectra</b> .....	477

## LIST OF SCHEMES

<b>Scheme 1.1</b> Two Major Mechanistic Pathways for C–C Bond Activation of Strained Cyclic Ketones .....	2
<b>Scheme 1.2</b> The Resonance Structure of Cyclopropenones .....	3
<b>Scheme 1.3</b> Stoichiometric Insertion of Platinum(0) into Cyclopropenone.....	4
<b>Scheme 1.4</b> Stoichiometric Insertion of Nickel(0) into Cyclopropenone .....	5
<b>Scheme 1.5</b> Stoichiometric Insertion of Rhodium(I) into Cyclopropenone .....	6
<b>Scheme 1.6</b> Stoichiometric Insertion of Cobalt(I) into Cyclopropenone .....	7
<b>Scheme 1.7</b> Nickel-Catalyzed Dimerization of Cyclopropenones .....	8
<b>Scheme 1.8</b> Nickel-Catalyzed Insertion of Ketene into Cyclopropenones .....	8
<b>Scheme 1.9</b> Transition-Metal Catalyzed Reaction between Cyclopropenones and Trimethylsilyl Cyanide .....	8
<b>Scheme 1.10</b> Ruthenium-Catalyzed Carbonylation of Cyclopropenones .....	10
<b>Scheme 1.11</b> Rhodium-Catalyzed [3+2]-Cycloaddition of Cyclopropenones with Alkynes .....	11
<b>Scheme 1.12</b> Rhodium-Catalyzed Aryl C–H Bond Insertion into Cyclopropenones .....	11
<b>Scheme 1.13</b> Cyclobutenediones and Cyclobutenones in C–C Bond Activation Reactions .....	12
<b>Scheme 1.14</b> Stoichiometric Reactions Involving Insertion of Transition-Metals into Cyclobutenediones .....	14
<b>Scheme 1.15</b> Stoichiometric Insertion of Transition-Metals into Cyclobutenones .....	15

<b>Scheme 1.16</b> Recent Examples of Stoichiometric Insertion of Transition-Metals into Benzocyclobutenones .....	16
<b>Scheme 1.17</b> Ruthenium-Catalyzed Decarbonylative C–C Bond Activation .....	18
<b>Scheme 1.18</b> Synthesis of Phenols through C–C Bond Activation.....	19
<b>Scheme 1.19</b> Rhodium or Ruthenium-Catalyzed Coupling between Cyclobutenones and Norbornene or Ketene.....	21
<b>Scheme 1.20</b> Rhodium-Catalyzed Intramolecular Ring Fusion Reaction.....	22
<b>Scheme 1.21</b> Rhodium-Catalyzed Carboacylation of Olefins through C–C Bond Activation of Benzocyclobutenones .....	23
<b>Scheme 1.22</b> Rhodium-Catalyzed Decarbonylative Spirocyclization through C–C Bond Activation of Benzocyclobutenones .....	24
<b>Scheme 1.23</b> Rhodium-Catalyzed Alkyne-Benzocyclobutenone Couplings .....	25
<b>Scheme 1.24</b> Rhodium-Catalyzed Carboacylation/Aromatization Cascade .....	25
<b>Scheme 1.25</b> Palladium-Catalyzed Insertion of Silacyclobutane into Benzocyclobutenones .....	26
<b>Scheme 1.26</b> Ruthenium-Catalyzed Insertion of Adjacent Diols into C–C Bond of Benzocyclobutenones and Benzocyclobutenediones.....	27
<b>Scheme 1.27</b> Nickel-Catalyzed Intermolecular Diene-Benzocyclobutenone Couplings .....	28
<b>Scheme 1.28</b> Decarbonylation of Cyclobutanones by Insertion of Stoichiometric Rhodium(I)..	29
<b>Scheme 1.29</b> Oxidative Addition of Cyclobutanone onto Rhodium(I) at Room Temperature ....	30
<b>Scheme 1.30</b> Rhodium(I)-Catalyzed Reductive Ring Opening of Cyclobutanones .....	31



<b>Scheme 1.31</b> Catalytic Decarbonylation of Cyclobutanones via Rhodium Catalysis .....	31
<b>Scheme 1.32</b> Rhodium(I)-Catalyzed Successive Cleavage of C–C and C–O Bonds .....	32
<b>Scheme 1.33</b> Intramolecular Olefin Insertion into C–C Bond of Cyclobutanones .....	33
<b>Scheme 1.34</b> Rhodium(I)-Catalyzed Bridged Ring Formation through C–C Bond Activation ..	34
<b>Scheme 1.35</b> Rhodium(I)-Catalyzed Vinyl Carbenoid Insertion into Cyclobutanones .....	35
<b>Scheme 1.36</b> Rhodium(I)-Catalyzed Decarbonylative Insertion of Olefins into Cyclobutanones .....	36
<b>Scheme 1.37</b> Rhodium(I)-Catalyzed Enantioselective Insertion of C=O Bonds into Cyclobutanones .....	36
<b>Scheme 1.38</b> Palladium(0)-Catalyzed Intramolecular Exchange of C–C and C–Si Bonds .....	37
<b>Scheme 1.40</b> Rhodium(I)-Catalyzed Addition/Ring-Opening of Cyclobutanones with Arylboronic Acids .....	38
<b>Scheme 1.41</b> Rhodium(I)-Catalyzed Arylative Ring Expansion of Cyclobutanones .....	39
<b>Scheme 1.42</b> Rhodium(I)-Catalyzed Enantioselective Lactone Synthesis from Cyclobutanones	39
<b>Scheme 1.43</b> Nickel(0)-Catalyzed Intermolecular Alkyne Insertion into Cyclobutanones .....	40
<b>Scheme 1.44</b> Nickel(0)-Catalyzed Enantioselective Intramolecular Olefin Insertion into Cyclobutanones .....	41
<b>Scheme 1.45</b> Nickel(0)-Catalyzed Enantioselective Intramolecular Allene Insertion into Cyclobutanones .....	42
<b>Scheme 2.1</b> Carboacylation of C=O Bonds via Transition-Metal-Catalyzed C–C Activation ....	49

<b>Scheme 2.2</b> General Process of Amide Bond Formation through “Cut-and-Sew” Approach .....	49
<b>Scheme 2.3</b> Carboacylation of C=N Bonds via Rh-Catalyzed C–C Activation .....	50
<b>Scheme 2.4</b> Representative Natural Products and Pharmaceuticals with Hydroisoquinolines ....	51
<b>Scheme 2.5</b> Crystal Structure of Compound <b>2a</b> .....	55
<b>Scheme 2.6</b> Cleavage of N–O Bond .....	62
<b>Scheme 2.7</b> Synthetic Applications I.....	62
<b>Scheme 2.8</b> Synthetic Applications II .....	63
<b>Scheme 3.1</b> The “Cut-and-Sew” Approach for Bridged and Fused Ring Synthesis.....	170
<b>Scheme 3.2</b> Structures of Representative Ergot Alkaloids.....	170
<b>Scheme 3.3</b> Prior Strategies towards Total Synthesis of Cycloclavine .....	171
<b>Scheme 3.4</b> Retrosynthetic Analysis for the Synthesis of (–)-Cycloclavine: a C–C Activation Strategy .....	172
<b>Scheme 3.5</b> Challenges for “Cut-and-Sew” Reactions.....	173
<b>Scheme 3.6</b> Synthesis of the Nitrogen-Tethered Benzocyclobutenone Substrate .....	174
<b>Scheme 3.7</b> Synthesis of Compound <b>3</b> as the Substrate for Cyclopropanation.....	179
<b>Scheme 3.8</b> Potential Side Reaction for Cyclopropanation.....	179
<b>Scheme 3.9</b> X-ray Structures of Compound <b>9b</b> (Racemic).....	181
<b>Scheme 3.10</b> Stereochemical Model for the Cyclopropanation Step .....	182
<b>Scheme 3.11</b> Synthesis of (–)-5- <i>epi</i> -Cycloclavine .....	183
<b>Scheme 3.12</b> Total Synthesis of (–)-Cycloclavine .....	184

<b>Scheme 3.13</b> A Summary of the Synthetic Efforts towards (–)-Cycloclavine .....	185
<b>Scheme 4.1</b> “Cut and Sew” Reactions with Cyclobutanones .....	282
<b>Scheme 4.2</b> Challenge for Fused Ring Formation.....	282
<b>Scheme 4.3</b> “Cut-and-Sew” with Cyclobutanones to Form Fused Rings .....	283
<b>Scheme 4.4</b> Precedents of Cyclohexenone-Fused Ring Formation via C–C Activation .....	284
<b>Scheme 4.5</b> Scope for Disubstituted Cyclobutanones .....	289
<b>Scheme 4.6</b> Unsuccessful Substrates.....	290
<b>Scheme 4.7</b> Control Experiments .....	291
<b>Scheme 4.8</b> <sup>13</sup> CO Exchange Experiment.....	292
<b>Scheme 4.9</b> Resting State Study .....	293
<b>Scheme 4.10</b> Kinetic Study with Different [Rh]/P Ratio .....	294
<b>Scheme 4.11</b> Synthetic Applications .....	295
<b>Scheme 5.1</b> Asymmetric Cyclohexenone-Bridged Ring Formation via C–C Activation .....	426
<b>Scheme 5.2</b> Representative Natural Products with the Fused Ring Systems Generated.....	427
<b>Scheme 5.3</b> Asymmetric Cyclohexenone-Fused or Bridged Ring Formation via C–C Activation .....	427
<b>Scheme 5.4</b> Representative Natural Products with Four-membered Ring .....	428
<b>Scheme 5.5</b> X-ray Structure of <b>2a</b> .....	434
<b>Scheme 5.6</b> Unsuccessful Substrates on Olefin- or Allene-Tethered Substrates.....	436
<b>Scheme 5.7</b> Unsuccessful Substrates on Alkyne-Tethered Substrates .....	437

## LIST OF TABLES

<b>Table 2.1</b> Evaluation of Solvents and Precatalysts <sup>a</sup> .....	52
<b>Table 2.2</b> Evaluation of Counter-Ion <sup>a</sup> .....	52
<b>Table 2.3</b> Evaluation of Chiral Ligands <sup>a</sup> .....	54
<b>Table 2.4</b> Further Screening with ( <i>R</i> )-xyl-SDP <sup>a</sup> .....	55
<b>Table 2.5</b> Studies of the Mixed-Ligand Conditions <sup>a</sup> .....	56
<b>Table 2.6</b> Control Experiments <sup>a</sup> .....	57
<b>Table 2.7</b> Substrate Scope I <sup>a</sup> .....	58
<b>Table 2.8</b> Substrate Scope II <sup>a</sup> .....	59
<b>Table 2.9</b> Unsuccessful Substrates <sup>a</sup> .....	60
<b>Table 2.10</b> Crystal Data and Structure Refinement for <b>2a</b> .....	106
<b>Table 2.11</b> Crystal Data and Structure Refinement for <b>2l</b> .....	108
<b>Table 2.12</b> Crystal Data and Structure Refinement for <b>2n</b> .....	110
<b>Table 2.13</b> Crystal Data and Structure Refinement for <b>6</b> .....	111
<b>Table 2.14</b> Crystal Data and Structure Refinement for <b>7</b> .....	113
<b>Table 3.1</b> Selected Optimization Study for the Rh-Catalyzed Asymmetric “Cut-and-Sew” Reaction <sup>a</sup> .....	175
<b>Table 3.2</b> Substrate Scope I <sup>a</sup> .....	177
<b>Table 3.3</b> Substrate Scope II <sup>a</sup> .....	178
<b>Table 3.4</b> Selected Condition Optimization for the Cyclopropanation Step <sup>a</sup> .....	181

<b>Table 3.5</b> Crystal Data and Structure Refinement for <b>12</b> (Racemic) .....	233
<b>Table 4.1</b> Selected Ligand Screening .....	285
<b>Table 4.2</b> Screening of the [Rh]/P Ratio <sup>a</sup> .....	286
<b>Table 4.3</b> Precatalyst/solvent Screening and Control Experiments <sup>a</sup> .....	287
<b>Table 4.4</b> Substrate Scope <sup>a</sup> .....	288
<b>Table 4.5</b> Series of <sup>13</sup> CO Exchange Experiment .....	293
<b>Table 4.6</b> Crystal Data and Structure Refinement for <b>2a</b> .....	353
<b>Table 4.7</b> Crystal Data and Structure Refinement for <b>3</b> .....	354
<b>Table 4.8</b> Crystal Data and Structure Refinement for <b>6</b> .....	356
<b>Table 5.1</b> Initial Condition Screening <sup>a</sup> .....	429
<b>Table 5.2</b> Selected Condition Screening with Different Precatalysts <sup>a</sup> .....	429
<b>Table 5.3</b> Selected Condition Screening with Different Ligands <sup>a</sup> .....	430
<b>Table 5.4</b> Selected Condition Screening with Different Additives <sup>a</sup> .....	431
<b>Table 5.5</b> Selected Condition Screening with In-Situ Generated Cationic Rhodium Catalysts <sup>a</sup> .....	432
<b>Table 5.6</b> Selected Condition Screening at Different Temperatures <sup>a</sup> .....	433
<b>Table 5.7</b> Selected Condition Screening for Acidic Additives <sup>a</sup> .....	433
<b>Table 5.8</b> Selected Control Experiments <sup>a</sup> .....	434
<b>Table 5.9</b> Substrate Scope <sup>a,b</sup> .....	435
<b>Table 5.10</b> Crystal Data and Structure Refinement for <b>2a</b> .....	475

## LIST OF FIGURES

<b>Figure 2.1</b> $^1\text{H}$ and $^{13}\text{C}$ NMR spectrum of compound <b>1a</b> .....	117
<b>Figure 2.2</b> $^1\text{H}$ and $^{13}\text{C}$ NMR spectrum of compound <b>1b</b> .....	118
<b>Figure 2.3</b> $^1\text{H}$ and $^{13}\text{C}$ NMR spectrum of compound <b>1c</b> .....	119
<b>Figure 2.4</b> $^1\text{H}$ and $^{13}\text{C}$ NMR spectrum of compound <b>1d</b> .....	120
<b>Figure 2.5</b> $^1\text{H}$ and $^{13}\text{C}$ NMR spectrum of compound <b>1e</b> .....	121
<b>Figure 2.6</b> $^1\text{H}$ and $^{13}\text{C}$ NMR spectrum of compound <b>1f</b> .....	122
<b>Figure 2.7</b> $^1\text{H}$ and $^{13}\text{C}$ NMR spectrum of compound <b>1g</b> .....	123
<b>Figure 2.8</b> $^1\text{H}$ and $^{13}\text{C}$ NMR spectrum of compound <b>1h</b> .....	124
<b>Figure 2.9</b> $^1\text{H}$ and $^{13}\text{C}$ NMR spectrum of compound <b>1i</b> .....	125
<b>Figure 2.10</b> $^1\text{H}$ and $^{13}\text{C}$ NMR spectrum of compound <b>1j</b> .....	126
<b>Figure 2.11</b> $^1\text{H}$ and $^{13}\text{C}$ NMR spectrum of compound <b>1k</b> .....	127
<b>Figure 2.12</b> $^1\text{H}$ and $^{13}\text{C}$ NMR spectrum of compound <b>1l</b> .....	128
<b>Figure 2.13</b> $^1\text{H}$ and $^{13}\text{C}$ NMR spectrum of compound <b>1m</b> .....	129
<b>Figure 2.14</b> $^1\text{H}$ and $^{13}\text{C}$ NMR spectrum of compound <b>1n</b> .....	130
<b>Figure 2.15</b> $^1\text{H}$ and $^{13}\text{C}$ NMR spectrum of compound <b>2a</b> .....	131
<b>Figure 2.16</b> $^1\text{H}$ and $^{13}\text{C}$ NMR spectrum of compound <b>2b</b> .....	132
<b>Figure 2.17</b> $^1\text{H}$ and $^{13}\text{C}$ NMR spectrum of compound <b>2c</b> .....	133
<b>Figure 2.18</b> $^1\text{H}$ and $^{13}\text{C}$ NMR spectrum of compound <b>2d</b> .....	134
<b>Figure 2.19</b> $^1\text{H}$ and $^{13}\text{C}$ NMR spectrum of compound <b>2e</b> .....	135

<b>Figure 2.20</b> $^1\text{H}$ and $^{13}\text{C}$ NMR spectrum of compound <b>2f</b> .....	136
<b>Figure 2.21</b> $^1\text{H}$ and $^{13}\text{C}$ NMR spectrum of compound <b>2g</b> .....	137
<b>Figure 2.22</b> $^1\text{H}$ and $^{13}\text{C}$ NMR spectrum of compound <b>2h</b> .....	138
<b>Figure 2.23</b> $^1\text{H}$ and $^{13}\text{C}$ NMR spectrum of compound <b>2i</b> .....	139
<b>Figure 2.24</b> $^1\text{H}$ and $^{13}\text{C}$ NMR spectrum of compound <b>2j</b> .....	140
<b>Figure 2.25</b> $^1\text{H}$ and $^{13}\text{C}$ NMR spectrum of compound <b>2k</b> .....	141
<b>Figure 2.26</b> $^1\text{H}$ and $^{13}\text{C}$ NMR spectrum of compound <b>2l</b> .....	142
<b>Figure 2.27</b> $^1\text{H}$ and $^{13}\text{C}$ NMR spectrum of compound <b>2m</b> .....	143
<b>Figure 2.28</b> $^1\text{H}$ and $^{13}\text{C}$ NMR spectrum of compound <b>2n</b> .....	144
<b>Figure 2.29</b> $^1\text{H}$ and $^{13}\text{C}$ NMR spectrum of compound <b>1j-II</b> .....	145
<b>Figure 2.30</b> $^1\text{H}$ and $^{13}\text{C}$ NMR spectrum of compound <b>1k-II</b> .....	146
<b>Figure 2.31</b> $^1\text{H}$ and $^{13}\text{C}$ NMR spectrum of compound <b>1l-II</b> .....	147
<b>Figure 2.32</b> $^1\text{H}$ and $^{13}\text{C}$ NMR spectrum of compound <b>1k-III</b> .....	148
<b>Figure 2.33</b> $^1\text{H}$ and $^{13}\text{C}$ NMR spectrum of compound <b>1k-IV</b> .....	149
<b>Figure 2.34</b> $^1\text{H}$ and $^{13}\text{C}$ NMR spectrum of compound <b>3</b> .....	150
<b>Figure 2.35</b> $^1\text{H}$ and $^{13}\text{C}$ NMR spectrum of compound <b>4</b> .....	151
<b>Figure 2.36</b> $^1\text{H}$ and $^{13}\text{C}$ NMR spectrum of compound <b>5</b> .....	152
<b>Figure 2.37</b> $^1\text{H}$ and $^{13}\text{C}$ NMR spectrum of compound <b>6</b> .....	153
<b>Figure 2.38</b> $^1\text{H}$ and $^{13}\text{C}$ NMR spectrum of compound <b>7</b> .....	154
<b>Figure 2.39</b> $^1\text{H}$ and $^{13}\text{C}$ NMR spectrum of compound <b>8</b> .....	155

<b>Figure 2.40</b> $^1\text{H}$ and $^{13}\text{C}$ NMR spectrum of compound <b>9</b> .....	156
<b>Figure 2.41</b> 2D NMR spectra of compound <b>2m</b> .....	157
<b>Figure 2.42</b> 2D NMR spectra of compound <b>2n</b> .....	159
<b>Figure 2.43</b> 2D NMR spectra of compound <b>8</b> .....	160
<b>Figure 3.1</b> $^1\text{H}$ and $^{13}\text{C}$ NMR spectrum of compound <b>6h</b> .....	238
<b>Figure 3.2</b> $^1\text{H}$ and $^{13}\text{C}$ NMR spectrum of compound <b>5</b> .....	239
<b>Figure 3.3</b> $^1\text{H}$ and $^{13}\text{C}$ NMR spectrum of compound <b>5a</b> .....	240
<b>Figure 3.4</b> $^1\text{H}$ and $^{13}\text{C}$ NMR spectrum of compound <b>5b</b> .....	241
<b>Figure 3.5</b> $^1\text{H}$ and $^{13}\text{C}$ NMR spectrum of compound <b>5c</b> .....	242
<b>Figure 3.6</b> $^1\text{H}$ and $^{13}\text{C}$ NMR spectrum of compound <b>5d</b> .....	243
<b>Figure 3.7</b> $^1\text{H}$ and $^{13}\text{C}$ NMR spectrum of compound <b>5e</b> .....	244
<b>Figure 3.8</b> $^1\text{H}$ , $^{13}\text{C}$ NMR and $^{19}\text{F}$ -NMR spectrum of compound <b>5f</b> .....	245
<b>Figure 3.9</b> $^1\text{H}$ and $^{13}\text{C}$ NMR spectrum of compound <b>5g</b> .....	247
<b>Figure 3.10</b> $^1\text{H}$ and $^{13}\text{C}$ NMR spectrum of compound <b>5h</b> .....	248
<b>Figure 3.11</b> $^1\text{H}$ and $^{13}\text{C}$ NMR spectrum of compound <b>5i</b> .....	249
<b>Figure 3.12</b> $^1\text{H}$ and $^{13}\text{C}$ NMR spectrum of compound <b>5j</b> .....	250
<b>Figure 3.13</b> $^1\text{H}$ and $^{13}\text{C}$ NMR spectrum of compound <b>5k</b> .....	251
<b>Figure 3.14</b> $^1\text{H}$ and $^{13}\text{C}$ NMR spectrum of compound <b>5l-I</b> .....	252
<b>Figure 3.15</b> $^1\text{H}$ and $^{13}\text{C}$ NMR spectrum of compound <b>5l</b> .....	253
<b>Figure 3.16</b> $^1\text{H}$ and $^{13}\text{C}$ NMR spectrum of compound <b>5m</b> .....	254



<b>Figure 3.17</b> $^1\text{H}$ and $^{13}\text{C}$ NMR spectrum of compound <b>5n</b> .....	255
<b>Figure 3.18</b> $^1\text{H}$ and $^{13}\text{C}$ NMR spectrum of compound <b>8</b> .....	256
<b>Figure 3.19</b> $^1\text{H}$ and $^{13}\text{C}$ NMR spectrum of compound <b>8a</b> .....	257
<b>Figure 3.20</b> $^1\text{H}$ and $^{13}\text{C}$ NMR spectrum of compound <b>8b</b> .....	258
<b>Figure 3.21</b> $^1\text{H}$ and $^{13}\text{C}$ NMR spectrum of compound <b>8c</b> .....	259
<b>Figure 3.22</b> $^1\text{H}$ and $^{13}\text{C}$ NMR spectrum of compound <b>8d</b> .....	260
<b>Figure 3.23</b> $^1\text{H}$ and $^{13}\text{C}$ NMR spectrum of compound <b>8e</b> .....	261
<b>Figure 3.24</b> $^1\text{H}$ , $^{13}\text{C}$ NMR and $^{19}\text{F}$ NMR spectrum of compound <b>8f</b> .....	262
<b>Figure 3.25</b> $^1\text{H}$ and $^{13}\text{C}$ NMR spectrum of compound <b>8g</b> .....	264
<b>Figure 3.26</b> $^1\text{H}$ and $^{13}\text{C}$ NMR spectrum of compound <b>8h</b> .....	265
<b>Figure 3.27</b> $^1\text{H}$ and $^{13}\text{C}$ NMR spectrum of compound <b>8i</b> .....	266
<b>Figure 3.28</b> $^1\text{H}$ and $^{13}\text{C}$ NMR spectrum of compound <b>8j</b> .....	267
<b>Figure 3.29</b> $^1\text{H}$ and $^{13}\text{C}$ NMR spectrum of compound <b>8k</b> .....	268
<b>Figure 3.30</b> $^1\text{H}$ and $^{13}\text{C}$ NMR spectrum of compound <b>8l</b> .....	269
<b>Figure 3.31</b> $^1\text{H}$ and $^{13}\text{C}$ NMR spectrum of compound <b>8m</b> .....	270
<b>Figure 3.32</b> $^1\text{H}$ and $^{13}\text{C}$ NMR spectrum of compound <b>8n</b> .....	271
<b>Figure 3.33</b> $^1\text{H}$ and $^{13}\text{C}$ NMR spectrum of compound <b>3</b> .....	272
<b>Figure 3.34</b> $^1\text{H}$ and $^{13}\text{C}$ NMR spectrum of compound <b>9b (major)</b> .....	273
<b>Figure 3.35</b> $^1\text{H}$ and $^{13}\text{C}$ NMR spectrum of compound <b>9b (minor)</b> .....	274
<b>Figure 3.36</b> $^1\text{H}$ and $^{13}\text{C}$ NMR spectrum of compound <b>10</b> .....	275

<b>Figure 3.37</b> $^1\text{H}$ and $^{13}\text{C}$ NMR spectrum of compound <b>2</b> .....	276
<b>Figure 3.38</b> $^1\text{H}$ and $^{13}\text{C}$ NMR spectrum of compound <b>1</b> .....	277
<b>Figure 3.39</b> $^1\text{H}$ and $^{13}\text{C}$ NMR spectrum of compound <b>11</b> .....	278
<b>Figure 3.40</b> $^1\text{H}$ (in $\text{CDCl}_3$ and $\text{CD}_2\text{Cl}_2$ ) and $^{13}\text{C}$ NMR spectrum of compound <b>12</b> .....	279
<b>Figure 4.1</b> $^1\text{H}$ and $^{13}\text{C}$ NMR spectrum of compound <b>1d-II</b> .....	361
<b>Figure 4.2</b> $^1\text{H}$ and $^{13}\text{C}$ NMR spectrum of compound <b>1j-II</b> .....	362
<b>Figure 4.3</b> $^1\text{H}$ and $^{13}\text{C}$ NMR spectrum of compound <b>1l-II</b> .....	363
<b>Figure 4.4</b> $^1\text{H}$ and $^{13}\text{C}$ NMR spectrum of compound <b>1m-II</b> .....	364
<b>Figure 4.5</b> $^1\text{H}$ and $^{13}\text{C}$ NMR spectrum of compound <b>1n-I</b> .....	365
<b>Figure 4.6</b> $^1\text{H}$ and $^{13}\text{C}$ NMR spectrum of compound <b>1u-I</b> .....	366
<b>Figure 4.7</b> $^1\text{H}$ and $^{13}\text{C}$ NMR spectrum of compound <b>1t-I</b> .....	367
<b>Figure 4.8</b> $^1\text{H}$ and $^{13}\text{C}$ NMR spectrum of compound <b>1a</b> .....	368
<b>Figure 4.9</b> $^1\text{H}$ and $^{13}\text{C}$ NMR spectrum of compound <b>1b</b> .....	369
<b>Figure 4.10</b> $^1\text{H}$ and $^{13}\text{C}$ NMR spectrum of compound <b>1c</b> .....	370
<b>Figure 4.11</b> $^1\text{H}$ and $^{13}\text{C}$ NMR spectrum of compound <b>1d</b> .....	371
<b>Figure 4.12</b> $^1\text{H}$ and $^{13}\text{C}$ NMR spectrum of compound <b>1e</b> .....	372
<b>Figure 4.13</b> $^1\text{H}$ and $^{13}\text{C}$ NMR spectrum of compound <b>1f</b> .....	373
<b>Figure 4.14</b> $^1\text{H}$ and $^{13}\text{C}$ NMR spectrum of compound <b>1g</b> .....	374
<b>Figure 4.15</b> $^1\text{H}$ and $^{13}\text{C}$ NMR spectrum of compound <b>1h</b> .....	375
<b>Figure 4.16</b> $^1\text{H}$ and $^{13}\text{C}$ NMR spectrum of compound <b>1i</b> .....	376

<b>Figure 4.17</b> $^1\text{H}$ and $^{13}\text{C}$ NMR spectrum of compound <b>1j</b> .....	377
<b>Figure 4.18</b> $^1\text{H}$ and $^{13}\text{C}$ NMR spectrum of compound <b>1k</b> .....	378
<b>Figure 4.19</b> $^1\text{H}$ and $^{13}\text{C}$ NMR spectrum of compound <b>1l</b> .....	379
<b>Figure 4.20</b> $^1\text{H}$ and $^{13}\text{C}$ NMR spectrum of compound <b>1m</b> .....	380
<b>Figure 4.21</b> $^1\text{H}$ and $^{13}\text{C}$ NMR spectrum of compound <b>1n</b> .....	381
<b>Figure 4.22</b> $^1\text{H}$ and $^{13}\text{C}$ NMR spectrum of compound <b>1o</b> .....	382
<b>Figure 4.23</b> $^1\text{H}$ and $^{13}\text{C}$ NMR spectrum of compound <b>1p</b> .....	383
<b>Figure 4.24</b> $^1\text{H}$ and $^{13}\text{C}$ NMR spectrum of compound <b>1q</b> .....	384
<b>Figure 4.25</b> $^1\text{H}$ and $^{13}\text{C}$ NMR spectrum of compound <b>1r</b> .....	385
<b>Figure 4.26</b> $^1\text{H}$ and $^{13}\text{C}$ NMR spectrum of compound <b>1s</b> .....	386
<b>Figure 4.27</b> $^1\text{H}$ and $^{13}\text{C}$ NMR spectrum of compound <b>1t</b> .....	387
<b>Figure 4.28</b> $^1\text{H}$ and $^{13}\text{C}$ NMR spectrum of compound <b>1u</b> .....	388
<b>Figure 4.29</b> $^1\text{H}$ and $^{13}\text{C}$ NMR spectrum of compound <b>1v</b> .....	389
<b>Figure 4.30</b> $^1\text{H}$ and $^{13}\text{C}$ NMR spectrum of compound <b>2a</b> .....	390
<b>Figure 4.31</b> $^1\text{H}$ and $^{13}\text{C}$ NMR spectrum of compound <b>2b</b> .....	391
<b>Figure 4.32</b> $^1\text{H}$ and $^{13}\text{C}$ NMR spectrum of compound <b>2c</b> .....	392
<b>Figure 4.33</b> $^1\text{H}$ and $^{13}\text{C}$ NMR spectrum of compound <b>2d</b> .....	393
<b>Figure 4.34</b> $^1\text{H}$ and $^{13}\text{C}$ NMR spectrum of compound <b>2e</b> .....	394
<b>Figure 4.35</b> $^1\text{H}$ and $^{13}\text{C}$ NMR spectrum of compound <b>2f</b> .....	395
<b>Figure 4.36</b> $^1\text{H}$ and $^{13}\text{C}$ NMR spectrum of compound <b>2g</b> .....	396

<b>Figure 4.37</b> $^1\text{H}$ and $^{13}\text{C}$ NMR spectrum of compound <b>2h</b> .....	397
<b>Figure 4.38</b> $^1\text{H}$ and $^{13}\text{C}$ NMR spectrum of compound <b>2i</b> .....	398
<b>Figure 4.39</b> $^1\text{H}$ and $^{13}\text{C}$ NMR spectrum of compound <b>2j</b> .....	399
<b>Figure 4.40</b> $^1\text{H}$ and $^{13}\text{C}$ NMR spectrum of compound <b>2k</b> .....	400
<b>Figure 4.41</b> $^1\text{H}$ and $^{13}\text{C}$ NMR spectrum of compound <b>2l</b> .....	401
<b>Figure 4.42</b> $^1\text{H}$ and $^{13}\text{C}$ NMR spectrum of compound <b>2m</b> .....	402
<b>Figure 4.43</b> $^1\text{H}$ and $^{13}\text{C}$ NMR spectrum of compound <b>2n</b> .....	403
<b>Figure 4.44</b> $^1\text{H}$ and $^{13}\text{C}$ NMR spectrum of compound <b>2o</b> .....	404
<b>Figure 4.45</b> $^1\text{H}$ and $^{13}\text{C}$ NMR spectrum of compound <b>2p</b> .....	405
<b>Figure 4.46</b> $^1\text{H}$ and $^{13}\text{C}$ NMR spectrum of compound <b>2q</b> .....	406
<b>Figure 4.47</b> $^1\text{H}$ and $^{13}\text{C}$ NMR spectrum of compound <b>2r</b> .....	407
<b>Figure 4.48</b> $^1\text{H}$ and $^{13}\text{C}$ NMR spectrum of compound <b>2s</b> .....	408
<b>Figure 4.49</b> $^1\text{H}$ and $^{13}\text{C}$ NMR spectrum of compound <b>2t</b> .....	409
<b>Figure 4.50</b> $^1\text{H}$ and $^{13}\text{C}$ NMR spectrum of compound <b>2u</b> .....	410
<b>Figure 4.51</b> $^1\text{H}$ and $^{13}\text{C}$ NMR spectrum of compound <b>2v (major)</b> .....	411
<b>Figure 4.52</b> $^1\text{H}$ and $^{13}\text{C}$ NMR spectrum of compound <b>3</b> .....	412
<b>Figure 4.53</b> $^1\text{H}$ and $^{13}\text{C}$ NMR spectrum of compound <b>4</b> .....	413
<b>Figure 4.54</b> $^1\text{H}$ and $^{13}\text{C}$ NMR spectrum of compound <b>5</b> .....	414
<b>Figure 4.55</b> $^1\text{H}$ and $^{13}\text{C}$ NMR spectrum of compound <b>6</b> .....	415
<b>Figure 4.56</b> $^1\text{H}$ and $^{13}\text{C}$ NMR spectrum of compound <b>7</b> .....	416

<b>Figure 4.57</b> $^1\text{H}$ and $^{13}\text{C}$ NMR spectrum of compound <b>8</b> .....	417
<b>Figure 4.58</b> $^1\text{H}$ and $^{13}\text{C}$ NMR spectrum of compound <b>9</b> .....	418
<b>Figure 4.59</b> $^1\text{H}$ and $^{13}\text{C}$ NMR spectrum of compound <b>2a'</b> .....	419
<b>Figure 4.60</b> 2D-NMR spectrum of compound <b>1u</b> .....	420
<b>Figure 4.61</b> 2D-NMR spectrum of compound <b>1v</b> .....	421
<b>Figure 4.62</b> 2D-NMR spectrum of compound <b>2u</b> .....	422
<b>Figure 4.63</b> 2D-NMR spectrum of compound <b>2v</b> .....	423
<b>Figure 4.64</b> 2D-NMR spectrum of compound <b>5</b> .....	424
<b>Figure 5.1</b> $^1\text{H}$ and $^{13}\text{C}$ NMR spectrum of compound <b>1a</b> .....	477
<b>Figure 5.2</b> $^1\text{H}$ and $^{13}\text{C}$ NMR spectrum of compound <b>1b</b> .....	478
<b>Figure 5.3</b> $^1\text{H}$ and $^{13}\text{C}$ NMR spectrum of compound <b>1c</b> .....	479
<b>Figure 5.4</b> $^1\text{H}$ and $^{13}\text{C}$ NMR spectrum of compound <b>1e</b> .....	480
<b>Figure 5.5</b> $^1\text{H}$ and $^{13}\text{C}$ NMR spectrum of compound <b>1f</b> .....	481
<b>Figure 5.6</b> $^1\text{H}$ and $^{13}\text{C}$ NMR spectrum of compound <b>1g</b> .....	482
<b>Figure 5.7</b> $^1\text{H}$ and $^{13}\text{C}$ NMR spectrum of compound <b>1h</b> .....	483
<b>Figure 5.8</b> $^1\text{H}$ and $^{13}\text{C}$ NMR spectrum of compound <b>1i</b> .....	484
<b>Figure 5.9</b> $^1\text{H}$ and $^{13}\text{C}$ NMR spectrum of compound <b>1j</b> .....	485
<b>Figure 5.10</b> $^1\text{H}$ and $^{13}\text{C}$ NMR spectrum of compound <b>1k</b> .....	486
<b>Figure 5.11</b> $^1\text{H}$ and $^{13}\text{C}$ NMR spectrum of compound <b>2a</b> .....	487
<b>Figure 5.12</b> $^1\text{H}$ and $^{13}\text{C}$ NMR spectrum of compound <b>2b</b> .....	488

<b>Figure 5.13</b> $^1\text{H}$ and $^{13}\text{C}$ NMR spectrum of compound <b>2c</b> .....	489
<b>Figure 5.14</b> $^1\text{H}$ and $^{13}\text{C}$ NMR spectrum of compound <b>2e</b> .....	490
<b>Figure 5.15</b> $^1\text{H}$ and $^{13}\text{C}$ NMR spectrum of compound <b>2f</b> .....	491
<b>Figure 5.16</b> $^1\text{H}$ and $^{13}\text{C}$ NMR spectrum of compound <b>2g</b> .....	492
<b>Figure 5.17</b> $^1\text{H}$ and $^{13}\text{C}$ NMR spectrum of compound <b>2h</b> .....	493
<b>Figure 5.18</b> $^1\text{H}$ and $^{13}\text{C}$ NMR spectrum of compound <b>2i</b> .....	494
<b>Figure 5.19</b> $^1\text{H}$ and $^{13}\text{C}$ NMR spectrum of compound <b>2j</b> .....	495
<b>Figure 5.20</b> $^1\text{H}$ and $^{13}\text{C}$ NMR spectrum of compound <b>2k</b> .....	496

## LIST OF ABBREVIATIONS

Ac	Acetyl
Acac	acetylacetonate
Ad	Adamantyl
Ar	Aryl
BARF	Tetrakis(perfluorophenyl)borate
BINAP	2,2'-bis(Diphenylphosphino)-1,1'-binaphthalene
Bn	Benzyl
Boc	<i>tert</i> -Butoxycarbonyl
Bu	Butyl
Bz	Benzoyl
COD	1,5-Cyclooctadienyl
COE	Cyclooctene
Cp	Cyclopentadienyl
Cp*	1,2,3,4,5-Pentamethylcyclopentadienyl
Cy	Cyclohexyl

$\delta$	Chemical shift
DCE	1,2-Dichloroethane
DCM	Dichloromethane
DIAD	Diisopropyl azodicarboxylate
DMF	<i>N,N</i> -Dimethylformamide
DMPU	<i>N, N'</i> -Dimethylpropyleneurea
DMSO	Dimethylsulphoxide
DPEphos	(Oxydi-2,1-phenylene)bis(diphenylphosphine)
dppb	1,4-bis(Diphenylphosphino)butane
dppe	1,2-bis(Diphenylphosphino)ethane
dppf	1,1'-bis(Diphenylphosphino)ferrocene
dppp	1,3-bis(Diphenylphosphino)propane
dppm	1,1-bis(Diphenylphosphino)methane
dr	Diastereomeric ratio
DG	Directing group
DTBMP	2,6-Di-tert-butyl-4-methylpyridine



ee	Enantiomeric excess
Et	Ethyl
equiv	Equivalent
HFIP	1,1,1,3,3,3-Hexafluoro-2-propanol
HPLC	High performance liquid chromatography
HRMS	High-resolution mass spectrometry
IBX	2-Iodoxybenzoic acid
IMes	1,3-Dimesitylimidazol-2-ylidene
<i>i</i> -Pr	Isopropyl
IR	Infrared
KPS	Potassium persulfate
<i>m</i>	Meta
mCPBA	<i>meta</i> -Chloroperoxybenzoic acid
Me	Methyl
Mes	Mesityl
MOM	Methoxymethyl

Ms	Methanesulphonyl
M.S.	Molecular Sieve
MW	Microwave
m/z	Mass charge ratio
nbd	2,5-Norbornadiene
NBS	<i>N</i> -Bromosuccinimide
<i>n</i> -Bu	<i>normal</i> -Butyl
NFSI	<i>N</i> -Fluorobenzenesulfonimide
NHC	<i>N</i> -Heterocyclic Carbene
NIS	<i>N</i> -Iodosuccinimide
NMR	Nuclear magnetic resonance
<i>n</i> -Pr	<i>normal</i> -Propyl
Ns	Nitrobenzenesulphonyl
<i>o</i>	Ortho
Oxone	2KHSO <sub>5</sub> ·KHSO <sub>4</sub> ·K <sub>2</sub> SO <sub>4</sub>
<i>p</i>	Para

PCC	Pyridinium chlorochromate
Ph	Phenyl
Phth	Phthaloyl
Pin	Pinacolyl
Piv	Pivaloyl
Py	Pyridyl
rr	Regioisomeric ratio
r.t.	Room temperature
TBS	<i>tert</i> -Butyldimethylsilyl
<i>t</i> -Bu	<i>tert</i> -Butyl
Tf	Trifluoromethanesulphonyl
Tfa	Trifluoroacetyl
THF	Tetrahydrofuran
TIPS	Tri- <i>iso</i> -propylsilyl
TLC	Thin-layer chromatography
TMS	Trimethylsilyl

Tol

Tolyl

Ts

*para*-Toluenesulphonyl

## ACKNOWLEDGEMENT

First of all, I would like to thank my advisor, Prof. Guangbin Dong, for taking the risk of recruiting me when I knew nothing about methodology development. Over the past five years, he has been a great mentor to me and taught me with his own example how to be an enthusiastic chemist and endure the ups and downs along the way. His creative ideas and solid understanding about catalysis have been vital to anything I have achieved in this thesis. I would like also to thank Professor Eric Anslyn, Professor Stephen Martin, and Professor Grant Willson, for the supportance during the two years I spent in University of Texas at Austin. I would also like to thank my committee members, Professor Viresh Rawal and Professor Scott Snyder, for agreeing to be my committee and attend my defense on a very short notice. The faculty members at University of Chicago are greatly appreciated for being very supportive since I moved to Chicago. Professor Viresh Rawal and Professor John Anderson have helped me a lot during my job searching process and I am really grateful for that.

Next, I want to thank all my collaborators during the past five years: Tao Xu, Jianchun Wang, Likun Jin, Mengqing Chen and Serena Lee; their helpful discussions and solid efforts contribute to every aspect of my research. I am especially grateful to Tao Xu for being my mentor in the first year of my Ph.D. study, who generously helped me both in research and life. All the Dong group members are greatly appreciated for being a super supportive and fun family in the past five year: Haye Min Ko, Rachel Whittaker, Zhi Ren, John Thompson, Xuan Zhou, Fanyang Mo, Hee Nam Lim, Yan Xu, Zhe Dong, Zhongxing Huang, Gang Li, Penghao Chen, Ki-Young

Yoon, Rong Zeng, Dong Xing, Saiyong Pan, Mike Young, Ying Xia, Jiabin Xie, Chengpeng Wang, Tatsuhiro Tsukamoto, Brent Billett, Ziqiang Rong, Ming Chen, Jun Zhu, Renhe Li, Alexander Rago, Sihua Hou, Xiaoyang Chen, Zhao Wu, Xukai Zhou, Hairong Lyu, Yibin Xue and Shusuke Ochi. It is my great honor to work with this group of talented and passionate chemists.

This last word of acknowledgment goes to my dearest family. I could not use any word to describe the gratitude I have for having them being my family. My parents have shown me how to love unconditionally and forgive radically. They encourage me and support me in every mountains and valleys. I dedicate this thesis to them.

Lin Deng  
*University of Chicago*  
May 2019

## **PREFACE**

Each chapter of this dissertation is numbered independently. A given compound may have a different number in different chapters. All experimental details, references, and notes for individual chapters are included at the end of each chapter.

## CHAPTER 1

### C–C Activation of Cyclic Ketones with Ring Strain: History and Recent Methodologies

#### 1.1 Introduction

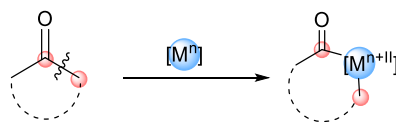
C–C and C–H bonds constitutes most of the organic compounds. In petroleum industry, the C–C bond cleavage and reorganization has been widely used in crude oil refining in a massive scale. When it goes to smaller scales, C–C bond activation has attracted the attention of synthetic chemists for decades because they often lead to interesting skeletal rearrangement and cracking. In the past four decades, significant progress in this field has been achieved, especially with transformations involving transition metals.<sup>1</sup> However, comparing with the selective C–H bond functionalization, studies around C–C  $\sigma$ -bond activations lag behind. One of the reasons is that C–C bonds are less abundant than C–H bonds. The other is that the highly directional character of the C–C bonds making its orbital overlap with transition metal not efficient. Nevertheless, highly strained alkanes, such as quadricyclane, cubanes etc.,<sup>1a</sup> have been shown to undergo C–C  $\sigma$ -bond activation rapidly and enabled the generation of a wide variety of complex ring systems. As more general and synthetically useful C–C  $\sigma$ -bond activation transformations were pursued, strained cyclic ketones have been found to privileged substrates for facile C–C bond cleavage. Ring strain is certainly the main driving force, but in addition to that, the stable acyl metal bond generated or



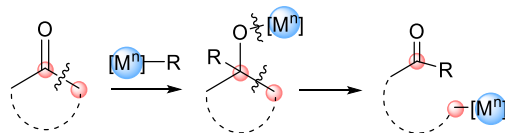
the downhill transformation after C–C bond cleavage also contributes. In addition, ketones are the most common functional groups existing in organic molecules and can also serve as a handle for further transformations, which significantly increases the synthetic utility of C–C bond activation reactions. Mechanistically, there are two major mechanistic pathways involved in the C–C bond cleavage reactions discussed here (Scheme 1.1). The pathway A is through the direct oxidative addition of ketones, which is the reverse reaction of the reductive elimination. Because of the stability of the C–C bond (ca. 90 kcal/mol) comparing with the C–M bond (ca. 30 kcal/mol),<sup>2</sup> the reductive elimination is often thermodynamically favoured. However, when the strained cyclic ketones are involved, this pathway would benefit from the releasing of ring strain and the stability of transition metal carbonyl bond. The other is pathway B, which starts with the addition of a nucleophile to the ketone, then  $\beta$ -carbon elimination driven by ring-strain would take place to cleave the C–C bond.

**Scheme 1.1** Two Major Mechanistic Pathways for C–C Bond Activation of Strained Cyclic Ketones

*Pathway A: Oxidative Addition*



*Pathway B:  $\beta$ -carbon Elimination*

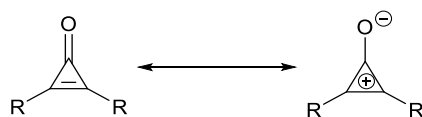


In following sessions, the history and recent development in C–C bond cleavages of several types of cyclic ketone with ring strain would be discussed in detail and we aim at giving a thorough background information for the further research we conducted in this thesis.

## 1.2 C–C Bond Activation of Cyclopropenones

Cyclopropenones have shown special stability attributing to its resonance structure, cyclopropenylum cation, which is the smallest member of the Hückel aromatic systems (Scheme 1.2). The chemical behavior of cyclopropenone is largely related to its polarized nature as well as the large ring strain in the three membered-ring. They have been found to undergo facile C–C bond cleavage due to its high ring strain.<sup>3</sup> In this review, we mainly focus on the transition metal-promoted C–C bond cleavage of cyclopropenones.

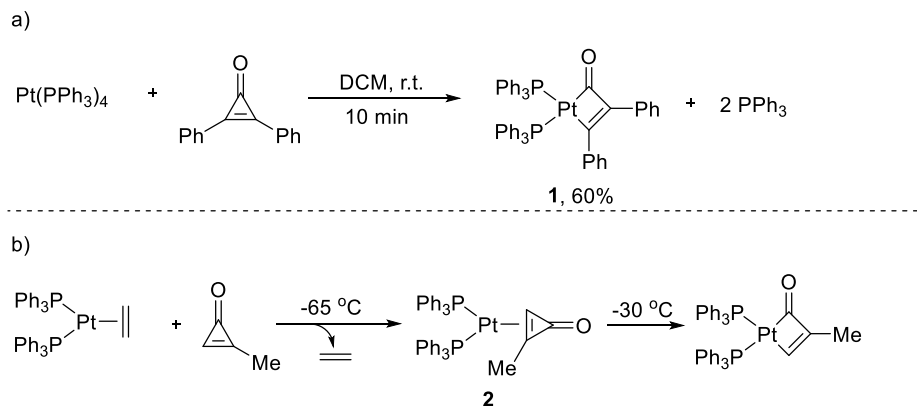
**Scheme 1.2** The Resonance Structure of Cyclopropenones



### 1.2.1 Reactions with stoichiometric metals

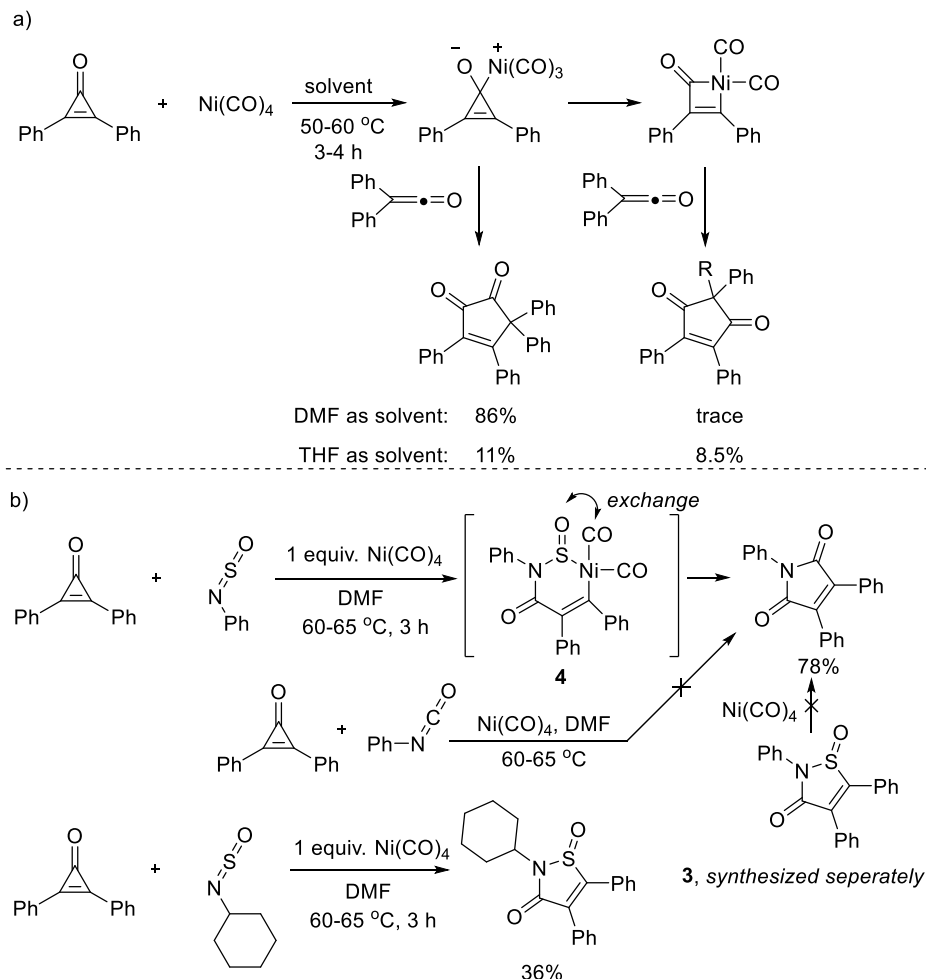
The generation of metallacyclobutenone intermediates were suggested by Bird in the decomposition of diarylcyclopropenones with complexes of Fe, Co as early as 1967.<sup>4</sup> In 1972, Baddley reported the stoichiometric insertion of platinum(0) into the C–C bond of diphenylcyclopropenone at room temperature. The platinacyclobutenone complex **1** was synthesized in 60% yield and was confirmed by X-ray crystallography (Scheme 1.3a).<sup>5</sup> Methylcyclopropenone was also found to undergo exchange with the ethylene ligand in a platinum(0) complex at -65 °C and the platinum further inserted to the C–C bond at slightly elevated temperature, which suggested that complex **2** was an intermediate for the C–C bond cleavage of cyclopropenones (Scheme 1.3b).<sup>6</sup>

### Scheme 1.3 Stoichiometric Insertion of Platinum(0) into Cyclopropenone



In addition to platinum(0) complex, nickel(0) carbonyl complex has also been reported by Baba and coworkers to generate nickelacyclobutenone complex and such intermediates can further react with ketene to generate cyclopenten-1,2-diones in good yield when one equivalent nickel was used (Scheme 1.4a).<sup>7</sup> They found that if *N*-thionylaniline was used as an addition partner, insertion reaction was observed but the S=O completely exchanged with the C=O on nickel. Formally, the product can be regarded as a 1:1 cycloadduct of diphenylcyclopropene and phenyl isocyanate. When phenyl isocyanate was tested in similar conditions, only trimerization of phenyl isocyanate was generated. When 2,4,5-triphenyl-3-isothiazolone-1-oxide **3** synthesized through other method reacted with  $\text{Ni(CO)}_4$ , the exchange product was not observed. These control experiments confirmed that the reaction might go through intermediate **4**, and the exchange happened before the product was generated (Scheme 1.4b). Interestingly, when diphenylcyclopropenone was reacted with *N*-thionylcyclohexylamine, such exchange was not observed.<sup>8</sup>

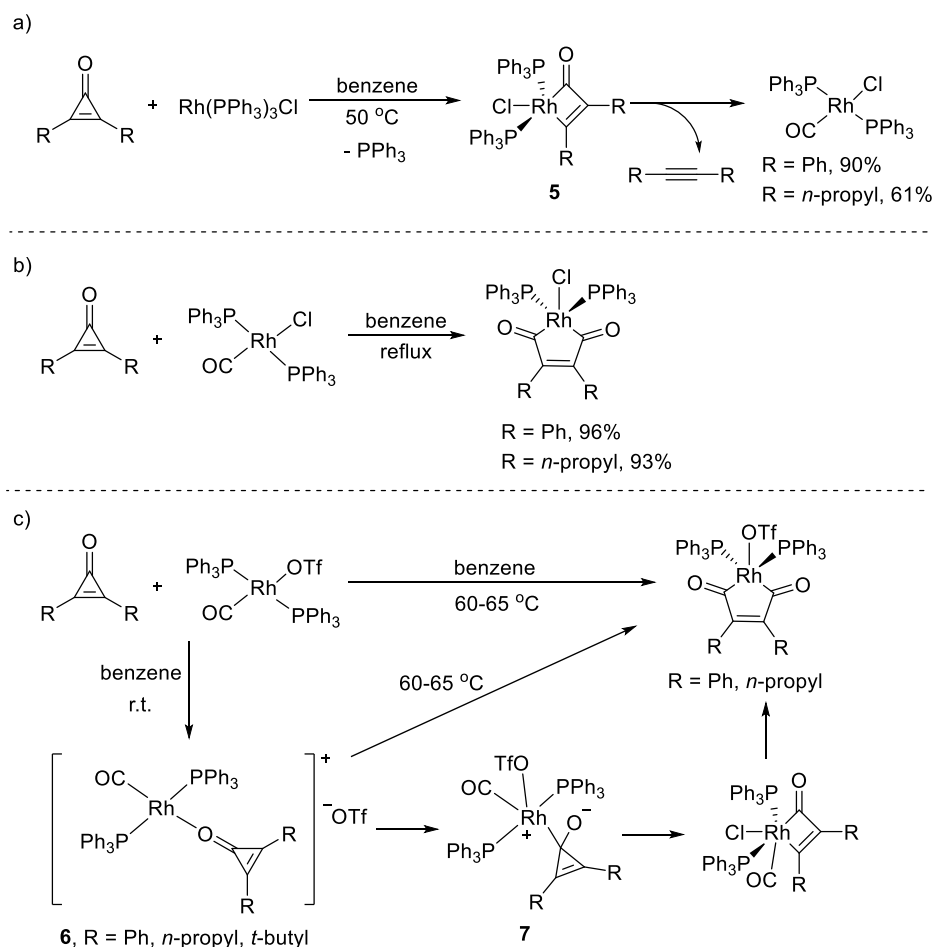
### Scheme 1.4 Stoichiometric Insertion of Nickel(0) into Cyclopropenone



Rhodium(I) complexes were also found to insert into the C–C bond of cyclopropenones by Stang in 1990 (Scheme 1.5).<sup>9</sup> They observed the generation of *trans*-Rh(PPh<sub>3</sub>)<sub>2</sub>(CO)Cl and alkyne products in high yield when heating the cyclopropenones with Wilkinson's catalyst (Scheme 1.5a). They proposed that the rhodacyclobutenone intermediate **5** was generated first, which then further decomposed through decarbonylation into alkynes and *trans*-Rh(PPh<sub>3</sub>)<sub>2</sub>(CO)Cl. When cyclopropenone reacted with the *trans*-Rh(PPh<sub>3</sub>)<sub>2</sub>(CO)Cl in refluxing benzene, air-stable 1-rhodacyclopentene-2,5-diones were isolated in high yields (Scheme 1.5b). When the rhodium complex was changed into *trans*-Rh(PPh<sub>3</sub>)<sub>2</sub>(CO)OTf, the reaction between cyclopropenones and

rhodium complex led to the generation of complex **6** at room temperature. At elevated temperature, the similar 1-rhodacyclopentene-2,5-diones can be generated (Scheme 1.5c). They proposed that the reaction proceed via a mechanism shown in scheme 1.5c. After the generation of complex **7**, rhodium inserted into the cyclopropenone, then CO insertion happened to generate the product.

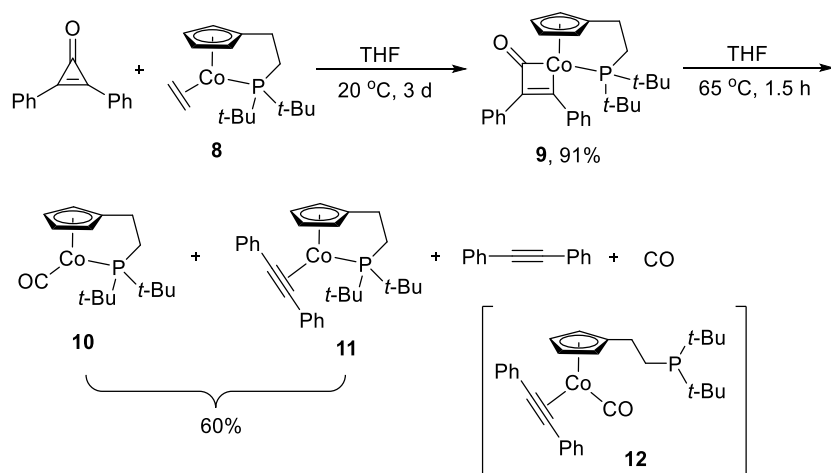
**Scheme 1.5** Stoichiometric Insertion of Rhodium(I) into Cyclopropenone



In 2000, Butenschön reported the insertion of cobalt(I) complex **8** into diphenylcyclopropenones after stirring in THF at  $20\text{ }^\circ\text{C}$  for 3 days with 91% yield (Scheme 1.6).<sup>10</sup> The structure of the metallacyclobutenone complex **9** was confirmed by X-ray crystallography and similar structural characters were observed comparing with the platinacyclobutenone reported by

Baddley (Scheme 1.3a). Upon heating, complex **9** would undergo decarbonylation to give a mixture of complex **10** and **11** in 60% yield and diphenylacetylene was also observed. It was known that carbonyl complex **10** does not undergo a thermal ligand exchange process with diphenylacetylene to give complex **11**. Such complex was proposed to come from intermediate **12**, which has a decoordinated phosphine sidearm directly generating from CO extrusion. Recombination of the sidearm would liberate either CO or diphenylacetylene and generate complex **10** or **11** respectively through an associative intramolecular ligand exchange reaction.

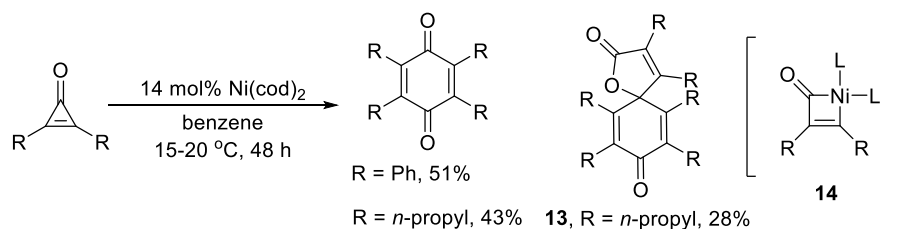
**Scheme 1.6** Stoichiometric Insertion of Cobalt(I) into Cyclopropanone



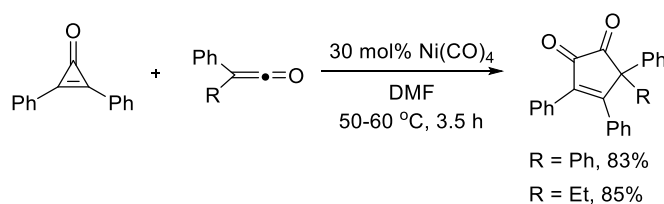
### 1.2.2 Catalytic reactions with different metals

The transition metal catalyzed C–C bond activation of cyclopropanones have been reported as early as the stoichiometric study. In 1972, Noyori reported a nickel(0)-catalyzed dimerization of cyclopropanone to generate benzoquinone. The interesting side product **13** observed in the reaction suggested the existence of the nickelcyclobutenone intermediate **14** (Scheme 1.7).<sup>11</sup> Shortly after that, Baba reported that the insertion of ketene into cyclopropanones can be catalyzed by a nickel carbonyl complex (Scheme 1.8).<sup>7</sup>

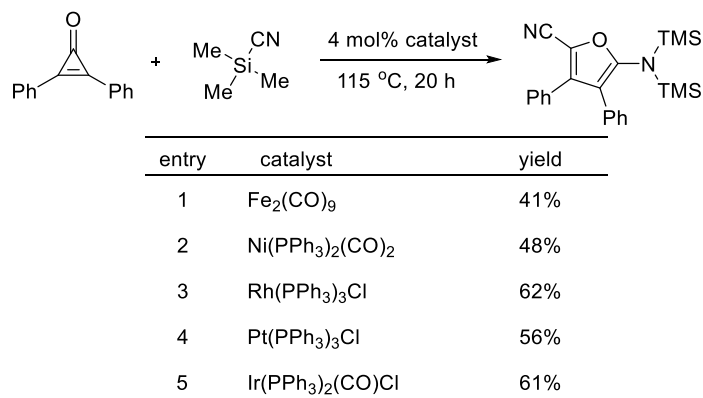
### Scheme 1.7 Nickel-Catalyzed Dimerization of Cyclopropenones



### Scheme 1.8 Nickel-Catalyzed Insertion of Ketene into Cyclopropenones



### Scheme 1.9 Transition-Metal Catalyzed Reaction between Cyclopropenones and Trimethylsilyl Cyanide



In 1987, Chatani reported that several transition-metal complexes can catalyze the reaction between cyclopropenones and trimethylsilyl cyanide to synthesize 5-amino-2-furancarbonitriles (Scheme 1.9).<sup>12</sup> The reaction mechanism was not described in the report. Based on the previous

study, it might proceed through nucleophilic addition of electron-rich transition metal catalyst to the cyclopropenone followed by ring-opening and further attacked the trimethylsilyl cyanide.

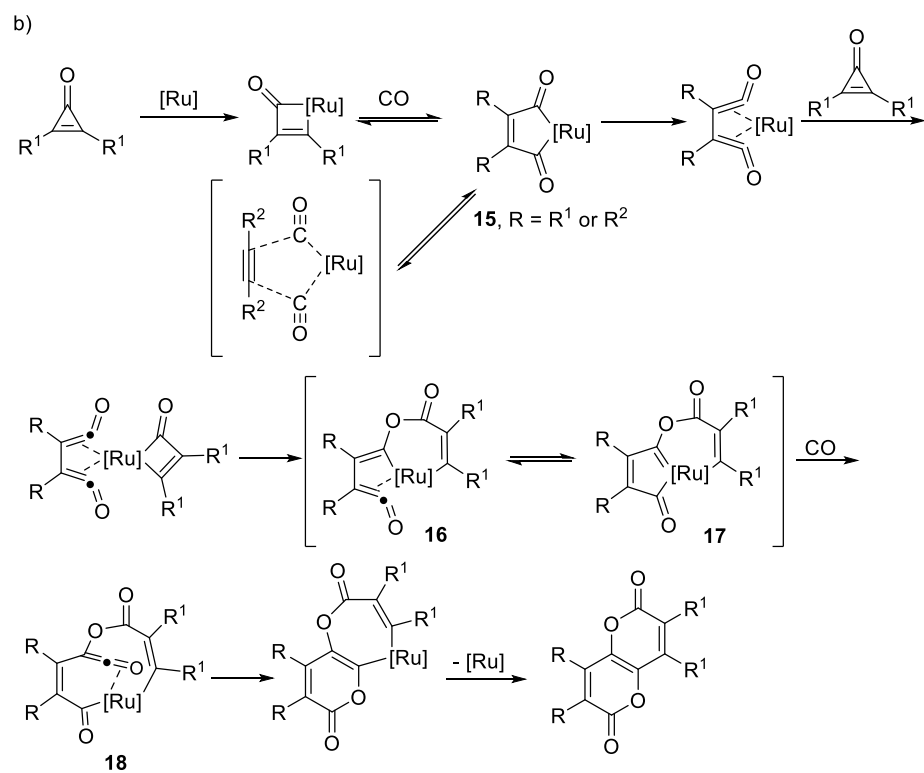
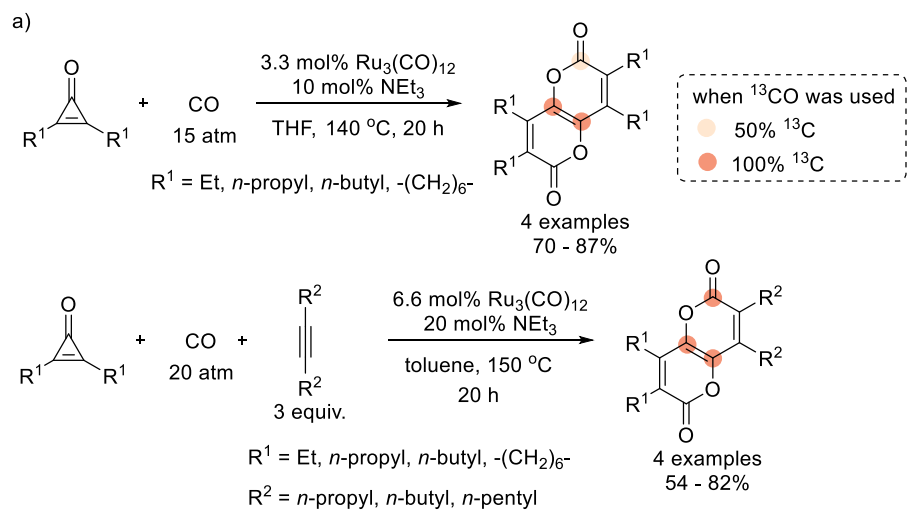
Mitsudo reported ruthenium-catalyzed carbonylative dimerizations of diaryl- or dialkylcyclopropenones as well as crossed reactions with internal alkynes to give substituted pyranopyrandiones (Scheme 1.10a).<sup>13</sup> When  $^{13}\text{C}$ O atmosphere was used in the reaction, carbons highlighted in Scheme 1.10a were labelled with  $^{13}\text{C}$  in corresponding ratio, which supported their mechanistic proposal (Scheme 1.10b). The reaction starts with oxidative addition of the C–C bond in cyclopropenone to give a ruthenacyclobutenone, following by carbonylation of ruthenacyclobutenone (or carbonylative cyclization of alkynes on the ruthenium), which led to a maleoylruthenium intermediate **15**. Such intermediate can further isomerize into an active ( $\eta^4$ -bisketene) ruthenium intermediate, which underwent oxidative addition into another molecule of cyclopropenone and insertion reactions to produce a (ketene)ruthenium intermediate **16**. After isomerizing into ruthenium carbene intermediate **17**, a molecule of carbon monoxide would insert into the carbene-ruthenium bond, which led to another ketene intermediate **18**. Final insertion of a ketene carbonyl group and reductive elimination give the desired product.

Wender later disclosed a rhodium(I)-catalyzed [3+2]-cycloaddition of cyclopropenones with alkynes forging cyclopentendiones (Scheme 1.11).<sup>14</sup> The rhodium catalyst underwent oxidative addition to the acyl-carbon bond of cyclopropenones and gave rhodacyclobutenones. Then alkyne migratory insertion followed by reductive elimination delivers cyclopentadienones. Diphenyl- and phenylmethylcyclopropenones can be used as the three carbon component in combination with aryl- and dialkyl-substituted alkynes or benzyne. Cyclopentendiones can be synthesized on a multigram scale through this transformation and 0.1 mol% catalyst loading still

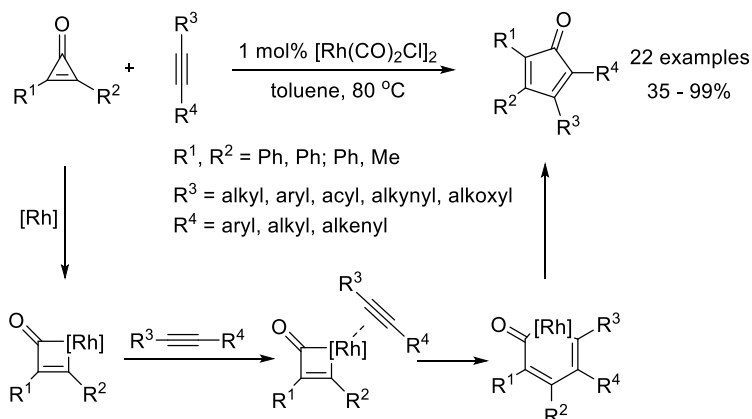


provided 69% yield. The regioselectivity is also excellent, consistent with the regioselectivity observed in Pauson-Khand reactions of analogous aryl alkynes.

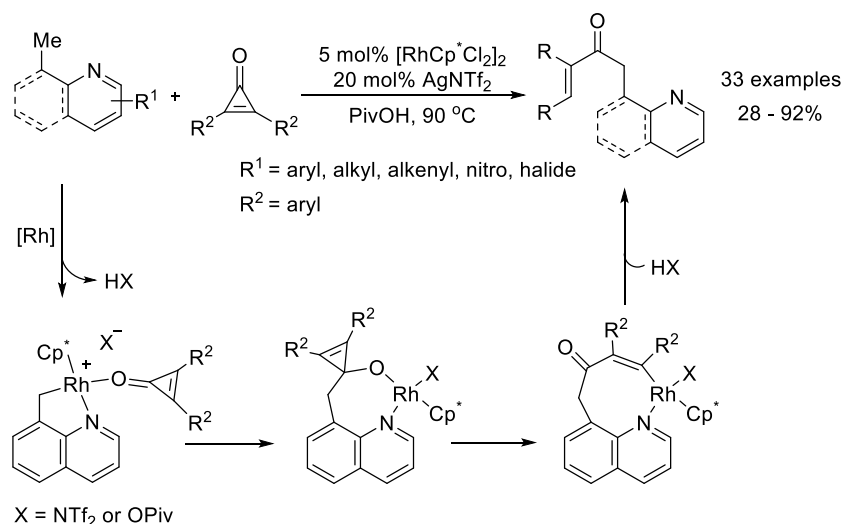
### Scheme 1.10 Ruthenium-Catalyzed Carbonylation of Cyclopropenones



**Scheme 1.11** Rhodium-Catalyzed [3+2]-Cycloaddition of Cyclopropenones with Alkynes



**Scheme 1.12** Rhodium-Catalyzed Aryl C–H Bond Insertion into Cyclopropenones



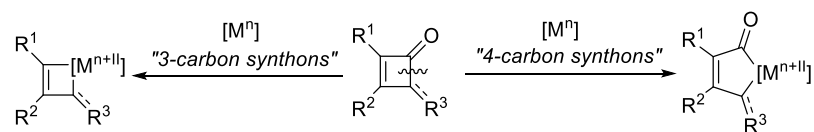
Recently, Li studied rhodium(III)-catalyzed C(sp<sup>3</sup>)–H bond insertion into cyclopropenones via C–H activation pathway.<sup>15</sup> This study is an extension of their previous report on rhodium(III)-catalyzed C(sp<sup>2</sup>)–H bond insertion into cyclopropenones.<sup>16</sup> The mechanism of both transformations are similar (Scheme 1.12). Initiated by C(sp<sup>3</sup>)–H bond activation, a five-membered rhodacyclic intermediate was generated and further coordinated to cyclopropenone. The carbonyl group of cyclopropenone then underwent migratory insertion followed by β-carbon

elimination to give a ring-opened alkenyl intermediate. At the end, protonolysis furnishes the final product.

### 1.3 C–C Bond Activation of Cyclobutenediones and Cyclobutenones

When it comes to four-membered ring ketones, early studies have been focused on cyclobutenediones and cyclobutenones, because they are more strained comparing to the saturated cyclobutanones thus more activated. Compared with cyclopropenones, their diverse structures and reactivities promise the product generated with an impressive level of complexity. In general, cyclobutenediones and cyclobutenones can either undergo direct C–C cleavage or decarbonylative C–C cleavage. As a result, they can be considered as either a four-carbon or three-carbon synthon (Scheme 1.13).<sup>1p</sup>

**Scheme 1.13** Cyclobutenediones and Cyclobutenones in C–C Bond Activation Reactions



#### 1.3.1 Reactions with stoichiometric metals

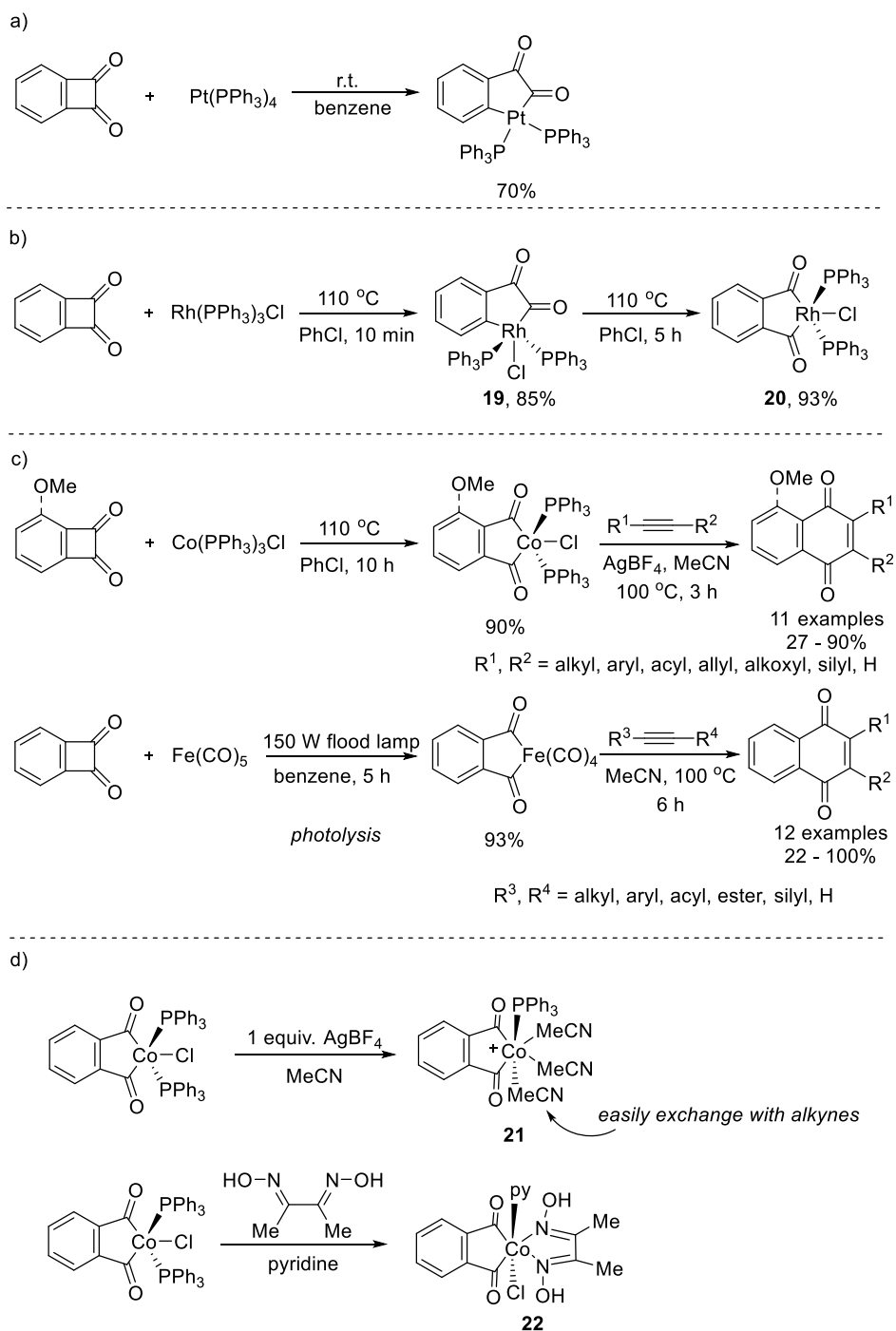
Benzocyclobutenediones are the initial candidate chosen to investigate the reactivity of four-membered ring ketones in C–C bond activation reaction. Metal insertion into the C–C bond of benzocyclobutenediones was first reported in 1973 by Kemmitt using Pt(PPh<sub>3</sub>)<sub>4</sub>. The structure of the platinabenzocyclopentenedione was confirmed by X-ray crystallography to be the unsymmetrical cleavage product (Scheme 1.14a).<sup>17</sup> Liebeskind later used Wilkinson's catalyst to generate the C–C bond cleavage product (Scheme 1.14b).<sup>18</sup> It was observed that the unsymmetrical cleavage product **19** was formed at first, which then isomerized to symmetrical cleavage product

**20**. This suggested that **19** is a kinetic product and **20** is a thermodynamic product. Cobalt and iron complex are also capable of inserting into the C–C bond of benzocyclobutenediones and the symmetrical cleavage products were observed.

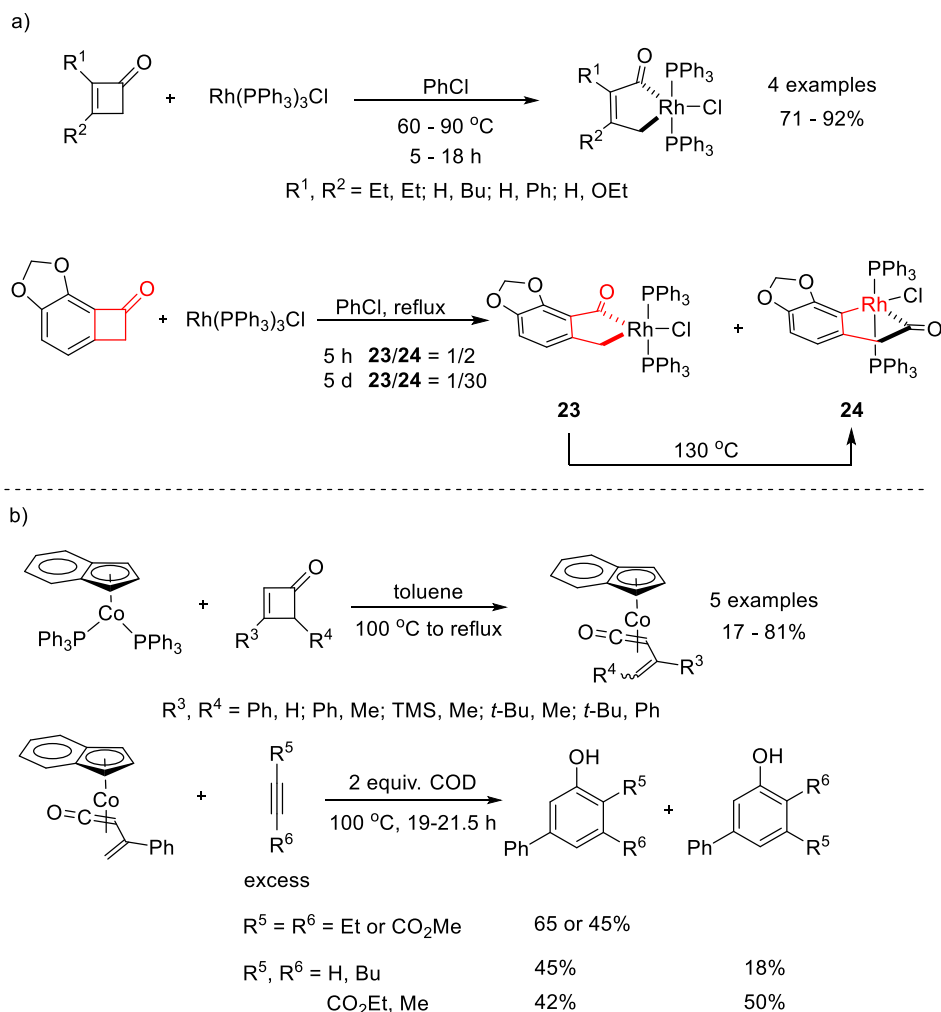
Following their stoichiometric study on the transition metal insertion into cyclobutenediones, Liebeskind systematically studied the naphthoquinone and benzoquinone synthesis realized by alkyne insertion to the metalla(benzo)cyclopentenediones.<sup>19</sup> Both cobalt and iron complexes were capable of reacting with a wide variety of alkynes to yield naphthoquinones with moderate to excellent efficiency and regioselectivity (Scheme 1.14c).<sup>20</sup> The cobalt system requires the activation using AgBF<sub>4</sub> to generate a 6-coordinated 18-electron cobalt complex and facilitate the ligand exchange with alkyne (Scheme 1.14d).<sup>21</sup> Compared with the iron system, the requirement of a silver salt might be a drawback, but the easy preparation of phthaloylcobalt complex **21** made it the primary system they further studied on.

Later this phthaloylcobalt complex was successfully applied to the regiospecific total synthesis of (±)-nanaomycin A enabled by an intramolecular directed regiochemical control.<sup>22</sup> To get rid of the silver salt in the cobalt system, they modified the cobalt complex with dimethylglyoxime in solvent amount of pyridine to give high yields of a 6-coordinated cobalt complex **22**, which enables a faster ligand exchange with alkynes and proved to be equally effective without silver salts (Scheme 1.14d).<sup>19</sup> In analogy to the naphthoquinone synthesis, the benzoquinone synthesis was achieved with good efficiency and regioselectivity.<sup>23</sup>

# **Scheme 1.14** Stoichiometric Reactions Involving Insertion of Transition-Metals into Cyclobutenediones



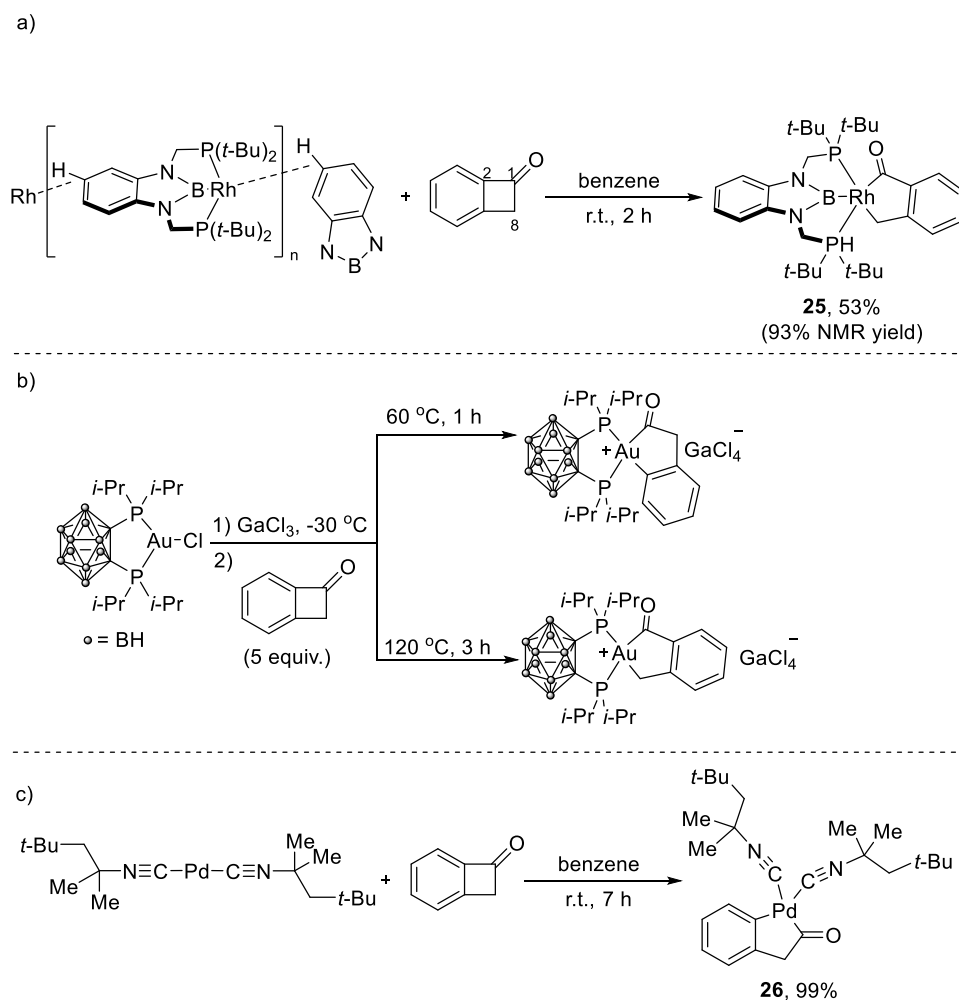
### Scheme 1.15 Stoichiometric Insertion of Transition-Metals into Cyclobutenones



Inspired by the success with activation and transformation of cyclobutenediones, Liebeskind casted attention on C–C bond cleavage of cyclobutenones and benzocyclobutenones (Scheme 1.15a).<sup>24</sup> Wilkinson's catalyst underwent oxidative addition to cyclobutenones and generated 5-rhoda-2-cyclopenten-1-ones with good efficiency. Mixtures of two regioisomeric insertion products were observed when benzocyclobutenones were employed. Interestingly, when the reaction time was extended to 5 days, complex **24** became the dominate product, which suggest that complex **24** is thermodynamically favored product. In contrast, when cyclobutenones reacted with  $(\eta^5\text{-C}_9\text{H}_7)\text{Co}(\text{PPh}_3)_2$ ,  $\eta^4$ -vinylketene complexes were formed as mixtures of *E/Z* isomers. The

monosubstituted vinylketene cobalt complex can react with various alkynes to generate phenols. For unsymmetrical alkynes, such a reaction would give a mixture of regioisomers (Scheme 1.15b).<sup>25</sup>

**Scheme 1.16** Recent Examples of Stoichiometric Insertion of Transition-Metals into Benzocyclobutenones



Recently, several stoichiometric reactions involving transition-metal insertion into benzocyclobutenones have been reported at much lower reaction temperature or with metals that are less explored in the field (Scheme 1.16). In 2013, Murakami, Nozaki and Yamashita observed

that an infinitely networked T-shape 14-electron rhodium(I) complex coordinating to a PBP pincer ligand was able to undergo oxidative addition into the C1–C8 bond of benzocyclobutenones, which delivered **25** with high efficiency at room temperature (Scheme 1.16a).<sup>26</sup>

Bourissou later disclosed that (diphosphinocarborane)gold(I) complexes can selectively cleave the C1–C2 or C1–C8 bond in benzocyclobutenone to generate the corresponding acyl gold(III) complexes at different reaction temperatures (Scheme 1.16b).<sup>27</sup> Moreover, when the palladium(0)-isocyanide complex was mixed with benzocyclobutenone in benzene at room temperature for 7 h, the C1–C2 bond of benzocyclobutenones were selectively cleaved and the five-membered palladacycle **26** was produced in a quantitative yield (Scheme 1.16c).<sup>28</sup>

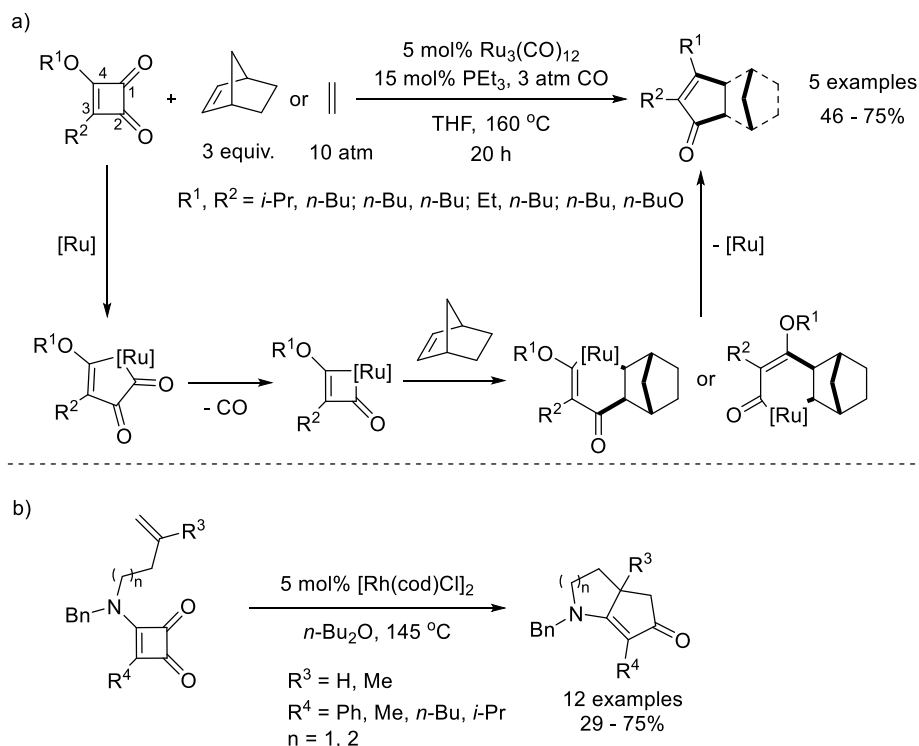
### 1.3.2 Catalytic reactions with different metals

On the basis of the stoichiometric study on C–C bond cleavage of cyclobutenediones, Mitsudo disclosed a ruthenium-catalyzed decarbonylative C–C bond activation of cyclobutenediones followed by coupling with alkenes (Scheme 1.17a).<sup>29</sup> Alkoxy group substitution on C4 position is required to selectively cleave the C1–C4 bond. When the 3,4-dialkylcyclobutenedione was subjected to the reaction condition, C1–C2 bond was selectively cleaved which led to the phenol product in 74% yield. The carbon monoxide pressure was found to be crucial for the transformation and 3 atm was the optimal pressure. Use of <sup>13</sup>CO would lead to 70% <sup>13</sup>C scrambling at the cyclopentenone product, which suggested that the external CO is needed to suppress the complete decarbonylation. Apart from norbornene, ethylene gas was also found to be an effective coupling partner. The proposed mechanism for this transformation started with the selective oxidative addition of ruthenium into the C1–C4 bond directed by the alkoxy substituent, followed by decarbonylation to generate a ruthenacyclobutenone intermediate. Subsequent migratory insertion of norbornene and reductive elimination gives the product



exclusively in its *exo* form. In 2006, Yamamoto reported an intramolecular version of this reaction using a nitrogen-tethered substrate (Scheme 1.17b).<sup>30</sup>

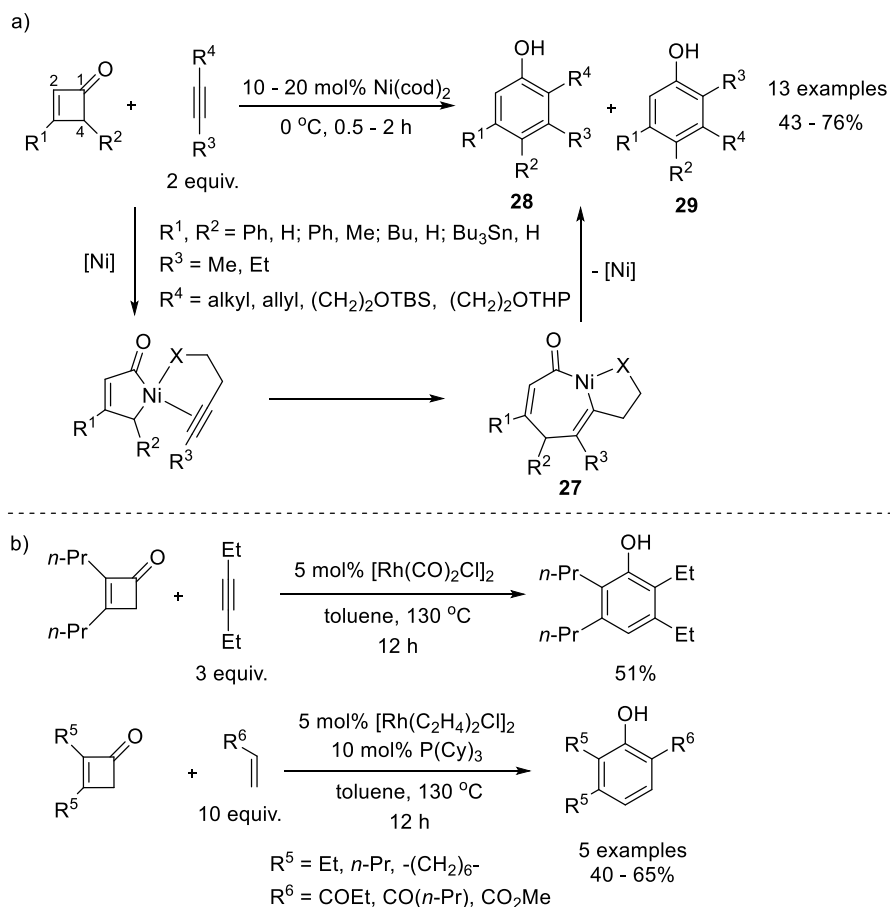
**Scheme 1.17** Ruthenium-Catalyzed Decarbonylative C–C Bond Activation



Compared with cyclobutenediones, cyclobutenones have been applied in a wide variety of catalytic transformations using transition metals. The catalytic reaction was pioneered by Liebeskind in 1991 to realize the synthesis of substituted phenols through nickel-catalyzed C–C bond cleavage of cyclobutenones (Scheme 1.18a).<sup>31</sup> The reaction was initiated by oxidative addition of the Ni(0) catalyst to the C1–C4 bond of cyclobutenones, and the coordinated alkyne would then undergo migratory insertion to generate intermediate **27**. After reductive elimination and aromatization, the product can be generated. For most of the examples, the ratio between **28** and **29** was close to 1:1. However, for alkyne substrates bearing an oxygen moiety two carbons away, the regioselectivity improves significantly to give a ratio of 3:1. The improvement on the

regioselectivity was attributed to the chelation between the nickel and the oxygen. This type of reactivity was later further explored by Kondo in 2007 using a rhodium catalyst.<sup>32</sup>

**Scheme 1.18** Synthesis of Phenols through C–C Bond Activation

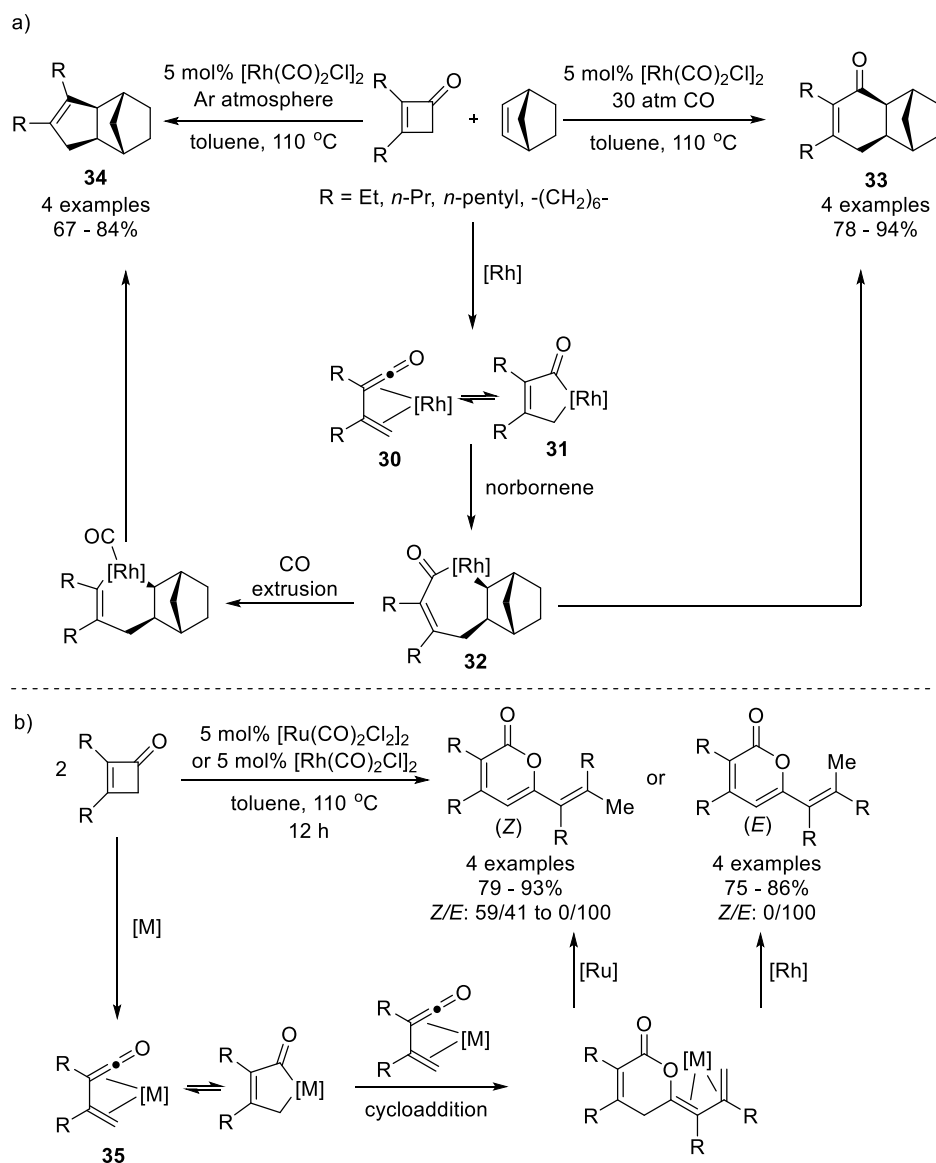


In Liebeskind's report, 2,3-disubstituted cyclobutenones were not viable substrates. However, using rhodium catalysts, these substrates could successfully yield the desired phenols in moderate yields (Scheme 1.18b). A more intriguing finding was that the cycloaddition between the proposed ( $\eta^4$ -vinylketene)rhodium intermediate and an electron-deficient olefin, followed by dehydrogenation and isomerization, would lead to a highly regioselective formation of phenol

products.<sup>32</sup> In 2015, Harrity investigated the regioselectivity in the nickel-catalyzed system and extended the insertion partner to alkynylboronates.<sup>33</sup>

Apart from catalytic reactions between cyclobutenones and alkenes to generate phenols, Mitsudo and Kondo reported on a rhodium-catalyzed decarbonylative coupling and direct coupling of cyclobutenones with norbornene to selectively synthesize cyclopentenones and cyclohexenones (Scheme 1.19a). Oxidative addition of rhodium into cyclobutenones generates the ( $\eta^4$ -vinylketene)rhodium intermediate **30** that may exist in an equilibrium with rhodacyclopentenone **31**. Migratory insertion of norbornene would lead to the rhodacycloheptenone intermediate **32**, from which direct reductive elimination produces cyclohexenones **33** and CO extrusion followed by reductive elimination yields cyclopentenones **34**. When  $^{13}\text{CO}$  atmosphere was used, 71% of the carbonyl group in the generated cyclohexenones was labeled by  $^{13}\text{C}$ , which suggested that the decarbonylation during the reaction process was facile but reversible. In addition to that, Mitsudo and Kondo disclosed that ruthenium or rhodium can both catalyze the C–C bond cleavage of cyclobutenones followed by insertion of another vinylketene generated in the reaction to yield 2-pyranones (Scheme 1.19b). The mechanism of this reaction includes the hetero-Diels-Alder reaction between two molecules of metal-bound  $\eta^4$ -vinylketene intermediate **35**. Interestingly ruthenium and rhodium gave different *Z/E* selectivity. Ruthenium catalysts gave good *Z* selectivity, while rhodium catalysts led to the *E* products exclusively. When cyclobutenone was fused with an eight-membered ring, both catalysts gave the *E* product.<sup>34</sup>

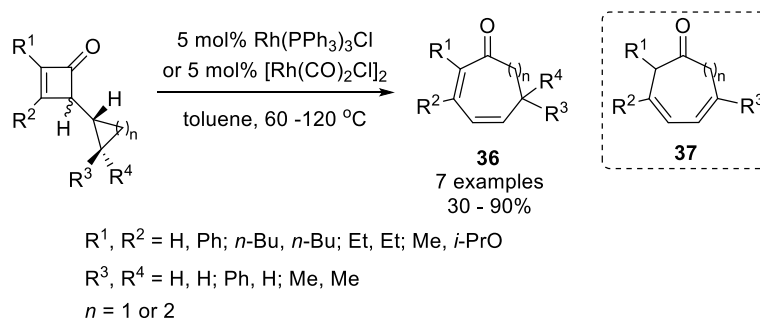
**Scheme 1.19** Rhodium or Ruthenium-Catalyzed Coupling between Cyclobutenones and Norbornene or Ketene



Apart from reacting cyclobutenones with unsaturated bonds, other coupling partners have been explored as well. In 1993, Liebeskind reported on a rhodium-catalyzed intramolecular ring fusion reaction between cyclobutenones and cyclopropanes or cyclobutanes (Scheme 1.20).<sup>35</sup> In the presence of a rhodium catalyst, cycloheptadienones or cyclooctadienones **36** was formed in good yields. At elevated temperature, 1,5-hydrogen shift can take place and generate the

isomerized products **37** in some cases. This ring fusion strategy provides a unique approach to obtain medium-size rings.

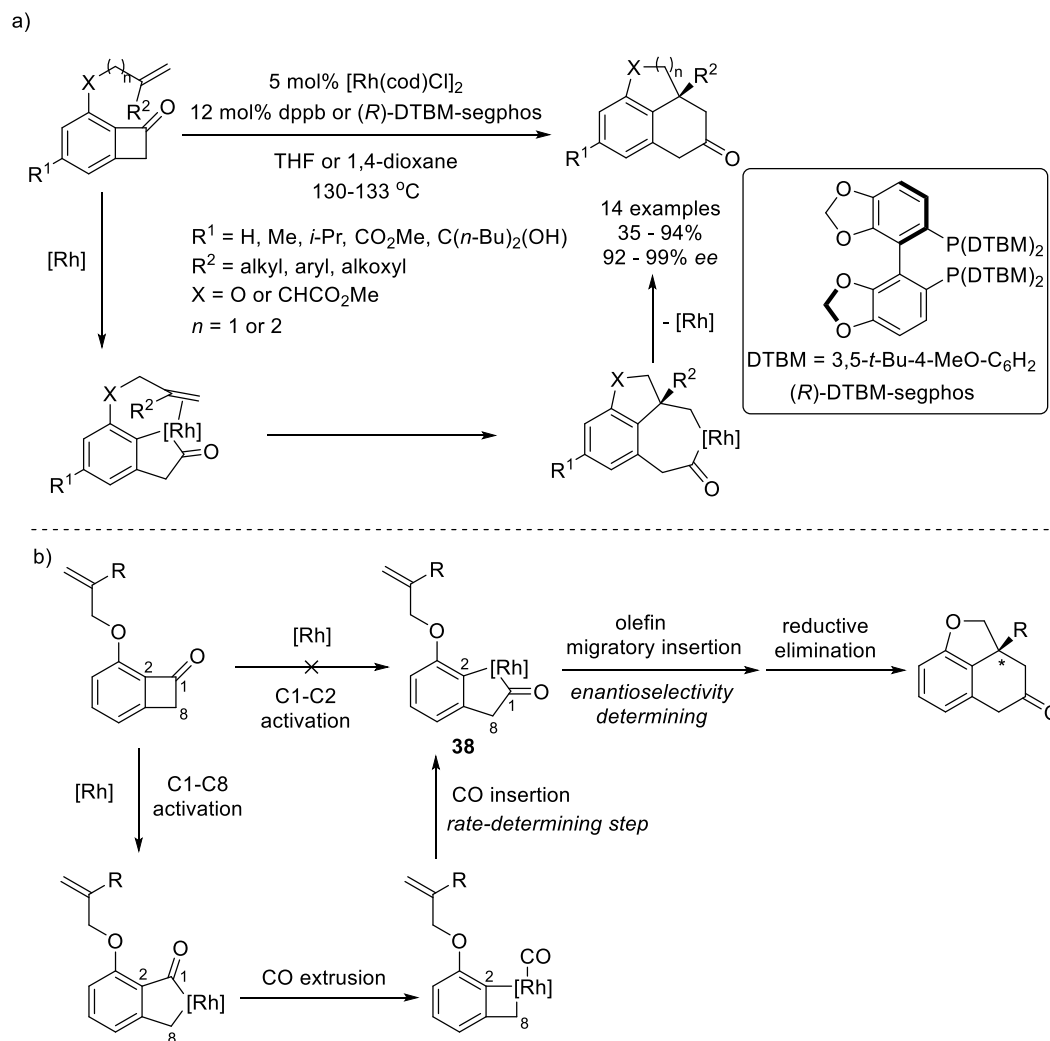
**Scheme 1.20** Rhodium-Catalyzed Intramolecular Ring Fusion Reaction



In Liebeskind's stoichiometric study, benzocyclobutenones have shown interesting regioselectivity in C–C bond cleavage (Scheme 1.15a), which intrigues the application of such intermediates in the catalytic transformations. Xu and Dong disclosed the rhodium-catalyzed intramolecular carboacylation of olefins through C–C bond activation of benzocyclobutenones in 2012 (Scheme 1.21a).<sup>36</sup> After the generation of rhodacycle, the intramolecular migratory insertion of olefins followed by reductive elimination would yield the tricyclic products.

Using (*R*)-DTBM-segphos, excellent enantioselectivity was obtained.<sup>37</sup> From the computational study by Liu (Scheme 1.21b), the C–C bond cleavage first occurs at the C1–C8 position, and then the CO extrusion and reinsertion takes place to afford the formal C1–C2 cleavage intermediate **38**. The CO reinsertion step was found to be the rate-determining step. After intermediate **38** is generated, the olefin would insert into the rhodacycle, which is the enantioselectivity determining step.<sup>38</sup>

**Scheme 1.21** Rhodium-Catalyzed Carboacylation of Olefins through C–C Bond Activation of Benzocyclobutenones

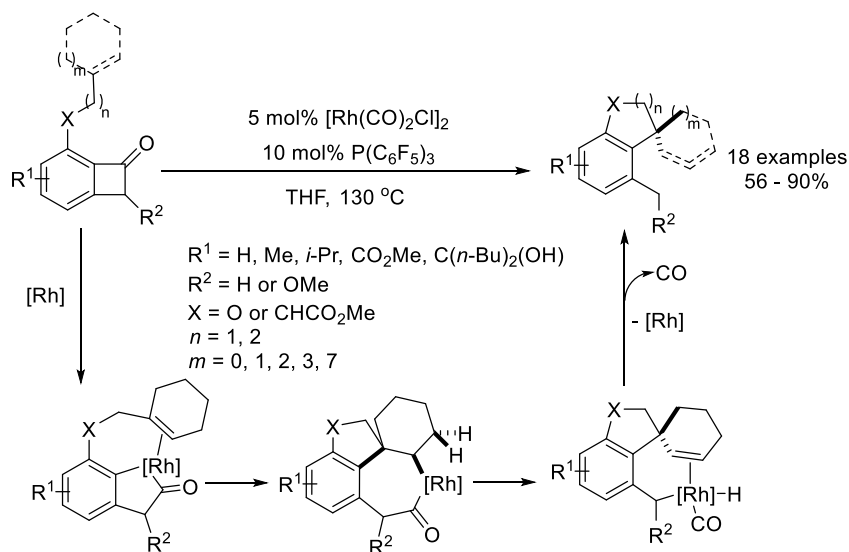


In analogy to the reaction between cyclobutenones and olefins (Scheme 1.19a), decarbonylative coupling between benzocyclobutenones and olefins can afford products with different ring structures. An intriguing spirocycle formation was observed by Dong when benzocyclobutenones tethered with cyclic olefins were subjected to the reaction catalyzed by  $[\text{Rh}(\text{CO})_2\text{Cl}]_2/\text{P}(\text{C}_6\text{F}_5)_3$  in tetrahydrofuran at 130 °C (Scheme 1.22).<sup>39</sup> The mechanism of this

transformation features a CO extrusion after migratory insertion of the olefin followed by a  $\beta$ -H elimination.

### Scheme 1.22 Rhodium-Catalyzed Decarbonylative Spirocyclization through C–C Bond

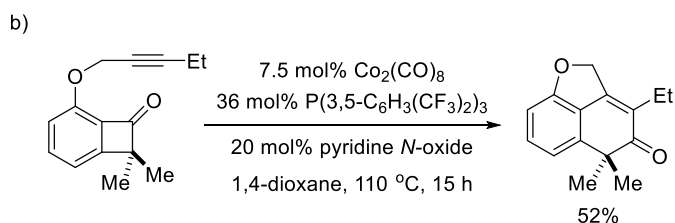
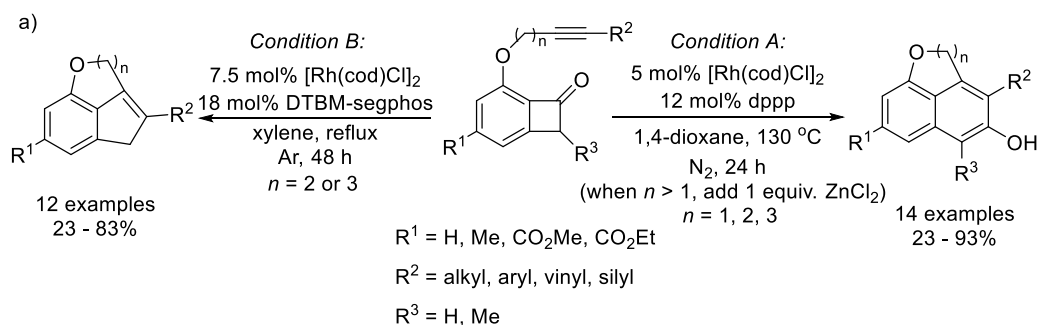
#### Activation of Benzocyclobutenones



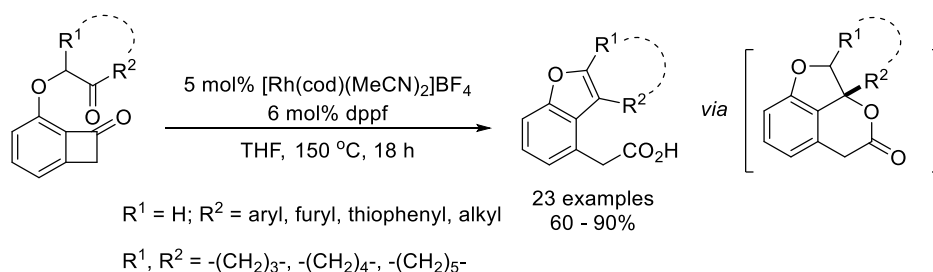
When alkynes were adopted as the coupling partner, both direct insertion products and decarbonylative insertion products were obtained through fine tuning of the reaction conditions (Scheme 1.23a).<sup>40</sup> Later, Dong disclosed that, using  $\text{Co}_2(\text{CO})_8/\text{P}(3,5\text{-C}_6\text{H}_3(\text{CF}_3)_2)_3$  as the optimal precatalyst/ligand combination, bulky benzocyclobutenones can be used as substrates to couple with alkynes intramolecularly (Scheme 1.23b).<sup>41</sup>

Apart from non-polarized  $2\pi$  units, recently, polarized ones such as  $\text{C}=\text{O}$  bonds have been reported to undergo similar insertion reactions to benzocyclobutenones. In 2018, Xu reported that a cationic rhodium(I) complex can catalyze the intramolecular carboacylation of  $\text{C}=\text{O}$  bonds with benzocyclobutenones followed by an aromatization-driven elimination to afford benzofurans (Scheme 1.24).<sup>42</sup>

### Scheme 1.23 Rhodium-Catalyzed Alkyne-Benzocyclobutenone Couplings



### Scheme 1.24 Rhodium-Catalyzed Carboacylation/Aromatization Cascade

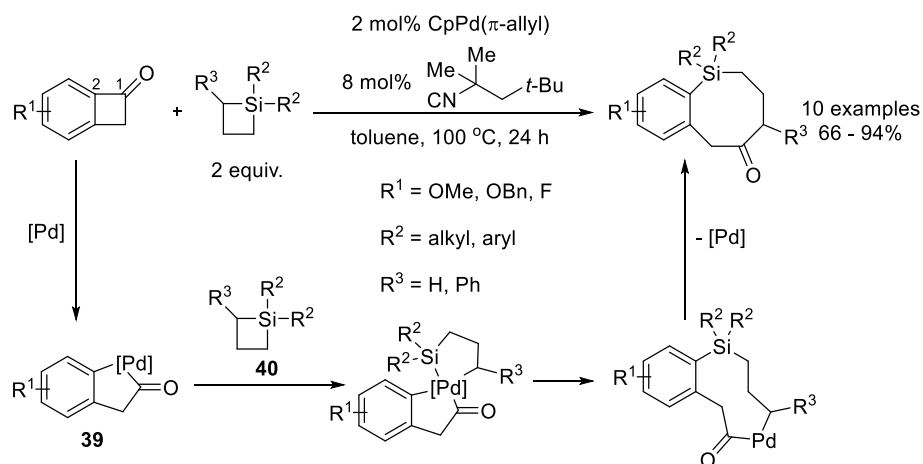


Murakami disclosed the insertion of silacyclobutanes into benzocyclobutenones using the *in-situ* generated palladium(0)-isocyanide complex as a catalyst. Firstly, the palladium(0) undergoes oxidative addition into C1–C2 bond in benzocyclobutenone to generate intermediate **39** (*vide supra*, Scheme 1.16c). The transmetalation of the C–Si bond in silacyclobutane **40** with the C–Pd bond of **39** takes place to give the nine-membered palladacycle. They proposed that the transmetalation happens through a sequence of oxidative addition and reductive elimination. Finally, C–C reductive elimination generates the eight-membered ring product and reforms the



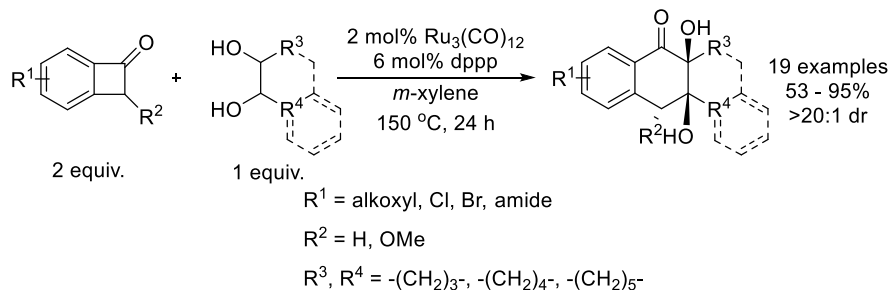
palladium(0) catalyst (Scheme 1.25).<sup>28</sup> Later, the computational study supported the proposed reaction pathway.<sup>43</sup>

**Scheme 1.25** Palladium-Catalyzed Insertion of Silacyclobutane into Benzocyclobutenones

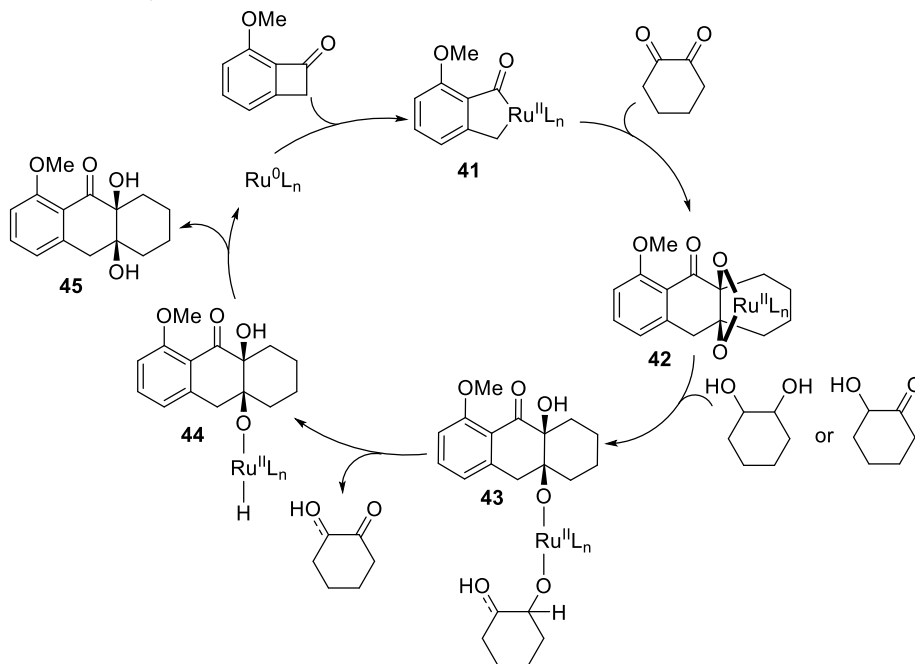


Recently, Krische reported that when a ruthenium(0) complex was used as the catalyst, the C1–C8 bond was selectively cleaved to generate ruthena-indanone **41**, which upon successive addition of the C–Ru bonds to 1,2-dione, generates the ruthenium(II) diolate complex **42**.<sup>44</sup> Protonolysis of intermediate **42** by the diol or ketol delivers the ruthenium(II) alkoxide **43**. After  $\beta$ -hydride elimination, the ruthenium hydride **44** and the ketol or 1,2-dione are generated. Lastly, O–H reductive elimination releases the product **45** and regenerated the ruthenium(0) catalyst. Diverse diols were found to undergo the cycloaddition reaction smoothly and the nonsymmetric diols gave high regioselectivity. It is noteworthy that the resulting cycloadduct **45** possesses the key structural motif in type II polyketides (Scheme 1.26). In 2018, the same group disclosed an analogous enantioselective cycloaddition between benzocyclobutenones and ketols by replacing the dppp ligand into (*R*)-segphos.<sup>45</sup>

**Scheme 1.26** Ruthenium-Catalyzed Insertion of Adjacent Diols into C–C Bond of  
Benzocyclobutenones and Benzocyclobutenediones



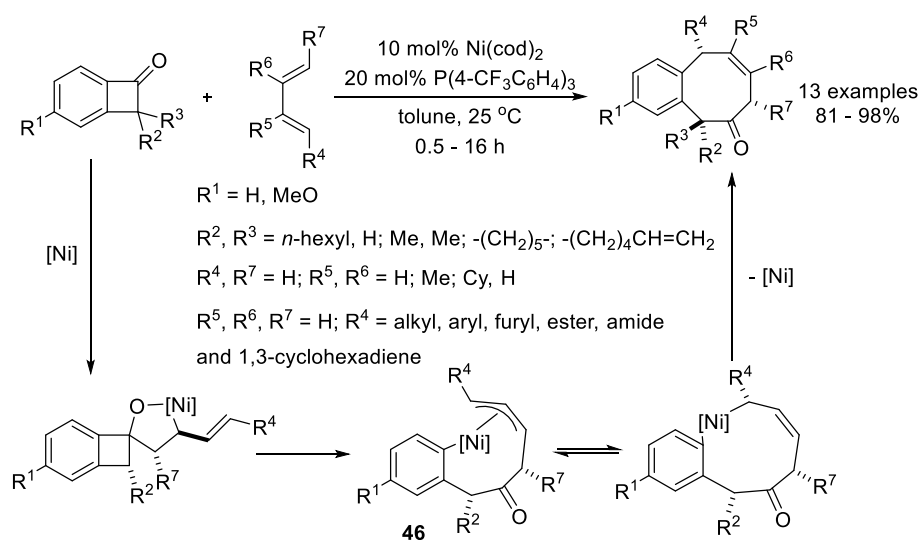
*Mechanistic Proposal:*



Apart from the oxidative addition pathway, the  $\beta$ -carbon elimination pathway has also been studied in C–C bond activation of benzocyclobutenones. In 2005, Martin reported that nickel(0) can catalyze the intermolecular insertion of dienes (or diphenylacetylene) into the benzocyclobutenones after the selective C1–C2 bond cleavage (Scheme 1.27).<sup>46</sup> The proposed mechanism started with oxidative cyclization of a low-valent nickel complex to 1,3-dienes and benzocyclobutenones. A subsequent  $\beta$ -carbon elimination leads to the formation of  $\pi$ -allyl nickel(II)

metallacycle **46**, which further undergoes reductive elimination to form the product. Later, computational studies suggested that this reaction could possibly go through an oxidative addition pathway.<sup>47</sup> When PPh<sub>3</sub> was adopted as the ligand with Ni(cod)<sub>2</sub> as precatalyst, analogous intermolecular insertion of diphenylacetylene into benzocyclobutenones was achieved with good efficiency.<sup>46</sup>

**Scheme 1.27** Nickel-Catalyzed Intermolecular Diene-Benzocyclobutenone Couplings



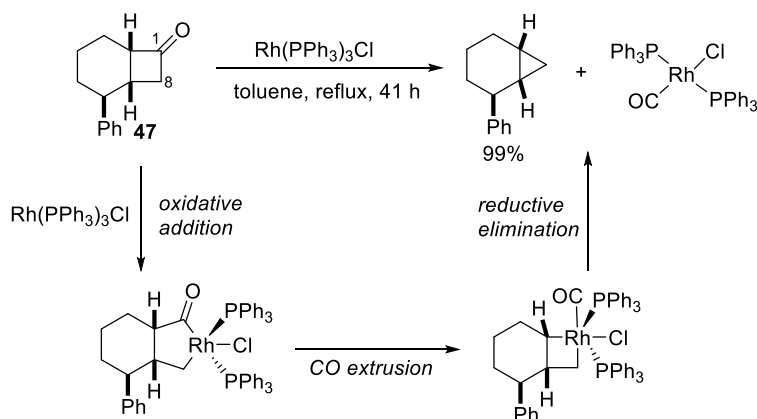
#### 1.4 C–C Bond Activation of Cyclobutanones

Cyclobutanones are another type of strained cyclic ketones which have been widely studied among C–C bond activation reactions. Compared with cyclobutenones and cyclobutenediones, they possess less ring strain and present a bigger challenge for transition-metal-mediated reactions. Nevertheless, different strategies have been applied to activate cyclobutanones and significant progress was made in the past two decades, especially in forging diverse ring systems and constructing quaternary carbon centers.

### 1.4.1 Reactions with stoichiometric metals

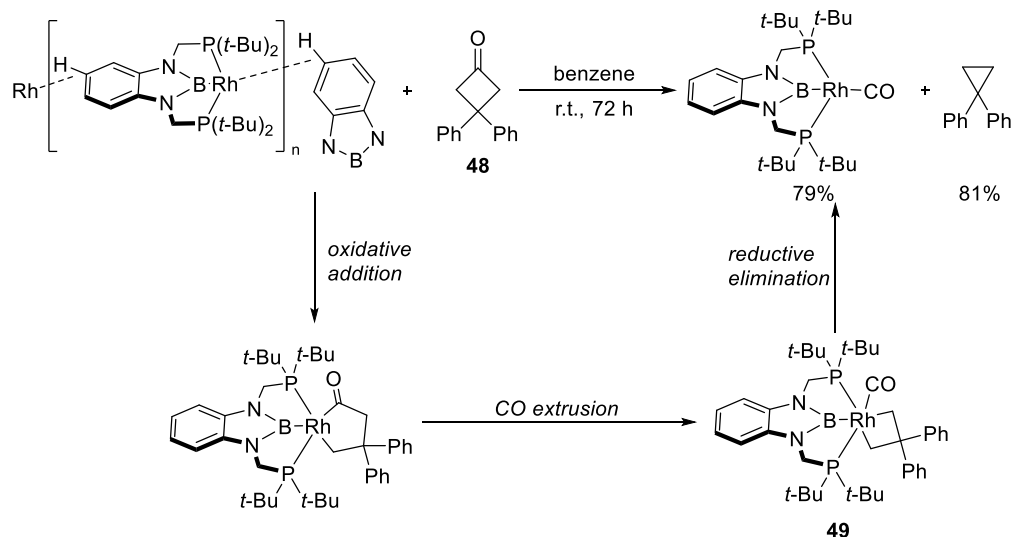
The C–C bond activation of cyclobutanones is pioneered by Murakami in 1994, when they observed the quantitative decarbonylation of cyclobutanones upon refluxing substrate **47** with Wilkinson's catalyst. The generation of stable *trans*-Rh(PPh<sub>3</sub>)<sub>2</sub>(CO)Cl was proposed to be crucial for the success of this transformation. The mechanism proposal starts with oxidative addition of Wilkinson's catalyst into the less hindered C1–C8 bond, and was followed by CO extrusion and reductive elimination to provide products (Scheme 1.28).<sup>48</sup> Similar stoichiometric reactions happened smoothly with simple 3-alkyl substituted cyclobutanones as well.<sup>49</sup>

**Scheme 1.28** Decarbonylation of Cyclobutanones by Insertion of Stoichiometric Rhodium(I)



In 2013, Murakami disclosed that an electron-rich rhodium(I) PBP complex can undergo oxidative addition into cyclobutanone **48** and proceed to the decarbonylation product with good efficiency at room temperature (Scheme 1.29).<sup>26</sup> The oxidative addition was proposed to be the rate-determining step. The hexa-coordinated intermediate **49** is thermodynamically unstable because of the steric congestion from the *t*-butyl group, which provide a driving force for the reductive elimination.

**Scheme 1.29** Oxidative Addition of Cyclobutanone onto Rhodium(I) at Room Temperature



#### 1.4.2 Catalytic reactions with different metals

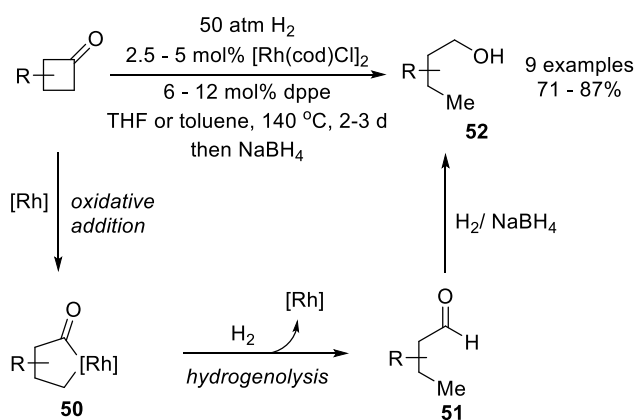
Upon the discovery of the reactivity between cyclobutanones and stoichiometric metals, the catalytic reactions have been the major focus for chemists to develop synthetically useful reactions utilizing the unique reaction mode of C–C bond activation. Through years of development, two major C–C cleavage pathways, direct oxidative addition and  $\beta$ -carbon elimination, have been heavily studied. The C–C bond activation of cyclobutanones followed by new bond formations has been demonstrated to be a highly efficient way to construct complex ring systems.

##### 1.4.2.1 C–C bond cleavage via oxidative addition pathway

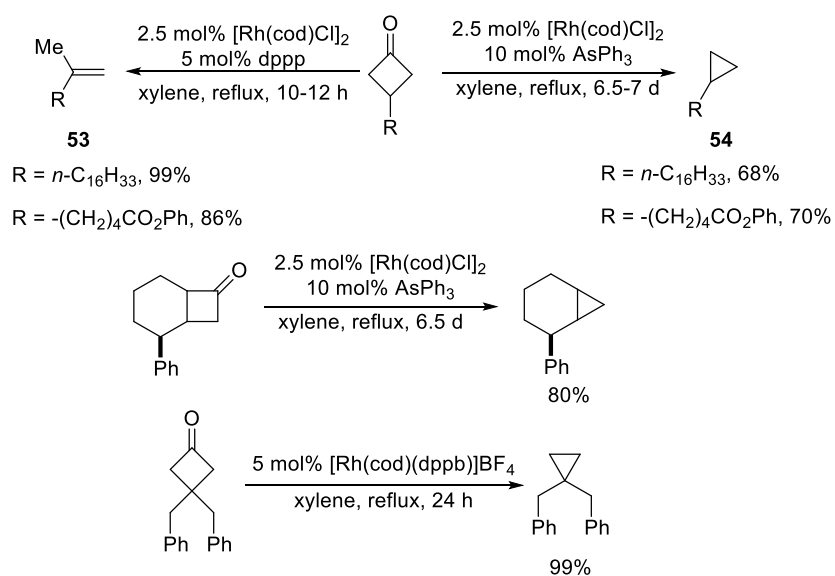
Catalytic reactions involving oxidative addition into cyclobutanone C–C bonds were discovered as early as the stoichiometric reactions. In the original report of the stoichiometric reaction (Scheme 1.28), Murakami disclosed a rhodium-catalyzed hydrogenolysis of cyclobutanones (Scheme 1.30).<sup>48</sup> After oxidative addition of rhodium into cyclobutanone to

generate rhodacyclopentanone **50**, hydrogenolysis happens to deliver the aldehyde product **51**. Part of the aldehyde product was further reduced under hydrogen atmosphere to give alcohol **52**, thus treatment of sodium borohydride was used to obtain the unified products. It was proposed that in addition to the relief of ring strain, the dihydrogen addition provides additional driving force for this reaction to take place.

**Scheme 1.30** Rhodium(I)-Catalyzed Reductive Ring Opening of Cyclobutanones

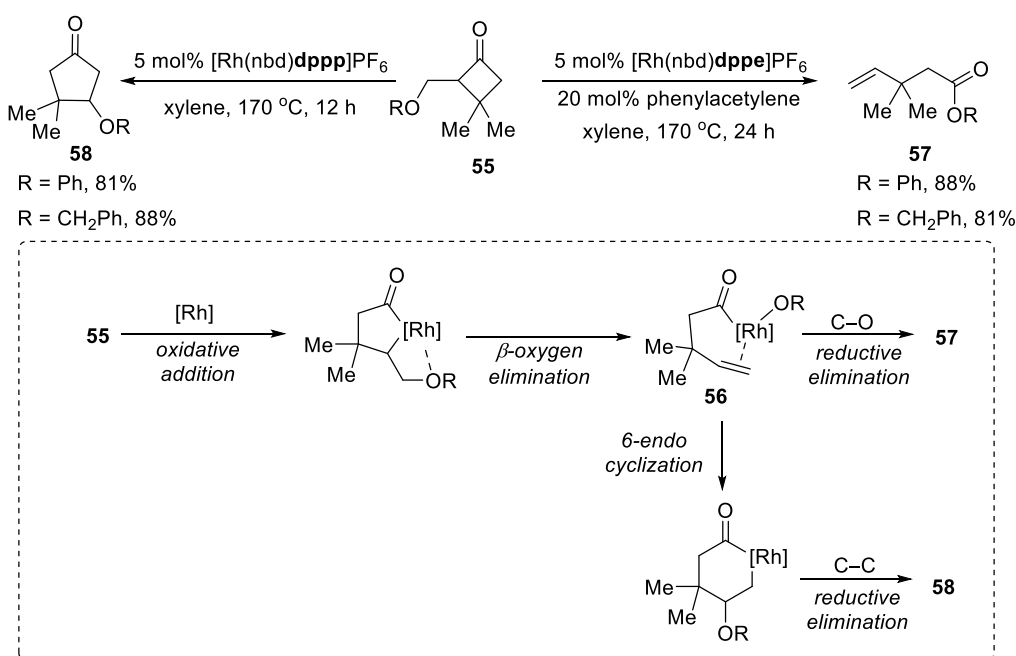


**Scheme 1.31** Catalytic Decarbonylation of Cyclobutanones via Rhodium Catalysis



In 1996, Murakami reported that through fine tuning of the ligand, cyclobutanones can undergo efficient decarbonylation into two different products **53** and **54**. Olefin **53** is generated through  $\beta$ -hydrogen elimination, while cyclopropane **54** through direct reductive elimination (Scheme 1.31).<sup>49</sup> Cyclobutanones fused with a cyclohexane is a viable substrate as well. Cationic rhodium catalysts can also yield the cyclopropane product.

**Scheme 1.32** Rhodium(I)-Catalyzed Successive Cleavage of C–C and C–O Bonds

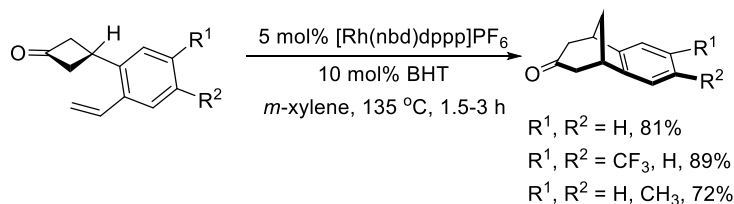


Other than using hydrogenolysis, Murakami further studied successive cleavage of C–C and C–O bonds in cyclobutanones containing an alkoxyl substituent at the  $\alpha$  position (Scheme 1.32).<sup>50</sup> After oxidative addition directed by the oxygen of the substituent at the more sterically hindered C–C bond, the resulting intermediate further undergoes  $\beta$ -oxygen elimination to generate **56**, which upon C–O bond reductive elimination yield the linear ester product **57**. Alternatively, **56** can go through a 6-*endo* cyclization followed by C–C bond reductive elimination to produce

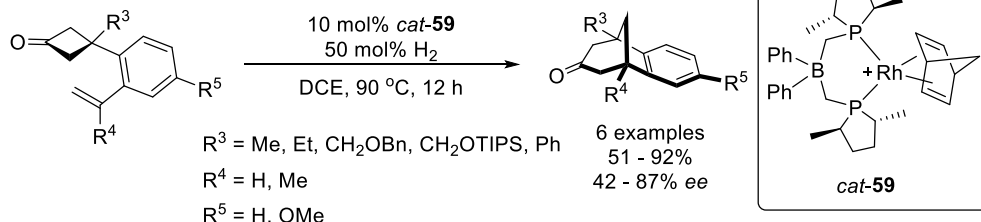
cyclized product **58**. For special spiro cyclobutanones, similar successive cleavage of two C–C bonds driven by ring strain was reported by the same group.<sup>51</sup>

### Scheme 1.33 Intramolecular Olefin Insertion into C–C Bond of Cyclobutanones

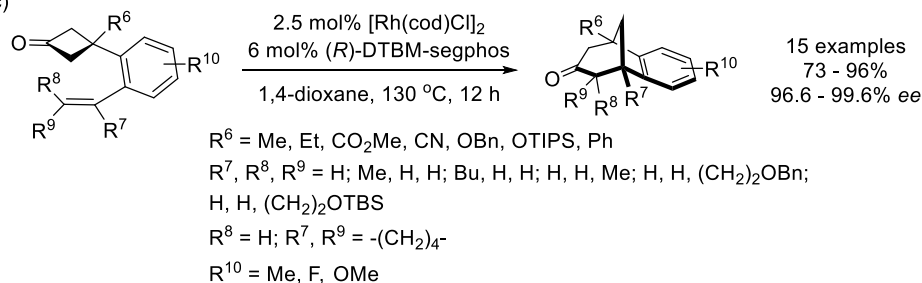
a)



b)



c)



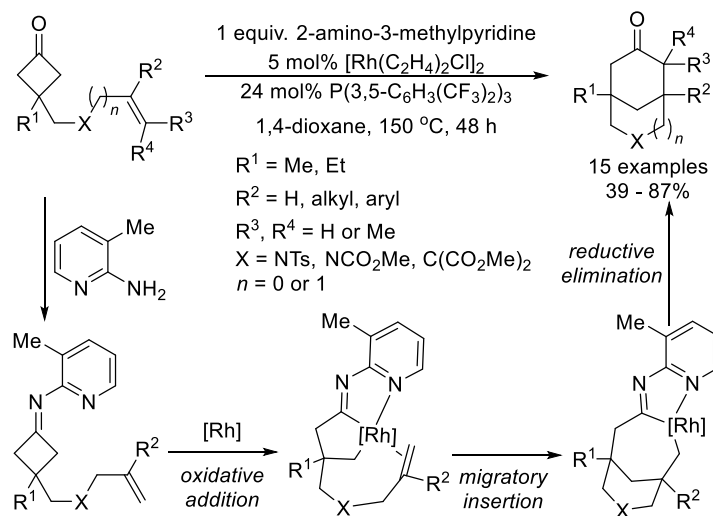
In 2002, Murakami disclosed the intramolecular olefin insertion into cyclobutanones to generate [3.2.1] bridged rings efficiently (Scheme 1.33a).<sup>52</sup> This transformation starts with oxidative addition of rhodium into the cyclobutanone. Then the olefin undergoes migratory insertion into the rhodacyclopentanone followed by C–C bond reductive elimination to generate the product. The substrate scope was restricted to three structurally similar examples. Later, Cramer developed a chiral rhodium catalyst **59** to realize the enantioselective version of this



reaction with moderate to good enantioselectivity and an extended substrate scope (Scheme 1.33b).<sup>53</sup> In 2014, Cramer discovered that the  $[\text{Rh}(\text{cod})\text{Cl}]_2/\text{DTBM-segphos}$  can realize a much better enantioselective transformation with excellent enantioselectivity (Scheme 1.33c).<sup>54</sup>

Intramolecular olefin insertion into cyclobutanones demonstrates the potential of this strategy in synthesizing complex bridged ring structures. However, the substrate was limited to styrene-tethered cyclobutanones due to competing decarbonylation side reactions. Extending the reaction scope to more general substrates requires addressing this challenge. In 2014, Ko and Dong reported the intramolecular carboacylation of various 1,1- or 1,2-disubstituted olefins with cyclobutanones (Scheme 1.34).<sup>55</sup> Other than the styrene-tethered cyclobutanones, the nitrogen-tethered and the malonate-tethered cyclobutanones underwent the transformation smoothly to deliver various [3.3.1] bridged ring systems.

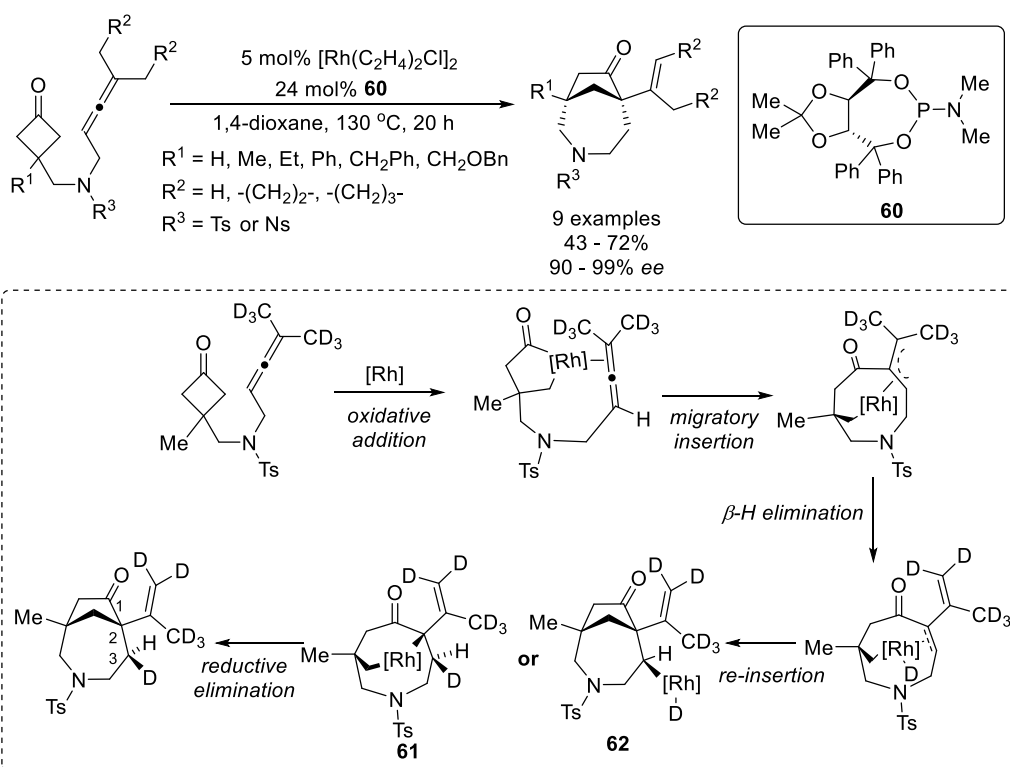
**Scheme 1.34** Rhodium(I)-Catalyzed Bridged Ring Formation through C–C Bond Activation



In 2015, Dong reported that allene can serve as a vinyl carbenoid equivalent to insert into cyclobutanones and generate [4.2.1] bridged cycles (Scheme 1.35).<sup>56</sup> An impressive level of

enantioselectivity and a broad substrate scope was observed in this transformation. During the mechanistic studies, they found that when the two terminal methyl groups on allene was labelled by deuterium, the hydrogen at C3 position was deuterated with a ratio greater than 95% and the C3 deuterium is *cis* to the alkenyl side chain. Based on this observation, they proposed a  $\beta$ -hydrogen elimination/re-insertion sequence after migratory insertion to generate intermediate **61** or **62**, both of which could deliver the product via reductive elimination.

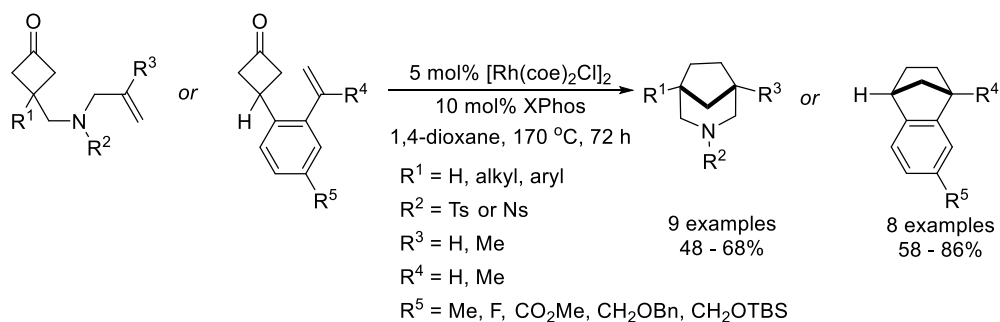
**Scheme 1.35** Rhodium(I)-Catalyzed Vinyl Carbenoid Insertion into Cyclobutanones



In comparison to cyclobutenones, it is more difficult to achieve decarbonylative insertion of unsaturated units into cyclobutanones because the  $\text{C}(\text{sp}^3)\text{--C}(\text{sp}^3)$  reductive elimination after CO extrusion is less favored compared with the original  $\text{C}(\text{sp}^2)\text{--C}(\text{sp}^3)$  case. Additionally, the potential side reaction leading to the formation of cyclopropanes needs to be prevented. Dong disclosed a

decarbonylative insertion of olefins into cyclobutanones making use of a bulky XPhos ligand, which promotes the reductive elimination step after the CO extrusion. Broad substrate scope was achieved with moderate to good yields (Scheme 1.36).<sup>57</sup>

**Scheme 1.36** Rhodium(I)-Catalyzed Decarbonylative Insertion of Olefins into Cyclobutanones



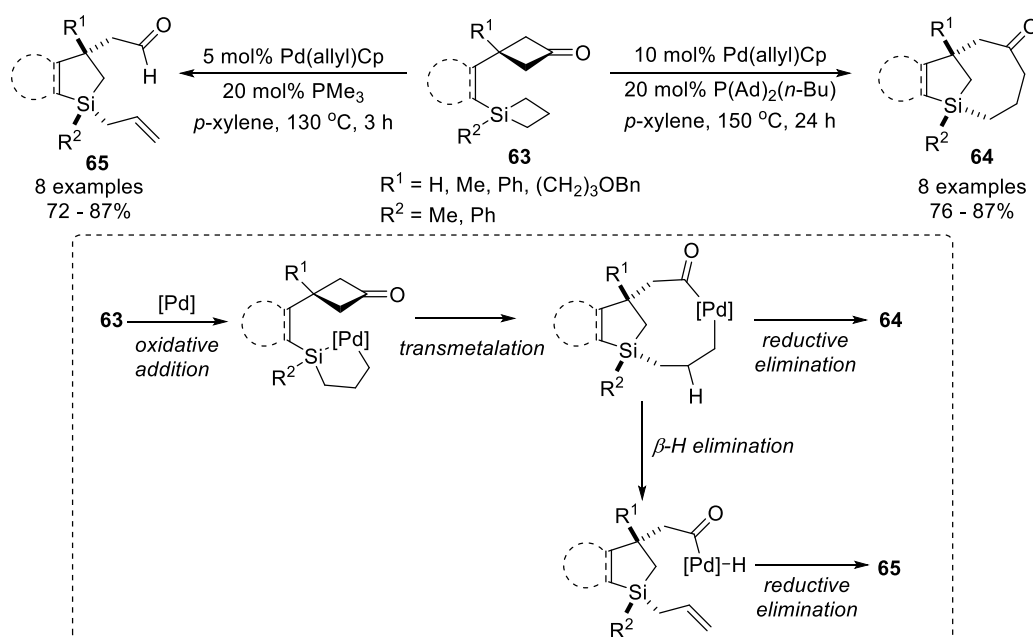
Apart from non-polar unsaturated bonds, Cramer reported that polarized C=O bonds can be successfully inserted into cyclobutanones after the rhodacyclopentanones were formed through oxidative addition of rhodium catalyst (Scheme 1.37).<sup>58</sup> With the help of DTBM-segphos, excellent enantioselectivity and broad substrate scope were achieved to obtain lactone-containing [3.2.1] bridged ring structures. It is impressive to see that with the presence of aldehyde C–H bonds, the rhodium catalyst selectively undergoes oxidative addition into the C–C bond other than the C–H bond.

**Scheme 1.37** Rhodium(I)-Catalyzed Enantioselective Insertion of C=O Bonds into Cyclobutanones



In addition to rhodium, palladium(0) catalysts can also promote C–C bond activation of cyclobutanones after initial oxidative insertion into Si–Si<sup>59</sup> or C–Si<sup>60</sup> bonds. In 2014, Murakami disclosed an intramolecular exchange of C–C and C–Si bond to generate interesting silabicyclo[5.2.1]decanes **64** diastereoselectively. The bulky phosphine ligand was used to promote the direct C–C bond reductive elimination after the transmetalation step. When less sterically hindered PMe<sub>3</sub> was applied, the  $\beta$ -hydrogen elimination would take place, followed by C–H reductive elimination to generate **65** (Scheme 1.38).<sup>60</sup>

**Scheme 1.38** Palladium(0)-Catalyzed Intramolecular Exchange of C–C and C–Si Bonds

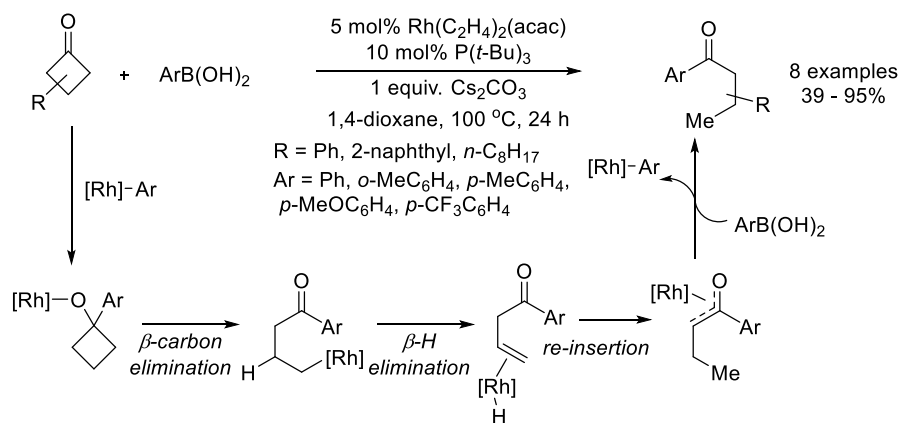


#### 1.4.2.2 C–C bond cleavage via $\beta$ -carbon elimination pathway

Apart from direct oxidative addition, the addition of a nucleophile to the C=O bond followed by  $\beta$ -carbon elimination represents another common pathway for C–C bond activation of cyclobutanones.

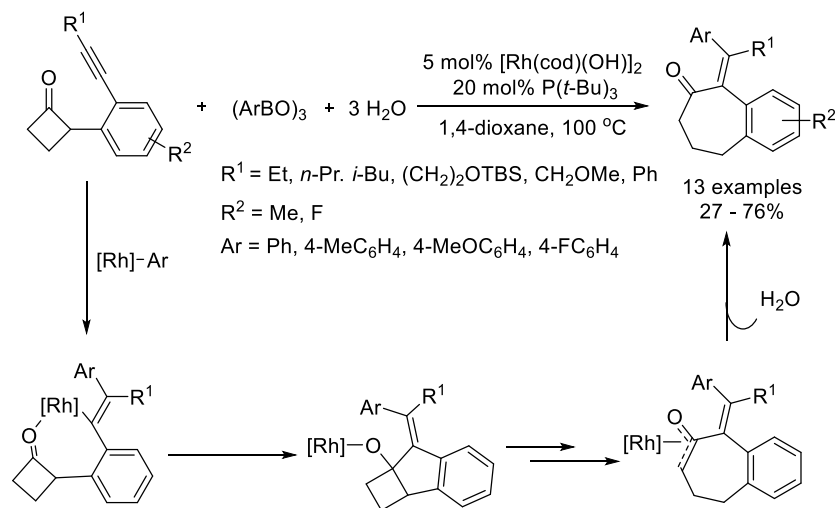
In 2004, Murakami reported that a more electron-rich arylrhodium(I) species generated from transmetalation can undergo addition to cyclobutanones. Then  $\beta$ -carbon elimination would happen to cleave the four-membered ring. After  $\beta$ -hydrogen elimination and re-insertion, the rhodium enolate intermediate would be generated and then undergo protonolysis to yield the product. The intermediacy of the rhodium enolate species was confirmed by a deuterium labeling study. Various arylboronic acids and cyclobutanones with different substitution are well-tolerated (Scheme 1.40).<sup>61</sup>

**Scheme 1.40** Rhodium(I)-Catalyzed Addition/Ring-Opening of Cyclobutanones with Arylboronic Acids

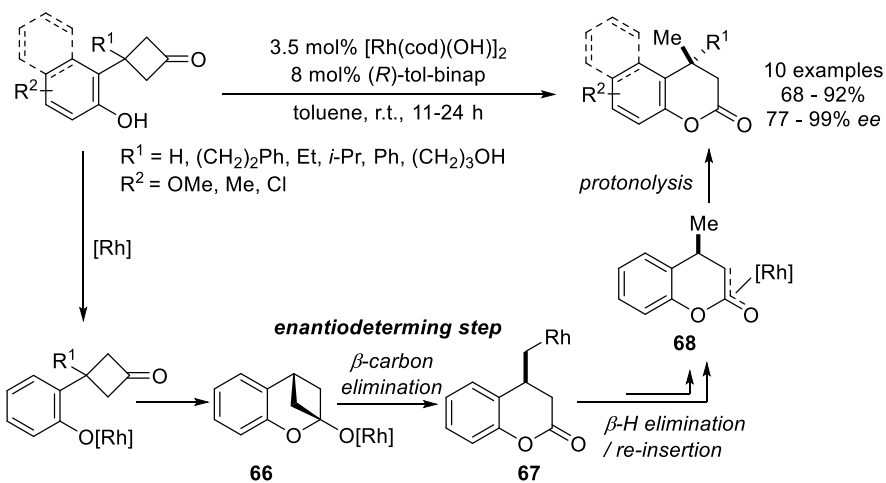


Murakami later disclosed that a similar reaction initiation mode can be applied to the ring expansion reaction of cyclobutanones using an alkyne-tethered substrate. The aryl rhodium can first undergo addition to the alkyne, then intramolecular addition of the rhodium to the  $\text{C}=\text{O}$  bond would take place. After  $\beta$ -hydrogen elimination, the rhodium enolate is generated and further undergoes protonolysis to yield the ring expansion product (Scheme 1.41).<sup>62</sup> Various functional groups and aryl boronic esters are well-tolerated. This method provides a unique way to synthesize medium-sized rings using C–C bond activation strategy.

**Scheme 1.41** Rhodium(I)-Catalyzed Arylative Ring Expansion of Cyclobutanones



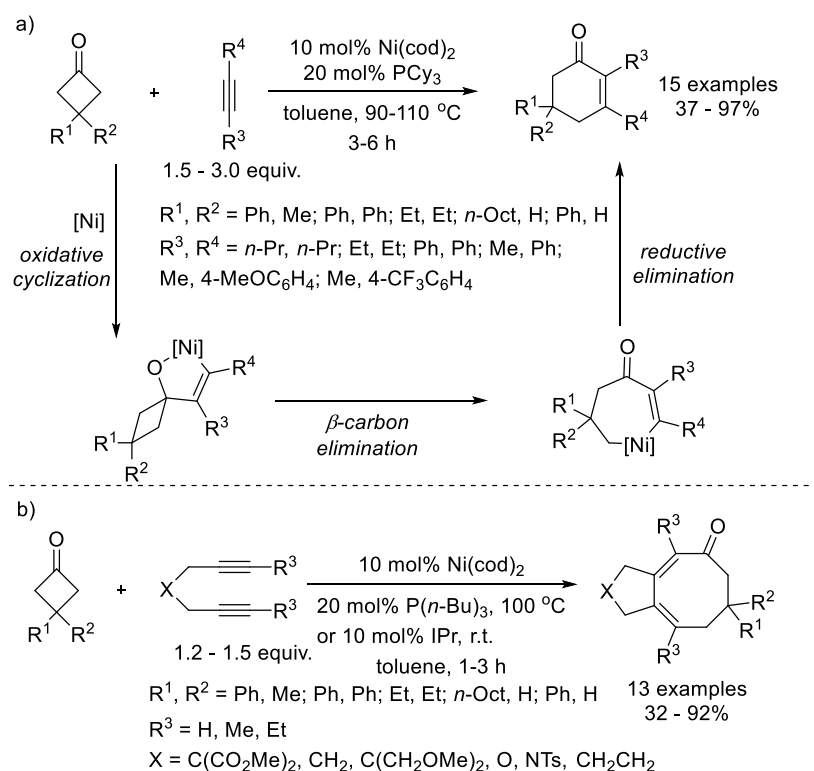
**Scheme 1.42** Rhodium(I)-Catalyzed Enantioselective Lactone Synthesis from Cyclobutanones



Instead of using arylboronic acids or esters to generate the rhodium aryl intermediate and further promote the  $\beta$ -carbon elimination, Murakami reported that rhodium catalysts can promote the C–C bond cleavage of cyclobutanones with phenols to form ester linkages inter-<sup>63</sup> or intramolecularly<sup>64</sup> through  $\beta$ -carbon elimination pathway. In 2007, they disclosed an enantioselective lactone formation using such a strategy (Scheme 1.42).<sup>65</sup> They proposed that the

reaction starts with generation of the rhodium aryloxide followed by its addition to the carbonyl group forming rhodium cyclobutanolate **66**. Then  $\beta$ -carbon elimination of **66** takes place to generate **67**, which is the enantiodetermining step. After a series of  $\beta$ -hydrogen elimination and reinsertion, intermediate **68** is generated and protonolysis of **68** affords the dihydrocoumarin product with moderate to excellent enantioselectivity. Different substitutions on the four-membered ring and the aryl linker are well-tolerated.

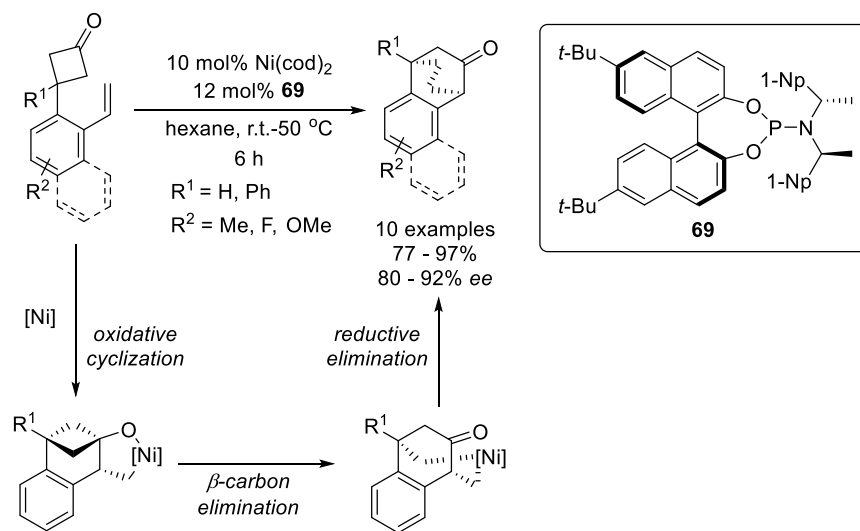
**Scheme 1.43** Nickel(0)-Catalyzed Intermolecular Alkyne Insertion into Cyclobutanones



Other than rhodium, nickel(0) catalysts have been found to be privileged in promoting the ring-opening of cyclobutanones through oxidative cyclization/ $\beta$ -carbon elimination pathway. In 2005, Murakami disclosed the intermolecular alkyne insertion into cyclobutanones using  $\text{Ni}(\text{cod})_2/\text{PCy}_3$  as an optimal precatalyst/ligand combination (Scheme 1.43a).<sup>66</sup> Various symmetrical or

unsymmetrical alkynes are viable substrates with moderate regioselectivity. The same group later reported a similar transformation between cyclobutanones and diynes, which afforded the bicyclic eight-membered ketones (Scheme 1.43b).<sup>67</sup> When *N*-heterocyclic carbene ligand IPr was used, the reaction can happen at room temperature. Different symmetrical diynes can successfully give the desired products. The unsymmetrical diyne gives higher yield but lower regioselectivity when PCy<sub>3</sub> is used as ligand, while in the case where IPr was used, the reactivity was lower but good regioselectivity was observed because of the steric bulkiness. Similar to cyclobutanones, azetidin-3-ones<sup>68</sup> and oxetan-3-ones<sup>69</sup> were reported by Louie, Murakami and Aïssa to be viable substrates to couple with alkynes or dienes through nickel catalysis.

**Scheme 1.44** Nickel(0)-Catalyzed Enantioselective Intramolecular Olefin Insertion into Cyclobutanones



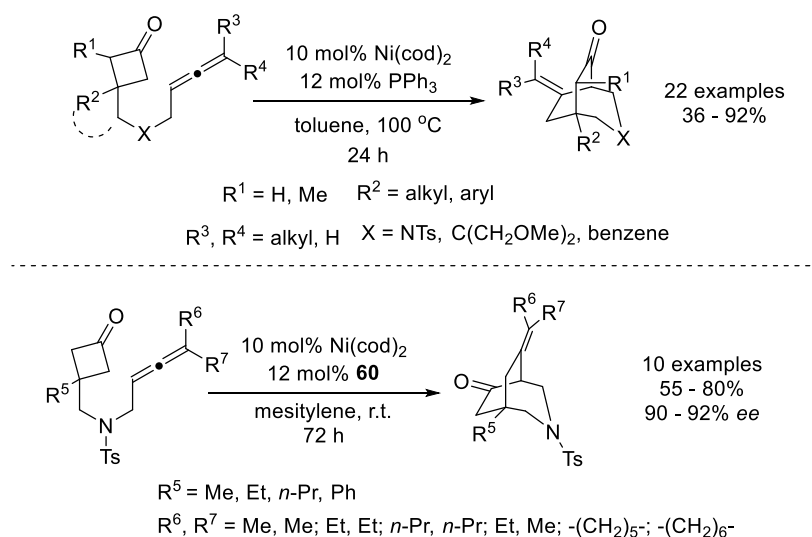
The intramolecular insertion of olefins into cyclobutanones catalyzed by nickel(0) was reported by Murakami in 2006.<sup>70</sup> The reaction was proposed to go through a similar mechanism as above. Later an enantioselective insertion was achieved with chiral phosphoramidite ligand **69**



and bioactive chiral benzobicyclo[2.2.2]octene structures were synthesized, which previously required multiple functional group manipulation and resolution processes (Scheme 1.44).<sup>71</sup> The oxidative cyclization is the enatiodetermining step.

Apart from alkynes or olefins, Dong reported that allene can also serve as the two carbon insertion unit for the intramolecular reaction with cyclobutanones. A broad substrate scope was achieved with the racemic transformation, which tolerates various types of linkage and substitution on cyclobutanones. With the help of phosphoramidite ligand **60**, a high level of enantiocontrol was achieved (Scheme 1.45).<sup>72</sup>

**Scheme 1.45** Nickel(0)-Catalyzed Enantioselective Intramolecular Allene Insertion into Cyclobutanones



## 1.5 Conclusions and Outlook

The C–C bond cleavage of cyclic ketones following by valuable new bond formations provides unique retro-synthetic strategies for organic synthesis. However, it remains a challenging task owing to the directional feature of the C–C bond. Releasing of the ring strain has been an

efficient driving force for such transformations. In this review, we have discussed how the three- and four-membered ring systems have been studied from stoichiometric reactions to a wide variety of catalytic transformations, which leads to the construction of valuable ring structures. However, the current methodologies still fall short considering the restrictions on substrates and harsh reaction conditions, which hinders its applications in natural product or pharmaceutical synthesis. Given these challenges, in this thesis, efforts were made to develop robust C–C bond activation reactions to obtain synthetically valuable ring systems including heterocycles and apply this unique reactivity into asymmetric synthesis and total synthesis of natural products.

## 1.6 References

- (1) (a) Crabtree, R. H. *Chem. Rev.* **1985**, *85*, 245. (b) Jones, W. D. *Nature* **1993**, *364*, 676. (c) Murakami, M.; Ito, Y., *Cleavage of Carbon–Carbon Single Bonds by Transition Metals*. In *Top. Organomet. Chem.*, 1999; Vol. 3, pp 97. (d) Rybtchinski, B.; Milstein, D. *Angew. Chem. Int. Ed.* **1999**, *38*, 870. (e) Jun, C.-H. *Chem. Soc. Rev.* **2004**, *33*, 610. (f) Necas, D.; Kotora, M. *Curr. Org. Chem.* **2007**, *11*, 1566. (g) Park, Y. J.; Park, J.-W.; Jun, C.-H. *Acc. Chem. Res.* **2008**, *41*, 222. (h) Murakami, M.; Matsuda, T. *Chem. Comm.* **2011**, *47*, 1100. (i) Seiser, T.; Saget, T.; Tran, D. N.; Cramer, N. *Angew. Chem. Int. Ed.* **2011**, *50*, 7740. (j) Korotvicka, A.; Necas, D.; Kotora, M. *Curr. Org. Chem.* **2012**, *16*, 1170. (k) Chen, F.; Wang, T.; Jiao, N. *Chem. Rev.* **2014**, *114*, 8613. (l) Dermenci, A.; Coe, J. W.; Dong, G. *Org. Chem. Front.* **2014**, *1*, 567. (m) Dong, G., *C–C bond activation*. Springer-Verlag: Berlin, 2014; Vol. 346. (n) Murakami, M.; Ishida, N., *Fundamental Reactions to Cleave Carbon–Carbon  $\sigma$ -Bonds with Transition Metal Complexes*. In *Cleavage of Carbon-Carbon Single Bonds by Transition Metals*, Wiley-VCH Verlag GmbH & Co. KGaA: 2015; pp 1. (o) Souillart, L.; Cramer, N. *Chem. Rev.* **2015**, *115*, 9410. (p) Chen, P.-h.; Dong, G. *Chem. Eur. J.* **2016**, *22*, 18290. (q) Chen, P.-h.; Billett, B. A.; Tsukamoto, T.; Dong, G. *ACS Cat.* **2017**, *7*, 1340. (r) Fumagalli, G.; Stanton, S.; Bower, J. F. *Chem. Rev.* **2017**, *117*, 9404. (s) Kim, D.-S.; Park, W.-J.; Jun, C.-H. *Chem. Rev.* **2017**, *117*, 8977. (t) Liang, Y.-F.; Jiao, N. *Acc. Chem. Res.* **2017**, *50*, 1640.
- (2) Halpern, J. *Acc. Chem. Res.* **1982**, *15*, 238.
- (3) Komatsu, K.; Kitagawa, T. *Chem. Rev.* **2003**, *103*, 1371.
- (4) Bird, C. W.; Briggs, E. M.; Hudec, J. *Journal of the Chemical Society C: Organic* **1967**, 1862.
- (5) Wong, W.; Singer, S. J.; Pitts, W. D.; Watkins, S. F.; Baddley, W. H. *J. Chem. Soc., Chem. Commun.* **1972**, 672.
- (6) Visser, J. P.; Ramakers-Blom, J. E. *J. Organomet. Chem.* **1972**, *44*, C63.

- (7) Baba, A.; Ohshiro, Y.; Agawa, T. *J. Organomet. Chem.* **1976**, *110*, 121.
- (8) Akio, B.; Yoshiki, O.; Toshio, A. *Chem. Lett.* **1976**, *5*, 11.
- (9) Song, L.; Arif, A. M.; Stang, P. J. *Organometallics* **1990**, *9*, 2792.
- (10) Foerstner, J.; Kakoschke, A.; Wartchow, R.; Butenschön, H. *Organometallics* **2000**, *19*, 2108.
- (11) Ryoji, N.; Isao, U.; Hidemasa, T. *Chem. Lett.* **1972**, *1*, 1189.
- (12) Chatani, N.; Hanafusa, T. *J. Org. Chem.* **1987**, *52*, 4408.
- (13) Kondo, T.; Kaneko, Y.; Taguchi, Y.; Nakamura, A.; Okada, T.; Shiotsuki, M.; Ura, Y.; Wada, K.; Mitsudo, T.-a. *J. Am. Chem. Soc.* **2002**, *124*, 6824.
- (14) Wender, P. A.; Paxton, T. J.; Williams, T. J. *J. Am. Chem. Soc.* **2006**, *128*, 14814.
- (15) Kong, L.; Zhou, X.; Xu, Y.; Li, X. *Org. Lett.* **2017**, *19*, 3644.
- (16) Yu, S.; Li, X. *Org. Lett.* **2014**, *16*, 1220.
- (17) Evans, J. A.; Everitt, G. F.; Kemmitt, R. D. W.; Russell, D. R. *J. Chem. Soc., Chem. Commun.* **1973**, 158.
- (18) Liebeskind, L. S.; Baysdon, S. L.; South, M. S.; Blount, J. F. *J. Organomet. Chem.* **1980**, *202*, C73.
- (19) Liebeskind, L. S.; Baysdon, S. L.; South, M. S.; Iyer, S.; Leeds, J. P. *Tetrahedron* **1985**, *41*, 5839.
- (20) Liebeskind, L. S.; Baysdon, S. L.; South, M. S. *J. Am. Chem. Soc.* **1980**, *102*, 7397.
- (21) Baysdon, S. L.; Liebeskind, L. S. *Organometallics* **1982**, *1*, 771.
- (22) South, M. S.; Liebeskind, L. S. *J. Am. Chem. Soc.* **1984**, *106*, 4181.
- (23) Liebeskind, L. S.; Leeds, J. P.; Baysdon, S. L.; Iyer, S. *J. Am. Chem. Soc.* **1984**, *106*, 6451.
- (24) Huffman, M. A.; Liebeskind, L. S.; Pennington, W. T. *Organometallics* **1990**, *9*, 2194.
- (25) Huffman, M. A.; Liebeskind, L. S. *J. Am. Chem. Soc.* **1990**, *112*, 8617.
- (26) Masuda, Y.; Hasegawa, M.; Yamashita, M.; Nozaki, K.; Ishida, N.; Murakami, M. *J. Am. Chem. Soc.* **2013**, *135*, 7142.
- (27) Joost, M.; Estévez, L.; Miqueu, K.; Amgoune, A.; Bourissou, D. *Angew. Chem. Int. Ed.* **2015**, *54*, 5236.
- (28) Okumura, S.; Sun, F.; Ishida, N.; Murakami, M. *J. Am. Chem. Soc.* **2017**, *139*, 12414.

- (29) Kondo, T.; Nakamura, A.; Okada, T.; Suzuki, N.; Wada, K.; Mitsudo, T.-a. *J. Am. Chem. Soc.* **2000**, *122*, 6319.
- (30) Yamamoto, Y.; Kuwabara, S.; Hayashi, H.; Nishiyama, H. *Adv. Synth. Catal.* **2006**, *348*, 2493.
- (31) Huffman, M. A.; Liebeskind, L. S. *J. Am. Chem. Soc.* **1991**, *113*, 2771.
- (32) Kondo, T.; Niimi, M.; Nomura, M.; Wada, K.; Mitsudo, T.-a. *Tetrahedron Lett.* **2007**, *48*, 2837.
- (33) Stalling, T.; Harker, W. R. R.; Auvinet, A.-L.; Cornel, E. J.; Harrierty, J. P. A. *Chem. Eur. J.* **2015**, *21*, 2701.
- (34) Kondo, T.; Taguchi, Y.; Kaneko, Y.; Niimi, M.; Mitsudo, T.-a. *Angew. Chem. Int. Ed.* **2004**, *43*, 5369.
- (35) Huffman, M. A.; Liebeskind, L. S. *J. Am. Chem. Soc.* **1993**, *115*, 4895.
- (36) Xu, T.; Dong, G. *Angew. Chem. Int. Ed.* **2012**, *51*, 7567.
- (37) Xu, T.; Ko, H. M.; Savage, N. A.; Dong, G. *J. Am. Chem. Soc.* **2012**, *134*, 20005.
- (38) Lu, G.; Fang, C.; Xu, T.; Dong, G.; Liu, P. *J. Am. Chem. Soc.* **2015**, *137*, 8274.
- (39) Xu, T.; Savage, N. A.; Dong, G. *Angew. Chem. Int. Ed.* **2014**, *53*, 1891.
- (40) Chen, P.-h.; Xu, T.; Dong, G. *Angew. Chem. Int. Ed.* **2014**, *53*, 1674.
- (41) Zhu, Z.; Li, X.; Chen, S.; Chen, P.-h.; Billett, B. A.; Huang, Z.; Dong, G. *ACS Cat.* **2018**, *8*, 845.
- (42) Sun, T.; Zhang, Y.; Qiu, B.; Wang, Y.; Qin, Y.; Dong, G.; Xu, T. *Angew. Chem. Int. Ed.* **2018**, *57*, 2859.
- (43) Xu, Z.-Y.; Zhang, S.-Q.; Liu, J.-R.; Chen, P.-P.; Li, X.; Yu, H.-Z.; Hong, X.; Fu, Y. *Organometallics* **2018**, *37*, 592.
- (44) Bender, M.; Turnbull, B. W. H.; Ambler, B. R.; Krische, M. J. *Science* **2017**, *357*, 779.
- (45) Ambler, B. R.; Turnbull, B. W. H.; Suravarapu, S. R.; Uteuliyev, M. M.; Huynh, N. O.; Krische, M. J. *J. Am. Chem. Soc.* **2018**, *140*, 9091.
- (46) Juliá-Hernández, F.; Ziadi, A.; Nishimura, A.; Martin, R. *Angew. Chem. Int. Ed.* **2015**, *54*, 9537.
- (47) (a) Yang, S.; Xu, Y.; Li, J. *Org. Lett.* **2016**, *18*, 6244. (b) Zou, H.; Wang, Z. L.; Huang, G. *Chemistry - A European Journal* **2017**, *23*, 12593.
- (48) Murakami, M.; Amii, H.; Ito, Y. *Nature* **1994**, *370*, 540.

- (49) Murakami, M.; Amii, H.; Shigeto, K.; Ito, Y. *J. Am. Chem. Soc.* **1996**, *118*, 8285.
- (50) Murakami, M.; Itahashi, T.; Amii, H.; Takahashi, K.; Ito, Y. *J. Am. Chem. Soc.* **1998**, *120*, 9949.
- (51) Murakami, M.; Takahashi, K.; Amii, H.; Ito, Y. *J. Am. Chem. Soc.* **1997**, *119*, 9307.
- (52) Murakami, M.; Itahashi, T.; Ito, Y. *J. Am. Chem. Soc.* **2002**, *124*, 13976.
- (53) Parker, E.; Cramer, N. *Organometallics* **2014**, *33*, 780.
- (54) Souillart, L.; Parker, E.; Cramer, N. *Angew. Chem. Int. Ed.* **2014**, *53*, 3001.
- (55) Ko, H. M.; Dong, G. *Nat. Chem.* **2014**, *6*, 739.
- (56) Zhou, X.; Dong, G. *J. Am. Chem. Soc.* **2015**, *137*, 13715.
- (57) Zhou, X.; Ko, H. M.; Dong, G. *Angew. Chem. Int. Ed.* **2016**, *55*, 13867.
- (58) Souillart, L.; Cramer, N. *Angew. Chem. Int. Ed.* **2014**, *53*, 9640.
- (59) Ishida, N.; Ikemoto, W.; Murakami, M. *Org. Lett.* **2012**, *14*, 3230.
- (60) Ishida, N.; Ikemoto, W.; Murakami, M. *J. Am. Chem. Soc.* **2014**, *136*, 5912.
- (61) Matsuda, T.; Makino, M.; Murakami, M. *Org. Lett.* **2004**, *6*, 1257.
- (62) Matsuda, T.; Makino, M.; Murakami, M. *Angew. Chem. Int. Ed.* **2005**, *44*, 4608.
- (63) Takanori, M.; Masanori, S.; Yohei, M.; Masahiro, M. *Chem. Lett.* **2007**, *36*, 744.
- (64) Murakami, M.; Tsuruta, T.; Ito, Y. *Angew. Chem. Int. Ed.* **2000**, *39*, 2484.
- (65) Matsuda, T.; Shigeno, M.; Murakami, M. *J. Am. Chem. Soc.* **2007**, *129*, 12086.
- (66) Murakami, M.; Ashida, S.; Matsuda, T. *J. Am. Chem. Soc.* **2005**, *127*, 6932.
- (67) Murakami, M.; Ashida, S.; Matsuda, T. *J. Am. Chem. Soc.* **2006**, *128*, 2166.
- (68) (a) Ho, K. Y. T.; Aïssa, C. *Chem. Eur. J.* **2012**, *18*, 3486. (b) Ishida, N.; Yuhki, T.; Murakami, M. *Org. Lett.* **2012**, *14*, 3898. (c) Kumar, P.; Louie, J. *Org. Lett.* **2012**, *14*, 2026. (d) Thakur, A.; Facer, M. E.; Louie, J. *Angew. Chem. Int. Ed.* **2013**, *52*, 12161. (e) Thakur, A.; Evangelista, J. L.; Kumar, P.; Louie, J. *J. Org. Chem.* **2015**, *80*, 9951. (f) Elwrfalli, F.; Esvan, Y. J.; Robertson, C. M.; Aïssa, C. *Chem. Comm.* **2019**, *55*, 497.
- (69) Barday, M.; Janot, C.; Clare, D.; Carr-Knox, C.; Higginson, B.; Ho, K. Y. T.; Aïssa, C. *Synthesis* **2017**, *49*, 3582.
- (70) Murakami, M.; Ashida, S. *Chem. Comm.* **2006**, 4599.

- (71) Liu, L.; Ishida, N.; Murakami, M. *Angew. Chem. Int. Ed.* **2012**, *51*, 2485.
- (72) Zhou, X.; Dong, G. *Angew. Chem. Int. Ed.* **2016**, *55*, 15091.

## CHAPTER 2

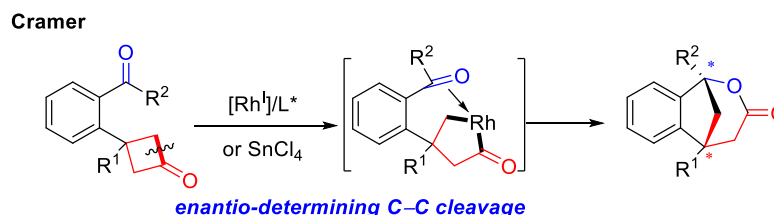
### Enantioselective Rh-catalyzed Carboacylation of C=N Bonds via C–C Activation of Benzocyclobutenones

#### 2.1 Introduction

Transition metal-catalyzed C–C  $\sigma$ -bond cleavage of cyclic compounds followed by  $2\pi$ -insertion, namely a “cut-and-sew” approach, has recently emerged as an attractive approach for complex bridged or fused ring formation.<sup>1</sup> Comparing with traditional approaches, these methods operate at near pH and redox neutral conditions, and usually in a highly atom-economical manner. However, as discussed in previous chapter, the unsaturated  $2\pi$ -units that have been applied to “cut-and-sew” sequence<sup>2</sup> are primarily non-polar carbon-carbon multiple bonds, such as alkenes, alkynes and 1,3-dienes.<sup>10</sup> It is evident that if polarized C=X bonds, such as aldehydes, imines etc., can be applied in “cut-and-sew” reactions, valuable heterocycles containing ring systems would be accessed efficiently. Potentially, it would provide new strategy for molecule disconnection in the synthesis of natural products and pharmaceuticals. Cramer and coworkers pioneered in applying the C=O bonds as the coupling partner with cyclobutanones to access bridged lactones. They demonstrated that rhodium precatalyst together with chiral phosphine ligand can provide a highly enantioselective transformation (Scheme 2.1).<sup>3</sup> In addition, through completely different

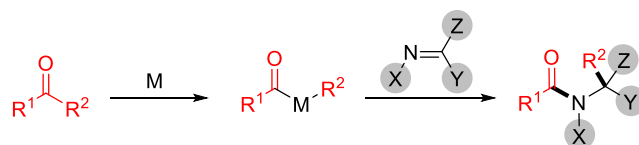
mechanistic pathways, the C–C bond cleavage of the same substrate can be observed when Lewis acid catalysts are used and generate different products.<sup>4</sup>

**Scheme 2.1** Carboacylation of C=O Bonds via Transition-Metal-Catalyzed C–C Activation



Stimulated by the pivotal role of amide bond formation in organic synthesis and the pharmaceutical importance of nitrogen-containing heterocycles, we have been fascinated by the transition metal-catalyzed carboacylation of C=N bonds, which, to the best of our knowledge, has not been reported previously. Based on the precedents on carboacylation of non-polar  $2\pi$  units with ketones, we proposed that initiated by oxidative addition of transition metal catalyst into ketone  $\alpha$  C–C bonds, the resulting two M–C bonds, including one M–acyl bond, can add across an imine C=N bond to form an amide (Scheme 2.2). Elegant work by Chi and coworkers, involving an organocatalyst-promoted ring-opening of cyclobutenones followed by a formal enantioselective hetero-Diels-Alder reaction with sulfonyl and isatin imines, represents the closest example.<sup>5</sup>

**Scheme 2.2** General Process of Amide Bond Formation through “Cut-and-Sew” Approach

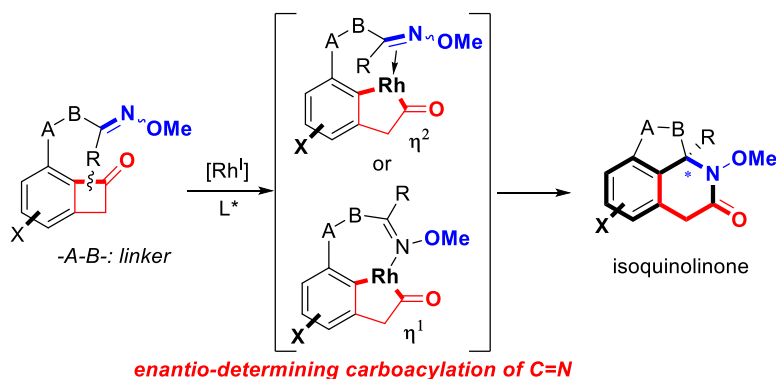


Given the importance of optically enriched lactam moieties in bioactive compounds,<sup>6</sup> herein we designed a Rh-catalyzed enantioselective intramolecular carboacylation of oximes



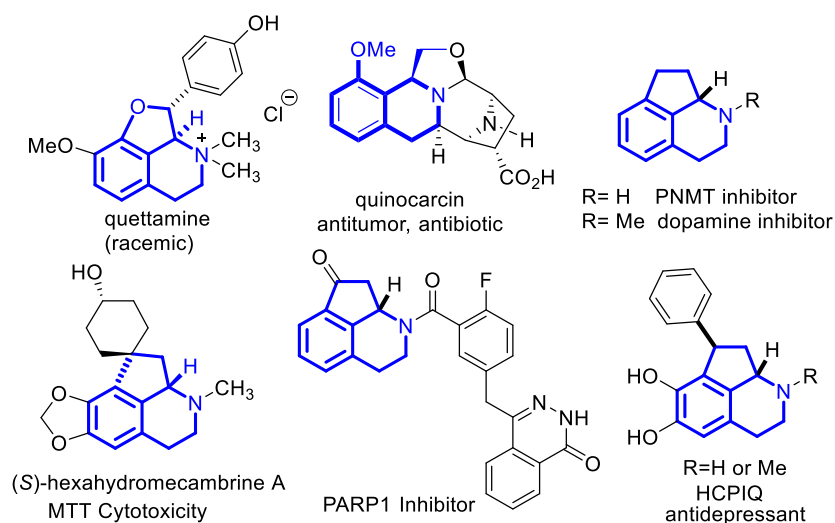
(imines) via C–C activation of benzocyclobutenones to access chiral fused lactams (Scheme 2.3). This design is supported by previous reported examples by our group where the selective C1–C2 bond cleavage happened and was followed by intramolecular insertion of alkenes and alkynes.<sup>7,8,9</sup> Mechanistically, the C–C bond cleavage might start with the C1–C8 bond cleavage, then go through CO extrusion and re-insertion to generate the selective C1–C2 bond cleavage intermediate.<sup>7c</sup> Considering the prevalence of hydroisoquinolines and isoquinolinones in natural products and pharmaceuticals,<sup>10</sup> this method would provide a significant impact to the synthesis of these scaffolds (Scheme 2.4).

**Scheme 2.3** Carboacylation of C=N Bonds via Rh-Catalyzed C–C Activation



There are three major challenges relating to the designed enantioselective carboacylation of C=N double bonds: a) distinct from ketones/aldehydes, imines tend to exist as a mixture of *E/Z* isomers, which may complicate the enantio-determining step; b) due to the Lewis basicity of the nitrogen, imines can coordinate with metals in either an  $\eta^1$  or  $\eta^2$  mode, which may influence the migratory insertion step;<sup>11</sup> (c) imine hydrolysis can be a competitive side reaction.

## Scheme 2.4 Representative Natural Products and Pharmaceuticals with Hydroisoquinolines



## 2.2 Results and Discussion

### 2.2.1 Condition optimization for rhodium-catalyzed carboacylation of C=N bonds

To explore the aforementioned challenges, we sought the use of oximes as an imine equivalent due to their bench stability and the ease of cleavage of N–O bond for introducing various substituents on the nitrogen (*vide infra*, Scheme 2.4 and Scheme 2.5). Benzocyclobutenone **1a** containing a ketoxime group with variable E/Z ratios (1:1 to 4:1) was employed as the initial substrate, and various catalytic conditions were explored (Table 2.1). Due to the different nature between C=C and C=N bonds, the conditions with [Rh(cod)Cl]<sub>2</sub> and dppb that previously worked best<sup>8a</sup> for olefin insertion only yielded a small amount of product (Table 2.1, entry 1). In contrast, through examining of various pre-catalysts, the corresponding cationic rhodium complex showed much higher reactivity (Table 2.1, entry 2). Regarding the solvent effect, THF was found to be optimal, and 1,4-dioxane also provided a reasonable yield (Table 2.1, entries 2-5). It is likely that both solvents can stabilize the active rhodium intermediates during the reaction via weak

coordination. In addition, the premade and in situ generated rhodium complexes (with dppb ligand) exhibited similar reactivity (Table 2.1, entry 6).

**Table 2.1** Evaluation of Solvents and Precatalysts<sup>a</sup>

1a  $\xrightarrow[110\text{ }^{\circ}\text{C, solvent}]{10\text{ mol\% [Rh]}, 12\text{ mol\% ligand}}$  2a

Entry	Catalyst/ Ligand	Solvent	Yield <sup>b</sup>
1	[Rh(COD)Cl] <sub>2</sub> /dppb	THF	<20%
2 <sup>c</sup>	[Rh(COD)dppb]BF <sub>4</sub>	THF	58% (66%)
3 <sup>c</sup>	[Rh(COD)dppb]BF <sub>4</sub>	1,4-dioxane	40% (60%)
4 <sup>c</sup>	[Rh(COD)dppb]BF <sub>4</sub>	PhCl	22% (47%)
5 <sup>c</sup>	[Rh(COD)dppb]BF <sub>4</sub>	Toluene	7% (8%) <sup>e</sup>
6 <sup>d</sup>	[Rh(COD)(CH <sub>3</sub> CN) <sub>2</sub> ]BF <sub>4</sub> /dppb	THF	57%

<sup>a</sup> Unless otherwise mentioned, the reaction was run with 10 mol % rhodium complex (based on the metal) and 12 mol % ligand on a 0.1 mmol scale at 110 °C for 48 h; numbers in parenthesis are yields based on recovered starting material (brsm). <sup>b</sup> Isolated yield. <sup>c</sup> Reactions were run at 110 °C for 12 h, 130 °C for 24 h. <sup>d</sup> 130 °C. <sup>e</sup> NMR yield using mesitylene as internal standard.

**Table 2.2** Evaluation of Counter-Ion<sup>a</sup>

1a  $\xrightarrow[130\text{ }^{\circ}\text{C, THF}]{10\text{ mol\% [Rh]}, 10\text{ mol\% ligand}, 10\text{ mol\% silver salt}}$  2a

Entry	Catalyst/ Ligand	Silver salt	Yield (BRSM)
1	[Rh(COD)dppb]BF <sub>4</sub>	none	58% (66%) <sup>a</sup>
2	[Rh(COD)Cl] <sub>2</sub> /dppb	AgOTf	6% (6%) <sup>b</sup>
3	[Rh(COD)Cl] <sub>2</sub> /dppb	AgPF <sub>6</sub>	0% (0%) <sup>b</sup>
4	[Rh(COD)Cl] <sub>2</sub> /dppb	AgSbF <sub>6</sub>	53% (53%) <sup>b</sup>
5	[Rh(COD)Cl] <sub>2</sub> /dppb	NaBARF	28% (42%) <sup>b</sup>
6	[Rh(COD)Cl] <sub>2</sub> /BIPHEP	AgSbF <sub>6</sub>	47% (48%) <sup>b</sup>
7	[Rh(COD)Cl] <sub>2</sub> /BIPHEP	AgBF <sub>4</sub>	49% (49%) <sup>b</sup>
8	[Rh(COD)Cl] <sub>2</sub> /(S)-BINAP	AgSbF <sub>6</sub>	20% (20%) <sup>b</sup>
9	[Rh(COD)Cl] <sub>2</sub> /(S)-BINAP	AgBF <sub>4</sub>	40% (57%) <sup>b</sup>

<sup>a</sup> isolated yield. <sup>b</sup> NMR yield using mesitylene as internal standard.

Meanwhile, a survey of the counter-ion effect was conducted, which indicated  $\text{BF}_4$  is the best counter-ion for this reaction (Table 2.2). Hence,  $[\text{Rh}(\text{cod})(\text{CH}_3\text{CN})_2]\text{BF}_4$  was selected as the pre-catalyst for further investigation of the enantioselective transformation.

A range of chiral bidentate phosphine ligands were examined (Table 2.3). DTBM-SEGPBOS and DIOP, which previously gave excellent enantioselectivity<sup>8b</sup> for the olefin insertion, only resulted in low yields and poor enantioselectivity (Table 2.3, entries 1 and 3). Surprisingly, xylyl-substituted SEGPBOS provided 86% ee (entry 2). Subsequently, ligands with different backbones, such as SYNPHOS, BINAP, H8-BINAP and MeO-BIPHEP, were evaluated (Table 2.3, entries 4-10). Again, the xylyl-based ligands showed significant higher enantioselectivity than their phenyl and tolyl analogues. In particular, good yield (72%) and excellent ee (92%) can be obtained with xyl-BINAP (Table 2.3, entry 7). While efforts to further improve the enantioselectivity using xyl-BINAP remained unfruitful, the xyl-SDP ligand, first developed by Zhou and coworkers,<sup>13</sup> was found to give almost perfect enantioselectivity (99% ee) (Table 2.3, entry 12). Such a high enantioselectivity of this transformation is remarkable, because it suggested that, although involving C–N formation, both *E* and *Z* isomers of the oxime substrate can be converted to the same enantiomer of the product. The absolute configuration of product **2a** (the *R* isomer) was confirmed by the micro-focused X-ray crystallography (Scheme 2.5).

**Table 2.3** Evaluation of Chiral Ligands<sup>a</sup>

Entry	Ligands	Yield	ee <sup>b</sup>
1	(R)-DTBM-SEGPHOS	23%	-23%
2	(R)-xyl-SEGPHOS	54%	-86%
3	(S,S)-DIOP	54%	3.2%
4	(R)-SYNPHOS	39%	-50%
5	(S)-BINAP	20%	56%
6	(R)-tol-BINAP	50%	-68%
7	(R)-xyl-BINAP	72%	-92%
8	(R)-H8-BINAP	71%	-80%
9	(R)-xyl-H8-BINAP	52%	-88%
10	(R)-xyl-MeO-BIPHEP	60%	-84%
11	(R)-SDP	32%	94%
12	(R)-xyl-SDP	46% (63%)	99%

(S,S)-DIOP

(R)-xyl-MeO-BIPHEP

(R)-SYNPHOS

Ar= Ph, (R)-BINAP  
Ar= tol, (R)-tol-BINAP  
Ar= xyl, (R)-xyl-BINAP

Ar= Ph, (R)-H8-BINAP  
Ar= xyl, (R)-xyl-H8-BINAP

Ar= Ph, (R)-SDP  
Ar= xyl, (R)-xyl-SDP

Ar= DTBM, (R)-DTBM-SEGPHOS  
Ar= xyl, (R)-xyl-SEGPHOS

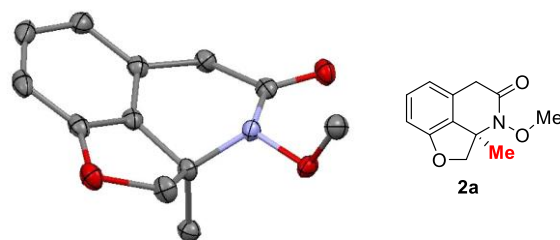
DTBM

xyl

tol

<sup>a</sup> Unless otherwise mentioned, the reaction was run with 10 mol % rhodium complex (based on the metal) and 12 mol % ligand on a 0.1 mmol scale at 110 °C for 48 h; numbers in parenthesis are yields based on recovered starting material (brsm). <sup>b</sup> Determined by chiral HPLC.

### Scheme 2.5 Crystal Structure of Compound 2a



at 50% probability level with absolute stereochemistry, Hydrogen atoms are omitted for clarity

**Table 2.4** Further Screening with (*R*)-xyl-SDP<sup>a</sup>

Entry	Additives	Conc.	<i>T</i> / °C	Time/h	Yield (BRSM)	e.e. <sup>b</sup>
1	none	0.1 M	110	36	53%	99%
2	none	0.1 M	110	48	53%	99%
3	none	0.1 M	110	96	32%	N/D
4	none	0.1 M	130	48	32% (35%)	N/D
5	none	0.05 M	130	48	44% (63%)	N/D
6	none	0.03 M	130	48	45% (59%)	97%
7	ZnCl <sub>2</sub>	0.1 M	130	48	24% (57%)	93%
8	BPh <sub>3</sub>	0.1 M	130	48	35% (35%)	N/D
9	Zn(OTf) <sub>2</sub>	0.1 M	130	48	<5%	N/D
10	portion-wise	0.1 M	110	96	61% (86%)	99%
11	none	0.1 M	110	36	53% (64%)	98%
12	PPh <sub>3</sub>	0.1 M	110	36	21% (65%)	N/D
13	P(C <sub>6</sub> F <sub>5</sub> ) <sub>3</sub>	0.1 M	110	36	16% (72%)	N/D

<sup>a</sup> Unless otherwise mentioned, the reaction was run with 10 mol % [Rh(COD)(CH<sub>3</sub>CN)<sub>2</sub>]BF<sub>4</sub> and 12 mol % (*R*)-xyl-SDP on a 0.1 mmol scale; numbers in parenthesis are yields based on recovered starting material (brsm). <sup>b</sup> Determined by chiral HPLC.

The reaction yield remained moderate despite intensive conditions screened with xyl-SDP ligand alone (Table 2.4). The impressively high enantioselectivity with the rigid SDP ligands suggested a well-controlled transition state, but the moderate yields indicated the stability of the catalyst could be an issue. Efforts of adding a mono-dentate ligand, such as PPh<sub>3</sub> or P(C<sub>6</sub>F<sub>5</sub>)<sub>3</sub>,<sup>14</sup> to

stabilize the catalyst intermediate remained unsuccessful due to side reactions triggered by these rhodium-monodentate-phosphine complexes (Table 2.4, entries 12 and 13).

**Table 2.5** Studies of the Mixed-Ligand Conditions<sup>a</sup>

Reaction scheme: 1a  $\xrightarrow[110\text{ }^{\circ}\text{C, 1,4-dioxane}]{10\text{ mol\% [Rh], 12 mol\% ligand}}$  2a

Entry	Catalyst	Ligand	Yield (BRSM)	e.e. <sup>b</sup>
1 <sup>c</sup>	[Rh(COD)(CH <sub>3</sub> CN) <sub>2</sub> ]BF <sub>4</sub>	( <i>R</i> )-xyl-SDP	46% (63%)	99%
2	[Rh(COD)(CH <sub>3</sub> CN) <sub>2</sub> ]BF <sub>4</sub>	( <i>R</i> )-xyl-SDP	51% (85%)	98%
3	[Rh(COD) <sub>2</sub> ]BF <sub>4</sub>	( <i>R</i> )-xyl-SDP	53% (90%)	98%
4 <sup>d</sup>	[Rh(COD) <sub>2</sub> ]BF <sub>4</sub>	( <i>R</i> )-xyl-SDP	55% (85%)	98%
5	[Rh(COD) <sub>2</sub> ]BF <sub>4</sub>	( <i>R</i> )-xyl-SDP : ( <i>R</i> )-xyl-BINAP 1:1	75%	-10%
6 <sup>e</sup>	[Rh(COD) <sub>2</sub> ]BF <sub>4</sub>	( <i>R</i> )-xyl-SDP : ( <i>R</i> )-xyl-BINAP 1:1	33% (82%)	-26%
7	[Rh(COD) <sub>2</sub> ]BF <sub>4</sub>	( <i>R</i> )-xyl-SDP : ( <i>rac</i> )-xyl-BINAP 1:1	74%	32%
8	[Rh(COD) <sub>2</sub> ]BF <sub>4</sub>	( <i>S</i> )-xyl-BINAP	79%	92%
9	[Rh(COD) <sub>2</sub> ]BF <sub>4</sub>	( <i>R</i> )-xyl-SDP : ( <i>S</i> )-xyl-BINAP 1:1	63%	94%
<b>10<sup>d</sup></b>	<b>[Rh(COD)<sub>2</sub>]BF<sub>4</sub></b>	<b>(<i>R</i>)-xyl-SDP : (<i>S</i>)-xyl-BINAP 1:1</b>	<b>70%</b>	<b>95%</b>
11 <sup>d</sup>	[Rh(COD)(CH <sub>3</sub> CN) <sub>2</sub> ]BF <sub>4</sub>	( <i>R</i> )-xyl-SDP : ( <i>S</i> )-xyl-BINAP 1:1	61%	94%
12 <sup>d</sup>	[Rh(COD) <sub>2</sub> ]BF <sub>4</sub>	( <i>R</i> )-xyl-SDP : ( <i>S</i> )-xyl-BINAP 2:1	60%	97%
13 <sup>d</sup>	[Rh(COD) <sub>2</sub> ]BF <sub>4</sub>	( <i>R</i> )-xyl-SDP : ( <i>S</i> )-xyl-BINAP 5:1	54%	98%

<sup>a</sup> Unless otherwise mentioned, the reaction was run with 10 mol % rhodium complex (based on the metal) and 12 mol % ligand on a 0.1 mmol scale at 110 °C for 48 h; numbers in parenthesis are yields based on recovered starting material (brsm). <sup>b</sup> Determined by chiral HPLC. <sup>c</sup> THF was used as the solvent. <sup>d</sup> Rhodium complex (5 mol%) and mixed ligands (6 mol%) were added initially; the reaction mixture was stirred at 110 °C for 24 h before another portion of the same catalyst was added. <sup>e</sup> the reaction was run for 14 h.

Although changing the solvent from THF to 1,4-dioxane slightly increased the yield (Table 2.5, entries 1 and 2), using [Rh(cod)<sub>2</sub>]BF<sub>4</sub> as the pre-catalyst gave a cleaner reaction (Table 2.5, entries 3 and 4). However, instead of using (*R*)-xyl-SDP alone, when 6 mol% (*R*)-xyl-BINAP was used together with 6 mol% (*R*)-xyl-SDP, the presence of xyl-BINAP indeed stabilize the catalyst and insured a good yield of 72% (Table 2.5, entry 5). It is worth noting that the *R* enantiomers of xyl-BINAP and xyl-SDP gave opposite enantioselectivity in our previous screening, so when they were used together in the reaction, they work against each other rendering a lower ee. So we further

tried to use (*R*)-xyl-SDP and (*S*)-xyl-BINAP together to make use of the advantages of both ligands. We were glad to see that they compromised each other and resulted in a significantly higher yield (70%) and excellent ee (95%) (Table 2.5, entry 10). We also compared both pre-catalysts and found [Rh(cod)<sub>2</sub>]<sub>2</sub>BF<sub>4</sub> provides best yield for current condition (Table 2.5, entry 11).

**Table 2.6** Control Experiments<sup>a</sup>

Entry	Variation	Additive	Yield <sup>b</sup>
1	w/o Rh catalyst	none	0%
2	w/o ligand	none	0%
3	w/o Rh catalyst and ligand	none	0%
4	w/o Rh catalyst and ligand	20 mol % ZnCl <sub>2</sub>	0%
5	w/o Rh catalyst and ligand	20 mol % AlCl <sub>3</sub>	0%
6	w/o Rh catalyst and ligand	20 mol % B(C <sub>6</sub> F <sub>5</sub> ) <sub>3</sub>	0%

<sup>a</sup> Unless otherwise mentioned, the reaction was run with 10 mol % rhodium complex (based on the metal) and 12 mol % ligand on a 0.1 mmol scale at 110 °C for 48 h. <sup>b</sup> NMR yield using 1,1,2,2-tetrachloroethane as the internal standard.

Further control experiments suggested that both rhodium catalyst and ligands are crucial for the reaction to take place (Table 2.6, entries 1-3). Given the literature precedents that Lewis acid alone can catalyze several C–C activation reactions<sup>4,12</sup>, we also explored some Lewis acids that proved to be efficient in other transformations. However, none of these Lewis acids were productive for our reaction (Table 2.6, entries 4-6).

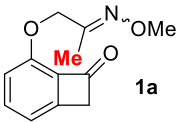
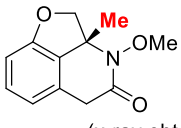
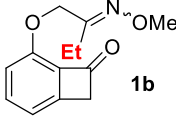
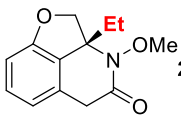
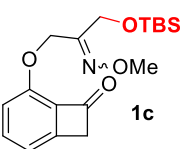
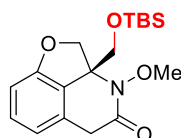
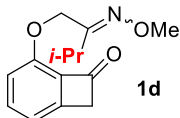
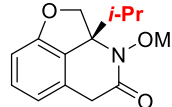
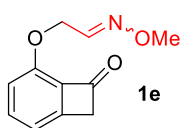
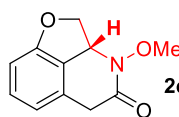
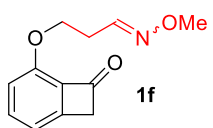
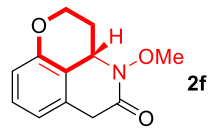
### 2.2.2 Substrate scope for rhodium-catalyzed carboacylation of C=N bonds

With the optimized conditions in hand (Table 2.5, entry 10), we next investigated the substrate scope. First, substitutes on the ketoxime with various steric properties all underwent the desired carboacylation giving excellent enantioselectivity (≥ 90% ee, Table 2.7). It is not surprising



that when the steric bulk of the oxime substituent increased from methyl to ethyl and to isopropyl, the reactivity diminished and a higher temperature (130 °C) was required (Table 2.7, entries 2-4).

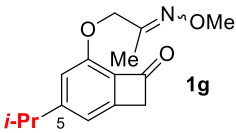
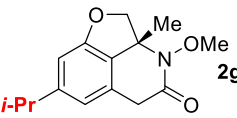
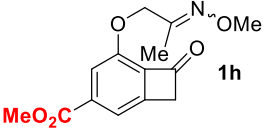
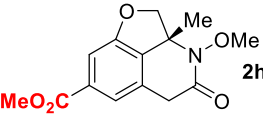
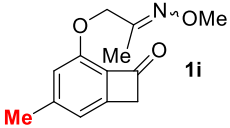
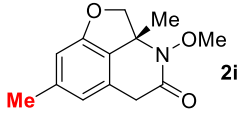
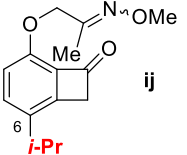
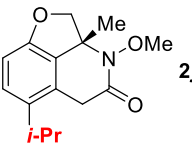
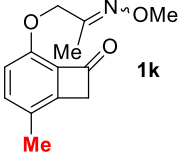
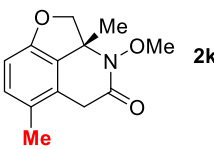
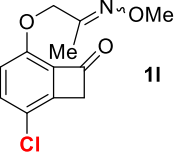
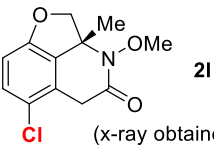
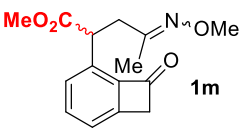
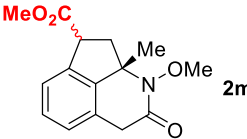
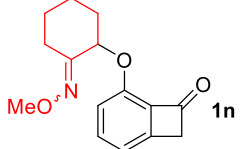
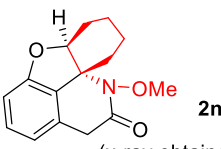
**Table 2.7** Substrate Scope I<sup>a</sup>

Entry	Substrate	Product	Yield <sup>c</sup>	ee <sup>d</sup>
1 <sup>b</sup>	 <b>1a</b>	 <b>2a</b> (x-ray obtained)	72%	95%
2	 <b>1b</b>	 <b>2b</b>	65%	94%
3	 <b>1c</b>	 <b>2c</b>	62%	90%
4	 <b>1d</b>	 <b>2d</b>	50%	90%
5 <sup>b,e</sup>	 <b>1e</b>	 <b>2e</b>	37%	92%
6 <sup>b</sup>	 <b>1f</b>	 <b>2f</b>	40%	81%

<sup>a</sup> Reaction conditions: [Rh(cod)<sub>2</sub>]BF<sub>4</sub> (5 mol %), (*R*)-xyl-SDP (3 mol %), (*S*)-xyl-BINAP (3 mol%), 1,4-dioxane, 130 °C; another portion of the same catalyst was added after 24h. <sup>b</sup> Reaction temperature was 110 °C. <sup>c</sup> Isolated yield; numbers in the parenthesis are brsm yields. <sup>d</sup> Determined by chiral HPLC. <sup>e</sup> (*R*)-xyl-SDP (12 mol%) alone was used.

Although the aldoxime substrate (**1e**) suffered from a competing β-H elimination side reaction and the lactam product (**2e**) was unstable at high temperatures, a moderate yield (37%) with an excellent ee (92%) can nevertheless be obtained by using xyl-SDP alone as the ligand (Table 2.7, entries 5). It is encouraging to observe that 6-membered rings can also be formed generating an interesting 6-6-6 fused lactam (Table 2.7, entry 6).

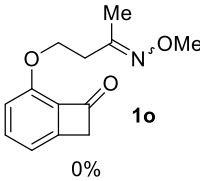
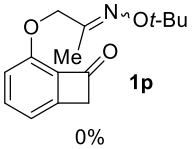
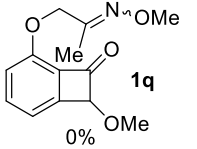
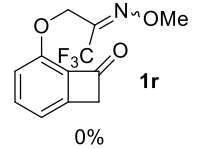
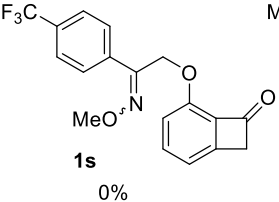
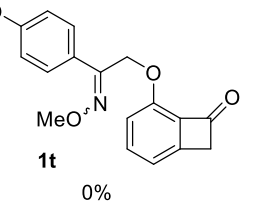
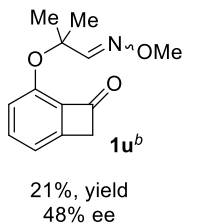
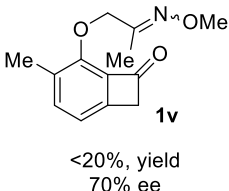
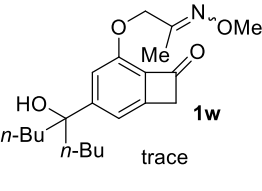
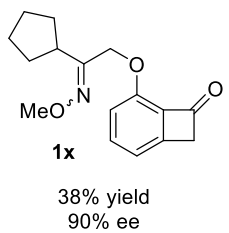
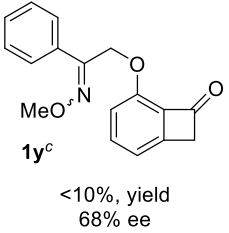
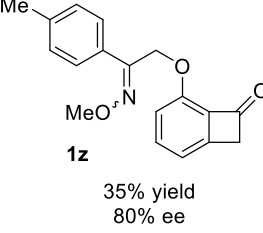
**Table 2.8 Substrate Scope II<sup>a</sup>**

Entry	Substrate	Product	Yield <sup>c</sup>	ee <sup>d</sup>
1	 <b>1g</b>	 <b>2g</b>	53% (74%)	90%
2 <sup>b</sup>	 <b>1h</b>	 <b>2h</b>	68%	94%
3 <sup>b</sup>	 <b>1i</b>	 <b>2i</b>	74%	89%
4 <sup>b</sup>	 <b>1j</b>	 <b>2j</b>	50%	86%
5	 <b>1k</b>	 <b>2k</b>	67%	90%
6	 <b>1l</b>	 <b>2l</b> (x-ray obtained)	72%	90%
7 <sup>b</sup>	 <b>1m</b>	 <b>2m</b>	70% d.r.=3:1	N/A
8 <sup>e</sup>	 <b>1n</b>	 <b>2n</b> (x-ray obtained)	66% d.r.>20:1	N/A

<sup>a</sup> Reaction conditions: [Rh(cod)<sub>2</sub>][BF<sub>4</sub>] (5 mol %), (*R*)-xyl-SDP (3 mol %), (*S*)-xyl-BINAP (3 mol %), 1,4-dioxane, 130 °C; another portion of the same catalyst was added after 24h. <sup>b</sup> Reaction temperature was 110 °C. <sup>c</sup> Isolated yield; numbers in the parenthesis are brsm yields. <sup>d</sup> Determined by chiral HPLC. <sup>e</sup> [Rh(CH<sub>3</sub>CN)<sub>2</sub>(COD)][BF<sub>4</sub>] (20 mol %) and (*R*)-xyl-BINAP (25 mol %) were used.

Moreover, both electron-donating and withdrawing groups on the arene can be well tolerated (Table 2.8, entries 1-6). In particular, both C5 and C6-substituted benzocyclobutenones are competent substrates.

**Table 2.9** Unsuccessful Substrates<sup>a</sup>

<sup>a</sup> Reaction conditions: [Rh(cod)<sub>2</sub>]BF<sub>4</sub> (5 mol %), (*R*)-xyl-SDP (3 mol %), (*S*)-xyl-BINAP (3 mol%), 1,4-dioxane, 130 °C; another portion of the same catalyst was added after 24h. <sup>b</sup> [Rh(cod)(CH<sub>3</sub>CN)]BF<sub>4</sub> (10 mol %) and (*R*)-xyl-BINAP (12 mol%) were used. <sup>c</sup> [Rh(cod)(CH<sub>3</sub>CN)]BF<sub>4</sub> (10 mol %) and (*R*)-xyl-SEGPHOS (12 mol%) were used.

Next, we aimed at replacing the ether linker with a carbon-based one. Substrate **1m** with a pre-existing stereocenter underwent smooth transformation to give the fused lactam in 70% yield with 3:1 dr (Table 2.8, entry 7). Finally, the substrate containing a cyclic oxime was examined for

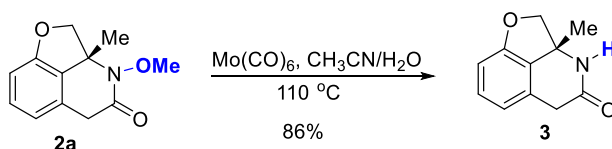
this transformation (Table 2.8, entry 8). We were concerned that the relatively rigid conformation of the six-membered ring with a fixed orientation would hinder the carboacylation process. To our delight, with a higher catalyst loading the desired tetracyclic scaffold containing two adjacent stereocenters can nonetheless be provided in good yield and excellent diastereoselectivity (>20:1 dr). The structure of product **2n** was confirmed by both 2D-NMR and X-ray diffraction analysis. Apart from the successful examples discussed above, we have synthesized other substrates which fail to deliver the desired product with synthetically useful yield or enantioselectivity (Table 2.9). When substrate **1o** was subjected to the standard condition, the 6-6-6 fused lactam product similar to product **2f** was not observed, mainly due to the steric hinderance. Increasing the steric on the oxygen of the oxime to tert-butyl (**1p**) would shut down the reaction. Methoxy substituent at C8 position (**1q**) cannot be tolerated. Replacing the methyl substituent with strongly electron-withdrawing trifluoromethyl group (**1r**) is not viable substrate due to substrate decomposition. Substrates with aryl substituents on the oxime are having low reactivity (**1s**, **1t**, **1y**, **1z**). Only **1y** and **1z** gave small amount of the product. Gem-dimethyl substituents on the linkage (**1u**) was proposed to bring the olefin closer to the rhodacycle intermediate, however it failed to give good yield and ee.

### 2.2.3 Synthetic applications for rhodium-catalyzed carboacylation of C=N bonds

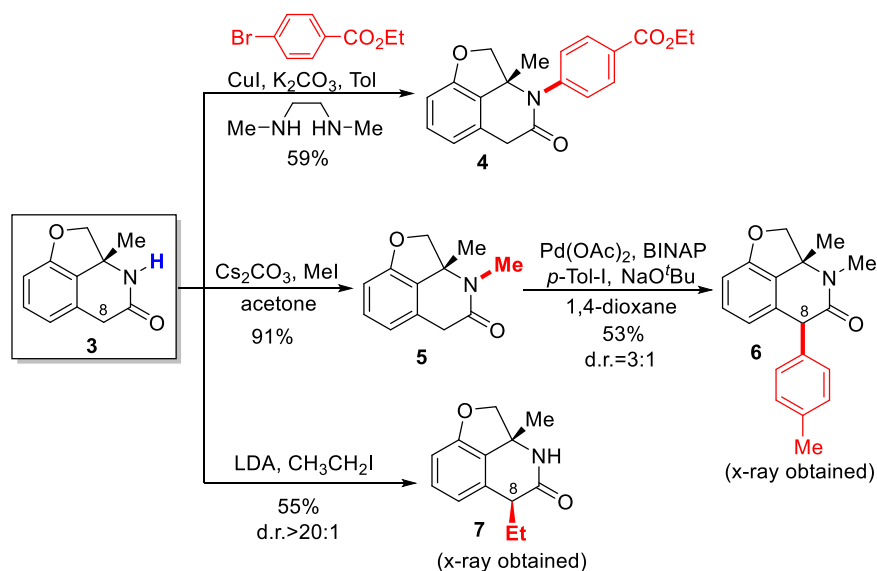
One advantage of using oximes as the C=N coupling partner is that the O–N bond can be easily cleaved using various reductants.<sup>15</sup> For example, treatment of lactam **2a** with Mo(CO)<sub>6</sub> provided the free amide in 86% yield (Scheme 2.6). *N*-arylated and alkylated lactams can be conveniently obtained under cross-coupling<sup>16</sup> and S<sub>N</sub>2 conditions (Scheme 2.7). While the benzocyclobutenone substrates with a C8 substituent were not reactive under carboacylation conditions, arylation and alkylation at the C8 position can be efficiently achieved through post

functionalization. In particular, complete diastereoselectivity was obtained for the alkylation reaction to generate **7**, suggesting an excellent convex-face-controlled situation. The relative stereochemistry was unambiguously confirmed by X-ray diffraction analysis.

### Scheme 2.6 Cleavage of N–O Bond

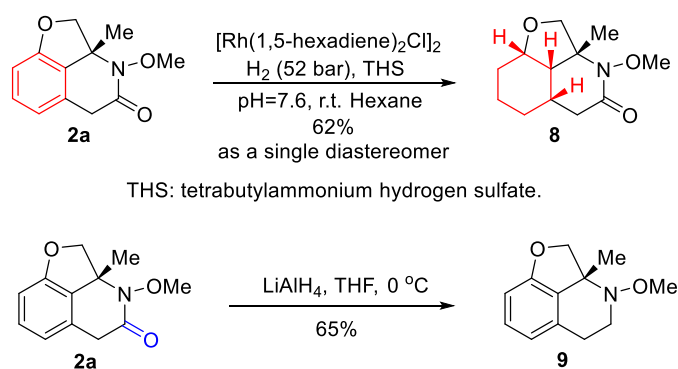


### Scheme 2.7 Synthetic Applications I



Furthermore, a new saturated scaffold **8** can be efficiently constructed using a mild Rh-catalyzed hydrogenation protocol (Scheme 2.8).<sup>17</sup> Two interesting features should be noted: 1) the reaction gives perfect diastereoselectivity; 2) the *N*-OMe bond and the amide moiety remained intact after the reaction. In addition, a complementary  $\text{LiAlH}_4$  reduction smoothly provided the corresponding *N*-OMe piperidine **9**.<sup>18</sup>

## Scheme 2.8 Synthetic Applications II



## 2.3 Conclusion

In summary, we have developed a highly enantioselective Rh-catalyzed carboacylation of oxime C=N bonds via C–C activation. Using this method, unique fused isoquinolinone scaffolds can be efficiently accessed from benzocyclobutenone-linked oximes. The reaction conditions do not use a strong acid or base and are overall redox neutral, which provide good functional group tolerance. High enantioselectivity can be achieved despite using a mixture of the *E/Z* isomers of the oximes. The resulting scaffolds were rendered to several derivatization conditions and among them, an interesting saturated fused lactam was successfully obtained. Considering the novelty of these structures, the potential pharmaceutical applications of the fused heterocyclic products are under investigation. Moreover, given the importance of amide-bond formation, this catalytic asymmetric C–C activation method provides an additional approach for their synthesis.

## 2.4 Experimental

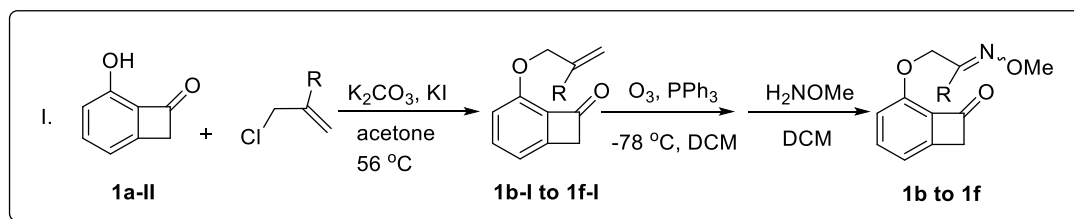
### 2.4.1 General information

Unless noted otherwise, all solvents were dried by filtration through a Pure-Solv MD-5 Solvent Purification System (Innovative Technology). And the solvents for the C–C Activation reactions were distilled freshly over sodium or calcium hydride and carefully freeze-pump-thawed. All the

C–C Activation reactions were carried out under nitrogen atmosphere with a stir bar in a sealed vial. Reaction temperatures were reported as the temperatures of the bath surrounding the flasks or vials. Sensitive ligands and rhodium catalysts and solvents were transferred under nitrogen into a nitrogen-filled glove-box with standard techniques. Analytical thin-layer chromatography (TLC) was carried out using 0.2 mm commercial silica gel plates (silica gel 60, F254, EMD chemical). Vials (17 x 60 mm (7.5mL) with PTFE lined cap attached) were purchased from Qorpak and flame-dried or put in an oven overnight. High-resolution mass spectra (HRSM) were obtained on a Karatos MS9 and are reported as  $m/z$  (relative intensity). Accurate masses are reported for the molecular ion  $[M+Na]^+$ ,  $[M+H]^+$ ,  $[M-H]^-$  or  $[M]$ . Infrared spectra were recorded on a Nicolet 380 FTIR using neat thin film technique. Nuclear magnetic resonance spectra ( $^1H$  NMR and  $^{13}C$  NMR) were recorded with a Varian Gemini (400 MHz,  $^1H$  at 400 MHz,  $^{13}C$  at 100 MHz). Unless otherwise noted, all spectra were acquired in  $CDCl_3$ . Chemical shifts are reported in parts per million (ppm,  $\delta$ ), downfield from tetramethylsilane (TMS,  $\delta=0.00$ ppm) and are referenced to residual solvent ( $CDCl_3$ ,  $\delta=7.26$  ppm ( $^1H$ ) and 77.00 ppm ( $^{13}C$ );  $CD_2Cl_2$ ,  $\delta=5.32$  ppm ( $^1H$ ) and 53.84 ppm ( $^{13}C$ )). Coupling constants were reported in Hertz (Hz). Data for  $^1H$  NMR spectra were reported as follows: chemical shift (ppm, referenced to protium; s = singlet, d = doublet, t = triplet, q = quartet, hept=heptuplet, dd = doublet of doublets, td = triplet of doublets, ddd = doublet of doublet of doublets, m = multiplet, coupling constant (Hz), and integration).

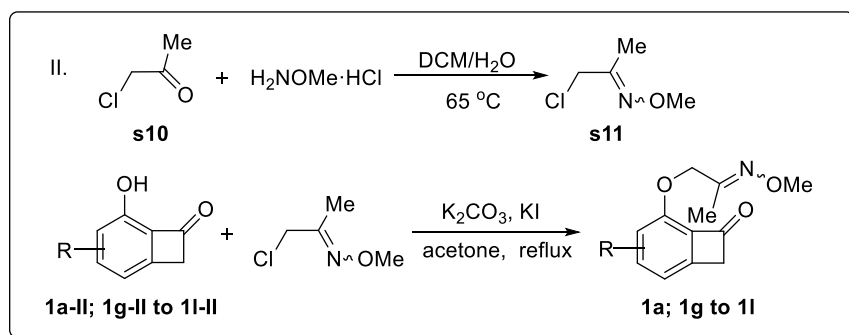
#### *2.4.2 Synthetic routes for substrate synthesis*

##### *Route I*



Substrates **1b** to **1f** were synthesized through **Route I**.

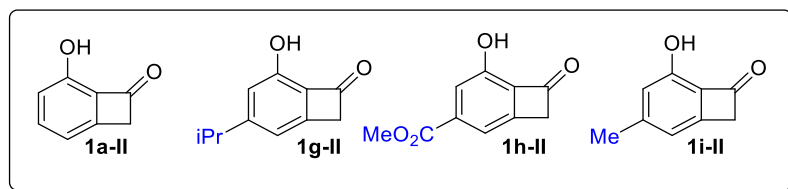
### Route II



Substrates **1a** and **1g** to **1i** were synthesized through **route II**.

### 2.4.3 Synthesis of precursors

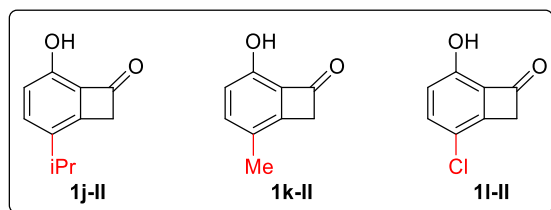
a) Synthesis of known compound **1a-II**, **1g-II**, **1h-II** and **1i-II**:



Compounds **1a-II**, **1g-II**, **1h-II** and **1i-II** were synthesized according to the reported procedure and match the data reported in literature.<sup>8a,8b,19</sup>

b) Synthesis of compound **1j-II**, **1k-II** and **1l-II**:

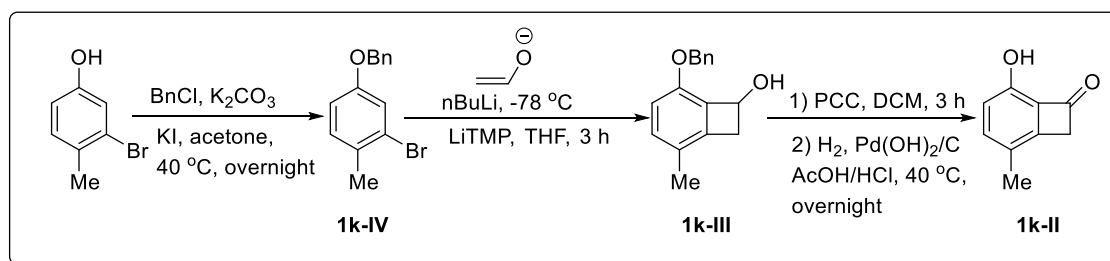




Compound **1j-II** was synthesized using same procedure as reported in literature.<sup>8a,8b</sup>

Compound **1j-II** was synthesized as a colorless oil in 30% yield (113.8 mg) in 4 steps from commercial available 4-(1-methylethyl)resorinol.  $R_f = 0.6$  (EtOAc/Hexane=1/5). **<sup>1</sup>H NMR (400 MHz, CDCl<sub>3</sub>)**:  $\delta$  7.28 (dd,  $J = 8.5, 0.5$  Hz, 1H), 6.75 (d,  $J = 8.5$  Hz, 1H), 3.91 (d,  $J = 0.7$  Hz, 2H), 3.53 (s, 1H), 2.93 (hept,  $J = 6.9$  Hz, 1H), 1.24 (d,  $J = 7.0$  Hz, 6H). **<sup>13</sup>C NMR (100 MHz, CDCl<sub>3</sub>)**:  $\delta$  189.20, 147.31, 147.04, 137.16, 135.56, 131.71, 116.88, 50.56, 31.10, 23.12. **IR**:  $\nu$  3271, 2961, 2871, 1741, 1619, 1591, 1501, 1276, 1147, 828, 672  $\text{cm}^{-1}$ ; **HRMS** calcd. for  $[M+H]^+$ : 177.0916. Found: 177.0912.

Compound **1k-II** was synthesized using the following procedure.<sup>19</sup>



Commercially available starting material 3-bromo-4-methylphenol (2.0 g, 10.7 mmol, 1 equiv.) was dissolved in a 40 mL vial (with stir bar) using acetone (20 mL). K<sub>2</sub>CO<sub>3</sub> (7.39 g, 53.5 mmol, 5 equiv.), KI (5.33 g, 32.1 mmol, 3 equiv.) and BnCl (4.57 g, 26.7 mmol, 2.5 equiv.) were added to the stirring solution. Then the reaction was heated to 40 °C and stirred overnight. Upon completion, the reaction mixture was transferred to a separation funnel and 40 mL of NH<sub>4</sub>Cl (sat.) solution was

added to quench the reaction. Then the mixture was extracted with ethyl acetate (EA) (3×20 mL). Afterwards, the organic phase was washed by saturated Na<sub>2</sub>S<sub>2</sub>O<sub>3</sub> solution twice and brine twice. The organic phase was then dried using Na<sub>2</sub>SO<sub>4</sub> and concentrated under reduced pressure. The residue was purified by silica gel flash column chromatography (EtOAc/Hexane=1/20) to obtain compound **1k-IV** as a colorless oil in 96% yield (2.85 g). *R<sub>f</sub>* = 0.7 (EtOAc/Hexane=1/5) **<sup>1</sup>H NMR (400 MHz, CDCl<sub>3</sub>):** δ 7.47 – 7.32 (m, 5H), 7.22 (s, 1H), 7.14 (dd, *J* = 8.5, 2.2 Hz, 1H), 6.85 (d, *J* = 8.4 Hz, 1H), 5.03 (s, 2H), 2.34 (s, 3H). **<sup>13</sup>C NMR (100 MHz, CDCl<sub>3</sub>):** δ 157.32, 157.30, 136.58, 136.56, 130.97, 130.96, 129.98, 128.58, 128.57, 128.03, 128.02, 127.44, 127.43, 124.84, 124.82, 118.60, 118.59, 114.12, 114.10, 70.24, 21.83, 21.82. **IR:** ν 3032, 2922, 1604, 1491, 1235, 1026, 736, 696, 450 cm<sup>-1</sup>; **HRMS** calcd. for [M]<sup>+</sup>: 276.0150. Found: 276.0150.

To a 100 mL flamed-dried Schlenk flask equipped with a stir bar and a nitrogen-filled balloon was added THF (20 mL). The system was cooled to 0 °C with an ice-water bath before *n*-BuLi (2.5 M in hexane, 3.2 mL, 8.1 mmol, 1.5 equiv.) was added dropwise. Upon completion, the system was warmed to r.t. and stirred for 16 h under nitrogen atmosphere. To a 30 mL flamed-dried Schlenk flask equipped with a stir bar and a nitrogen-filled balloon were added 2,2,6,6-tetramethylpiperidine (918.13 mg, 6.5 mmol, 1.2 equiv.) and THF (15 mL). After cooled to 0 °C with an ice-water bath, *n*-BuLi (2.5 M in hexane, 2.6 mL, 6.5 mmol, 1.2 equiv.) was added dropwise and the reaction was stirred at 0 °C for 0.5 h to provide lithium tetramethylpiperidine solution. The previous 100 mL flask was cooled to –78 °C with an acetone-dry ice bath and compound **1k-IV** (1.5 g, 5.4 mmol, 1 equiv) in THF (5 mL) was added before *in situ* generated lithium tetramethylpiperidine was added dropwise. The reaction was stirred at –78 °C for 3h and was warmed to r.t. before quenched by adding saturated NH<sub>4</sub>Cl solution (30 mL). The mixture was extracted with ethyl acetate (3×30 mL), washed with brine, and dried with Na<sub>2</sub>SO<sub>4</sub>. The combined

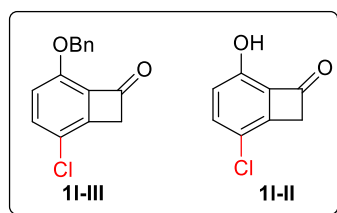
organic extract was concentrated under reduced pressure and purified by silica gel flash column chromatography (EtOAc/Hexane=1/10) on silica gel to afford compound **1k-III** as a colorless oil in 56% yield (723.5 mg).  $R_f = 0.4$  (EtOAc/Hexane=1/5)  **$^1\text{H}$  NMR (400 MHz,  $\text{CDCl}_3$ )**:  $\delta$  7.46 – 7.41 (m, 2H), 7.37 (ddd,  $J = 8.0, 6.9, 1.0$  Hz, 2H), 7.31 (d,  $J = 7.2$  Hz, 1H), 7.01 (dt,  $J = 8.4, 0.7$  Hz, 1H), 6.74 (d,  $J = 8.4$  Hz, 1H), 5.33 (d,  $J = 12.3$  Hz, 1H), 5.23 (d,  $J = 12.2$  Hz, 1H), 5.18 (ddd,  $J = 9.6, 4.6, 1.8$  Hz, 1H), 3.50 (dd,  $J = 14.3, 4.6$  Hz, 1H), 2.96 – 2.87 (m, 1H), 2.17 (d,  $J = 9.6$  Hz, 1H), 2.12 (s, 3H), 1.56 (s, 3H).  **$^{13}\text{C}$  NMR (100 MHz,  $\text{CDCl}_3$ )**:  $\delta$  151.50, 142.07, 137.59, 131.84, 130.40, 128.49, 127.78, 127.17, 127.16, 125.40, 115.33, 71.11, 70.02, 41.19, 15.77. **IR**:  $\nu$  3302, 2920, 1582, 1490, 1454, 1262, 1112, 1047, 1007, 825, 729, 667  $\text{cm}^{-1}$ ; **HRMS** calcd. for  $[\text{M}]^+$ : 240.1150. Found: 240.1150.

Compound **1k-III** (480.6 mg, 2.0 mmol, 1 equiv.) was dissolved in dichloromethane (10 mL). Pyridinium chlorochromate (PCC) (689.8 mg, 3.2 mmol, 1.6 equiv.) and silica gel (1.03 g, mass ratio to PCC is 1.5:1) were added to the solution. The reaction was monitored by TLC and stopped at 3 h when all the starting material was consumed. The resulting mixture was filtered through a silica pad and concentrated. The crude product was used directly in the next step without further purification.

The crude product from the previous step was dissolved in 10 mL AcOH in a 50 mL Schlenk tube and 2 mL of 6M HCl (aq.) was added into the solution. Then the  $\text{Pd}(\text{OH})_2$  (20 wt% on carbon) (137.0 mg, 0.97 mmol, 0.5 equiv.) was added to the solution. A  $\text{H}_2$  balloon was equipped and a pump with low vacuum was used to degas and pump  $\text{H}_2$  three times. The reaction was heated at 40 °C overnight. When the reaction was finished, the reaction mixture was filtered through a celite pad and the solid was washed with acetone. After concentrating the solution under reduced pressure, the crude product was purified by silica gel flash column chromatography

(EtOAc/Hexane=1/5) on silica gel to afford compound **1k-II** as a colorless oil in 81% yield for two steps (242.6 mg).  $R_f = 0.3$  (EtOAc/Hexane = 1/5).  **$^1\text{H}$  NMR (400 MHz,  $\text{CDCl}_3$ )**:  $\delta$  7.23 (dd,  $J = 8.3, 0.8$  Hz, 1H), 6.72 (d,  $J = 8.4$  Hz, 1H), 3.83 (s, 2H), 2.25 (s, 3H).  **$^{13}\text{C}$  NMR (100 MHz,  $\text{CDCl}_3$ )**:  $\delta$  188.52, 148.59, 147.34, 139.70, 131.10, 124.46, 116.94, 49.77, 16.41. **IR**:  $\nu$  2923, 1753, 1620, 1585, 1501, 1451, 1270, 1149, 1012, 822, 631  $\text{cm}^{-1}$ ; **HRMS** calcd. for  $[\text{M}]^+$ : 148.0524. Found: 148.0523.

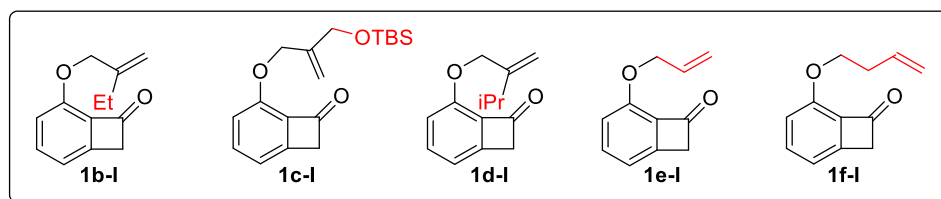
Compound **1l-II** was synthesized using same procedure as **1k-II**.<sup>19</sup>



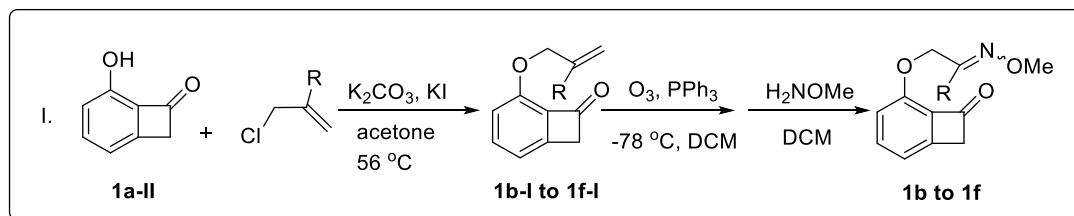
Compound **1l-III** matched the reported data<sup>19</sup> and **1l-II** was obtained using similar deprotection procedure used in **1k-II** synthesis. **1l-II** was obtained as a colorless oil in 89% yield (105.2 mg).  $R_f = 0.4$  (EtOAc/Hexane=1/5).  **$^1\text{H}$  NMR (400 MHz,  $\text{CDCl}_3$ )**:  $\delta$  7.36 (d,  $J = 8.8$  Hz, 1H), 6.77 (d,  $J = 8.8$  Hz, 1H), 3.92 (s, 2H).  **$^{13}\text{C}$  NMR (100 MHz,  $\text{CDCl}_3$ )**:  $\delta$  187.03, 148.65, 147.07, 138.57, 132.34, 119.14, 119.07, 50.28, 29.68. **IR**:  $\nu$  3079, 2921, 1780, 1755, 1732, 1597, 1440, 1414, 1294, 1154, 984, 818, 750, 714  $\text{cm}^{-1}$ ; **HRMS** calcd. for  $[\text{M}]^+$ : 167.9978. Found: 167.9981.

### c) Synthesis of known compounds **1b-I** to **1f-I**:

From compound **1a-II**, compound **1b-I** to **1f-I** were synthesized according to the reported procedure and matched the data reported in literature.<sup>8a,8b,19</sup>



#### 2.4.4 **Route I** synthesis of substrates **1b** to **1f**

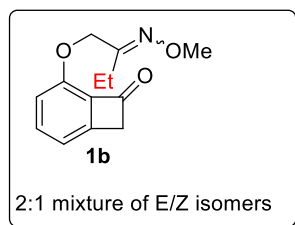


Substrates **1b** to **1f** were synthesized through **Route I**.

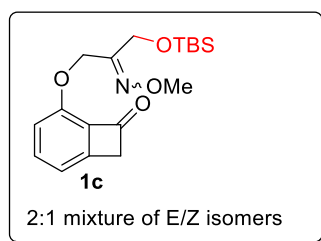
#### *General Procedure for the Synthesis of Oxime Substrates from **1b-I** to **1f-I** in **Route I***

##### One-pot ozonolysis and oxime formation

*Using the synthesis of substrate **1b** as an example:* A round bottom flask was charged with a stir bar, and the alkene precursor **1b-I** in DCM (633.1 mg, 3.13 mmol, 1 equiv.; 0.2 mol/L). The flask was sealed with plastic stopper on top and cooled to -78 °C in an acetone-dry ice bath. A needle was inserted through the stopper to keep a static pressure inside the flask while inserting an oxygen gas line into the reaction system. The ozone generator was opened. After the solution turned pale blue, a DCM solution of PPh<sub>3</sub> (4.11 g, 15.7 mmol; 5equiv. for small scale reactions and 2 equiv. for large scale reactions) was injected to quench the reaction and the reaction was stirred at room temperature for 15 minutes. NH<sub>2</sub>OMe·HCl (261.4 mg, 3.13 mmol, 1equiv.) was then added to the reaction and the flask was kept stirring at room temperature (also **1c-I**, **1e-I**, **1f-I**) or 65 °C with 4 Å molecule sieves (10 equiv.) (**1d-I**) overnight. [For substrate **1c-I** the TBS group was removed during this reaction, thus the protection method used in literature<sup>1</sup> was used to re-protect the OH group] The reaction mixture was concentrated using rovacator (if 4 Å molecule sieves were used, the reaction mixture was filtered before concentrating the mixture) before purifying by silica gel column chromatography (EtOAc/Hexane=1/10).

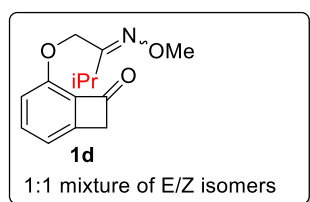


**1b** was isolated as a colorless oil in 54% yield (395.2 mg) on a 2 mmol scale as an inseparable 2:1 mixture of E/Z isomers from **1b-I** and  $\text{NH}_2\text{OME}\cdot\text{HCl}$ .  $R_f = 0.5$  (EtOAc/Hexane=1/5).  **$^1\text{H}$  NMR (400 MHz,  $\text{CDCl}_3$ ):**  $\delta$  (major) 7.44 (dd,  $J = 8.4, 7.1$  Hz, 0.68H), 7.06 (dd,  $J = 0.7, 0.5$  Hz, 0.68H), 6.86 (dd,  $J = 8.5, 0.7$  Hz, 0.68H), 4.93 (s, 1.33H), 3.93 (s, 1.33H), 3.88 (s, 2H), 2.45 (q,  $J = 7.6$  Hz, 1.36H), 1.11 (t,  $J = 7.7$  Hz, 2.47H). );  $\delta$  (minor) 7.45 (dd,  $J = 8.4, 7.1$  Hz, 0.33H), 7.07 (dd,  $J = 0.7, 0.5$  Hz, 0.33H), 6.84 (dd,  $J = 8.5, 0.7$  Hz, 0.33H), 5.22 (s, 0.68H), 3.93 (s, 0.68H), 3.89 (s, 1.02H), 2.37 (q,  $J = 7.4$  Hz, 0.71H), 1.13 (t,  $J = 7.4$  Hz, 0.75H).  **$^{13}\text{C}$  NMR (100 MHz,  $\text{CDCl}_3$ ):**  $\delta$  184.71, 184.54, 157.92, 157.16, 151.83, 151.72, 150.71, 150.54, 137.70, 132.61, 132.49, 116.17, 115.79, 115.68, 115.56, 72.03, 66.73, 61.74, 51.39, 51.30, 24.30, 19.92, 11.16, 9.96. **IR:**  $\nu$  2973, 2938, 2818, 1765, 1603, 1575, 1473, 1450, 1270, 1048, 896, 784  $\text{cm}^{-1}$ ; **HRMS** calcd. For  $[\text{M}+\text{Na}]^+$ : 256.0944. Found: 256.0947.

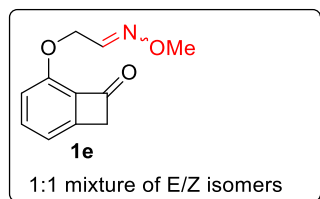


**1c** was isolated as a colorless oil in 69% yield (730 mg) on a 3 mmol scale as an inseparable 2:1 mixture of E/Z isomers from **1c-I** and  $\text{NH}_2\text{OME}\cdot\text{HCl}$ .  $R_f = 0.7$  (EtOAc/Hexane=1/5).  **$^1\text{H}$  NMR (400 MHz,  $\text{CDCl}_3$ ):**  $\delta$  (major) 7.42 (dd,  $J = 8.4, 7.0$  Hz, 0.67H), 7.02 (dd,  $J = 7.0, 0.7$  Hz, 0.67H), 6.83 (dd,  $J = 8.4, 0.8$  Hz, 0.67H), 5.08 (s, 1.36H), 4.59 (s, 1.36H), 3.91 (s, 1.39H), 3.87 (s, 2.09H),

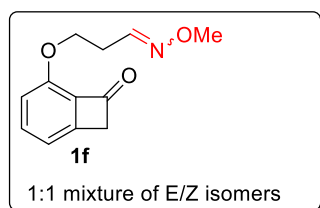
0.81 (s, 6.04H), 0.03 (s, 4.09H).  $\delta$  (minor) 7.43 (dd,  $J = 8.4, 7.0$  Hz, 0.33H), 7.05 (dd,  $J = 7.0, 0.7$  Hz, 0.33H), 6.83 (dd,  $J = 8.4, 0.8$  Hz, 0.33H), 5.24 (s, 0.65H), 4.34 (s, 0.65H), 3.93 (s, 0.69H), 3.91 (s, 1.01H), 0.83 (s, 2.90H), 0.03 (s, 1.91H).  **$^{13}\text{C}$  NMR (100 MHz,  $\text{CDCl}_3$ ):**  $\delta$  184.61, 156.39, 154.67, 152.06, 151.95, 150.57, 150.37, 137.50, 132.39, 116.16, 115.89, 115.50, 115.20, 69.26, 64.37, 62.16, 62.08, 61.59, 57.65, 51.31, 51.19, 25.63, 18.11, -5.44, -5.73. **IR:**  $\nu$  2930, 2898, 2857, 1770, 1603, 1575, 1473, 1273, 1128, 1048, 837, 780  $\text{cm}^{-1}$ ; **HRMS** calcd. For  $[\text{M}+\text{Na}]^+$ : 372.1602. Found: 372.1605.



**1d** was isolated as a colorless oil in 58% yield (298.7 mg) on a 2 mmol scale as an inseparable 1:1 mixture of E/Z isomers from **1d-I** and  $\text{NH}_2\text{OMe}\cdot\text{HCl}$ .  $R_f = 0.6$  (EtOAc/Hexane=1/5).  **$^1\text{H}$  NMR (400 MHz,  $\text{CDCl}_3$ ):**  $\delta$  7.42 (ddd,  $J = 8.4, 7.1, 2.6$  Hz, 1H), 7.04 (ddd,  $J = 7.1, 3.5, 0.7$  Hz, 1H), 6.83 (ddd,  $J = 8.5, 4.3, 0.7$  Hz, 1H), 5.17 (s, 1H), 4.94 (s, 1H), 3.92 (s, 2H), 3.87 (d,  $J = 1.8$  Hz, 3H), 3.30 (hept,  $J = 7.0$  Hz, 0.5H), 2.76 (hept,  $J = 6.9$  Hz, 0.5H), 1.14 (dd,  $J = 7.0, 5.4$  Hz, 6H).  **$^{13}\text{C}$  NMR (100 MHz,  $\text{CDCl}_3$ ):**  $\delta$  184.64, 184.50, 159.83, 159.54, 151.73, 151.64, 150.60, 150.44, 137.60, 132.53, 132.42, 116.19, 115.80, 115.53, 115.43, 70.93, 65.63, 61.70, 51.30, 51.22, 30.52, 26.66, 20.00, 18.87. **IR:**  $\nu$  2968, 2937, 2901, 2875, 2818, 1767, 1602, 1575, 1473, 1273, 1047, 905, 783  $\text{cm}^{-1}$ ; **HRMS** calcd. for  $[\text{M}+\text{Na}]^+$ : 270.1101. Found: 270.1099.



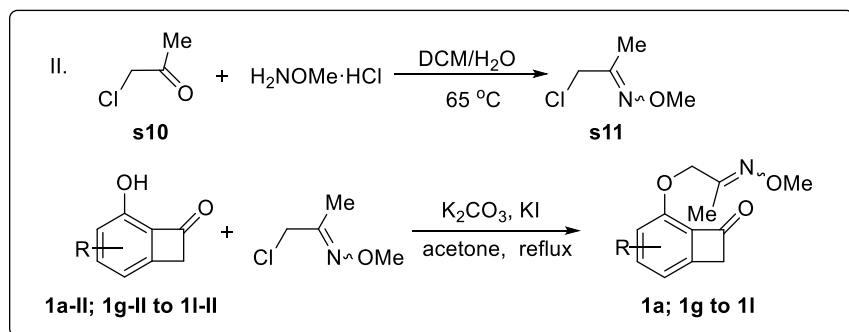
**1e** was isolated as white solid in 43% yield (160 mg) on a 1 mmol scale as an inseparable 1:1 mixture of E/Z isomers from **1e-I** and  $\text{NH}_2\text{OMe}\cdot\text{HCl}$ .  $R_f = 0.6$  (EtOAc/Hexane=1/5). M.P.=66-68 °C.  **$^1\text{H}$  NMR (400 MHz,  $\text{CDCl}_3$ )**  $\delta$  7.56 (t,  $J = 5.6$  Hz, 0.5H), 7.45 (ddd,  $J = 8.4, 7.1, 3.0$  Hz, 1H), 7.07 (ddq,  $J = 7.1, 3.6, 0.7$  Hz, 1H), 6.91 (t,  $J = 3.6$  Hz, 0.5H), 6.85 (ddd,  $J = 8.4, 2.6, 0.6$  Hz, 1H), 5.18 (d,  $J = 3.6$  Hz, 1H), 4.99 (d,  $J = 5.6$  Hz, 1H), 3.95 (m, 1.5H), 3.95 – 3.93 (m, 2H), 3.89 (m, 1.5H).  **$^{13}\text{C}$  NMR (100 MHz,  $\text{CDCl}_3$ )**:  $\delta$  184.68, 184.46, 151.46, 151.26, 150.67, 150.52, 147.32, 144.82, 137.83, 137.78, 132.56, 132.30, 116.23, 115.94, 115.86, 115.76, 68.55, 66.18, 62.40, 61.94, 51.41, 51.32. **IR**:  $\nu$  2938, 1765, 1602, 1573, 1473, 1269, 1046, 870, 785  $\text{cm}^{-1}$ ; **HRMS** calcd. for  $[\text{M}+\text{Na}]^+$ : 228.0631. Found: 228.0631.



**1f** was isolated as a colorless oil in 60% yield (410.2 mg) on a 3 mmol scale as an inseparable 1:1 mixture of E/Z isomers from **1f-I** and  $\text{NH}_2\text{OMe}\cdot\text{HCl}$ .  $R_f = 0.6$  (EtOAc/Hexane=1/5).  **$^1\text{H}$  NMR (400 MHz,  $\text{CDCl}_3$ )**:  $\delta$  7.48 (t,  $J = 6.1$  Hz, 0.5H), 7.43 (ddd,  $J = 8.5, 7.1, 1.5$  Hz, 1H), 7.05 – 7.00 (m, 1H), 6.84 – 6.77 (m, 1.5H), 4.52 (q,  $J = 6.3$  Hz, 2H), 3.92 (dd,  $J = 1.8, 0.9$  Hz, 2H), 3.89 (s, 1.5H), 3.83 (s, 1.6H), 2.80 (d,  $J = 6.3$  Hz, 1H), 2.67 (q,  $J = 6.2$  Hz, 1H).  **$^{13}\text{C}$  NMR (100 MHz,  $\text{CDCl}_3$ )**:  $\delta$  184.90, 184.89, 152.00, 151.99, 150.48, 147.73, 147.31, 137.73, 132.22, 132.20, 116.27, 115.30, 115.28, 69.28, 68.87, 61.72, 61.39, 51.20, 29.80, 26.07. **IR**:  $\nu$  2938, 1765, 1603, 1573, 1461, 1275, 1050, 785  $\text{cm}^{-1}$ ; **HRMS** calcd. for  $[\text{M}+\text{Na}]^+$ : 242.0788. Found: 242.0781.

#### 2.4.5 *Route II* synthesis of substrates **1a** and **1g** to **1m**





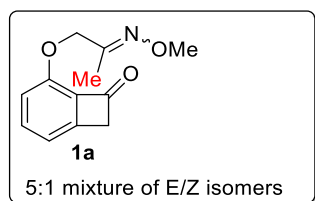
Substrates **1a** and **1g to 1l** were synthesized through **route II**.

**S11** was synthesized according to a reported procedure<sup>20</sup> and matched the reported data.

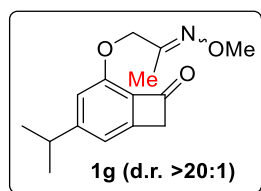
### General Procedures for the Synthesis of Oxime Substrates from **1a-II** and **1g-II** to **1l-II**

#### Substitution reaction with pre-formed oxime chloride

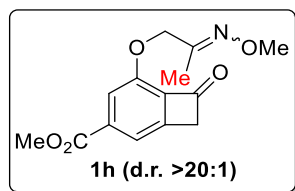
*Using the synthesis of substrate **II** as an example:* To a solution of compound **1l-II** (105.2 mg, 0.62 mmol, 1 equiv.) in acetone (10 mL),  $\text{K}_2\text{CO}_3$  (256.7 mg, 1.86 mmol, 3 equiv.), KI (206.7 mg, 1.24 mmol, 2 equiv.) and **S11** (114.3 mg, 0.94 mmol, 1.5 equiv.) were added to the stirring solution. Then the reaction was heated to 70 °C and stirred overnight. After the reaction was complete, 10 mL of  $\text{NH}_4\text{Cl}$  (sat.) solution was used to quench the reaction. The mixture was extracted with ethyl acetate (EA) (3×10 mL). Then the organic phase was washed by saturated  $\text{Na}_2\text{S}_2\text{O}_3$  (aq.) solution (2×10 mL) and brine (2×10 mL). The organic phase was then dried using  $\text{Na}_2\text{SO}_4$  and concentrated under reduced pressure. The residue was purified by silica gel flash column chromatography (EtOAc/Hexane=1/10). to obtain the compound **1l** as a white solid in 83% yield (2.85 g).



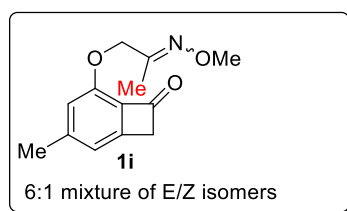
**1a** was isolated following the general procedure as a white solid in 68% yield (250 mg) on a 3 mmol scale as an inseparable 5:1 mixture of E/Z isomers from **1a-II** and **S11**.  $R_f = 0.5$  (EtOAc/Hexane=1/5). M.P. = 53-54 °C **<sup>1</sup>H NMR (400 MHz, CDCl<sub>3</sub>)**:  $\delta$  (major) 7.44 (ddd,  $J = 8.4, 7.1, 3.9$  Hz, 0.84H), 7.07 – 7.01 (m, 0.84H), 6.86 (m, 0.84H), 4.90 (s, 1.71H), 3.93 (d,  $J = 0.9$  Hz, 1.71H), 3.89 (s, 2.5H), 1.95 (s, 2.5H).  $\delta$  (minor) 7.45 (ddd,  $J = 8.4, 7.1, 3.9$  Hz, 0.20H), 7.09 – 7.05 (m, 0.20H), 6.84 (m, 0.2H), 5.21 (m, 0.32H), 3.93 (d,  $J = 0.9$  Hz, 0.32H), 3.89 (s, 0.47H), 1.97 (s, 0.47H). **<sup>13</sup>C NMR (100 MHz, CDCl<sub>3</sub>)**:  $\delta$  184.73, 184.52, 154.56, 152.68, 151.84, 150.53, 137.74, 137.72, 132.45, 116.14, 115.59, 73.31, 67.48, 61.80, 61.73, 51.39, 51.28, 16.51, 12.22. **IR**:  $\nu$  2963, 2937, 1763, 1602, 1576, 1474, 1289, 1267, 1159, 1129, 1051, 899, 784 cm<sup>-1</sup>; **HRMS** calcd. for [M+Na]<sup>+</sup>: 242.0788. Found: 242.0789.



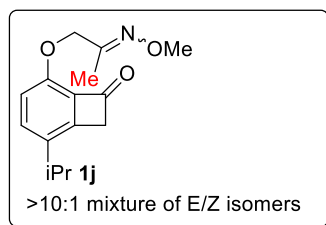
**1g** was isolated as a colorless oil in 70% yield (98 mg) on a 1 mmol scale from **1g-II** and **S11**.  $R_f = 0.6$  (EtOAc/Hexane=1/5). **<sup>1</sup>H NMR (400 MHz, CDCl<sub>3</sub>)**:  $\delta$  6.94 (s, 1H), 6.74 (s, 1H), 4.89 (s, 2H), 3.89 (s, 3H), 3.87 (s, 2H), 2.91 (hept,  $J = 6.9$  Hz, 1H), 1.95 (s, 3H), 1.25 (d,  $J = 6.9$  Hz, 6H). **<sup>13</sup>C NMR (100 MHz, CDCl<sub>3</sub>)**:  $\delta$  184.19, 160.91, 152.77, 151.94, 150.47, 130.27, 114.28, 114.11, 73.34, 61.70, 50.68, 35.09, 23.63, 12.24. **IR**:  $\nu$  2962, 1780, 1609, 1571, 1448, 1329, 1223, 1142, 1057, 899, 842, 668 cm<sup>-1</sup>; **HRMS** calcd. for [M+Na]<sup>+</sup>: 284.12570. Found: 284.12550.



**1h** was isolated as a colorless oil in 54% yield (78 mg) on a 1 mmol scale from **1h-II** and **S11**.  $R_f$  = 0.5 (EtOAc/Hexane=1/5).  **$^1\text{H}$  NMR (400 MHz,  $\text{CDCl}_3$ )**:  $\delta$  7.68 (s, 1H), 7.58 (s, 1H), 4.91 (s, 2H), 3.97 (s, 2H), 3.94 (s, 3H), 3.89 (s, 3H), 1.95 (s, 3H), 1.55 (s, 3H).  **$^{13}\text{C}$  NMR (100 MHz,  $\text{CDCl}_3$ )**:  $\delta$  184.12, 165.88, 152.28, 151.54, 150.53, 138.62, 135.72, 118.17, 116.19, 73.63, 61.77, 52.63, 51.12, 22.99, 12.16. **IR**:  $\nu$  2955, 1769, 1726, 1611, 1572, 1436, 1371, 1293, 1278, 1228, 1137, 1059, 900, 872, 774, 668, 601, 455  $\text{cm}^{-1}$ ; **HRMS** calcd. for  $[\text{M}+\text{Na}]^+$ : 300.08420. Found: 300.08440.

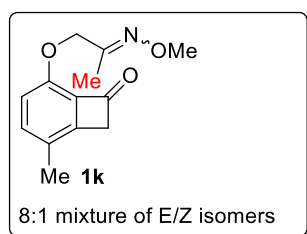


**1i** was isolated as white solid in 72% yield (167.5 mg) on a 2 mmol scale as an inseparable 6:1 mixture of E/Z isomers from **1i-II** and **S11**.  $R_f$  = 0.6 (EtOAc/Hexane=1/5). M.P.= 96-98 °C  **$^1\text{H}$  NMR (400 MHz,  $\text{CDCl}_3$ )**:  $\delta$  (major) 6.88 (s, 1H), 6.68 (s, 1H), 4.88 (s, 2H), 3.89 (s, 3H), 3.86 (s, 3H), 2.38 (s, 3H), 1.94 (s, 3H).  **$^{13}\text{C}$  NMR (100 MHz,  $\text{CDCl}_3$ )**:  $\delta$  184.10, 152.78, 151.76, 150.44, 149.77, 129.94, 116.66, 73.28, 61.70, 50.69, 22.49, 12.18. **IR**:  $\nu$  2980, 2944, 1770, 1753, 1613, 1569, 1466, 1444, 1353, 1276, 1130, 1065, 911, 847, 600  $\text{cm}^{-1}$ ; **HRMS** calcd. for  $[\text{M}+\text{Na}]^+$ : 256.09440. Found: 256.09450.

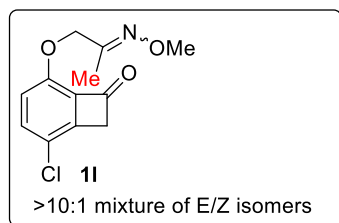


**1j** was isolated as a colorless oil in 87% yield (150 mg) on a 1 mmol scale as an inseparable >10:1 mixture of E/Z isomers from **1j-II** and **S11**.  $R_f$  = 0.5 (EtOAc/Hexane=1/5).  **$^1\text{H}$  NMR (400 MHz,**

**CDCl<sub>3</sub>**:  $\delta$  (major) 7.28 – 7.26 (m, 1H), 6.81 (dt,  $J = 8.5, 0.8$  Hz, 1H), 4.88 (s, 2H), 3.93 (d,  $J = 0.9$  Hz, 2H), 3.89 (s, 3H), 2.95 (hept,  $J = 6.9$  Hz, 1H), 1.94 (s, 3H), 1.26 (s, 3H), 1.25 (s, 3H). **<sup>13</sup>C** **NMR (100 MHz, CDCl<sub>3</sub>)**:  $\delta$  184.93, 152.92, 149.82, 147.17, 136.01, 132.47, 116.71, 77.19, 73.20, 61.72, 50.86, 31.13, 23.08, 12.21. **IR**:  $\nu$  2962, 2936, 1763, 1621, 1569, 1492, 1458, 1420, 1290, 1213, 1143, 1048, 899, 840, 668, 606, 456 cm<sup>-1</sup>; **HRMS** calcd. for [M+Na]<sup>+</sup>: 284.12570. Found: 284.12590.

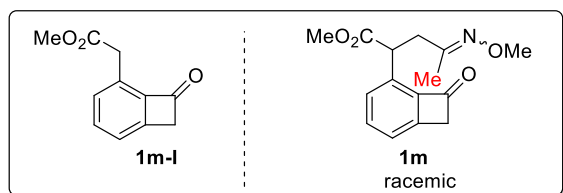


**1k** was isolated as a white solid in 83% yield (242.4 mg) on a 2 mmol scale as an inseparable 8:1 mixture of E/Z isomers from **1k-II** and **S11**.  $R_f = 0.5$  (EtOAc/Hexane=1/5). M.P. = 77-79 °C **<sup>1</sup>H** **NMR (400 MHz, CDCl<sub>3</sub>)**:  $\delta$  (major) 7.22 (dd,  $J = 8.4, 0.7$  Hz, 1H), 6.78 (dd,  $J = 8.4, 1.0$  Hz, 1H), 4.86 (s, 2H), 3.88 (s, 3H), 3.84 (s, 2H), 2.26 (s, 3H), 1.93 (s, 3H). **<sup>13</sup>C** **NMR (100 MHz, CDCl<sub>3</sub>)**:  $\delta$  184.46, 184.27, 154.83, 152.86, 149.88, 149.70, 148.85, 148.65, 138.72, 131.82, 131.70, 129.43, 125.45, 125.29, 116.77, 116.39, 110.66, 73.60, 73.15, 72.57, 69.44, 67.36, 61.77, 61.69, 61.66, 50.16, 50.06, 17.86, 16.47, 16.46, 12.19, 11.80. **IR**:  $\nu$  2937, 1764, 1621, 1576, 1492, 1268, 1063, 900, 838, 749, 436 cm<sup>-1</sup>; **HRMS** calcd. for [M+H]<sup>+</sup>: 234.1130. Found: 234.1127.



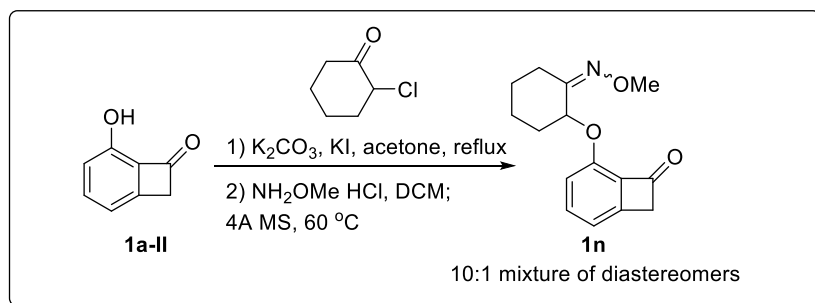
**1l** was isolated as white solid in 83% yield (130.4 mg) on a 1 mmol scale from **1l-II** and **S11**.  $R_f$  = 0.6 (EtOAc/Hexane=1/5).  **$^1\text{H}$  NMR (400 MHz,  $\text{CDCl}_3$ )**:  $\delta$  7.36 (d,  $J$  = 8.9 Hz, 1H), 6.84 (d,  $J$  = 8.8 Hz, 1H), 4.87 (s, 2H), 3.96 (d,  $J$  = 0.8 Hz, 2H), 3.89 (s, 3H), 1.94 (s, 3H).  **$^{13}\text{C}$  NMR (100 MHz,  $\text{CDCl}_3$ )**:  $\delta$  152.31, 150.71, 147.27, 137.55, 120.29, 118.81, 77.20, 73.69, 61.81, 50.76, 12.23. **IR**:  $\nu$  2937, 1781, 1759, 1570, 1472, 1449, 1411, 1369, 1287, 1266, 1051, 965, 901, 668  $\text{cm}^{-1}$ ; **HRMS** calcd. for  $[\text{M}+\text{Na}]^+$ : 276.03980. Found: 276.04000.

### Synthesis of **1m**

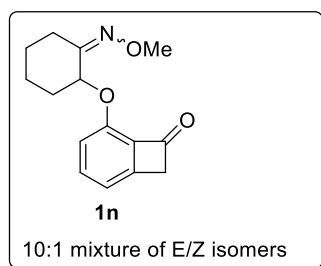


**1m-I** was synthesized according to the reported procedure and matched the reported data<sup>8a</sup>. Following the general procedure, **1m** was isolated as a colorless oil in 66% yield as a racemic mixture from **1m-I** and **S11**.  $R_f$  = 0.3 (EtOAc/Hexane=1/5).  **$^1\text{H}$  NMR (400 MHz,  $\text{CDCl}_3$ )**:  $\delta$  7.45 (t,  $J$  = 7.4 Hz, 1H), 7.42 – 7.39 (m, 1H), 7.34 – 7.31 (m, 1H), 4.21 (dd,  $J$  = 8.6, 6.6 Hz, 1H), 3.95 (t,  $J$  = 0.8 Hz, 2H), 3.73 (s, 3H), 3.66 (s, 3H), 3.14 (ddd,  $J$  = 16.2, 8.6, 0.6 Hz, 1H), 2.73 (ddd,  $J$  = 16.2, 6.6, 0.5 Hz, 1H), 1.79 (s, 3H).  **$^{13}\text{C}$  NMR (100 MHz,  $\text{CDCl}_3$ )**:  $\delta$  187.47, 172.47, 153.95, 151.25, 146.13, 135.30, 134.19, 128.34, 122.46, 61.27, 52.24, 52.06, 45.25, 37.91, 14.68. **IR**:  $\nu$  2952, 1750, 1739, 1581, 1437, 1162, 1051, 952, 893, 853, 783, 550, 436  $\text{cm}^{-1}$ ; **HRMS** calcd. for  $[\text{M}+\text{Na}]^+$ : 298.10500. Found: 298.10520.

### 2.4.6 Synthesis of substrates **1n**



**1n** was synthesized using the procedure shown above. Using the general procedure for substitution as before, the ketone substrate was obtained. Then it was used without further purification to condense with  $\text{NH}_2\text{OMe} \cdot \text{HCl}$  using the general procedure for **route I**.

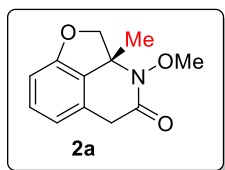


**1n** was isolated as a colorless oil in 50% yield as an inseparable 10:1 mixture of E/Z isomers for two steps.  $R_f = 0.5$  (EtOAc/Hexane=1/5).  **$^1\text{H}$  NMR (400 MHz,  $\text{CDCl}_3$ ):**  $\delta$  (major) 7.43 (dd,  $J = 8.5, 7.1$  Hz, 1H), 7.01 (d,  $J = 6.8$  Hz, 1H), 6.87 (d,  $J = 8.4$  Hz, 1H), 5.35 (d,  $J = 5.5$  Hz, 1H), 3.89 (d,  $J = 2.6$  Hz, 2H), 3.79 (s, 3H), 2.83 – 2.70 (m, 1H), 2.54 – 1.59 (m, 7H).  **$^{13}\text{C}$  NMR (100 MHz,  $\text{CDCl}_3$ ):**  $\delta$  184.71, 156.89, 151.03, 150.41, 137.61, 132.57, 116.55, 115.06, 78.38, 61.51, 51.09, 32.33, 25.18, 22.74, 21.05. **IR:**  $\nu$  2937, 1762, 1601, 1570, 1469, 1269, 1127, 1046, 962, 870, 782, 668  $\text{cm}^{-1}$ ; **HRMS** calcd. for  $[\text{M}+\text{Na}]^+$ : 282.11010. Found: 282.11040.

#### 2.4.7 General procedure for C–C activation reactions

(reaction was usually performed at 0.1mmol scale at 0.05 M concentration)

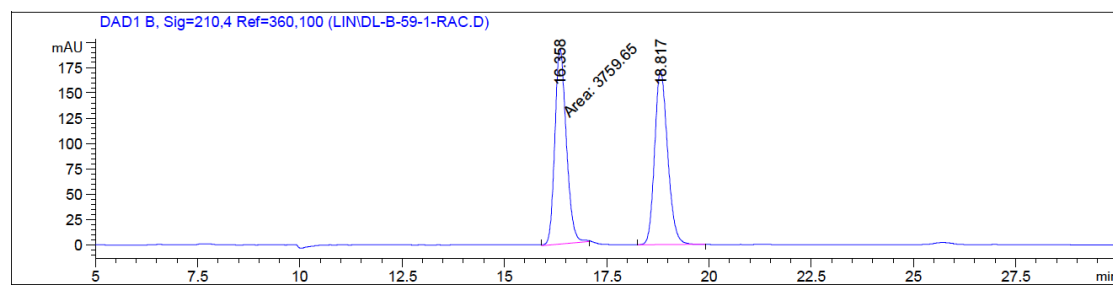
In a nitrogen filled glove box, a 8 mL vial was charged with the benzocyclobutenone substrates (**1a** to **1n**, 0.1 mmol), Rh(COD)<sub>2</sub>BF<sub>4</sub> (5 mol%, 0.005 mmol, 2.1 mg) or [Rh(CH<sub>3</sub>CN)<sub>2</sub>(COD)]BF<sub>4</sub> (5 mol%, 0.005 mmol, 1.9 mg) and ligand (6 mol%, 0.006 mmol). After adding 2 mL 1,4-dioxane, the vial was capped and the solution was maintained at certain temperature for 24h before another portion of same catalyst was added. After the reaction was maintained at the same temperature for another 24h, it was cooled to room temperature and purified by silica gel flash chromatography.



**2a** (15.8 mg) was isolated as a colorless oil in 72% yield. Rh(COD)<sub>2</sub>BF<sub>4</sub> (10 mol%, 0.01 mmol, 4.1 mg) (*R*)-xyl-SDP (6 mol %, 0.006 mmol, 4.2 mg), (*S*)-xyl-BINAP (6 mol%, 0.006 mmol, 4.4 mg) were used and the reaction was maintained at 110 °C. *R<sub>f</sub>* = 0.6 (EtOAc/Hexane=1/1). **<sup>1</sup>H NMR (400 MHz, CDCl<sub>3</sub>):** δ 7.19 (t, *J* = 7.7 Hz, 1H), 6.78 – 6.68 (m, 2H), 4.60 (dd, *J* = 8.4, 0.9 Hz, 1H), 4.54 (d, *J* = 8.4 Hz, 1H), 3.90-3.85 (td, *J* = 20.5, 1.3 Hz, 1H), 3.87 (s, 3H), 3.69 (d, *J* = 20.6 Hz, 1H), 1.63 (d, *J* = 0.9 Hz, 3H). **<sup>13</sup>C NMR (100 MHz, CDCl<sub>3</sub>):** δ 170.69, 157.55, 130.64, 128.77, 128.74, 118.68, 108.75, 83.32, 66.57, 64.34, 37.04, 22.65. **IR:** ν 2972, 2933, 1691, 1639, 1612, 1473, 1279, 1047, 935, 771, 668, 633 cm<sup>-1</sup>; **HRMS** calcd. for [M+Na]<sup>+</sup>: 242.0788. Found: 242.0789.

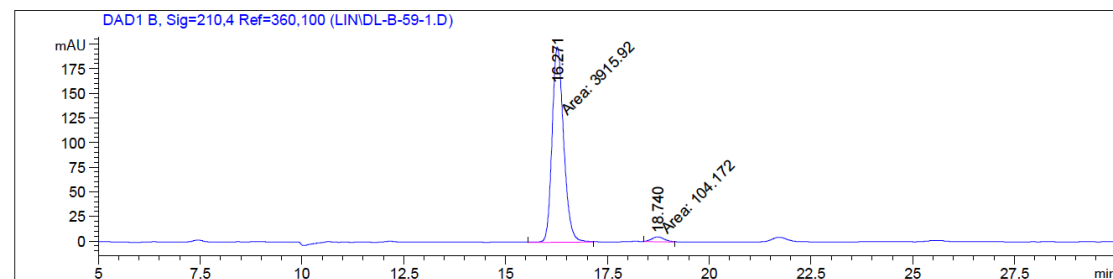
Chiral HPLC (Chiralpak IA, hexane:isopropanol = 97:3, 1 mL/min, 210 nm), *t*<sub>minor</sub> = 18.740 min, *t*<sub>major</sub> = 16.271 min. [α]<sub>D</sub><sup>20</sup> = -53 (c=0.75, CH<sub>2</sub>Cl<sub>2</sub>) at 95 % e.e.

### **Racemic Sample 2a**

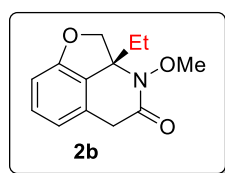


Peak #	RetTime [min]	Type	Width [min]	Area [mAU*s]	Height [mAU]	Area %
1	16.358	MM	0.3248	3759.64697	192.91611	49.7686
2	18.817	BB	0.3399	3794.61060	171.68166	50.2314

### Enantiomeric Sample 2a



Peak #	RetTime [min]	Type	Width [min]	Area [mAU*s]	Height [mAU]	Area %
1	16.271	MM	0.3287	3915.92285	198.56981	97.4087
2	18.740	MM	0.3535	104.17199	4.91210	2.5913



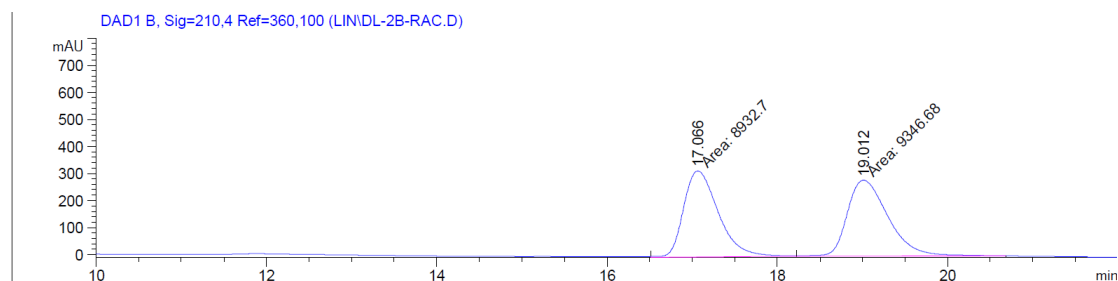
**2b** (15.2 mg) was isolated as light yellow oil in 65% yield.  $\text{Rh}(\text{COD})_2\text{BF}_4$  (10 mol%, 0.01 mmol, 4.1 mg) (*R*)-xyl-SDP (6 mol %, 0.006 mmol, 4.2 mg), (*S*)-xyl-BINAP (6 mol%, 0.006 mmol, 4.4



mg) were used and the reaction was maintained at 130 °C.  $R_f$  = 0.6 (EtOAc/Hexane=1/1).  **$^1\text{H}$  NMR (400 MHz,  $\text{CDCl}_3$ )**:  $\delta$  7.18 (t,  $J$  = 7.8 Hz, 1H), 6.72 (d,  $J$  = 8.0 Hz, 2H), 4.62 – 4.52 (m, 2H), 3.92 (dt,  $J$  = 20.7, 1.1 Hz, 1H), 3.84 (s, 3H), 3.64 (d,  $J$  = 20.8 Hz, 1H), 2.10 (d,  $J$  = 7.5 Hz, 2H), 0.86 (t,  $J$  = 7.5 Hz, 3H).  **$^{13}\text{C}$  NMR (100 MHz,  $\text{CDCl}_3$ )**:  $\delta$  170.39, 158.31, 130.65, 129.85, 126.74, 118.63, 108.65, 82.57, 70.28, 64.20, 37.56, 30.24, 8.09. **IR**:  $\nu$  2970, 2937, 2883, 1688, 1635, 1812, 1471, 1279, 1057, 943, 773  $\text{cm}^{-1}$ ; **HRMS** calcd. for  $[\text{M}+\text{Na}]^+$ : 256.0944. Found: 256.0947.

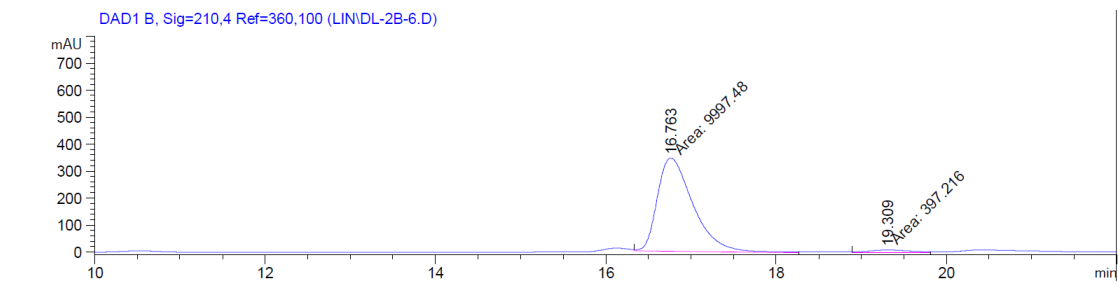
Chiral HPLC (Chiralpak IA, hexane:isopropanol = 98:2, 1 mL/min, 210 nm):  $t_{\text{minor}}$  = 19.309 min,  $t_{\text{major}}$  = 16.763 min.  $[\alpha]_D^{20}$  = -43 ( $c$  = 0.63,  $\text{CH}_2\text{Cl}_2$ ) at 92% e.e..

### **Racemic Sample 2b**

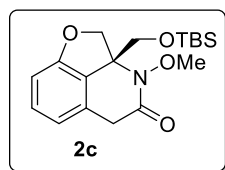


Peak #	RetTime [min]	Type	Width [min]	Area [mAU*s]	Height [mAU]	Area %
1	17.066	MM	0.4705	8932.69531	316.40082	48.8676
2	19.012	MM	0.5553	9346.68262	280.52795	51.1324

### **Enantiomeric Sample 2b**



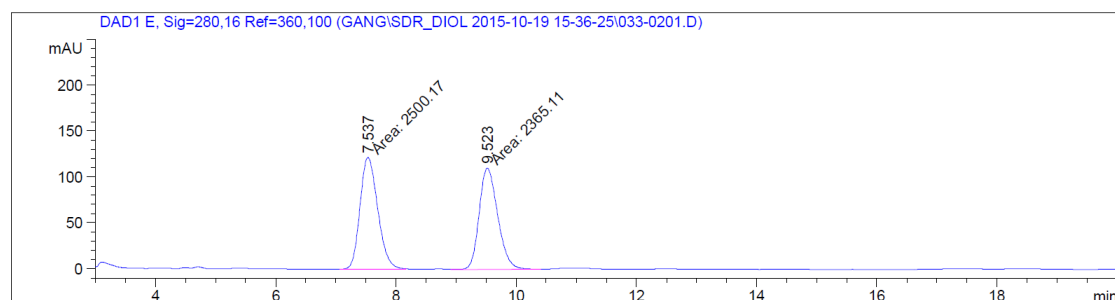
Peak #	RetTime [min]	Type	Width [min]	Area [mAU*s]	Height [mAU]	Area %
1	16.763	MM	0.4836	9997.48438	344.55362	96.1787
2	19.309	MM	0.6114	397.21585	10.82889	3.8213



**2c** (21.7 mg) was isolated as a colorless oil in 62% yield. Rh(COD)<sub>2</sub>BF<sub>4</sub> (10 mol%, 0.01 mmol, 4.1 mg) (*R*)-xyl-SDP (6 mol %, 0.006 mmol, 4.2 mg), (*S*)-xyl-BINAP (6 mol%, 0.006 mmol, 4.4 mg) were used and the reaction was maintained at 130 °C. *R<sub>f</sub>*=0.7 (EtOAc/Hexane=1/1). **<sup>1</sup>H NMR (400 MHz, CDCl<sub>3</sub>):** δ 7.19 (dd, *J* = 7.4, 3.1 Hz, 1H), 6.72 (d, *J* = 8.1 Hz, 2H), 4.58 (d, *J* = 8.9 Hz, 1H), 4.40 (d, *J* = 9.0 Hz, 1H), 4.21 (d, *J* = 10.1 Hz, 1H), 4.02 (d, *J* = 20.4 Hz, 1H), 3.84 (s, 2H), 3.78 (d, *J* = 10.1 Hz, 1H), 3.56 (d, *J* = 20.4 Hz, 1H), 0.79 (s, 9H), -0.06 (d, *J* = 1.0 Hz, 6H). **<sup>13</sup>C NMR (100 MHz, CDCl<sub>3</sub>):** δ 171.95, 158.03, 131.55, 130.63, 125.68, 118.51, 109.99, 108.28, 79.09, 71.25, 64.48, 64.14, 38.18, 25.75, 18.40, -5.76. **IR:** ν 2955, 2930, 2857, 1762, 1698, 1612, 1471, 1361, 1254, 1124, 1093, 1058, 948, 840, 777, 662 cm<sup>-1</sup>; **HRMS** calcd. for [M+Na]<sup>+</sup>: 372.16020. Found: 372.16040.

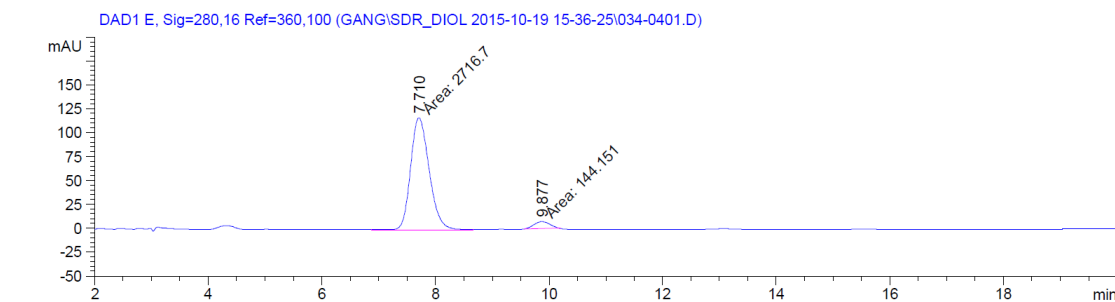
Chiral HPLC (Chiralpak IA, hexane:isopropanol = 98:2, 1 mL/min, 280 nm): *t*<sub>minor</sub>=9.877 min, *t*<sub>major</sub>=7.710 min. [α]<sub>D</sub><sup>20</sup> = -40 (c=0.82, CH<sub>2</sub>Cl<sub>2</sub>) at 90% e.e.

### **Racemic Sample 2c**

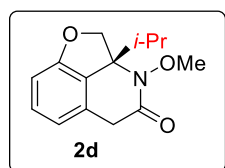


Peak #	RetTime [min]	Type	Width [min]	Area [mAU*s]	Height [mAU]	Area %
1	7.537	MF	0.3421	2500.16699	121.80779	51.3880
2	9.523	MM	0.3576	2365.10986	110.23833	48.6120

### Enantiomeric Sample 2c



Peak #	RetTime [min]	Type	Width [min]	Area [mAU*s]	Height [mAU]	Area %
1	7.710	MM	0.3845	2716.70483	117.76103	94.9613
2	9.877	MM	0.3244	144.15134	7.40620	5.0387

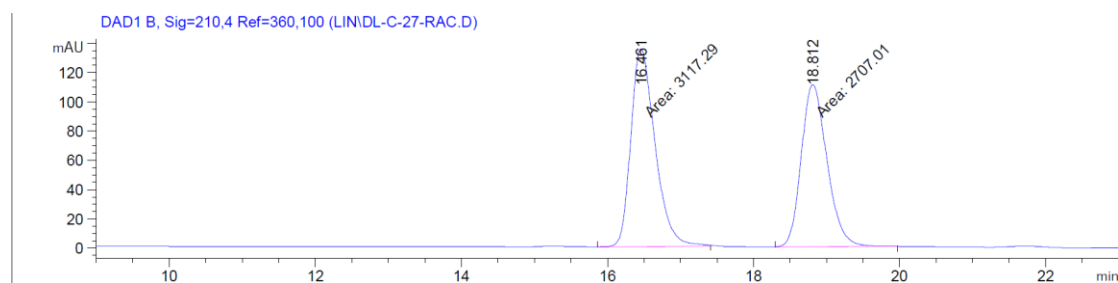


**2d** (12.4 mg) was isolated as a colorless oil in 50% yield. Rh(COD)<sub>2</sub>BF<sub>4</sub> (10 mol%, 0.01 mmol, 4.1 mg) (*R*)-xyl-SDP (6 mol %, 0.006 mmol, 4.2 mg), (*S*)-xyl-BINAP (6 mol%, 0.006 mmol, 4.4

mg) were used and the reaction was maintained at 130 °C.  $R_f = 0.5$  (EtOAc/Hexane=1/1).  **$^1\text{H}$  NMR (400 MHz,  $\text{CDCl}_3$ ):**  $\delta$  7.20 (t,  $J = 7.8$  Hz, 1H), 6.72 (dd,  $J = 8.1, 4.6$  Hz, 2H), 4.73 (d,  $J = 8.8$  Hz, 1H), 4.62 (d,  $J = 8.8$  Hz, 1H), 3.96 (dt,  $J = 20.7, 1.2$  Hz, 1H), 3.85 (s, 3H), 3.61 (d,  $J = 20.8$  Hz, 1H), 2.50 (hept,  $J = 6.9$  Hz, 1H), 1.02 (d,  $J = 6.9$  Hz, 3H), 0.91 (d,  $J = 6.8$  Hz, 3H).  **$^{13}\text{C}$  NMR (100 MHz,  $\text{CDCl}_3$ ):**  $\delta$  169.75, 158.94, 130.72, 130.49, 125.40, 118.74, 108.36, 81.04, 73.15, 64.25, 38.11, 36.81, 17.61, 16.87. **IR:**  $\nu$  2970, 2936, 1687, 1470, 1279, 1116, 1057, 943, 773, 667  $\text{cm}^{-1}$ . **HRMS** calcd. for  $[\text{M}+\text{Na}]^+$ : 270.11010. Found: 270.11020.

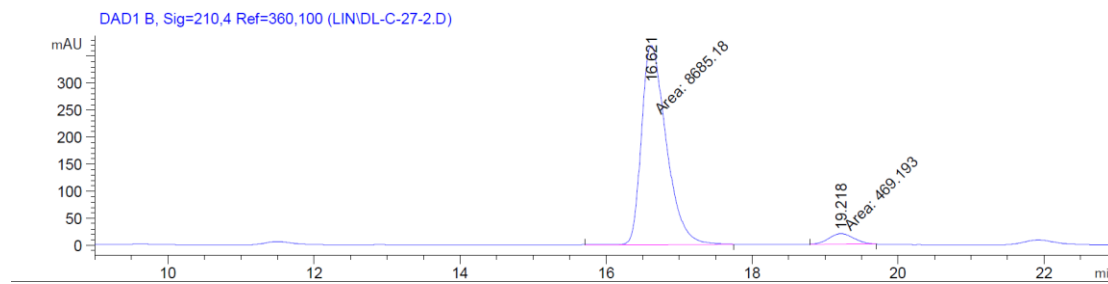
Chiral HPLC (Chiralpak IA, hexane:isopropanol = 98:2, 1 mL/min, 210 nm):  $t_{\text{minor}} = 19.218$  min,  $t_{\text{major}} = 16.621$  min.  $[\alpha]_D^{20} = -11$  ( $c = 0.88$ ,  $\text{CH}_2\text{Cl}_2$ ) at 90% e.e.

### Racemic Sample 2d

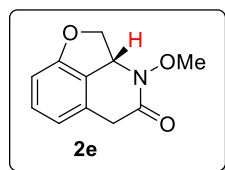


Peak #	RetTime [min]	Type	Width [min]	Area [mAU*s]	Height [mAU]	Area %
1	16.461	MM	0.3840	3117.28613	135.29062	53.5221
2	18.812	MM	0.4075	2707.00903	110.72683	46.4779

### Enantiomeric Sample 2d



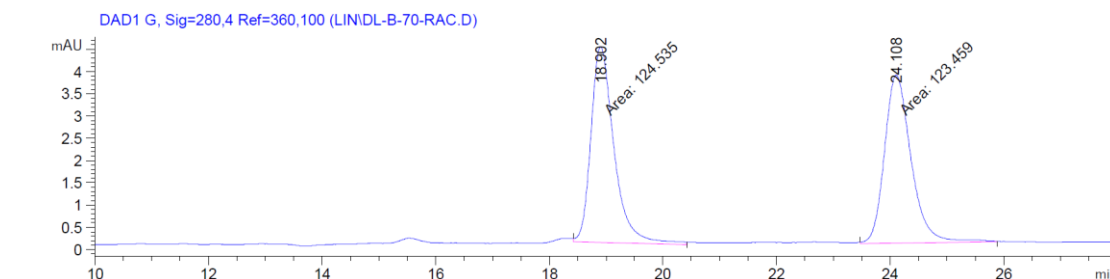
Peak #	RetTime [min]	Type	Width [min]	Area [mAU*s]	Height [mAU]	Area %
1	16.621	MM	0.3928	8685.17773	368.51218	94.8747
2	19.218	MM	0.3981	469.19284	19.64262	5.1253



**2e** (7.6 mg) was isolated as light yellow oil in 37% yield.  $\text{Rh}(\text{COD})_2\text{BF}_4$  (10 mol%, 0.01 mmol, 4.1 mg) (*R*)-xyl-SDP (12 mol %, 0.012 mmol, 8.2 mg) were used and the reaction was maintained at 110 °C.  $R_f$  = 0.3 (EtOAc/Hexane=1/1).  **$^1\text{H}$  NMR (400 MHz,  $\text{CDCl}_3$ ):**  $\delta$  7.20 (t,  $J$  = 7.9 Hz, 1H), 6.73 (d,  $J$  = 7.5 Hz, 2H), 5.50 – 5.40 (m, 1H), 4.95 (dd,  $J$  = 8.8, 7.4 Hz, 1H), 4.49 (dd,  $J$  = 10.0, 8.8 Hz, 1H), 3.90 (dd,  $J$  = 20.5, 1.6 Hz, 1H), 3.87 (s, 3H), 3.70 (dd,  $J$  = 20.5, 1.6 Hz, 1H).  **$^{13}\text{C}$  NMR (100 MHz,  $\text{CDCl}_3$ ):**  $\delta$  170.96, 158.51, 130.95, 129.87, 123.14, 118.47, 108.56, 77.97, 63.71, 59.69, 37.86. **IR:**  $\nu$  2927, 2854, 1691, 1640, 1612, 1471, 1266, 1072, 1041, 938, 770  $\text{cm}^{-1}$ ; **HRMS** calcd. for  $[\text{M}+\text{Na}]^+$ : 228.0631. Found: 228.0631.

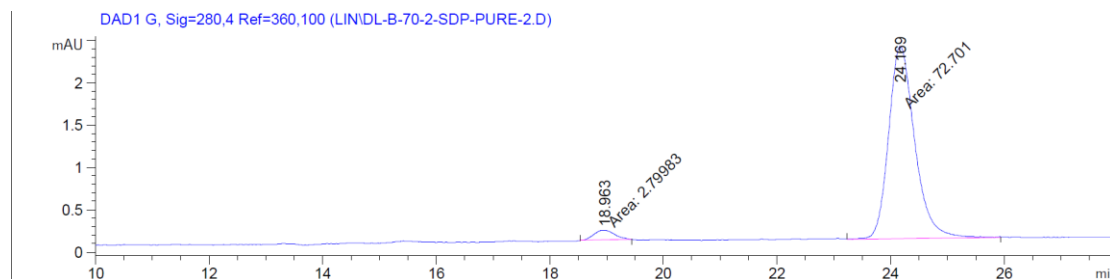
Chiral HPLC (Chiralpak IB, hexane:isopropanol = 92:8, 1 mL/min, 210 nm):  $t_{\text{minor}}$  = 18.963 min,  $t_{\text{major}}$  = 24.169 min.  $[\alpha]_D^{20}$  = -6 ( $c$  = 0.48,  $\text{CH}_2\text{Cl}_2$ ) at 92% e.e..

### Racemic Sample 2e

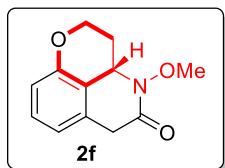


Peak #	RetTime [min]	Type	Width [min]	Area [mAU*s]	Height [mAU]	Area %
1	18.902	MM	0.4723	124.53470	4.39498	50.2168
2	24.108	MM	0.5450	123.45930	3.77538	49.7832

### Enantiomeric Sample 2e



Peak #	RetTime [min]	Type	Width [min]	Area [mAU*s]	Height [mAU]	Area %
1	18.963	MM	0.4140	2.79983	1.12716e-1	3.7083
2	24.169	MM	0.5333	72.70095	2.27205	96.2917



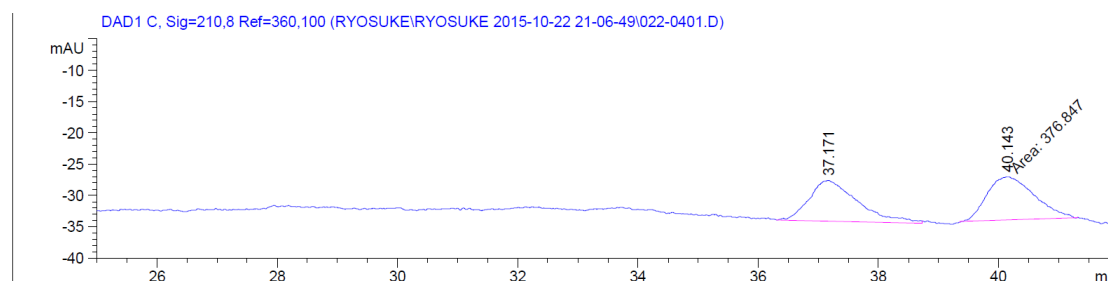
**2f** (8.8 mg) was isolated as yellow oil in 40% yield. Rh(COD)<sub>2</sub>BF<sub>4</sub> (10 mol%, 0.01 mmol, 4.1 mg)

(*R*)-xyl-SDP (6 mol %, 0.006 mmol, 4.2 mg), (*S*)-xyl-BINAP (6 mol%, 0.006 mmol, 4.4 mg) were

used and the reaction was maintained at 110 °C.  $R_f = 0.5$  (EtOAc/Hexane=1/1).  **$^1\text{H}$  NMR (400 MHz,  $\text{CDCl}_3$ ):**  $\delta$  7.17 (t,  $J = 7.9$  Hz, 1H), 6.74 (d,  $J = 8.3$  Hz, 1H), 6.69 (d,  $J = 7.5$  Hz, 1H), 4.83 (dd,  $J = 11.5, 5.3$  Hz, 1H), 4.52 (ddd,  $J = 11.6, 4.0, 2.5$  Hz, 1H), 4.20 (ddd,  $J = 13.4, 11.7, 1.9$  Hz, 1H), 3.89 (s, 3H), 3.78 – 3.63 (m, 2H), 2.65 – 2.59 (m, 1H), 2.20 – 2.07 (m, 1H).  **$^{13}\text{C}$  NMR (100 MHz,  $\text{CDCl}_3$ ):**  $\delta$  168.76, 152.76, 131.58, 129.63, 118.66, 116.75, 114.62, 77.30, 76.98, 76.66, 64.25, 64.06, 54.05, 38.12, 29.67, 26.49. **IR:**  $\nu$  2926, 2654, 1688, 1596, 1475, 1462, 1263, 1082, 1052, 778  $\text{cm}^{-1}$ ; **HRMS** calcd. for  $[\text{M}+\text{Na}]^+$ : 242.07880. Found: 242.07870.

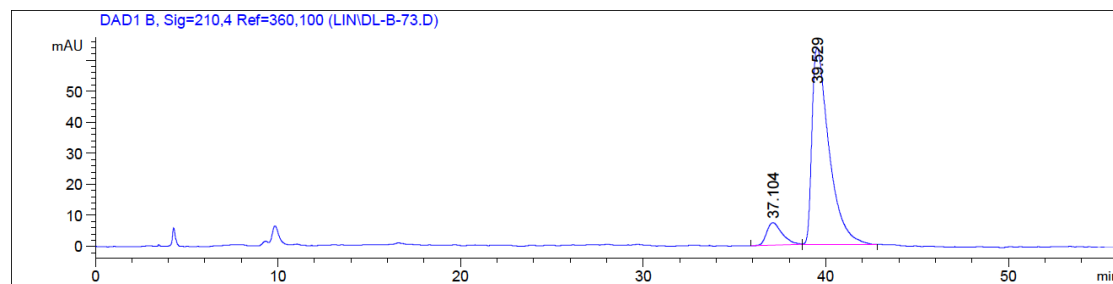
Chiral HPLC (Chiralpak IB, hexane:isopropanol = 95:5, 1 mL/min, 210 nm):  $t_{\text{minor}} = 37.104$  min,  $t_{\text{major}} = 39.529$  min.  $[\alpha]_{\text{D}}^{20} = -15$  ( $c = 0.78$ ,  $\text{CH}_2\text{Cl}_2$ ) at 81% e.e.

### Racemic Sample 2f

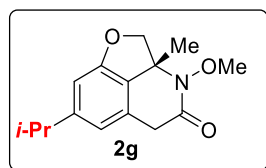


Peak #	RetTime [min]	Type	Width [min]	Area [mAU*s]	Height [mAU]	Area %
1	37.171	BB	0.6614	361.47104	6.49435	48.9587
2	40.143	MM	0.9032	376.84689	6.95430	51.0413

### Enantiomeric Sample 2f



Peak #	RetTime [min]	Type	Width [min]	Area [mAU*s]	Height [mAU]	Area %
1	37.104	BB	0.8485	423.66238	7.19950	9.3731
2	39.529	BB	0.9368	4096.33301	63.48286	90.6269

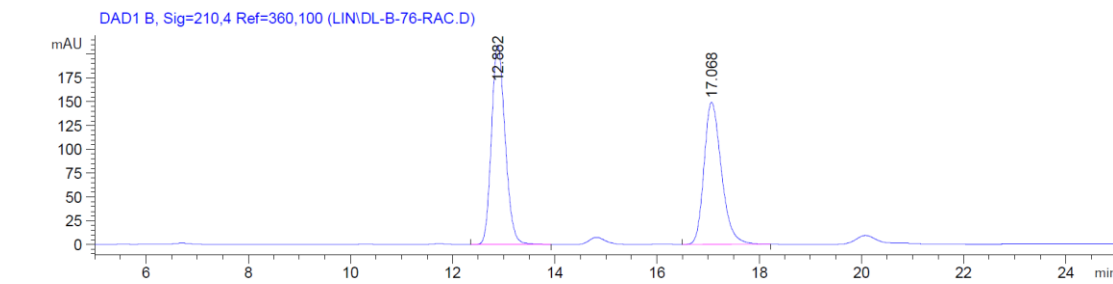


**2g** (13.8 mg) was isolated as a colorless oil in 53% yield. Rh(COD)<sub>2</sub>BF<sub>4</sub> (10 mol%, 0.01 mmol, 4.1 mg) (*R*)-xyl-SDP (6 mol %, 0.006 mmol, 4.2 mg), (*S*)-xyl-BINAP (6 mol%, 0.006 mmol, 4.4 mg) were used and the reaction was maintained at 130 °C. *R<sub>f</sub>*=0.6 (EtOAc/Hexane=1/1). **<sup>1</sup>H NMR (400 MHz, CDCl<sub>3</sub>):** δ 6.62 (s, 1H), 6.60 (s, 1H), 4.59 (dd, *J* = 8.4, 0.8 Hz, 1H), 4.52 (d, *J* = 8.4 Hz, 1H), 3.85 (s, 3H), 3.85 (td, 1H), 3.65 (d, *J* = 20.6 Hz, 1H), 2.87 (hept, *J* = 6.9 Hz, 1H), 1.62 (d, *J* = 0.8 Hz, 3H), 1.23 (d, *J* = 6.9 Hz, 6H). **<sup>13</sup>C NMR (100 MHz, CDCl<sub>3</sub>):** δ 170.93, 157.88, 152.89, 128.31, 126.37, 116.77, 106.89, 83.61, 77.19, 66.44, 64.27, 37.18, 34.70, 24.14, 22.74. **IR:** ν 2960, 1700, 1638, 1490, 1436, 1302, 1282, 1067, 1040, 969, 953, 847, 668, 651, 635 cm<sup>-1</sup>; **HRMS** calcd. for [M+Na]<sup>+</sup>: 284.12570. Found: 284.12620.

Chiral HPLC (Chiralpak IA, hexane:isopropanol = 97:3, 1 mL/min, 210 nm): *t*<sub>minor</sub>=16.687 min, *t*<sub>major</sub>=12.655 min. [α]<sub>D</sub><sup>20</sup> = -28 (c=1.53, CH<sub>2</sub>Cl<sub>2</sub>) at 90% ee..

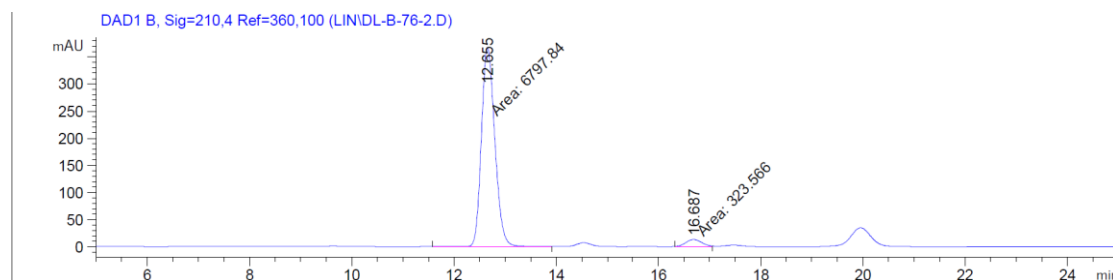


## Racemic Sample 2g

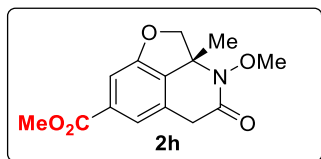


Peak #	RetTime [min]	Type	Width [min]	Area [mAU*s]	Height [mAU]	Area %
1	12.882	BB	0.2889	3893.11011	209.39294	52.3654
2	17.068	BB	0.3647	3541.40527	149.33739	47.6346

## Enantiomeric Sample 2g



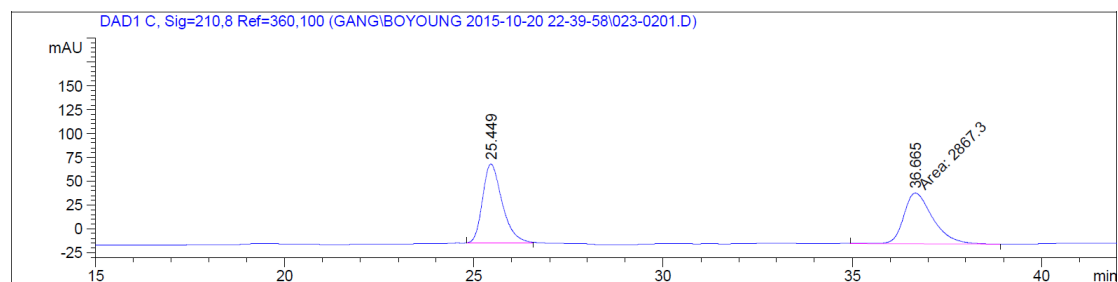
Peak #	RetTime [min]	Type	Width [min]	Area [mAU*s]	Height [mAU]	Area %
1	12.655	MM	0.3078	6797.84375	368.13293	95.4564
2	16.687	MM	0.3856	323.56555	13.98700	4.5436



**2h** (18.8 mg) was isolated as yellow oil in 68% yield. Rh(COD)<sub>2</sub>BF<sub>4</sub> (10 mol%, 0.01 mmol, 4.1 mg) (*R*)-xyl-SDP (6 mol %, 0.006 mmol, 4.2 mg), (*S*)-xyl-BINAP (6 mol%, 0.006 mmol, 4.4 mg) were used and the reaction was maintained at 110 °C. *R<sub>f</sub>* = 0.7 (EtOAc/Hexane=1/1). **<sup>1</sup>H NMR (400 MHz, CDCl<sub>3</sub>):** δ 7.49 (s, 1H), 7.39 (t, *J* = 0.9 Hz, 1H), 4.64 (dd, *J* = 8.5, 0.7 Hz, 1H), 4.59 (d, *J* = 8.5 Hz, 1H), 3.90 (s, 3H), 3.87 (s, 4H), 3.73 (d, *J* = 20.7 Hz, 1H), 1.64 (d, *J* = 1.8 Hz, 3H). **<sup>13</sup>C NMR (100 MHz, CDCl<sub>3</sub>):** δ 170.13, 166.36, 157.58, 133.50, 133.15, 128.59, 120.92, 110.02, 83.66, 66.37, 64.43, 52.39, 36.78, 22.49. **IR:** ν 2951, 2362, 1720, 1693, 1433, 1364, 1289, 1243, 1215, 1075, 1049, 989, 838, 770, 644 cm<sup>-1</sup> **HRMS** calcd. for [M+Na]<sup>+</sup>: 300.08420. Found: 300.08480.

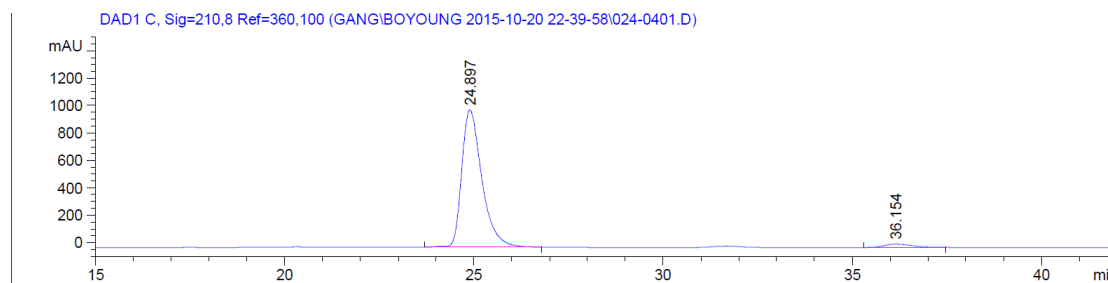
Chiral HPLC (Chiralpak IA, hexane:isopropanol = 95:5, 1 mL/min, 210 nm): *t*<sub>minor</sub> = 36.154 min, *t*<sub>major</sub> = 24.897 min. [α]<sub>D</sub><sup>20</sup> = -23 (c=1.49, CH<sub>2</sub>Cl<sub>2</sub>) at 94% e.e.

### Racemic Sample 2h

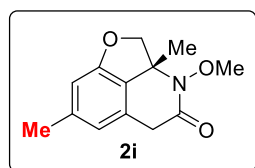


Peak #	RetTime [min]	Type	Width [min]	Area [mAU*s]	Height [mAU]	Area %
1	25.449	BB	0.5494	2970.20825	82.62710	50.8815
2	36.665	MM	0.8960	2867.29541	53.33685	49.1185

### Enantiomeric Sample 2h



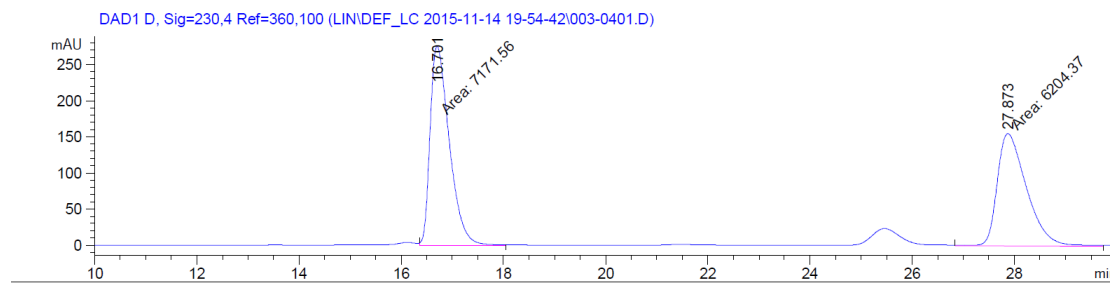
Peak #	RetTime [min]	Type	Width [min]	Area [mAU*s]	Height [mAU]	Area %
1	24.897	BB	0.5672	3.71310e4	1000.04425	96.7187
2	36.154	BB	0.7647	1259.72632	24.54700	3.2813



**2i** (17.2 mg) was isolated as a colorless oil in 74% yield. Rh(COD)<sub>2</sub>BF<sub>4</sub> (10 mol%, 0.01 mmol, 4.1 mg) (*R*)-xyl-SDP (6 mol %, 0.006 mmol, 4.2 mg), (*S*)-xyl-BINAP (6 mol%, 0.006 mmol, 4.4 mg) were used and the reaction was maintained at 110 °C. *R<sub>f</sub>* = 0.6 (EtOAc/Hexane=1/1). **<sup>1</sup>H NMR (400 MHz, CDCl<sub>3</sub>):** δ 6.56 (s, 2H), 4.58 (dd, *J* = 8.4, 0.8 Hz, 1H), 4.52 (d, *J* = 8.4 Hz, 1H), 3.85 (s, 3H), 3.84 (d, *J* = 20.5 Hz, 1H), 3.63 (d, *J* = 20.6 Hz, 1H), 2.33 (s, 3H), 1.61 (d, *J* = 0.7 Hz, 3H). **<sup>13</sup>C NMR (100 MHz, CDCl<sub>3</sub>):** δ 170.87, 157.86, 141.38, 128.33, 126.09, 119.23, 109.44, 83.60, 66.41, 64.30, 37.04, 22.76, 21.93. **IR:** ν 2928, 1689, 1637, 1497, 1449, 1289, 1087, 1063, 1048, 972, 954, 923, 833, 654, 634 cm<sup>-1</sup>; **HRMS** calcd. for [M+Na]<sup>+</sup>: 256.09440. Found: 256.09480.

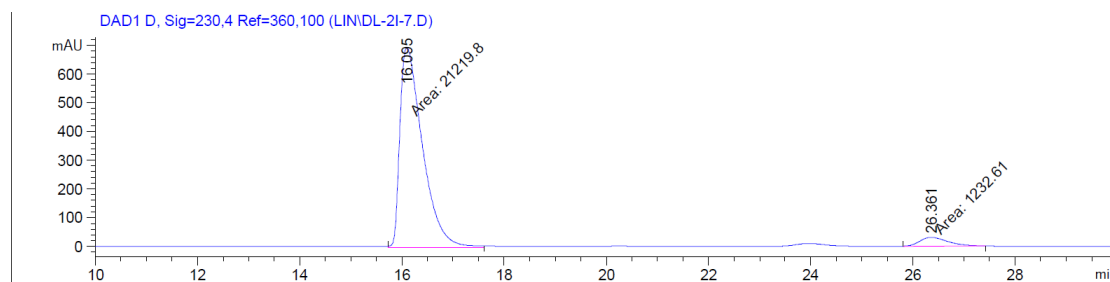
Chiral HPLC (Chiralpak IA, hexane:isopropanol = 98:2, 1 mL/min, 230 nm): *t*<sub>minor</sub> = 26.361 min, *t*<sub>major</sub> = 16.095 min. [α]<sub>D</sub><sup>20</sup> = -33 (c=1.50, CH<sub>2</sub>Cl<sub>2</sub>) at 89% ee.

### Racemic Sample 2i

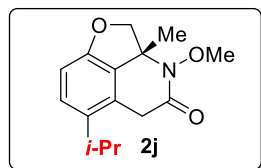


Peak #	RetTime [min]	Type	Width [min]	Area [mAU*s]	Height [mAU]	Area %
1	16.701	FM	0.4343	7171.55713	275.19339	53.6154
2	27.873	MM	0.6656	6204.37305	155.36742	46.3846

### Enantiomeric Sample 2i



Peak #	RetTime [min]	Type	Width [min]	Area [mAU*s]	Height [mAU]	Area %
1	16.095	MM	0.5090	2.12198e4	694.79749	94.5101
2	26.361	MM	0.6548	1232.60718	31.37551	5.4899

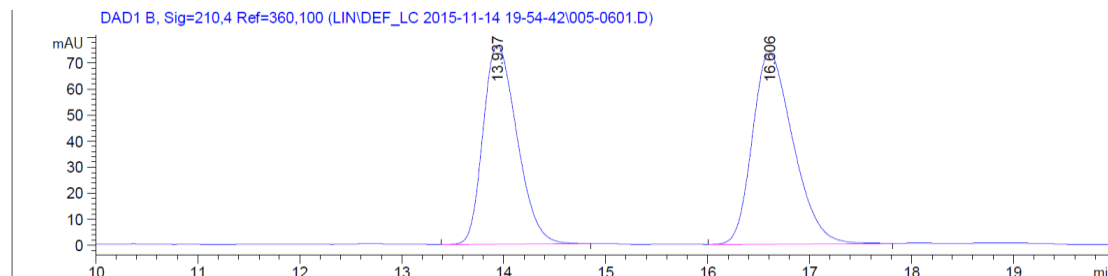


**2j** (13.0 mg) was isolated as yellow oil in 50% yield. Rh(COD)<sub>2</sub>BF<sub>4</sub> (10 mol%, 0.01 mmol, 4.1 mg) (*R*)-xyl-SDP (6 mol %, 0.006 mmol, 4.2 mg), (*S*)-xyl-BINAP (6 mol%, 0.006 mmol, 4.4 mg)

were used and the reaction was maintained at 110 °C.  $R_f = 0.6$  (EtOAc/Hexane=1/1).  **$^1\text{H}$  NMR (400 MHz,  $\text{CDCl}_3$ ):**  $\delta$  7.11 (d,  $J = 8.3$  Hz, 1H), 6.72 (d,  $J = 9.1$  Hz, 1H), 4.59 (dd,  $J = 8.3, 0.8$  Hz, 1H), 4.51 (d,  $J = 8.3$  Hz, 1H), 3.87 (s, 3H), 3.83 – 3.67 (m, 2H), 2.91 (hept,  $J = 6.9$  Hz, 1H), 1.61 (d,  $J = 2.2$  Hz, 3H), 1.21 (dd,  $J = 6.9, 3.0$  Hz, 6H).  **$^{13}\text{C}$  NMR (100 MHz,  $\text{CDCl}_3$ ):**  $\delta$  170.91, 155.32, 138.15, 128.57, 126.75, 125.76, 108.95, 83.13, 66.63, 64.30, 35.10, 28.73, 23.57, 23.23, 22.69. **IR:** 2961, 2928, 2360, 2342, 1691, 1487, 1459, 1277, 1154, 1067, 1037, 955, 935, 814, 668  $\text{v cm}^{-1}$ . **HRMS** calcd. for  $[\text{M}+\text{Na}]^+$ : 284.12570. Found: 284.12600.

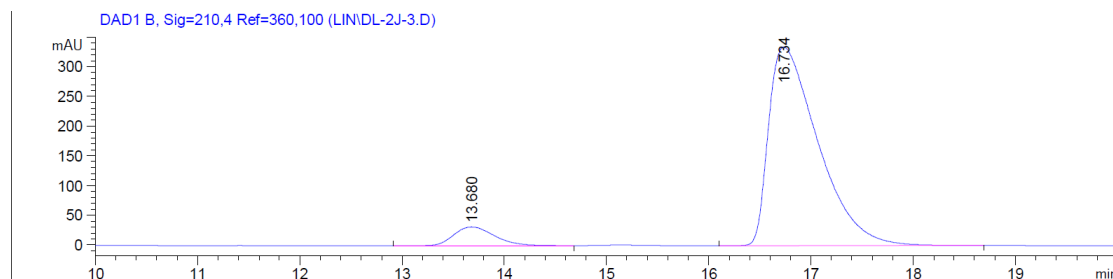
Chiral HPLC (Chiralpak IA, hexane:isopropanol = 98:2, 1 mL/min, 210 nm):  $t_{\text{minor}} = 13.680$  min,  $t_{\text{major}} = 16.734$  min.  $[\alpha]_D^{20} = -45$  ( $c = 0.88$ ,  $\text{CH}_2\text{Cl}_2$ ) at 86% e.e..

### **Racemic Sample 2j**

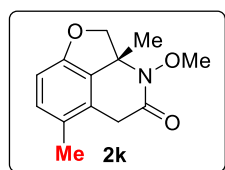


Peak #	RetTime [min]	Type	Width [min]	Area [mAU*s]	Height [mAU]	Area %
1	13.937	BB	0.3630	1762.46692	76.43552	46.3320
2	16.606	BB	0.4284	2041.52405	73.41205	53.6680

### **Enantiomeric Sample 2j**



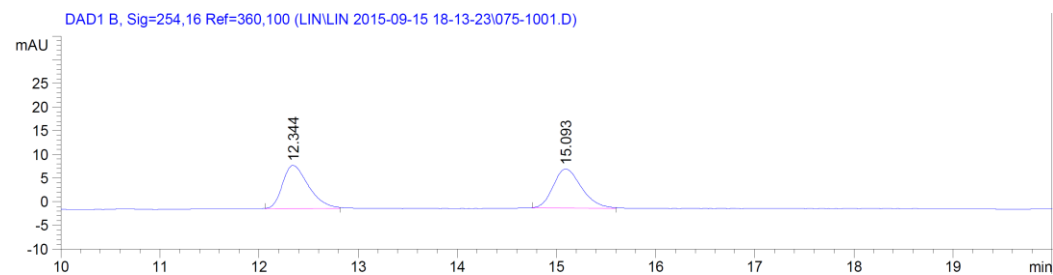
Peak #	RetTime [min]	Type	Width [min]	Area [mAU*s]	Height [mAU]	Area %
1	13.680	BB	0.4344	881.44708	31.70377	7.2612
2	16.734	BB	0.5146	1.12576e4	334.51941	92.7388



**2k** (15.6 mg) was isolated as a colorless oil in 67% yield. Rh(COD)<sub>2</sub>BF<sub>4</sub> (10 mol%, 0.01 mmol, 4.1 mg) (*R*)-xyl-SDP (6 mol %, 0.006 mmol, 4.2 mg), (*S*)-xyl-BINAP (6 mol%, 0.006 mmol, 4.4 mg) were used and the reaction was maintained at 130 °C. *R<sub>f</sub>* = 0.4 (EtOAc/Hexane=1/1). **<sup>1</sup>H NMR (400 MHz, CDCl<sub>3</sub>):** δ 7.00 (dd, *J* = 8.1, 0.8 Hz, 1H), 6.65 (d, *J* = 8.1 Hz, 1H), 4.57 (dd, *J* = 8.3, 0.9 Hz, 1H), 4.51 (d, *J* = 8.3 Hz, 1H), 3.86 (s, 3H), 3.71 (s, 2H), 2.18 (d, *J* = 0.7 Hz, 3H), 1.61 (d, *J* = 0.9 Hz, 3H). **<sup>13</sup>C NMR (100 MHz, CDCl<sub>3</sub>):** δ <sup>13</sup>C NMR (101 MHz, cdcl<sub>3</sub>) δ 170.85, 155.54, 131.11, 128.70, 127.20, 126.92, 108.65, 83.23, 66.59, 64.27, 35.42, 22.71, 17.09. **IR:** ν 2982, 2963, 2940, 1682, 1488, 1274, 1194, 1037, 936, 817, 659, 638 cm<sup>-1</sup>; **HRMS** calcd. for [M+H]<sup>+</sup>: 233.1052. Found: 233.1049.

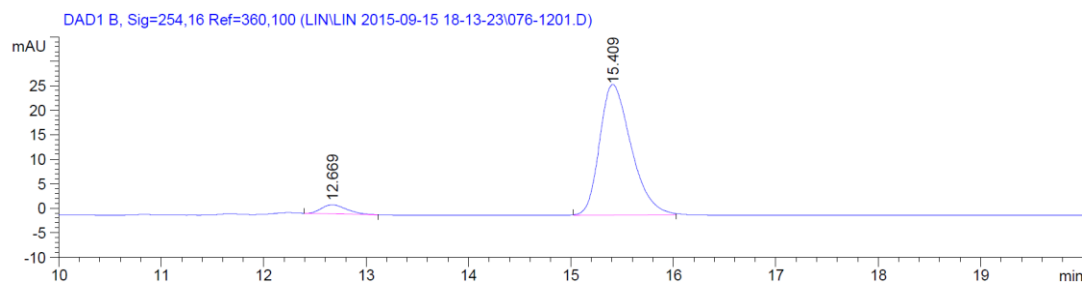
Chiral HPLC (Chiralpak IA, hexane:isopropanol = 97:3, 1 mL/min, 254 nm), *t*<sub>minor</sub> = 12.669 min, *t*<sub>major</sub> = 15.409 min. [α]<sub>D</sub><sup>20</sup> = -25 (c=1.22, CH<sub>2</sub>Cl<sub>2</sub>) at 90 % ee.

### Racemic Sample 2k

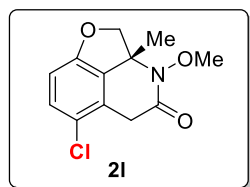


Peak #	RetTime [min]	Type	Width [min]	Area [mAU*s]	Height [mAU]	Area %
1	12.344	BB	0.2754	165.13733	9.11349	50.1464
2	15.093	BB	0.3043	164.17308	8.24353	49.8536

### Enantiomeric Sample 2k



Peak #	RetTime [min]	Type	Width [min]	Area [mAU*s]	Height [mAU]	Area %
1	12.669	BB	0.2658	31.48661	1.83901	5.2409
2	15.409	BB	0.3273	569.30206	26.64713	94.7591

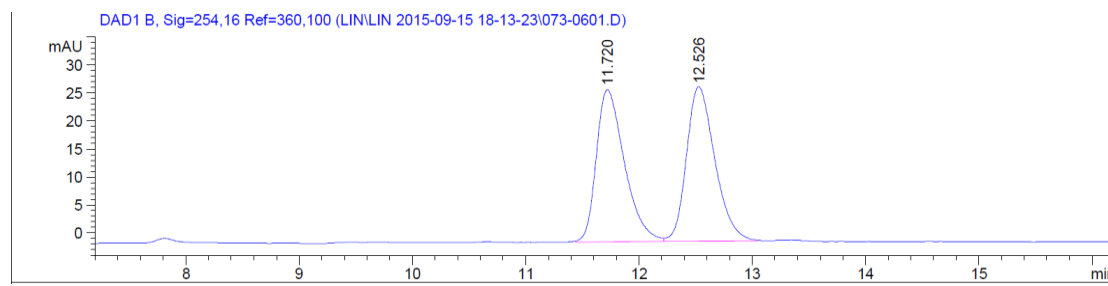


**2l** (18.2 mg) was isolated as yellow solid in 72% yield. Rh(COD)<sub>2</sub>BF<sub>4</sub> (10 mol%, 0.01 mmol, 4.1 mg) (*R*)-xyl-SDP (6 mol %, 0.006 mmol, 4.2 mg), (*S*)-xyl-BINAP (6 mol%, 0.006 mmol, 4.4 mg) were used and the reaction was maintained at 130 °C. R<sub>f</sub> = 0.4 (EtOAc/Hexane=1/1). <sup>1</sup>H NMR

(400 MHz, CDCl<sub>3</sub>):  $\delta$  7.18 (d, J = 8.5 Hz, 1H), 6.71 – 6.68 (m, 1H), 4.61 (dd, J = 8.4, 0.8 Hz, 1H), 4.55 (d, J = 8.4 Hz, 1H), 3.87 (d, J = 21.2 Hz, 1H), 3.86 (s, 3H), 3.71 (dd, J = 21.2, 0.9 Hz, 1H), 1.62 (d, J = 0.8 Hz, 3H). <sup>13</sup>C NMR (100 MHz, CDCl<sub>3</sub>):  $\delta$  169.98, 156.07, 130.35, 126.77, 123.17, 110.31, 83.76, 66.61, 64.36, 35.23, 29.68, 22.76. IR:  $\nu$  2924, 1684, 1472, 1457, 1274, 1100, 1042, 943, 817 cm<sup>-1</sup>; HRMS calcd. for [M+Na]<sup>+</sup>: 276.03980. Found: 276.04000.

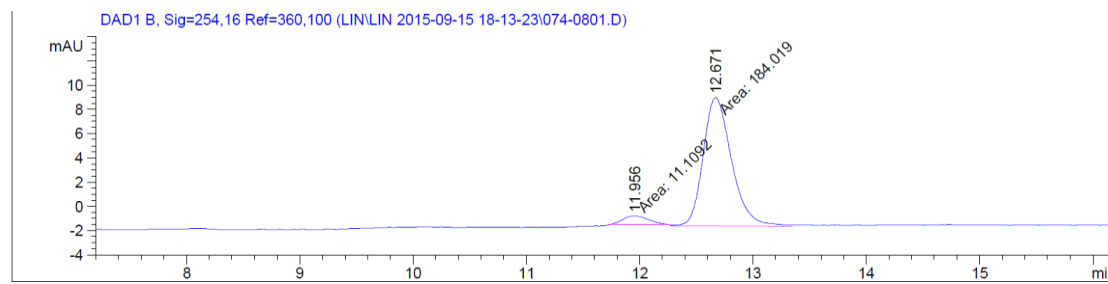
Chiral HPLC (Chiralpak IA, hexane:isopropanol = 95:5, 1 mL/min, 210 nm),  $t_{\text{minor}}$  = 10.463 min,  $t_{\text{major}}$  = 10.926 min.  $[\alpha]_{\text{D}}^{20}$  = -18 (c=1.69, CH<sub>2</sub>Cl<sub>2</sub>) at 89 % ee.

### Racemic Sample 2l



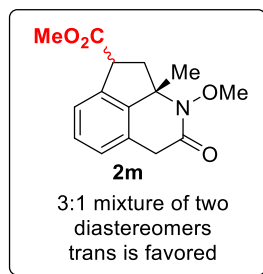
Peak #	RetTime [min]	Type	Width [min]	Area [mAU*s]	Height [mAU]	Area %
1	11.720	BV	0.2647	467.11456	27.15729	49.3527
2	12.526	VB	0.2670	479.36838	27.55320	50.6473

### Enantiomeric Sample 2l

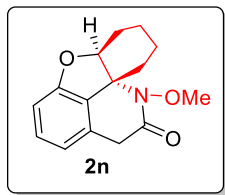




Peak #	RetTime [min]	Type	Width [min]	Area [mAU*s]	Height [mAU]	Area %
1	11.956	MM	0.2596	11.10922	7.13351e-1	5.6933
2	12.671	MM	0.2899	184.01852	10.57862	94.3067



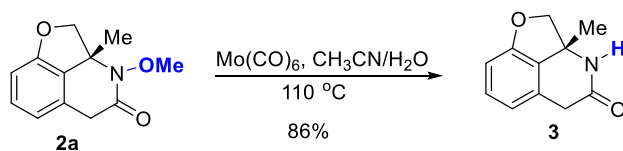
**2m** (19.2 mg) was isolated as a colorless oil in 70% yield. d.r. = 3:1. Rh(COD)<sub>2</sub>BF<sub>4</sub> (10 mol%, 0.01 mmol, 4.1 mg) (*R*)-xyl-SDP (6 mol %, 0.006 mmol, 4.2 mg), (*S*)-xyl-BINAP (6 mol%, 0.006 mmol, 4.4 mg) were used and the reaction was maintained at 110 °C. *R*<sub>f</sub> = 0.5 (EtOAc/Hexane=1/1). **<sup>1</sup>H NMR (400 MHz, CDCl<sub>3</sub>):** δ (major) 7.34 (d, *J* = 7.6 Hz, 1H), 7.32 – 7.27 (t, *J* = 7.2 Hz, 1H), 7.07 (d, *J* = 7.2 Hz, 1H), 4.13 (d, *J* = 9.5 Hz, 0.79H), 3.90 (s, 2.4H), 3.85 (d, *J* = 20.5 Hz, 0.9H), 3.66 (d, *J* = 20.5 Hz, 0.9 H), 3.76 (s, 2.4H), 2.86 (dd, *J* = 13.0, 1.0 Hz, 0.84H), 2.72 (d, *J* = 10.0 Hz, 0.9H), 1.54 (d, *J* = 0.9 Hz, 2.56H). [major and minor E/Z isomers are inseparable in aromatic region] δ (minor) 4.26 (dd, *J* = 10.8, 6.4 Hz, 0.20H), 3.94 (d, *J* = 10.2 Hz, 0.35H), 3.92 (s, 0.7H), 3.83 (s, 0.7H), 3.73 (d, *J* = 10.2 Hz, 0.35H), 2.69 – 2.61 (m, 0.50H), 1.48 (d, *J* = 0.9 Hz, 0.64H). **<sup>13</sup>C NMR (100 MHz, CDCl<sub>3</sub>):** δ 172.87, 170.20, 143.32, 136.78, 129.33, 128.07, 125.61, 124.68, 69.28, 64.43, 52.47, 48.33, 41.54, 37.16, 24.49. **IR:** ν 2925, 2852, 1735, 1686, 1436, 1325, 1261, 1199, 1174, 1061, 1032, 783, 762, 669, 623 cm<sup>-1</sup>; **HRMS** calcd. for [M+Na]<sup>+</sup>: 298.10500. Found: 298.10430. The relative stereochemistry is also determined by 2D-NMR (See Data-2D NMR).



**2n** (17.0 mg) was isolated as a colorless oil in 66% yield. d.r.  $\geq$  20:1.  $[\text{Rh}(\text{CH}_3\text{CN})_2(\text{COD})]\text{BF}_4$  (20 mol%, 0.02 mmol, 7.6 mg), (*R*)-xyl-BINAP (25 mol%, 0.025 mmol, 18.4 mg) were used and the reaction was maintained at 130 °C.  $R_f = 0.5$  (EtOAc/Hexane=1/1).  **$^1\text{H}$  NMR (400 MHz,  $\text{CDCl}_3$ ):**  $\delta$  7.16 (t,  $J = 7.8$  Hz, 1H), 6.71 (t,  $J = 8.3$  Hz, 2H), 4.85 (t,  $J = 2.7$  Hz, 1H), 3.84 (s, 4H), 3.67 (d,  $J = 20.6$  Hz, 1H), 2.45 – 1.51 (m, 8H).  **$^{13}\text{C}$  NMR (100 MHz,  $\text{CDCl}_3$ ):**  $\delta$  170.28, 156.49, 131.12, 130.08, 128.23, 118.37, 108.76, 89.04, 65.06, 64.20, 37.04, 34.34, 26.02, 20.56, 18.82, -0.03. **IR:**  $\nu$  2936, 1687, 1639, 1465, 1292, 1265, 1137, 1072, 1056, 1035, 934, 820, 776, 736, 638, 431  $\text{cm}^{-1}$ ; **HRMS.** calcd. for  $[\text{M}+\text{Na}]^+$ : 282.11010. Found: 282.11050. The relative stereochemistry is determined by both 2D-NMR and X-ray analysis (see attached data).

#### 2.4.8 Synthetic applications

a) N-O bond cleavage reaction: synthesis of **3**

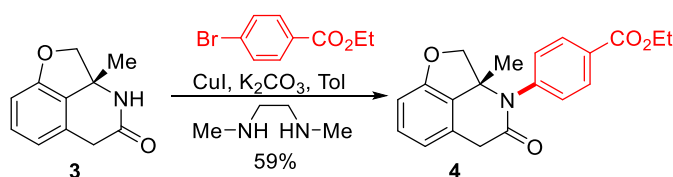


Compound **2a** (100.0 mg, 0.45 mmol, 1 equiv., 95% e.e.) was dissolved in a 20 mL vial (with stir bar) using acetonitrile (12 mL).  $\text{Mo(CO)}_6$  (133.5 mg, 0.90 mmol, 2 equiv.) and  $\text{H}_2\text{O}$  (4 mL) was added to the stirring solution. Then the reaction was sealed and heated to 110 °C and stirred overnight. When reaction was complete, the mixture was filtered with Celite pad, then concentrated under reduced pressure. The residue was purified by silica gel flash column

chromatography (EtOAc/Hexane=1/2 with 20% MeOH). Compound **3** was obtained as a white solid in 86% yield (75 mg).

Compound **3**:  $R_f = 0.2$  (EtOAc/Hexane=1/1).  $[\alpha]_D^{20} = -22$  ( $c=0.97$ ,  $\text{CH}_2\text{Cl}_2$ ).  **$^1\text{H}$  NMR (400 MHz,  $\text{CDCl}_3$ )**:  $\delta$  7.50 (s, 1H), 7.17 (t,  $J = 7.8$  Hz, 1H), 6.73 (ddt,  $J = 12.3, 8.1, 0.7$  Hz, 2H), 4.50 (d,  $J = 8.2$  Hz, 1H), 4.32 (dd,  $J = 8.2, 0.9$  Hz, 1H), 3.73 (dt,  $J = 19.4, 1.2$  Hz, 1H), 3.46 (d,  $J = 19.5$  Hz, 1H), 1.61 (d,  $J = 1.0$  Hz, 3H).  **$^{13}\text{C}$  NMR (100 MHz,  $\text{CDCl}_3$ )**:  $\delta$  173.59, 157.13, 130.28, 129.86, 128.53, 119.08, 108.62, 84.59, 59.48, 35.37, 26.80. **IR**:  $\nu$  3292, 2925, 2853, 1654, 1458, 1376, 1149, 1050, 972, 749, 648  $\text{cm}^{-1}$ ; **HRMS**. calcd. for  $[\text{M}+\text{Na}]^+$ : 212.06820. Found: 212.06830.

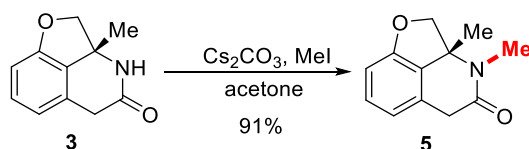
b) Cu-catalyzed C-N bond formation: synthesis of **4**



An 8 mL vial was charged with starting material compound **3** (10 mg, 0.05 mmol, 1equiv., synthesized from 95% e.e. **2a**) and another 8 mL vial was charged with aryl bromide (12.1 mg, 0.05 mmol, 1equiv.), CuI (6.1 mg, 0.03 mmol, 0.6 equiv.),  $\text{K}_2\text{CO}_3$  (175.5 mg, 1.3 mmol, 24 equiv.) and  $\text{N}_1,\text{N}_2$ -Dimethylethane-1,2-diamine (5.6 mg, 0.06 mmol, 1.2 equiv.). Both vials were transferred to a nitrogen-filled glove box. Toluene (0.5 mL) was added to the second vial and the solution was stirred for 2 mins. Using another 1 mL toluene to dissolve and transfer the compound **3** into the pre-stirred mixture of other components. The vial was sealed and took outside the glovebox. The reaction was stirred at 130  $^\circ\text{C}$  overnight. After the reaction was complete, it was concentrated and purified by silica gel flash chromatography. Compound **4** was obtained as a light yellow oil in 59% yield (10.2 mg).

Compound **4**:  $R_f = 0.6$  (EtOAc/Hexane=1/1).  $[\alpha]_D^{20} = -2$  ( $c=1.06$ ,  $\text{CH}_2\text{Cl}_2$ ).  **$^1\text{H}$  NMR (400 MHz,  $\text{CDCl}_3$ )**:  $\delta$  8.14 – 8.09 (m, 2H), 7.32 – 7.27 (m, 2H), 7.23 (d,  $J = 7.8$  Hz, 1H), 6.84 – 6.81 (m, 1H), 6.75 (dt,  $J = 8.1, 0.7$  Hz, 1H), 4.43 – 4.33 (m, 4H), 4.08 (d,  $J = 8.6$  Hz, 1H), 4.00 – 3.91 (m, 1H), 3.76 (d,  $J = 19.4$  Hz, 1H), 1.80 (d,  $J = 0.9$  Hz, 3H), 1.40 (t,  $J = 7.1$  Hz, 3H).  **$^{13}\text{C}$  NMR (100 MHz,  $\text{CDCl}_3$ )**:  $\delta$  170.84, 165.72, 156.65, 142.81, 130.90, 130.57, 130.08, 129.60, 128.79, 128.35, 118.92, 108.71, 83.25, 65.09, 61.23, 36.85, 25.61, 14.32. **IR**:  $\nu$  2924, 2853, 1717, 1669, 1605, 1508, 1472, 1458, 1305, 1276, 1174, 1101, 1020, 958, 936, 768, 742, 713, 580  $\text{cm}^{-1}$ ; **HRMS**. calcd. for  $[\text{M}+\text{Na}]^+$ : 360.12060. Found: 360.12040.

c) Substitution reaction: synthesis of **5**

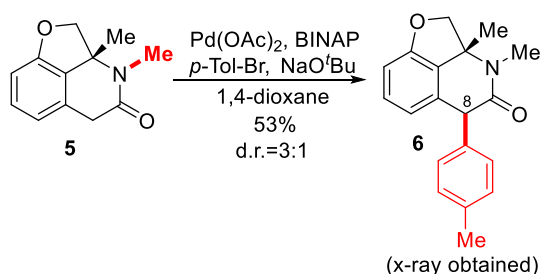


Compound **3** (15.0 mg, 0.08 mmol, 1 equiv., synthesized from 95% e.e. **2a**) was dissolved in a 20 mL vial (with stir bar) using acetone (10 mL).  $\text{Cs}_2\text{CO}_3$  (172.2 mg, 0.53 mmol, 7 equiv.) and MeI (67.5 mg, 29.6  $\mu\text{L}$ , 0.048 mmol, 6 equiv.) were added to the stirring solution. The reaction was then sealed and heated to 40  $^\circ\text{C}$  with stirring for 36 h. Upon completion, the reaction mixture was transferred to a separation funnel and 10 mL of  $\text{NH}_4\text{Cl}$  (sat.) solution was added to quench the reaction. The mixture was further extracted with ethyl acetate (EA) (3 $\times$ 10 mL) and washed by brine twice. The organic phase was then dried using  $\text{Na}_2\text{SO}_4$  and concentrated under reduced pressure. The residue was purified by silica gel flash column chromatography (EtOAc/Hexane=1/10) to obtain the compound **5** as a colorless oil in 91% yield (14.6 mg).

Compound **5**:  $R_f = 0.5$  (EtOAc/Hexane=1/1).  $[\alpha]_D^{20} = -12$  ( $c=1.46$ ,  $\text{CH}_2\text{Cl}_2$ ).  **$^1\text{H}$  NMR (400 MHz,  $\text{CDCl}_3$ )**:  $\delta$  7.17 (t,  $J = 7.8$  Hz, 1H), 6.74 (dd,  $J = 7.6, 0.6$  Hz, 1H), 6.71 (d,  $J = 8.0$  Hz, 1H), 4.45 (d,  $J = 8.0$  Hz, 1H), 4.41 (dd,  $J = 8.1, 0.8$  Hz, 1H), 3.71 (d,  $J = 19.4$  Hz, 1H), 3.58 (d,  $J = 19.4$  Hz,

1H), 2.92 (s, 3H), 1.54 (d,  $J = 0.8$  Hz, 3H).  **$^{13}\text{C}$  NMR (100 MHz,  $\text{CDCl}_3$ ):**  $\delta$  170.60, 156.94, 130.26, 130.12, 128.42, 118.79, 108.43, 83.36, 63.57, 36.01, 29.01, 22.76. **IR:**  $\nu$  3205, 2964, 2923, 1655, 1473, 1356, 1305, 1242, 1164, 1026, 934, 751, 447  $\text{cm}^{-1}$ ; **HRMS.** calcd. for  $[\text{M}+\text{Na}]^+$ : 226.08380. Found: 226.08380.

d)  $\alpha$ -arylation of **5**: synthesis of **6**

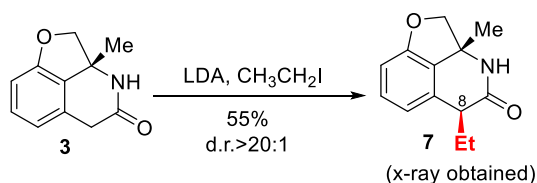


An 8 mL vial was charged with Compound **5** (10 mg, 0.044 mmol, 1 equiv.) and another 8 mL vial was charged with aryl bromide (11.3 mg, 0.066 mmol, 1.5equiv.),  $\text{Pd}(\text{OAc})_2$  (1.2 mg, 0.0044 mmol, 0.1 equiv.),  $\text{NaOtBu}$  (12.7 mg, 0.132 mmol, 3 equiv.) and BINAP (2.7 mg, 0.0044 mmol, 0.1 equiv.). Both vials were transferred to a nitrogen filled glove box. 0.5 mL 1,4-dioxane was added to the second vial and the solution was stirred for 2 mins. Using 1 mL of 1,4-dioxane to dissolve and transfer the compound **5** into the pre-stirred mixture of other components. The vial was sealed and took outside the glovebox. The reaction was stirred at 90  $^{\circ}\text{C}$  overnight. After the reaction was complete, it was concentrated and purified by silica gel flash chromatography. Compound **6** was obtained as a colorless oil in 53% yield as an inseparable 3:1 mixture of diastereomers (6.6 mg). The structure was also confirmed by X-Ray analysis. In the crystal we obtained, 17% of the hydrogen atom at carbon 8 was oxidized to OH.

Compound **6** (a 3:1 mixture of diastereomers):  $R_f = 0.6$  (EtOAc/Hexane=1/1).  **$^1\text{H}$  NMR (400 MHz,  $\text{CDCl}_3$ ):**  $\delta$  (major) 7.54 (d,  $J = 0.7$  Hz, 1H), 7.47 – 7.44 (m, 2H), 7.09 (td,  $J = 7.9, 5.3$  Hz, 1H),

6.89 (dd,  $J = 8.6, 0.7$  Hz, 2H), 6.70 (ddd,  $J = 8.0, 3.4, 0.7$  Hz, 1H), 5.27 (s, 1H), 3.55 (dd,  $J = 12.8, 7.7$  Hz, 1H), 3.45 – 3.38 (m, 1H), 2.35 (s, 3H), 1.99 (s, 3H), 0.70 (d,  $J = 1.0$  Hz, 3H).  **$^{13}\text{C}$  NMR (100 MHz,  $\text{CDCl}_3$ )**:  $\delta$  (major) 173.84, 157.13, 139.75, 138.32, 135.54, 130.72, 129.29, 127.86, 126.89, 118.18, 109.58, 84.19, 75.49, 62.95, 51.13, 29.70, 23.83, 21.25, 21.05. **IR**:  $\nu$  3240, 2924, 1659, 1467, 1241, 1166, 954, 933, 788, 751, 450  $\text{cm}^{-1}$ ; **HRMS**. calcd. for  $[\text{M}+\text{H}]^+$ : 294.1494. Found: 294.1486.

e)  $\alpha$ -alkylation of **3**: synthesis of **7**



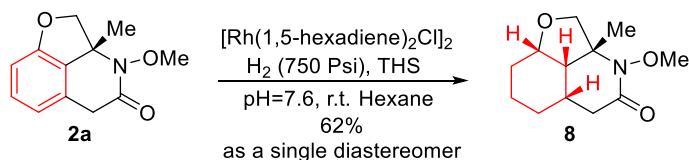
To a 10 mL flamed-dried Schlenk flask equipped with a stir bar and a nitrogen-filled balloon was added THF (2.3 mL) and freshly distilled  $i\text{-Pr}_2\text{NH}$  (506.0 mg, 0.7 mL, 5.0 mmol, 1 equiv.). The system was cooled to  $-78^\circ\text{C}$  with an acetone-dry ice bath before  $n\text{-BuLi}$  (2.5 M in hexane, 2.0 mL, 5 mmol, 1 equiv.) was added dropwise. Upon completion, the system was warmed to  $0^\circ\text{C}$  and stirred for 0.5 h under nitrogen atmosphere. Meanwhile, to another 10 mL flamed-dried flask equipped with a stir bar and a nitrogen-filled balloon were added compound **3** (9.5 mg, 0.05 mmol, 1 equiv., synthesized from 95% e.e. **2a**) and THF (5 mL). After cooled to  $-78^\circ\text{C}$  with an acetone-dry ice bath, the newly made LDA solution as indicated above (1 M in THF/Hexane, 1.0 mL, 1.00 mmol, 20 equiv.) was added dropwise and the reaction was warmed up to  $-20^\circ\text{C}$  for 0.5 h. After that, the reaction was cooled to  $-78^\circ\text{C}$  again and  $\text{EtI}$  (389.9 mg, 0.2 mL, 2.5 mmol, 50 equiv.) was added dropwisely. The reaction was gradually warmed up to R.T. for 4h and was quenched by adding  $\text{NH}_4\text{Cl}$  (sat.) 5 mL. The mixture was extracted with ethyl acetate (10 mL $\times$ 3), washed with brine, and dried with  $\text{Na}_2\text{SO}_4$ . The combined organic extract was concentrated under reduced

pressure and purified by silica gel flash column chromatography (EtOAc/Hexane=1/10) on silica gel to afford compound **7** as a colorless oil in 55% yield (6.0 mg). The relative stereochemistry was determined by X-ray analysis (see in **X-Ray data**). The sample used for X-Ray analysis was synthesized from compound **3** with 40% e.e.

Compound **7**:  $R_f = 0.5$  (EtOAc/Hexane=1/1).  $[\alpha]_D^{20} = 8$  (c=0.50, CH<sub>2</sub>Cl<sub>2</sub>). **<sup>1</sup>H NMR (400 MHz, CDCl<sub>3</sub>)**:  $\delta$  7.18 (d,  $J = 7.6$  Hz, 1H), 6.73 (dd,  $J = 7.8, 2.8$  Hz, 2H), 6.61 (d,  $J = 53.6$  Hz, 1H), 4.44 (d,  $J = 7.8$  Hz, 1H), 4.25 (dd,  $J = 7.8, 1.0$  Hz, 1H), 3.32 (m, 1H), 2.21 (dq,  $J = 12.9, 7.5, 5.4$  Hz, 1H), 1.81 (ddq,  $J = 13.2, 10.0, 7.3$  Hz, 1H), 1.68 (d,  $J = 1.0$  Hz, 3H), 1.18 (t,  $J = 7.4$  Hz, 3H). **<sup>13</sup>C NMR (100 MHz, CDCl<sub>3</sub>)**:  $\delta$  176.05, 157.87, 134.42, 130.03, 127.99, 120.34, 108.62, 85.37, 59.12, 55.97, 48.45, 28.94, 28.92, 12.66.

. **IR**:  $\nu$  3432, 2923, 1654, 1473, 1365, 1242, 1088, 959, 864, 749 cm<sup>-1</sup>; **HRMS**. calcd. for [M+Na]<sup>+</sup>: 240.0995. Found: 240.0993.

f) Rh-catalyzed hydrogenation: synthesis of **8**

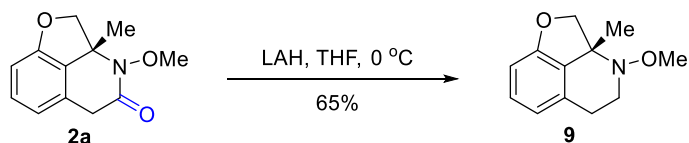


A 20 mL vial was charged with **2a** (18.4 mg, 0.084 mmol, 1 equiv.),  $[\text{Rh}(1,5\text{-pentadiene})\text{Cl}]_2$  (3.7 mg, 0.0084 mmol, 0.1 equiv.), tetrabutylammonium hydrogen sulfate (THS) (11.4 mg, 0.034 mmol, 0.4 equiv.), a buffer solution of pH=7.6 (2 mL), Et<sub>2</sub>O (0.5 mL) and hexane (5 mL). The vial was put into a high-pressure hydrogenation reactor and H<sub>2</sub> gas was introduced and maintained at 850 psi. The vessel was sealed and stirred at r.t. for 24 h. Then H<sub>2</sub> pressure was carefully released. The solution was extracted with EtOAc (3 × 10 mL). The combined organic extract was dried over anhydrous sodium sulfate, filtered, and concentrated under reduced pressure. The residue was

purified by silica gel flash column chromatography (EtOAc/Hexane=1/10) to afford product compound **8** (11.8 mg) as a colorless oil in 62% yield. The relative stereochemistry was determined by 2D-NMR (see in **NMR Spectra**).

Compound **8**:  $R_f$  = 0.5 (EtOAc/Hexane=1/1).  $[\alpha]_D^{20}$  = -42 ( $c$ =1.18,  $\text{CH}_2\text{Cl}_2$ ).  **$^1\text{H}$  NMR (400 MHz,  $\text{CDCl}_3$ )**:  $\delta$  4.04 (d,  $J$  = 9.9 Hz, 1H), 3.95 (td,  $J$  = 4.6, 2.2 Hz, 1H), 3.81 (s, 3H), 3.52 (d,  $J$  = 9.9 Hz, 1H), 2.78 (dd,  $J$  = 16.5, 10.5 Hz, 1H), 2.33 – 2.13 (m, 3H), 2.00 (dtd,  $J$  = 10.5, 4.1, 1.3 Hz, 1H), 1.75 – 1.55 (m, 2H), 1.53 (s, 3H), 1.46 – 1.32 (m, 1H), 0.91 – 0.79 (m, 2H).  **$^{13}\text{C}$  NMR (100 MHz,  $\text{CDCl}_3$ )**:  $\delta$  173.05, 79.15, 69.96, 64.16, 49.50, 37.70, 27.71, 27.08, 26.55, 25.24, 15.40. **IR**:  $\nu$  2924, 1638, 1472, 1368, 1308, 1243, 1153, 1106, 1022, 957, 936, 793, 771, 601  $\text{cm}^{-1}$ ; **HRMS**. calcd. for  $[\text{M}+\text{Na}]^+$ : 248.1257. Found: 248.1260.

g) LAH reduction: synthesis of **9**<sup>21</sup>



To a suspension of  $\text{LiAlH}_4$  (17.4 mg, 0.45 mmol, 10 equiv.) in THF (0.5 mL) in 10 mL flamed-dried Schlenk flask equipped with stir bar and a nitrogen-filled balloon was added Compound **2a** (12.3 mg, 0.056 mmol, 1 equiv., 95% e.e.) solution in 0.5 mL THF dropwise at 0 °C. The reaction was then allowed to warm to r.t. and reflux overnight. When the reaction was complete, the flask was cooled to 0 °C again and 0.3 mL water and 0.2 mL 15% NaOH was added to quench the reaction. The mixture was then filtered through a silica pad and washed with acetone. The solution was concentrated under reduced pressure and the residue was purified by silica gel flash column



chromatography (EtOAc/Hexane=1/10) to afford product compound **9** (7.5 mg) as a colorless oil in 65% yield.

Compound **9**:  $R_f = 0.7$  (EtOAc/Hexane=1/1).  $[\alpha]_D^{20} = -16$  ( $c=0.51$ ,  $\text{CH}_2\text{Cl}_2$ ).  **$^1\text{H}$  NMR (400 MHz,  $\text{CDCl}_3$ )**:  $\delta$  7.18 (td,  $J = 7.9, 1.0$  Hz, 1H), 6.72 (dd,  $J = 7.8, 1.0$  Hz, 1H), 4.70 (dd,  $J = 9.6, 1.0$  Hz, 1H), 4.06 (dd,  $J = 9.6, 1.0$  Hz, 1H), 3.99 (dddd,  $J = 10.7, 5.4, 4.3, 1.0$  Hz, 1H), 3.74 (dddd,  $J = 10.8, 9.5, 3.5, 1.1$  Hz, 1H), 3.56 (s, 3H), 3.14 (dddd,  $J = 14.0, 9.5, 4.3, 1.0$  Hz, 1H), 2.92 (dd,  $J = 14.1, 4.4$  Hz, 1H), 1.71 (s, 3H).  **$^{13}\text{C}$  NMR (100 MHz,  $\text{CDCl}_3$ )**:  $\delta$  161.09, 138.66, 130.54, 126.40, 123.04, 108.66, 78.60, 67.57, 63.82, 62.84, 35.44, 20.46. **IR**:  $\nu$  3347, 2928, 1654, 1591, 1466, 1446, 1264, 1046, 999, 785, 746, 416  $\text{cm}^{-1}$ ; **HRMS**. calcd. for  $[\text{M}+\text{H}]^+$ : 206.1181. Found: 206.1185.

#### 2.4.9 X-ray data

##### I. X-ray data for **2a**

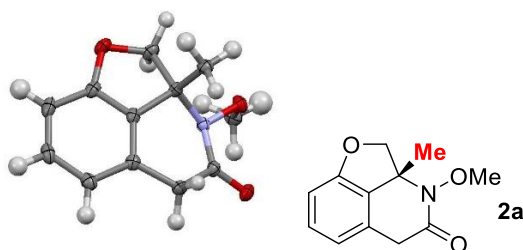


**Table 2.10** Crystal Data and Structure Refinement for **2a**

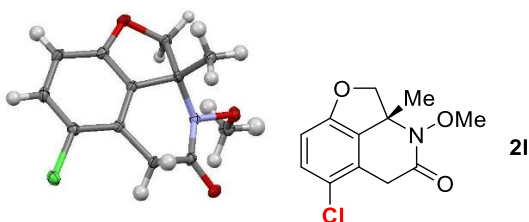
Empirical formula	$\text{C}_{12}\text{H}_{13}\text{N O}_3$
Formula weight	219.23
Temperature	100(2) K
Wavelength	1.54184 Å
Crystal system	monoclinic
Space group	P 21

**Table 2.10** Continued Crystal Data and Structure Refinement for **2a**

Unit cell dimensions	$a = 8.3112(15) \text{ \AA}$	$\alpha = 90^\circ$ .
	$b = 7.2566(13) \text{ \AA}$	$\beta = 95.146(2)^\circ$ .
	$c = 8.9068(17) \text{ \AA}$	$\gamma = 90^\circ$ .
Volume	$535.01(17) \text{ \AA}^3$	
Z	2	
Density (calculated)	$1.361 \text{ Mg/m}^3$	
Absorption coefficient	$0.812 \text{ mm}^{-1}$	
F(000)	232	
Crystal size	$0.310 \times 0.290 \times 0.140 \text{ mm}^3$	
Theta range for data collection	$4.986$ to $74.282^\circ$ .	
Index ranges	$-10 \leq h \leq 10$ , $-8 \leq k \leq 8$ , $-11 \leq l \leq 10$	
Reflections collected	5543	
Independent reflections	2019 [ $R(\text{int}) = 0.0140$ ]	
Completeness to $\theta = 67.684^\circ$	100.0 %	
Absorption correction	Semi-empirical from equivalents	
Max. and min. transmission	1.00 and 0.909	
Refinement method	Full-matrix least-squares on $F^2$	
Data / restraints / parameters	2019 / 1 / 199	
Goodness-of-fit on $F^2$	1.064	
Final R indices [ $I > 2\sigma(I)$ ]	$R1 = 0.0236$ , $wR2 = 0.0632$	
R indices (all data)	$R1 = 0.0236$ , $wR2 = 0.0633$	
Absolute structure parameter	$-0.06(19)$	

**Table 2.10** Continued Crystal Data and Structure Refinement for **2a**

Extinction coefficient	0.0129(17)
Largest diff. peak and hole	0.218 and -0.111 e.Å <sup>-3</sup>

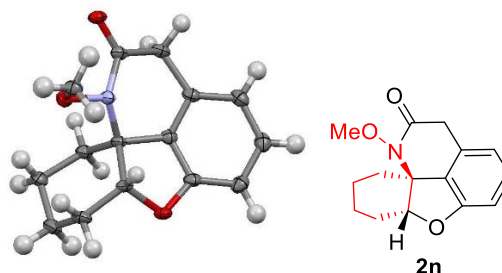
II. X-ray data for **2l****Table 2.11** Crystal Data and Structure Refinement for **2l**

Empirical formula	C <sub>12</sub> H <sub>12</sub> Cl N O <sub>3</sub>	
Formula weight	253.68	
Temperature	100(2) K	
Wavelength	1.54184 Å	
Crystal system	monoclinic	
Space group	P 2 <sub>1</sub>	
Unit cell dimensions	a = 8.7567(12) Å	α = 90°.
	b = 7.2460(10) Å	β = 96.915(7)°.
	c = 9.0118(14) Å	γ = 90°.
Volume	567.65(14) Å <sup>3</sup>	
Z	2	
Density (calculated)	1.484 Mg/m <sup>3</sup>	
Absorption coefficient	2.964 mm <sup>-1</sup>	
F(000)	264	

**Table 2.11** Continued Crystal Data and Structure Refinement for **2l**

Crystal size	0.24 x 0.15 x 0.12 mm <sup>3</sup>
Theta range for data collection	4.943 to 74.278°.
Index ranges	-10<=h<=10, -8<=k<=9, -11<=l<=11
Reflections collected	5799
Independent reflections	2182 [R(int) = 0.0184]
Completeness to theta = 67.684°	99.9 %
Absorption correction	Semi-empirical from equivalents
Max. and min. transmission	1.00 and 0.881
Refinement method	Full-matrix least-squares on F <sup>2</sup>
Data / restraints / parameters	2182 / 103 / 203
Goodness-of-fit on F <sup>2</sup>	1.063
Final R indices [I>2sigma(I)]	R1 = 0.0207, wR2 = 0.0547
R indices (all data)	R1 = 0.0209, wR2 = 0.0550
Absolute structure parameter	0.008(12)
Extinction coefficient	n/a
Largest diff. peak and hole	0.204 and -0.218 e.Å <sup>-3</sup>

### III. X-ray data for **2n**

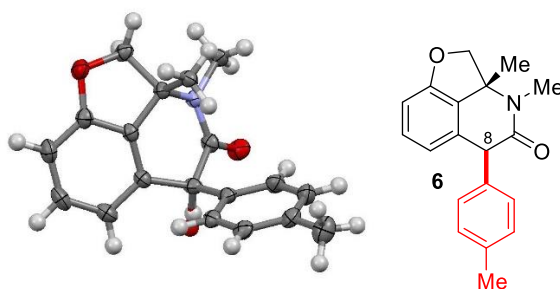


**Table 2.12** Crystal Data and Structure Refinement for **2n**

Identification code	DL-C-59	
Empirical formula	C <sub>15</sub> H <sub>17</sub> N O <sub>3</sub>	
Formula weight	259.29	
Temperature	100(2) K	
Wavelength	1.54184 Å	
Crystal system	Monoclinic	
Space group	P 2 <sub>1</sub> /c	
Unit cell dimensions	a = 9.6015(3) Å	α = 90°.
	b = 14.9637(5) Å	β = 104.171(3)°.
	c = 8.9947(3) Å	γ = 90°.
Volume	1252.98(7) Å <sup>3</sup>	
Z	4	
Density (calculated)	1.375 Mg/m <sup>3</sup>	
Absorption coefficient	0.780 mm <sup>-1</sup>	
F(000)	552	
Crystal size	0.400 x 0.020 x 0.010 mm <sup>3</sup>	
Theta range for data collection	4.750 to 74.174°.	
Index ranges	-11 ≤ h ≤ 11, -18 ≤ k ≤ 15, -10 ≤ l ≤ 10	
Reflections collected	9340	
Independent reflections	2497 [R(int) = 0.0432]	
Completeness to theta = 67.684°	99.9 %	
Absorption correction	Semi-empirical from equivalents	

**Table 2.12** Continued Crystal Data and Structure Refinement for **2n**

Max. and min. transmission	0.992 and 0.732
Refinement method	Full-matrix least-squares on F <sup>2</sup>
Data / restraints / parameters	2497 / 0 / 173
Goodness-of-fit on F <sup>2</sup>	1.087
Final R indices [I>2sigma(I)]	R1 = 0.0520, wR2 = 0.2109
R indices (all data)	R1 = 0.0632, wR2 = 0.2144
Extinction coefficient	n/a
Largest diff. peak and hole	0.379 and -0.331 e.Å <sup>-3</sup>

IV. X-ray data for **6****Table 2.13** Crystal Data and Structure Refinement for **6**

Empirical formula	C19 H19 N O2.20		
Formula weight	296.55		
Temperature	100(2) K		
Wavelength	1.54184 Å		
Crystal system	orthorhombic		
Space group	P 21 21 21		
Unit cell dimensions	a = 8.2495(3) Å	α= 90°.	
	b = 12.0484(3) Å	β= 90°.	

**Table 2.13** Continued Crystal Data and Structure Refinement for **6**

	$c = 14.9606(7) \text{ \AA}$	$\gamma = 90^\circ$ .
Volume	1486.98(10) $\text{\AA}^3$	
Z	4	
Density (calculated)	1.325 $\text{Mg/m}^3$	
Absorption coefficient	0.689 $\text{mm}^{-1}$	
F(000)	630	
Crystal size	0.210 x 0.100 x 0.030 $\text{mm}^3$	
Theta range for data collection	4.712 to 74.417°.	
Index ranges	$-10 \leq h \leq 10$ , $-14 \leq k \leq 15$ , $-18 \leq l \leq 15$	
Reflections collected	9736	
Independent reflections	2909 [ $R(\text{int}) = 0.0376$ ]	
Completeness to $\theta = 67.684^\circ$	99.9 %	
Absorption correction	Semi-empirical from equivalents	
Max. and min. transmission	1.00 and 0.849	
Refinement method	Full-matrix least-squares on $F^2$	
Data / restraints / parameters	2909 / 0 / 206	
Goodness-of-fit on $F^2$	1.050	
Final R indices [ $I > 2\sigma(I)$ ]	$R1 = 0.0410$ , $wR2 = 0.1030$	
R indices (all data)	$R1 = 0.0434$ , $wR2 = 0.1049$	
Absolute structure parameter	0.13(17)	
Extinction coefficient	n/a	
Largest diff. peak and hole	0.162 and -0.277 $\text{e.\AA}^{-3}$	

# V. X-ray data for **7**

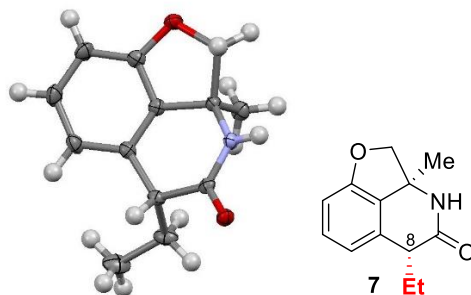


**Table 2.14** Crystal Data and Structure Refinement for **7**

Empirical formula	C <sub>13</sub> H <sub>15</sub> N O <sub>2</sub>	
Formula weight	217.26	
Temperature	100(2) K	
Wavelength	1.54184 Å	
Crystal system	monoclinic	
Space group	P 2 <sub>1</sub>	
Unit cell dimensions	a = 7.5087(2) Å	α = 90°.
	b = 19.9025(6) Å	β = 93.255(3)°.
	c = 11.5097(5) Å	γ = 90°.
Volume	1717.26(10) Å <sup>3</sup>	
Z	6	
Density (calculated)	1.261 Mg/m <sup>3</sup>	
Absorption coefficient	0.685 mm <sup>-1</sup>	
F(000)	696	
Crystal size	0.370 x 0.050 x 0.020 mm <sup>3</sup>	
Theta range for data collection	3.847 to 74.282°.	



**Table 2.14** Continued Crystal Data and Structure Refinement for **7**

Index ranges	-8<=h<=9, -20<=k<=24, -14<=l<=14
Reflections collected	16617
Independent reflections	6404 [R(int) = 0.0280]
Completeness to theta = 67.684°	100.0 %
Absorption correction	Semi-empirical from equivalents
Max. and min. transmission	1.00 and 0.672
Refinement method	Full-matrix least-squares on F <sup>2</sup>
Data / restraints / parameters	6404 / 1 / 452
Goodness-of-fit on F <sup>2</sup>	1.047
Final R indices [I>2sigma(I)]	R1 = 0.0308, wR2 = 0.0791
R indices (all data)	R1 = 0.0318, wR2 = 0.0801
Absolute structure parameter	0.00(16)
Extinction coefficient	n/a
Largest diff. peak and hole	0.182 and -0.202 e.Å <sup>-3</sup>

## 2.5 References

- (1) For selected reviews on C–C activation, see: (a) Jones, W. D. *Nature* **1993**, *364*, 676. (b) Murakami, M.; Ito, Y. *Top. Organomet. Chem.* **1999**, *3*, 97. (c) Rybtchinski, B.; Milstein, D. *Angew. Chem., Int. Ed.* **1999**, *38*, 870. (d) Jun, C.-H. *Chem. Soc. Rev.* **2004**, *33*, 610. (e) Satoh, T.; Miura, M. *Top. Organomet. Chem.* **2005**, *14*, 1. (f) Necas, D.; Kotora, M. *Curr. Org. Chem.* **2007**, *11*, 1566. (g) Crabtree, R. H. *Chem. Rev.* **1985**, *85*, 245. (h) Ruhland, K. *Eur. J. Org. Chem.* **2012**, 2683. (i) Korotvicka, A.; Necas, D.; Kotora, M. *Curr. Org. Chem.* **2012**, *16*, 1170. (j) Seiser, T.; Saget, T.; Tran, D. N.; Cramer, N. *Angew. Chem., Int. Ed.* **2011**, *50*, 7740. (k) Murakami, M.; Matsuda, T. *Chem. Commun.* **2011**, *47*, 1100. (l) Dermenci, A.; Coe, J. W.; Dong, G. *Org. Chem. Front.* **2014**, *1*, 567. (m) C–C bond activation. In *Topics in Current Chemistry*; Dong, G., Ed.; Springer-Verlag: Berlin, **2014**, Vol. 346. (n) Chen, F.; Wang, T.; Jiao, N. *Chem. Rev.* **2014**, *114*, 8613. (o) Souillart, L.; Cramer, N. *Chem. Rev.* **2015**, *115*, 9410.

- (2) For two seminal works: (a) South, M. S.; Liebeskind, L. S. *J. Am. Chem. Soc.* **1984**, *106*, 4181. (b) Murakami, M.; Itahashi, T.; Ito, Y. *J. Am. Chem. Soc.* **2002**, *124*, 13976.
- (3) Souillart, L.; Cramer, N. *Angew. Chem. Int. Ed.* **2014**, *53*, 9640.
- (4) Souillart, L.; Cramer, N. *Chem. Eur. J.* **2015**, *21*, 1863.
- (5) Li, B.-S.; Wang, Y.; Jin, Z.; Zheng, P.; Ganguly, R.; Chi, Y. R. *Nature Comm.* **2015**, *6*, 6207.
- (6) For examples of drugs containing a chiral lactam moiety, see: (a) St Georgiev, V.; Van Inwegen, R. G.; Carlson, P. *Eur. J. Med. Chem.* **1990**, *25*, 375. (b) Mekonnen, B.; Weiss, E.; Katz, E.; Ma, J.; Ziffer, H.; Kyle, D. E. *Biorg. Med. Chem.* **2000**, *8*, 1111. (c) Ding, Y.-S.; Lin, K.-S.; Logan, J.; Benveniste, H.; Carter, P. *J. Neurochem.* **2005**, *94*, 337. (d) Lin, K.-S.; Ding, Y.-S. *Biorg. Med. Chem.* **2005**, *13*, 4658. (e) Altomare, C.; Carotti, A.; Casini, G.; Cellamare, S.; Ferappi, M.; Gavuzzo, E.; Mazza, F.; Pantaleoni, G.; Giorgi, R. *J. Med. Chem.* **1988**, *31*, 2153. (f) Altomare, C.; Cellamare, S.; Carotti, A.; Casini, G.; Ferappi, M.; Gavuzzo, E.; Mazza, F.; Carrupt, P.-A.; Gaillard, P.; Testa, B. *J. Med. Chem.* **1995**, *38*, 170.
- (7) For a seminal mechanistic study on the metal cleavage of benzocyclobutenone C–C bond, see: (a) Huffman, M. A.; Liebeskind, L. S.; Pennington, W. T. *Organometallics*, **1990**, *9*, 2194. (b) Huffman, M. A.; Liebeskind, L. S.; Pennington, W. T. *Organometallics*, **1992**, *11*, 255. For a detailed computational mechanism study of benzocyclobutenones with Rh(I) complex, see: (c) Lu, G.; Fang, C.; Xu, T.; Dong, G.; Liu, P. *J. Am. Chem. Soc.* **2015**, *137*, 8274.
- (8) For selected examples involving  $2\pi$ -insertion to rhodaindanones via oxidative addition of Rh(I)-catalysts into C(sp<sup>2</sup>)-acyl bonds: (a) Xu, T.; Dong, G. *Angew. Chem. Int. Ed.* **2012**, *51*, 7567. (b) Xu, T.; Ko, H. M.; Sagave, N. A.; Dong, G. *J. Am. Chem. Soc.* **2012**, *134*, 20005. (c) Xu, T.; Savage, N. A.; Dong, G. *Angew. Chem., Int. Ed.* **2014**, *53*, 1891. (d) Xu, T.; Dong, G. *Angew. Chem., Int. Ed.* **2014**, *53*, 10733. (e) Chen, P.-h.; Xu, T.; Dong, G. *Angew. Chem., Int. Ed.* **2014**, *53*, 1674.
- (9) For selected examples involving  $2\pi$ -insertion to related rhodacyclopentanones: reference 2b, 3 and (a) Matsuda, T.; Fujimoto, A.; Ishibashi, M.; Murakami, M. *Chem. Lett.* **2004**, *33*, 876. (b) Shaw, M. H.; Melikhova, E. Y.; Kloer, D. P.; Whittingham, W. G.; Bower, J. F. *J. Am. Chem. Soc.* **2013**, *135*, 4992. (c) Ko, H. M.; Dong, G. *Nature Chemistry* **2014**, *6*, 739. (d) Parker, E.; Cramer, N. *Organometallics* **2014**, *33*, 780. (e) Souillart, L.; Parker, E.; Cramer, N. *Angew. Chem., Int. Ed.* **2014**, *53*, 3001. (f) Shaw, M. H.; McCreanor, N. G.; Whittingham, W. G.; Bower, J. F. *J. Am. Chem. Soc.* **2015**, *137*, 463. (g) Shaw, M. H.; Croft, R. A.; Whittingham, W. G.; Bower, J. F. *J. Am. Chem. Soc.* **2015**, *137*, 8054.
- (10) For examples of drugs containing a tetrahydroisoquinoline moiety, see: (a) Omar, H.; Hashim, N. M.; Zajmi, A.; Nordin, N.; Abdelwahab, S. I.; Azizan, A. H. S.; Hadi, A. H. A.; Ali, H. M. *Molecules* **2013**, *18*, 8994. (b) Zarga, M. A.; Miana, G. A.; Shamma, M. *Tetrahedron Lett.* **1981**, *22*, 541. (c) Grunewald, G. L.; Sall, D. J.; Monn, J. A. *J. Med. Chem.* **1988**, *31*, 433. (d) Kim, J. H.; Ryu, Y. B.; Lee, W. S.; Kim, Y. H. *Bioorg. Med. Chem.* **2014**, *22*, 6047. (e) Ye, N.; Chen, C. H.; Chen, T.; Song, Z.; He, J. X.; Huan, X. J.; Song, S. S.; Liu, Q.; Chen, Y.; Ding, J.; Xu, Y.; Miao, Z. H.; Zhang, A. *J. Med. Chem.* **2013**, *56*, 2885. (f) Parraga, J.; Galan, A.; Sanz, M. J.; Cabedo, N.; Cortes, D. *Eur. J. Med. Chem.* **2015**, *90*, 101. For a

- comprehensive review of the chemistry and biology of the tetrahydroisoquinoline alkaloids, see: (g) Scott, J. D.; Williams, R. M. *Chem. Rev.* **2002**, *102*, 1669. For isoquinolinones with novel vasorelaxation activity, see: (h) Lin, C. H.; Lin, M. S.; Lin, Y. H.; Chen, I. M.; Lin, P. R.; Cheng, C. Y.; Tsai, M. C. *Pharmacology* **2003**, *67*, 202.
- (11) (a) Ittel, S. D.; Johnson, L. K. *Chem. Rev.* **2000**, *100*, 1169. (b) Milios, C. J.; Stamatatos, T. C.; Perlepes, S. P. *Polyhedron* **2006**, *25*, 134.
- (12) Pan, Z.; Pound, S. M.; Rondla, N. R.; Douglas, C. J. *Angew. Chem. Int. Ed.* **2014**, *53*, 5170.
- (13) (a) Xie, J.-H.; Zhou, Q.-L. *Acc. Chem. Res.* **2008**, *41*, 581. (b) Xie, J.-H.; Zhu, S.-F.; Zhou, Q.-L. *Chem. Rev.* **2011**, *111*, 1713. (c) Fan, B.-M.; Xie, J.-H.; Li, S.; Wang, L.-X.; Zhou, Q.-L. *Angew. Chem. Int. Ed.* **2007**, *46*, 1275. (d) Liu, S.; Xie, J.-H.; Wang, L.-X.; Zhou, Q.-L. *Angew. Chem. Int. Ed.* **2007**, *46*, 7506.
- (14) Yang, Y.; Shi, S.-L.; Liu, P.; Buchwald, S. L. *Science* **2015**, *349*, 62.
- (15) For examples of reductive cleavage of N–O bonds: (a) using samarium(II) iodide: Myers, R. M.; Langston, S. P.; Conway, S. P.; Abell, C. *Org. Lett.* **2000**, *2*, 1349. (b) using ruthenium: Fukuzawa, H.; Ura, Y.; Kataoka, Y. *J. Organomet. Chem.* **2011**, *696*, 3643. (c) using zinc or molybdenum: (e) Atobe, M.; Yamazaki, N.; Kibayashi, C. *J. Org. Chem.* **2004**, *69*, 5595. (d) Ren, Z.; Schulz, J. E.; Dong, G. *Org Lett* **2015**, *17*, 2696.
- (16) For reviews on C–N bond formations: (a) Muci, A.R.; Buchwald, S. L. *Topics in Curr. Chem.* **2002**, *219*, 131. (b) Hartwig, J. F. *Acc. Chem. Res.* **1998**, *31*, 852. (c) Wolfe, J. P.; Wagaw, S.; Marcoux, J. F.; Buchwald, S. L. *Acc. Chem. Res.* **1998**, *31*, 805. (d) Bariwalab, J.; Eycken, E. V. *Chem. Soc. Rev.* **2013**, *42*, 9283. (e) Beletskaya, I.; Cheprakov, A. *Coord. Chem. Rev.* **2004**, *248*, 2337.
- (17) Januszkiewicz, K. R.; Alper, H. *Organometallics* **1983**, *2*, 1055 and reference 8b.
- (18) Wardrop, D. J.; Basak, A. *Org. Lett.* **2001**, *3*, 1053.
- (19) Chen, P. H.; Savage, N. A.; Dong, G. *Tetrahedron* **2014**, *70*, 4135.
- (20) Godfrey, J. D., Jr; Mueller, R. H.; Sedergran, T. C.; Soundararajan, N.; Colandrea, V. J. *Tetrahedron Letters* **1994**, *35*, 6405.
- (21) Karanfil, A.; Balta, B.; Eskici, M. *Tetrahedron* **2012**, *68*, 10218.

## 2.6 NMR Spectra

**Figure 2.1**  $^1\text{H}$  and  $^{13}\text{C}$  NMR spectrum of compound **1a**

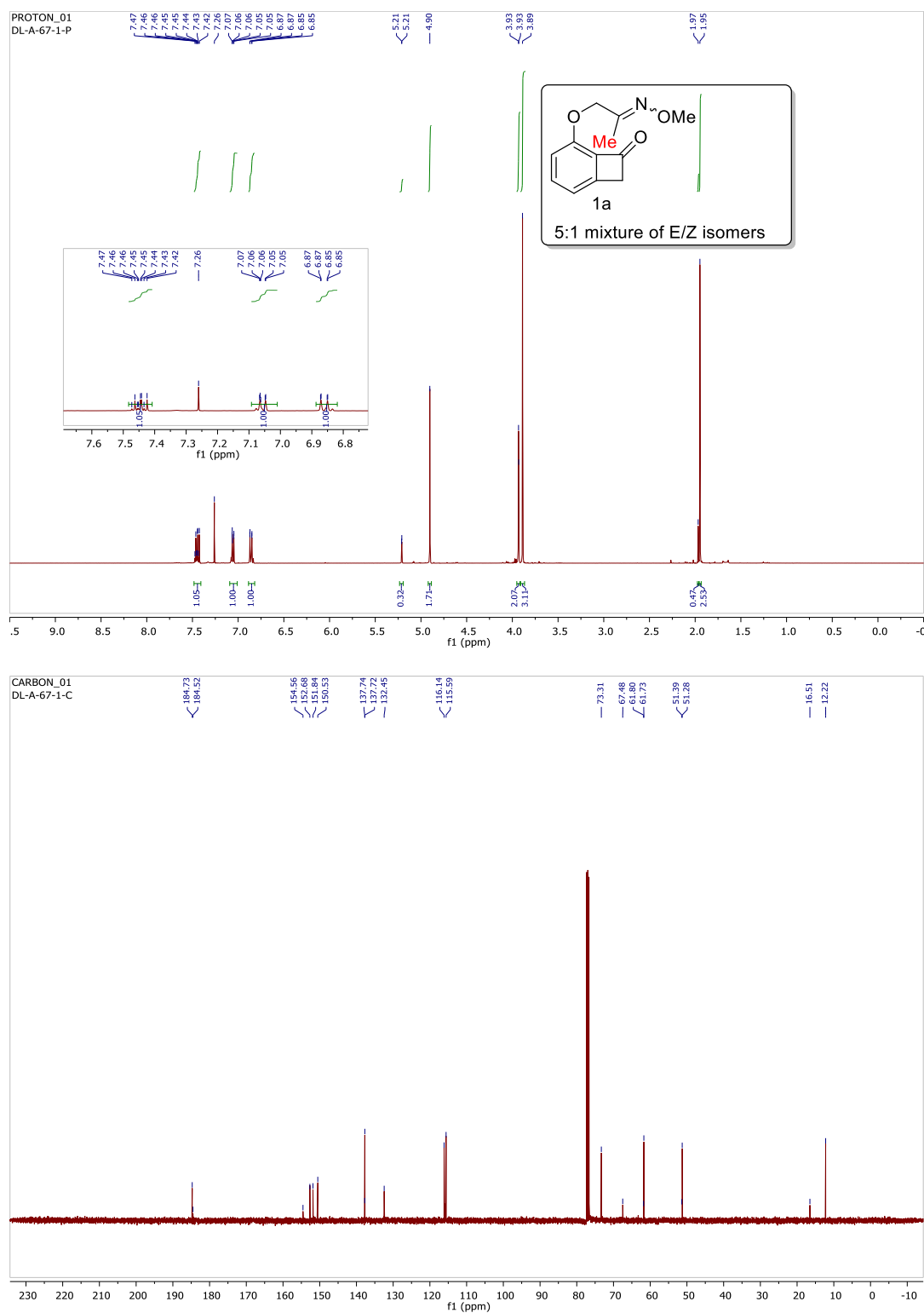


**Figure 2.2**  $^1\text{H}$  and  $^{13}\text{C}$  NMR spectrum of compound **1b**

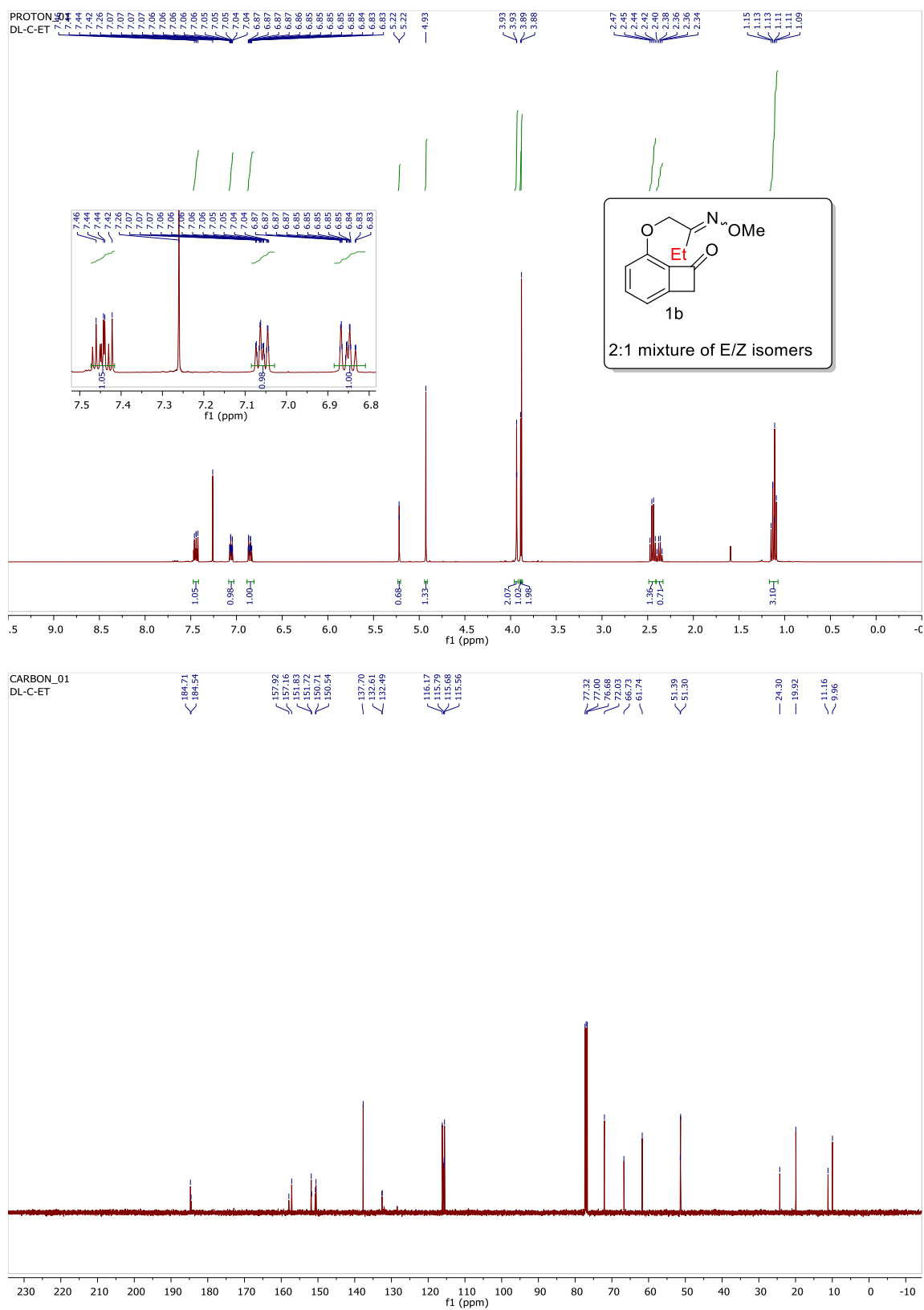


**Figure 2.3**  $^1\text{H}$  and  $^{13}\text{C}$  NMR spectrum of compound **1c**

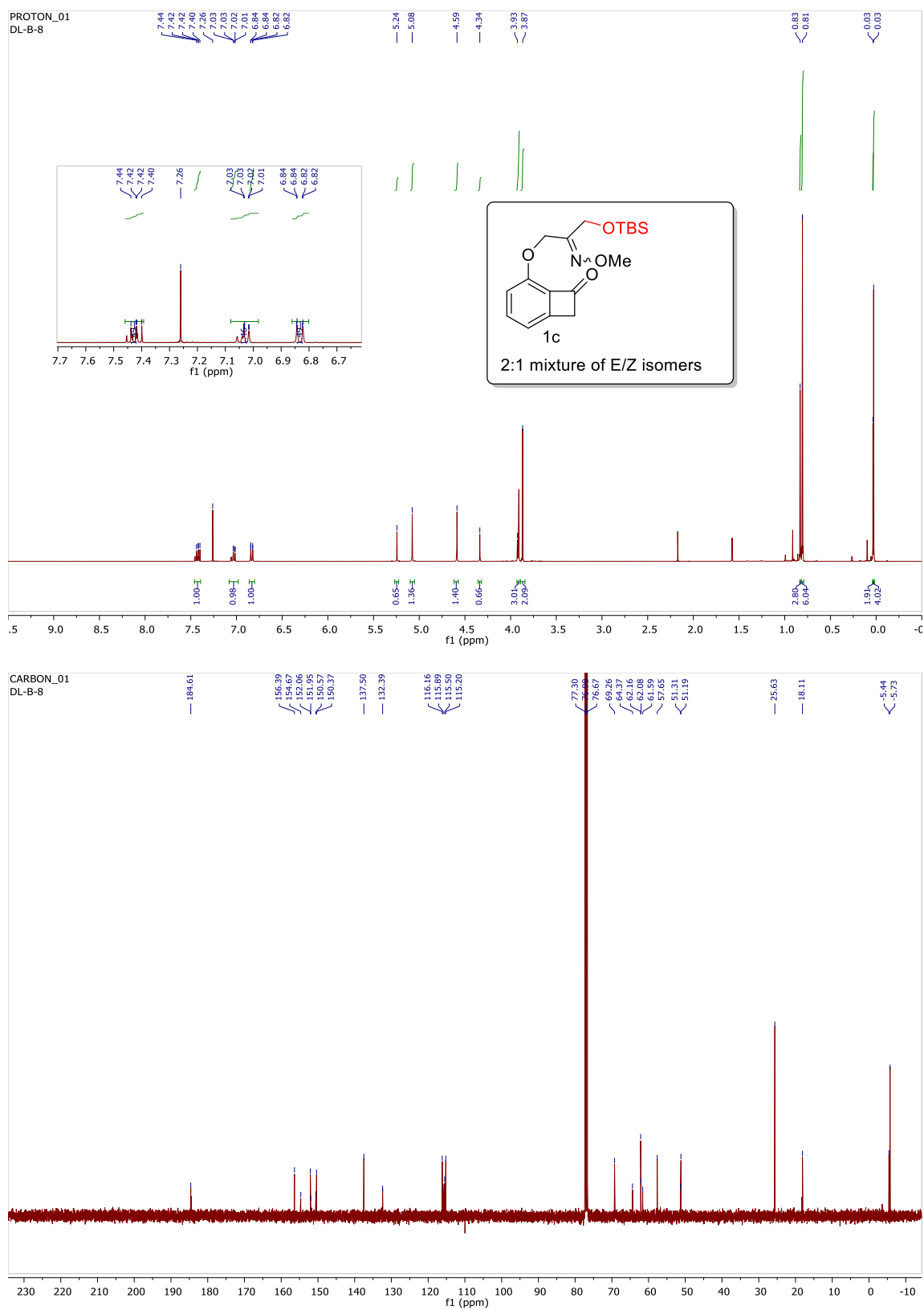


**Figure 2.4**  $^1\text{H}$  and  $^{13}\text{C}$  NMR spectrum of compound **1d**

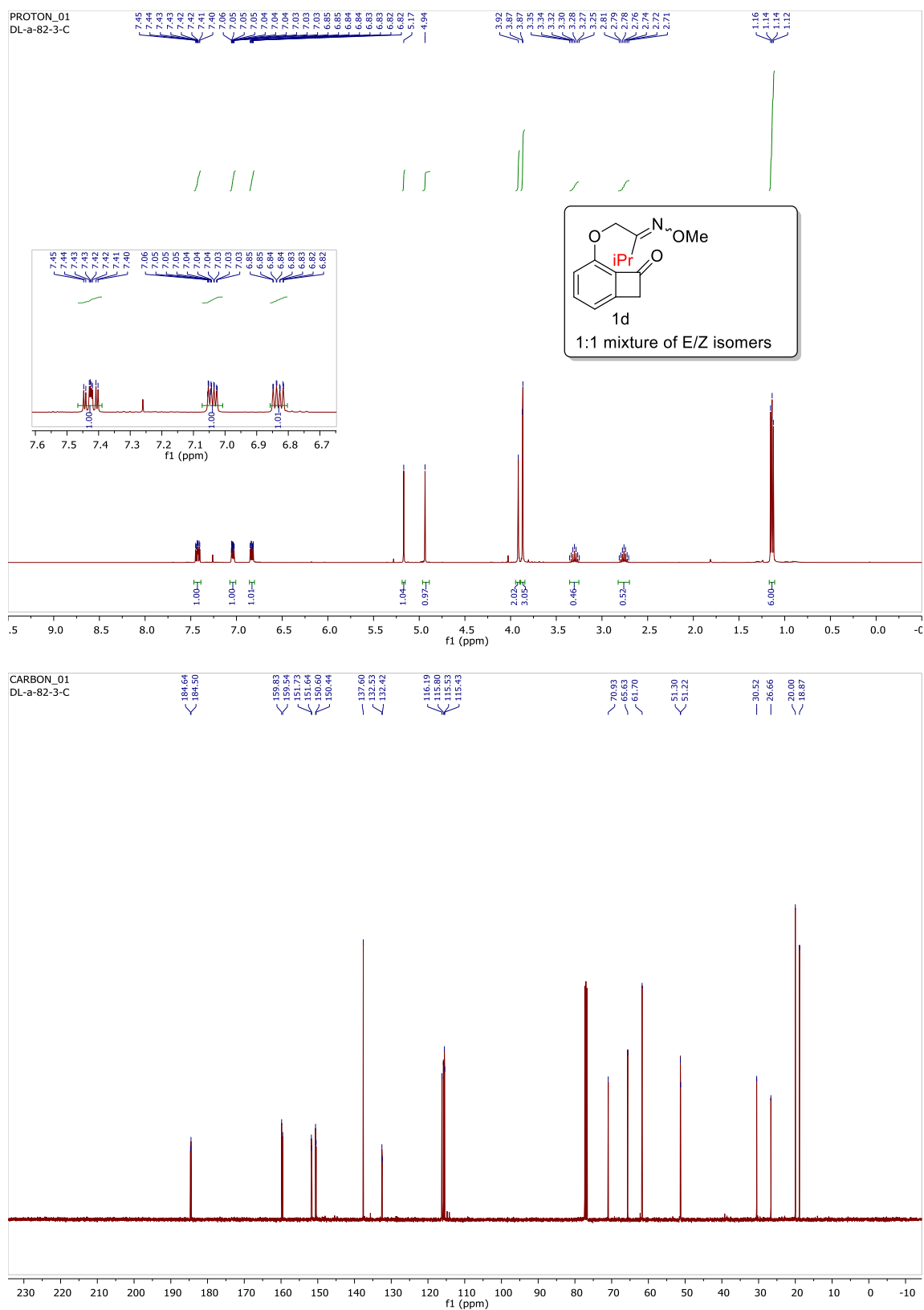


**Figure 2.5**  $^1\text{H}$  and  $^{13}\text{C}$  NMR spectrum of compound **1e**

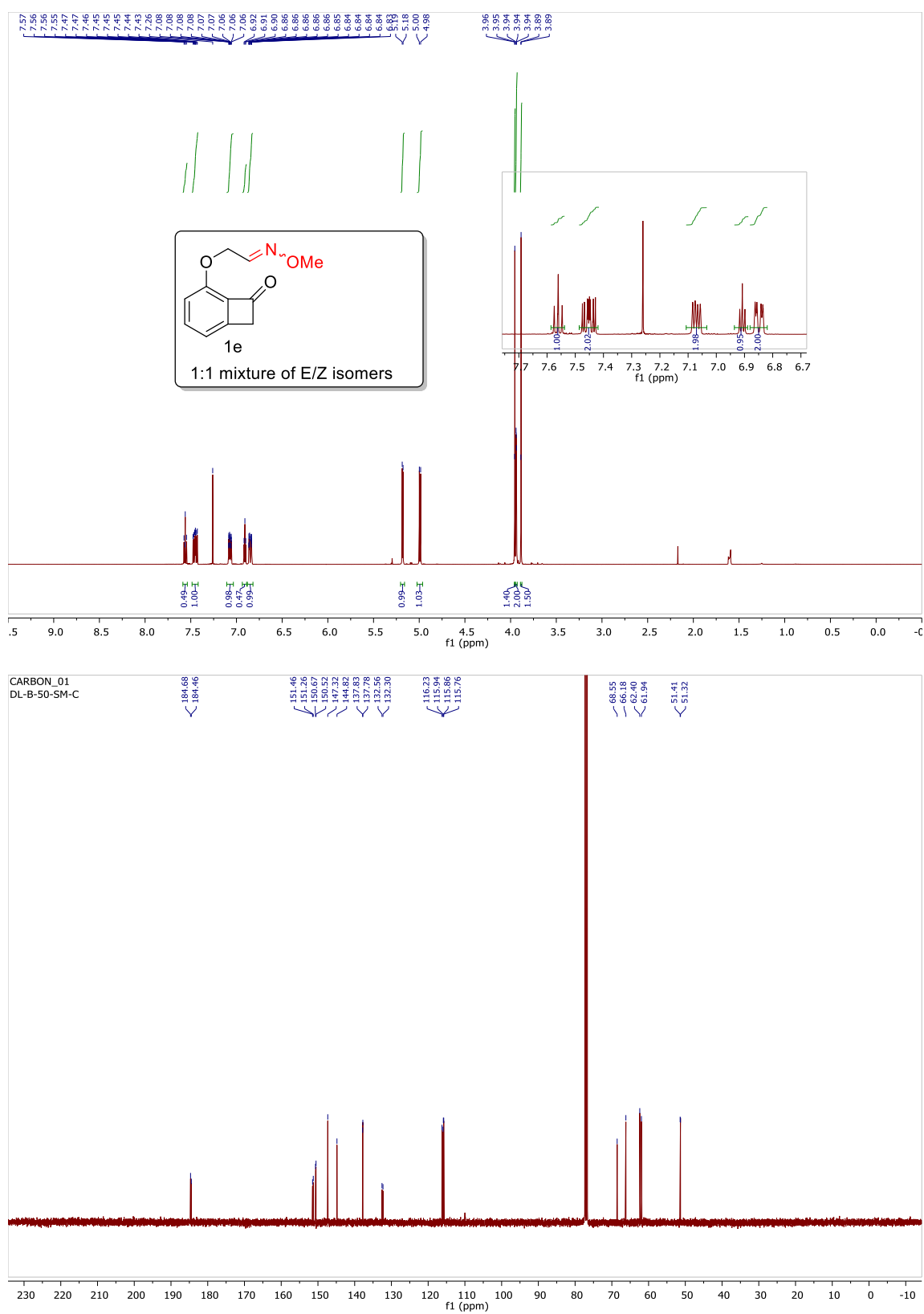




**Figure 2.6**  $^1\text{H}$  and  $^{13}\text{C}$  NMR spectrum of compound **1f**

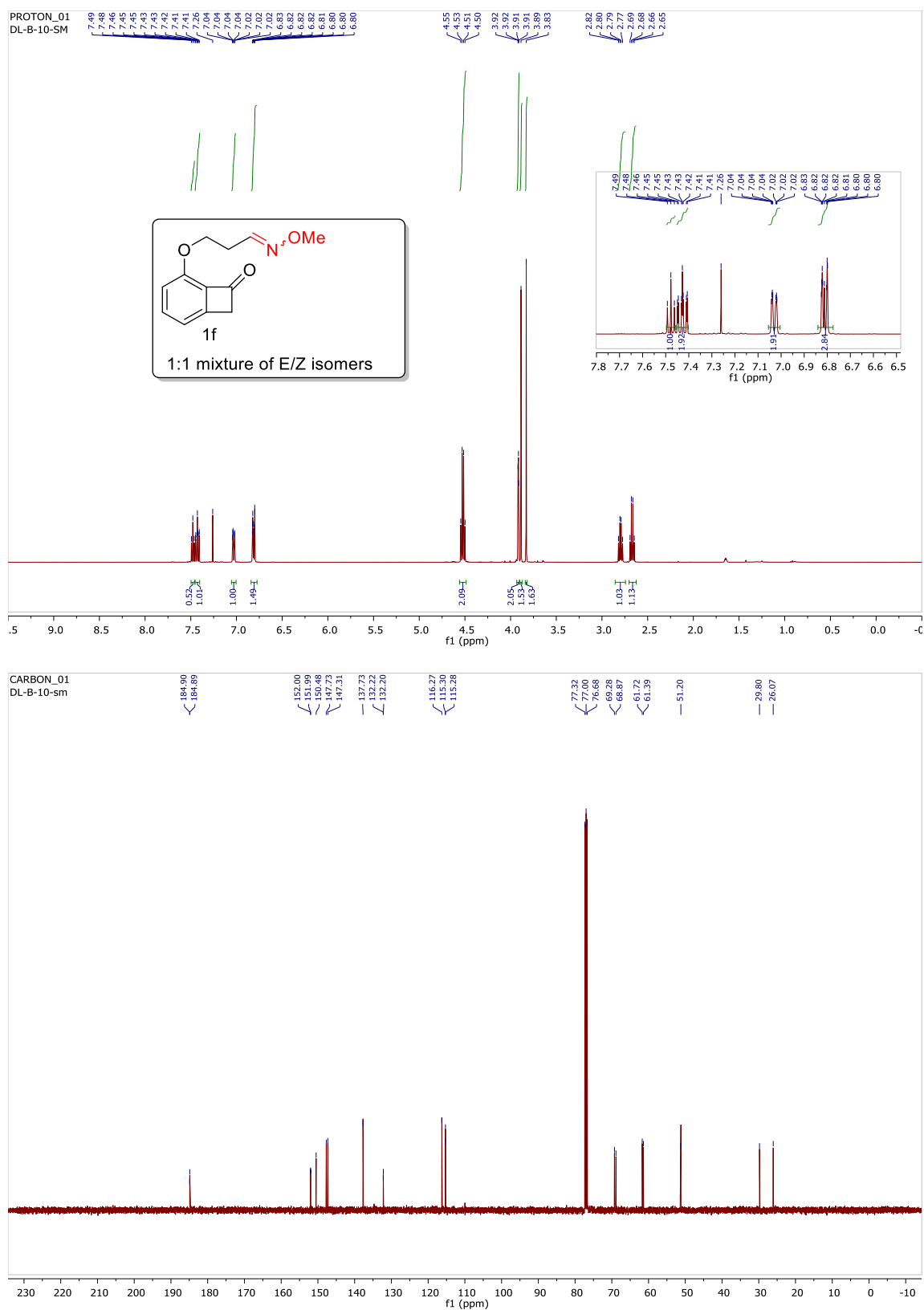


**Figure 2.7**  $^1\text{H}$  and  $^{13}\text{C}$  NMR spectrum of compound **1g**

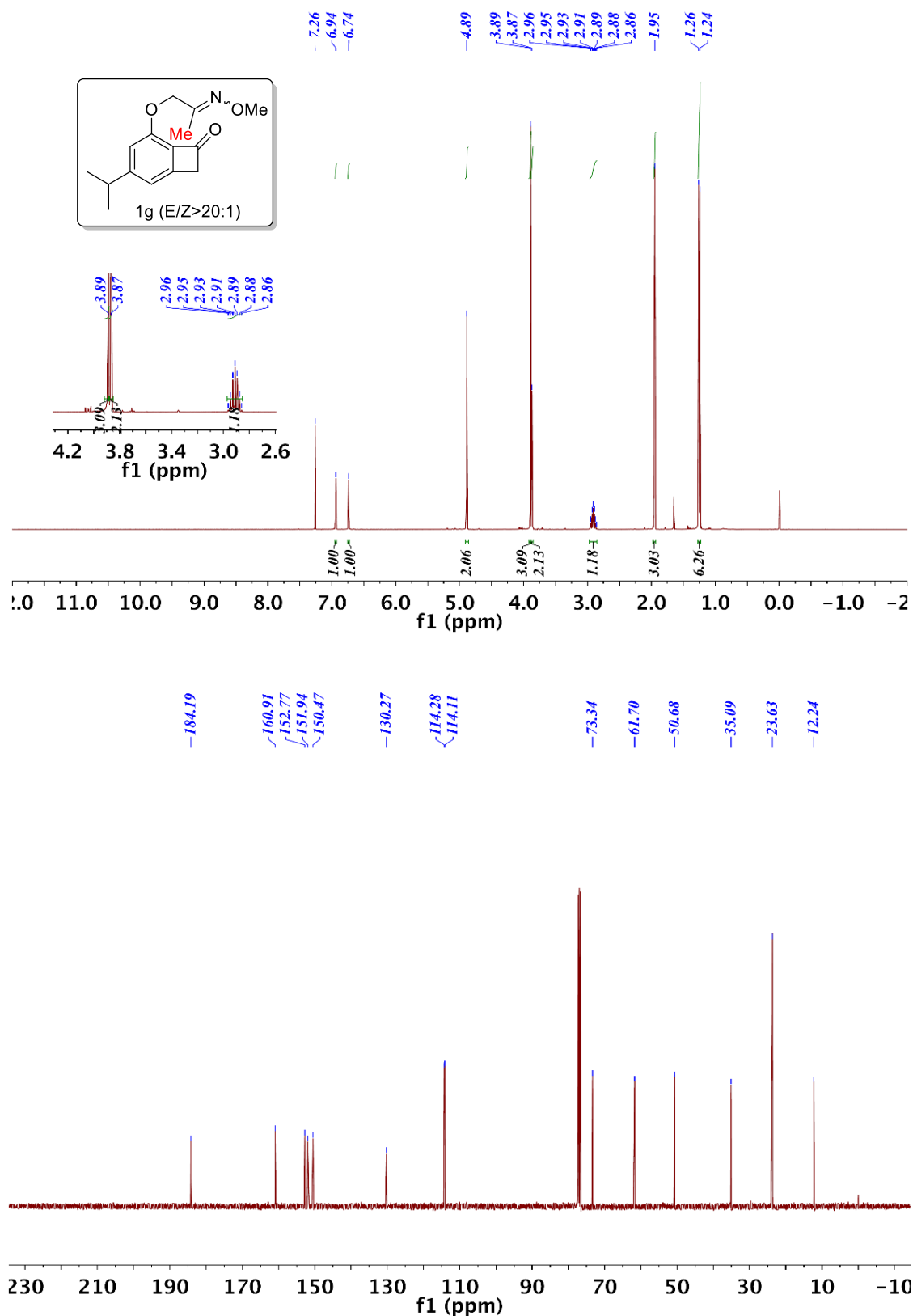


**Figure 2.8**  $^1\text{H}$  and  $^{13}\text{C}$  NMR spectrum of compound **1h**

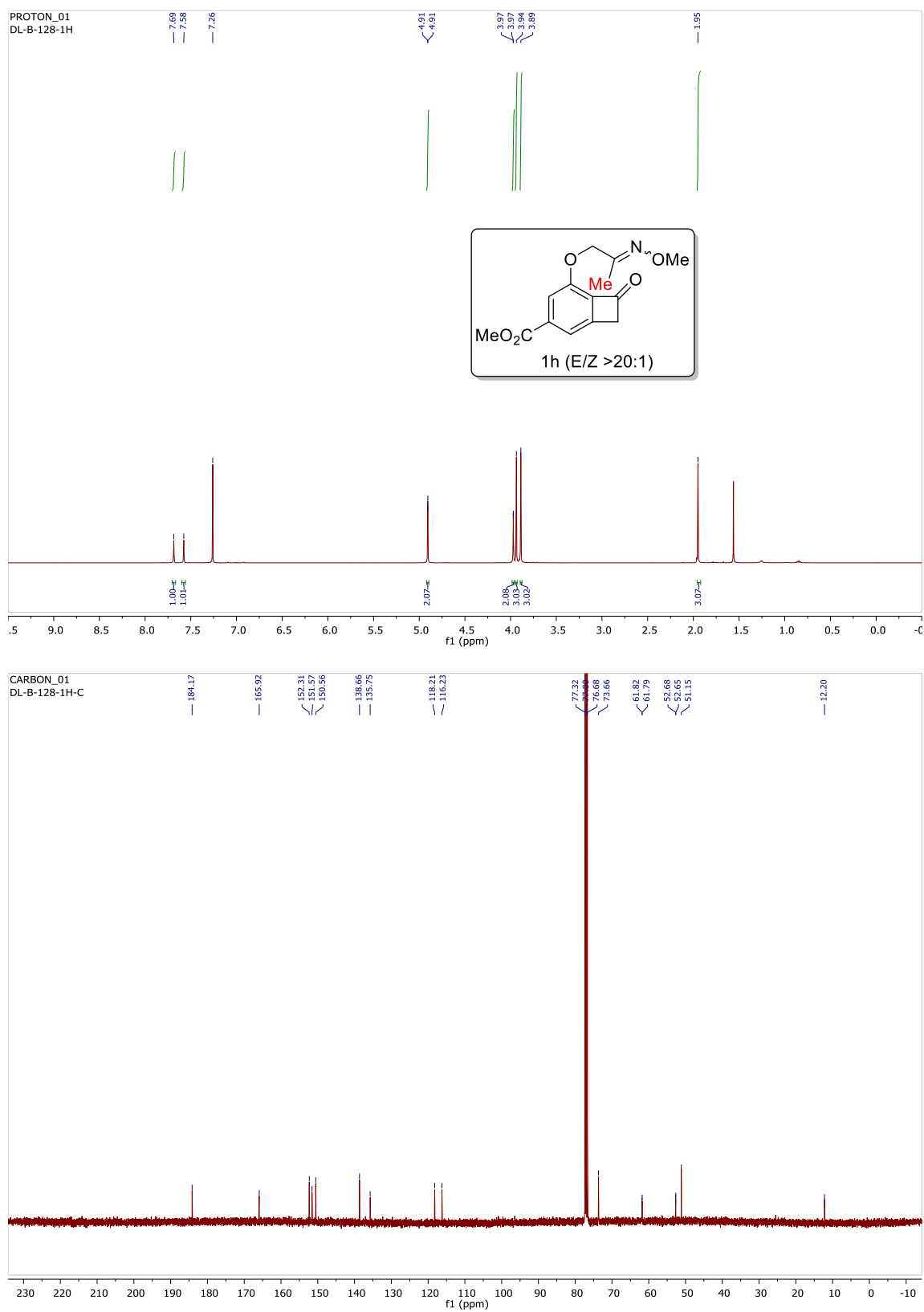


**Figure 2.9**  $^1\text{H}$  and  $^{13}\text{C}$  NMR spectrum of compound **1i**

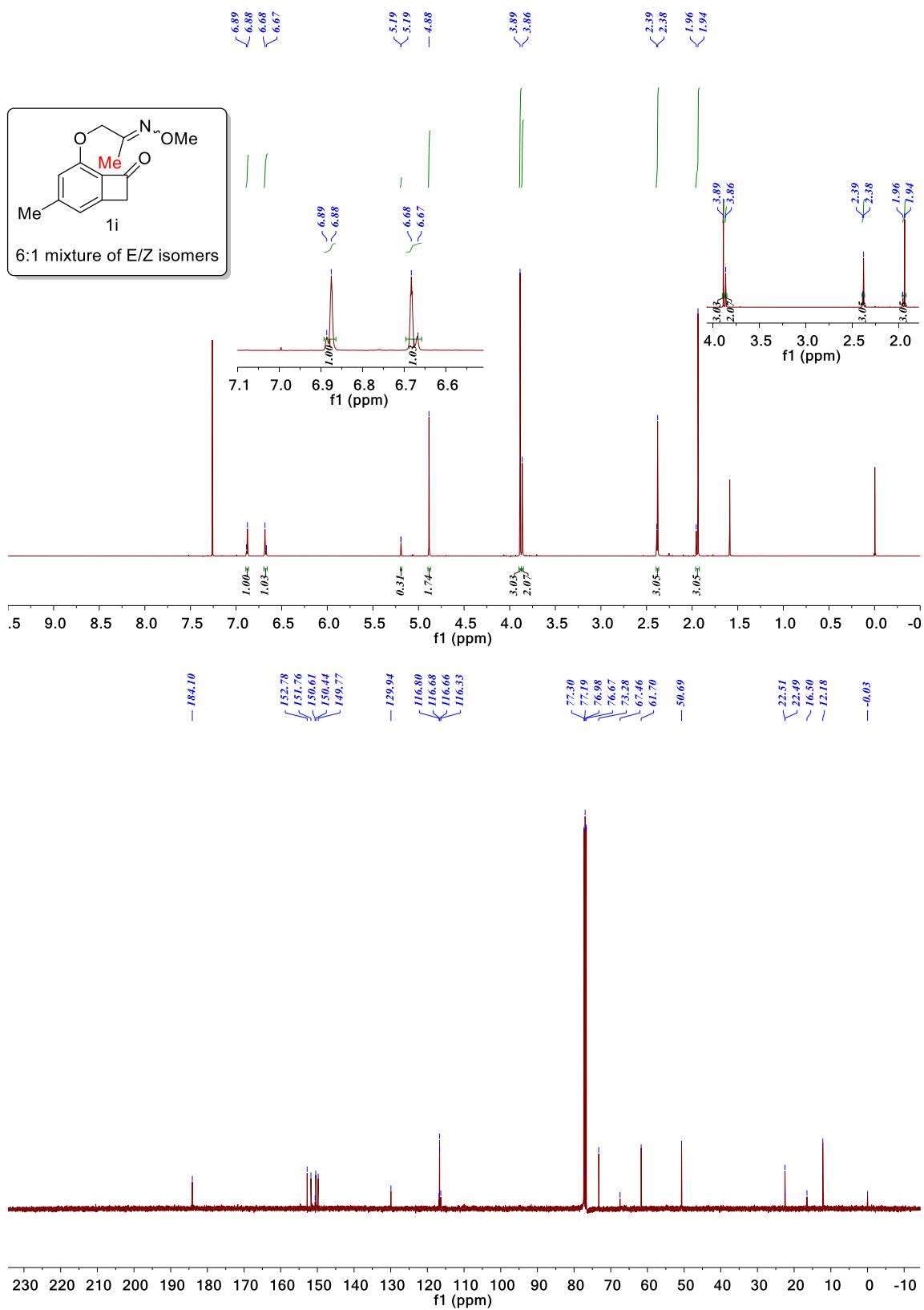


**Figure 2.10**  $^1\text{H}$  and  $^{13}\text{C}$  NMR spectrum of compound **1j**

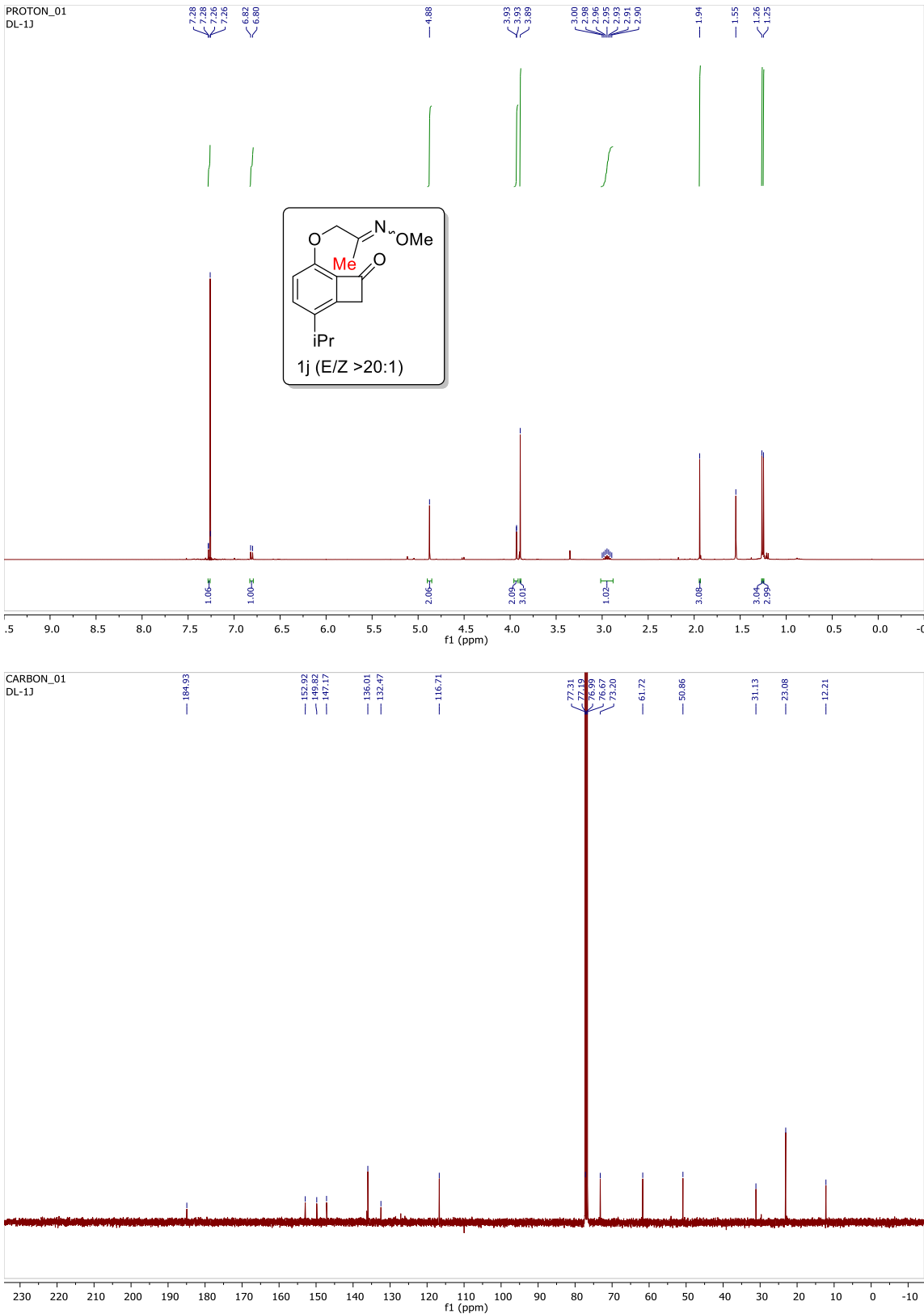


**Figure 2.11**  $^1\text{H}$  and  $^{13}\text{C}$  NMR spectrum of compound **1k**

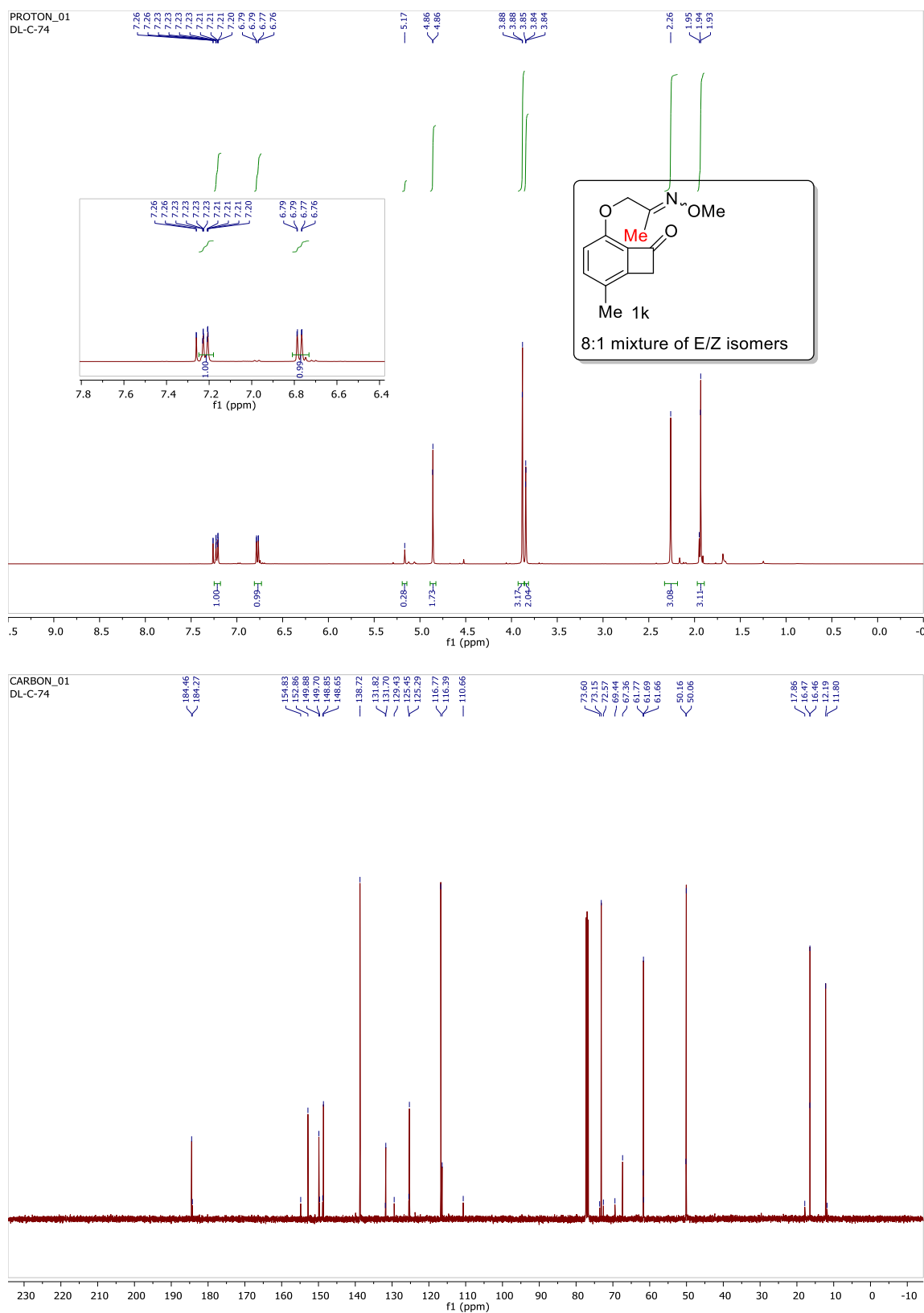


**Figure 2.12**  $^1\text{H}$  and  $^{13}\text{C}$  NMR spectrum of compound **11**

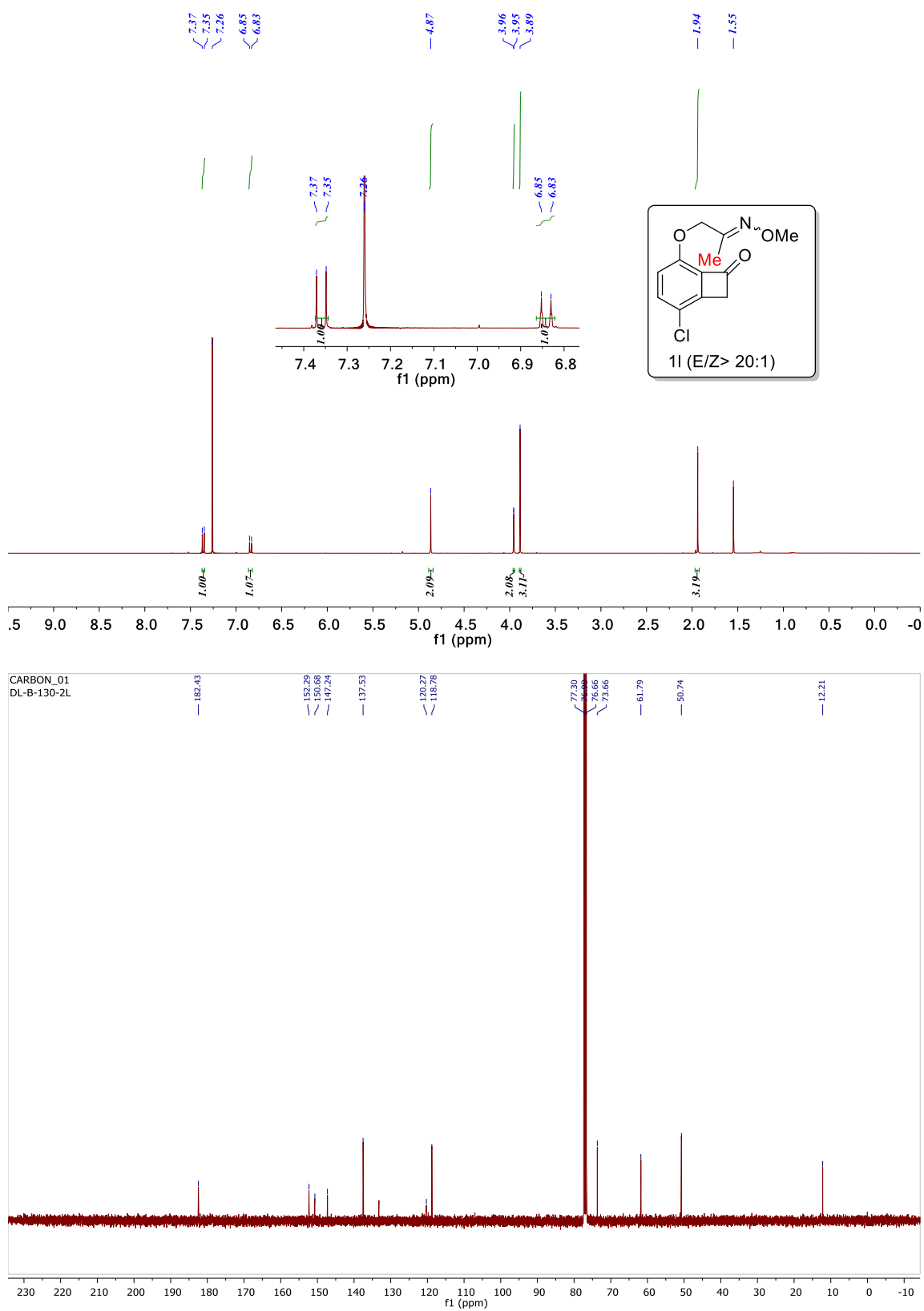


**Figure 2.13**  $^1\text{H}$  and  $^{13}\text{C}$  NMR spectrum of compound **1m**

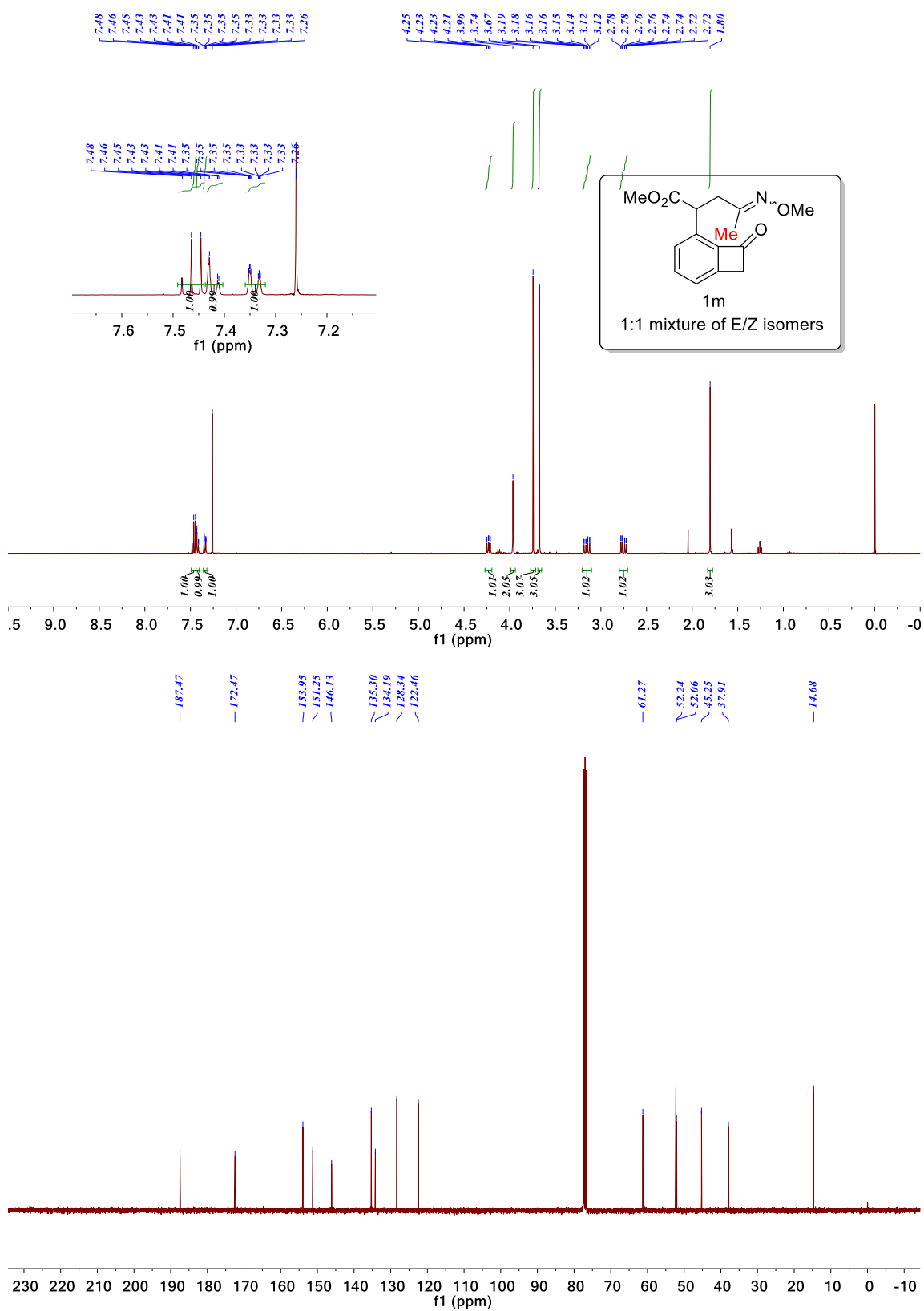




**Figure 2.14**  $^1\text{H}$  and  $^{13}\text{C}$  NMR spectrum of compound **1n**

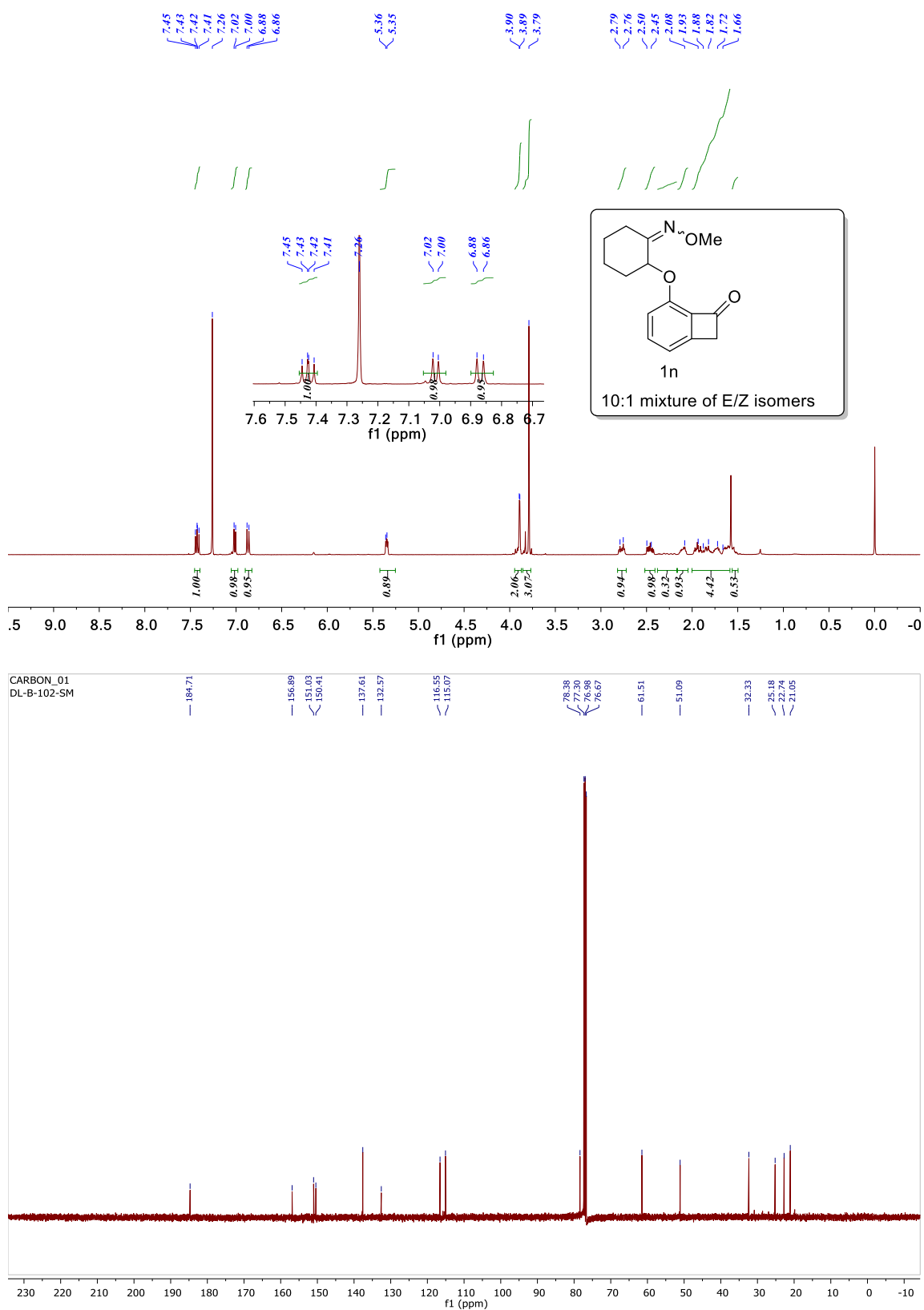


**Figure 2.15**  $^1\text{H}$  and  $^{13}\text{C}$  NMR spectrum of compound **2a**

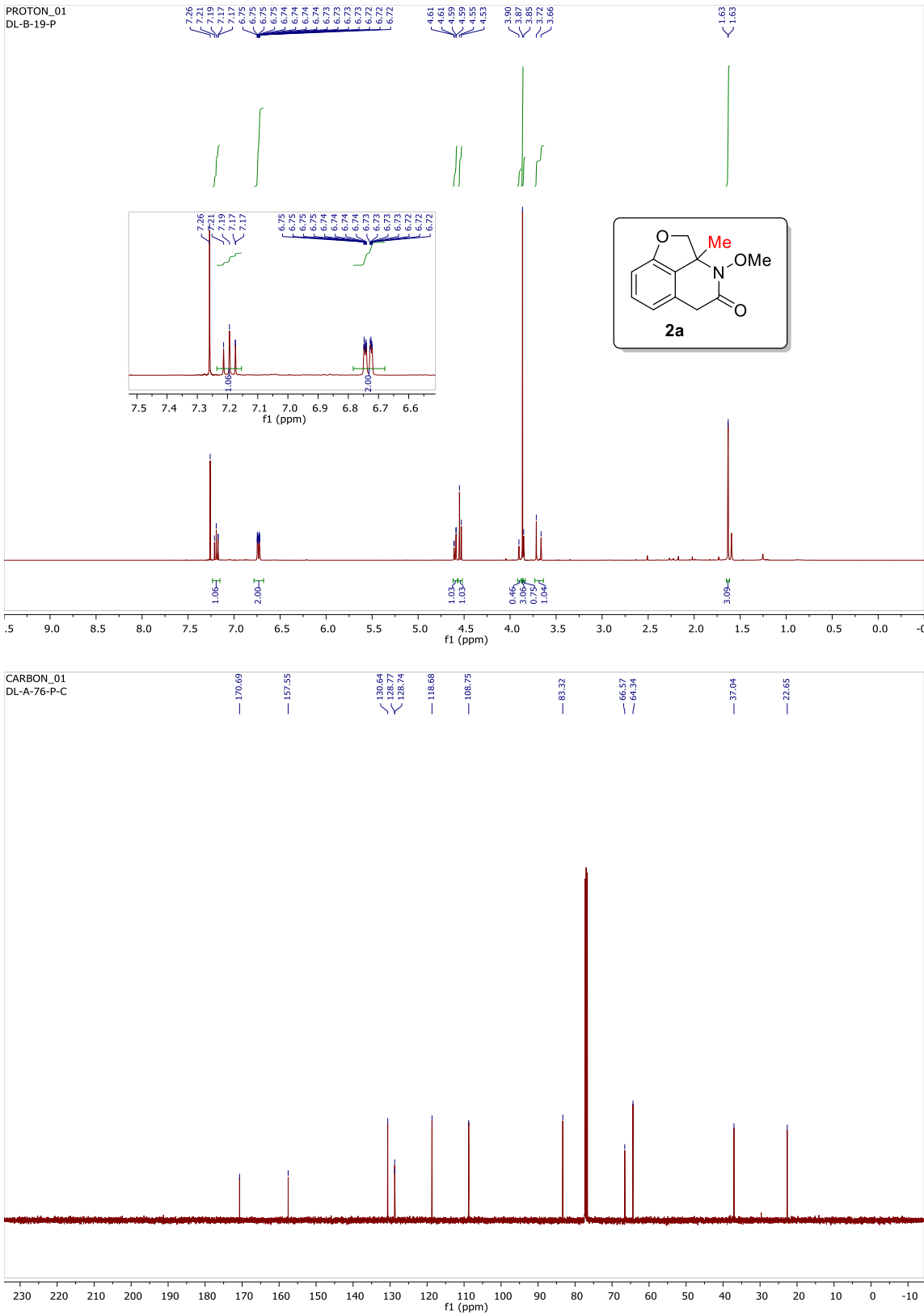


**Figure 2.16**  $^1\text{H}$  and  $^{13}\text{C}$  NMR spectrum of compound **2b**

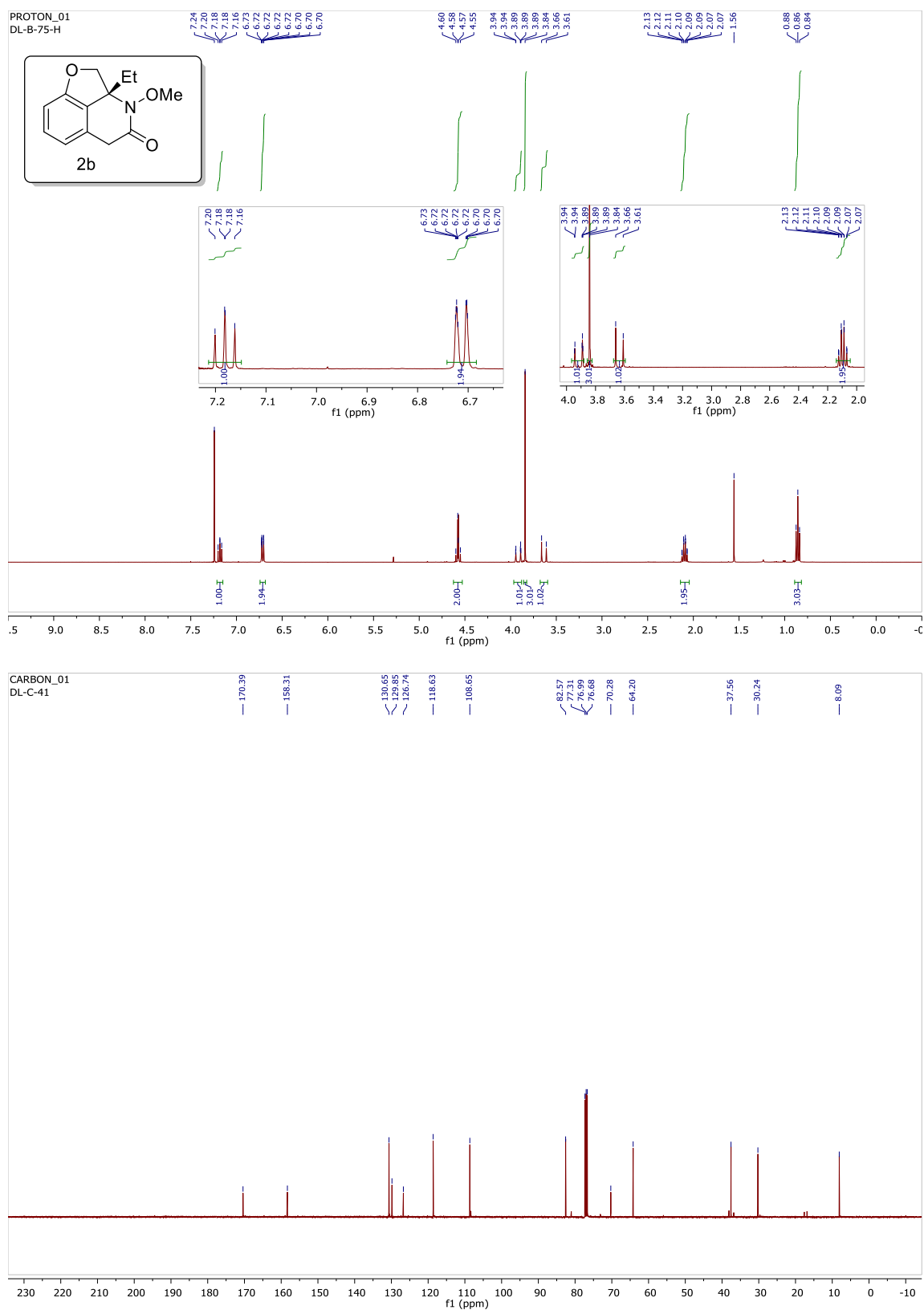


**Figure 2.17**  $^1\text{H}$  and  $^{13}\text{C}$  NMR spectrum of compound **2c**

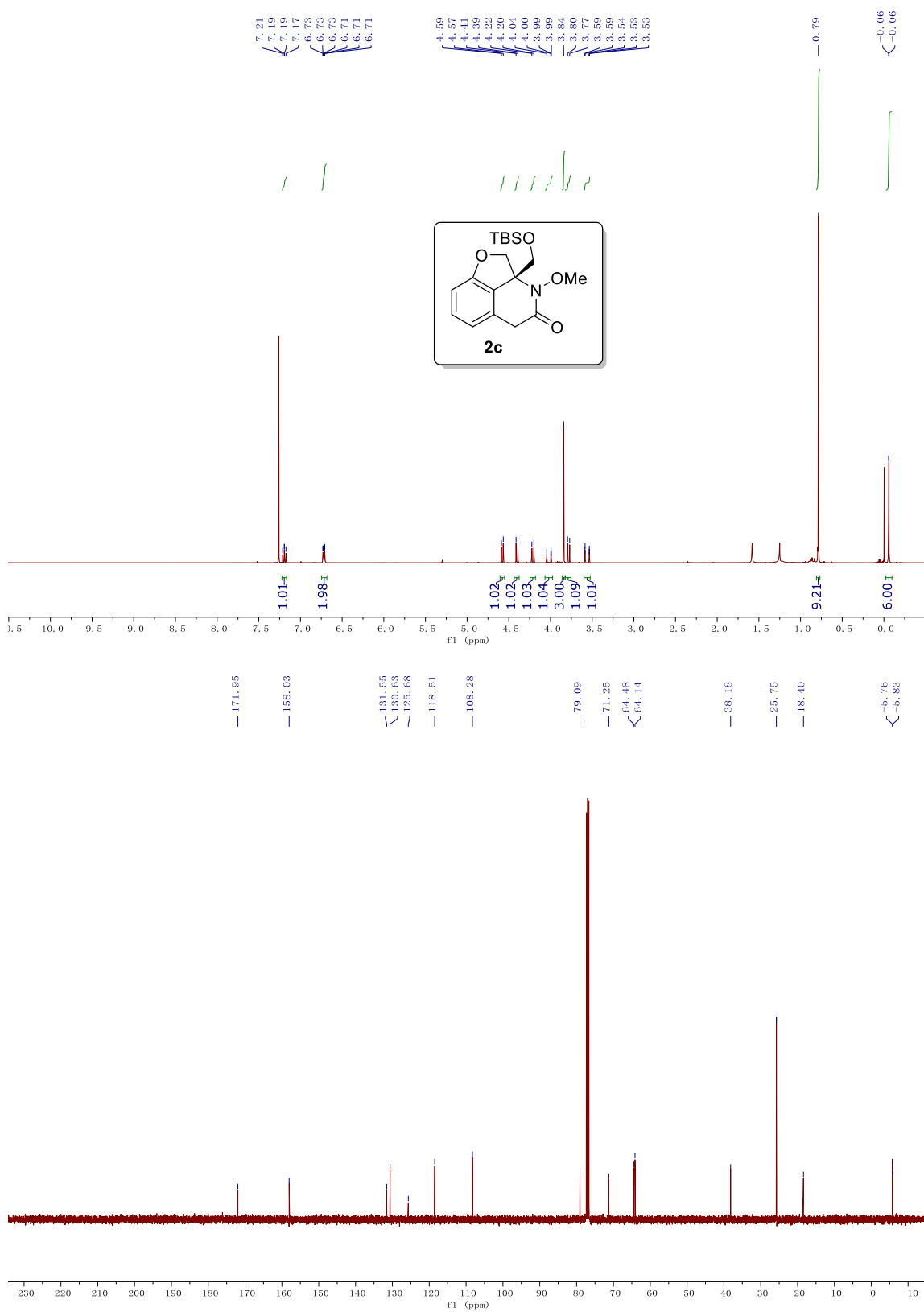


**Figure 2.18**  $^1\text{H}$  and  $^{13}\text{C}$  NMR spectrum of compound **2d**

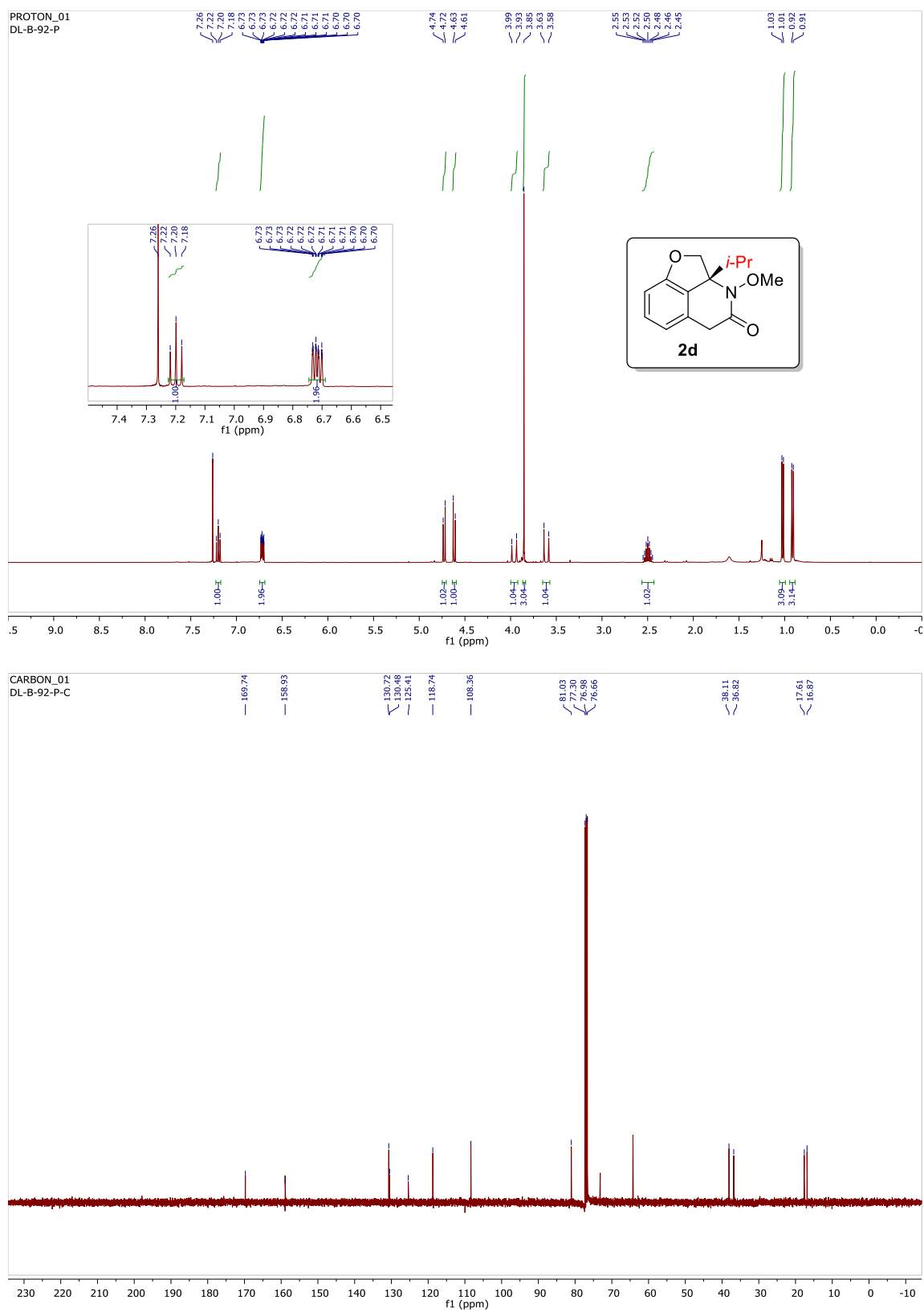


**Figure 2.19**  $^1\text{H}$  and  $^{13}\text{C}$  NMR spectrum of compound **2e**

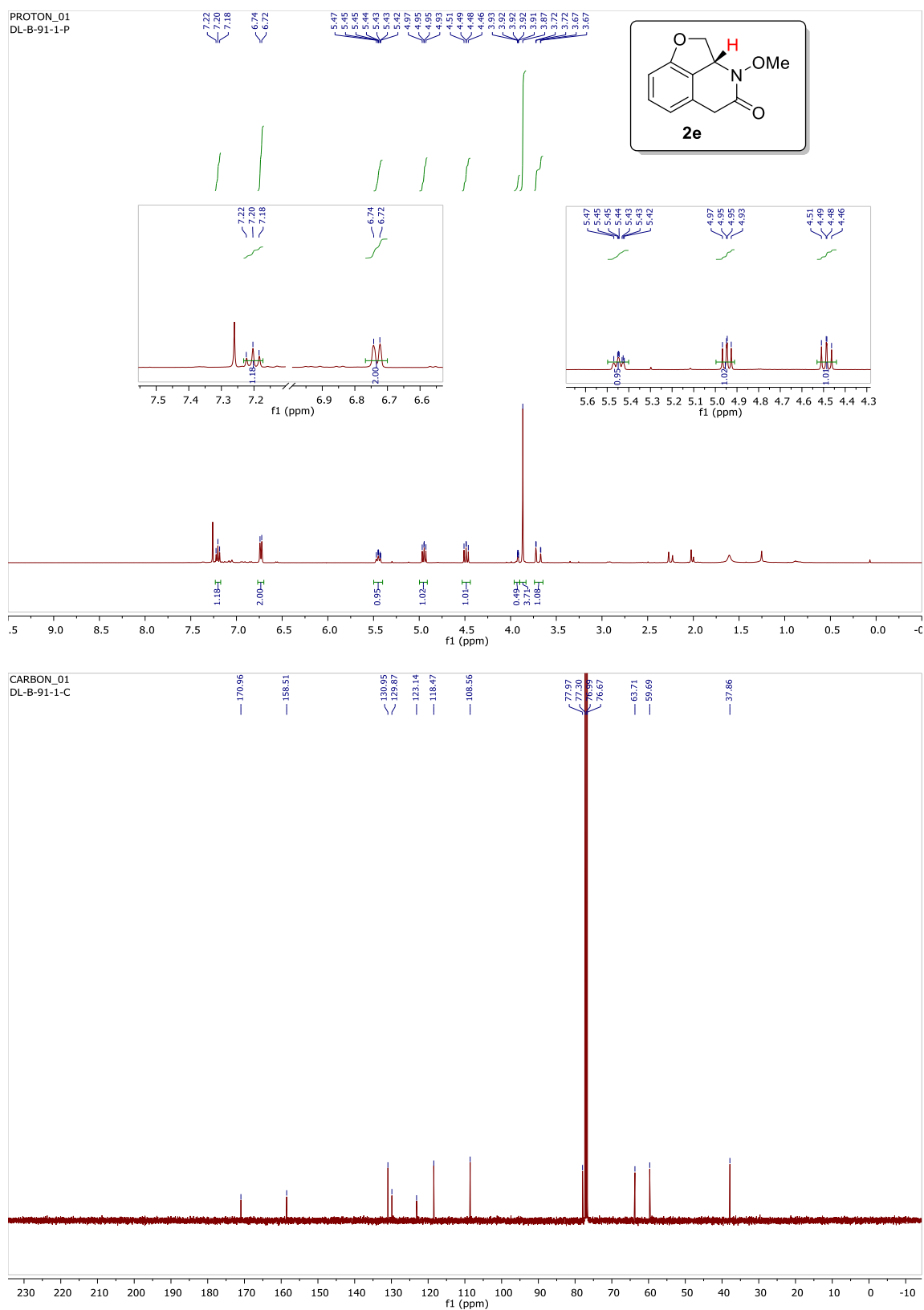


**Figure 2.20**  $^1\text{H}$  and  $^{13}\text{C}$  NMR spectrum of compound **2f**

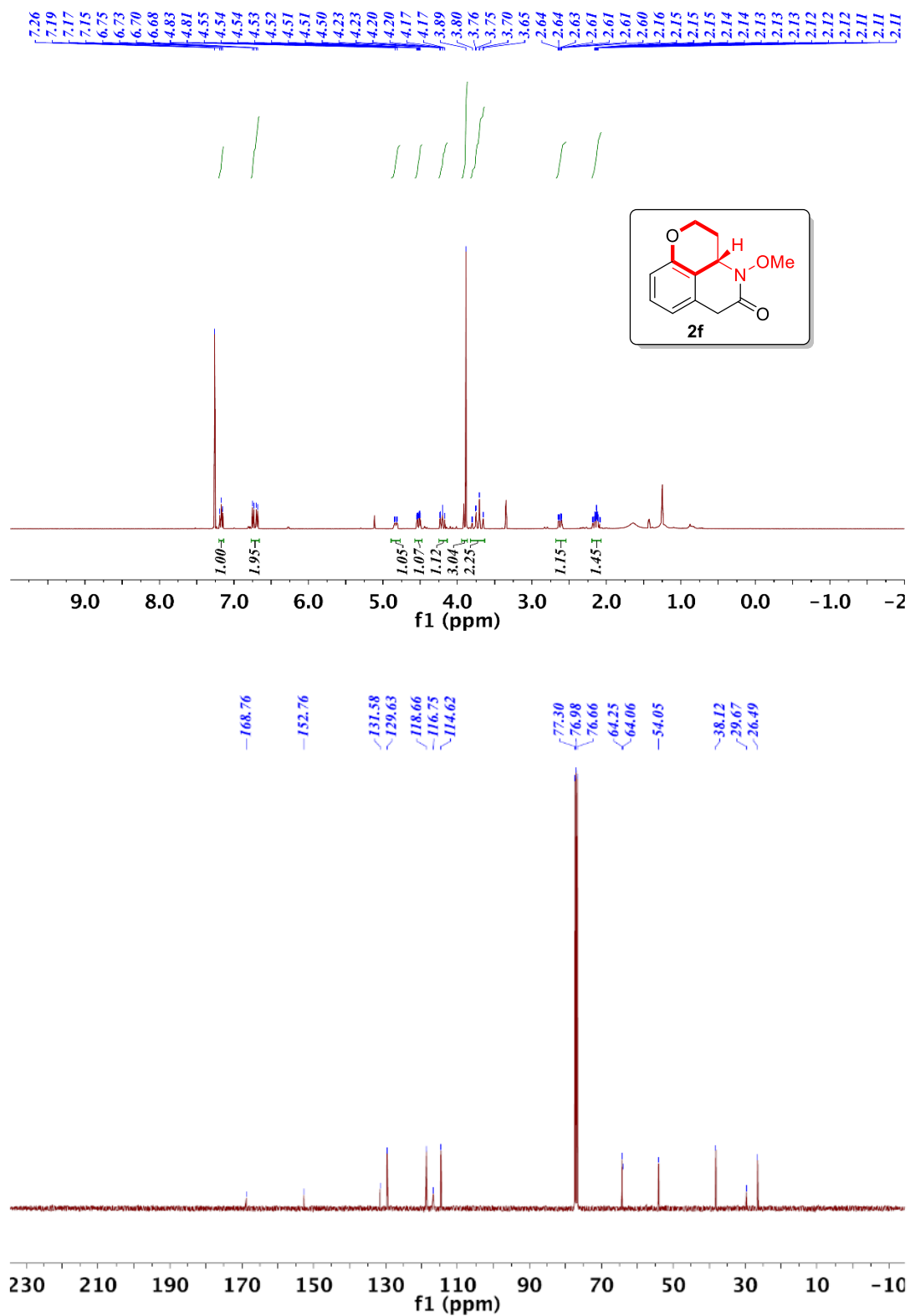


**Figure 2.21**  $^1\text{H}$  and  $^{13}\text{C}$  NMR spectrum of compound **2g**

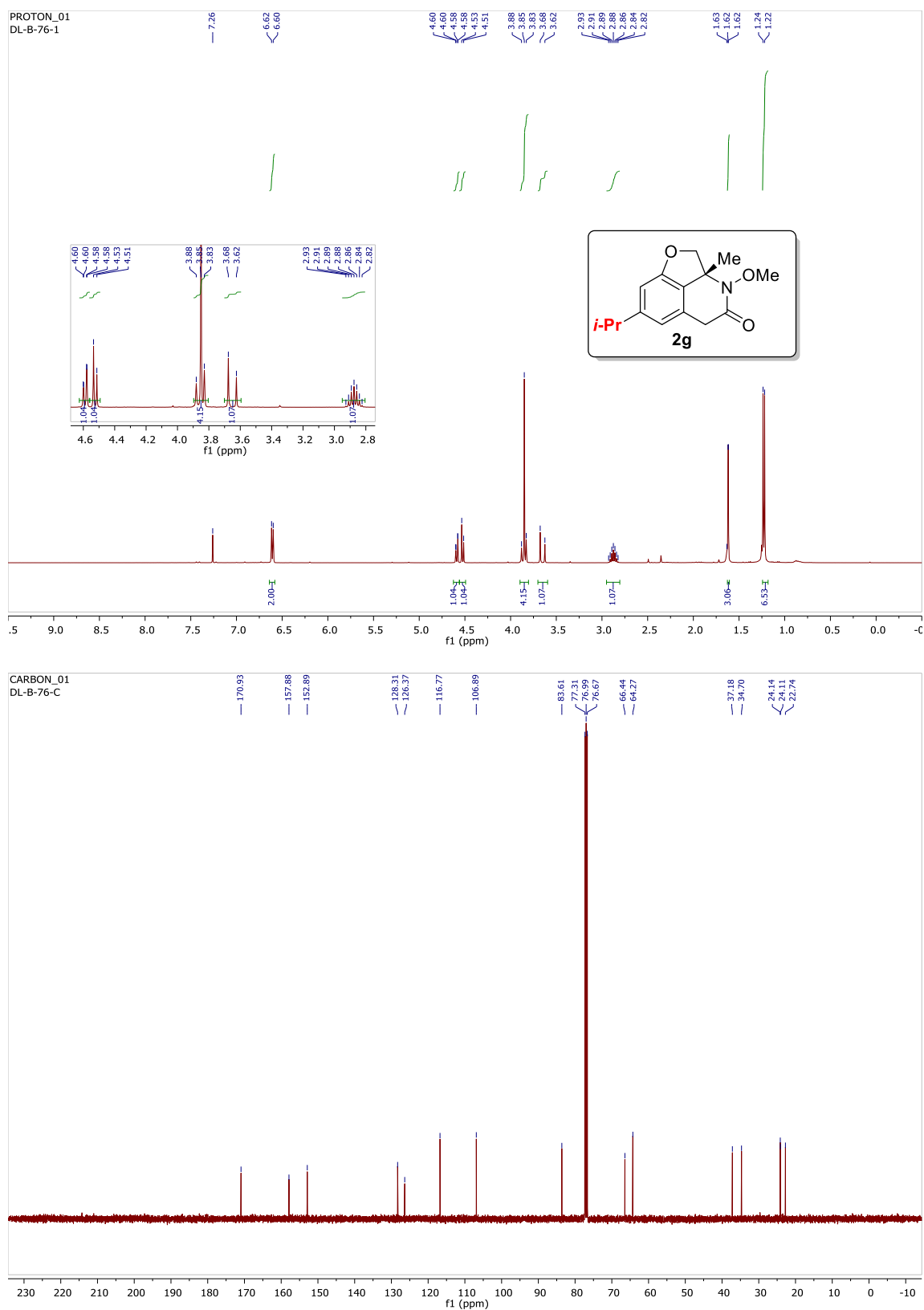




**Figure 2.22**  $^1\text{H}$  and  $^{13}\text{C}$  NMR spectrum of compound **2h**

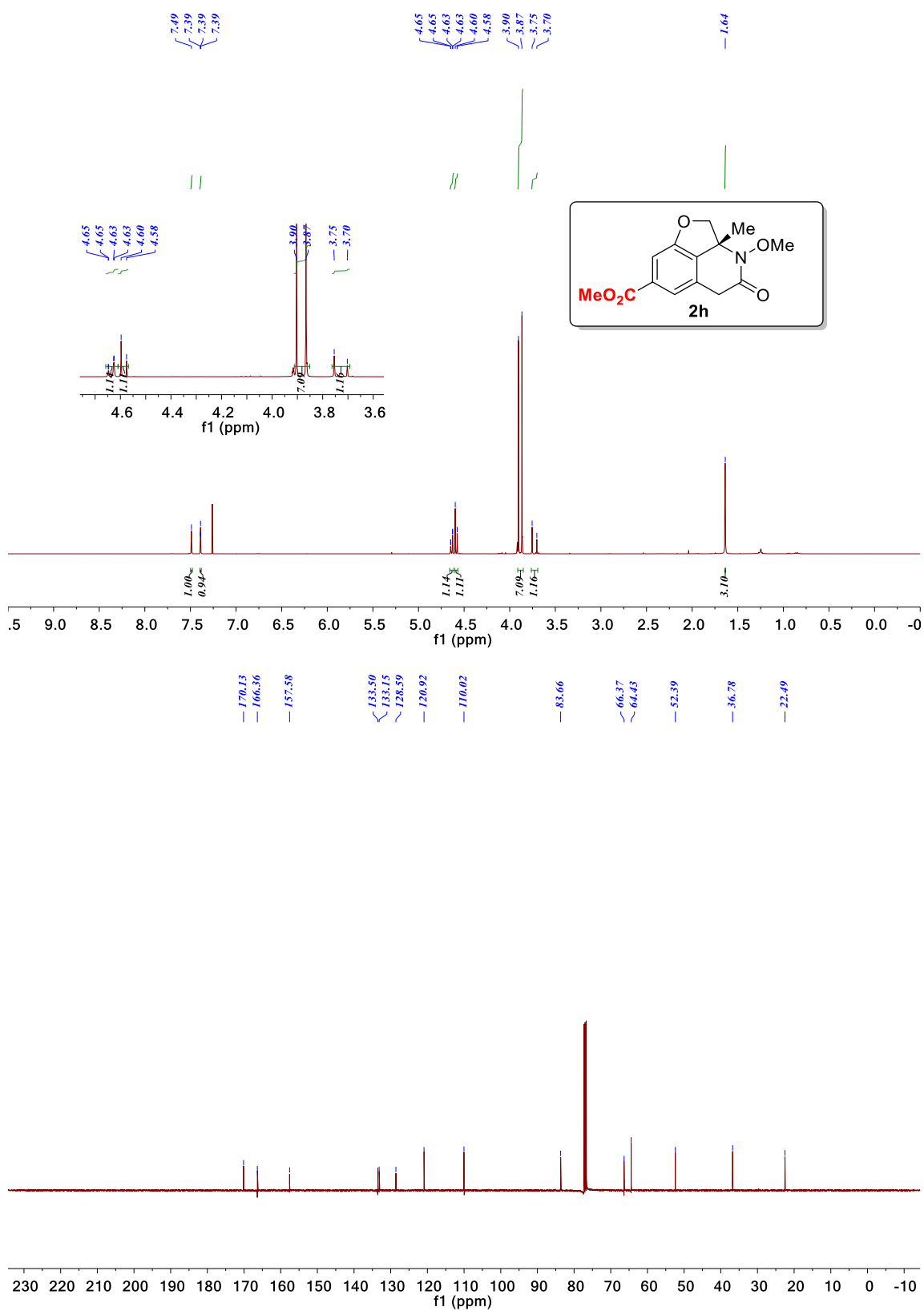


**Figure 2.23**  $^1\text{H}$  and  $^{13}\text{C}$  NMR spectrum of compound **2i**

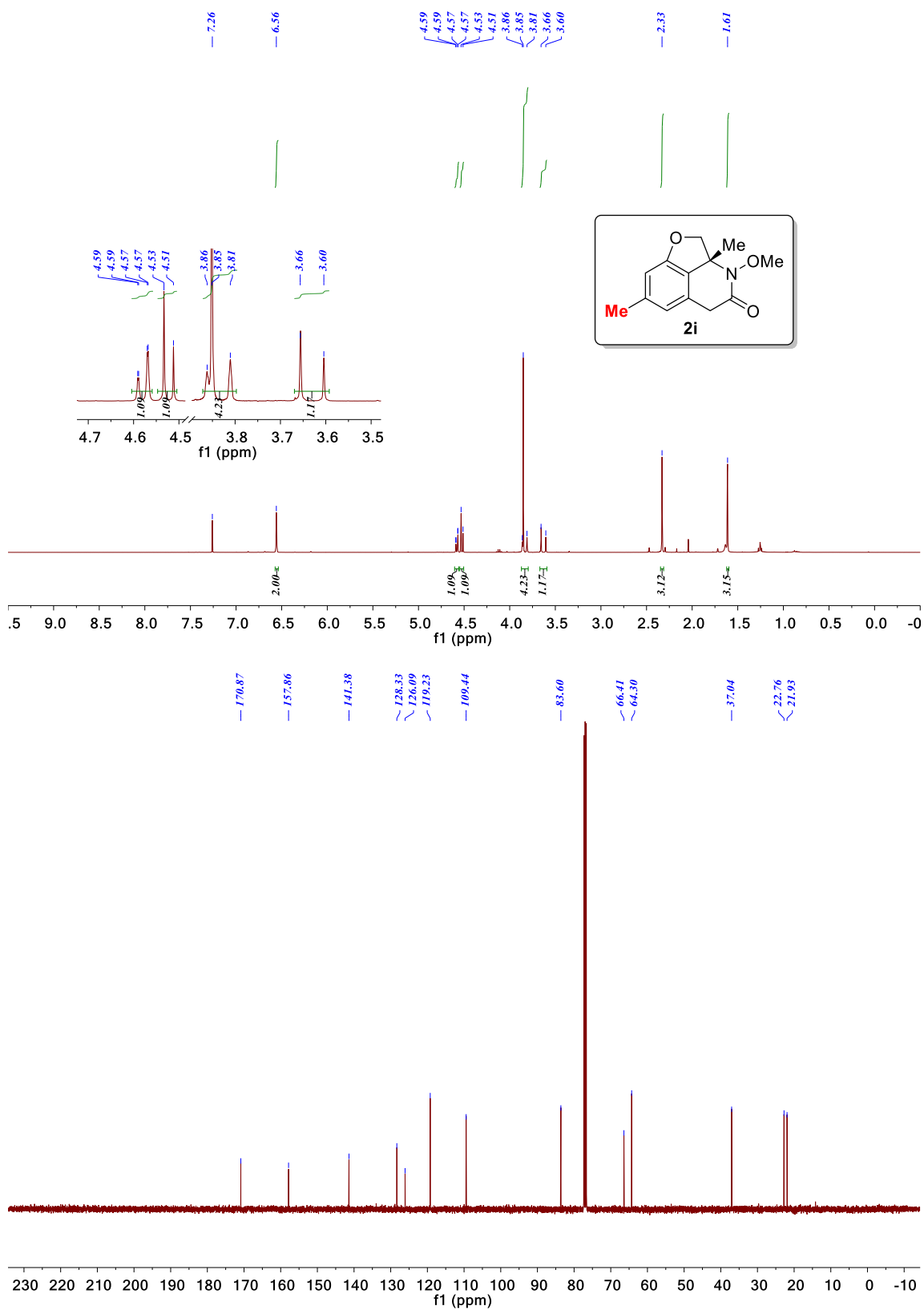


**Figure 2.24**  $^1\text{H}$  and  $^{13}\text{C}$  NMR spectrum of compound **2j**

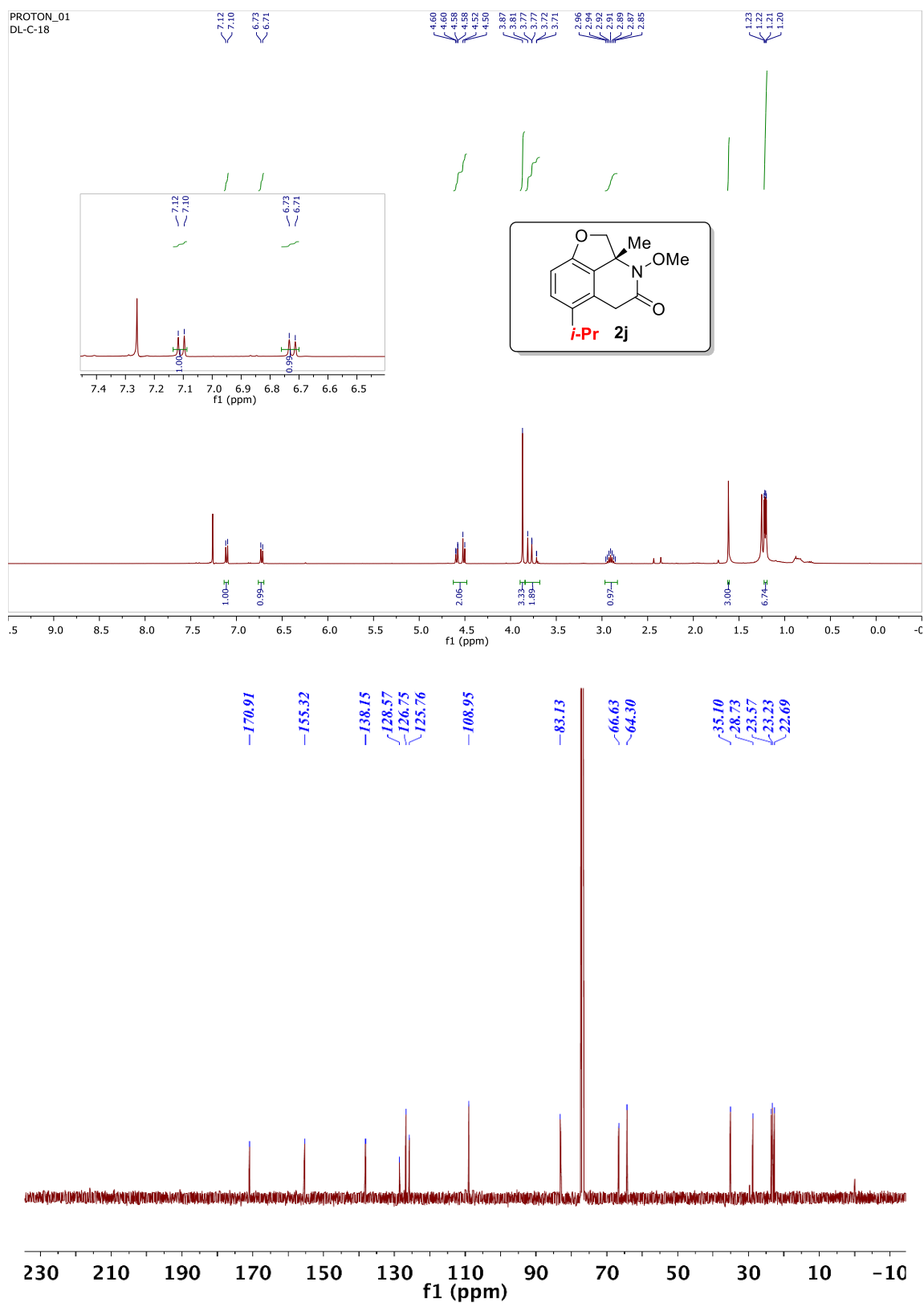


**Figure 2.25**  $^1\text{H}$  and  $^{13}\text{C}$  NMR spectrum of compound **2k**

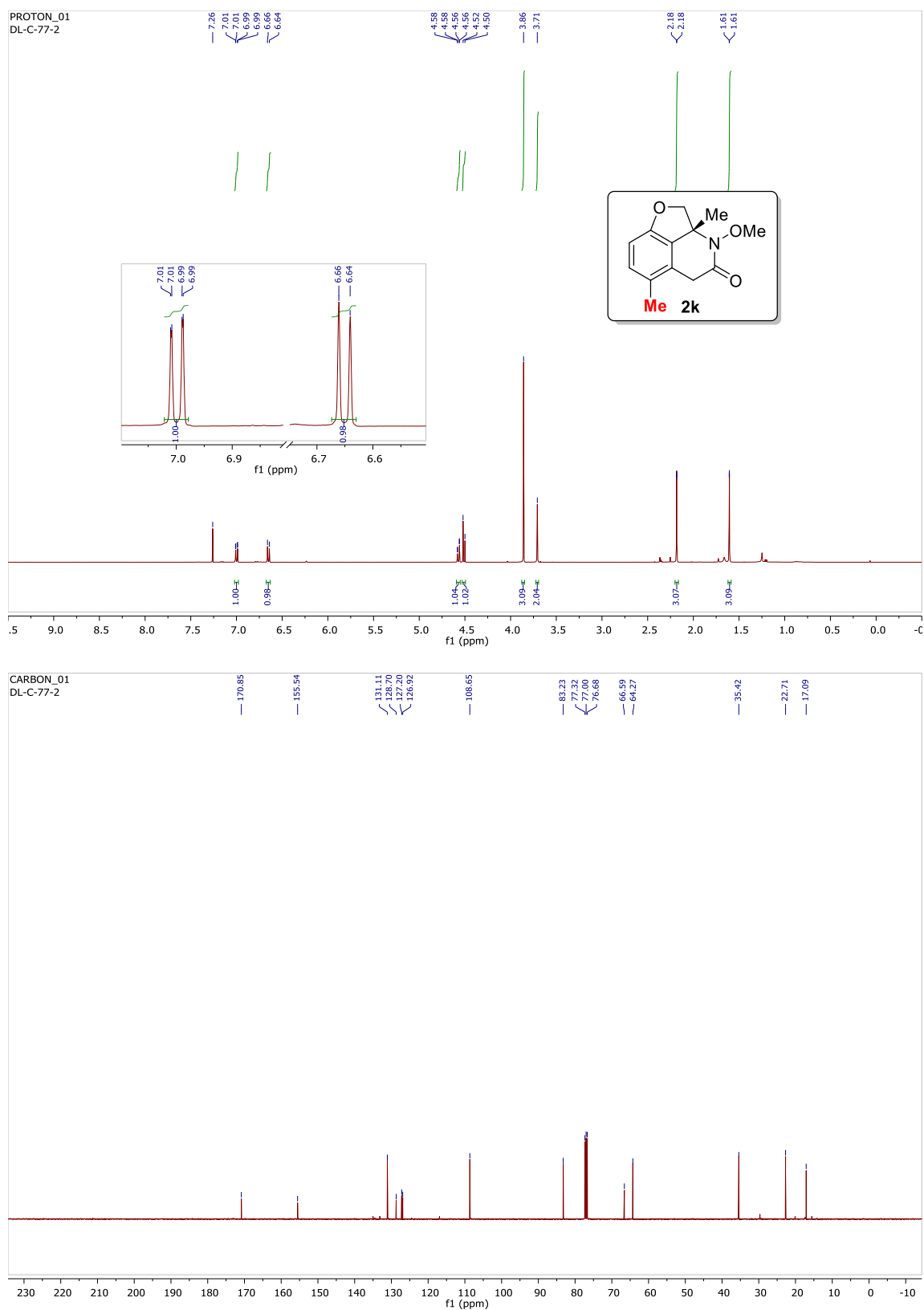


**Figure 2.26**  $^1\text{H}$  and  $^{13}\text{C}$  NMR spectrum of compound **21**

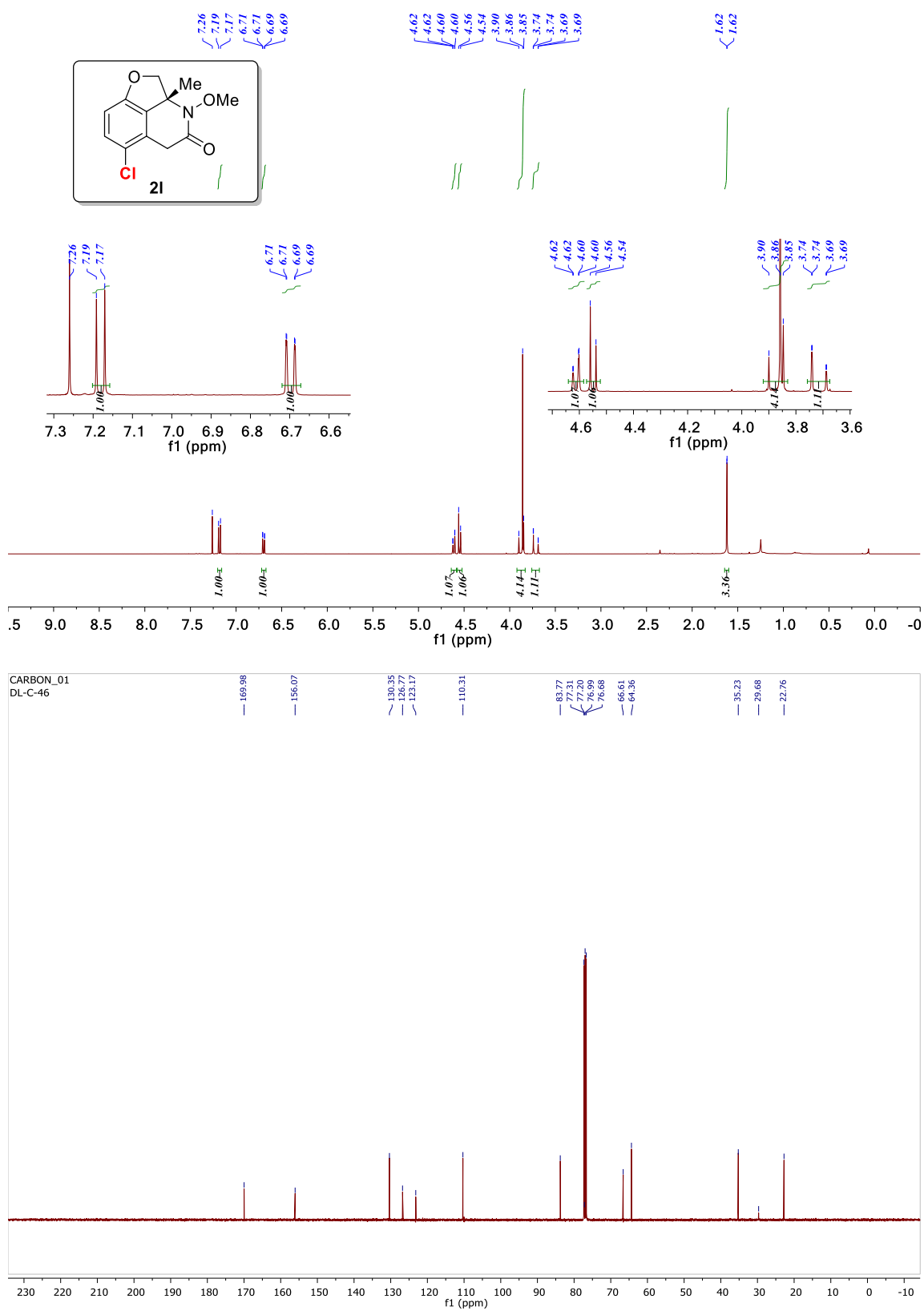


**Figure 2.27**  $^1\text{H}$  and  $^{13}\text{C}$  NMR spectrum of compound **2m**

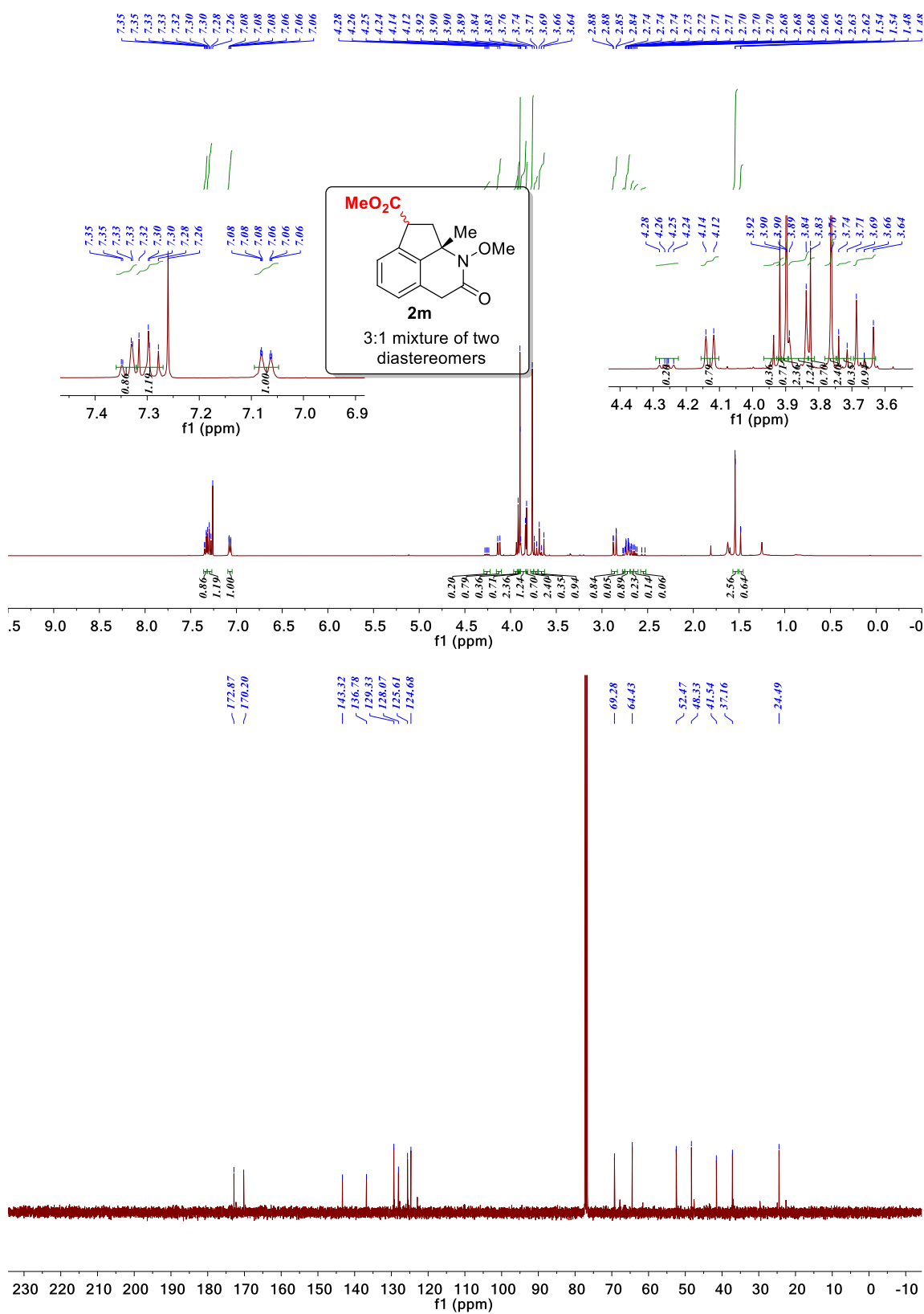


**Figure 2.28**  $^1\text{H}$  and  $^{13}\text{C}$  NMR spectrum of compound **2n**

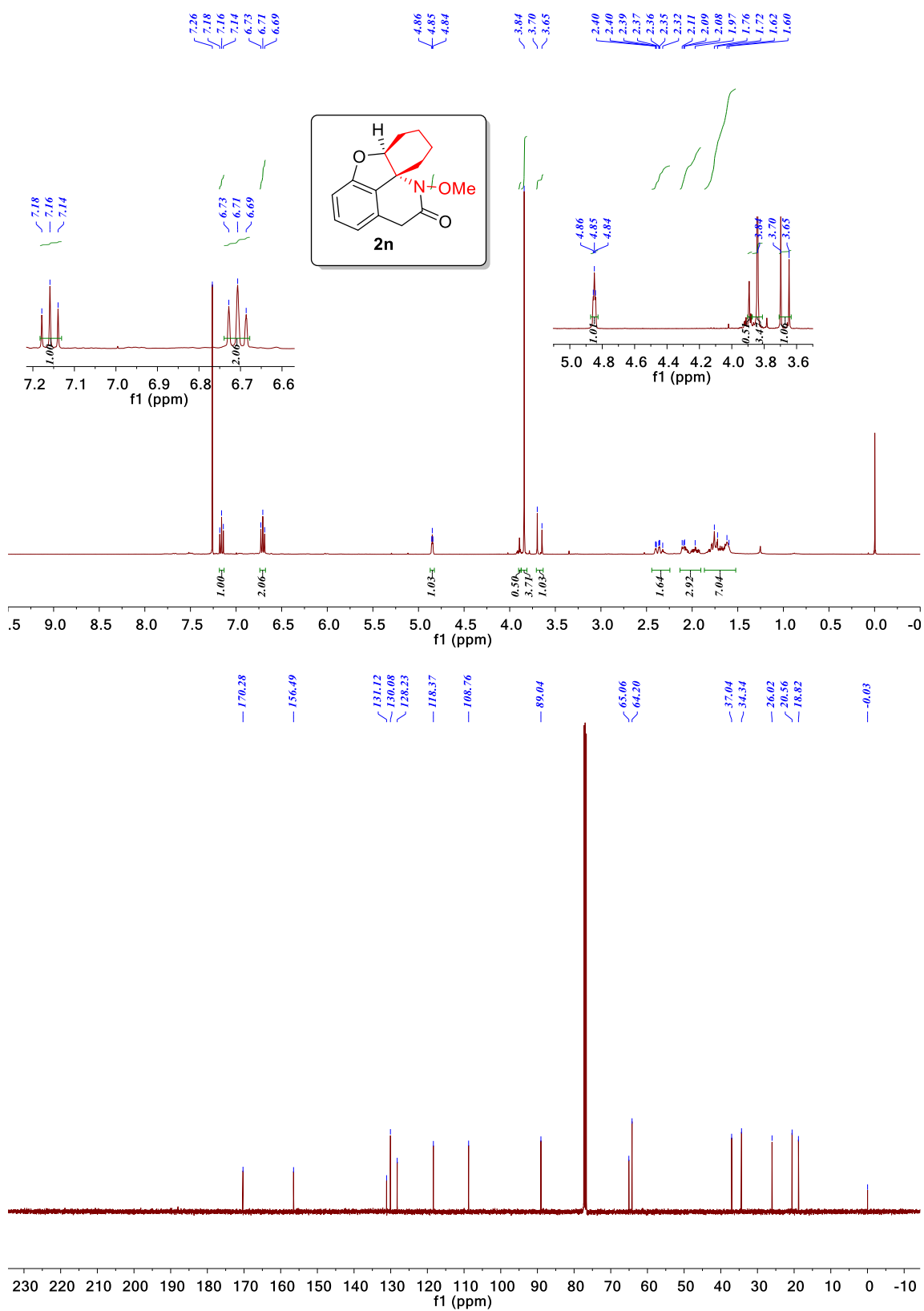


**Figure 2.29**  $^1\text{H}$  and  $^{13}\text{C}$  NMR spectrum of compound **1j-II**

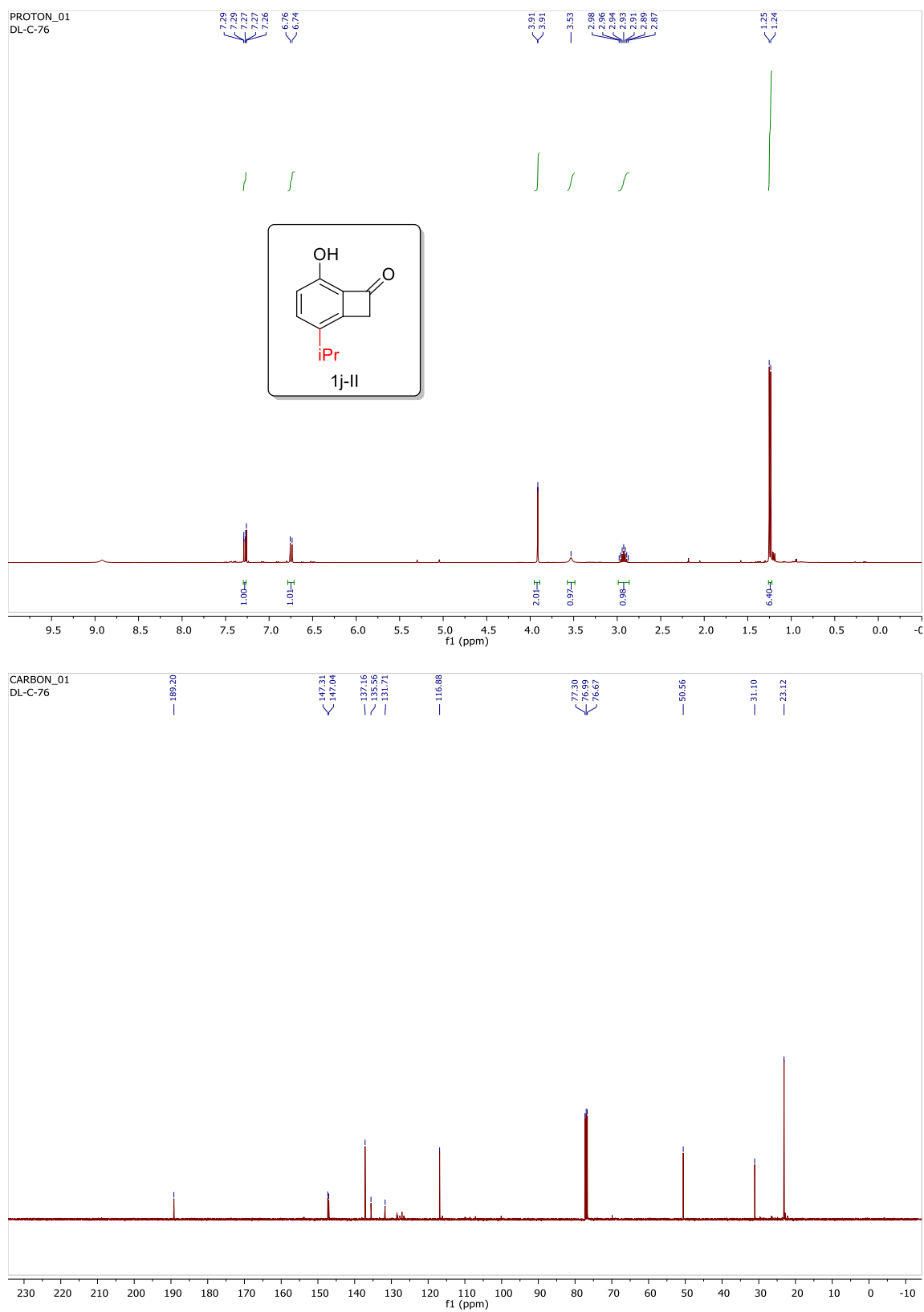




**Figure 2.30**  $^1\text{H}$  and  $^{13}\text{C}$  NMR spectrum of compound **1k-II**

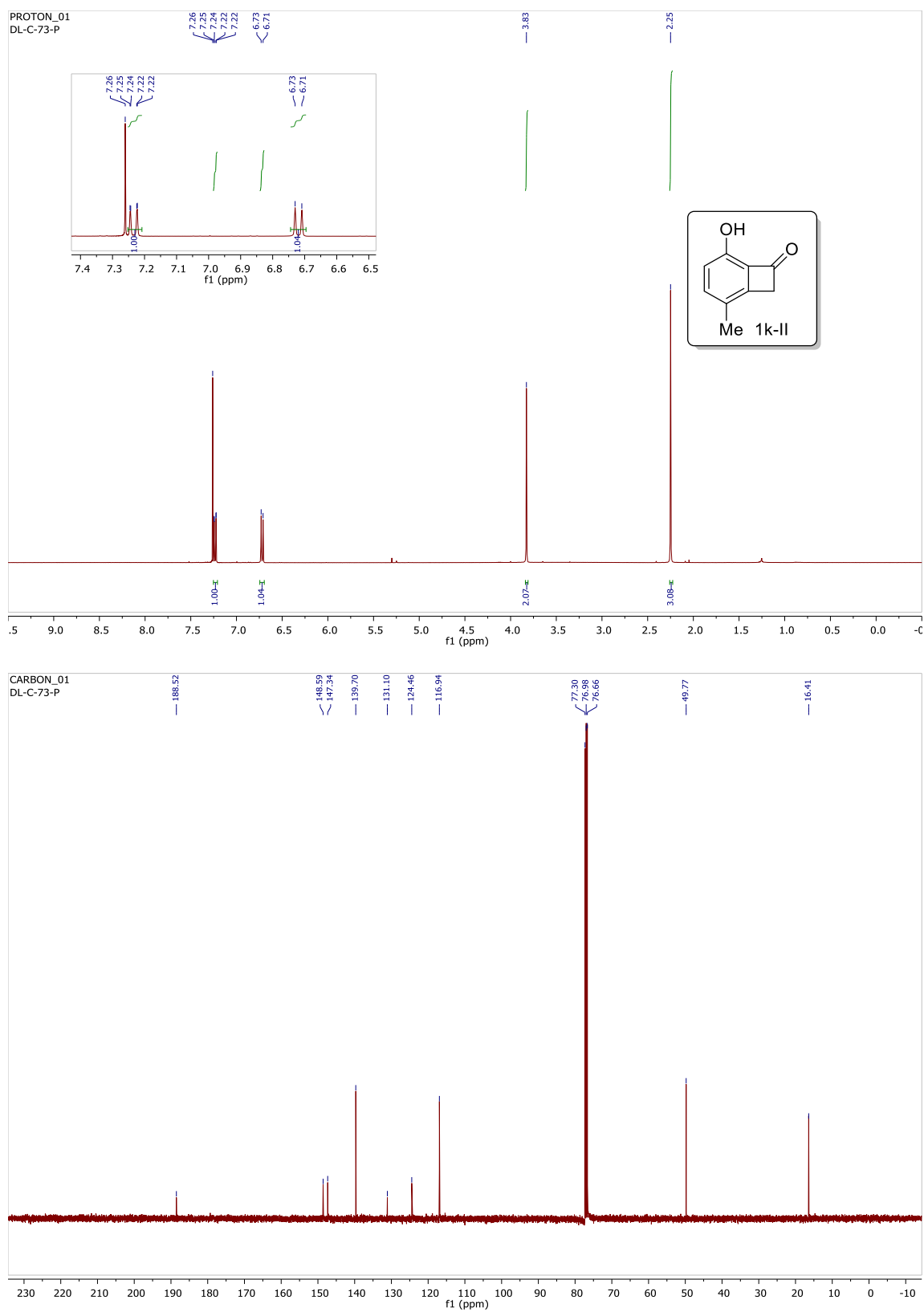


**Figure 2.31**  $^1\text{H}$  and  $^{13}\text{C}$  NMR spectrum of compound **11-II**

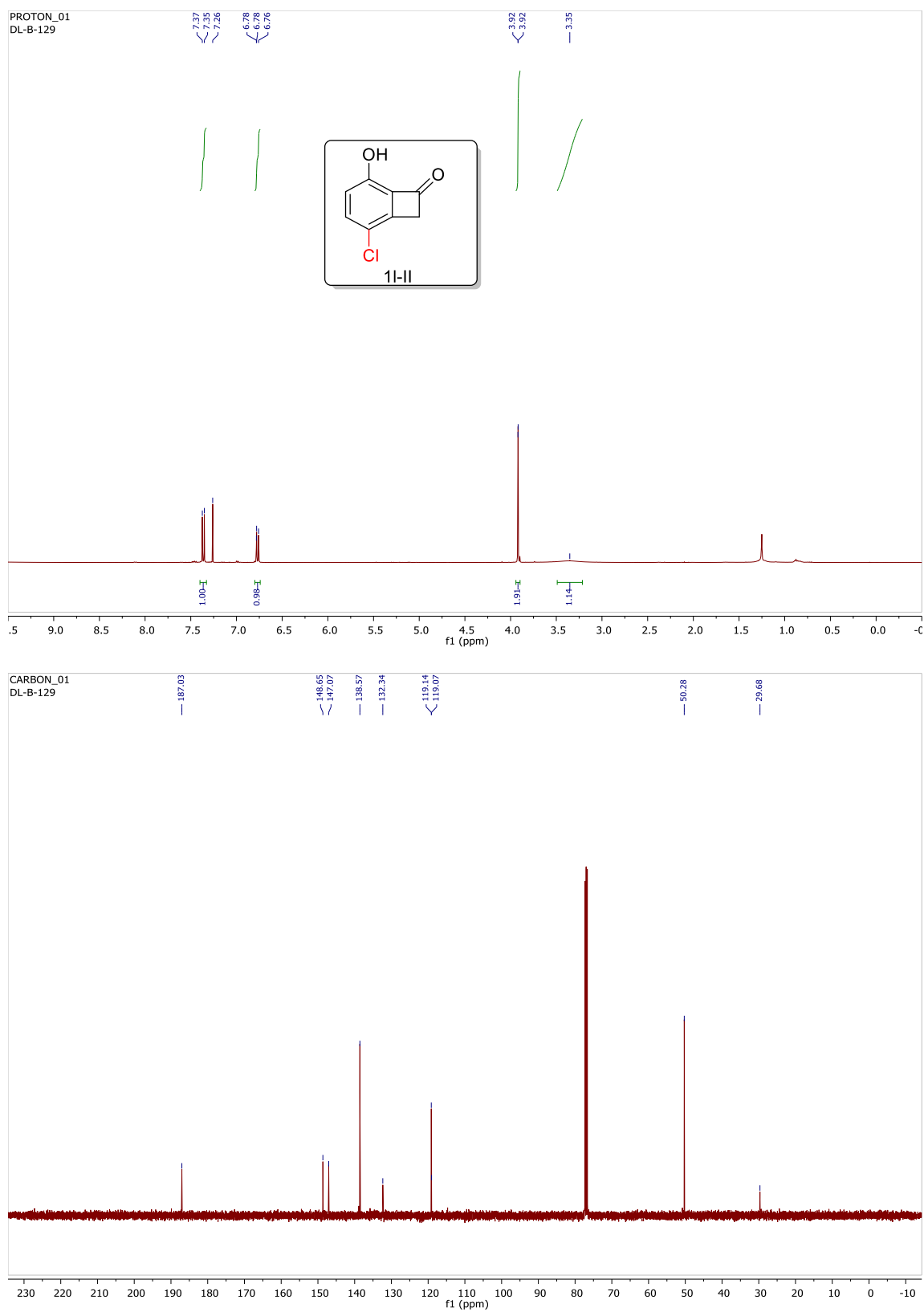


**Figure 2.32**  $^1\text{H}$  and  $^{13}\text{C}$  NMR spectrum of compound **1k-III**

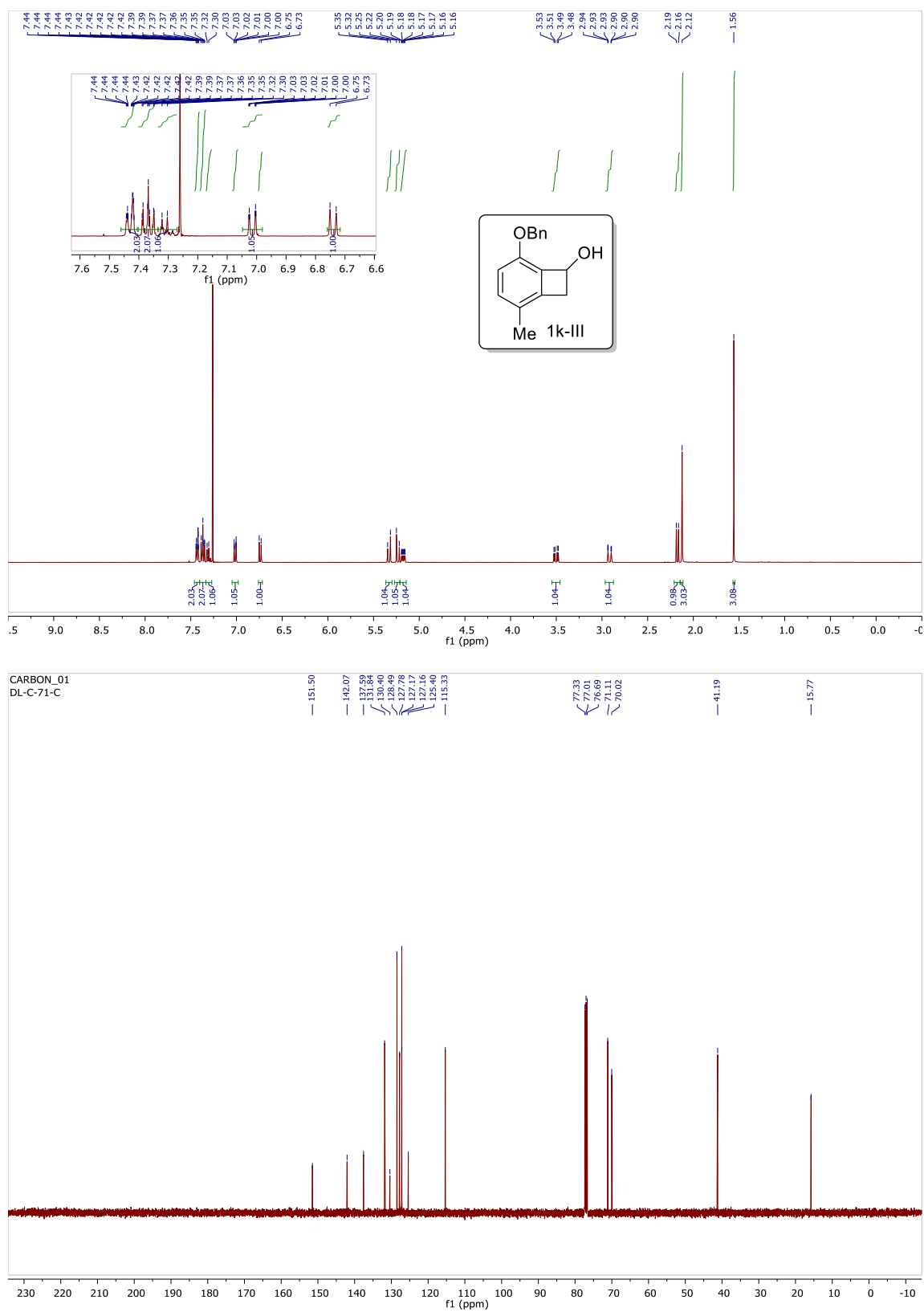


**Figure 2.33**  $^1\text{H}$  and  $^{13}\text{C}$  NMR spectrum of compound **1k-IV**

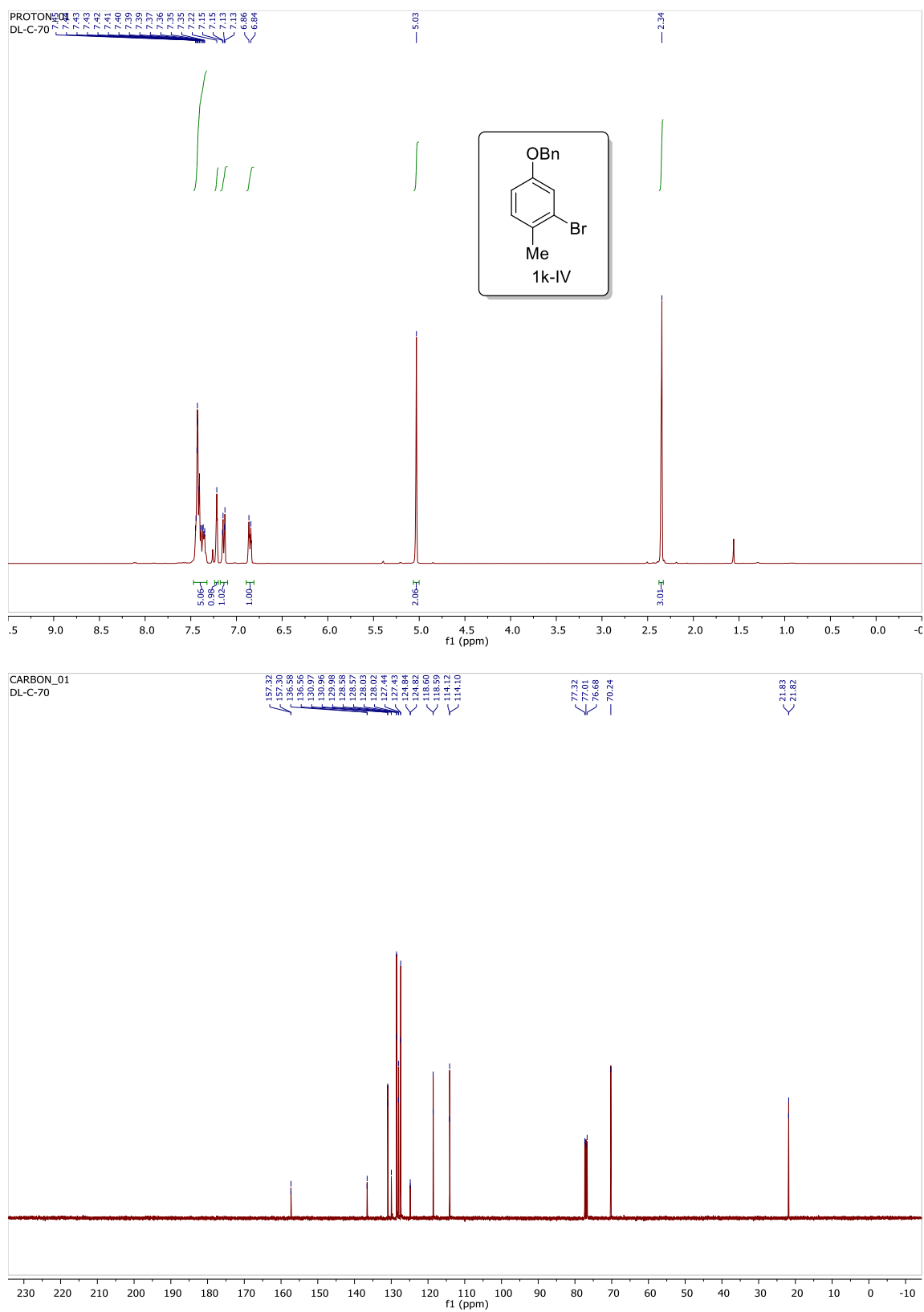


**Figure 2.34**  $^1\text{H}$  and  $^{13}\text{C}$  NMR spectrum of compound **3**

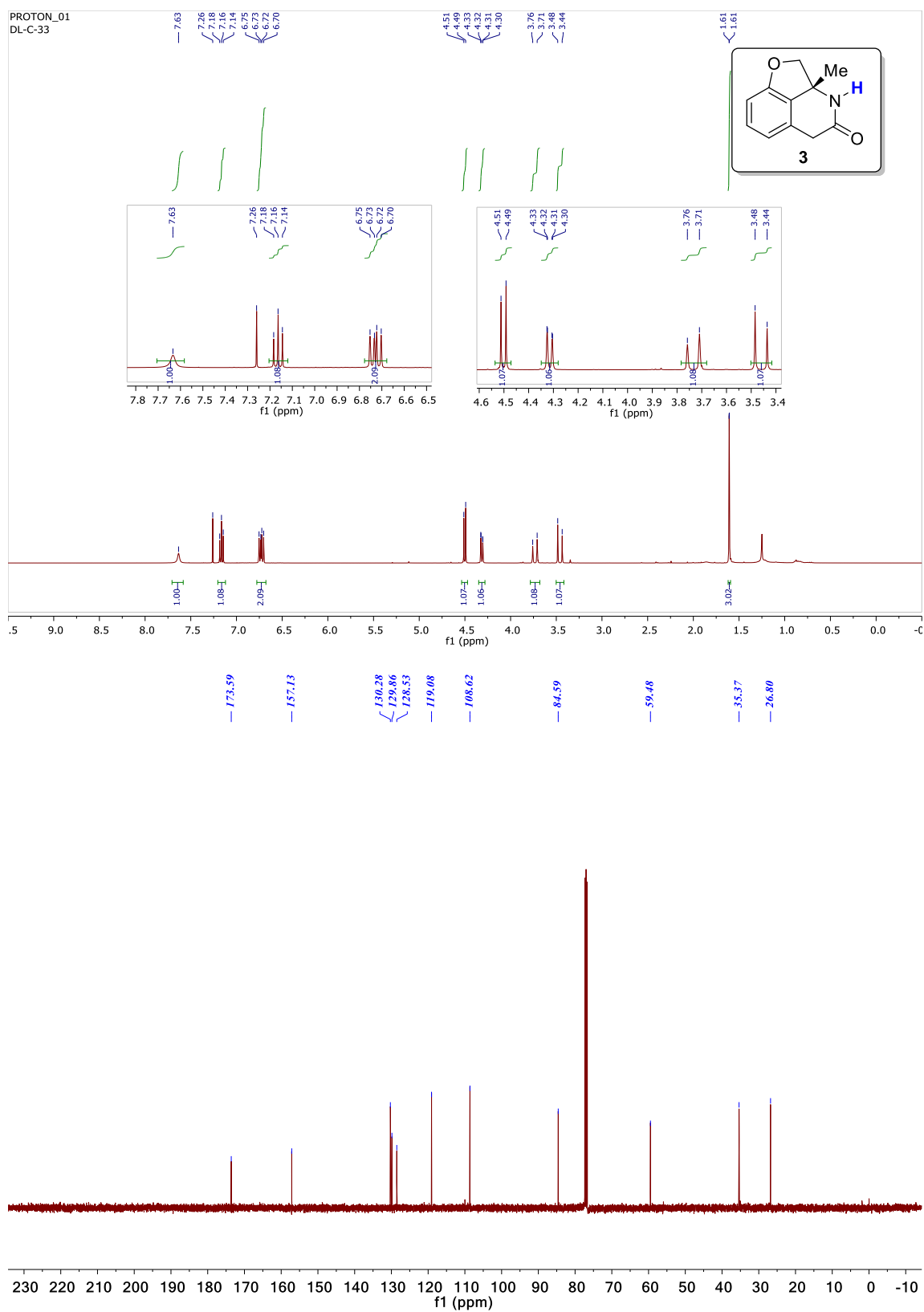


**Figure 2.35**  $^1\text{H}$  and  $^{13}\text{C}$  NMR spectrum of compound **4**

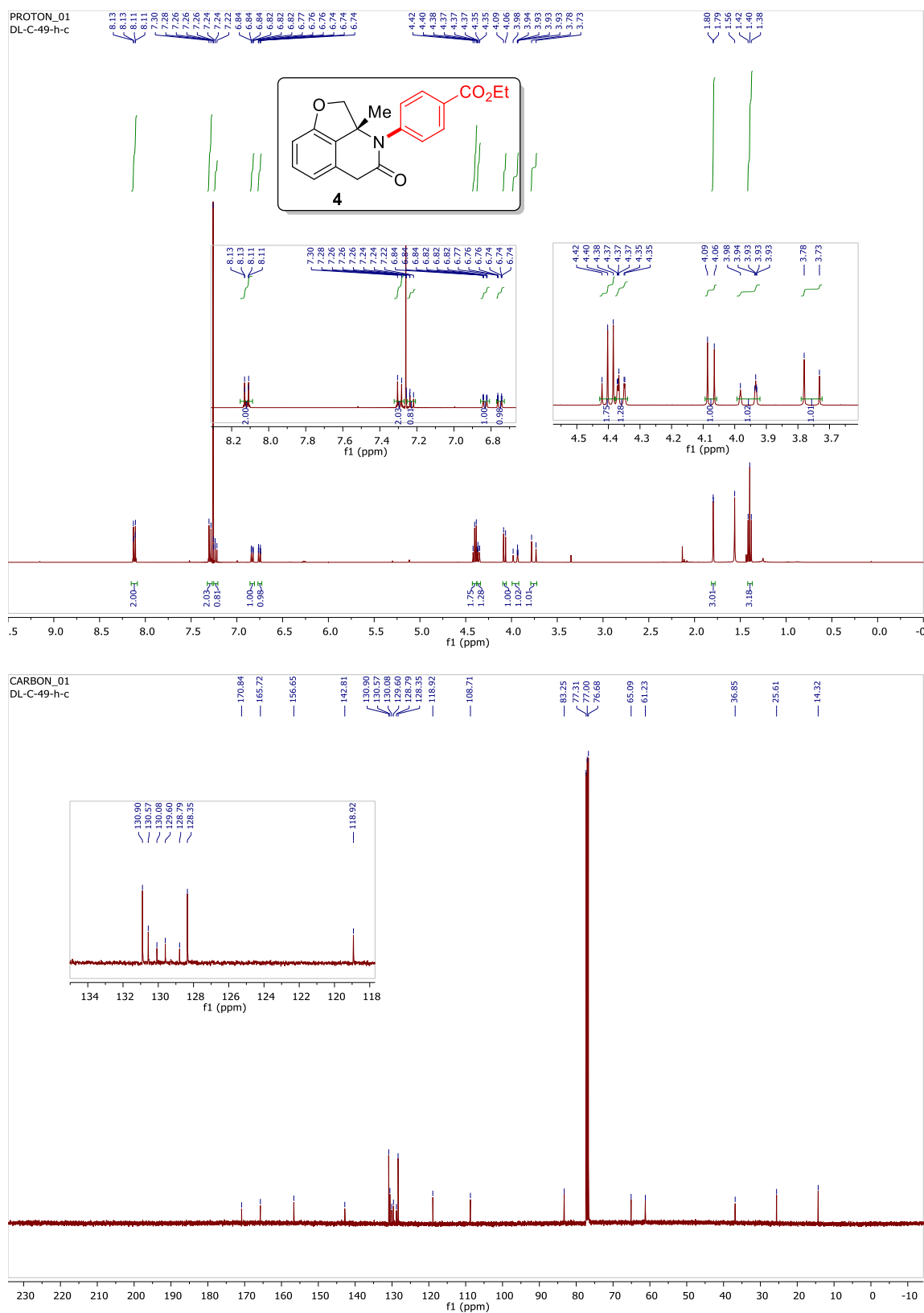


**Figure 2.36**  $^1\text{H}$  and  $^{13}\text{C}$  NMR spectrum of compound **5**

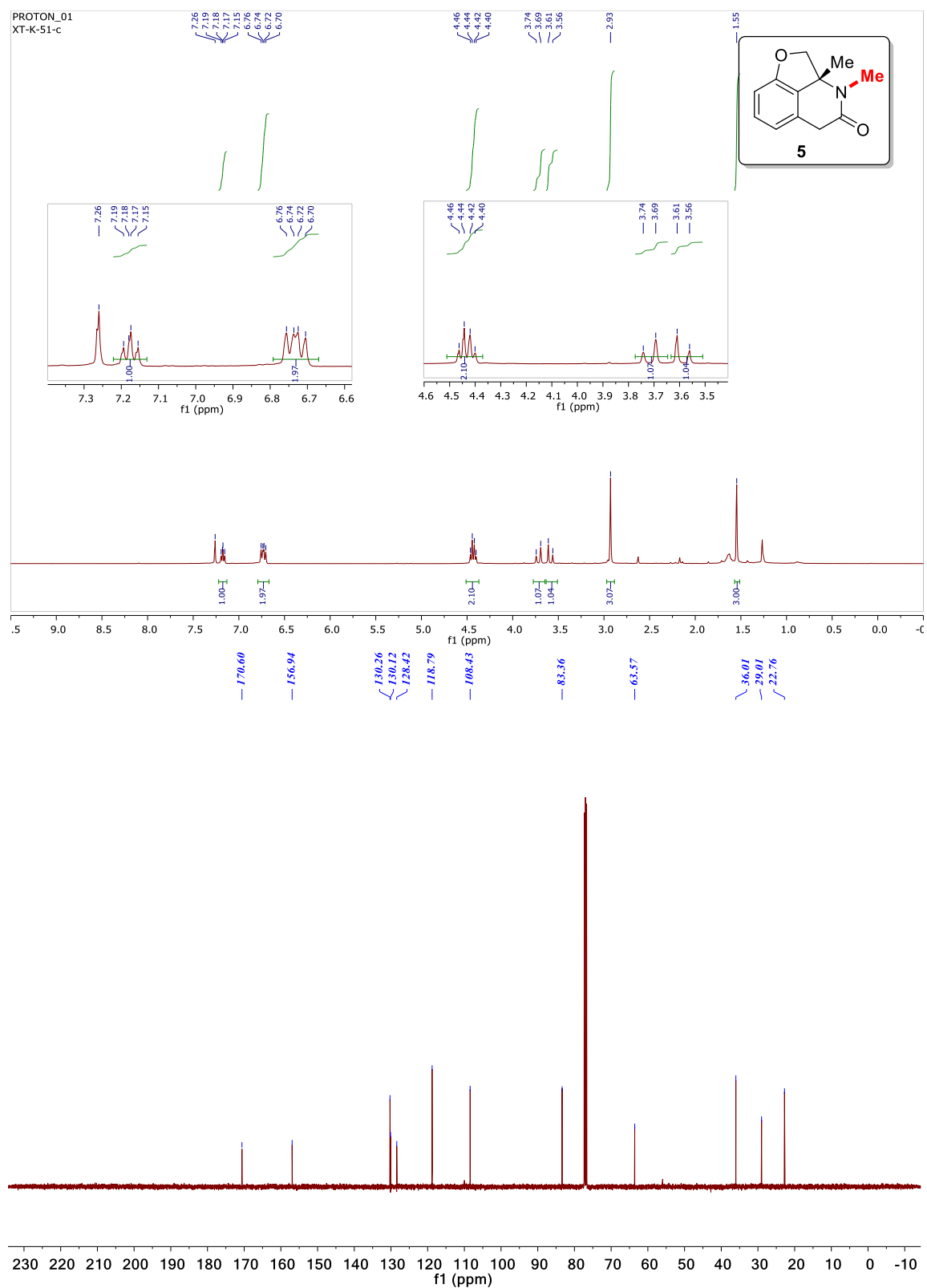


**Figure 2.37**  $^1\text{H}$  and  $^{13}\text{C}$  NMR spectrum of compound **6**

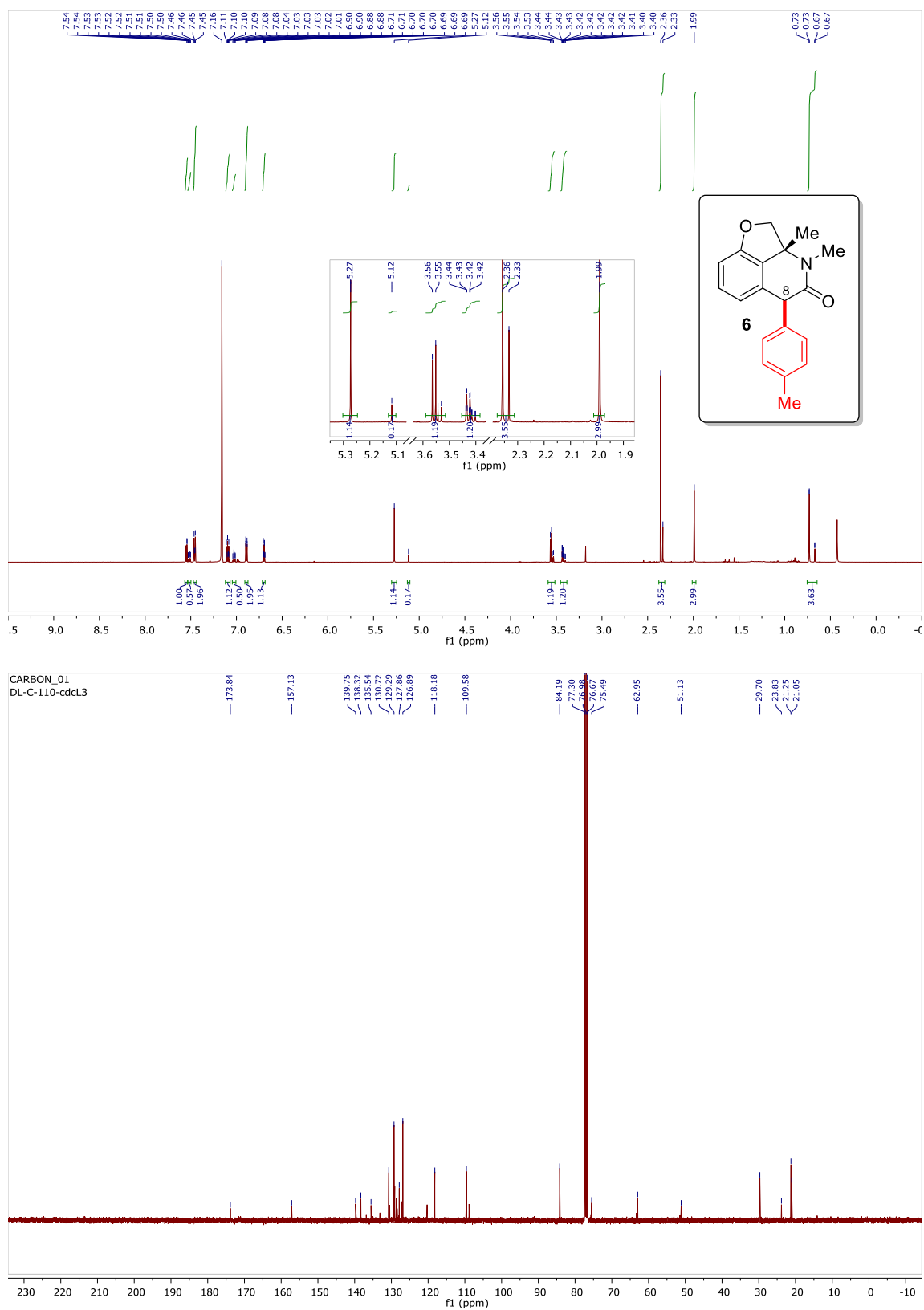




**Figure 2.38**  $^1\text{H}$  and  $^{13}\text{C}$  NMR spectrum of compound **7**

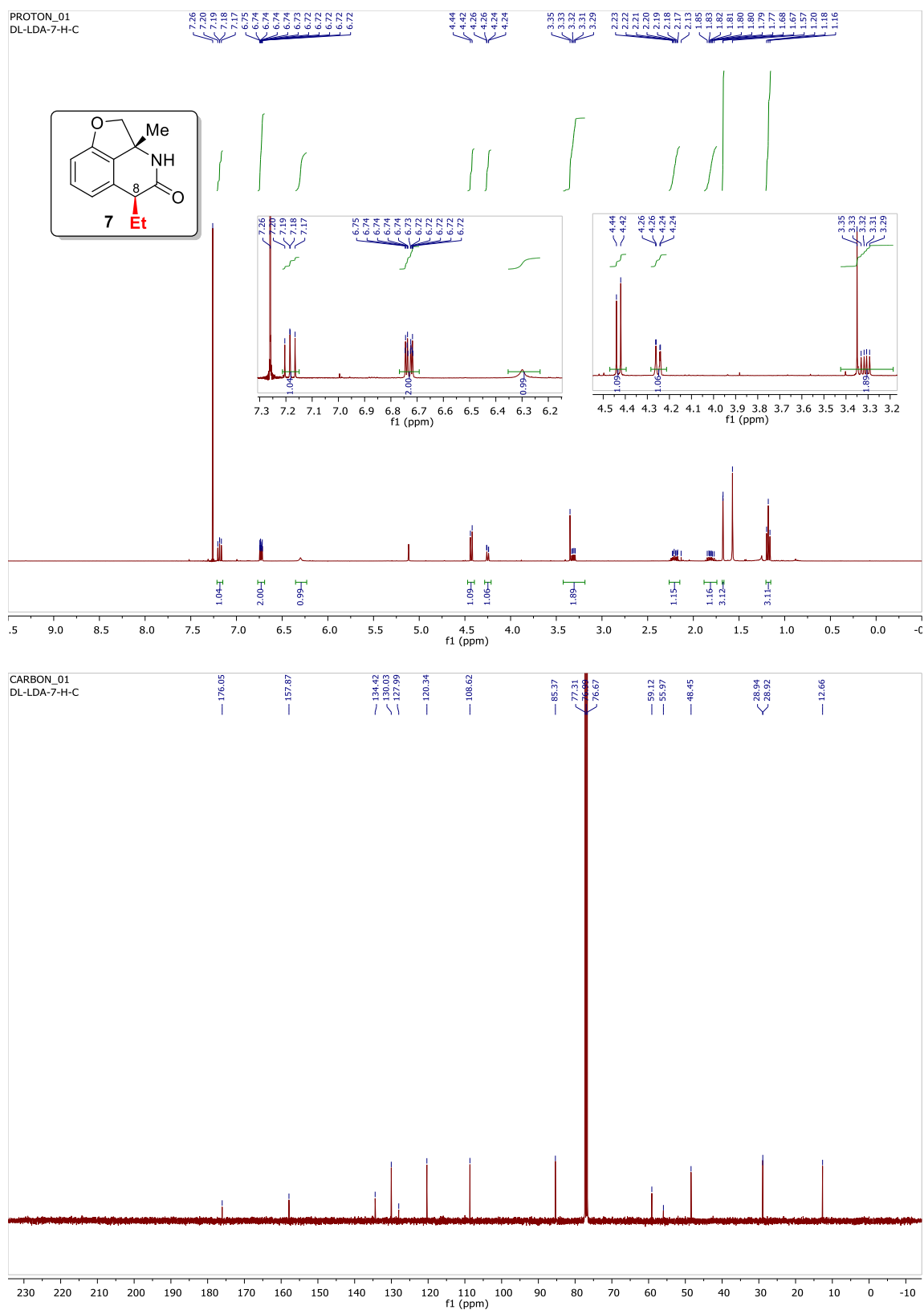


**Figure 2.39**  $^1\text{H}$  and  $^{13}\text{C}$  NMR spectrum of compound **8**

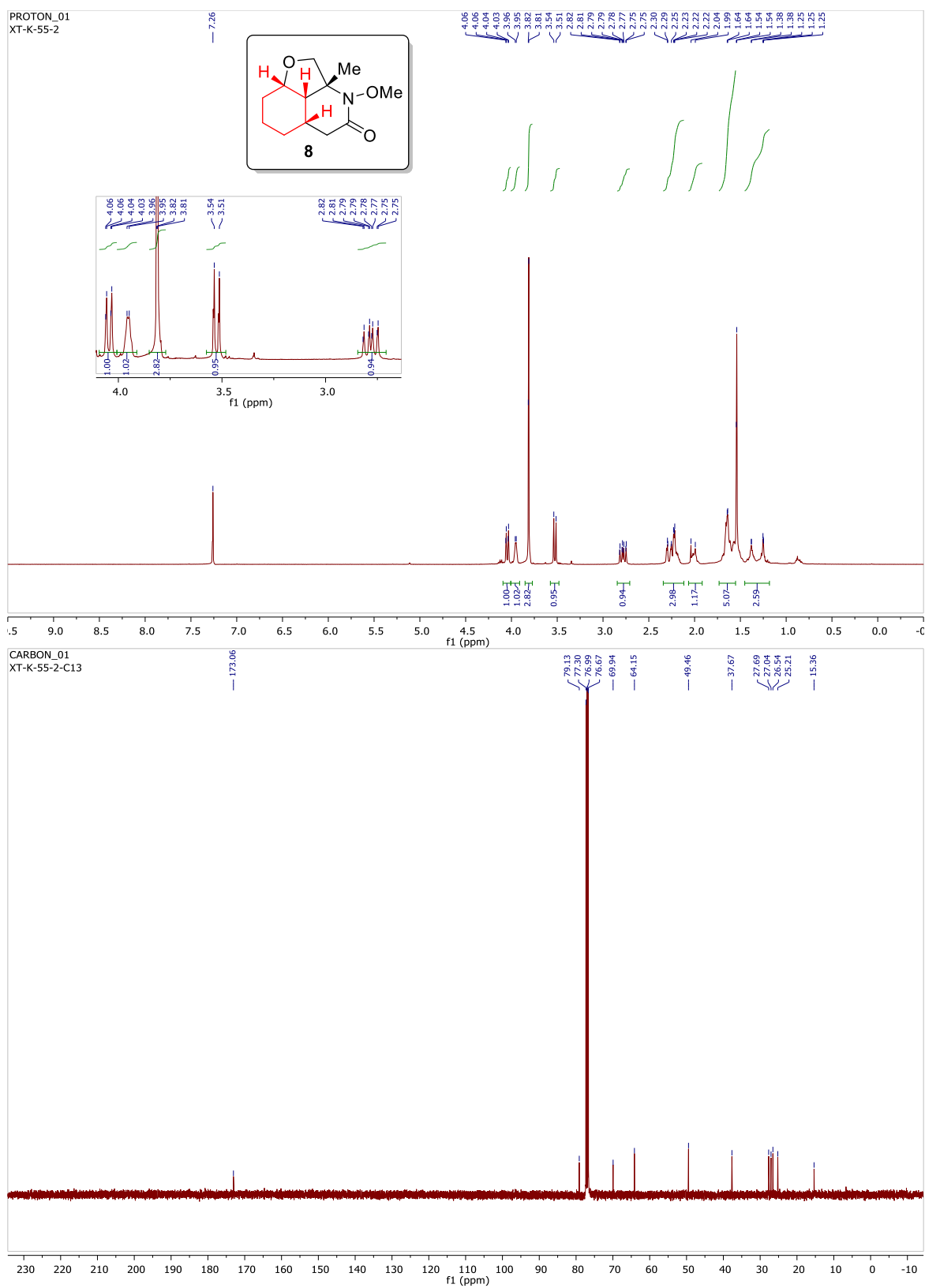


**Figure 2.40**  $^1\text{H}$  and  $^{13}\text{C}$  NMR spectrum of compound **9**

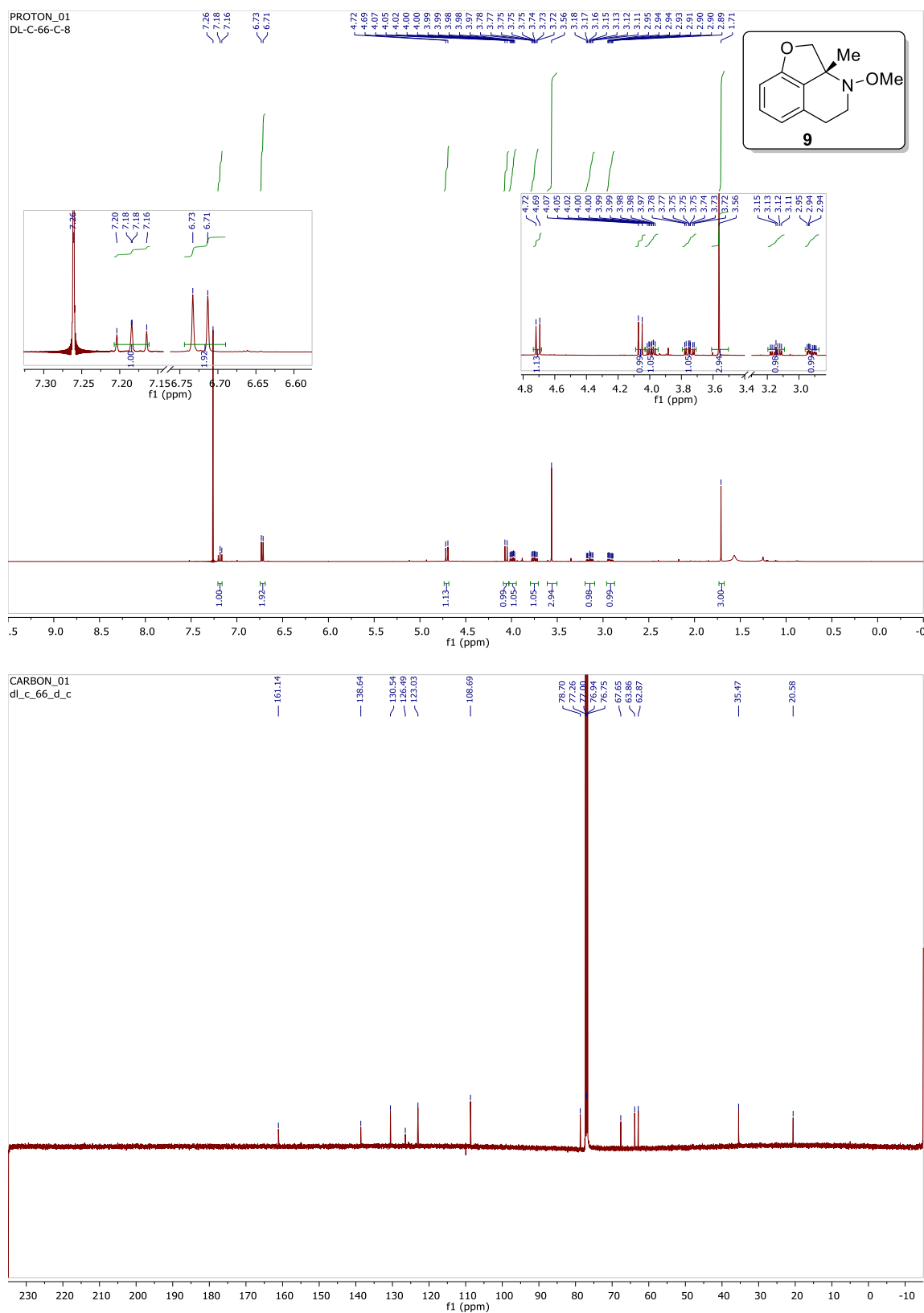


**Figure 2.41** 2D NMR spectra of compound **2m**

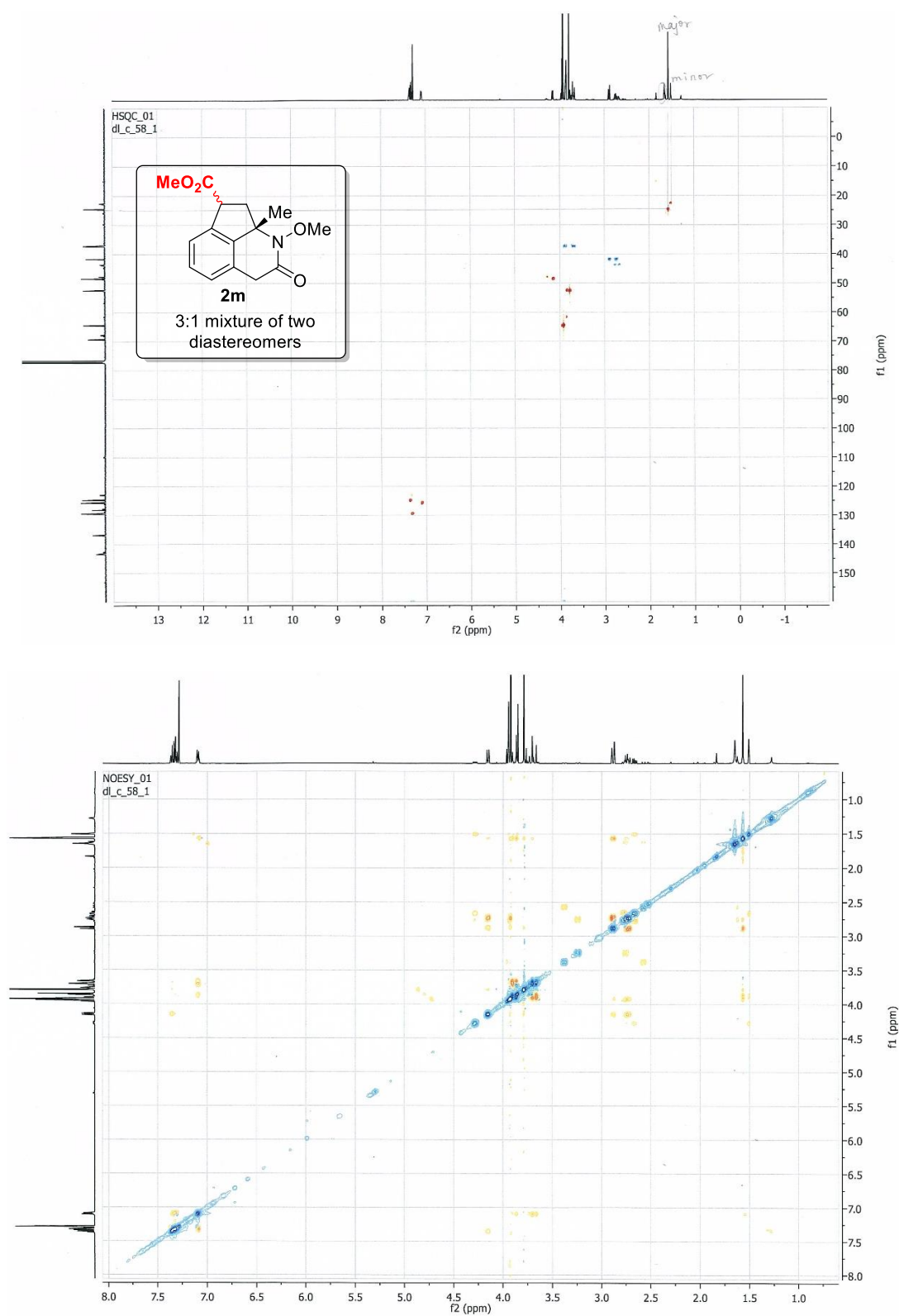


**Figure 2.41** Continued 2D NMR spectra of compound **2m**

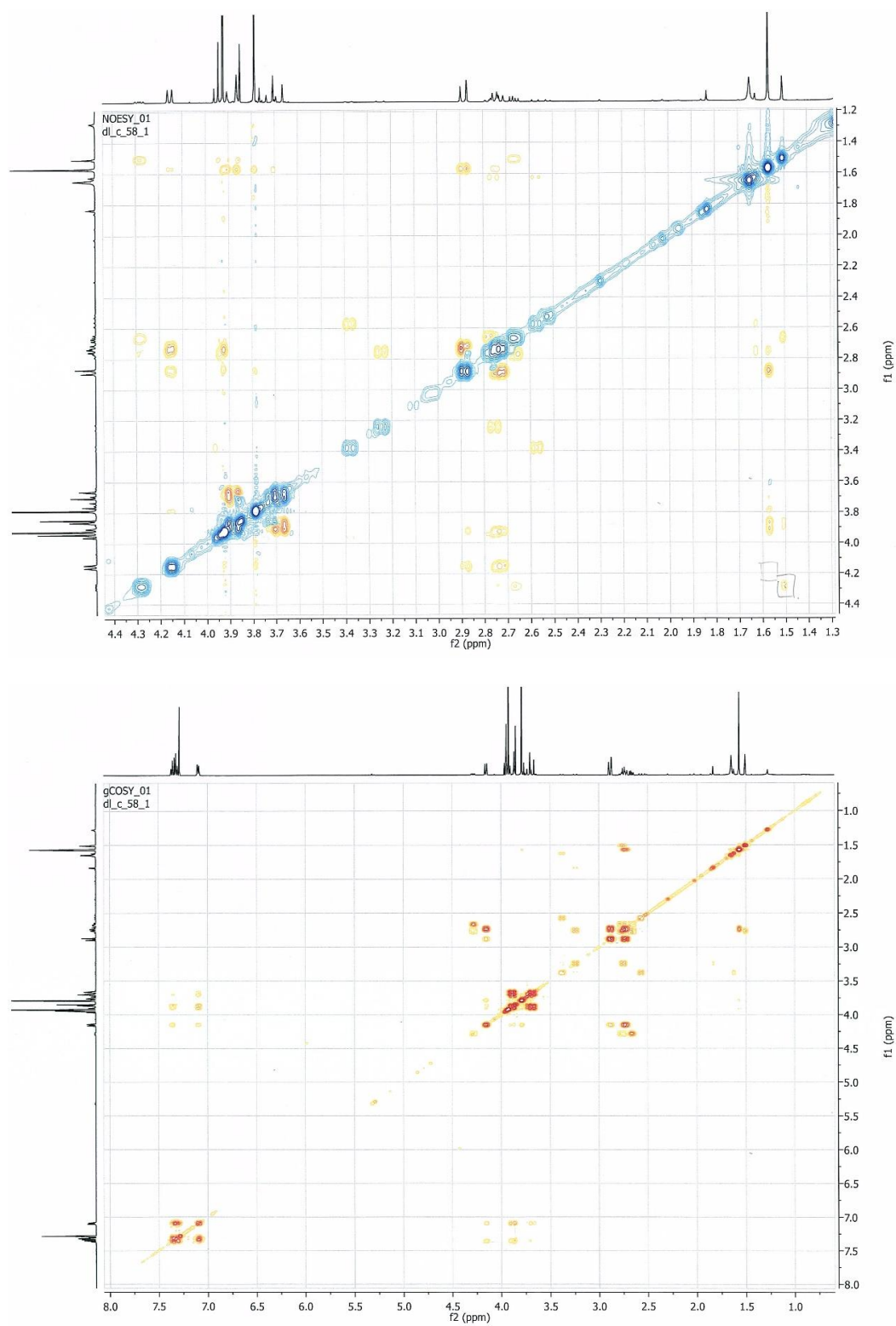


**Figure 2.42** 2D NMR spectra of compound **2n**

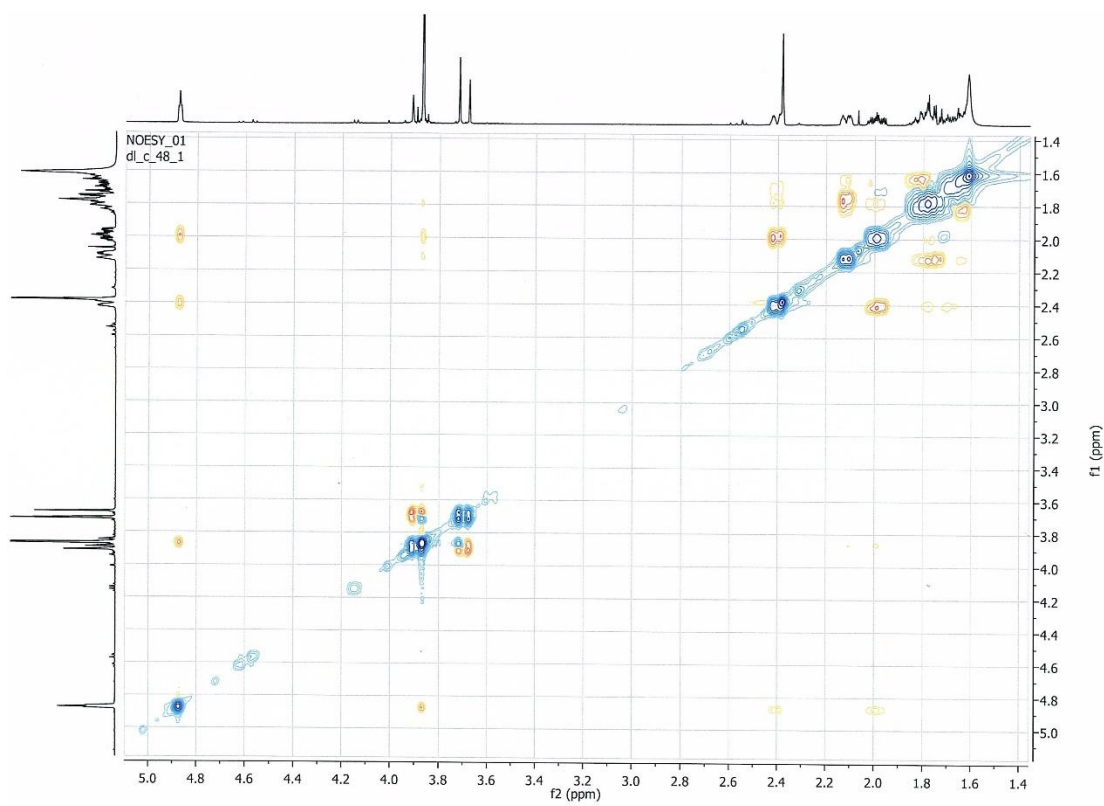
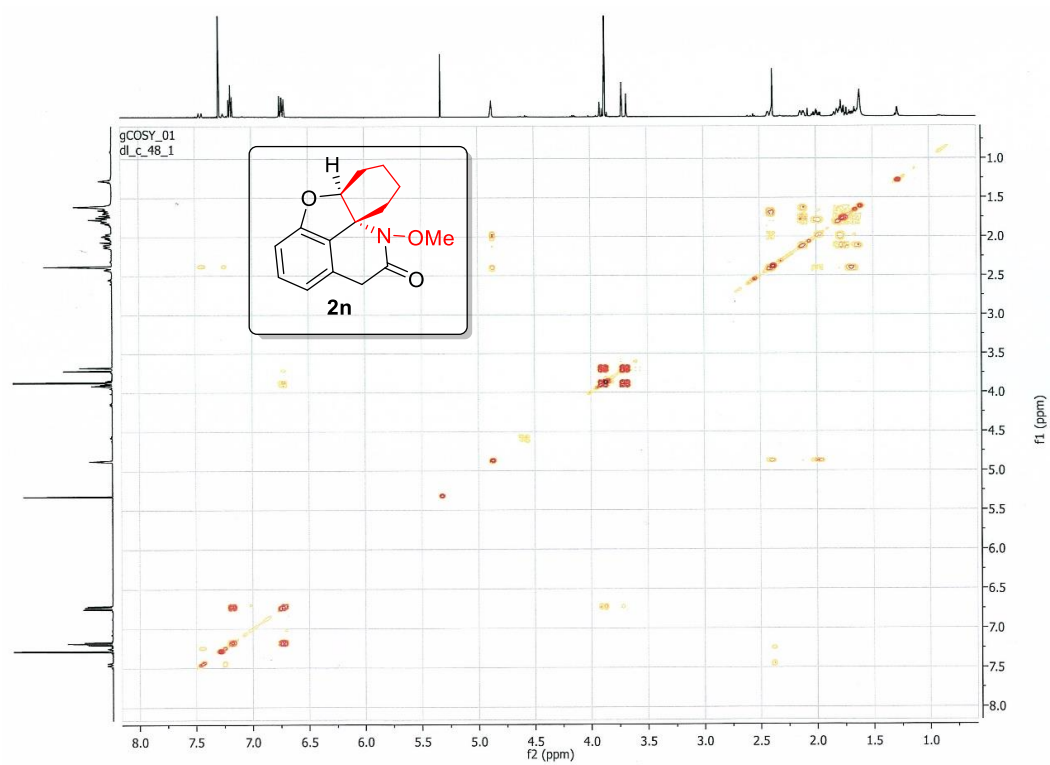
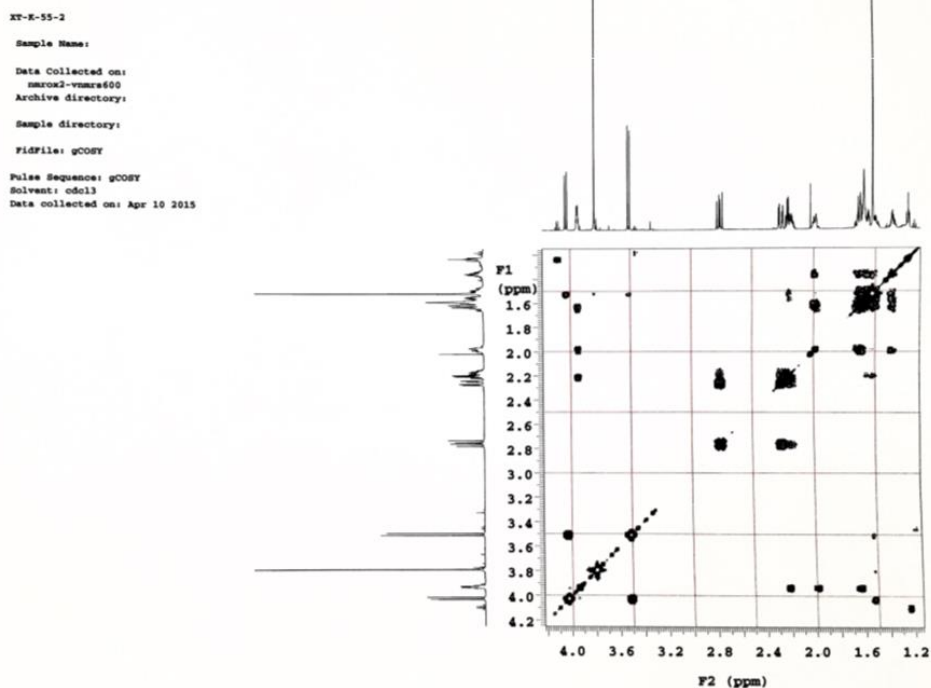
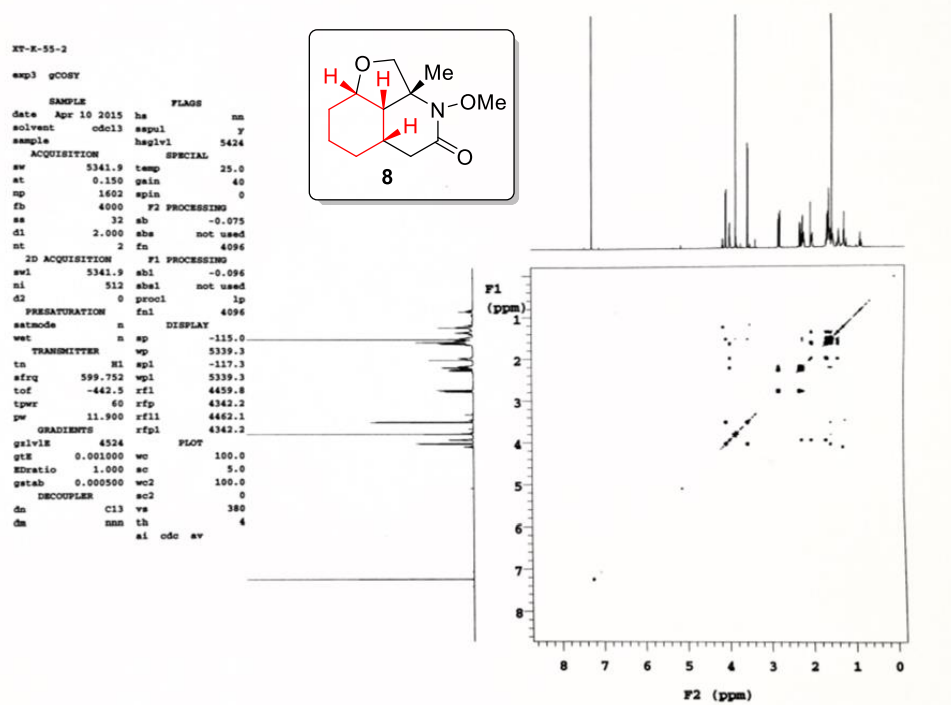


Figure 2.43 2D NMR spectra of compound 8



**Figure 2.43** Continued 2D NMR spectra of compound **8**

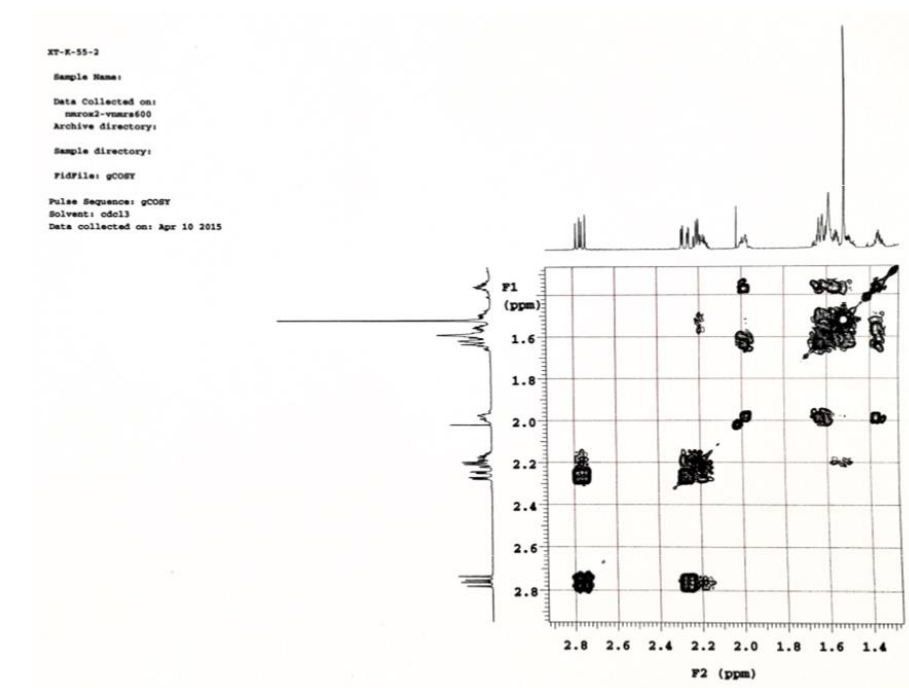
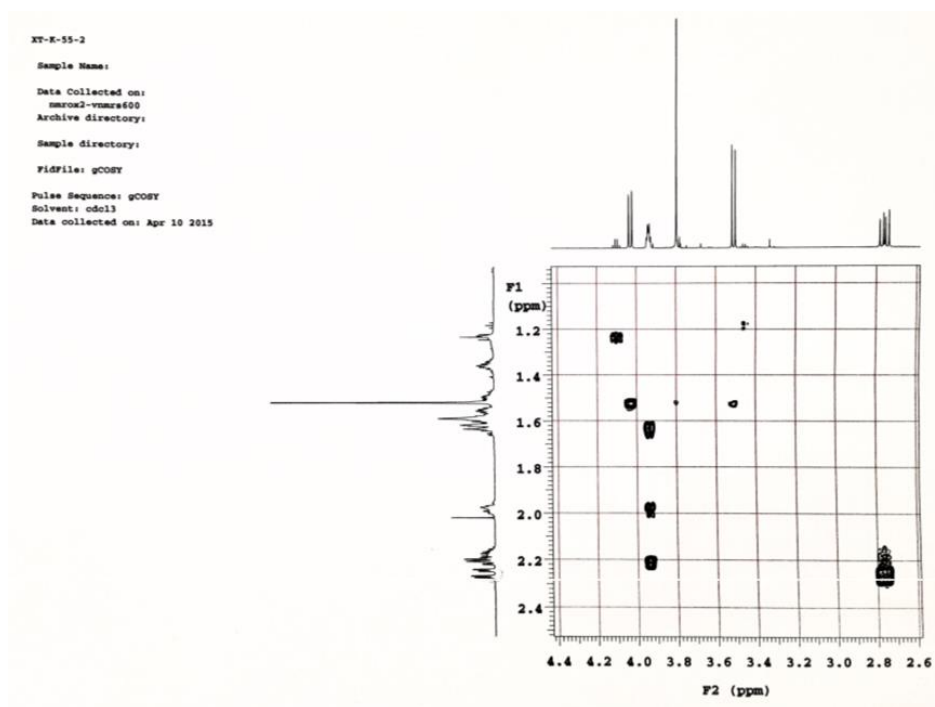
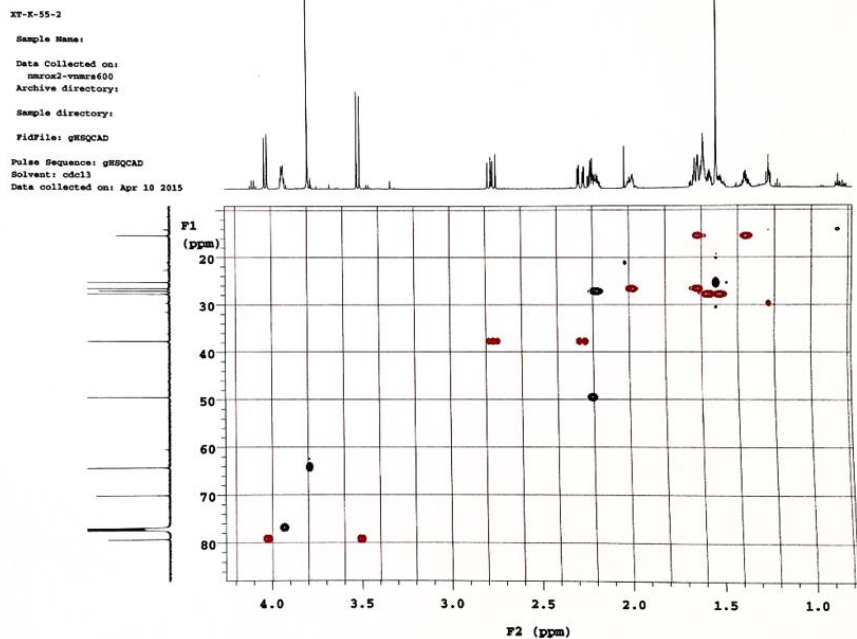
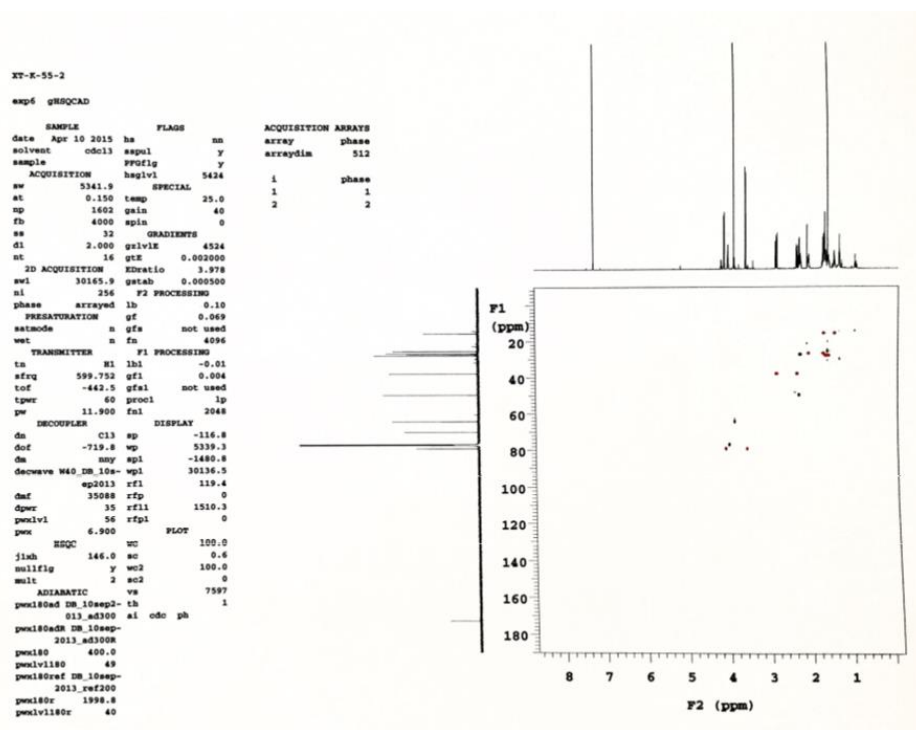




Figure 2.43 Continued 2D NMR spectra of compound 8



**Figure 2.43** Continued 2D NMR spectra of compound **8**

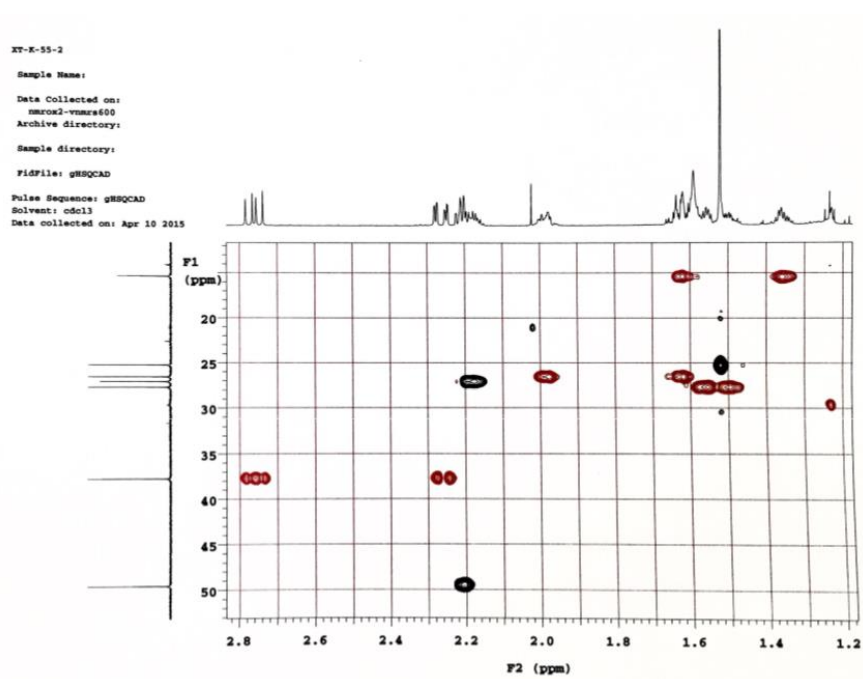
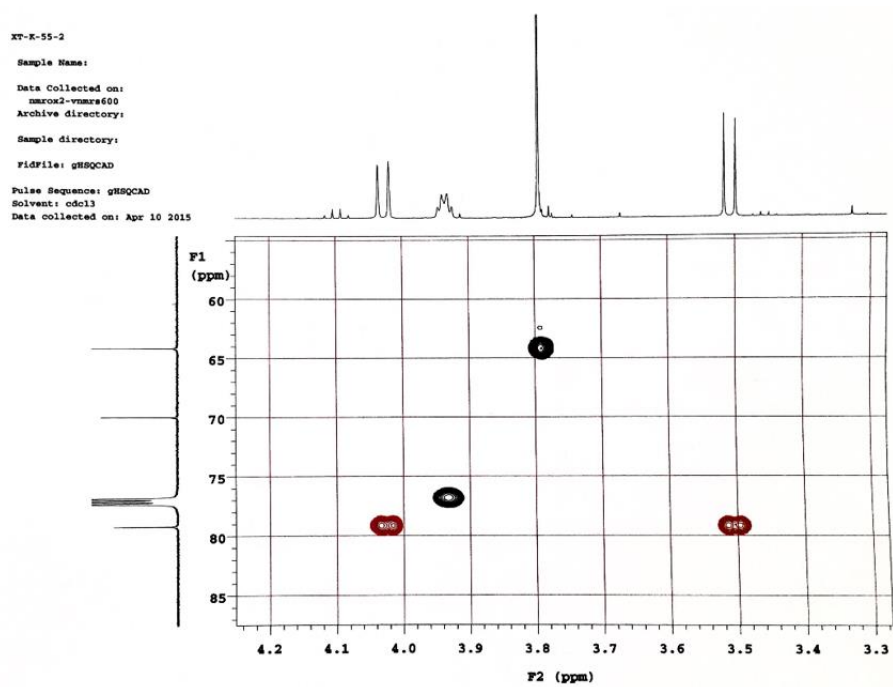
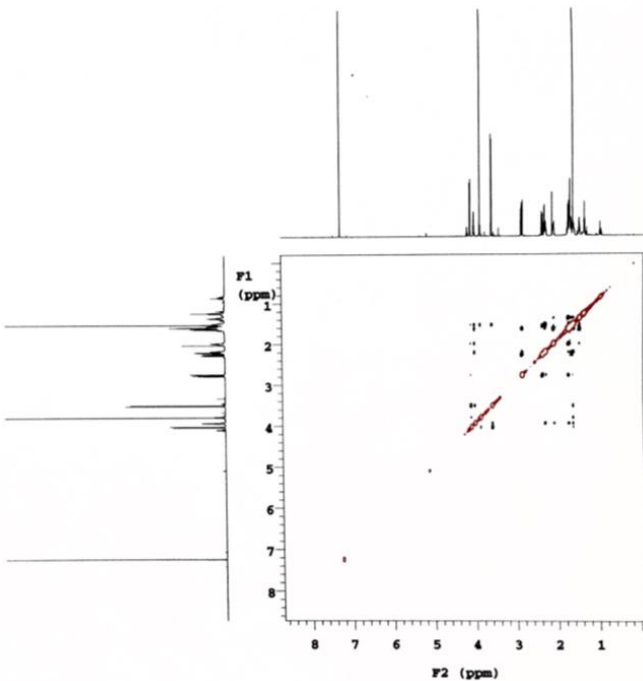


Figure 2.43 Continued 2D NMR spectra of compound 8

KT-K-55-2

exp8 NOESY

SAMPLE		FLAGS	
date	Apr 10 2015	ha	nn
solvent	odc13	aspl	y
sample		PPUfig	y
ACQUISITION		hagiv1	5424
sw	5341.9	SPECIAL	
at	0.150	temp	25.0
np	1602	gain	40
fb	4000	spin	0
ss	32	F2 PROCESSING	
dl	2.000	gf	0.046
nt	16	gfs	not used
2D ACQUISITION		fn	2048
sw1	5341.9	F1 PROCESSING	
nl	256	gf1	0.019
TRANSMITTER		gfal	not used
tn	81	procl	lp
sfreq	599.752	fn1	2048
tof	-442.5	DISPLAY	
tpwr	60	sp	-114.5
pw	11.900	wp	5336.7
	NOESY	sp1	-114.8
mlw	0.800	wpl	5336.7
PRESATURATION		rfl	4461.9
satmode	n	rfp	4342.2
wet	n	rfl1	4462.2
DECOUPLER		rflp1	4342.2
dn	C13	PLOT	
dm	mm	wc	100.0
		ac	0
		wc2	100.0
		ac2	0
		ve	1092
		th	2
		al	odc ph



KT-K-55-2

Sample Name:

Data Collected on:  
nmr02-vnmr600

Archive directory:

Sample directory:

Fidfile: NOESY

Pulse Sequence: NOESY

Solvent: odc13

Data collected on: Apr 10 2015

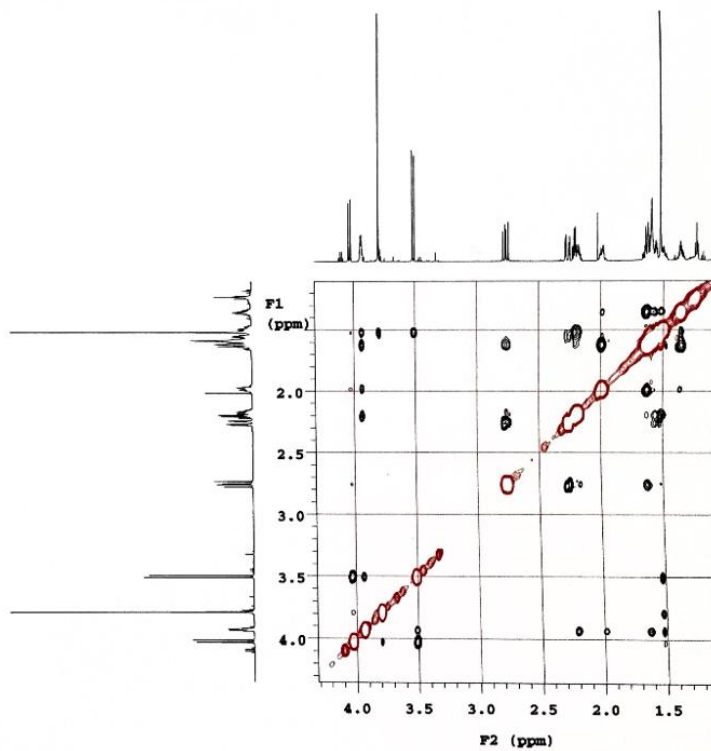
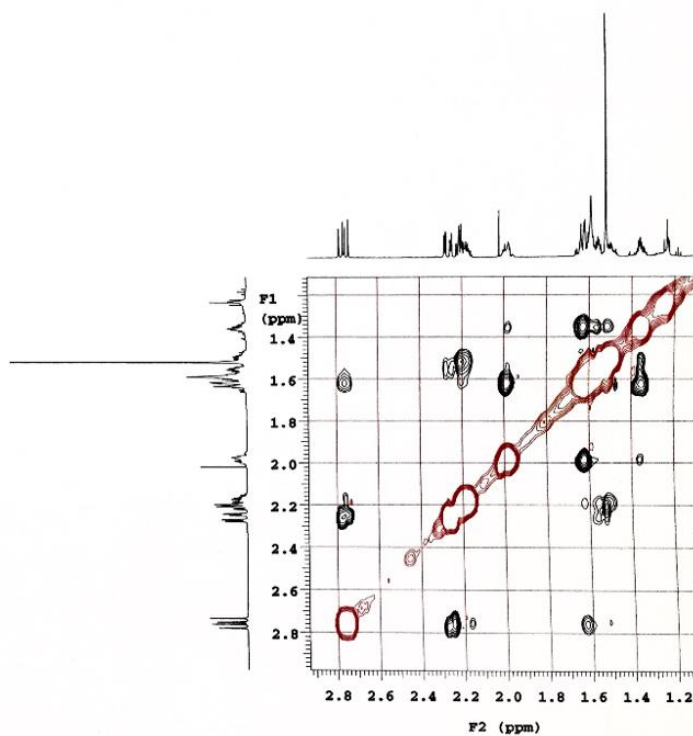


**Figure 2.43** Continued 2D NMR spectra of compound **8**

XT-K-55-2  
 Sample Name:  
 Data Collected on:  
 nmrox2-vnmr600  
 Archive directory:  
 Sample directory:  
 FidFile: NOESY  
 Pulse Sequence: NOESY  
 Solvent: cdcl3  
 Data collected on: Apr 10 2015



XT-K-55-2  
 Sample Name:  
 Data Collected on:  
 nmrox2-vnmr600  
 Archive directory:  
 Sample directory:  
 FidFile: NOESY  
 Pulse Sequence: NOESY  
 Solvent: cdcl3  
 Data collected on: Apr 10 2015

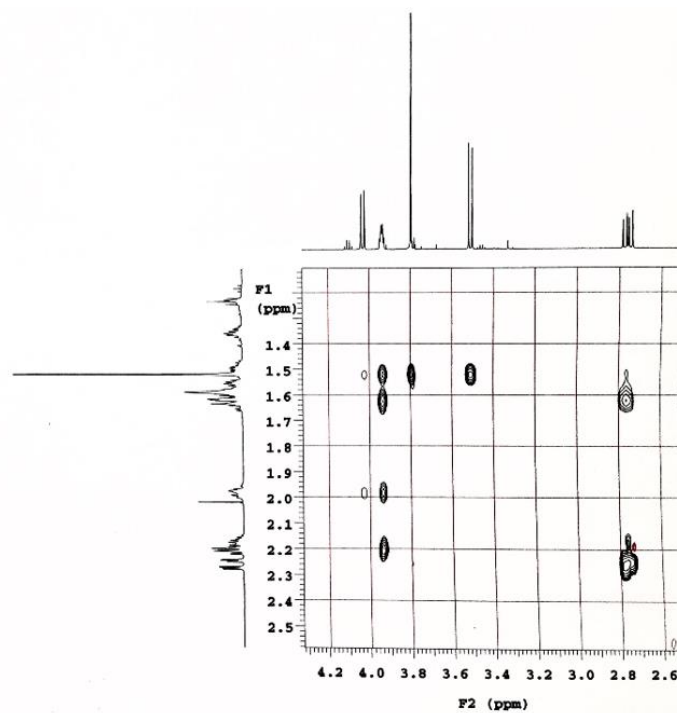
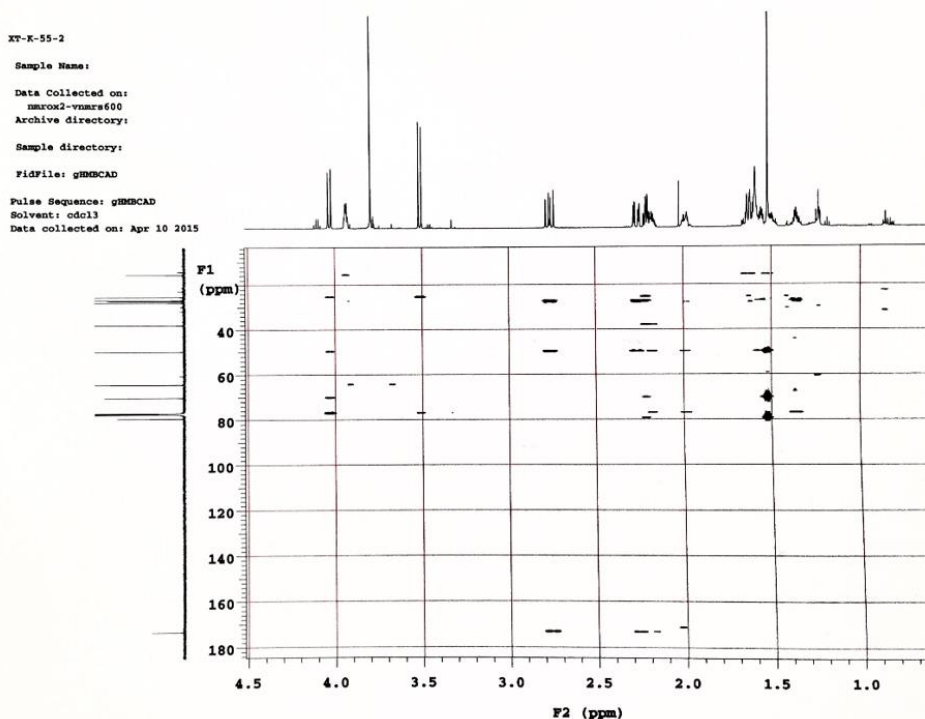
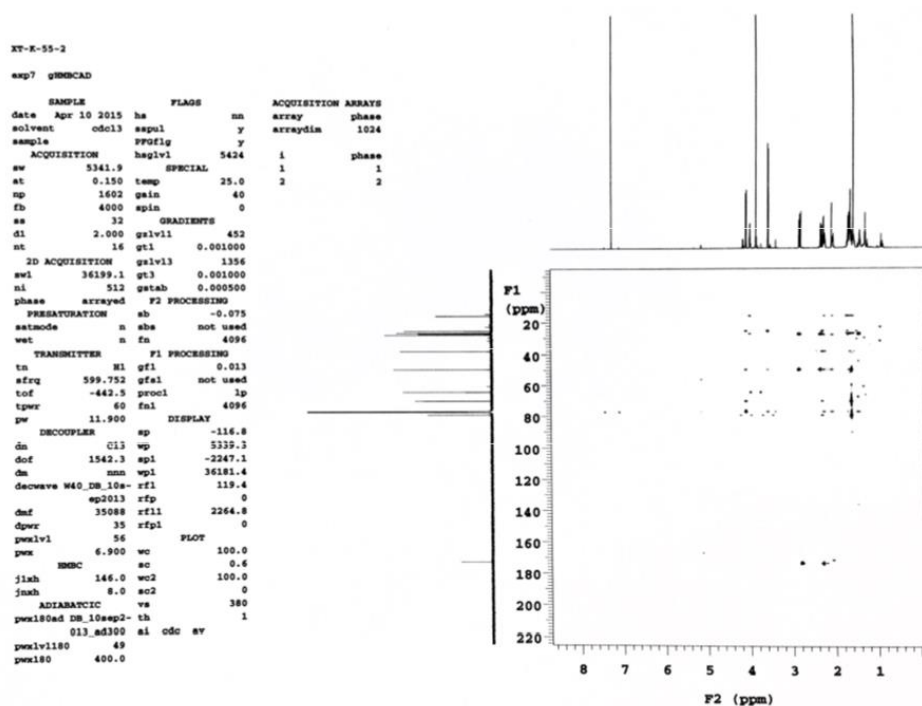


Figure 2.43 Continued 2D NMR spectra of compound 8



**Figure 2.43** Continued 2D NMR spectra of compound **8**

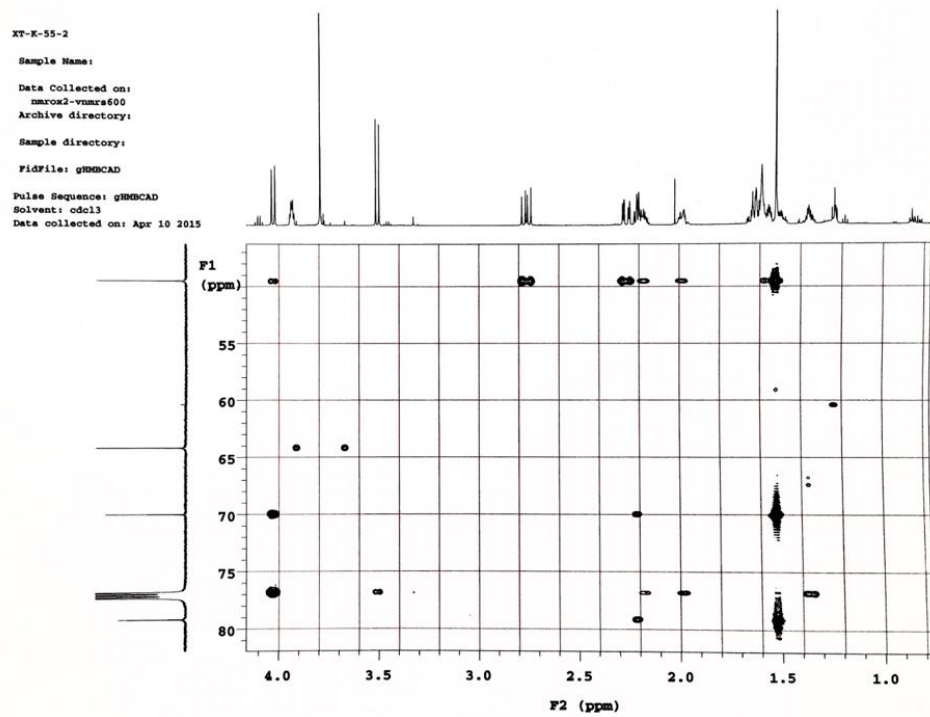
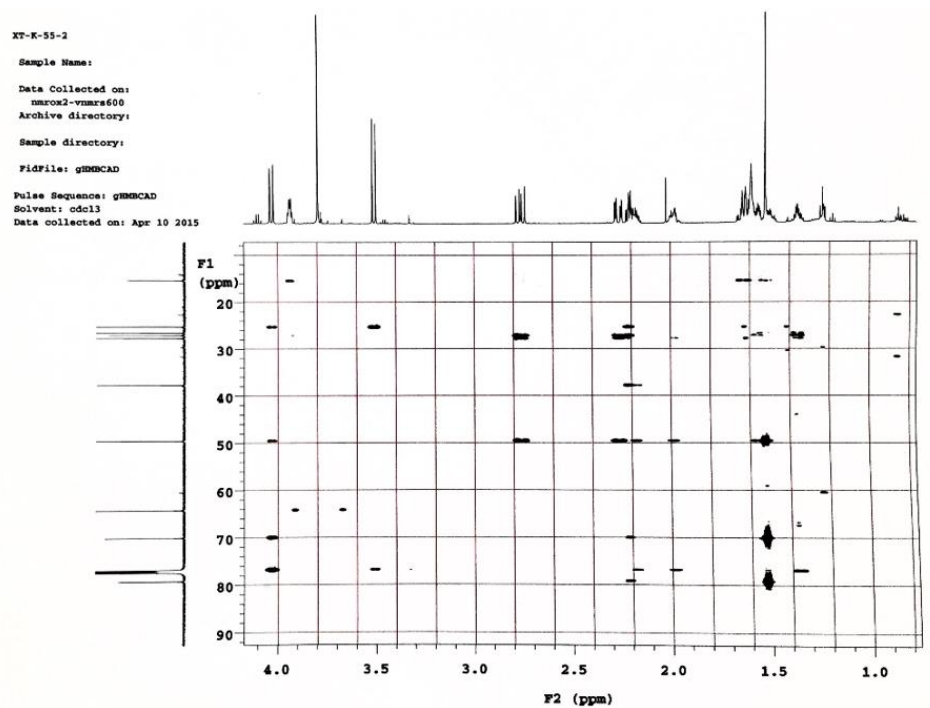
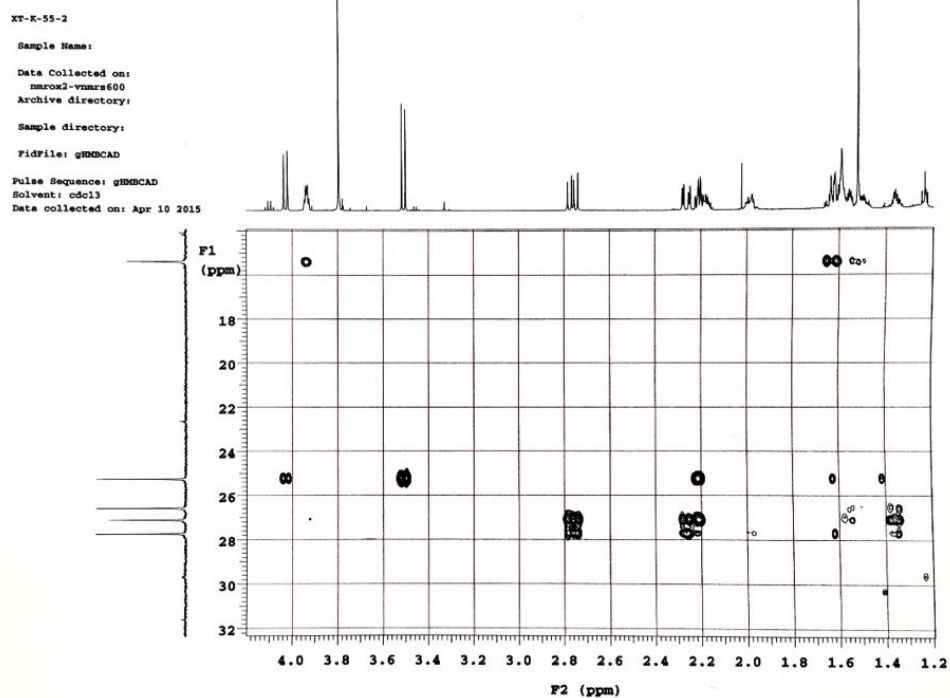
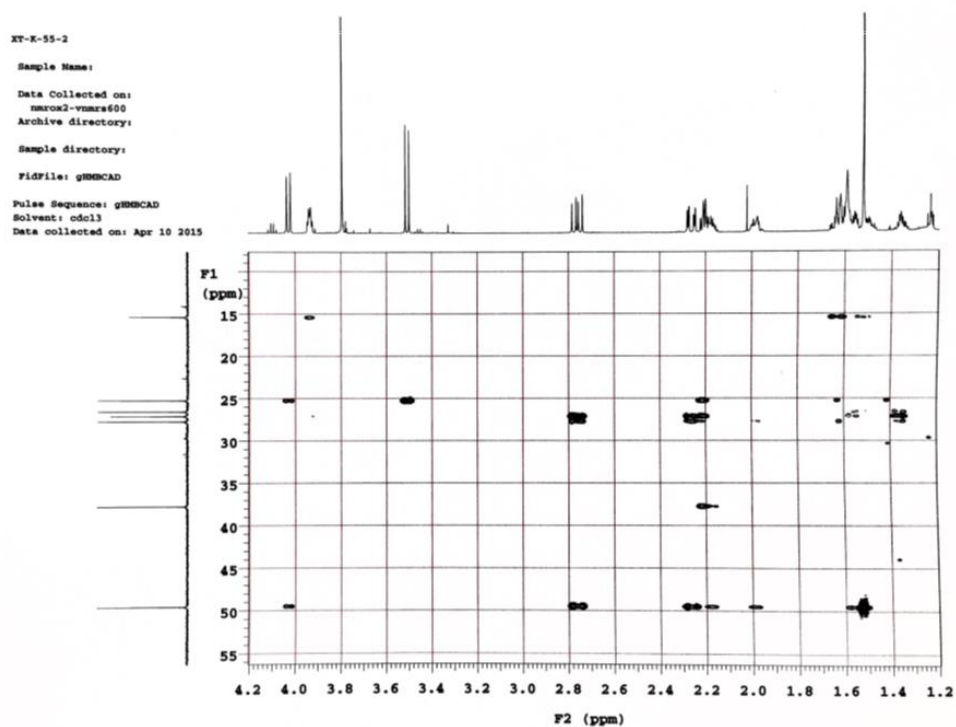


Figure 2.43 Continued 2D NMR spectra of compound 8



## CHAPTER 3

### Concise Synthesis of (–)-Cycloclavine and (–)-5-*epi*-Cycloclavine via Asymmetric C–C Activation

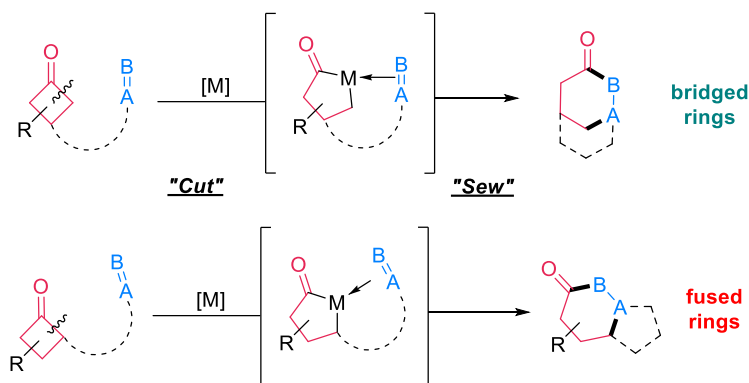
#### 3.1 Introduction

With the rapid development of transition metal (TM)-catalyzed carbon–carbon bond (C–C) activation,<sup>1</sup> new bond disconnection strategies have been made possible to access complex ring structures. However, beyond intriguing methodology development, the potential synthetic utility of these new C–C activation methods remains unexplored. Arguably, one of the most attractive ways to examine the efficacy and scope of new synthetic methods is to use them in the context of complex molecule syntheses. On the other hand, the potential challenges in complex molecule synthesis would provide valuable feedbacks and insights for further development of methodology. To date, only a handful of examples have been reported on using C–C activation as the key strategy in total synthesis of natural products,<sup>2</sup> particularly in an asymmetric manner.<sup>2h</sup> The namely “Cut-and-Sew” strategy developed over past decades by our group and others provides new opportunities for the construction of bridged and fused rings through intramolecular insertion of an unsaturated unit into  $\alpha$  C–C bond of a cyclic ketone.<sup>1q,3</sup> (Scheme 3.1). As discussed in previous chapter, we successfully achieved a highly enantioselective carboacylation of C=N bonds. Apart from aiming to tackle the challenge of applying polarized C=X bonds in “Cut-and-Sew” reactions, we also envision the synthetic significance of N-containing heterocycles and the potential



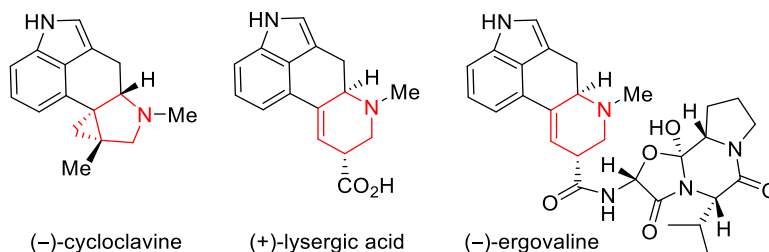
application of this type of transformation in atom-economical total synthesis of related natural products. In this chapter, we will describe a complete story on the concise total synthesis of indole alkaloid (–)-cycloclavine and its unnatural analogue enabled by a highly enantioselective “Cut-and-Sew” transformation<sup>4,5,6</sup> with nitrogen-tethered benzocyclobutenones and olefins.

**Scheme 3.1** The “Cut-and-Sew” Approach for Bridged and Fused Ring Synthesis



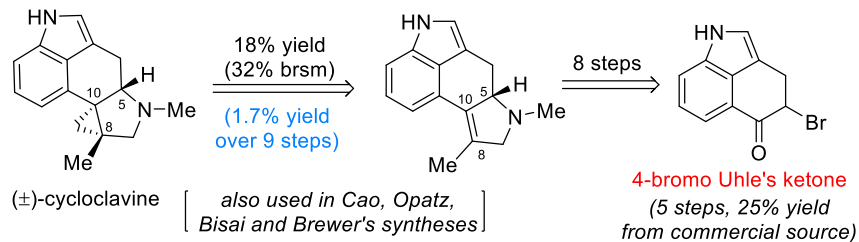
As an indole alkaloid, cycloclavine was first isolated from the seeds of *Ipomoea hildebrandtii* by Hofmann and co-workers in 1969<sup>7</sup> and later from *Aspergillus japonicus* in 1982 (Scheme 3.2).<sup>8</sup> It represents the only member in the ergot alkaloid family that contains a cyclopropane ring. During the past decade, ergot alkaloids have attracted significant attention of synthetic chemists due to their striking polycyclic fused scaffolds as well as a broad spectrum of biological activities for potential pharmaceutical and agrichemical applications.<sup>9</sup> While the full biological profile of cycloclavine remains to be disclosed, a recent study showed that cycloclavine exhibits promising insecticidal and antiparasitic properties.<sup>10</sup>

**Scheme 3.2** Structures of Representative Ergot Alkaloids

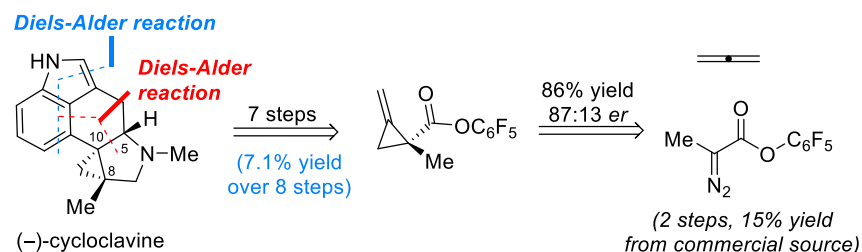


### Scheme 3.3 Prior Strategies towards Total Synthesis of Cycloclavine

#### a. Szántay's approach



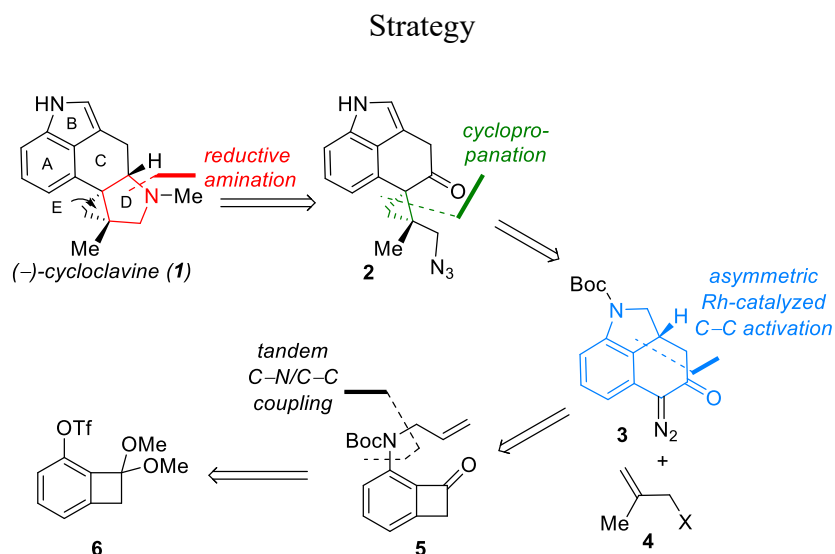
#### b. Wipf's approach



Distinct from other members in the ergot alkaloids family, cycloclavine possesses a pentacyclic core with a unique [3.1.0] structural motif.<sup>9k</sup> The sterically congested cyclopropane ring along with three contiguous stereogenic centers including two adjacent quaternary carbons presents a considerable challenge for asymmetric total synthesis. The first total synthesis of (±)-cycloclavine was described in 2008 by Szántay.<sup>11</sup> In this seminal work, the [3.1.0] fused ring was constructed in the late stage through cyclopropanation of the tetrasubstituted olefin (Scheme 3.3), which unfortunately gave only 18% yield (32% based on recovered starting material) likely owing to the steric hindrance of the olefin as well as the presence of nucleophilic indole and pyrrolidine moieties in the substrate. Subsequently, a number of formal syntheses of cycloclavine have been reported utilizing such a late-stage cyclopropanation strategy.<sup>12</sup> In contrast, a unique and elegant approach was developed by Wipf in 2011, in which cyclopropane was introduced at the very beginning of the synthesis followed by two intramolecular Diels-Alder cycloaddition to furnish the fused 6-5-6-5 ring systems (Scheme 1b).<sup>13</sup> In 2017, the Wipf group reported the first asymmetric total synthesis of (-)-cycloclavine.<sup>14</sup> Despite the high novelty and step-efficiency of

the synthetic route, the moderate enantioselectivity initially obtained from the asymmetric cyclopropanation step and a low overall yield still leave room for developing an alternative enantioselective synthesis of cycloclavine.

**Scheme 3.4** Retrosynthetic Analysis for the Synthesis of (-)-Cycloclavine: a C–C Activation



From a retrosynthetic viewpoint (Scheme 3.4), we envisioned that the pyrrolidine D ring could be installed in the end through an intramolecular reductive amination, and the tetrasubstituted cyclopropane E ring could be constructed via a diastereoselective cyclopropanation between a less bulky 1,1-disubstituted olefin **4** with aryl  $\alpha$ -diazoketone **3**. The indoline-fused tricycle (A/B/C rings) in intermediate **3** is expected to be synthesized from an enantioselective nitrogen-tethered “Cut-and-Sew” reaction via C–C activation of benzocyclobutenone **5**, which could be conveniently prepared from the known aryl triflate **6**.<sup>15</sup>

### 3.2 Results and Discussion

#### 3.2.1 Rh-catalyzed enantioselective “cut-and-sew” reactions to construct fused indolines

To explore the proposed synthetic strategy, the key “Cut-and-Sew” reaction was investigated first. In 2012, we reported a highly enantioselective Rh-catalyzed carboacylation of olefins through cleavage of benzocyclobutenone C–C  $\sigma$ -bonds.<sup>5a</sup> This reaction is atom-economical and operates under pH- and redox-neutral conditions. While a range of substrates have been demonstrated in this preliminary report, including different substitution patterns on benzocyclobutenones and olefins, the tethering structure has nevertheless been largely restricted to a more flexible oxygen linker.<sup>3,5a,5f</sup> Thus, to enable the synthesis of cycloclavine, the key questions are 1) whether high efficiency and enantioselectivity could be obtained for the “Cut-and-Sew” reaction with a more rigid nitrogen-tethered substrate (Scheme 3.5), and 2) whether a rapid and efficient route could be established for preparing such nitrogen-substituted benzocyclobutenones.

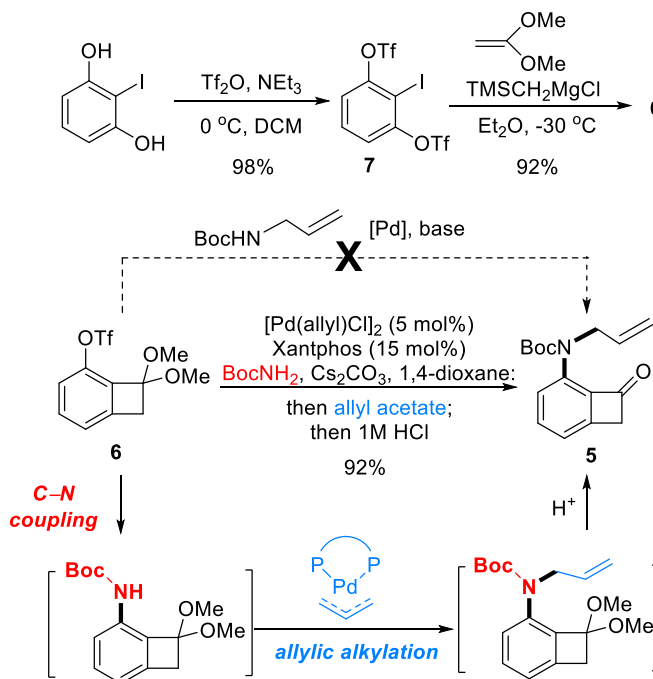
**Scheme 3.5** Challenges for “Cut-and-Sew” Reactions



In a forward manner, following a reported procedure by Hosoya,<sup>15</sup> the ketal-protected OTf-substituted benzocyclobutenone (**6**) was prepared with an excellent overall yield from commercially available 2-iodoresorcinol through a sequence of triflation and benzyne-mediated [2+2] cycloaddition (Scheme 3.6). Attempts to directly couple Boc-protected allylamine with triflate **6** were unfruitful likely owing to the steric hindrance of both substrates. However, a Pd-catalyzed C–N bond coupling<sup>16</sup> between triflate **6** and *tert*-butyl carbamate, followed by an allylic alkylation catalyzed by the same Pd species and then acidic workup, provided the nitrogen-tethered benzocyclobutenone **5** in an excellent yield. Hence, this three-step route offers a rapid and

high-yielding entry to substrate **5** for the subsequent C–C activation, which otherwise would take around 6 steps using the prior preparation routes.<sup>3,17</sup>

**Scheme 3.6** Synthesis of the Nitrogen-Tethered Benzocyclobutenone Substrate



With substrate **5** in hand, the key “Cut-and-Sew” reaction was explored (Table 3.1). Unsurprisingly, under the previous optimal (racemic<sup>3</sup> and asymmetric<sup>5a</sup>) conditions for the ether-linked substrates, the desired tricycle product was only obtained in low yields (Table 3.1, entries 1 and 2) and moderate enantioselectivity (Table 3.1, entry 2). We hypothesized that the reduced reactivity was likely due to the increased bulkiness and rigidity of the nitrogen linkage, thus use of a less bulky and more electron-deficient Rh catalyst might enhance the binding with the olefin moiety thereby promoting the subsequent 2 $\pi$  insertion. Indeed, the combination of a monodentate phosphine ligand, i.e. PMe<sub>2</sub>Ph, with  $\pi$ -acidic [Rh(CO)<sub>2</sub>Cl]<sub>2</sub> afforded indoline product **8** in an excellent yield (Table 3.1, entry 3). Interestingly, [Rh(CO)<sub>2</sub>Cl]<sub>2</sub> as a precatalyst alone still gave 49% yield (Table 3.1, entry 4). However, developing enantioselective transformations based on

the  $[\text{Rh}(\text{CO})_2\text{Cl}]_2$  system proved to be challenging due to the limitation of using monodentate electron-rich ligands. On the other hand, while a promising level of enantioselectivity could be achieved using chloro-Rh(I)/olefin precatalysts, the yield was difficult to be improved (Table 3.1, entries 5-7).

**Table 3.1** Selected Optimization Study for the Rh-Catalyzed Asymmetric “Cut-and-Sew”

Reaction<sup>a</sup>

Entry	Precatalyst/ Ligand	Temperature (°C)	Yield <sup>b</sup>	ee <sup>c</sup>
1	5 mol% $[\text{Rh}(\text{cod})\text{Cl}]_2$ / 10 mol% dppb	130	18% <sup>g,h</sup>	N/A
2	5 mol% $[\text{Rh}(\text{cod})\text{Cl}]_2$ / 10 mol% ( <i>R</i> )-DTBM-segphos	130	12% (57%)	75%
3	5 mol% $[\text{Rh}(\text{CO})_2\text{Cl}]_2$ / 10 mol% $\text{PMe}_2\text{Ph}$	120	86%	N/A
4 <sup>d</sup>	5 mol% $[\text{Rh}(\text{CO})_2\text{Cl}]_2$	120	49% <sup>g</sup>	N/A
5	5 mol% $[\text{Rh}(\text{cod})\text{Cl}]_2$ / 10 mol% ( <i>R</i> )-DM-segphos	130	22% (71%)	26%
6	5 mol% $[\text{Rh}(\text{cod})\text{Cl}]_2$ / 10 mol% ( <i>R</i> )-tol-binap	130	7% (37%)	72%
7	5 mol% $[\text{Rh}(\text{coe})_2\text{Cl}]_2$ / 10 mol% ( <i>R</i> )-DTBM-segphos	110	12% (44%)	85%
8	10 mol% $\text{Rh}(\text{nbd})_2\text{BF}_4$ / 12 mol% ( <i>R</i> )-DTBM-segphos	100	61%	97.5%
9	10 mol% $\text{Rh}(\text{cod})_2\text{BF}_4$ / 12 mol% ( <i>R</i> )-DTBM-segphos	120	22%	98%
10 <sup>e</sup>	10 mol% $\text{Rh}(\text{cod})_2\text{BF}_4$ / 12 mol% ( <i>R</i> )-DTBM-Segphos	90	95%	97%
11 <sup>e</sup>	5 mol% $\text{Rh}(\text{cod})_2\text{BF}_4$ / 6 mol% ( <i>R</i> )-DTBM-segphos	90	96%	97.5%
12 <sup>e,f</sup>	3 mol% $\text{Rh}(\text{cod})_2\text{BF}_4$ / 3.6 mol% ( <i>R</i> )-DTBM-segphos	90	95%	97.5%

<sup>a</sup> Unless otherwise mentioned, the reaction was run on a 0.1 mmol scale at specified temperature for 24 h. <sup>b</sup> Isolated yield; numbers in parenthesis are yields based on recovered starting material (brsm). <sup>c</sup> Determined by chiral HPLC.

<sup>d</sup> Reaction time was 72 h. <sup>e</sup> Reaction time was 12 h. <sup>f</sup> Reaction scale was 2.0 mmol. <sup>g</sup> NMR yields using 1,1,2,2-tetrachloroethane as internal standard. <sup>h</sup> Tetrahydrofuran (THF) was used as solvent.

Finally, we turned our attention to cationic Rh(I) precatalysts, because the olefin coordination would likely be enhanced due to the cationic nature of the metal. To our delight, using  $\text{Rh}(\text{nbd})_2\text{BF}_4$  and DTBM-segphos as the metal/ligand combination, 61% yield and 97.5% ee were achieved (Table 3.1, entry 8). The  $\text{Rh}(\text{cod})_2\text{BF}_4$  was found to be more reactive than  $\text{Rh}(\text{nbd})_2\text{BF}_4$ , and a 95% yield was reached at a lower reaction temperature (90 °C) with the same ee (Table 3.1, entry 10); in contrast, at 120 °C significant catalyst decomposition was observed leading to a much

lower yield (Table 3.1, entry 9). Remarkably, with this new catalyst system, the catalyst loading and reaction time could be further reduced. For example, using 3 mol% Rh, tricycle **8** was isolated in 95% yield and 97.5% ee in 12 h on a 2.0 mmol scale.

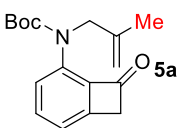
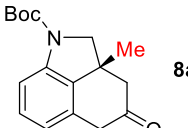
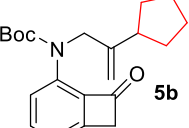
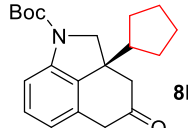
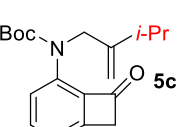
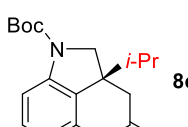
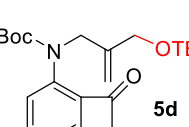
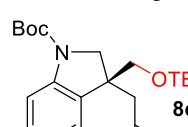
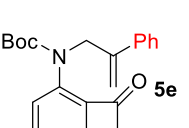
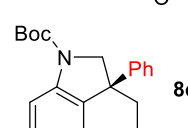
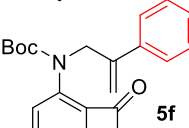
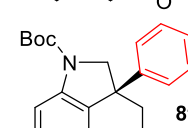
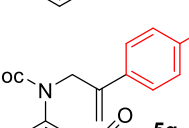
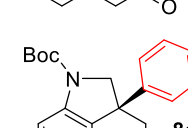
Comparing with our first-generation conditions for the ether-linked benzocyclobutenones, the current one shows several advantages: first, the reaction temperature is significantly lower (90 vs 130 °C); second, the loading of the rhodium catalyst could be reduced to 3 mol% (previously, 10 mol%); and finally, the reaction is much faster (12 vs 48 h).<sup>5a</sup>

### 3.2.2 Substrate scope for the Rh-catalyzed synthesis of tricyclic indolines via C–C activation

After obtaining the optimal conditions for the Rh-catalyzed carboacylation of olefins with nitrogen-tethered benzocyclobutenones, the substrate scope was further investigated (Table 3.2). First, alkyl substituents on the olefin with various steric properties all underwent the desired carboacylation reaction giving excellent enantioselectivity ( $\geq 97\%$  ee, Table 3.2, entries 1-4). It is not surprising that with increased bulkiness around the olefin, the yield of the reaction slightly decreased from methyl to cyclopentyl to isopropyl, while the enantioselectivity remained the same. Given the pH and redox-neutral reaction conditions, the TBS-protected primary alcohol is well tolerated (Table 3.2, entry 4). Both electron-rich and poor aryl substituents are compatible, giving good yields and excellent enantioselectivity (Table 3.2, entries 5-7).

In addition, C5 and C6-substituted benzocyclobutenones are competent substrates (Table 3.3, entries 1 and 2). Furthermore, besides the Boc moiety, other protecting groups at the nitrogen, such as acyl or tosyl group, are also suitable for this reaction, providing products in 80-91% yields and 99% ee (Table 3.3, entries 3-5). Gratifyingly, 1,2-disubstituted and trisubstituted olefins undergo the desired transformation with good yields and ee, which were not viable substrates for our first generation condition (Table 3.3, entries 6 and 7).

**Table 3.2** Substrate Scope I<sup>a</sup>

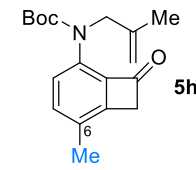
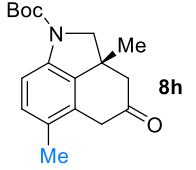
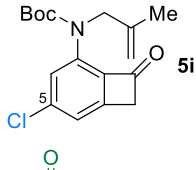
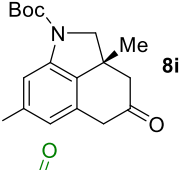
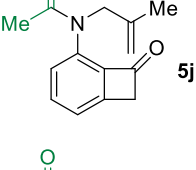
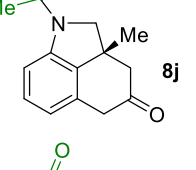
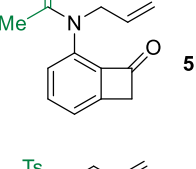
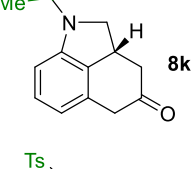
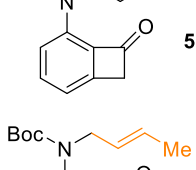
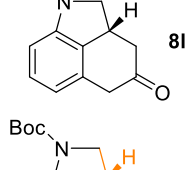
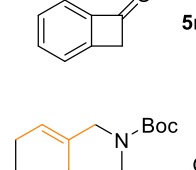
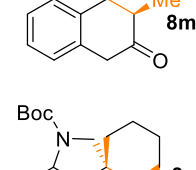
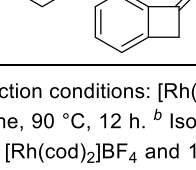
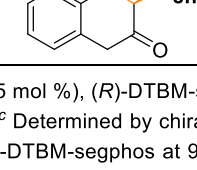
Entry	Substrate	Product	Yield <sup>b</sup>	e.e. <sup>c</sup>
1			88%	98%
2			78%	98%
3			71%	98%
4			71%	97%
5			78%	97%
6			93%	98%
7			76%	99%

<sup>a</sup> Reaction conditions: [Rh(cod)<sub>2</sub>]BF<sub>4</sub> (5 mol %), (*R*)-DTBM-segphos (6 mol%), 1,4-dioxane, 90 °C, 12 h. <sup>b</sup> Isolated yield. <sup>c</sup> Determined by chiral HPLC.

In summary, the improved catalytic conditions show a general feature for the nitrogen-tethered substrates, giving high yields and excellent enantioselectivity. The reaction conditions do not contain strong acids/bases or stoichiometric oxidants/reductants, which could be the key for the good functional group tolerance. Thus, this method is expected to be useful for enantioselective synthesis of various indole or indoline-containing complex target molecules.



**Table 3.3 Substrate Scope II<sup>a</sup>**

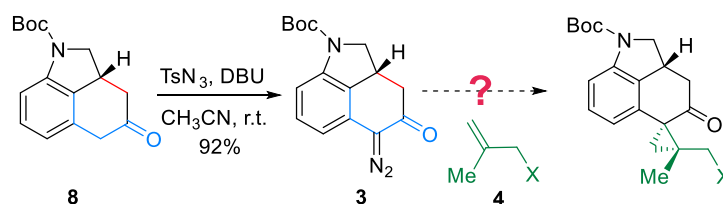
Entry	Substrate	Product	Yield <sup>b</sup>	e.e. <sup>c</sup>
1			95%	98%
2			76%	98%
3			90%	99%
4			80%	99%
5 <sup>d</sup>			91%	99%
6 <sup>e</sup>			75%	94%
7 <sup>e</sup>			82%	98%

<sup>a</sup> Reaction conditions: [Rh(cod)<sub>2</sub>]BF<sub>4</sub> (5 mol %), (R)-DTBM-segphos (6 mol%), 1,4-dioxane, 90 °C, 12 h. <sup>b</sup> Isolated yield. <sup>c</sup> Determined by chiral HPLC. <sup>d</sup> Run with 10 mol% [Rh(cod)<sub>2</sub>]BF<sub>4</sub> and 12 mol% (R)-DTBM-segphos at 90 °C for 12 h and then 110 °C for 12 h. <sup>e</sup> Run with 10 mol% [Rh(cod)<sub>2</sub>]BF<sub>4</sub> and 12 mol% (R)-DTBM-segphos. <sup>f</sup> Compound **5m** is an inseparable 4:1 mixture of *trans/cis* isomers. From our control experiment, *cis* isomer cannot undergo the desired reaction, so the product obtained was generated exclusively from the *trans* isomer. The yield was calculated based on the amount of *trans* starting material.

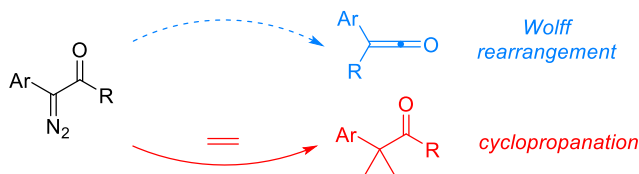
### 3.2.3 Rh-catalyzed diastereoselective cyclopropanation

With a reliable route to access key intermediate **8**, we continued to explore the forward synthesis of (–)-cycloclavine. First, the diazo-transfer reaction proceeded smoothly to afford compound **3** in 92% yield (Scheme 3.7). Clearly, the next formidable challenge is to construct the tetra-substituted cyclopropane E ring in an efficient and diastereoselective fashion. While cyclopropanation with donor–acceptor carbenoids, pioneered by the Davies group,<sup>18</sup> has been extensively developed, the use of ketone-derived diazo compounds is less common compared to the widely used ester-derived ones.<sup>19</sup> In particular, the  $\alpha$ -diazoketone-based cyclopropanation with 1,1-disubstituted olefins to construct tetrasubstituted cyclopropanes diastereoselectively remains elusive.

**Scheme 3.7** Synthesis of Compound **3** as the Substrate for Cyclopropanation



**Scheme 3.8** Potential Side Reaction for Cyclopropanation



One potential side reaction with  $\alpha$ -diazoketones could be the Wolff rearrangement,<sup>20</sup> which would possibly lead to ring contraction (Scheme 3.8). However, due to the low temperature of the dirhodium-catalyzed cyclopropanation, the Wolff rearrangement was expected to be unlikely to happen. Thus, the reactions with racemic  $\alpha$ -diazoketone **3** were tested initially under various dinuclear Rh(II)-catalyzed cyclopropanation conditions (Table 3.4, entries 1-4). Davies' DOSP catalyst<sup>21</sup> was found to give higher reactivity than other commercially available Rh(II) catalysts.

While the use of protected allyl amine **4a** could indeed provide the desired cyclopropane product **9a**, the efficiency was not satisfying, likely owing to the bulkiness or chelating effect of the carbamate moiety. Hence, less sterically hindered 2-methylallyl chloride **4b** was then employed as the olefin substrate. To our delight, **4b** exhibited significantly enhanced reactivity and could even yield the desired cyclopropane product **9b** at  $-60\text{ }^{\circ}\text{C}$  using  $\text{Rh}_2(R\text{-DOSP})_4$  as the catalyst (Table 3.4, entry 5). After a further survey of the reaction temperature and solvent (Table 3.4, entries 6-8),  $-40\text{ }^{\circ}\text{C}$  and hexane/toluene as a mixed solvent proved to be more efficient; cyclopropane **9b** could be isolated in 78-80% yield and  $\sim 6:1$  d.r favoring the desired diastereomer with either enantiopure or racemic catalyst (Table 3.4, entries 7 and 8). It is noteworthy that both diastereomers are easily separable, and the relative stereochemistry of the major diastereomer **9b** was confirmed by X-ray crystallography (Scheme 3.9).

The optimal reaction conditions have also been applied to compound **3** with 97.5% e.e. using 1 mol%  $\text{Rh}_2(R\text{-DOSP})_4$  as the catalyst (Table 3.4, entry 9). On a larger scale the desired product **9b** was still isolated in 85% yield with satisfactory diastereoselectivity. Interestingly, use of the other enantiomer of the Rh catalyst, i.e.  $\text{Rh}_2(S\text{-DOSP})_4$ , gave diminished diastereoselectivity, suggesting a mismatched situation (Table 3.4, entry 10). Given that both enantiomers of the Rh catalysts gave the same major diastereomer of the product, it indicates that the diastereoselectivity was majorly controlled by the substrate. Finally, as a control experiment, the achiral Du Bois'  $\text{Rh}_2(\text{esp})_2^{22}$  catalyst was also found to be effective under the optimized conditions (Table 3.4, entry 11), though the yield was lower than the DOSP one.

**Table 3.4** Selected Condition Optimization for the Cyclopropanation Step<sup>a</sup>

$\text{3} + \text{Me-CH=CH-X} \xrightarrow[\text{hexane/DCM, slow addition of 3}]{\text{conditions}}$

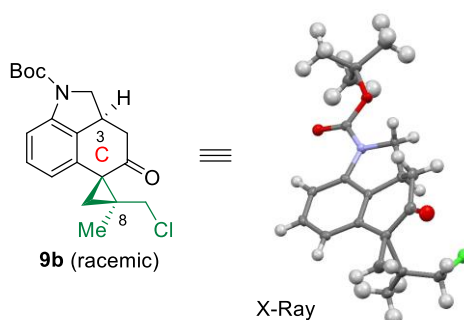
$\text{X=MeNBoc, 4a}$   
 $\text{X=Cl, 4b}$

$\text{X=MeNBoc, 9a}$   
 $\text{X=Cl, 9b}$

Entry	X	Catalyst (1 mol%)	T[°C]	Yield <sup>b</sup>	d.r. <sup>b</sup>
1	MeNBoc	Rh <sub>2</sub> (OAc) <sub>4</sub>	40	<10%	N/D
2	MeNBoc	Rh <sub>2</sub> (esp) <sub>2</sub>	r.t.	trace	N/D
3	MeNBoc	Rh <sub>2</sub> ( <i>R</i> -DOSP) <sub>4</sub>	r.t.	25%	N/D
4	MeNBoc	Rh <sub>2</sub> ( <i>R</i> -DOSP) <sub>4</sub>	-40	trace	N/D
5	Cl	Rh <sub>2</sub> ( <i>R</i> -DOSP) <sub>4</sub>	-60	27%	5:1
6	Cl	Rh <sub>2</sub> ( <i>R</i> -DOSP) <sub>4</sub>	-40	45%	6:1
7 <sup>c</sup>	Cl	Rh <sub>2</sub> ( <i>R</i> -DOSP) <sub>4</sub>	-40	80%	5.9:1
8 <sup>c,d</sup>	Cl	Rh <sub>2</sub> ( <i>R/S</i> -DOSP) <sub>4</sub>	-40	78%	5.8:1
<b>9<sup>c,e,f</sup></b>	<b>Cl</b>	<b>Rh<sub>2</sub>(<i>R</i>-DOSP)<sub>4</sub></b>	<b>-40</b>	<b>85%</b>	<b>5.8:1</b>
10 <sup>c,e</sup>	Cl	Rh <sub>2</sub> ( <i>S</i> -DOSP) <sub>4</sub>	-40	52%	4.3:1
11 <sup>c,e</sup>	Cl	Rh <sub>2</sub> (esp) <sub>2</sub>	-40	67%	6.3:1

<sup>a</sup> Unless otherwise mentioned, the reaction was run on a 0.1 mmol scale at specified temperature for 6 h using racemic compound **3**; compound **3** was added to the stirring solution of catalyst and **4a** or **4b** with a speed of 2 mL/h. <sup>b</sup> Yield and d.r. were determined based on isolated compounds. <sup>c</sup> Using hexane/toluene (10:1) as a mixed solvent. <sup>d</sup> 0.5 mol% of Rh<sub>2</sub>(*R*-DOSP)<sub>4</sub> and 0.5 mol% of Rh<sub>2</sub>(*S*-DOSP)<sub>4</sub> were mixed to provide the racemic catalyst. <sup>e</sup> Starting material **3** was prepared from compound **8** with 97.5% ee. <sup>f</sup> Reaction was run on a 0.7 mmol scale.

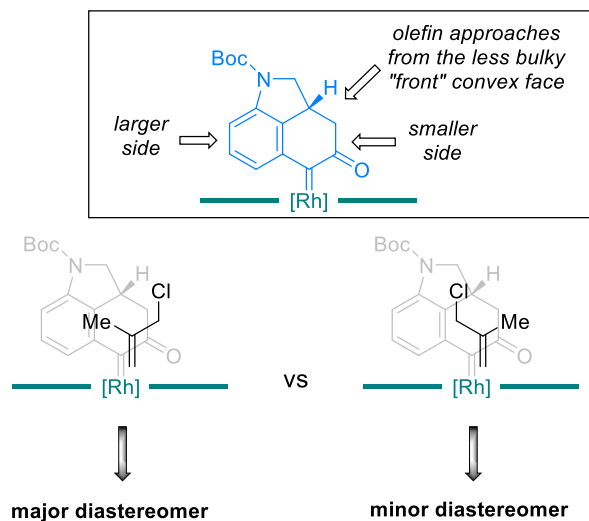
**Scheme 3.9** X-ray Structures of Compound **9b** (Racemic)



A plausible model has been proposed to explain the observed diastereoselectivity (Scheme 3.10). According to Davies' model on the cyclopropanation with donor-accepter carbenoids,<sup>23</sup> the aryl group is generally considered as a larger group and the acceptor part is considered as a smaller

group. Thus, we rationalized that during the transition state for the cyclopropanation, first, the olefin would approach to the less bulky convex face of the tricycle; second, the smaller methyl substituent of the olefin would prefer to stay at the more sterically hindered side (the aryl side) of the carbenoid and the bulkier chloromethyl group of the olefin would favor the less sterically hindered side (the ketone side). The minor diastereomer likely comes from the other olefin orientation relative to the carbenoid due to the moderate steric difference between methyl and chloromethyl groups.

**Scheme 3.10** Stereochemical Model for the Cyclopropanation Step

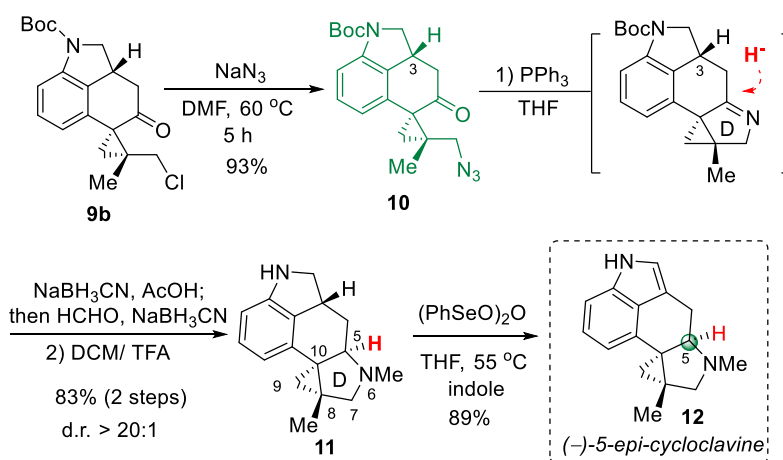


### 3.2.4 End game

The stage is now set for closing of the last D ring. A  $S_N2$  reaction between alkyl chloride **9b** and sodium azide went smoothly to deliver azido compound **10** in an excellent yield (Scheme 3.11). The subsequent one-pot aza-Wittig, imine reduction and reductive amination sequence<sup>24</sup> furnished the pyrrolidine ring and *N*-methyl substitution in a high overall efficiency and complete diastereoselectivity. However, the C5 stereocenter was found to be opposite from the one of natural cycloclavine **1**. Nevertheless, removal of the Boc protecting group with TFA, followed by a

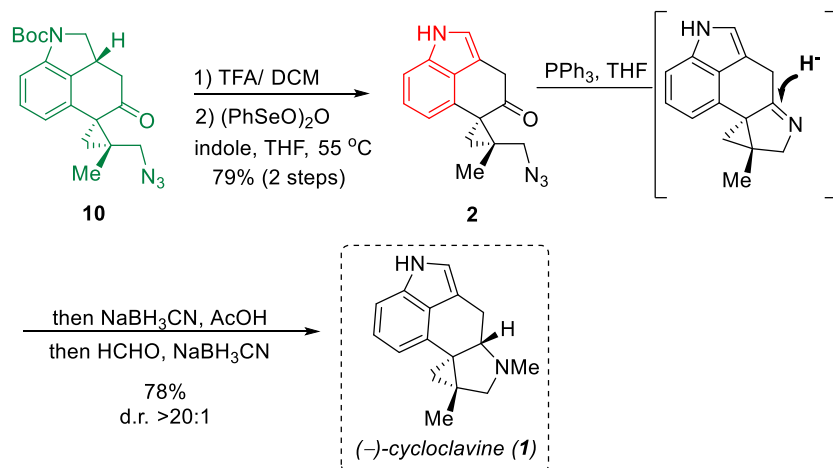
selenium-mediated dehydrogenation,<sup>25</sup> accomplished the synthesis of (–)-5-*epi*-cycloclavine **12**, which spectroscopically matched the one reported by Wipf and coworkers.<sup>13</sup> It is noteworthy that indole was added as a scavenger to avoid oxidative decomposition of product **12** formed.<sup>25c</sup>

### Scheme 3.11 Synthesis of (–)-5-*epi*-Cycloclavine



We postulated that the undesired diastereoselectivity during the imine reduction step is likely influenced by the remote C3 stereocenter. As depicted from the X-ray crystal structure (Scheme 3.9) of **9b**, the cyclohexanone C ring is highly twisted, which forces the C8 quaternary center pointing to the same face as the C3 hydrogen. Thus, we hypothesized that removing the C3 stereocenter might significantly alter the conformation of the imine intermediate, thereby providing a different stereochemical outcome for the reduction. To test this hypothesis, the indoline moiety in azide **10** was then converted to a flat indole structural motif through Boc-deprotection and then dehydrogenation (Scheme 3.12). Using indole **2** as the substrate, to our delight, the same aza-Wittig reduction/reductive amination sequence indeed provided (–)-cycloclavine in 78% yield as a single diastereomer, which is spectroscopically identical to the reported natural sample.<sup>7,14</sup>

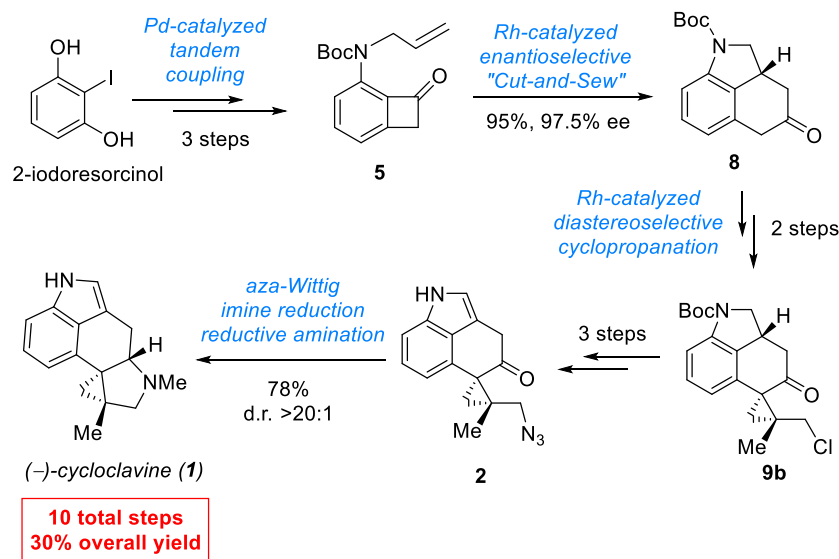
### Scheme 3.12 Total Synthesis of (–)-Cycloclavine



### 3.3 Conclusion

In summary, concise enantioselective total synthesis of (–)-cycloclavine has been accomplished in 10 steps with 30% overall yield (Scheme 3.13). The high efficiency of the synthetic strategy is enabled by a number of transition metal-catalyzed transformations. First, a Pd-catalyzed tandem C–N bond coupling/allylic alkylation offers a rapid and high-yielding route to access nitrogen-tethered benzocyclobutenone substrates. Second, an asymmetric Rh-catalyzed “Cut-and-Sew” reaction has been employed to build the fused A/B/C core structure in a highly enantioselective manner. Third, a diastereoselective Rh-catalyzed cyclopropanation between  $\alpha$ -diazoketone and 1,1-substituted olefin effectively constructs two adjacent quaternary centers, which addresses the “late-stage cyclopropanation challenge” in cycloclavine synthesis.<sup>11</sup> In particular, the C–C activation method has served as the key strategy in this total synthesis, which could have further implications beyond this work. It is anticipated that the unique “Cut-and-Sew” strategy may inspire future development of novel bond disconnections for the syntheses of other natural products and bioactive compounds that contain complex bridged or fused rings.

**Scheme 3.13** A Summary of the Synthetic Efforts towards (–)-Cycloclavine



### 3.4 Experimental

#### 3.4.1 General information

Unless otherwise noted, all screening reactions were carried out in 4-mL vial sealed with PTFE lined caps. Solvents for the rhodium catalyzed C–C bond activation reaction were distilled over corresponding drying agents then freeze-pump-thawed three times before use. Methyl acetate was distilled over phosphorus pentoxide and freeze-pump-thawed three times before use. Rhodium precatalysts were purchased from Strem. All commercially available substrates were used without further purification. Thin layer chromatography (TLC) analysis was run on silica gel plates purchased from EMD Chemical (silica gel 60, F254). Infrared spectra were recorded on a Nicolet iS5 FT-IR Spectrometer using neat thin film technique. High-resolution mass spectra (HRMS) were obtained on an Agilent 6224 TOF-MS spectrometer and are reported as  $m/z$ . Nuclear magnetic resonance spectra ( $^1\text{H}$  NMR and  $^{13}\text{C}$  NMR) were recorded with a Bruker Model DMX 400 (400 MHz,  $^1\text{H}$  at 400 MHz,  $^{13}\text{C}$  at 101 MHz). For  $\text{CDCl}_3$  solutions, the chemical shifts were

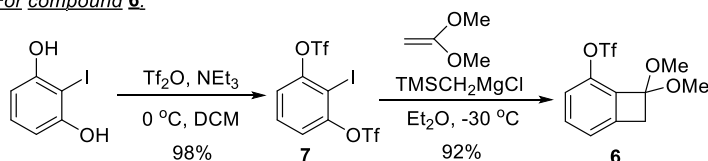


reported as parts per million (ppm) referenced to residual protium or carbon of the solvents:  $\text{CHCl}_3$   $\delta$  H (7.26 ppm) and  $\text{CDCl}_3$   $\delta$  C (77.00 ppm). Coupling constants were reported in Hertz (Hz). Data for  $^1\text{H}$  NMR spectra were reported as following: chemical shift ( $\delta$ , ppm), multiplicity (br = broad, s = singlet, d = doublet, t = triplet, q = quartet, dd = doublet of doublets, td = triplet of doublets, ddd = doublet of doublet of doublets, m = multiplet), coupling constant (Hz), and integration. Analytical HPLC was carried out on an Angilent 1260 infinity HPLC with DAD, Chiralpak IA-IF, served as columns, and mixtures of *n*-hexane and *i*-PrOH were used for elution.

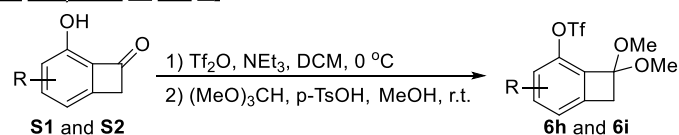
### 3.4.2 Synthetic routes for substrate synthesis

The substrates for the C–C activation reactions were synthesized following the route shown below:

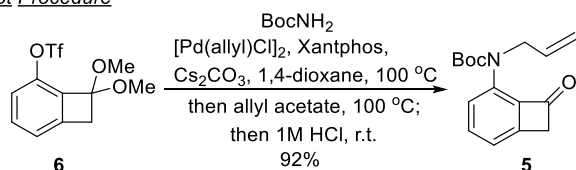
For compound 6:



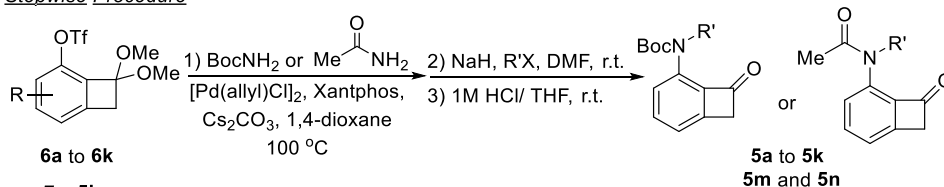
For compound 6h and 6i:



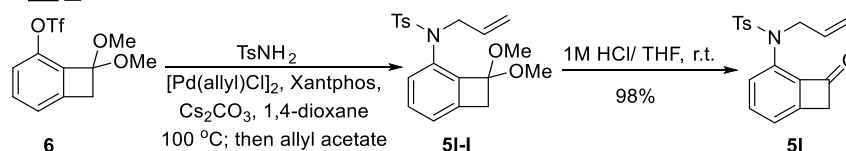
One-pot Procedure



Stepwise Procedure



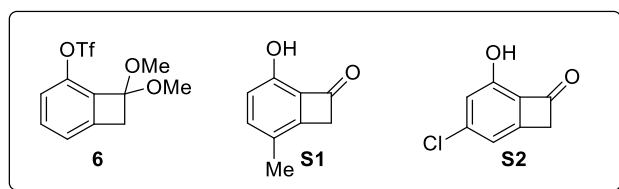
For 5l



Compound **6** was synthesized according to the reported procedure<sup>15</sup>. Compounds **6h** and **6i** were synthesized in two steps from literature known benzocyclobutenone precursors<sup>5f</sup> **S1** and **S2**. For the following C–N bond coupling reaction, alkylation and deprotection sequence, substrate **5** was synthesized using a one-pot procedure<sup>16d</sup>, while substrates **5a-5k** and **5m** to **5n** were synthesized following the stepwise procedure. For compound **5l**, because the C–N bond coupling was not efficient enough, we purified the intermediate **5l-I** and subjected it to the following reactions.

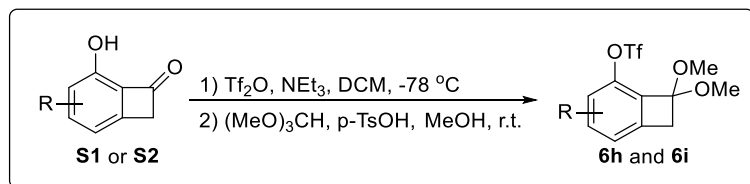
### 3.4.2.1 Synthesis of intermediates and substrates **5** to **5n**

a) Synthesis of known compounds **6**, **S1** and **S2**:



Compounds **6**, **S1** and **S2** were synthesized according to the reported procedure, Their spectroscopic data match those reported in literature<sup>5f,15</sup>.

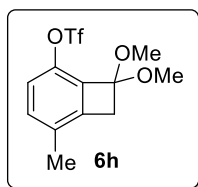
b) Synthesis of compounds **6h** and **6i**:



### Representative procedure:

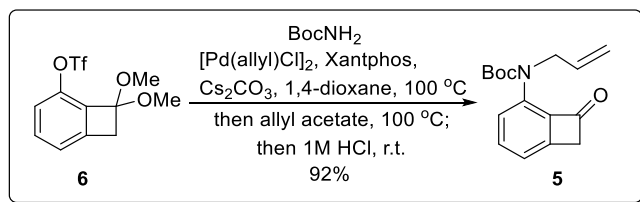
To a 100 mL flamed-dried Schlenk flask equipped with a stir bar and a nitrogen-filled balloon was added **S1** (843.7 mg, 5.7 mmol, 1.0 equiv.) in dichloromethane (30 mL). The system was cooled to -78 °C with a dry ice-acetone bath before NEt<sub>3</sub> (1.58 mL, 11.4 mmol, 2.0 equiv.) and Tf<sub>2</sub>O (1.15

mL, 6.84 mmol, 1.2 equiv.) were added dropwisely. Upon completion of the addition, the system was kept at -78 °C and stirred for 1 h under nitrogen atmosphere. After the starting material was fully consumed, the reaction mixture was quenched with saturated aqueous NH<sub>4</sub>Cl solution (20 mL) and warmed to room temperature. The mixture was extracted with ethyl acetate (3×20 mL), washed with brine, and dried over Na<sub>2</sub>SO<sub>4</sub>. The combined organic extract was concentrated under reduced pressure and subjected to next step without further purification. The crude product was dissolved in MeOH (20 mL) before (MeO)<sub>3</sub>CH (5.61 mL, 51.3 mmol, 9.0 equiv.) and *p*-TsOH (108.4 mg, 0.57 mmol, 0.1 equiv.) were added to the stirring solution. The reaction was stirred at room temperature overnight. The reaction was quenched by saturated aqueous NaHCO<sub>3</sub> solution (20 mL) and the mixture was extracted with ethyl acetate (3×20 mL), washed with brine, and dried over Na<sub>2</sub>SO<sub>4</sub>. The crude product was purified by silica gel flash column chromatography (EtOAc/Hexane=1/10) to afford compound **6h** as a colorless oil in 96% yield over two steps (1.78 g).



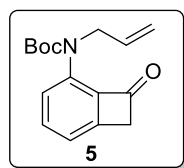
Compound **6h** was isolated as a colorless oil in 96% yield over two steps (1.78 g).  $R_f = 0.6$  (EtOAc/Hexane=1/5). **<sup>1</sup>H NMR (400 MHz, CDCl<sub>3</sub>):**  $\delta$  7.17 (dd,  $J = 8.6, 0.9$  Hz, 1H), 7.05 (d,  $J = 8.5$  Hz, 1H), 3.45 (s, 6H), 3.31 (s, 2H), 2.23 (s, 3H). **<sup>13</sup>C NMR (101 MHz, CDCl<sub>3</sub>):**  $\delta$  143.1, 138.6, 135.6, 134.6, 132.5, 120.1, 120.0, 117.0, 104.5, 51.8, 42.4, 16.4. **IR:**  $\nu$  3446, 2065, 1635, 1423, 1256, 1211, 860, 750, 618 cm<sup>-1</sup>; **HRMS** calcd. For [M+Na]<sup>+</sup>: 349.0328 Found: 349.0323.

c) Synthesis of compound **5**:



### **Procedure:**

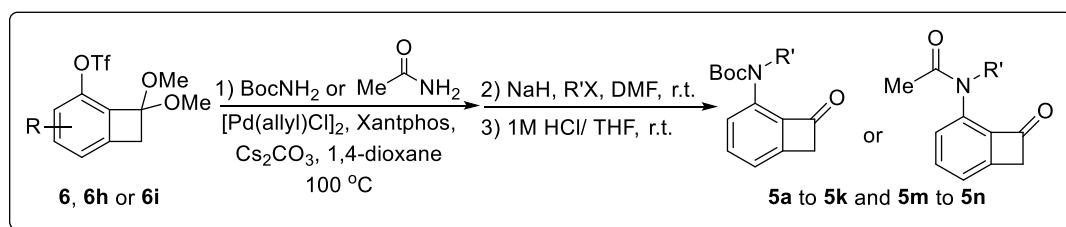
To a 20 mL flamed-dried vial equipped with a stir bar was added **6** (312.3 mg, 1 mmol, 1.0 equiv.), BocNH<sub>2</sub> (175.8 mg, 1.5 mmol, 1.5 equiv.), [Pd(allyl)Cl]<sub>2</sub> (18.3 mg, 0.05 mmol, 5 mol%), Xantphos (86.8 mg, 0.15 mmol, 15 mol%) and Cs<sub>2</sub>CO<sub>3</sub> (975 mg, 3.0 mmol, 3.0 equiv.). Then the vial was loosely capped and transferred into a nitrogen-filled glovebox and 1,4-dioxane (10 mL) was added to the mixture before the vial was tightly capped and transferred out. The system was heated to 100 °C overnight. The reaction was then cooled down to room temperature and allyl acetate (0.54 mL, 5 mmol, 5.0 equiv.) was added to the mixture inside glovebox. The mixture was stirred at 100 °C for another 10 min. After cooling the reaction back to room temperature, 1M HCl (6 mL) was added dropwisely to the vial and the mixture was stirred for 1 h at room temperature. The reaction was then quenched by saturated aqueous NaHCO<sub>3</sub> solution (30 mL) and the mixture was extracted with ethyl acetate (3×20 mL), washed with brine, and dried over Na<sub>2</sub>SO<sub>4</sub>. The crude product was purified by silica gel flash column chromatography (EtOAc/Hexane=1/10) to afford compound **5** as a colorless oil in 92% yield (252 mg).



Compound **5** was isolated as a colorless oil in 92% yield in one pot (252 mg).  $R_f$  = 0.4 (EtOAc/Hexane=1/5). <sup>1</sup>H NMR (500 MHz, CDCl<sub>3</sub>): δ 7.52 (d,  $J$  = 8.4 Hz, 1H), 7.48 – 7.41 (m, 1H), 7.18 (d,  $J$  = 7.1 Hz, 1H), 5.80 (ddt,  $J$  = 17.5, 10.4, 5.3 Hz, 1H), 5.13 – 5.01 (m, 2H), 4.57 (d,

$J = 5.1$  Hz, 2H), 3.89 (s, 2H), 1.49 (s, 9H).  $^{13}\text{C}$  NMR (101 MHz,  $\text{CDCl}_3$ ):  $\delta$  185.4, 153.1, 150.5, 139.0, 135.9, 135.7, 133.8, 123.4, 118.5, 116.0, 81.7, 51.2, 51.1, 28.1. **IR**:  $\nu$  2977, 2929, 1765, 1707, 1599, 1478, 1367, 1239, 1147, 976, 787, 575  $\text{cm}^{-1}$ ; **HRMS** calcd. For  $[\text{M}+\text{Na}]^+$ : 296.1257. Found: 296.1256.

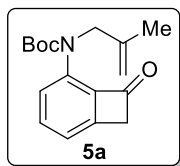
d) Synthesis of compounds **5a** to **5k** and **5m** to **5n**:



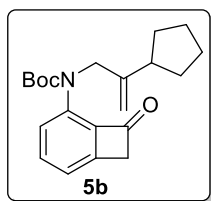
**Procedure** (using **5a** as an example):

To a 20 mL flamed-dried vial equipped with a stir bar was added **6** (665.2 mg, 2.13 mmol, 1.0 equiv.),  $\text{BocNH}_2$  (391.9 mg, 3.34 mmol, 1.5 equiv.),  $[\text{Pd}(\text{allyl})\text{Cl}]_2$  (38.9 mg, 0.11 mmol, 5 mol%), Xantphos (184.9 mg, 0.32 mmol, 15 mol%) and  $\text{Cs}_2\text{CO}_3$  (2.08 g, 6.4 mmol, 3.0 equiv.). Then the vial was loosely capped and transferred into a nitrogen-filled glovebox and 1,4-dioxane (10 mL) was added to the mixture before the vial was tightly capped and transferred out. The system was then heated to  $100^\circ\text{C}$  overnight. Upon completion, the reaction was cooled to room temperature and filtered through a pad of celite. The filtrate was concentrated under reduced pressure and the crude product was dissolved in DMF (10 mL).  $\text{NaH}$  (74.88 mg, 3.12 mmol, 1.5 equiv.) was added to the mixture, followed by 3-chloro-2-methyl-1-propene (0.42 mL, 3.12 mmol, 1.5 equiv.). The mixture was stirred overnight at room temperature. Upon completion, the reaction was quenched with water and extracted with ethyl acetate ( $3 \times 20$  mL), washed with brine, and dried over  $\text{Na}_2\text{SO}_4$ . The crude product was dissolved in 6 mL tetrahydrofuran and transferred to a 20 mL vial charged with a stir bar. While stirring, 2 mL of 1M  $\text{HCl}$  aqueous solution was added to the mixture. After

stirring for 1 h at room temperature, saturated NaHCO<sub>3</sub> aqueous solution was added dropwisely to quench the reaction. The mixture was extracted with ethyl acetate (3×20 mL), washed with brine, and dried over Na<sub>2</sub>SO<sub>4</sub>. The crude product was purified by silica gel flash column chromatography (EtOAc/Hexane=1/5) to afford compound **5a** as a colorless oil in 94% yield (575 mg) over 3 steps. [All the R'X used in substrate preparation were literature known compounds<sup>3,5a</sup>]

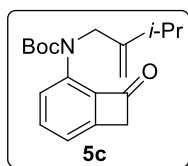


Compound **5a** was isolated as a colorless oil in 94% yield over 3 steps.  $R_f$  = 0.5 (EtOAc/Hexane=1/5). **<sup>1</sup>H NMR (500 MHz, CDCl<sub>3</sub>):**  $\delta$  7.51 (d,  $J$  = 8.4 Hz, 1H), 7.48 – 7.42 (m, 1H), 7.18 (d,  $J$  = 7.0 Hz, 1H), 4.76 – 4.73 (m, 1H), 4.70 (s, 1H), 4.51 (s, 2H), 3.88 (s, 2H), 1.68 (s, 3H), 1.49 (s, 9H). **<sup>13</sup>C NMR (101 MHz, CDCl<sub>3</sub>):**  $\delta$  185.4, 153.3, 150.5, 141.3, 139.2, 135.9, 135.7, 123.5, 118.5, 110.7, 81.6, 53.9, 51.1, 28.1, 19.9. **IR:**  $\nu$  3080, 2976, 2931, 1766, 1708, 1599, 1478, 1367, 1240, 1159, 975, 788, 576 cm<sup>-1</sup>; **HRMS** calcd. For [M+Na]<sup>+</sup>: 310.1414. Found: 310.1414.

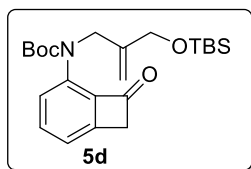


Compound **5b** was isolated as a colorless oil in 86% yield over 3 steps.  $R_f$  = 0.6 (EtOAc/Hexane=1/5). **<sup>1</sup>H NMR (500 MHz, CDCl<sub>3</sub>):**  $\delta$  7.52 (d,  $J$  = 8.4 Hz, 1H), 7.49 – 7.42 (m, 1H), 7.18 (d,  $J$  = 7.0 Hz, 1H), 4.78 (s, 1H), 4.68 (s, 1H), 4.55 (s, 2H), 3.89 (s, 2H), 2.35 (p,  $J$  = 8.5 Hz, 1H), 1.82 (td,  $J$  = 11.2, 6.8 Hz, 2H), 1.72 – 1.62 (m, 2H), 1.61 – 1.52 (m, 2H), 1.49 (s, 9H), 1.44 – 1.34 (m, 2H). **<sup>13</sup>C NMR (101 MHz, CDCl<sub>3</sub>):**  $\delta$  185.3, 153.2, 150.4, 148.5, 139.1, 136.0, 135.8, 123.3, 118.4, 106.3, 81.5, 52.8, 51.0, 43.6, 31.2, 28.0, 24.8. **IR:**  $\nu$  2955, 2869, 1766, 1708,

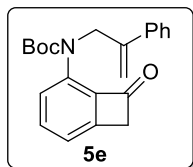
1599, 1478, 1367, 1243, 1157, 981, 787, 575  $\text{cm}^{-1}$ ; **HRMS** calcd. For  $[\text{M}+\text{Na}]^+$ : 364.1883. Found: 364.1880.



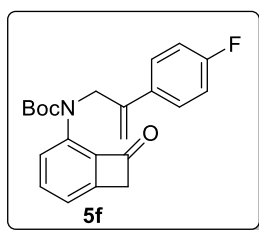
Compound **5c** was isolated as a colorless oil in 97% yield over 3 steps.  $R_f = 0.6$  (EtOAc/Hexane=1/5).  **$^1\text{H}$  NMR (500 MHz,  $\text{CDCl}_3$ )**:  $\delta$  7.51 (d,  $J = 8.4$  Hz, 1H), 7.48 – 7.42 (m, 1H), 7.18 (d,  $J = 7.0$  Hz, 1H), 4.76 (s, 1H), 4.67 (s, 1H), 4.56 (s, 2H), 3.88 (s, 2H), 2.23 (hept,  $J = 6.4$  Hz, 1H), 1.48 (s, 9H), 1.03 (d,  $J = 7.0$  Hz, 6H).  **$^{13}\text{C}$  NMR (101 MHz,  $\text{CDCl}_3$ )**:  $\delta$  185.4, 153.3, 151.1, 150.5, 139.2, 136.0, 135.9, 123.4, 118.5, 106.6, 81.6, 52.1, 51.1, 31.6, 28.1, 21.6. **IR**:  $\nu$  3435, 2965, 2930, 1766, 1708, 1599, 1478, 1367, 1243, 1155, 981, 786  $\text{cm}^{-1}$ ; **HRMS** calcd. For  $[\text{M}+\text{H}]^+$ : 316.1907. Found: 316.1906.



Compound **5d** was isolated as a colorless oil in 91% yield over 3 steps.  $R_f = 0.7$  (EtOAc/Hexane=1/5).  **$^1\text{H}$  NMR (500 MHz,  $\text{CDCl}_3$ )**:  $\delta$  7.49 (d,  $J = 8.3$  Hz, 1H), 7.45 (dd,  $J = 8.3$ , 6.8 Hz, 1H), 7.18 (d,  $J = 6.8$  Hz, 1H), 5.05 (d,  $J = 1.5$  Hz, 1H), 4.83 (d,  $J = 1.4$  Hz, 1H), 4.58 (s, 2H), 4.09 (s, 2H), 3.88 (s, 2H), 1.48 (s, 9H), 0.87 (s, 9H), 0.02 (s, 6H).  **$^{13}\text{C}$  NMR (101 MHz,  $\text{CDCl}_3$ )**:  $\delta$  185.4, 153.2, 150.5, 144.3, 139.4, 135.9, 135.6, 123.5, 118.6, 109.7, 81.7, 64.1, 51.2, 50.7, 28.1, 25.8, 18.3, -5.5. **IR**:  $\nu$  2929, 2856, 1766, 1711, 1600, 1478, 1367, 1257, 1158, 977, 838, 765  $\text{cm}^{-1}$ ; **HRMS** calcd. For  $[\text{M}+\text{H}]^+$ : 418.2408. Found: 418.2410.

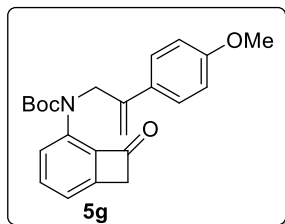


Compound **5e** was isolated as a colorless oil in 30% yield over 3 steps.  $R_f = 0.5$  (EtOAc/Hexane=1/5).  **$^1\text{H}$  NMR (500 MHz,  $\text{CDCl}_3$ ):**  $\delta$  7.40 (dd,  $J = 8.4, 7.1$  Hz, 1H), 7.35 – 7.24 (m, 6H), 7.18 (d,  $J = 7.1$  Hz, 1H), 5.25 (s, 1H), 5.05 (s, 1H), 5.02 (s, 2H), 3.90 (s, 2H), 1.47 (s, 9H).  **$^{13}\text{C}$  NMR (101 MHz,  $\text{CDCl}_3$ ):**  $\delta$  185.5, 153.1, 150.4, 144.5, 139.5, 139.1, 135.8, 135.2, 128.2, 127.7, 126.4, 124.1, 118.7, 112.7, 81.7, 51.9, 51.2, 28.0. **IR:**  $\nu$  2977, 2926, 1766, 1707, 1599, 1478, 1368, 1241, 1157, 981, 750, 704  $\text{cm}^{-1}$ ; **HRMS** calcd. For  $[\text{M}+\text{H}]^+$ : 350.1751. Found: 350.1761.

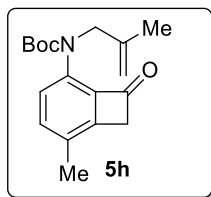


Compound **5f** was isolated as a light yellow solid in 75% yield over 3 steps. Melting Point: 91-92  $^{\circ}\text{C}$ .  $R_f = 0.4$  (EtOAc/Hexane=1/5).  **$^1\text{H}$  NMR (500 MHz,  $\text{CDCl}_3$ ):**  $\delta$  7.40 (t,  $J = 7.7$  Hz, 1H), 7.34 – 7.26 (m, 3H), 7.19 (d,  $J = 7.1$  Hz, 1H), 6.97 (t,  $J = 8.5$  Hz, 2H), 5.18 (s, 1H), 5.03 (s, 1H), 5.00 (s, 2H), 3.90 (s, 2H), 1.47 (s, 9H).  **$^{13}\text{C}$  NMR (101 MHz,  $\text{CDCl}_3$ ):**  $\delta$  185.6, 162.4 (d,  $J = 246.7$  Hz), 153.1, 150.4, 143.6, 139.4, 135.8, 135.2 (d,  $J = 3.4$  Hz), 135.1, 128.1 (d,  $J = 8.0$  Hz), 124.2, 118.8, 115.0 (d,  $J = 21.4$  Hz), 112.9, 81.8, 51.8, 51.2, 28.0.  **$^{19}\text{F}$  NMR (470 MHz,  $\text{CDCl}_3$ ):**  $\delta$  -68.4. **IR:**  $\nu$  3435, 2930, 1764, 1707, 1600, 1510, 1368, 1234, 1157, 981, 841, 750  $\text{cm}^{-1}$ ; **HRMS** calcd. For  $[\text{M}+\text{Na}]^+$ : 390.1476. Found: 390.1483.

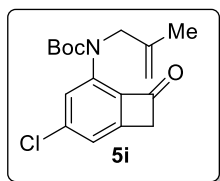




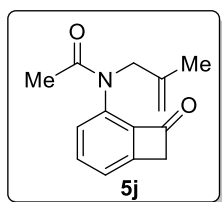
Compound **5g** was isolated as a colorless oil in 37% yield over 3 steps.  $R_f = 0.4$  (EtOAc/Hexane=1/5).  **$^1\text{H}$  NMR (500 MHz,  $\text{CDCl}_3$ ):**  $\delta$  7.40 (t,  $J = 7.7$  Hz, 1H), 7.31 (d,  $J = 8.3$  Hz, 1H), 7.29 – 7.25 (m, 2H), 7.18 (d,  $J = 7.1$  Hz, 1H), 6.83 (d,  $J = 8.6$  Hz, 2H), 5.18 (s, 1H), 4.96 (s, 1H), 4.99 (s, 2H), 3.89 (s, 2H), 3.80 (s, 3H), 1.47 (s, 9H).  **$^{13}\text{C}$  NMR (101 MHz,  $\text{CDCl}_3$ ):**  $\delta$  185.5, 159.2, 153.2, 150.4, 143.7, 139.5, 135.7, 135.2, 131.6, 127.4, 124.2, 118.7, 113.5, 111.2, 81.7, 55.2, 51.8, 51.2, 28.1. **IR:**  $\nu$  3454, 2978, 2932, 1763, 1706, 1600, 1513, 1368, 1249, 1156, 1033, 981, 836, 749, 576  $\text{cm}^{-1}$ ; **HRMS** calcd. For  $[\text{M}+\text{Na}]^+$ : 402.1676 Found: 402.1669.



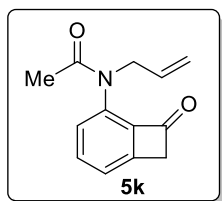
Compound **5h** was isolated as a colorless oil in 87% yield over 3 steps.  $R_f = 0.6$  (EtOAc/Hexane=1/5).  **$^1\text{H}$  NMR (400 MHz,  $\text{CDCl}_3$ ):**  $\delta$  7.39 (d,  $J = 8.3$  Hz, 1H), 7.24 (d,  $J = 8.4$  Hz, 1H), 4.74 (s, 1H), 4.70 (s, 1H), 4.49 (s, 2H), 3.82 (s, 2H), 2.30 (s, 3H), 1.67 (s, 3H), 1.48 (s, 9H).  **$^{13}\text{C}$  NMR (101 MHz,  $\text{CDCl}_3$ ):**  $\delta$  185.3, 153.4, 149.2, 141.4, 138.9, 136.8, 133.2, 128.8, 124.7, 110.8, 81.4, 53.9, 50.0, 28.1, 19.9, 16.9. **IR:**  $\nu$  2976, 2922, 1761, 1706, 1577, 1497, 1389, 1366, 1242, 1154, 1088, 979, 764  $\text{cm}^{-1}$ ; **HRMS** calcd. For  $[\text{M}+\text{H}]^+$ : 302.1751 Found: 302.1749.



Compound **5i** was isolated as a colorless oil in 60% yield over 3 steps.  $R_f = 0.4$  (EtOAc/Hexane=1/5).  **$^1\text{H}$  NMR (400 MHz,  $\text{CDCl}_3$ )**:  $\delta$  7.67 (s, 1H), 7.17 (d,  $J = 1.3$  Hz, 1H), 4.80 – 4.71 (m, 1H), 4.67 (s, 1H), 4.53 (s, 2H), 3.86 (s, 2H), 1.69 (s, 3H), 1.50 (s, 9H).  **$^{13}\text{C}$  NMR (101 MHz,  $\text{CDCl}_3$ )**:  $\delta$  183.6, 152.9, 151.2, 141.8, 141.0, 137.0, 136.7, 123.6, 118.9, 110.6, 82.3, 54.0, 50.7, 28.0, 19.9. **IR**:  $\nu$  2977, 2930, 1766, 1713, 1594, 1446, 1366, 1275, 1155, 1071, 980, 764, 749  $\text{cm}^{-1}$ ; **HRMS** calcd. For  $[\text{M}+\text{Na}]^+$ : 344.1024 Found: 344.1028.

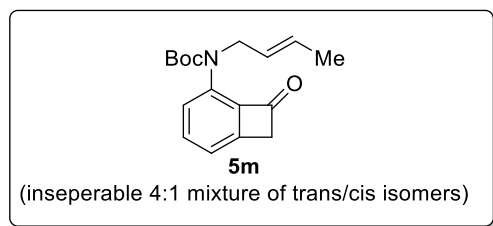


Compound **5j** was isolated as a colorless oil in 78% yield over 3 steps.  $R_f = 0.4$  (acetone/Hexane=1/5).  **$^1\text{H}$  NMR (400 MHz,  $\text{CDCl}_3$ )**:  $\delta$  7.53 (dd,  $J = 8.1, 7.3$  Hz, 1H), 7.36 (d,  $J = 7.3$  Hz, 1H), 7.30 (s, 1H), 4.76 (s, 1H), 4.72 (s, 1H), 4.50 (s, 2H), 3.97 (s, 2H), 2.15 (s, 3H), 1.67 (s, 3H).  **$^{13}\text{C}$  NMR (101 MHz,  $\text{CDCl}_3$ )**:  $\delta$  185.5, 170.0, 151.4, 140.5, 136.3, 135.1, 125.7, 121.0, 112.2, 53.9, 51.8, 22.5, 20.0. **IR**:  $\nu$  3005, 1762, 1665, 1596, 1477, 1377, 1275, 1260, 764, 750  $\text{cm}^{-1}$ ; **HRMS** calcd. For  $[\text{M}+\text{H}]^+$ : 230.1176 Found: 230.1179.

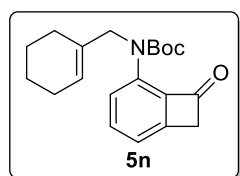


Compound **5k** was isolated as a colorless oil in 85% yield over 3 steps.  $R_f = 0.4$  (acetone/Hexane=1/5).  **$^1\text{H}$  NMR (400 MHz,  $\text{CDCl}_3$ )**:  $\delta$  7.54 (dd,  $J = 8.1, 7.3$  Hz, 1H), 7.38 (d,  $J = 7.3$  Hz, 1H), 7.29 (s, 1H), 5.78 (ddt,  $J = 17.2, 10.6, 5.5$  Hz, 1H), 5.18 – 5.03 (m, 2H), 4.53 (d,  $J = 5.5$  Hz, 2H), 3.99 (s, 2H), 2.13 (s, 3H).  **$^{13}\text{C}$  NMR (101 MHz,  $\text{CDCl}_3$ )**:  $\delta$  185.5, 169.8, 151.6,

136.3, 135.1, 133.0, 126.0, 121.3, 117.1, 51.9, 51.3, 22.6. **IR:**  $\nu$  2922, 1762, 1668, 1596, 1478, 1375, 1275, 1139, 970, 750, 570  $\text{cm}^{-1}$ ; **HRMS** calcd. For  $[\text{M}+\text{H}]^+$ : 216.1019 Found: 216.1015.

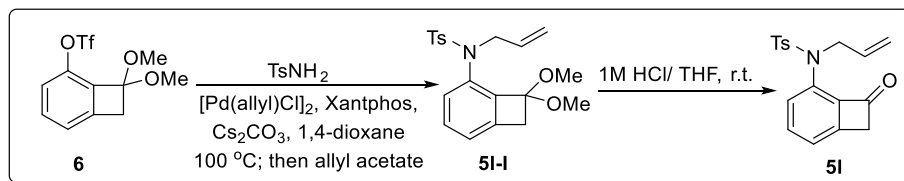


Compound **5m** was isolated as a colorless oil in 88% yield over 3 steps.  $R_f = 0.6$  (EtOAc/Hexane=1/5).  **$^1\text{H}$  NMR (400 MHz,  $\text{CDCl}_3$ ):**  $\delta$  (reported as a E/Z mixture) 7.53 – 7.40 (m, 2H), 7.19 (td,  $J = 7.1, 1.4$  Hz, 1H), 5.59 – 5.29 (m, 2H), 4.63 – 4.57 (m, 0.4H), 4.48 (dt,  $J = 5.6, 1.3$  Hz, 1.6H), 3.93 – 3.85 (m, 2H), 1.64 – 1.57 (m, 3H), 1.49 (s, 9H).  **$^{13}\text{C}$  NMR (101 MHz,  $\text{CDCl}_3$ ):**  $\delta$  (reported as a E/Z mixture) 185.52, 185.46, 153.2, 150.6, 150.5, 139.5, 139.1, 135.9, 135.84, 135.82, 135.7, 127.8, 126.6, 126.51, 126.48, 124.1, 123.6, 118.7, 118.4, 81.6, 81.5, 51.2, 51.1, 50.7, 46.2, 28.2, 28.1, 17.7, 13.0. **IR:**  $\nu$  2975, 2927, 1763, 1704, 1599, 1580, 1477, 1366, 1308, 1232, 1159, 1138, 974  $\text{cm}^{-1}$ ; **HRMS** calcd. For  $[\text{M}+\text{H}]^+$ : 288.1594; Found: 288.1591.



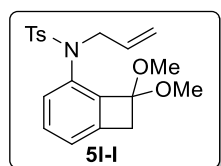
Compound **5n** was isolated as a colorless oil in 80% yield over 3 steps.  $R_f = 0.6$  (EtOAc/Hexane=1/5).  **$^1\text{H}$  NMR (400 MHz,  $\text{CDCl}_3$ ):**  $\delta$  7.45 (d,  $J = 4.4$  Hz, 2H), 7.22 – 7.16 (m, 1H), 5.45 – 5.37 (m, 1H), 4.43 (s, 2H), 3.89 (s, 2H), 1.94 – 1.82 (m, 4H), 1.56 – 1.50 (m, 2H), 1.48 (s, 9H), 1.47 – 1.43 (m, 2H).  **$^{13}\text{C}$  NMR (101 MHz,  $\text{CDCl}_3$ ):**  $\delta$  185.6, 153.5, 150.5, 139.6, 135.8, 135.8, 133.7, 123.8, 122.6, 118.5, 81.4, 54.3, 51.2, 28.1, 26.0, 24.9, 22.5, 22.3. **IR:**  $\nu$  3450, 2976, 2928, 1764, 1704, 1634, 1478, 1366, 1234, 1157, 1137, 980  $\text{cm}^{-1}$ ; **HRMS** calcd. For  $[\text{M}+\text{H}]^+$ : 328.1907; Found: 328.1903.

e) Synthesis of compound **5I**:



**Procedure (step 1):**

To a 8 mL flamed-dried vial equipped with a stir bar was added **6** (156.2 mg, 1 mmol, 1.0 equiv.), TsNH<sub>2</sub> (205.4 mg, 1.2 mmol, 2.4 equiv.), [Pd(allyl)Cl]<sub>2</sub> (36.6 mg, 0.10 mmol, 20 mol%), Xantphos (173. mg, 0.30 mmol, 60 mol%) and Cs<sub>2</sub>CO<sub>3</sub> (488.7 mg, 1.5 mmol, 3.0 equiv.). Then the vial was loosely capped and transferred into a nitrogen-filled glovebox and 1,4-dioxane (4 mL) was added to the mixture before the vial was tightly capped and transferred out. The system was then heated to 100 °C overnight. Upon completion, the reaction was cooled to room temperature and filtered through a pad of celite. The filtrate was concentrated under reduced pressure and the crude product was dissolved in DMF (10 mL). NaH (20.0 mg, 0.5 mmol, 2 equiv.) was added to the mixture, followed by allyl bromide (121.0 mg, 1.0 mmol, 2.0 equiv.). The mixture was stirred overnight at room temperature. Upon completion, the reaction was quenched with water and extracted with ethyl acetate (3×20 mL), washed with brine, and dried over Na<sub>2</sub>SO<sub>4</sub>. The crude product was purified by silica gel flash column chromatography (EtOAc/Hexane=1/3) to afford compound **5I-I** as a colorless oil in 47% yield (88 mg).

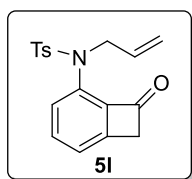


Compound **5I-I** was isolated as a colorless oil in 47% yield.  $R_f = 0.4$  (EtOAc/Hexane=1/3). <sup>1</sup>H NMR (500 MHz, CDCl<sub>3</sub>):  $\delta$  7.60 (d,  $J = 8.3$  Hz, 2H), 7.20 (d,  $J = 7.7$  Hz, 2H), 7.15 (d,  $J = 7.6$

Hz, 1H), 7.10 (d,  $J = 7.3$  Hz, 1H), 6.82 (d,  $J = 7.8$  Hz, 1H), 5.41 (t,  $J = 6.7$  Hz, 1H), 5.37 (s, 1H), 5.27 (d,  $J = 1.3$  Hz, 1H), 4.09 (d,  $J = 6.7$  Hz, 2H), 3.33 (s, 6H), 3.32 (s, 2H), 2.41 (s, 3H).  **$^{13}\text{C}$  NMR (101 MHz,  $\text{CDCl}_3$ )**:  $\delta$  142.8, 142.8, 141.5, 141.2, 137.6, 133.6, 130.5, 129.3, 127.1, 126.4, 123.0, 117.2, 106.1, 52.0, 47.6, 41.5, 21.5. **IR**:  $\nu$  3278, 2935, 2831, 1639, 1599, 1451, 1328, 1238, 1160, 1104, 1061, 1034, 850, 791, 664, 550  $\text{cm}^{-1}$ ; **HRMS** calcd. For  $[\text{M}+\text{H}]^+$ : 374.1421; Found: 374.1417.

**Procedure (step 2):**

Compound **51-I** (136 mg, 0.36 mmol, 1.0 equiv.) was dissolved in 6 mL tetrahydrofuran and transferred to a 20 mL vial charged with a stir bar. While stirring, 2 mL of 1M HCl aqueous solution was added to the mixture. After stirring for 1 h at room temperature, saturated  $\text{NaHCO}_3$  aqueous solution was added dropwisely to quench the reaction. The mixture was extracted with ethyl acetate (3 $\times$ 20 mL), washed with brine, and dried over  $\text{Na}_2\text{SO}_4$ . The crude product was purified by silica gel flash column chromatography (EtOAc/Hexane=1/5) to afford compound **51** as a colorless oil in 98% yield (117.5 mg).



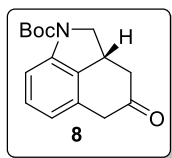
Compound **51** was isolated as a colorless oil in 98% yield from **51-I**.  $R_f = 0.3$  (EtOAc/Hexane=1/3).  **$^1\text{H}$  NMR (400 MHz,  $\text{CDCl}_3$ )**:  $\delta$  7.64 (dd,  $J = 8.2, 0.8$  Hz, 1H), 7.54 (dd,  $J = 8.2, 7.2$  Hz, 1H), 7.42 (d,  $J = 8.4$  Hz, 2H), 7.33 (dd,  $J = 7.2, 0.7$  Hz, 1H), 7.21 (d,  $J = 7.8$  Hz, 2H), 5.69 (ddt,  $J = 17.1, 10.3, 5.8$  Hz, 1H), 5.09 (dq,  $J = 17.2, 1.6$  Hz, 1H), 5.00 (dq,  $J = 10.3, 1.4$  Hz, 1H), 4.49 (dt,  $J = 5.8, 1.6$  Hz, 2H), 3.80 (s, 2H), 2.39 (s, 3H).  **$^{13}\text{C}$  NMR (101 MHz,  $\text{CDCl}_3$ )**:  $\delta$  184.4, 150.8, 144.0, 141.2, 136.3, 134.4, 132.9, 132.6, 129.5, 128.0, 127.3, 121.1, 118.3, 52.2, 51.2, 21.6. **IR**:  $\nu$  2924,

1766, 1595, 1473, 1354, 1164, 1090, 973, 814, 748, 662, 545  $\text{cm}^{-1}$ ; **HRMS** calcd. For  $[\text{M}+\text{H}]^+$ : 328.1002 Found: 328.1003.

### 3.4.3 Procedure for C–C bond activation and characterization of compounds 8 to 8l

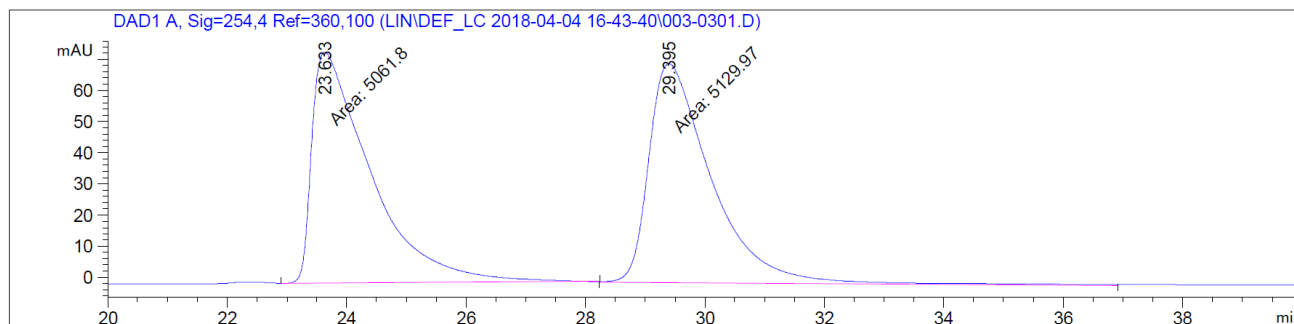
#### **Procedure:**

In a nitrogen filled glove box, a 4 mL vial was charged with the benzocyclobutenone substrates (**5** to **5l**, 0.1 mmol),  $\text{Rh}(\text{COD})_2\text{BF}_4$  (5 mol%, 0.005 mmol, 2.1 mg) and (*R*)-DTBM-segphos (6 mol%, 0.006 mmol, 7.1 mg). After adding 1 mL 1,4-dioxane, the vial was capped and the solution was maintained at certain temperature (90 °C or 110 °C) for 12h. Upon completion, it was cooled to room temperature and the solvent was removed by rotavap under reduced pressure. The crude product was directly purified by silica gel flash chromatography to yield **8** to **8l**.



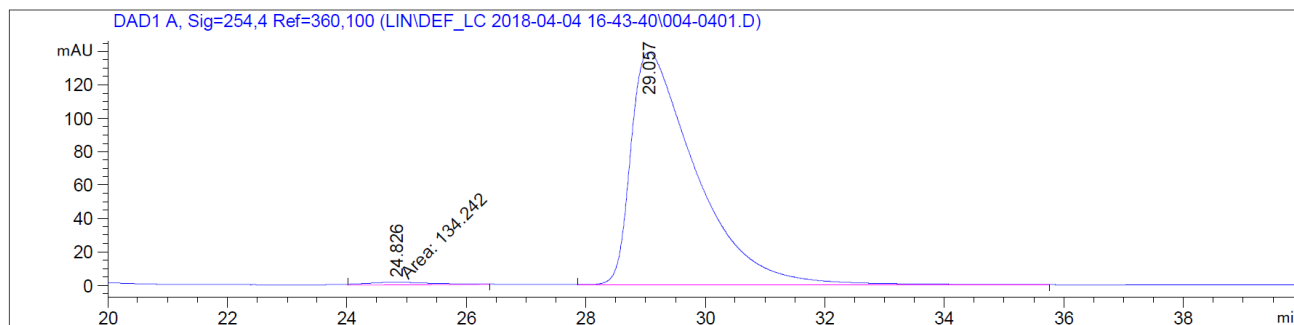
**8** (518.2 mg) was isolated as a white solid in 95% yield. Melting Point: 115-116 °C.  $\text{Rh}(\text{COD})_2\text{BF}_4$  (3 mol%, 0.06 mmol, 24.4 mg) and (*R*)-DTBM-segphos (3.6 mol%, 0.072 mmol, 84.9 mg) were used and the reaction was maintained at 90 °C.  $R_f = 0.4$  (EtOAc/Hexane=1/3).  **$^1\text{H}$  NMR (400 MHz,  $\text{CDCl}_3$ ):**  $\delta$  7.72 – 7.20 (m, 1H), 7.18 (t,  $J = 7.7$  Hz, 1H), 6.77 (d,  $J = 7.6$  Hz, 1H), 4.41 (s, 1H), 3.79 – 3.63 (m, 1H), 3.63 – 3.54 (m, 1H), 3.52 (s, 2H), 2.95 (dd,  $J = 16.2, 5.3$  Hz, 1H), 2.30 (dd,  $J = 16.2, 12.3$  Hz, 1H), 1.57 (s, 9H).  **$^{13}\text{C}$  NMR (101 MHz,  $\text{CDCl}_3$ ):**  $\delta$  208.7, 152.4, 130.3, 129.1, 121.0, 112.9, 81.1, 55.3, 44.0, 42.2, 34.0, 28.4. **IR:**  $\nu$  2975, 1700, 1462, 1389, 1351, 1252, 1161, 1135, 948, 856, 784, 762, 735  $\text{cm}^{-1}$ ; **HRMS** calcd. For  $[\text{M}+\text{Na}]^+$ : 296.1257. Found: 296.1254. Chiral HPLC (Chiralpak IF, hexane:isopropanol = 98:2, 1 mL/min, 254 nm),  $t_{\text{minor}} = 24.8$  min,  $t_{\text{major}} = 29.0$  min.  $[\alpha]_{\text{D}}^{21.5} = -139$  ( $c = 2.20$ ,  $\text{CHCl}_3$ ) at 97.5 % e.e.

## Racemic Sample 8

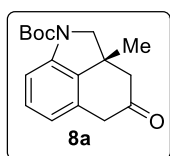


Peak #	RetTime [min]	Type	Width [min]	Area [mAU*s]	Height [mAU]	Area %
1	23.633	MM	1.1375	5061.79883	74.16519	49.6656
2	29.395	MM	1.2159	5129.96924	70.31551	50.3344

## Enantiomeric Sample 8



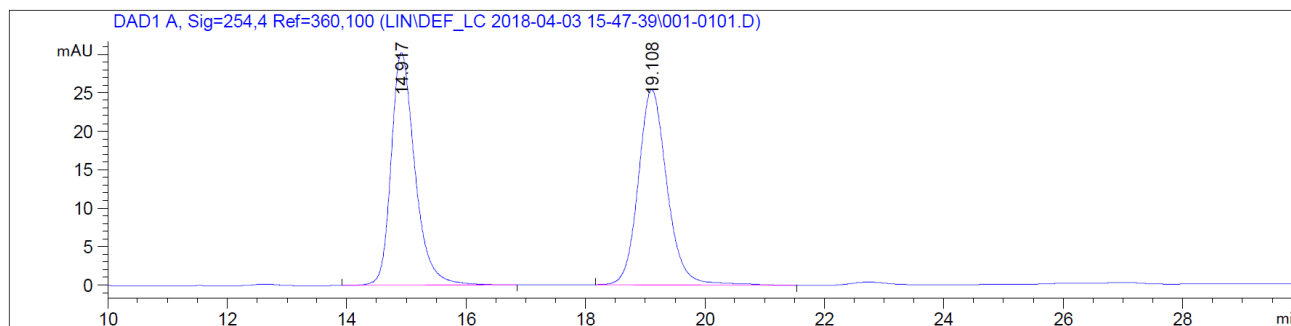
Peak #	RetTime [min]	Type	Width [min]	Area [mAU*s]	Height [mAU]	Area %
1	24.826	MM	1.4330	134.24211	1.56128	1.2608
2	29.057	BB	1.1122	1.05130e4	139.02695	98.7392



**8a** (25.0 mg) was isolated as a white solid in 88% yield. Melting Point: 154-156 °C. Rh(COD)<sub>2</sub>BF<sub>4</sub> (5 mol%, 0.005 mmol, 2.1 mg) and (*R*)-DTBM-segphos (6 mol%, 0.006 mmol, 7.1 mg) were used and the reaction was maintained at 90 °C. *R<sub>f</sub>* = 0.4 (EtOAc/Hexane=1/3). **<sup>1</sup>H NMR (400 MHz, CDCl<sub>3</sub>)**: δ 7.73 – 7.20 (m, 1H), 7.18 (t, *J* = 7.8 Hz, 1H), 6.77 (d, *J* = 7.5 Hz, 1H), 3.99 (s, 1H), 3.71 (d, *J* = 10.8 Hz, 1H), 3.60 (d, *J* = 21.7 Hz, 1H), 3.50 (d, *J* = 21.7 Hz, 1H), 2.80 (d, *J* = 15.6 Hz, 1H), 2.52 (d, *J* = 15.6 Hz, 1H), 1.58 (s, 9H), 1.26 (s, 3H). **<sup>13</sup>C NMR (101 MHz, CDCl<sub>3</sub>)**: δ 208.8, 152.6, 140.5, 129.5, 129.0, 121.3, 113.1, 81.7, 62.3, 50.9, 40.7, 39.7, 28.4, 25.8. **IR**: ν 3444, 2975, 1700, 1621, 1475, 1389, 1337, 1162, 1136, 855, 750 cm<sup>-1</sup>; **HRMS** calcd. For [M+Na]<sup>+</sup>: 310.1414. Found: 310.1415.

Chiral HPLC (Chiralpak IF, hexane:isopropanol = 98:2, 1 mL/min, 254 nm), *t*<sub>minor</sub> = 18.4 min, *t*<sub>major</sub> = 14.1 min. [α]<sub>D</sub><sup>21.5</sup> = -91.2 (c= 1.04, CHCl<sub>3</sub>) at 98 % e.e.

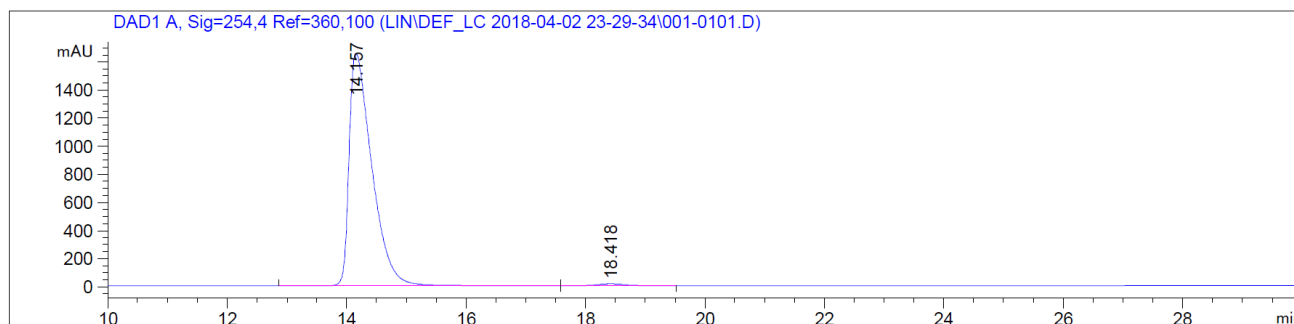
### Racemic Sample 8a



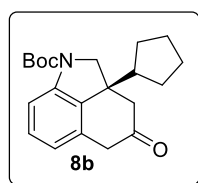
Peak #	RetTime [min]	Type	Width [min]	Area [mAU*s]	Height [mAU]	Area %
1	14.917	BB	0.4215	838.23456	30.22814	49.6893
2	19.108	BB	0.5101	848.71851	25.38437	50.3107

### Enantiomeric Sample 8a





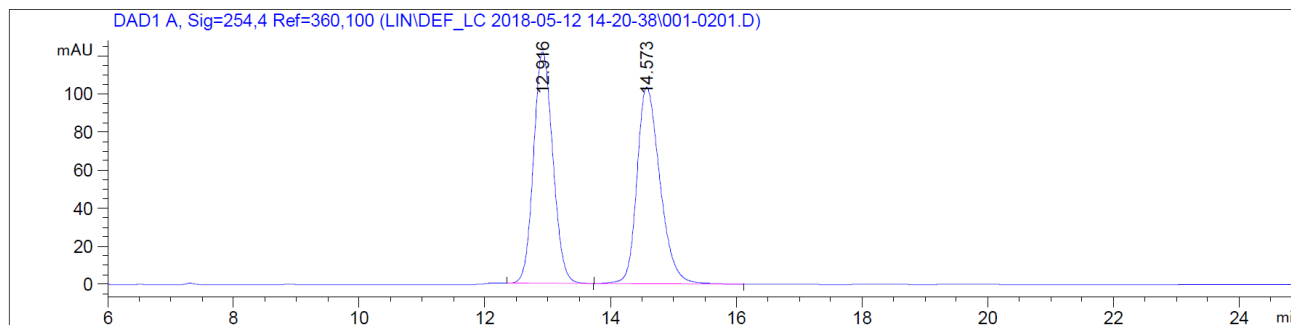
Peak #	RetTime [min]	Type	Width [min]	Area [mAU*s]	Height [mAU]	Area %
1	14.157	BB	0.3958	4.36475e4	1654.24170	98.9617
2	18.418	BB	0.4994	457.95563	14.08207	1.0383



**8b** (26.6 mg) was isolated as a colorless oil in 78% yield.  $\text{Rh}(\text{COD})_2\text{BF}_4$  (5 mol%, 0.005 mmol, 2.1 mg) and (*R*)-DTBM-segphos (6 mol%, 0.006 mmol, 7.1 mg) were used and the reaction was maintained at 90 °C.  $R_f = 0.4$  (EtOAc/Hexane=1/3).  **$^1\text{H}$  NMR (400 MHz,  $\text{CDCl}_3$ )**:  $\delta$  7.75 – 7.19 (m, 1H), 7.18 (s, 1H), 6.77 (d,  $J = 7.6$  Hz, 1H), 4.13 (m, 1H), 3.65 (d,  $J = 21.9$  Hz, 1H), 3.57 (d,  $J = 11.4$  Hz, 1H), 3.45 (d,  $J = 22.0$  Hz, 1H), 2.92 (d,  $J = 15.7$  Hz, 1H), 2.46 (d,  $J = 15.7$  Hz, 1H), 1.88 (d,  $J = 8.4$  Hz, 1H), 1.77 (dtd,  $J = 11.0, 7.3, 3.0$  Hz, 1H), 1.66 – 1.49 (m, 12H), 1.44 – 1.29 (m, 2H), 1.28 – 1.10 (m, 2H).  **$^{13}\text{C}$  NMR (101 MHz,  $\text{CDCl}_3$ )**:  $\delta$  209.4, 152.0, 140.5, 129.9, 129.0, 121.4, 120.9, 113.0, 81.8, 57.0, 50.2, 48.3, 45.5, 41.1, 28.4, 28.4, 27.6, 27.2, 25.1, 24.8. **IR**:  $\nu$  3442, 2957, 1699, 1618, 1461, 1388, 1275, 1162, 1137, 750, 521  $\text{cm}^{-1}$ ; **HRMS** calcd. For  $[\text{M}+\text{H}]^+$ : 342.2064. Found: 342.2062.

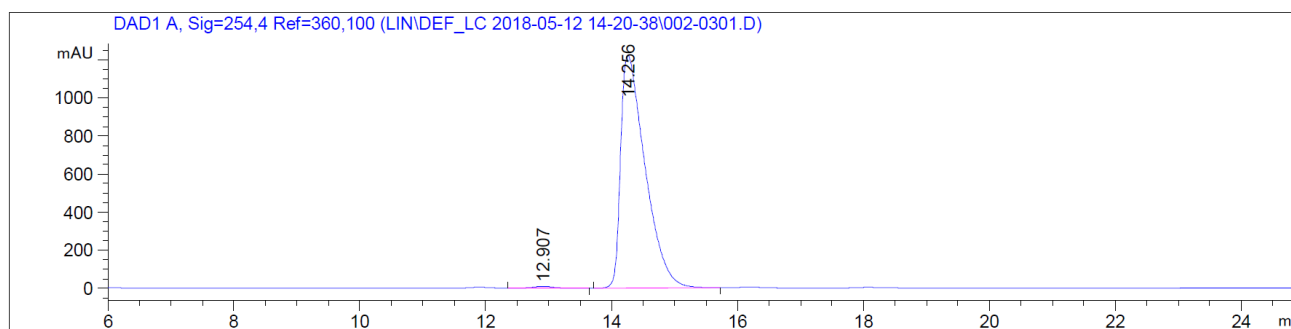
Chiral HPLC (Chiralpak IF, hexane:isopropanol = 98:2, 1 mL/min, 254 nm),  $t_{\text{minor}} = 12.9$  min,  
 $t_{\text{major}} = 14.2$  min.  $[\alpha]_{\text{D}}^{21.5} = -68.4$  ( $c = 0.70$ ,  $\text{CHCl}_3$ ) at 98% e.e.

### **Racemic Sample 8b**

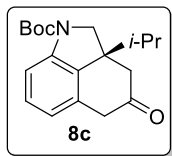


Peak #	RetTime [min]	Type	Width [min]	Area [mAU*s]	Height [mAU]	Area %
1	12.916	BB	0.3328	2595.53271	121.70525	49.6854
2	14.573	BB	0.3905	2628.40674	103.41245	50.3146

### **Enantiomeric Sample 8b**



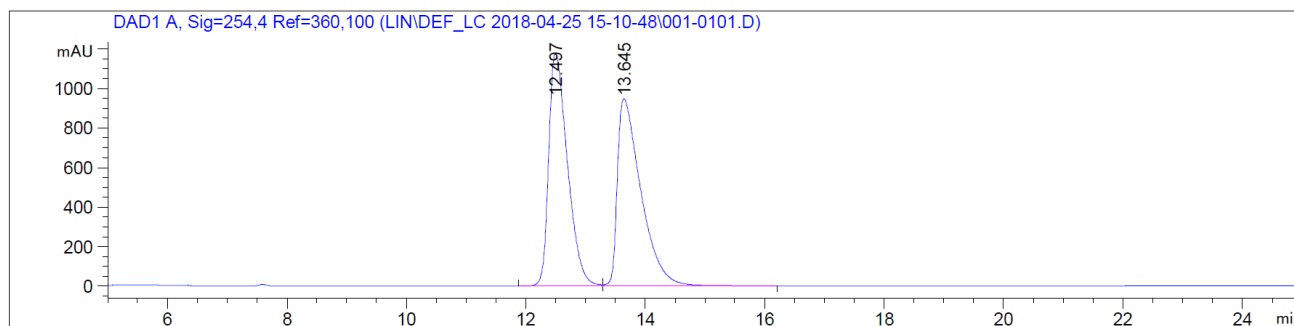
Peak #	RetTime [min]	Type	Width [min]	Area [mAU*s]	Height [mAU]	Area %
1	12.907	BB	0.3278	206.30048	9.79096	0.6215
2	14.256	BB	0.4024	3.29901e4	1224.24268	99.3785



**8c** (22.0 mg) was isolated as a white solid in 71% yield. Melting Point: 122-124 °C. Rh(COD)<sub>2</sub>BF<sub>4</sub> (5 mol%, 0.005 mmol, 2.1 mg) and (*R*)-DTBM-segphos (6 mol%, 0.006 mmol, 7.1 mg) were used and the reaction was maintained at 90 °C. *R<sub>f</sub>* = 0.4 (EtOAc/Hexane=1/3). **<sup>1</sup>H NMR (400 MHz, CDCl<sub>3</sub>):** δ 7.71 – 7.16 (m, 1H), 7.19 (s, 1H), 6.78 (d, *J* = 7.6 Hz, 1H), 4.17 (m, 1H), 3.63 (d, *J* = 22.0 Hz, 1H), 3.54 – 3.38 (m, 2H), 3.03 (d, *J* = 15.7 Hz, 1H), 2.41 (d, *J* = 15.7 Hz, 1H), 1.71 (dq, *J* = 13.6, 6.8 Hz, 1H), 1.59 (m, 9H), 0.97 (d, *J* = 6.7 Hz, 3H), 0.77 (d, *J* = 6.8 Hz, 3H). **<sup>13</sup>C NMR (101 MHz, CDCl<sub>3</sub>):** δ 209.3, 152.0, 130.1, 129.0, 121.5, 112.9, 80.9, 55.8, 48.8, 46.2, 41.0, 34.4, 28.4, 17.5, 16.8. **IR:** ν 3441, 1699, 1635, 1457, 1386, 1275, 1260, 1139, 750 cm<sup>-1</sup>; **HRMS** calcd. For [M+Na]<sup>+</sup>: 338.1727. Found: 338.1716.

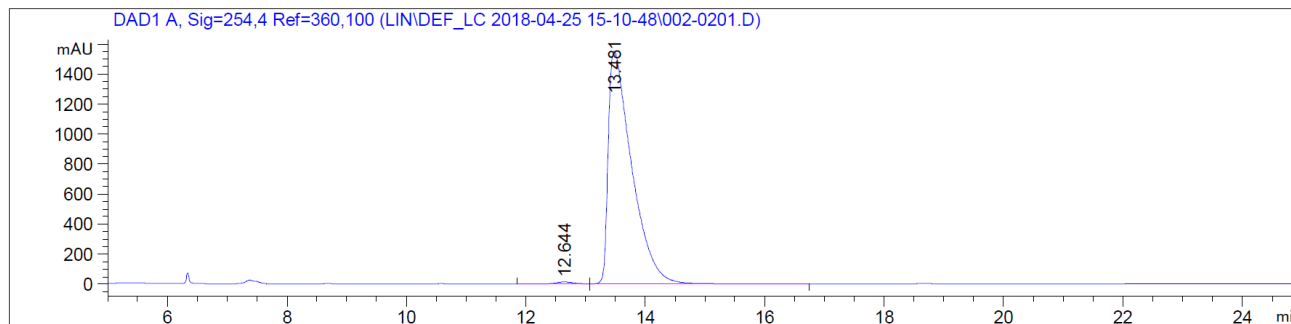
Chiral HPLC (Chiralpak IF, hexane:isopropanol = 99:1, 1 mL/min, 254 nm), *t*<sub>minor</sub> = 12.6 min, *t*<sub>major</sub> = 13.5 min. [α]<sub>D</sub><sup>21.5</sup> = -63.5 (c= 0.95, CHCl<sub>3</sub>) at 98% e.e.

### **Racemic Sample 8c**

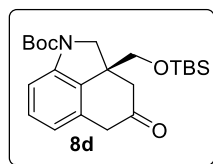


Peak #	RetTime [min]	Type	Width [min]	Area [mAU*s]	Height [mAU]	Area %
1	12.497	BV	0.3366	2.57255e4	1178.75208	49.7820
2	13.645	VB	0.4073	2.59508e4	948.21454	50.2180

### Enantiomeric Sample 8c



Peak #	RetTime [min]	Type	Width [min]	Area [mAU*s]	Height [mAU]	Area %
1	12.644	BV	0.3301	304.48911	14.20492	0.7134
2	13.481	VB	0.4005	4.23781e4	1552.24231	99.2866

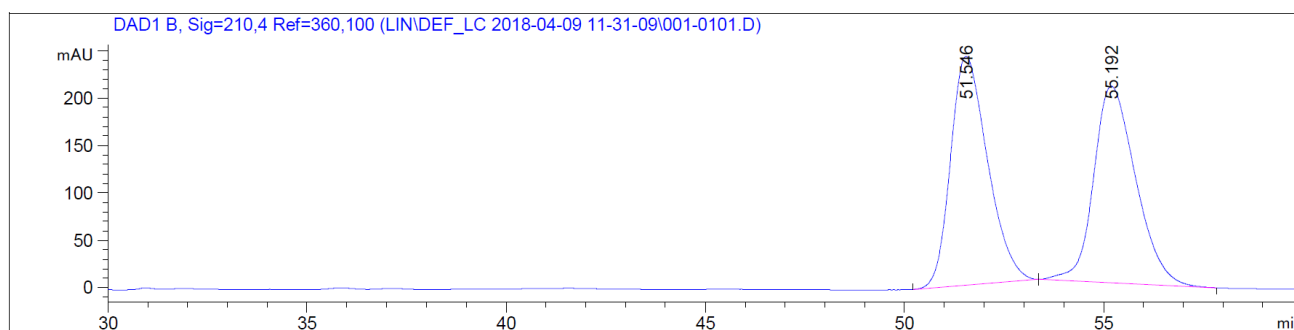


**8d** (28.5 mg) was isolated as a white solid in 71% yield. Melting Point: 95-97 °C. Rh(COD)<sub>2</sub>BF<sub>4</sub> (5 mol%, 0.005 mmol, 2.1 mg) and (*R*)-DTBM-segphos (6 mol%, 0.006 mmol, 7.1 mg) were used and the reaction was maintained at 90 °C. *R<sub>f</sub>* = 0.5 (EtOAc/Hexane=1/3). **<sup>1</sup>H NMR (400 MHz, CDCl<sub>3</sub>):** δ 7.74 – 7.19 (m, 1H), 7.20 (t, *J* = 7.7 Hz, 1H), 6.76 (d, *J* = 7.6 Hz, 1H), 4.07 (m, 1H), 3.70 – 3.54 (m, 4H), 3.40 (d, *J* = 21.6 Hz, 1H), 2.96 (d, *J* = 16.1 Hz, 1H), 2.40 (d, *J* = 16.1 Hz, 1H), 1.57 (s, 9H), 0.81 (s, 9H), -0.06 (d, *J* = 3.0 Hz, 6H). **<sup>13</sup>C NMR (101 MHz, CDCl<sub>3</sub>):** δ 208.1,

152.5, 131.5, 129.4, 121.2, 112.9, 80.9, 68.3, 58.3, 46.6, 41.4, 28.4, 25.8, 18.3, -5.7, -5.9. **IR:**  $\nu$  2929, 2885, 2856, 1705, 1459, 1388, 1347, 1256, 1163, 1137, 1099, 838, 782  $\text{cm}^{-1}$ ; **HRMS** calcd. For  $[\text{M}+\text{K}]^+$ : 456.1967. Found: 456.1980.

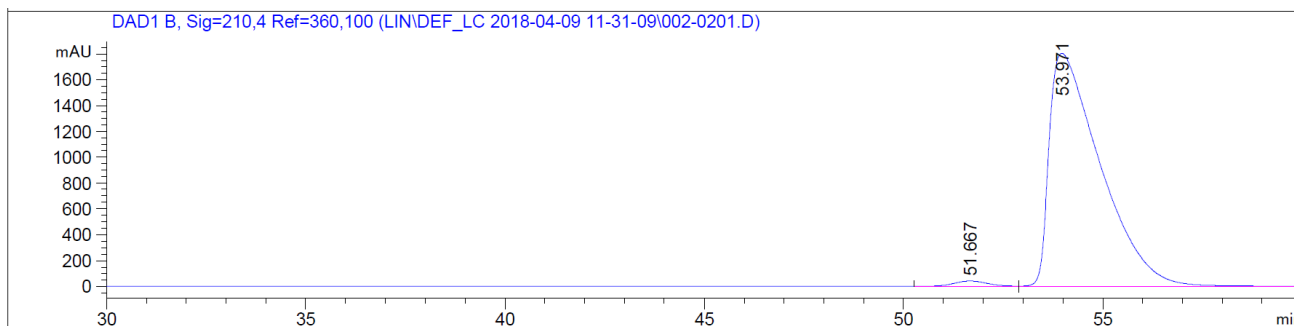
Chiral HPLC (Chiralpak IF, hexane:isopropanol = 99:1, 0.3 mL/min, 210 nm),  $t_{\text{minor}} = 51.7$  min,  $t_{\text{major}} = 54.0$  min.  $[\alpha]_{\text{D}}^{21.5} = -28.2$  ( $c = 1.31$ ,  $\text{CHCl}_3$ ) at 97% e.e.

### **Racemic Sample 8d**

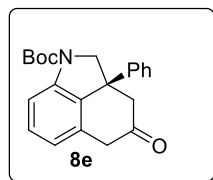


Peak #	RetTime [min]	Type	Width [min]	Area [mAU*s]	Height [mAU]	Area %
1	51.546	BB	1.0015	1.55841e4	241.28061	50.5455
2	55.192	BB	1.1354	1.52477e4	207.47116	49.4545

### **Enantiomeric Sample 8d**



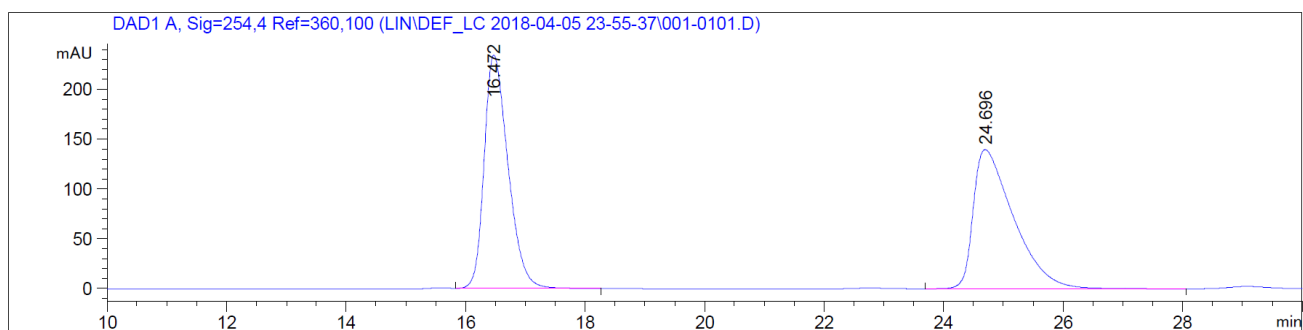
Peak #	RetTime [min]	Type	Width [min]	Area [mAU*s]	Height [mAU]	Area %
1	51.667	BB	0.8834	2295.71265	40.49353	1.4071
2	53.971	BBA	1.2752	1.60853e5	1802.44165	98.5929



**8e** (26.8 mg) was isolated as a colorless oil in 78% yield. Rh(COD)<sub>2</sub>BF<sub>4</sub> (5 mol%, 0.005 mmol, 2.1 mg) and (*R*)-DTBM-segphos (6 mol%, 0.006 mmol, 7.1 mg) were used and the reaction was maintained at 90 °C. R<sub>f</sub> = 0.4 (EtOAc/Hexane=1/3). **<sup>1</sup>H NMR (400 MHz, CDCl<sub>3</sub>):** δ 7.88 – 7.30 (m, 1H), 7.34 – 7.24 (m, 3H), 7.24 – 7.16 (m, 1H), 7.03 (d, *J* = 6.3 Hz, 2H), 6.85 (d, *J* = 7.6 Hz, 1H), 4.28 (m, 1H), 4.07 (d, *J* = 10.9 Hz, 1H), 3.48 (d, *J* = 16.2 Hz, 1H), 3.41 (d, *J* = 21.0 Hz, 1H), 3.24 (d, *J* = 21.0 Hz, 1H), 2.75 (d, *J* = 16.2 Hz, 1H), 1.66 – 1.43 (m, 9H). **<sup>13</sup>C NMR (101 MHz, CDCl<sub>3</sub>):** δ 208.1, 152.3, 143.3, 140.9, 132.5, 130.8, 129.7, 129.0, 127.3, 126.1, 121.4, 113.2, 81.1, 64.5, 51.0, 47.1, 41.8, 28.4. **IR:** ν 3443, 1699, 1634, 1474, 1385, 1275, 1162, 1137, 750, 701 cm<sup>-1</sup>; **HRMS** calcd. For [M+H]<sup>+</sup>: 350.1751. Found: 350.1745.

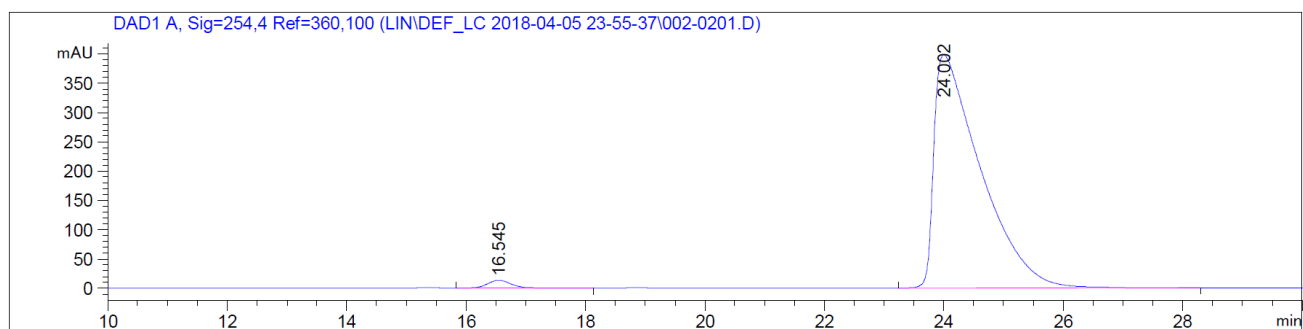
Chiral HPLC (Chiralpak IF, hexane:isopropanol = 98:2, 1 mL/min, 254 nm), t<sub>minor</sub> = 16.5 min, t<sub>major</sub> = 24.0 min. [α]<sub>D</sub><sup>21.5</sup> = -118.9 (c = 0.95, CHCl<sub>3</sub>) at 97% e.e.

### **Racemic Sample 8e**

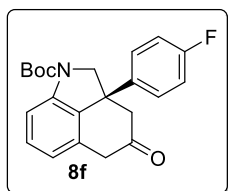


Peak #	RetTime [min]	Type	Width [min]	Area [mAU*s]	Height [mAU]	Area %
1	16.472	BB	0.4282	6509.98535	234.23973	49.8598
2	24.696	BB	0.7025	6546.60889	139.75941	50.1402

### Enantiomeric Sample 8e



Peak #	RetTime [min]	Type	Width [min]	Area [mAU*s]	Height [mAU]	Area %
1	16.545	BB	0.4256	371.59622	13.39684	1.6909
2	24.002	BB	0.7812	2.16053e4	398.07251	98.3091

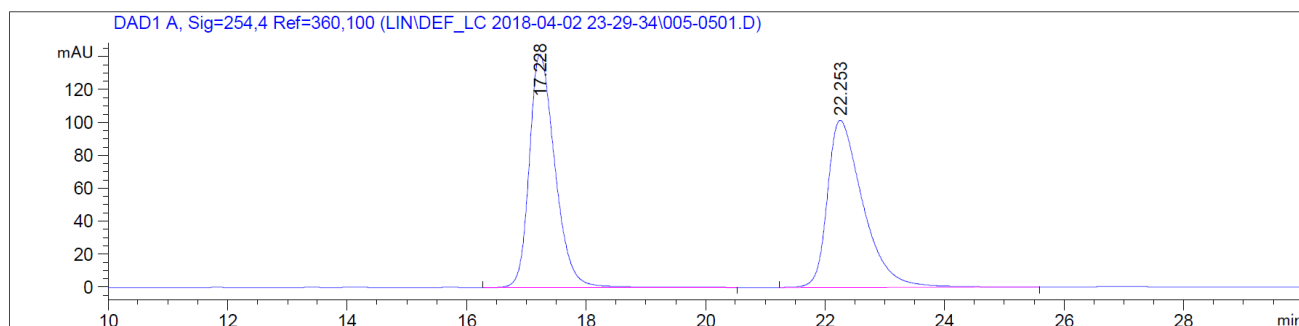


**8f** (34.0 mg) was isolated as a colorless oil in 93% yield. Melting Point: 97-99 °C. Rh(COD)<sub>2</sub>BF<sub>4</sub> (5 mol%, 0.005 mmol, 2.1 mg) and (*R*)-DTBM-segphos (6 mol%, 0.006 mmol, 7.1 mg) were used

and the reaction was maintained at 90 °C.  $R_f = 0.3$  (EtOAc/Hexane=1/3).  **$^1\text{H}$  NMR (400 MHz,  $\text{CDCl}_3$ ):**  $\delta$  7.90 – 7.25 (m, 1H), 7.31 (t,  $J = 7.8$  Hz, 1H), 7.07 – 6.90 (m, 4H), 6.86 (d,  $J = 7.5$  Hz, 1H), 4.22 (m, 1H), 4.05 (d,  $J = 10.9$  Hz, 1H), 3.45 (s, 1H), 3.40 (d,  $J = 5.7$  Hz, 1H), 3.22 (d,  $J = 21.1$  Hz, 1H), 2.76 (d,  $J = 16.1$  Hz, 1H), 1.64 – 1.42 (m, 9H).  **$^{13}\text{C}$  NMR (101 MHz,  $\text{CDCl}_3$ ):**  $\delta$  207.8, 161.8 (d,  $J = 247.0$  Hz), 152.3, 139.0, 129.9, 127.9 (d,  $J = 8.2$  Hz), 121.6, 115.9 (d,  $J = 21.4$  Hz), 113.3, 64.2, 51.1, 46.2, 41.7, 28.4.  **$^{19}\text{F}$  NMR (470 MHz,  $\text{CDCl}_3$ ):**  $\delta$  -68.4. **IR:**  $\nu$  3442, 1635, 1507, 1474, 1386, 1337, 1275, 1161, 1138, 750, 516  $\text{cm}^{-1}$ ; **HRMS** calcd. For  $[\text{M}+\text{Na}]^+$ : 390.1476. Found: 390.1464.

Chiral HPLC (Chiralpak IF, hexane:isopropanol = 98:2, 1 mL/min, 254 nm),  $t_{\text{minor}} = 17.7$  min,  $t_{\text{major}} = 21.5$  min.  $[\alpha]_{\text{D}}^{21.5} = -89.9$  ( $c = 0.88$ ,  $\text{CHCl}_3$ ) at 98% e.e.

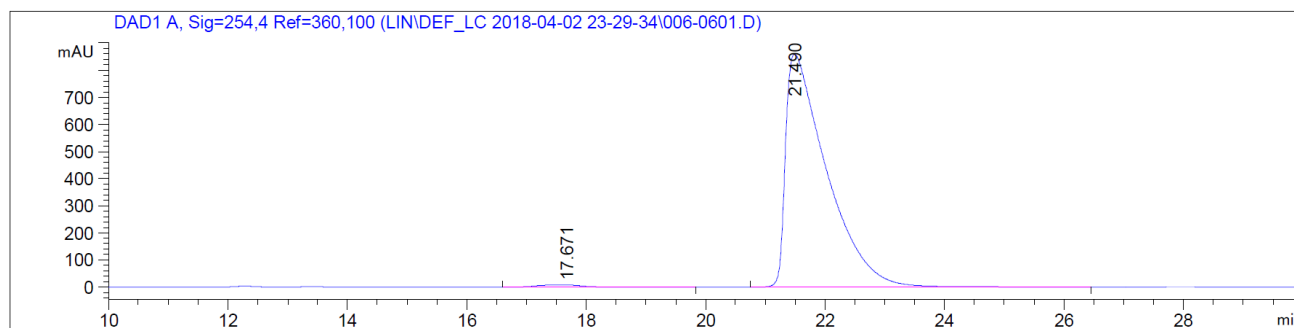
### Racemic Sample 8f



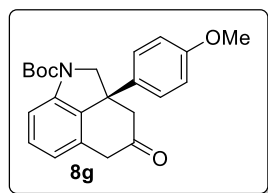
Peak #	RetTime [min]	Type	Width [min]	Area [mAU*s]	Height [mAU]	Area %
1	17.228	BB	0.4557	4224.91748	141.76109	50.1852
2	22.253	BB	0.6238	4193.74316	101.54588	49.8148

### Enantiomeric Sample 8f





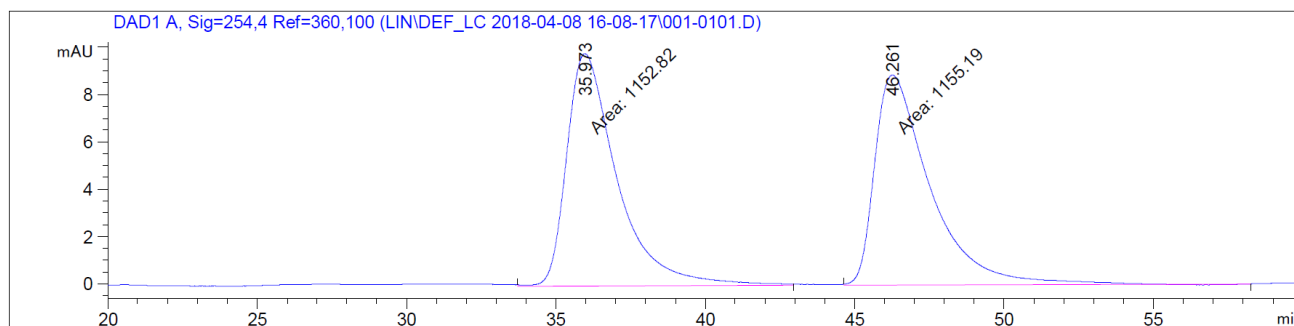
Peak #	RetTime [min]	Type	Width [min]	Area [mAU*s]	Height [mAU]	Area %
1	17.671	BB	0.6837	401.00906	7.90668	0.9663
2	21.490	BB	0.6845	4.10976e4	861.54816	99.0337



**8g** (31.3 mg) was isolated as a colorless oil in 76% yield.  $\text{Rh}(\text{COD})_2\text{BF}_4$  (5 mol%, 0.005 mmol, 2.1 mg) and (*R*)-DTBM-segphos (6 mol%, 0.006 mmol, 7.1 mg) were used and the reaction was maintained at 90 °C.  $R_f = 0.3$  (EtOAc/Hexane=1/3).  **$^1\text{H}$  NMR (400 MHz,  $\text{CDCl}_3$ ):**  $\delta$  7.85 – 7.23 (m, 1H), 7.29 (t,  $J = 7.7$  Hz, 1H), 6.93 (d,  $J = 8.3$  Hz, 2H), 6.84 (d,  $J = 7.6$  Hz, 1H), 6.79 (d,  $J = 8.8$  Hz, 2H), 4.24 (m, 1H), 4.03 (d,  $J = 10.9$  Hz, 1H), 3.75 (s, 3H), 3.53 – 3.33 (m, 2H), 3.24 (d,  $J = 21.0$  Hz, 1H), 2.73 (d,  $J = 16.1$  Hz, 1H), 1.62 – 1.36 (m, 9H).  **$^{13}\text{C}$  NMR (101 MHz,  $\text{CDCl}_3$ ):**  $\delta$  208.2, 158.6, 152.3, 141.0, 135.3, 132.8, 130.8, 129.6, 127.3, 121.4, 114.3, 113.2, 81.0, 64.6, 55.2, 51.1, 46.3, 41.8, 28.4. **IR:**  $\nu$  3442, 2056, 1699, 1621, 1511, 1474, 1386, 1337, 1275, 1256, 1162, 1137, 1029, 833, 750  $\text{cm}^{-1}$ ; **HRMS** calcd. For  $[\text{M}+\text{Na}]^+$ : 402.1676. Found: 402.1673.

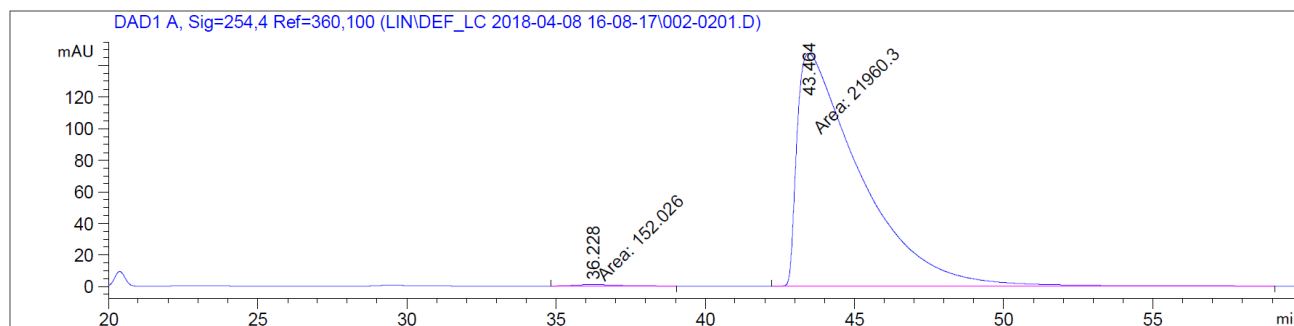
Chiral HPLC (Chiralpak ID, hexane:isopropanol = 98:2, 1 mL/min, 254 nm),  $t_{\text{minor}} = 36.2$  min,  $t_{\text{major}} = 43.5$  min.  $[\alpha]_D^{21.5} = -104.9$  ( $c = 1.06$ ,  $\text{CHCl}_3$ ) at 99% e.e.

### Racemic Sample 8g

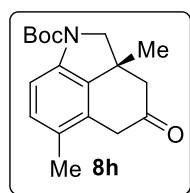


Peak #	RetTime [min]	Type	Width [min]	Area [mAU*s]	Height [mAU]	Area %
1	35.973	MM	1.9547	1152.81665	9.82926	49.9486
2	46.261	MM	2.1657	1155.18762	8.89003	50.0514

### Enantiomeric Sample 8g



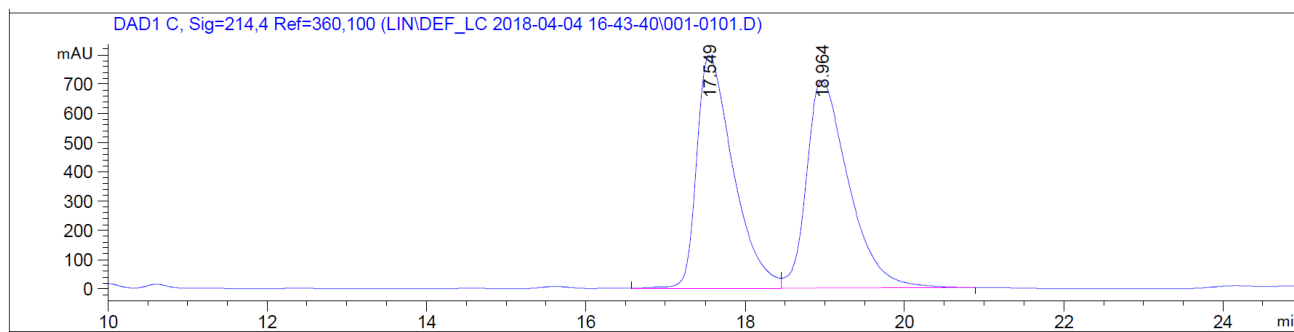
Peak #	RetTime [min]	Type	Width [min]	Area [mAU*s]	Height [mAU]	Area %
1	36.228	MM	2.2703	152.02570	1.11607	0.6875
2	43.464	MM	2.4780	2.19603e4	147.70340	99.3125



**8h** (28.5 mg) was isolated as a white solid in 95% yield. Melting Point: 140-142 °C. Rh(COD)<sub>2</sub>BF<sub>4</sub> (5 mol%, 0.005 mmol, 2.1 mg) and (*R*)-DTBM-segphos (6 mol%, 0.006 mmol, 7.1 mg) were used and the reaction was maintained at 90 °C. *R<sub>f</sub>* = 0.4 (EtOAc/Hexane=1/3). **<sup>1</sup>H NMR (400 MHz, CDCl<sub>3</sub>):** δ 7.64 – 7.11 (m, 1H), 7.02 (d, *J* = 8.0 Hz, 1H), 3.98 (m, 1H), 3.69 (d, *J* = 10.7 Hz, 1H), 3.48 (d, *J* = 22.0 Hz, 1H), 3.40 (d, *J* = 22.1 Hz, 1H), 2.78 (d, *J* = 15.1 Hz, 1H), 2.54 (d, *J* = 15.1 Hz, 1H), 2.18 (s, 3H), 1.57 (s, 9H), 1.23 (s, 3H). **<sup>13</sup>C NMR (101 MHz, CDCl<sub>3</sub>):** δ 208.9, 152.6, 129.5, 127.8, 112.8, 80.8, 62.0, 50.8, 39.5, 38.9, 29.7, 28.4, 25.9, 17.7. **IR:** ν 3443, 2974, 1699, 1626, 1484, 1387, 1369, 1338, 1257, 1159, 1137, 816, 751 cm<sup>-1</sup>; **HRMS** calcd. For [M+H]<sup>+</sup>: 324.1570. Found: 324.1568.

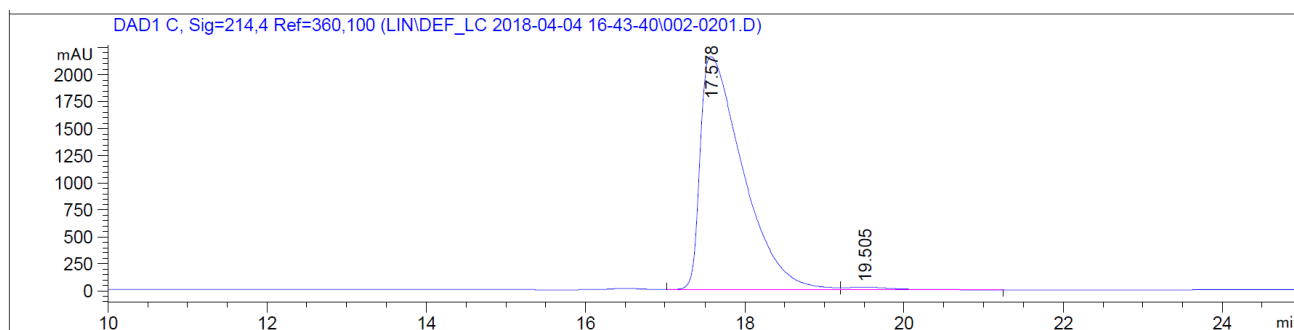
Chiral HPLC (Chiralpak IF, hexane:isopropanol = 99:1, 1 mL/min, 214 nm), *t*<sub>minor</sub> = 19.5 min, *t*<sub>major</sub> = 17.6 min. [α]<sub>D</sub><sup>21.5</sup> = -88.7 (c = 1.19, CHCl<sub>3</sub>) at 98% e.e.

### Racemic Sample 8h

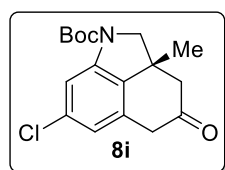


Peak #	RetTime [min]	Type	Width [min]	Area [mAU*s]	Height [mAU]	Area %
1	17.549	BV	0.4790	2.51541e4	795.31250	49.2640
2	18.964	VB	0.5527	2.59057e4	708.27655	50.7360

### Enantiomeric Sample 8h



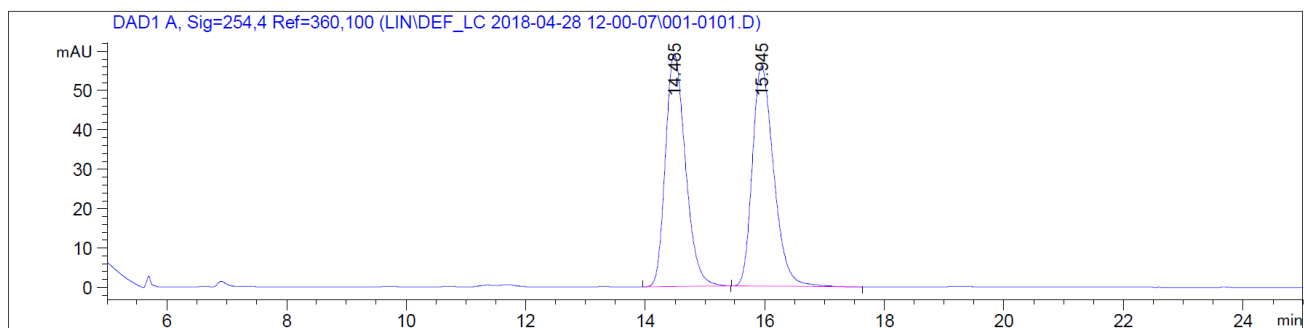
Peak #	RetTime [min]	Type	Width [min]	Area [mAU*s]	Height [mAU]	Area %
1	17.578	VV	0.5570	8.04349e4	2157.27026	98.7408
2	19.505	VB	0.6250	1025.72388	23.88517	1.2592



**8i** (24.0 mg) was isolated as a colorless oil in 76% yield.  $\text{Rh}(\text{COD})_2\text{BF}_4$  (5 mol%, 0.005 mmol, 2.1 mg) and (*R*)-DTBM-segphos (6 mol%, 0.006 mmol, 7.1 mg) were used and the reaction was maintained at 90 °C.  $R_f = 0.4$  (EtOAc/Hexane=1/3).  **$^1\text{H}$  NMR (400 MHz,  $\text{CDCl}_3$ )**:  $\delta$  7.80 – 7.19 (m, 1H), 6.78 (d,  $J = 1.2$  Hz, 1H), 3.98 (m, 1H), 3.73 (d,  $J = 10.8$  Hz, 1H), 3.57 (d,  $J = 21.8$  Hz, 1H), 3.45 (d,  $J = 21.8$  Hz, 1H), 2.80 (d,  $J = 15.6$  Hz, 1H), 2.50 (d,  $J = 15.6$  Hz, 1H), 1.58 (s, 9H), 1.25 (s, 3H).  **$^{13}\text{C}$  NMR (101 MHz,  $\text{CDCl}_3$ )**:  $\delta$  207.7, 166.8, 152.4, 141.6, 121.1, 113.8, 109.6, 50.7, 40.4, 29.7, 28.4, 25.8. **IR**:  $\nu$  3400, 2975, 1705, 1618, 1479, 1437, 1371, 1337, 1275, 1157, 1139, 859, 751, 592  $\text{cm}^{-1}$ ; **HRMS** calcd. For  $[\text{M}+\text{Na}]^+$ : 344.1024. Found: 344.1027.

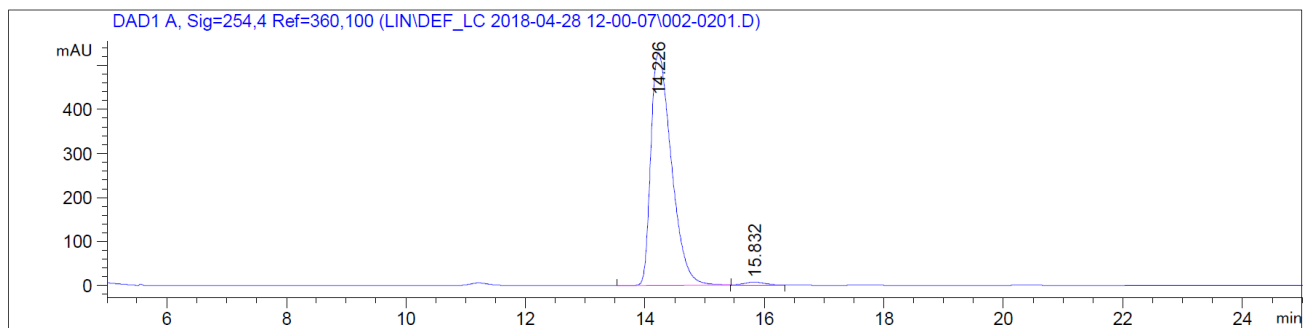
Chiral HPLC (Chiralpak IF, hexane:isopropanol = 99:1, 1 mL/min, 254 nm),  $t_{\text{minor}} = 15.8$  min,  $t_{\text{major}} = 14.2$  min.  $[\alpha]_D^{21.5} = -69.8$  ( $c = 0.43$ ,  $\text{CHCl}_3$ ) at 98% e.e.

### Racemic Sample 8i

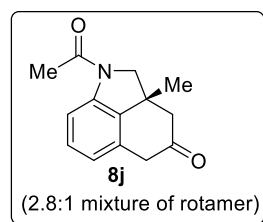


Peak #	RetTime [min]	Type	Width [min]	Area [mAU*s]	Height [mAU]	Area %
1	14.485	BB	0.3618	1377.60852	59.13932	49.7598
2	15.945	BB	0.3870	1390.90991	55.76566	50.2402

### Enantiomeric Sample 8i



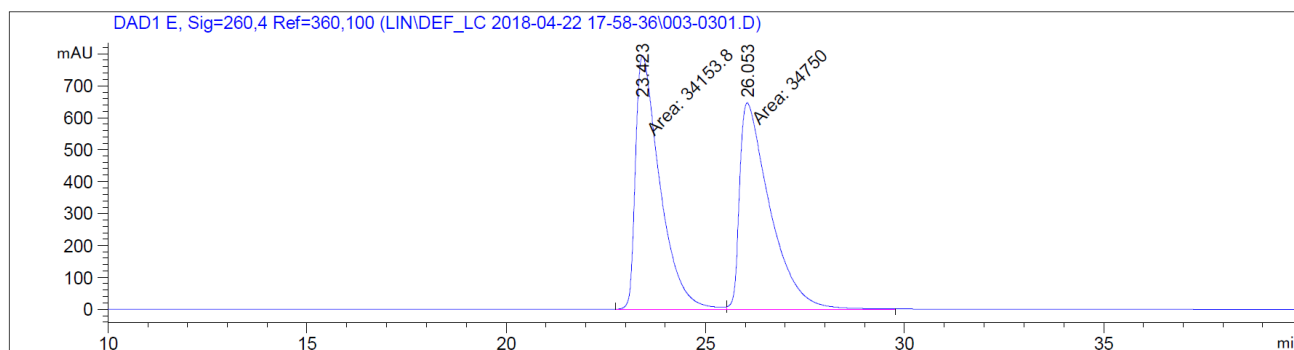
Peak #	RetTime [min]	Type	Width [min]	Area [mAU*s]	Height [mAU]	Area %
1	14.226	BB	0.3681	1.26037e4	528.79913	98.8756
2	15.832	BB	0.3521	143.32492	6.38088	1.1244



**8j** (20.7 mg, 2.8:1 mixture of rotamer) was isolated as a colorless oil in 90% yield. Rh(COD)<sub>2</sub>BF<sub>4</sub> (5 mol%, 0.005 mmol, 2.1 mg) and (*R*)-DTBM-segphos (6 mol%, 0.006 mmol, 7.1 mg) were used and the reaction was maintained at 90 °C. *R<sub>f</sub>* = 0.4 (acetone/Hexane=1/3). **<sup>1</sup>H NMR (400 MHz, CDCl<sub>3</sub>):** δ (major rotamer) 7.95 (d, *J* = 8.0 Hz, 1H), 7.22 (t, *J* = 7.8 Hz, 1H), 6.86 (d, *J* = 7.6 Hz, 1H), 3.96 (d, *J* = 9.9 Hz, 1H), 3.90 (d, *J* = 10.0 Hz, 1H), 3.66 – 3.57 (m, 1H), 3.52 (d, *J* = 21.8 Hz, 1H), 2.83 (d, *J* = 15.5 Hz, 1H), 2.55 (d, *J* = 15.6 Hz, 1H), 2.24 (s, 3H), 1.30 (s, 3H). **<sup>13</sup>C NMR (101 MHz, CDCl<sub>3</sub>):** δ (all the peaks observed) 208.3, 168.8, 140.3, 134.4, 131.0, 129.32, 129.27, 128.97, 126.7, 122.8, 122.5, 115.4, 112.8, 63.8, 62.5, 50.7, 50.6, 40.7, 40.6, 39.0, 25.9, 25.3, 24.1, 23.9. **IR:** ν 3442, 2064, 1636, 1472, 1399, 1276, 750, 569 cm<sup>-1</sup>; **HRMS** calcd. For [M+H]<sup>+</sup>: 230.1176. Found: 230.1176.

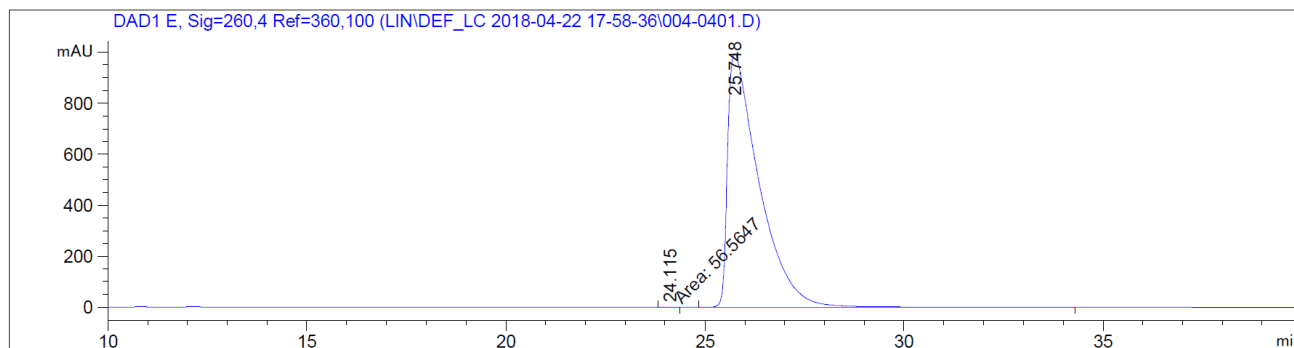
Chiral HPLC (Chiralpak IF, hexane:isopropanol = 85:15, 1 mL/min, 260 nm), *t*<sub>minor</sub> = 24.1 min, *t*<sub>major</sub> = 25.7 min. [ $\alpha$ ]<sub>D</sub><sup>21.5</sup> = -135.3 (c = 0.91, CHCl<sub>3</sub>) at 99% e.e.

### Racemic Sample 8j

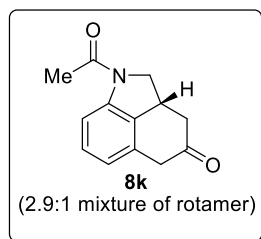


Peak #	RetTime [min]	Type	Width [min]	Area [mAU*s]	Height [mAU]	Area %
1	23.423	MF	0.7142	3.41538e4	796.97180	49.5674
2	26.053	FM	0.8927	3.47500e4	648.80408	50.4326

## Enantiomeric Sample 8j



Peak #	RetTime [min]	Type	Width [min]	Area [mAU*s]	Height [mAU]	Area %
1	24.115	MM	0.5411	56.56469	1.74236	0.1032
2	25.748	BB	0.7927	5.47543e4	993.96942	99.8968



**8k** (17.2 mg, 2.9:1 mixture of rotamer) was isolated as a white solid in 80% yield. Melting Point: 154-156 °C. Rh(COD)<sub>2</sub>BF<sub>4</sub> (5 mol%, 0.005 mmol, 2.1 mg) and (*R*)-DTBM-segphos (6 mol%, 0.006 mmol, 7.1 mg) were used and the reaction was maintained at 90 °C. *R<sub>f</sub>* = 0.4 (acetone/Hexane=1/3). **<sup>1</sup>H NMR (400 MHz, CDCl<sub>3</sub>):** δ (major rotamer) 7.94 (d, *J* = 8.0 Hz, 1H), 7.22 (t, *J* = 7.8 Hz, 1H), 6.86 (d, *J* = 7.6 Hz, 1H), 4.41 (t, *J* = 9.1 Hz, 1H), 3.88 – 3.78 (m, 1H), 3.74 (t, *J* = 9.6 Hz, 1H), 3.55 (s, 2H), 2.97 (dd, *J* = 16.1, 5.3 Hz, 1H), 2.33 (dd, *J* = 16.1, 12.0 Hz, 1H), 2.24 (s, 3H). **<sup>13</sup>C NMR (101 MHz, CDCl<sub>3</sub>):** δ (all the peaks observed) 208.2, 168.5, 141.1, 131.7, 130.4, 130.2, 129.3, 129.0, 122.4, 122.1, 115.2, 112.5, 56.4, 55.6, 43.8, 43.7, 42.1, 35.0,

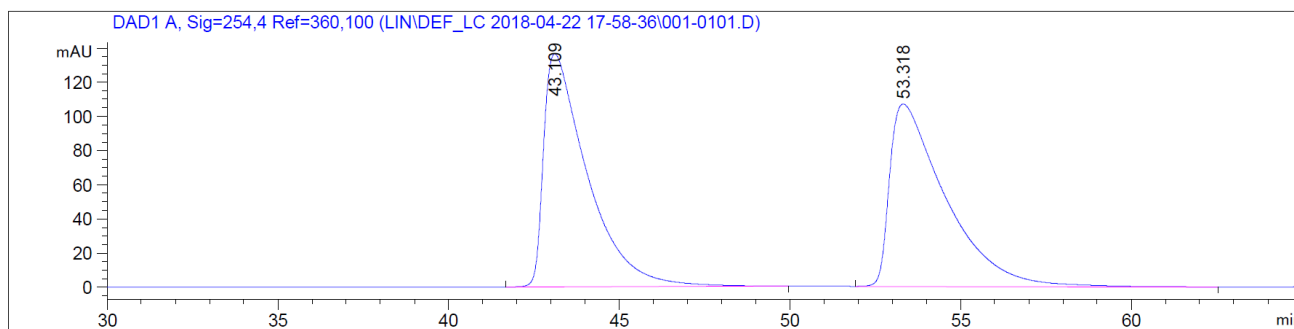
33.6, 29.7, 24.2, 23.9. **IR:**  $\nu$  3440, 2050, 1635, 1472, 1416, 1275, 749, 578  $\text{cm}^{-1}$ ; **HRMS** calcd.

For  $[\text{M}+\text{H}]^+$ : 216.1019. Found: 216.1010.

Chiral HPLC (Chiralpak IF, hexane:isopropanol = 85:15, 1 mL/min, 254 nm),  $t_{\text{minor}} = 44.6$  min,

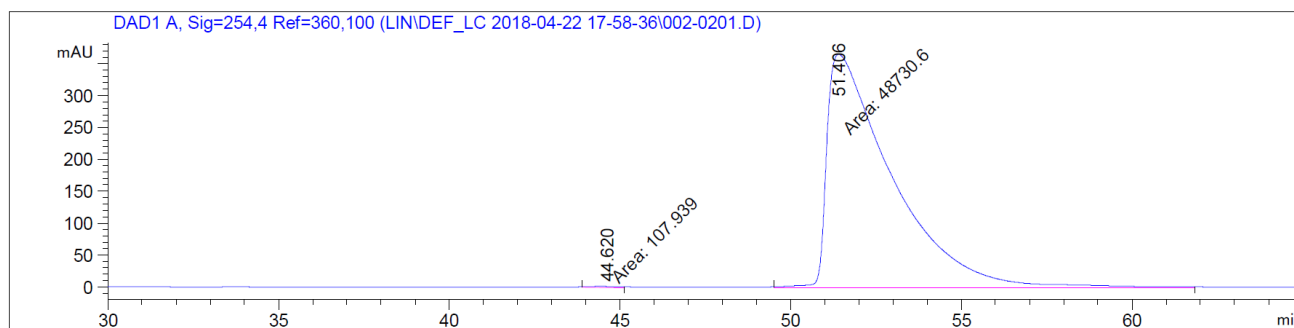
$t_{\text{major}} = 51.4$  min.  $[\alpha]_{\text{D}}^{21.5} = -177.9$  ( $c = 0.95$ ,  $\text{CHCl}_3$ ) at 99% e.e.

### Racemic Sample 8k



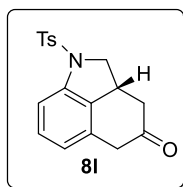
Peak #	RetTime [min]	Type	Width [min]	Area [mAU*s]	Height [mAU]	Area %
1	43.109	BB	1.2759	1.21946e4	136.54861	49.9805
2	53.318	BB	1.6252	1.22041e4	106.79595	50.0195

### Enantiomeric Sample 8k





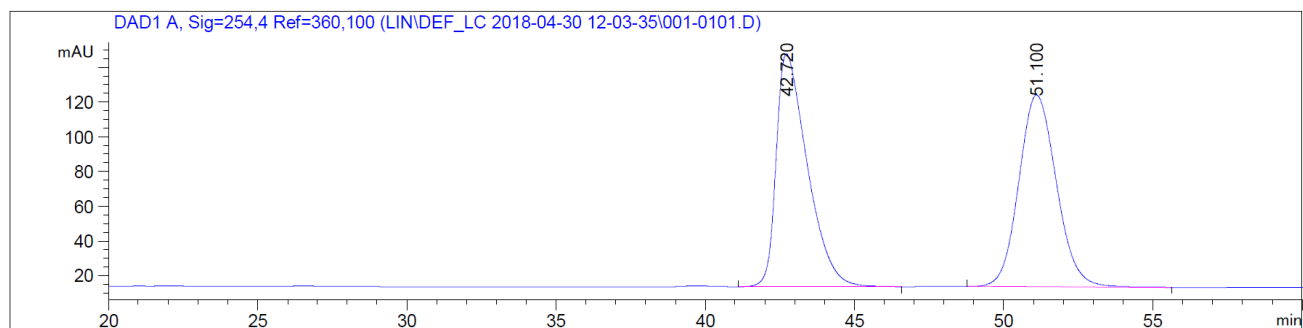
Peak #	RetTime [min]	Type	Width [min]	Area [mAU*s]	Height [mAU]	Area %
1	44.620	MM	1.0347	107.93900	1.73873	0.2210
2	51.406	MM	2.2181	4.87306e4	366.16602	99.7790



**8l** (32.0 mg) was isolated as white solid in 91% yield. Melting Point: 127-129 °C. Rh(COD)<sub>2</sub>BF<sub>4</sub> (10 mol%, 0.01 mmol, 4.2 mg) and (*R*)-DTBM-segphos (12 mol%, 0.012 mmol, 14.2 mg) were used and the reaction was maintained at 90 °C for 12 h then at 110 °C for 12 h. *R<sub>f</sub>* = 0.2 (EtOAc/Hexane=1/3). **<sup>1</sup>H NMR (400 MHz, CDCl<sub>3</sub>):** δ 7.71 (d, *J* = 8.4 Hz, 2H), 7.47 (dd, *J* = 8.1, 0.8 Hz, 1H), 7.26 (d, *J* = 1.4 Hz, 2H), 7.25 – 7.18 (m, 1H), 6.81 (dd, *J* = 7.6, 0.9 Hz, 1H), 4.40 (dd, *J* = 9.9, 8.4 Hz, 1H), 3.55 – 3.47 (m, 1H), 3.46 – 3.44 (s, 2H), 3.38 (dd, *J* = 10.7, 10.0 Hz, 1H), 2.85 (dd, *J* = 16.1, 5.4 Hz, 1H), 2.38 (s, 3H), 2.11 (dd, *J* = 16.1, 12.1 Hz, 1H). **<sup>13</sup>C NMR (101 MHz, CDCl<sub>3</sub>):** δ 207.7, 144.4, 140.6, 133.7, 130.9, 129.8, 129.4, 127.3, 122.5, 113.3, 57.8, 43.6, 41.8, 34.7, 21.6. **IR:** ν 3441, 2064, 1707, 1635, 1456, 1353, 1275, 1165, 1095, 750, 660, 581, 543 cm<sup>-1</sup>; **HRMS** calcd. For [M+H]<sup>+</sup>: 328.1002. Found: 328.1002.

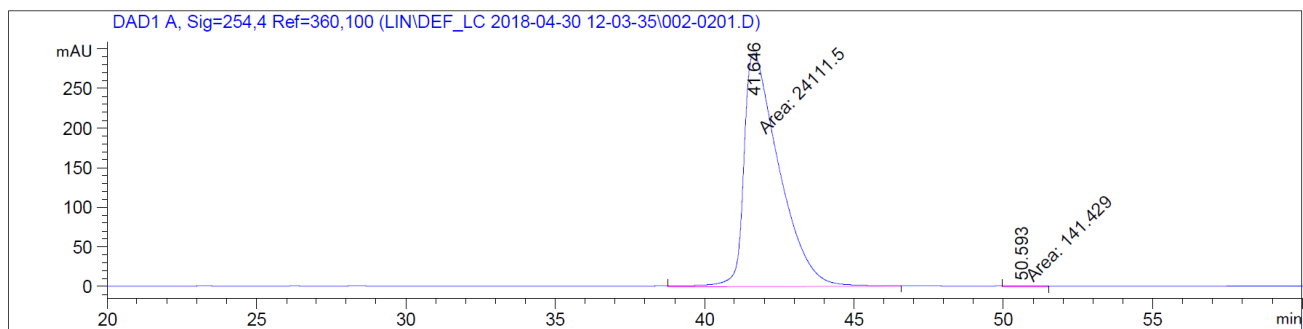
Chiral HPLC (Chiralpak IF, hexane:isopropanol = 85:15, 1 mL/min, 254 nm), *t*<sub>minor</sub> = 50.6 min, *t*<sub>major</sub> = 41.6 min. [α]<sub>D</sub><sup>21.5</sup> = -134.5 (c = 0.62, CHCl<sub>3</sub>) at 99% e.e.

### **Racemic Sample 8l**

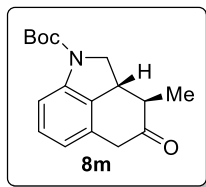


Peak #	RetTime [min]	Type	Width [min]	Area [mAU*s]	Height [mAU]	Area %
1	42.720	BB	1.1037	9729.44531	134.22519	50.1079
2	51.100	BB	1.3663	9687.53711	110.55894	49.8921

### Enantiomeric Sample 8l

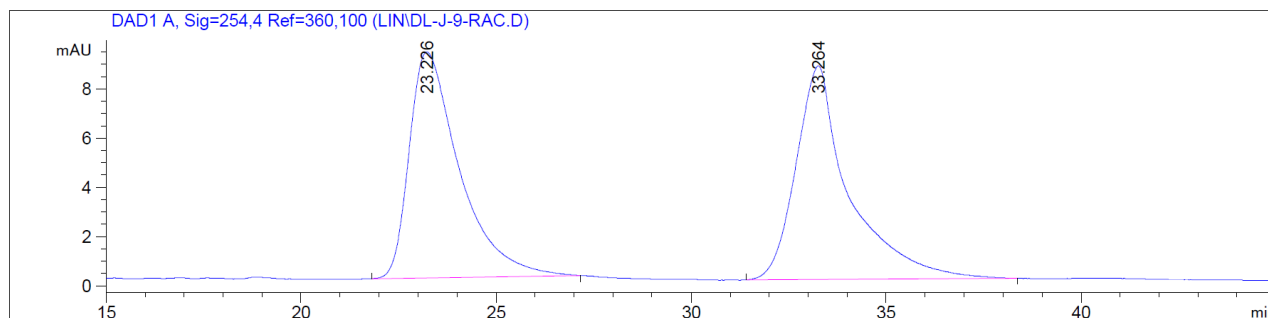


Peak #	RetTime [min]	Type	Width [min]	Area [mAU*s]	Height [mAU]	Area %
1	41.646	MM	1.3625	2.41115e4	294.94385	99.4169
2	50.593	MM	1.3283	141.42949	1.77458	0.5831



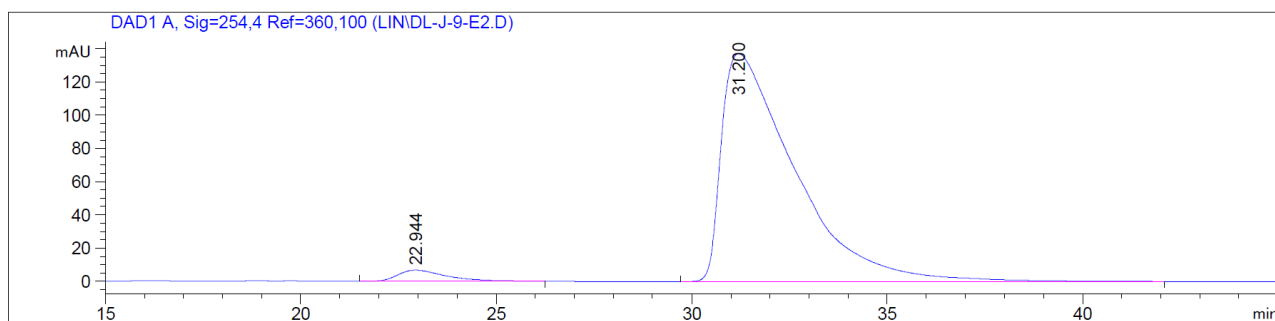
**8m** (17.1 mg) was isolated as a white solid in 75% yield. Melting Point: 155-159 °C. Rh(COD)<sub>2</sub>BF<sub>4</sub> (10 mol%, 0.01 mmol, 4.2 mg) and (*R*)-DTBM-segphos (12 mol%, 0.012 mmol, 14.2 mg) were used and the reaction was maintained at 90 °C for 12 h. *R<sub>f</sub>* = 0.6 (EtOAc/Hexane=1/5). **<sup>1</sup>H NMR (400 MHz, CDCl<sub>3</sub>)**: δ 7.76-7.20 (m, 1H), 7.18 (t, *J* = 7.7 Hz, 1H), 6.88 – 6.69 (m, 1H), 4.38 (br, 1H), 3.64 (t, *J* = 10.5 Hz, 1H), 3.57 (s, 2H), 3.40 – 3.24 (m, 1H), 2.35 (dq, *J* = 12.0, 6.6 Hz, 1H), 1.58 (s, 9H), 1.23 (d, *J* = 6.7 Hz, 3H). **<sup>13</sup>C NMR (101 MHz, CDCl<sub>3</sub>)**: δ 210.0, 152.4, 130.4, 129.0, 120.9, 112.8, 81.0, 54.7, 48.4, 41.8, 40.6, 28.4, 12.4. **IR**: ν 2966, 2925, 2853, 1702, 1475, 1462, 1389, 1354, 1162, 1136, 776 cm<sup>-1</sup>; **HRMS** calcd. For [M+Na]<sup>+</sup>: 310.1414. Found: 310.1406. Chiral HPLC (Chiralpak IF, hexane:isopropanol = 98:2, 1 mL/min, 254 nm), *t*<sub>minor</sub> = 22.9 min, *t*<sub>major</sub> = 31.2 min. [*α*]<sub>D</sub><sup>21.5</sup> = -114.8 (c = 1.08, CHCl<sub>3</sub>) at 94% e.e.

### Racemic Sample 8m

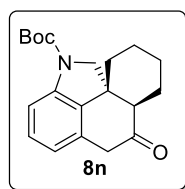


Peak #	RetTime [min]	Type	Width [min]	Area [mAU*s]	Height [mAU]	Area %
1	23.226	BB	1.2728	819.87750	9.17241	49.9569
2	33.264	BB	1.2774	821.29224	8.66851	50.0431

### Enantiomeric Sample 8m



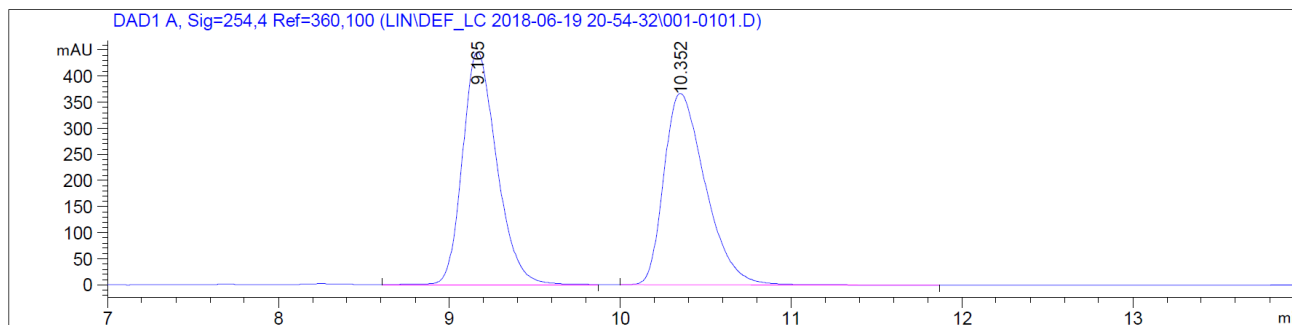
Peak #	RetTime [min]	Type	Width [min]	Area [mAU*s]	Height [mAU]	Area %
1	22.944	BB	1.2073	581.18683	6.73112	3.1409
2	31.200	BB	1.8371	1.79224e4	137.27806	96.8591



**8n** (26.7 mg) was isolated as a colorless oil in 82% yield.  $\text{Rh}(\text{COD})_2\text{BF}_4$  (10 mol%, 0.01 mmol, 4.2 mg) and (*R*)-DTBM-segphos (12 mol%, 0.012 mmol, 14.2 mg) were used and the reaction was maintained at 90 °C for 12 h.  $R_f = 0.6$  (EtOAc/Hexane=1/5).  **$^1\text{H}$  NMR (400 MHz,  $\text{CDCl}_3$ ):**  $\delta$  7.76 – 7.21 (m, 1H), 7.17 (t,  $J = 7.8$  Hz, 1H), 6.76 (d,  $J = 7.6$  Hz, 1H), 4.47 – 4.08 (m, 1H), 3.65 – 3.47 (m, 3H), 2.55 – 2.42 (m, 1H), 2.41 – 2.33 (m, 1H), 1.82 – 1.73 (m, 1H), 1.71 – 1.64 (m, 1H), 1.60 (s, 9H), 1.55 – 1.48 (m, 1H), 1.41 – 1.19 (m, 3H).  **$^{13}\text{C}$  NMR (101 MHz,  $\text{CDCl}_3$ ):**  $\delta$  210.1, 152.6, 139.9, 135.3, 129.8, 128.8, 121.1, 112.9, 80.9, 58.7, 52.9, 42.6, 41.2, 32.4, 28.4, 22.6, 22.0, 21.2. **IR:**  $\nu$  2924, 2853, 1705, 1620, 1460, 1387, 1351, 1162, 1138, 1081, 777  $\text{cm}^{-1}$ ; **HRMS** calcd. For  $[\text{M}+\text{Na}]^+$ : 350.1727. Found: 350.1722.

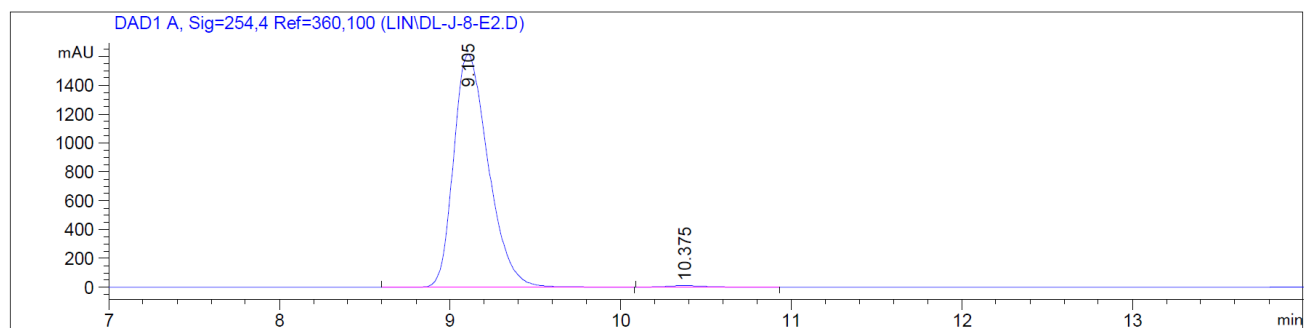
Chiral HPLC (Chiralpak IA, hexane:isopropanol = 99:1, 1 mL/min, 254 nm),  $t_{\text{minor}} = 10.4$  min,  
 $t_{\text{major}} = 9.1$  min.  $[\alpha]_{\text{D}}^{21.5} = -97.6$  (c= 2.67,  $\text{CHCl}_3$ ) at 98% e.e.

### **Racemic Sample 8n**



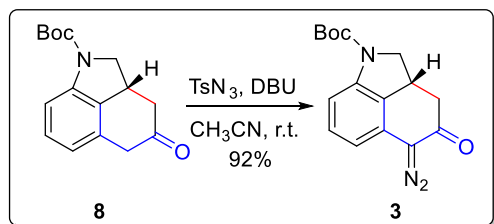
Peak #	RetTime [min]	Type	Width [min]	Area [mAU*s]	Height [mAU]	Area %
1	9.165	BB	0.2130	6234.80469	446.14462	50.2401
2	10.352	BB	0.2606	6175.20605	366.40610	49.7599

### **Enantiomeric Sample 8n**



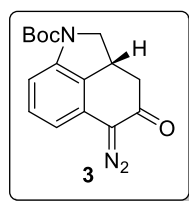
Peak #	RetTime [min]	Type	Width [min]	Area [mAU*s]	Height [mAU]	Area %
1	9.105	BB	0.2165	2.27470e4	1613.47888	99.2855
2	10.375	BB	0.2537	163.69363	10.06678	0.7145

### 3.4.4 Procedure and characterization data for the total synthesis of (–)-cycloclavine

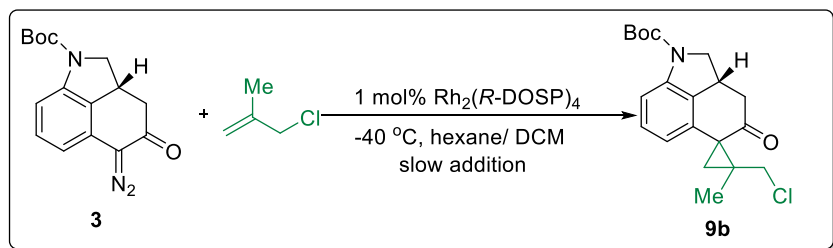


#### **Procedure:**

A 20 mL vial with a stir bar was charged with **8** (672 mg, 2.46 mmol, 1.0 equiv.) and  $\text{TsN}_3$  (581.9 mg, 2.95 mmol, 1.2 equiv.) in  $\text{CH}_3\text{CN}$  (10 mL). After adding DBU (441  $\mu\text{L}$ , 2.95 mmol, 1.2 equiv.) at 0 °C, the vial was capped and the mixture was stirred at 0 °C for 2 h. Upon completion, it was warmed up to room temperature and the solvent was removed by rotavap under reduced pressure. The crude product was purified by silica gel flash chromatography (hexane:ethyl acetate= 10:1) to yield the desired product **3**.

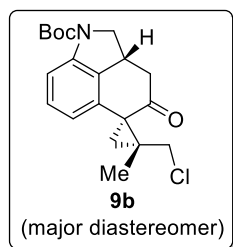


Compound **3** was isolated as a bright yellow solid in 92% yield (670 mg). Melting Point: 148-150 °C (decomposed).  $R_f = 0.5$  (EtOAc/Hexane=1/5).  **$^1\text{H}$  NMR (400 MHz,  $\text{CDCl}_3$ ):**  $\delta$  7.64 – 7.02 (m, 1H), 7.23 (t,  $J = 7.9$  Hz, 1H), 6.61 (d,  $J = 7.9$  Hz, 1H), 4.40 (m, 1H), 3.74 – 3.49 (m, 2H), 2.93 (dd,  $J = 15.6, 5.3$  Hz, 1H), 2.50 (dd,  $J = 15.5, 13.1$  Hz, 1H), 1.57 (s, 9H).  **$^{13}\text{C}$  NMR (101 MHz,  $\text{CDCl}_3$ ):**  $\delta$  192.3, 152.3, 130.0, 124.5, 122.0, 113.2, 111.5, 81.2, 70.3, 55.4, 42.1, 34.2, 28.4. **IR:**  $\nu$  3453, 2084, 1698, 1651, 1475, 1459, 1391, 1356, 1275, 1261, 1163, 1141, 859, 750  $\text{cm}^{-1}$ ; **HRMS** calcd. For  $[\text{M}+\text{H}]^+$ : 300.1343. Found: 300.1339.  $[\alpha]_D^{21.5} = -167.8$  ( $c = 1.57$ ,  $\text{CHCl}_3$ ).



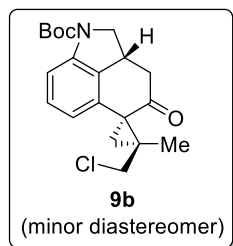
### **Procedure<sup>21</sup>:**

To a 50 mL flamed-dried Schlenk flask equipped with a stir bar and a nitrogen-filled balloon was added Rh<sub>2</sub>(R-DOSP)<sub>4</sub> (12.7 mg, 0.0068 mmol, 1 mol%) and 3-chloro-2-methyl-1-propene (604.9 mg, 6.68 mmol, 10 equiv.) in hexane (15 mL). The system was cooled to -40 °C before **3** (200 mg, 0.67 mmol, 1.0 equiv.) in hexane/toluene (4 mL/ 2 mL) was added using slow-addition pump with a speed of 2 mL/ h. After the addition of **3** was finished, the system was kept at -40 °C for another 20 min. After the starting material was fully consumed, the reaction solution was directly loaded to a silica gel column while the temperature was still below 0 °C. The crude product was purified by silica gel flash column chromatography (EtOAc/Hexane=1/50) to afford compound **9b** as a white solid in 85% yield. Two diastereomers of compound **9b** were isolated through silica gel chromatography, with a ratio of 5.8:1. The relative stereochemistry of the major isomer was determined by X-ray crystallography.



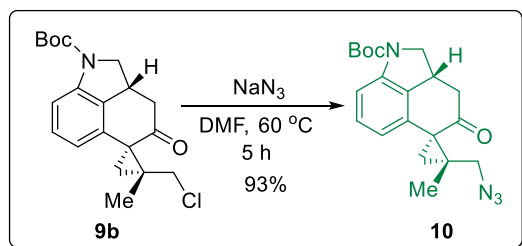
Compound **9b** (major diastereomer) was isolated as a white solid in 73% yield (175.8 mg). Melting Point: 183-184 °C (decomposed). *R<sub>f</sub>* = 0.4 (EtOAc/Hexane=1/5). <sup>1</sup>H NMR (400 MHz, CDCl<sub>3</sub>): δ 7.74 – 7.22 (m, 1H), 7.19 (t, *J* = 7.8 Hz, 1H), 6.55 (d, *J* = 7.8 Hz, 1H), 4.46 (s, 1H), 3.93 (d, *J* =

8.0 Hz, 1H), 3.75 (d,  $J = 11.4$  Hz, 1H), 3.68 – 3.55 (m, 2H), 3.07 (dd,  $J = 17.7, 5.8$  Hz, 1H), 2.29 (dd,  $J = 17.7, 11.9$  Hz, 1H), 2.12 (d,  $J = 5.4$  Hz, 1H), 1.67 (d,  $J = 5.4$  Hz, 1H), 1.57 (s, 9H), 1.06 (s, 3H).  **$^{13}\text{C}$  NMR (101 MHz,  $\text{CDCl}_3$ )**:  $\delta$  206.7, 152.4, 141.1, 133.7, 128.5, 118.9, 113.0, 81.5, 54.9, 48.8, 44.7, 43.0, 39.9, 32.7, 28.4, 22.9, 17.2. **IR**:  $\nu$  3444, 2977, 2098, 1694, 1617, 1462, 1390, 1350, 1258, 1142, 750  $\text{cm}^{-1}$ ; **HRMS** calcd. For  $[\text{M}+\text{H}]^+$ : 362.1517. Found: 362.1513.  $[\alpha]_{\text{D}}^{21.5} = -132.3$  ( $c = 1.10, \text{CHCl}_3$ ).



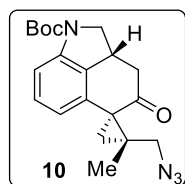
Compound **9b** (minor diastereomer) was isolated as a colorless oil in 12% yield (30.3 mg). The stereochemistry was tentatively assigned based on preliminary experimental results. After subjecting this minor diastereomer to further deprotection and oxidation of the indoline to the indole, we found the compound obtained is likely the diastereomer of compound **2** according to the  $^1\text{H}$ -NMR spectrum. This experiment suggested that the diastereomer observed here should arise from the stereocenter close to the methyl and methylene chloride group.  $R_f = 0.3$  (EtOAc/Hexane=1/5).  **$^1\text{H}$  NMR (400 MHz,  $\text{CDCl}_3$ )**:  $\delta$  7.77 – 7.25 (m, 1H), 7.20 (t,  $J = 7.8$  Hz, 1H), 6.59 (d,  $J = 7.7$  Hz, 1H), 4.42 (s, 1H), 3.93 – 3.75 (m, 1H), 3.60 (dd,  $J = 13.9, 10.3$  Hz, 2H), 3.21 (d,  $J = 11.3$  Hz, 1H), 3.00 (dd,  $J = 17.8, 5.1$  Hz, 1H), 2.35 (dd,  $J = 18.1, 11.9$  Hz, 1H), 1.99 (d,  $J = 5.6$  Hz, 1H), 1.64 (d,  $J = 5.6$  Hz, 1H), 1.57 (s, 9H), 1.33 (s, 3H).  **$^{13}\text{C}$  NMR (101 MHz,  $\text{CDCl}_3$ )**:  $\delta$  206.0, 152.4, 134.1, 131.0, 128.8, 118.4, 113.2, 80.8, 54.8, 50.5, 44.9, 44.1, 37.3, 33.2, 28.4, 21.1, 16.5. **IR**:  $\nu$  2976, 2930, 1698, 1477, 1462, 1391, 1351, 1322, 1256, 1166, 1143, 736  $\text{cm}^{-1}$ ; **HRMS** calcd. For  $[\text{M}+\text{H}]^+$ : 362.1517. Found: 362.1516.





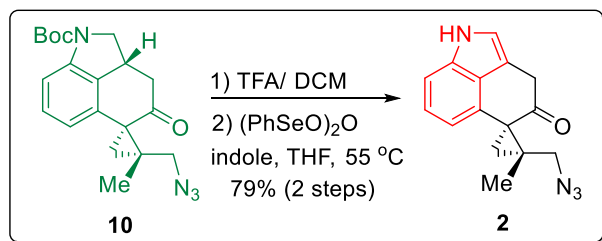
### **Procedure:**

A 20 mL vial with a stir bar was charged with **9b** (150 mg, 0.41 mmol, 1.0 equiv. the major diastereomer) and  $\text{NaN}_3$  (161.7 mg, 2.49 mmol, 6.0 equiv.) in DMF (10 mL). The vial was capped and the mixture was stirring at  $60\text{ }^\circ\text{C}$  for 5 h. Upon completion, it was cooled down to room temperature and the reaction mixture was quenched with brine (10 mL). The mixture was extracted with ethyl acetate (3×20 mL), washed with brine, and dried over  $\text{Na}_2\text{SO}_4$ . The combined organic extract was concentrated under reduced pressure. The crude product was purified by silica gel flash chromatography (hexane:ethyl acetate= 20:1) to yield the desired product **10**.



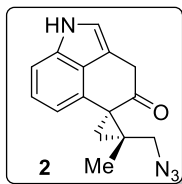
Compound **10** was isolated as a white solid in 93% yield (140 mg). Melting Point:  $116\text{--}118\text{ }^\circ\text{C}$ .  $R_f = 0.6$  (EtOAc/Hexane=1/5).  **$^1\text{H}$  NMR (400 MHz,  $\text{CDCl}_3$ ):**  $\delta$  7.75 – 7.22 (m, 1H), 7.18 (t,  $J = 7.7$  Hz, 1H), 6.54 (d,  $J = 7.8$  Hz, 1H), 4.47 (s, 1H), 3.96 – 3.76 (m, 1H), 3.63 (dd,  $J = 11.3, 8.9$  Hz, 1H), 3.55 (d,  $J = 12.7$  Hz, 1H), 3.39 (d,  $J = 12.8$  Hz, 1H), 3.04 (dd,  $J = 17.6, 5.3$  Hz, 1H), 2.29 (dd,  $J = 17.6, 12.0$  Hz, 1H), 2.00 (d,  $J = 5.5$  Hz, 1H), 1.58 (d,  $J = 5.6$  Hz, 9H), 1.54 (d,  $J = 5.5$  Hz, 1H), 0.99 (s, 3H).  **$^{13}\text{C}$  NMR (101 MHz,  $\text{CDCl}_3$ ):**  $\delta$  206.9, 152.4, 133.5, 131.7, 128.5, 118.9, 112.9, 80.8, 55.1, 44.8, 42.2, 37.8, 32.8, 28.4, 21.1, 17.8. **IR:**  $\nu$  3439, 2096, 1694, 1635, 1462, 1390, 1259,

1166, 1139, 1079, 749  $\text{cm}^{-1}$ ; **HRMS** calcd. For  $[\text{M}+\text{H}]^+$ : 369.1921. Found: 369.1922.  $[\alpha]_{\text{D}}^{21.5} = -167.8$  ( $c = 0.87$ ,  $\text{CHCl}_3$ ).

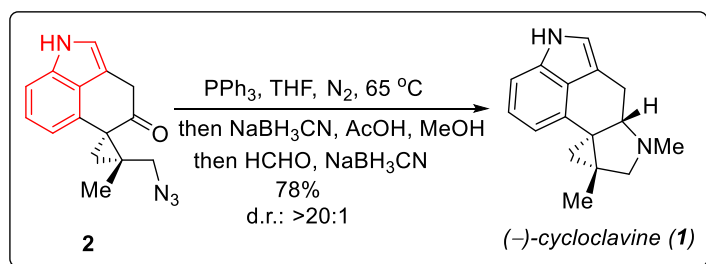


### **Procedure**<sup>25c</sup>:

A 20 mL vial with a stir bar was charged with **10** (36.8 mg, 0.1 mmol, 1.0 equiv.) in dichloromethane (5 mL). TFA (1 mL) was added dropwisely to the stirring solution and the mixture was stirred at room temperature for 1 h. The reaction mixture was then quenched with saturated aqueous  $\text{NaHCO}_3$  solution (10 mL) and extracted with dichloromethane ( $3 \times 10$  mL), washed with brine, and dried over  $\text{Na}_2\text{SO}_4$ . The combined organic extract was concentrated under reduced pressure. The crude product was transferred to a flame-dried 8 mL vial and  $(\text{PhSeO})_2\text{O}$  (18.0 mg, 0.05 mmol, 0.5 equiv.) and indole (23.4 mg, 0.2 mmol, 2.0 equiv.) was added. The vial was loosely capped and transferred into a nitrogen-filled glovebox, where anhydrous THF (2 mL) was used to dissolve the mixture. After stirring at 55 °C for 2 h, the vial was cooled down to room temperature and the solvent was removed under reduced pressure. The crude product was purified by silica gel flash chromatography (dichloromethane:methanol= 100:0 to 100:1) to yield the desired product **2**. Compound **2** is unstable even under nitrogen atmosphere at low temperature, normally directly subjected to the next step right after purification. Here we provide  $^1\text{H}$ -NMR and  $^{13}\text{C}$ -NMR data for compound **2**.



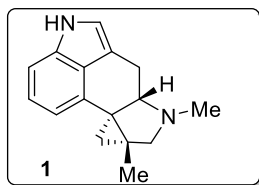
Compound **2** was isolated as a colorless oil in 79% yield over 2 steps (21.2 mg).  $R_f = 0.5$  (DCM/MeOH=20/1).  **$^1\text{H}$  NMR (500 MHz,  $\text{CDCl}_3$ ):**  $\delta$  8.10 (s, 1H), 7.25 – 7.13 (m, 2H), 6.96 (s, 1H), 6.57 (d,  $J = 6.6$  Hz, 1H), 4.03 (d,  $J = 19.5$  Hz, 1H), 3.87 (d,  $J = 19.6$  Hz, 1H), 3.59 (d,  $J = 12.8$  Hz, 1H), 3.30 (d,  $J = 12.7$  Hz, 1H), 2.21 – 2.12 (m, 1H), 1.56 – 1.44 (m, 1H), 1.28 (s, 3H).  **$^{13}\text{C}$  NMR (101 MHz,  $\text{CDCl}_3$ ):**  $\delta$  204.0, 133.4, 128.5, 126.8, 123.0, 118.0, 114.8, 109.4, 108.7, 56.4, 41.8, 39.2, 36.8, 21.6, 16.6.



### **Procedure:**

An 8 mL vial was charged with **2** (35.0 mg, 0.13 mmol, 1.0 equiv.) and  $\text{PPh}_3$  (103.4 mg, 0.39 mmol, 3.0 equiv.). After adding THF (1 mL) inside a nitrogen-filled glovebox, the vial was capped and the mixture was stirred at 65 °C for 2 h. After that, MeOH (5 mL) was added to the solution as well as  $\text{NaBH}_3\text{CN}$  (10.3 mg, 0.16 mmol, 1.3 equiv.) and AcOH (100  $\mu\text{L}$ ). The mixture was then stirred for 30 min at room temperature, before HCHO (37 wt% solution in water, 270  $\mu\text{L}$ ) and another portion of  $\text{NaBH}_3\text{CN}$  (10.3 mg, 0.16 mmol, 1.3 equiv.) was added. The mixture was further stirred for 30 min. Upon completion, the reaction was quenched by brine (10 mL). The mixture was extracted with dichloromethane (3 $\times$ 10 mL), washed with brine, and dried over  $\text{Na}_2\text{SO}_4$ . The

crude product was purified by silica gel flash chromatography (dichloromethane:methanol= 100:0 to 50:1) to yield the desired natural product **1**. The characterization data of compound **1** matches the reported data<sup>13,14</sup>.



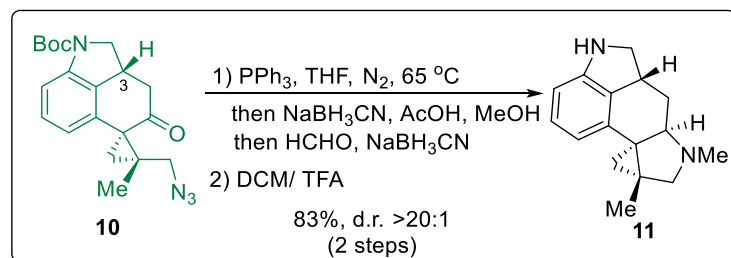
Compound **1** was isolated as a white solid in 78% yield (24.3 mg). Melting Point: 158-160 °C.  $R_f$  = 0.4 (DCM/MeOH=20/1). **<sup>1</sup>H NMR (400 MHz, CDCl<sub>3</sub>):**  $\delta$  7.92 (br, 1H), 7.14 (d,  $J$  = 8.0 Hz, 1H), 7.09 (t,  $J$  = 7.6 Hz, 1H), 6.90 (s, 1H), 6.83 (d,  $J$  = 6.9 Hz, 1H), 3.17 (d,  $J$  = 9.0 Hz, 1H), 3.14 (dd,  $J$  = 14.2, 3.2 Hz, 1H), 2.79 (dd,  $J$  = 11.5, 3.7 Hz, 1H), 2.61 (t,  $J$  = 12.2 Hz, 1H), 2.41 (d,  $J$  = 8.6 Hz, 1H), 2.37 (s, 3H), 1.69 (s, 3H), 1.61 (d,  $J$  = 3.4 Hz, 1H), 0.46 (d,  $J$  = 3.5 Hz, 1H). **<sup>13</sup>C NMR (101 MHz, CDCl<sub>3</sub>):**  $\delta$  135.4, 133.6, 128.7, 122.9, 118.1, 113.2, 110.4, 107.9, 69.6, 65.6, 39.9, 34.4, 27.8, 24.9, 24.2, 16.5. **IR:**  $\nu$  3416, 2076, 1634, 1448, 1276, 749, 616 cm<sup>-1</sup>; **HRMS** calcd. For [M+Na]<sup>+</sup>: 261.1362. Found: 261.1360.  $[\alpha]_D^{21.5}$  = -45.3 ( $c$  = 0.86, CHCl<sub>3</sub>). [Reported  $[\alpha]_D^{21.5}$  = -58.9 ( $c$  = 0.23, CHCl<sub>3</sub>)]

Comparison of the NMR Data between Synthesized **1** and Reported **1**<sup>13,14</sup>

H-NMR of Synthesized <b>1</b>	H-NMR of Reported <b>1</b>	<sup>13</sup> C-NMR of Synthesized <b>1</b>	<sup>13</sup> C-NMR of Reported <b>1</b>
7.92 (br, 1H)	7.92 (br, 1 H)	135.4	135.4
7.14 (d, $J$ = 8.0 Hz, 1H)	7.15 (d, $J$ = 8.4 Hz, 1H)	133.6	133.5
7.09 (t, $J$ = 7.6 Hz, 1H)	7.10 (app t, $J$ = 7.7 Hz, 1H)	128.7	128.7
6.90 (s, 1H)	6.91 (s, 1 H)	122.9	122.9
6.83 (d, $J$ = 6.9 Hz, 1H)	6.84 (d, $J$ = 7.0 Hz, 1H)	118.1	118.1
3.17 (d, $J$ = 9.0 Hz, 1H)	3.17 (d, $J$ = 9.1 Hz, 1H)	113.2	113.2
3.14 (dd, $J$ = 14.2, 3.2 Hz, 1H)	3.15 (dd, $J$ = 14.0, 4.2 Hz, 1H)	110.4	110.3
2.79 (dd, $J$ = 11.5, 3.7 Hz, 1H)	2.79 (dd, $J$ = 11.2, 3.5 Hz, 1H)	107.9	107.9
2.61 (t, $J$ = 12.2 Hz, 1H)	2.61 (t, $J$ = 12.6 Hz, 1H)	69.6	69.6

2.41 (d, $J = 8.6$ Hz, 1H)	2.42 (d, $J = 8.4$ Hz, 1H)	65.6	65.6
2.37 (s, 3H)	2.37 (s, 3 H)	39.9	39.9
1.69 (s, 3H)	1.70 (s, 3 H)	34.4	34.3
1.61 (d, $J = 3.4$ Hz, 1H)	1.61 (d, $J = 2.8$ Hz, 1H)	27.8	27.8
0.46 (d, $J = 3.5$ Hz, 1H)	0.46 (d, $J = 3.5$ Hz, 1H)	24.9	24.9
		24.2	24.2
		16.5	16.5

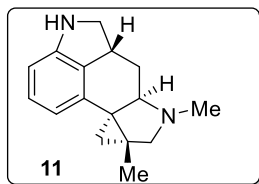
### 3.4.5 Procedure and characterization data of total synthesis of (–)-5-*epi*-cycloclavine



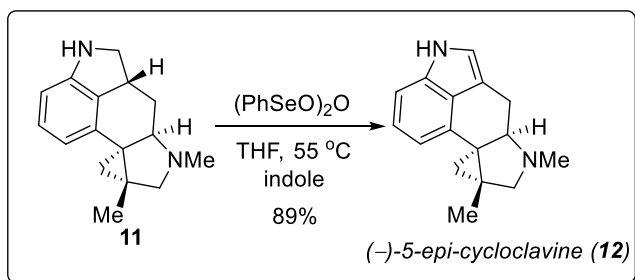
### **Procedure:**

An 8 mL vial was charged with **10** (51.4 mg, 0.14 mmol, 1.0 equiv.) and  $\text{PPh}_3$  (109.8 mg, 0.42 mmol, 3.0 equiv.). After adding THF (1 mL) inside a nitrogen-filled glovebox, the vial was capped and the mixture was stirred at  $65^\circ\text{C}$  for 2 h. After that, MeOH (5 mL) was added to the solution as well as  $\text{NaBH}_3\text{CN}$  (13.2 mg, 0.21 mmol, 1.5 equiv.), AcOH (97  $\mu\text{L}$ , 1.68 mmol, 12 equiv.). The mixture was then stirred for 30 min at room temperature, before HCHO (37 wt% solution in water, 240  $\mu\text{L}$ ) and another portion of  $\text{NaBH}_3\text{CN}$  (13.2 mg, 0.21 mmol, 1.5 equiv.) was added. The mixture was further stirred for 30 min. Upon completion, the reaction was quenched by brine (10 mL). The mixture was extracted with dichloromethane ( $3 \times 10$  mL), washed with brine, and dried over  $\text{Na}_2\text{SO}_4$ . The crude product was dissolved in 5 mL dichloromethane and 1 mL of trifluoroacetic acid was added dropwisely to the stirring solution. After the mixture was stirred for 1 h, the reaction was quenched by saturated  $\text{NaHCO}_3$  aqueous solution (10 mL). The mixture was extracted with dichloromethane ( $3 \times 10$  mL), washed with brine, and dried over  $\text{Na}_2\text{SO}_4$ . The crude

product was purified by silica gel flash chromatography (dichloromethane:methanol= 100:0 to 20:1) to yield the desired product **11**.



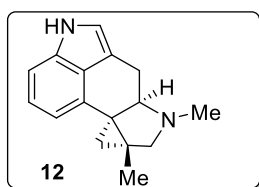
Compound **11** was isolated as a white solid in 83% yield (28.0 mg). Melting Point: 119-120 °C.  $R_f = 0.2$  (DCM/MeOH=20/1).  **$^1\text{H}$  NMR (400 MHz,  $\text{CDCl}_3$ ):**  $\delta$  6.97 (td,  $J = 7.7, 0.9$  Hz, 1H), 6.49 (d,  $J = 7.6$  Hz, 1H), 6.24 (d,  $J = 7.7$  Hz, 1H), 3.83 (t,  $J = 8.4$  Hz, 1H), 3.34 (ddd,  $J = 12.1, 8.5, 4.4$  Hz, 1H), 3.23 (dd,  $J = 10.9, 8.4$  Hz, 2H), 2.51 (d,  $J = 4.5$  Hz, 1H), 2.33 (d,  $J = 9.5$  Hz, 1H), 2.29 – 2.23 (m, 4H), 1.58 (d,  $J = 4.8$  Hz, 1H), 1.39 (ddd,  $J = 13.2, 11.9, 4.8$  Hz, 1H), 1.03 (s, 3H), 0.91 (d,  $J = 4.9$  Hz, 1H).  **$^{13}\text{C}$  NMR (101 MHz,  $\text{CDCl}_3$ ):**  $\delta$  149.4, 133.4, 133.3, 127.1, 113.7, 106.1, 72.5, 67.3, 55.1, 39.5, 38.8, 35.2, 34.4, 33.2, 30.7, 17.3. **IR:**  $\nu$  3443, 2065, 1635, 1275, 1260, 764, 750, 566  $\text{cm}^{-1}$ ; **HRMS** calcd. For  $[\text{M}+\text{H}]^+$ : 241.1699. Found: 241.1704.  $[\alpha]_D^{21.5} = -138$  ( $c = 0.71$ ,  $\text{CHCl}_3$ ).



### **Procedure:**

To a flame-dried 8 mL vial charged with **11** (14.4 mg, 0.06 mmol, 1.0 equiv.) was added  $(\text{PhSeO})_2\text{O}$  (10.8 mg, 0.03 mmol, 0.5 equiv.) and indole (21.1 mg, 0.18 mmol, 3.0 equiv.). The vial was loosely capped and transferred into a nitrogen-filled glovebox, where anhydrous THF (1

mL) was used to dissolve the mixture. After stirring at 55 °C for 2 h, the vial was cooled down to room temperature and the solvent was removed by rotavap under reduced pressure. The crude product was purified by silica gel flash chromatography (dichloromethane:methanol= 100:0 to 20:1) to yield the desired product **12**. The characterization data of compound **12** matches the reported data<sup>13</sup>.



Compound **12** was isolated as a white solid in 89% yield (12.7 mg). Melting Point: 175-176 °C (decomposed).  $R_f$  = 0.4 (DCM/MeOH=20/1). **<sup>1</sup>H NMR (400 MHz, CDCl<sub>3</sub>):**  $\delta$  7.92 (br, 1H), 7.20 – 7.13 (m, 2H), 6.90 (t,  $J$  = 1.9 Hz, 1H), 6.62 (dd,  $J$  = 5.1, 2.7 Hz, 1H), 3.54 (dd,  $J$  = 11.0, 5.6 Hz, 1H), 3.08 – 2.97 (m, 2H), 2.67 (d,  $J$  = 8.8 Hz, 1H), 2.62 (ddd,  $J$  = 14.5, 11.0, 1.8 Hz, 1H), 2.51 (s, 3H), 1.59 (d,  $J$  = 4.4 Hz, 1H), 1.15 (d,  $J$  = 6.3 Hz, 4H). **<sup>1</sup>H NMR (400 MHz, CD<sub>2</sub>Cl<sub>2</sub>):**  $\delta$  8.05 (br, 1H), 7.18 – 7.07 (m, 2H), 6.92 (t,  $J$  = 1.8 Hz, 1H), 6.58 (dd,  $J$  = 6.4, 1.4 Hz, 1H), 3.47 (dd,  $J$  = 10.8, 5.6 Hz, 1H), 3.01 (dd,  $J$  = 14.6, 5.6 Hz, 1H), 2.98 (d,  $J$  = 8.8 Hz, 1H), 2.66 (d,  $J$  = 8.8 Hz, 1H), 2.60 (ddd,  $J$  = 14.5, 11.0, 1.8 Hz, 1H), 2.49 (s, 3H), 1.60 – 1.52 (m, 1H), 1.12 (s, 3H), 1.11 (d,  $J$  = 4.5 Hz, 1H). **<sup>13</sup>C NMR (101 MHz, CDCl<sub>3</sub>):**  $\delta$  133.3, 130.4, 127.4, 122.9, 118.1, 112.9, 111.6, 107.6, 62.9, 59.7, 35.8, 35.4, 33.2, 20.1, 18.6, 14.9. **IR:**  $\nu$  3420, 1635, 1275, 1260, 764, 749, 528 cm<sup>-1</sup>; **HRMS** calcd. For [M+H]<sup>+</sup>: 239.1543. Found: 239.1550.  $[\alpha]_D^{21.5}$  = -42 (c= 0.64, CHCl<sub>3</sub>).

Comparison of the NMR Data between Synthesized **12** and Reported **12**<sup>13</sup>

H-NMR of Synthesized <b>12</b> (in CD <sub>2</sub> Cl <sub>2</sub> )	H-NMR of Reported <b>12</b> (in CD <sub>2</sub> Cl <sub>2</sub> )	<sup>13</sup> C-NMR of Synthesized <b>12</b> (in CDCl <sub>3</sub> )	<sup>13</sup> C-NMR of Reported <b>12</b> (in CDCl <sub>3</sub> )
8.05 (br, 1H)	8.04 (br s, 1 H)	133.3	133.3
7.18 – 7.07 (m, 2H)	7.15-7.10 (m, 2 H)	130.4	130.5

6.92 (t, $J = 1.8$ Hz, 1H)	6.92 (dd, $J = 1.8$ Hz, 1H)	127.4	127.4
6.58 (dd, $J = 6.4, 1.4$ Hz, 1H)	6.58 (dd, $J = 6.6, 0.6$ Hz, 1H)	122.9	122.9
3.47 (dd, $J = 10.8, 5.6$ Hz, 1H)	3.47 (dd, $J = 10.8, 6.0$ Hz, 1H)	118.1	118.1
3.01 (dd, $J = 14.6, 5.6$ Hz, 1H)	3.01 (dd, $J = 14.4, 6.0$ Hz, 1H)	112.9	112.9
2.98 (d, $J = 8.8$ Hz, 1H)	2.98 (d, $J = 8.4$ Hz, 1H)	111.6	111.7
2.66 (d, $J = 8.8$ Hz, 1H)	2.66 (d, $J = 9.0$ Hz, 1H)	107.6	107.6
2.60 (ddd, $J = 14.5, 11.0, 1.8$ Hz, 1H)	2.59 (ddd, $J = 16.2, 11.4, 1.8$ Hz, 1H)	62.9	62.9
2.49 (s, 3H)	2.48 (s, 3 H)	59.7	59.8
1.60 – 1.52 (m, 1H)	1.57 (d, $J = 3.0$ Hz, 1H)	35.8	35.8
1.12 (s, 3H)	1.12 (s, 3 H)	35.4	35.4
1.11 (d, $J = 4.5$ Hz, 1H)	1.11 (d, $J = 4.2$ Hz, 1H)	33.2	33.2
		20.1	20.1
		18.6	18.6
		14.9	14.9

### 3.4.6 X-ray data

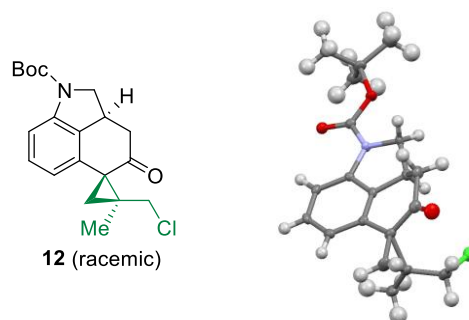


**Table 3.5** Crystal Data and Structure Refinement for **12** (Racemic)

Empirical formula	C <sub>20</sub> H <sub>24</sub> ClNO <sub>3</sub>
Formula weight	361.85
Temperature/K	100(2)
Crystal system	orthorhombic
Space group	P2 <sub>1</sub> 2 <sub>1</sub> 2 <sub>1</sub>
a/Å	9.2522(8)



**Table 3.5** Continued Crystal Data and Structure Refinement for **12**  
(Racemic)

b/Å	10.3247(9)
c/Å	19.5321(16)
$\alpha/^\circ$	90
$\beta/^\circ$	90
$\gamma/^\circ$	90
Volume/Å <sup>3</sup>	1865.8(3)
Z	4
$\rho_{\text{calc}}/\text{cm}^3$	1.288
$\mu/\text{mm}^{-1}$	0.223
F(000)	768.0
Crystal size/mm <sup>3</sup>	0.04 × 0.03 × 0.03
Radiation	MoK $\alpha$ ( $\lambda$ = 0.71073)
2 $\Theta$ range for data collection/ $^\circ$	4.17 to 56.626
Index ranges	-12 ≤ h ≤ 8, -13 ≤ k ≤ 10, -26 ≤ l ≤ 26
Reflections collected	13956
Independent reflections	4589 [ $R_{\text{int}}$ = 0.0471, $R_{\text{sigma}}$ = 0.0647]
Data/restraints/parameters	4589/0/230
Goodness-of-fit on F <sup>2</sup>	1.041
Final R indexes [ $I \geq 2\sigma(I)$ ]	$R_1$ = 0.0485, $wR_2$ = 0.1097
Final R indexes [all data]	$R_1$ = 0.0689, $wR_2$ = 0.1175
Largest diff. peak/hole / e Å <sup>-3</sup>	0.36/-0.36
Flack parameter	-0.09(5)

### 3.5 References

- (1) For selected reviews, see: (a) Crabtree, R. H. *Chem. Rev.* **1985**, *85*, 245. (b) Jones, W. D. *Nature* **1993**, *364*, 676. (c) Murakami, M.; Ito, Y., *Cleavage of Carbon–Carbon Single Bonds by Transition Metals*. In *Top. Organomet. Chem.*, 1999; Vol. 3, pp 97. (d) Rybtchinski, B.; Milstein, D. *Angew. Chem. Int. Ed.* **1999**, *38*, 870. (e) Jun, C.-H. *Chem. Soc. Rev.* **2004**, *33*, 610. (f) Necas, D.; Kotorá, M. *Curr. Org. Chem.* **2007**, *11*, 1566. (g) Park, Y. J.; Park, J.-W.; Jun, C.-H. *Acc. Chem. Res.* **2008**, *41*, 222. (h) Murakami, M.; Matsuda, T. *Chem. Comm.* **2011**, *47*, 1100. (i) Seiser, T.; Saget, T.; Tran, D. N.; Cramer, N. *Angew. Chem. Int. Ed.* **2011**, *50*, 7740. (j) Korotvicka, A.; Necas, D.; Kotorá, M. *Curr. Org. Chem.* **2012**, *16*, 1170. (k) Chen, F.; Wang, T.; Jiao, N. *Chem. Rev.* **2014**, *114*, 8613. (l) Dermenci, A.; Coe, J. W.; Dong, G. *Org. Chem. Front.* **2014**, *1*, 567. (m) Dong, G., *C–C bond activation*. Springer-Verlag: Berlin, 2014; Vol. 346. (n) Murakami, M.; Ishida, N., *Fundamental Reactions to Cleave Carbon–Carbon  $\sigma$ -Bonds with Transition Metal Complexes*. In *Cleavage of Carbon-Carbon Single Bonds by Transition Metals*, Wiley-VCH Verlag GmbH & Co. KGaA: 2015; pp 1. (o) Souillart, L.; Cramer, N. *Chem. Rev.* **2015**, *115*, 9410. (p) Chen, P.-h.; Dong, G. *Chem. Eur. J.* **2016**, *22*, 18290. (q) Chen, P.-h.; Billett, B. A.; Tsukamoto, T.; Dong, G. *ACS Cat.* **2017**, *7*, 1340. (r) Fumagalli, G.; Stanton, S.; Bower, J. F. *Chem. Rev.* **2017**, *117*, 9404. (s) Kim, D.-S.; Park, W.-J.; Jun, C.-H. *Chem. Rev.* **2017**, *117*, 8977.
- (2) For a recent review, see: (a) Murakami, M.; Ishida, N., *Total Syntheses of Natural Products and Biologically Active Compounds by Transition-Metal-Catalyzed C–C Cleavage*. In *Cleavage of Carbon-Carbon Single Bonds by Transition Metals*, Wiley-VCH Verlag GmbH & Co. KGaA: 2015; pp 253. For selected examples, see: (b) South, M. S.; Liebeskind, L. S. *J. Am. Chem. Soc.* **1984**, *106*, 4181. (c) Wender, P. A.; Fuji, M.; Husfeld, C. O.; Love, J. A. *Org. Lett.* **1999**, *1*, 137. (d) Trost, B. M.; Waser, J.; Meyer, A. *J. Am. Chem. Soc.* **2007**, *129*, 14556. (e) Jiao, L.; Yuan, C.; Yu, Z.-X. *J. Am. Chem. Soc.* **2008**, *130*, 4421. (f) Nakao, Y.; Ebata, S.; Yada, A.; Hiyama, T.; Ikawa, M.; Ogoshi, S. *J. Am. Chem. Soc.* **2008**, *130*, 12874. (g) Hirata, Y.; Yukawa, T.; Kashihara, N.; Nakao, Y.; Hiyama, T. *J. Am. Chem. Soc.* **2009**, *131*, 10964. (h) Liang, Y.; Jiang, X.; Yu, Z.-X. *Chem. Comm.* **2011**, *47*, 6659. (i) Evans, P. A.; Inglesby, P. A.; Kilbride, K. *Org. Lett.* **2013**, *15*, 1798. (j) Xu, T.; Dong, G. *Angew. Chem. Int. Ed.* **2014**, *53*, 10733. (k) Sun, T.; Zhang, Y.; Qiu, B.; Wang, Y.; Qin, Y.; Dong, G.; Xu, T. *Angew. Chem. Int. Ed.* **2018**, *57*, 2859.
- (3) Xu, T.; Dong, G. *Angew. Chem. Int. Ed.* **2012**, *51*, 7567.
- (4) Souillart, L.; Parker, E.; Cramer, N., *Asymmetric Transformations via C–C Bond Cleavage*. In *C–C Bond Activation*, Dong, G., Ed. Springer Berlin Heidelberg: Berlin, Heidelberg, 2014; pp 163.
- (5) For asymmetric C–C activation reactions via oxidative addition, see: (a) Xu, T.; Ko, H. M.; Savage, N. A.; Dong, G. *J. Am. Chem. Soc.* **2012**, *134*, 20005. (b) Parker, E.; Cramer, N. *Organometallics* **2014**, *33*, 780. (c) Souillart, L.; Cramer, N. *Angew. Chem. Int. Ed.* **2014**, *53*, 9640. (d) Souillart, L.; Parker, E.; Cramer, N. *Angew. Chem. Int. Ed.* **2014**, *53*, 3001. (e) Zhou, X.; Dong, G. *J. Am. Chem. Soc.* **2015**, *137*, 13715. (f) Deng, L.; Xu, T.; Li, H.; Dong, G. *J. Am. Chem. Soc.* **2016**, *138*, 369.

- (6) For asymmetric C–C activation reactions via  $\beta$ -carbon elimination, see: (a) Matsuda, T.; Shigeno, M.; Makino, M.; Murakami, M. *Org. Lett.* **2006**, *8*, 3379. (b) Seiser, T.; Cramer, N. *Angew. Chem. Int. Ed.* **2008**, *47*, 9294. (c) Seiser, T.; Roth, O. A.; Cramer, N. *Angew. Chem. Int. Ed.* **2009**, *48*, 6320. (d) Shigeno, M.; Yamamoto, T.; Murakami, M. *Chem. Eur. J.* **2009**, *15*, 12929. (e) Seiser, T.; Cramer, N. *Chem. Eur. J.* **2010**, *16*, 3383. (f) Seiser, T.; Cramer, N. *Angew. Chem. Int. Ed.* **2010**, *49*, 10163. (g) Liu, L.; Ishida, N.; Murakami, M. *Angew. Chem. Int. Ed.* **2012**, *51*, 2485. (h) Zhou, X.; Dong, G. *Angew. Chem. Int. Ed.* **2016**, *55*, 15091.
- (7) Stauffacher, D.; Niklaus, P.; Tschertter, H.; Weber, H. P.; Hofmann, A. *Tetrahedron* **1969**, *25*, 5879.
- (8) Furuta, T.; Koike, M.; Abe, M. *Agric. Biol. Chem.* **1982**, *46*, 1921.
- (9) (a) MacLeod, R. M.; Lehmyer, J. E. *Cancer Research* **1973**, *33*, 849. (b) Berde, B.; Stürmer, E., *Introduction to the Pharmacology of Ergot Alkaloids and Related Compounds as a Basis of Their Therapeutic Application*. In *Ergot Alkaloids and Related Compounds*, Berde, B., Schild, H. O., Eds. Springer Berlin Heidelberg: Berlin, Heidelberg, 1978; pp 1. (c) Horwell, D. C. *Tetrahedron* **1980**, *36*, 3123. (d) Lyons, P. C.; Plattner, R. D.; Bacon, C. W. *Science* **1986**, *232*, 487. (e) de Groot, A. N. J. A.; van Dongen, P. W. J.; Vree, T. B.; Hekster, Y. A.; van Roosmalen, J. *Drugs* **1998**, *56*, 523. (f) Somei, M.; Yokoyama, Y.; Murakami, Y.; Ninomiya, I.; Kiguchi, T.; Naito, T., *Recent synthetic studies on the ergot alkaloids and related compounds*. In *The Alkaloids: Chemistry and Biology*, Academic Press: 2000; Vol. 54, pp 191. (g) Boichenko, L. V.; Boichenko, D. M.; Vinokurova, N. G.; Reshetilova, T. A.; Arinbasarov, M. U. *Microbiology* **2001**, *70*, 306. (h) Schardl, C. L.; Panaccione, D. G.; Tudzynski, P., *Chapter 2 Ergot Alkaloids – Biology and Molecular Biology*. In *The Alkaloids: Chemistry and Biology*, Cordell, G. A., Ed. Academic Press: 2006; Vol. 63, pp 45. (i) Schiff, P. L. *Am. J. Pharm. Educ.* **2006**, *70*, 98. (j) Liu, Q.; Jia, Y. *Org. Lett.* **2011**, *13*, 4810. (k) Wallwey, C.; Li, S.-M. *Nat. Prod. Rep.* **2011**, *28*, 496. (l) McCabe, S. R.; Wipf, P. *Org. Bio. Chem.* **2016**, *14*, 5894.
- (10) Kırber, K.; Song, D.; Rheinheimer, J.; Kaiser, F.; Dickhaut, J.; Narine, A.; Culbertson, D. L.; Thompson, S.; Rieder, J. WO2014096238 A1, **2014**.
- (11) Incze, M.; Dörnyei, G.; Moldvai, I.; Temesvári-Major, E.; Egyed, O.; Szántay, C. *Tetrahedron* **2008**, *64*, 2924.
- (12) (a) Jabre, N. D.; Watanabe, T.; Brewer, M. *Tetrahedron Lett.* **2014**, *55*, 197. (b) Wang, W.; Lu, J.-T.; Zhang, H.-L.; Shi, Z.-F.; Wen, J.; Cao, X.-P. *J. Org. Chem.* **2014**, *79*, 122. (c) Netz, N.; Opatz, T. *J. Org. Chem.* **2016**, *81*, 1723. (d) Chen, J.-Q.; Song, L.-L.; Li, F.-X.; Shi, Z.-F.; Cao, X.-P. *Chem. Comm.* **2017**, *53*, 12902. (e) Chaudhuri, S.; Ghosh, S.; Bhunia, S.; Bisai, A. *Chem. Comm.* **2018**, *54*, 940.
- (13) Petronijevic, F. R.; Wipf, P. *J. Am. Chem. Soc.* **2011**, *133*, 7704.
- (14) McCabe, S. R.; Wipf, P. *Angew. Chem. Int. Ed.* **2017**, *56*, 324.
- (15) Yoshida, S.; Uchida, K.; Igawa, K.; Tomooka, K.; Hosoya, T. *Chem. Comm.* **2014**, *50*, 15059.

- (16) For selected reviews, see: (a) Hartwig, J. F. *Acc. Chem. Res.* **1998**, *31*, 852. (b) Wolfe, J. P.; Wagaw, S.; Marcoux, J.-F.; Buchwald, S. L. *Acc. Chem. Res.* **1998**, *31*, 805. (c) Yang, B. H.; Buchwald, S. L. *J. Organomet. Chem.* **1999**, *576*, 125. (d) Yin, J.; Buchwald, S. L. *Org. Lett.* **2000**, *2*, 1101. (e) Hartwig, J. F. *Acc. Chem. Res.* **2008**, *41*, 1534. (f) S., S. D.; L., B. S. *Angew. Chem. Int. Ed.* **2008**, *47*, 6338.
- (17) Chen, P. H.; Savage, N. A.; Dong, G. *Tetrahedron* **2014**, *70*, 4135.
- (18) (a) Davies, H. M. L.; Antoulinakis, E. G. *Org. React.* **2001**, *57*, 1. (b) Lebel, H.; Marcoux, J.-F.; Molinaro, C.; Charette, A. B. *Chem. Rev.* **2003**, *103*, 977. (c) Reissig, H.-U.; Zimmer, R. *Chem. Rev.* **2003**, *103*, 1151. (d) Bartoli, G.; Bencivenni, G.; Dalpozzo, R. *Synthesis* **2014**, *46*, 979.
- (19) (a) Denton, J. R.; Davies, H. M. L. *Org. Lett.* **2009**, *11*, 787. (b) Lindsay, V. N. G.; Nicolas, C.; Charette, A. B. *J. Am. Chem. Soc.* **2011**, *133*, 8972.
- (20) Wolfgang, K. *Eur. J. Org. Chem.* **2002**, 2193.
- (21) Davies, H. M. L.; Nagashima, T.; Klino, J. L. *Org. Lett.* **2000**, *2*, 823.
- (22) Espino, C. G.; Fiori, K. W.; Kim, M.; Du Bois, J. *J. Am. Chem. Soc.* **2004**, *126*, 15378.
- (23) Qin, C.; Boyarskikh, V.; Hansen, J. H.; Hardcastle, K. I.; Musaev, D. G.; Davies, H. M. L. *J. Am. Chem. Soc.* **2011**, *133*, 19198.
- (24) (a) Feng, P.; Fan, Y.; Xue, F.; Liu, W.; Li, S.; Shi, Y. *Org. Lett.* **2011**, *13*, 5827. (b) Hou, S. H.; Tu, Y. Q.; Liu, L.; Zhang, F. M.; Wang, S. H.; Zhang, X. M. *Angew. Chem. Int. Ed.* **2013**, *52*, 11373.
- (25) (a) Barton, D. H. R.; Lusinch, X.; Milliet, P. *Tetrahedron Lett.* **1982**, *23*, 4949. (b) Ninomiya, I.; Hashimoto, C.; Kiguchi, T.; Barton, D. H. R.; Lusinch, X.; Milliet, P. *Tetrahedron Lett.* **1985**, *26*, 4187. (c) Ninomiya, I.; Kiguchi, T.; Hashimoto, C.; Barton, D. H. R.; Lusinch, X.; Milliet, P. *Tetrahedron Lett.* **1985**, *26*, 4183.

### 3.6 NMR Spectra

**Figure 3.1**  $^1\text{H}$  and  $^{13}\text{C}$  NMR spectrum of compound **6h**

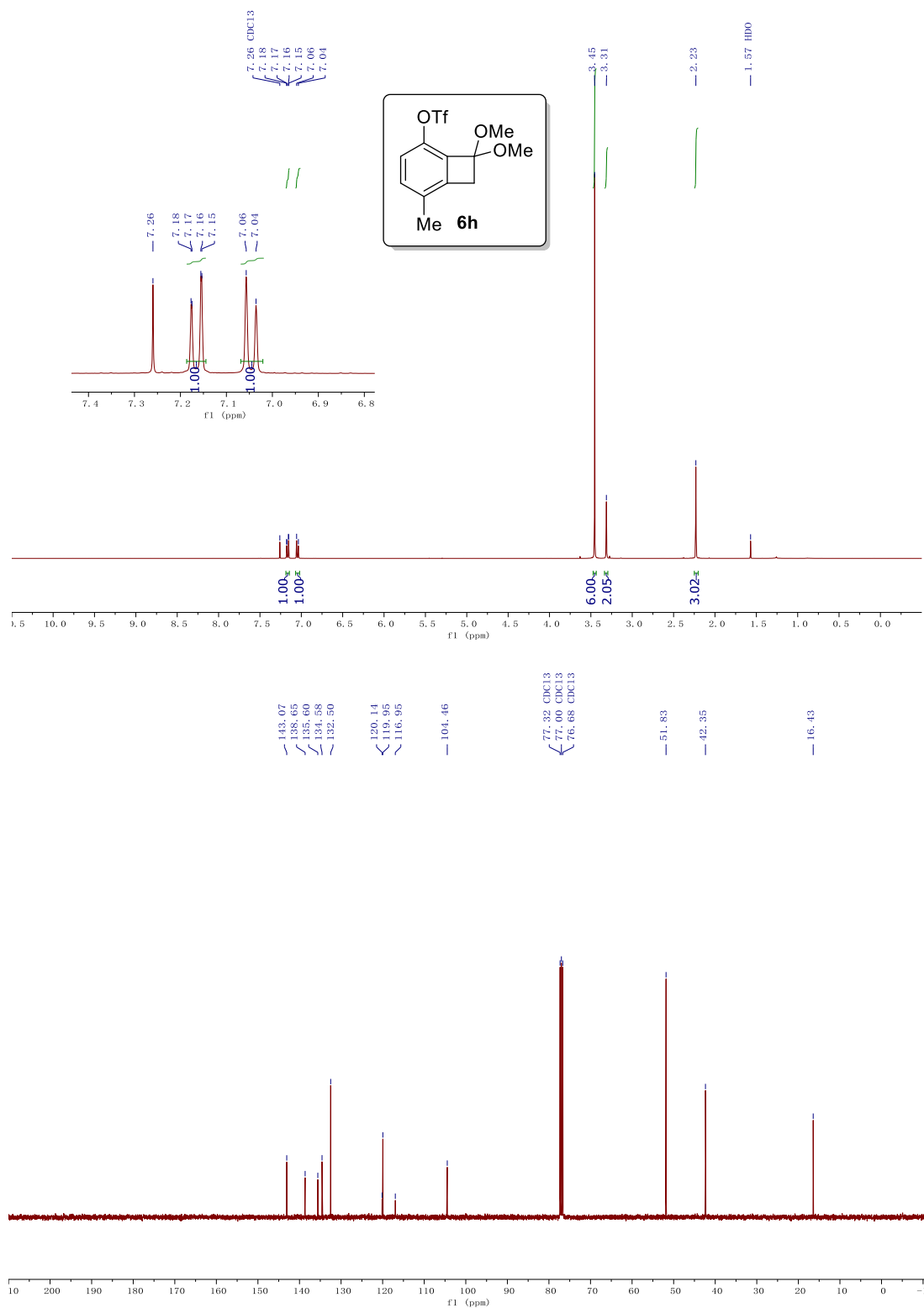


**Figure 3.2**  $^1\text{H}$  and  $^{13}\text{C}$  NMR spectrum of compound **5**

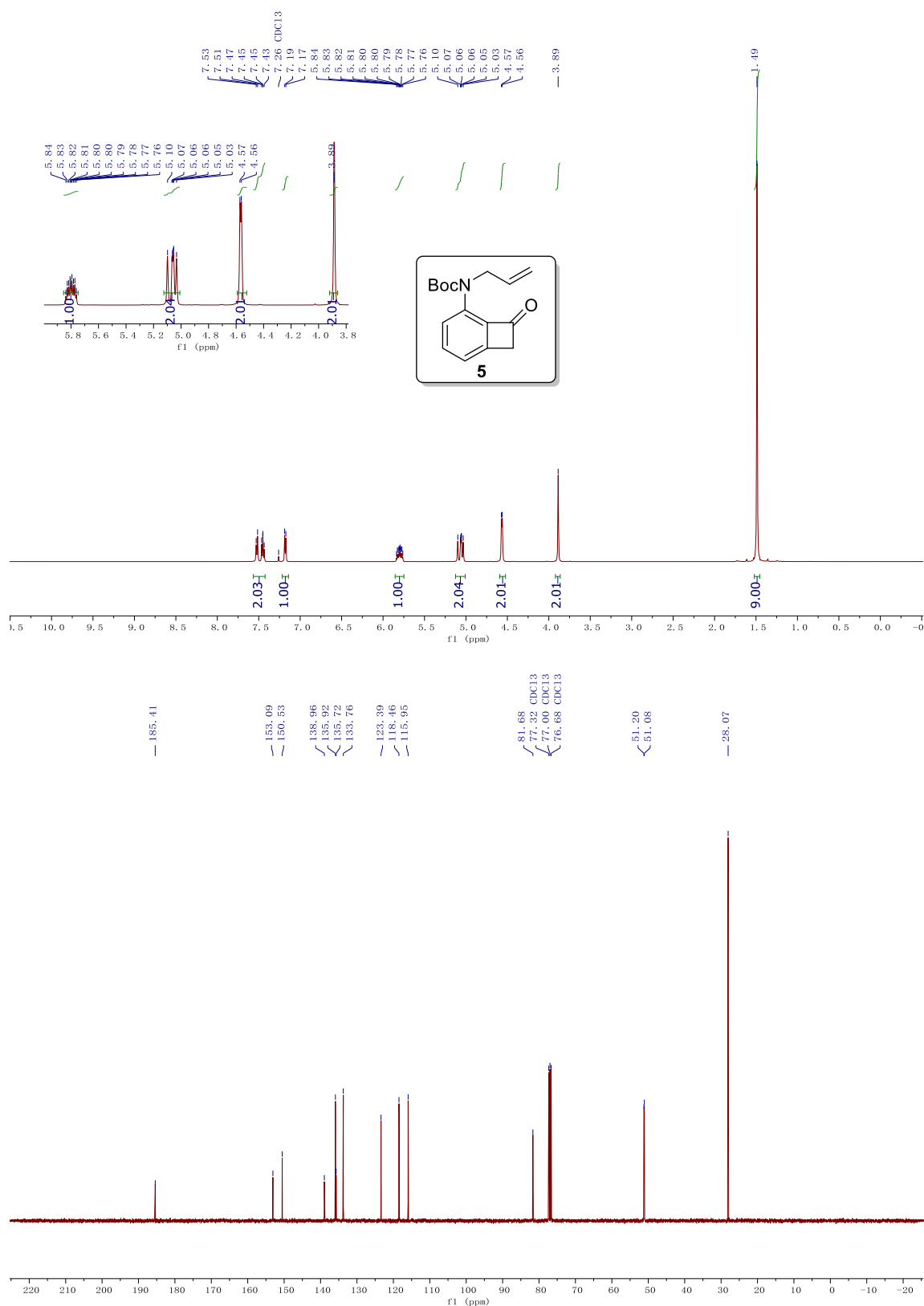


**Figure 3.3**  $^1\text{H}$  and  $^{13}\text{C}$  NMR spectrum of compound **5a**

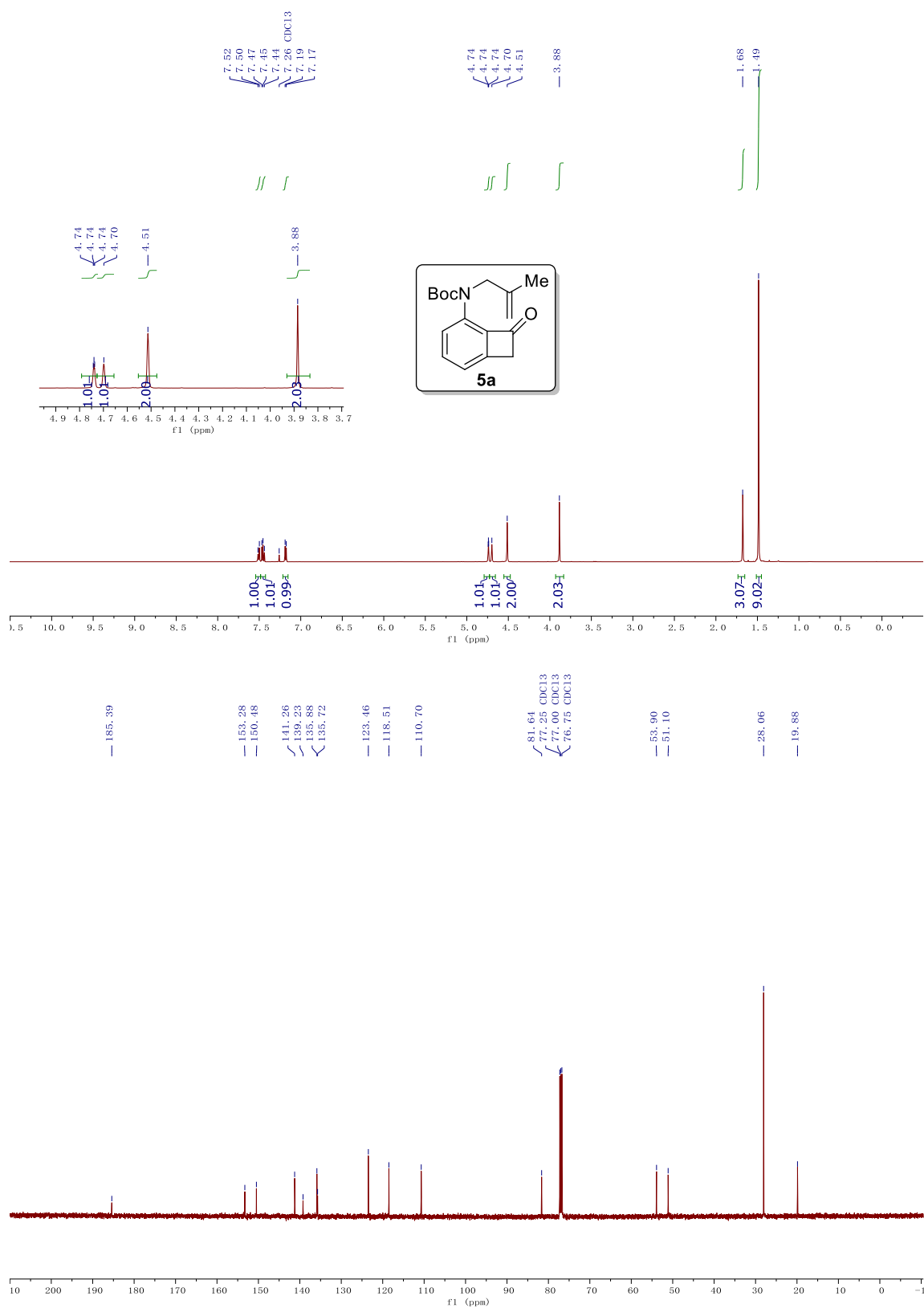


**Figure 3.4**  $^1\text{H}$  and  $^{13}\text{C}$  NMR spectrum of compound **5b**

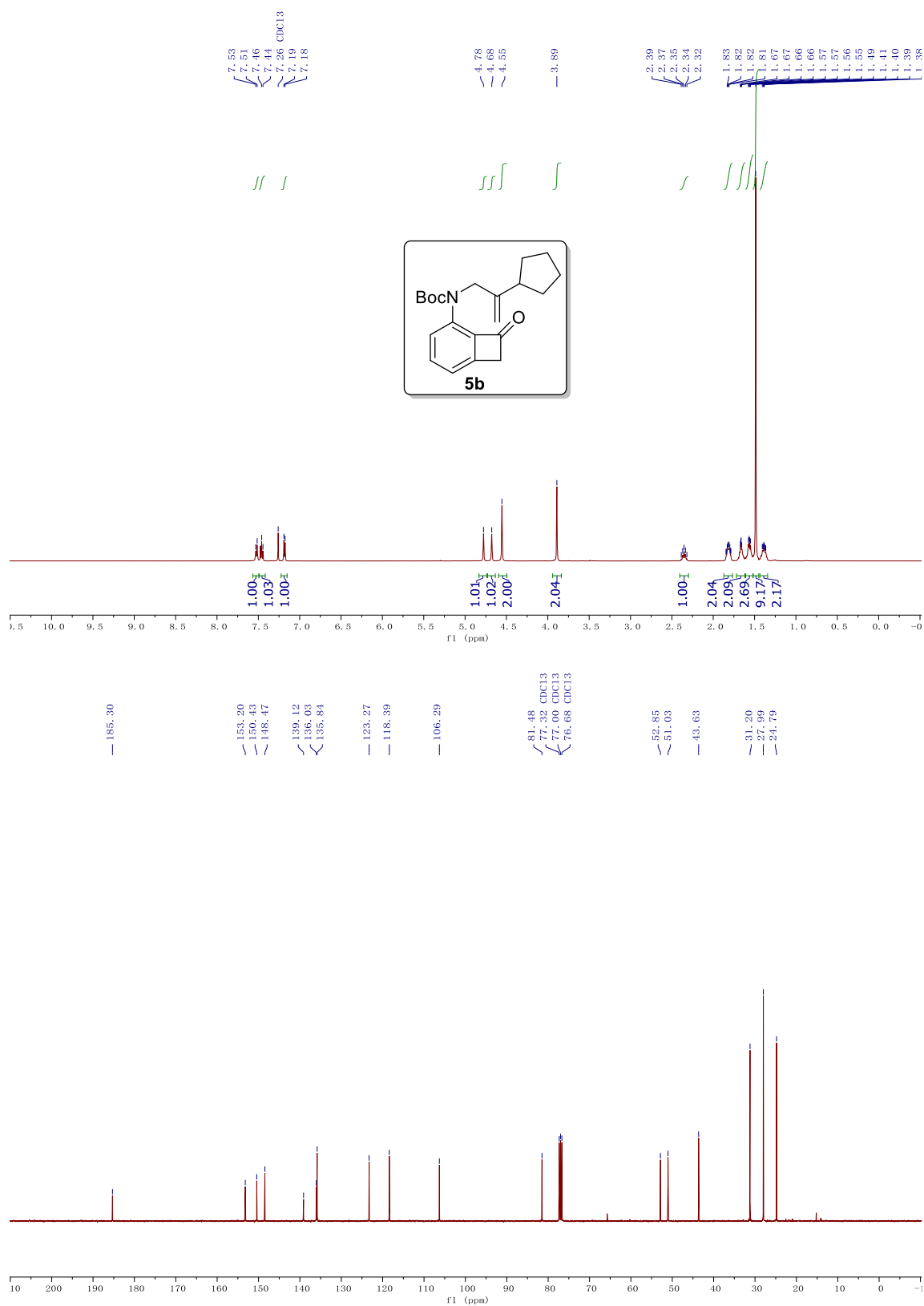




**Figure 3.5**  $^1\text{H}$  and  $^{13}\text{C}$  NMR spectrum of compound **5c**

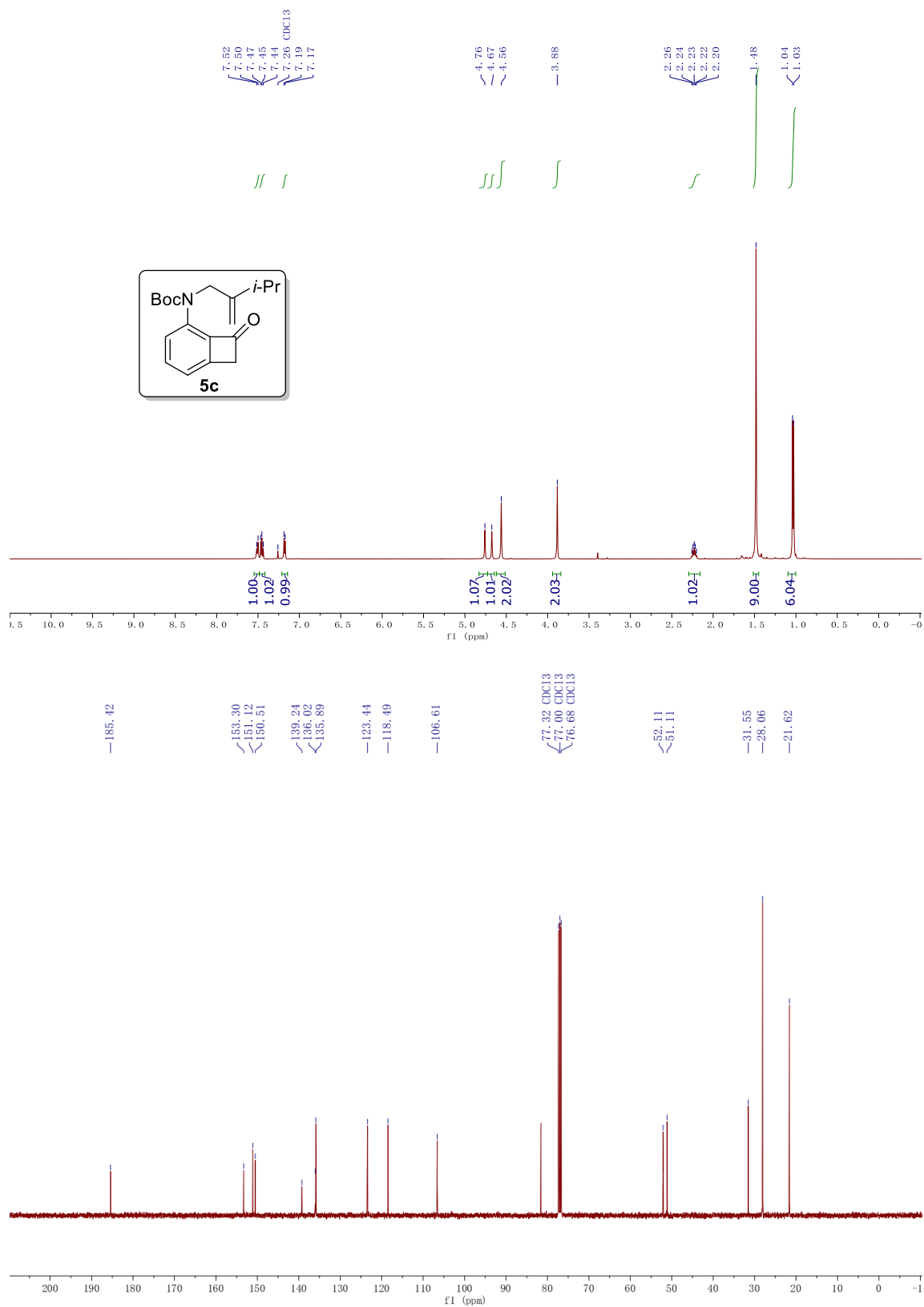


**Figure 3.6**  $^1\text{H}$  and  $^{13}\text{C}$  NMR spectrum of compound **5d**

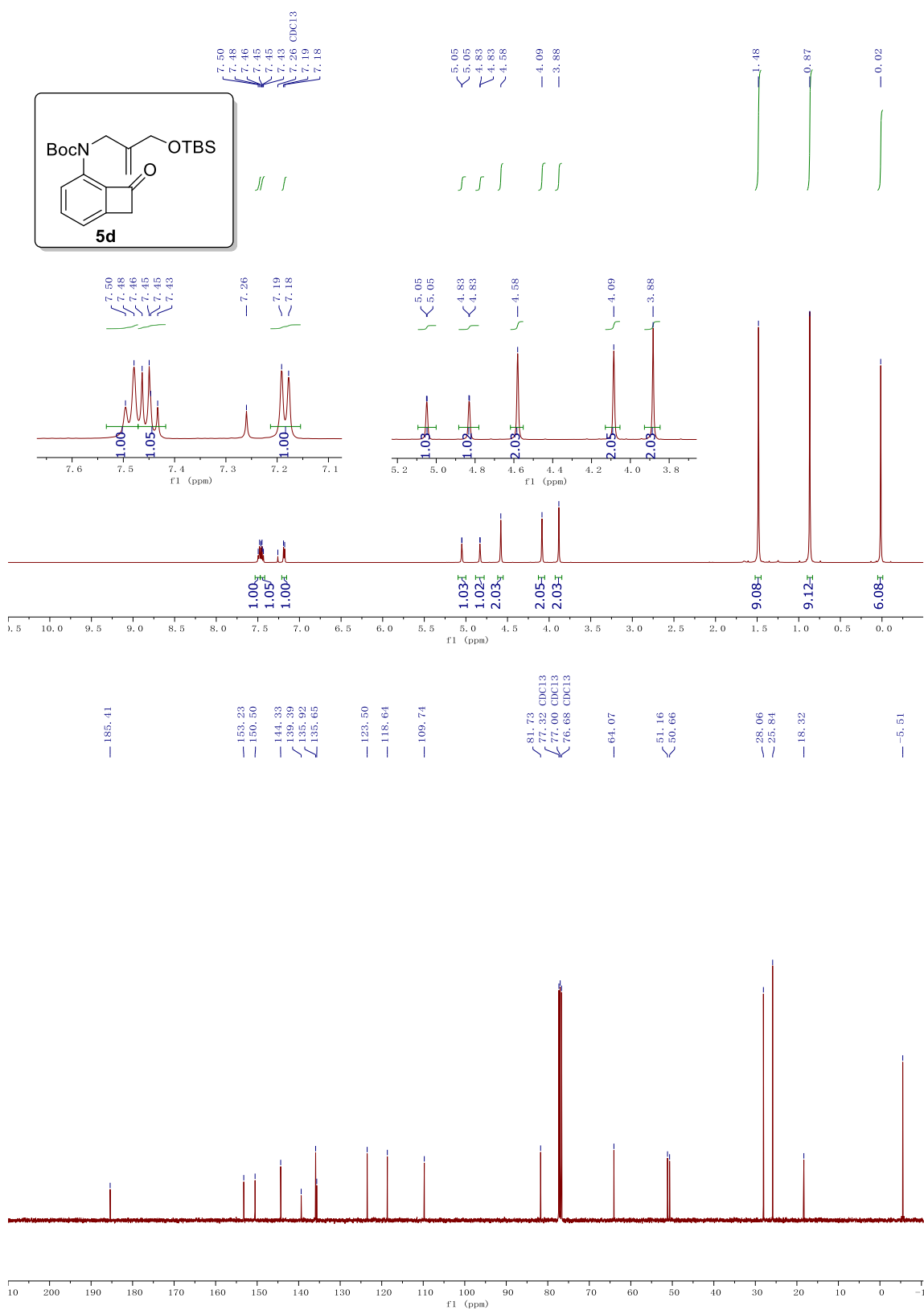


**Figure 3.7**  $^1\text{H}$  and  $^{13}\text{C}$  NMR spectrum of compound **5e**

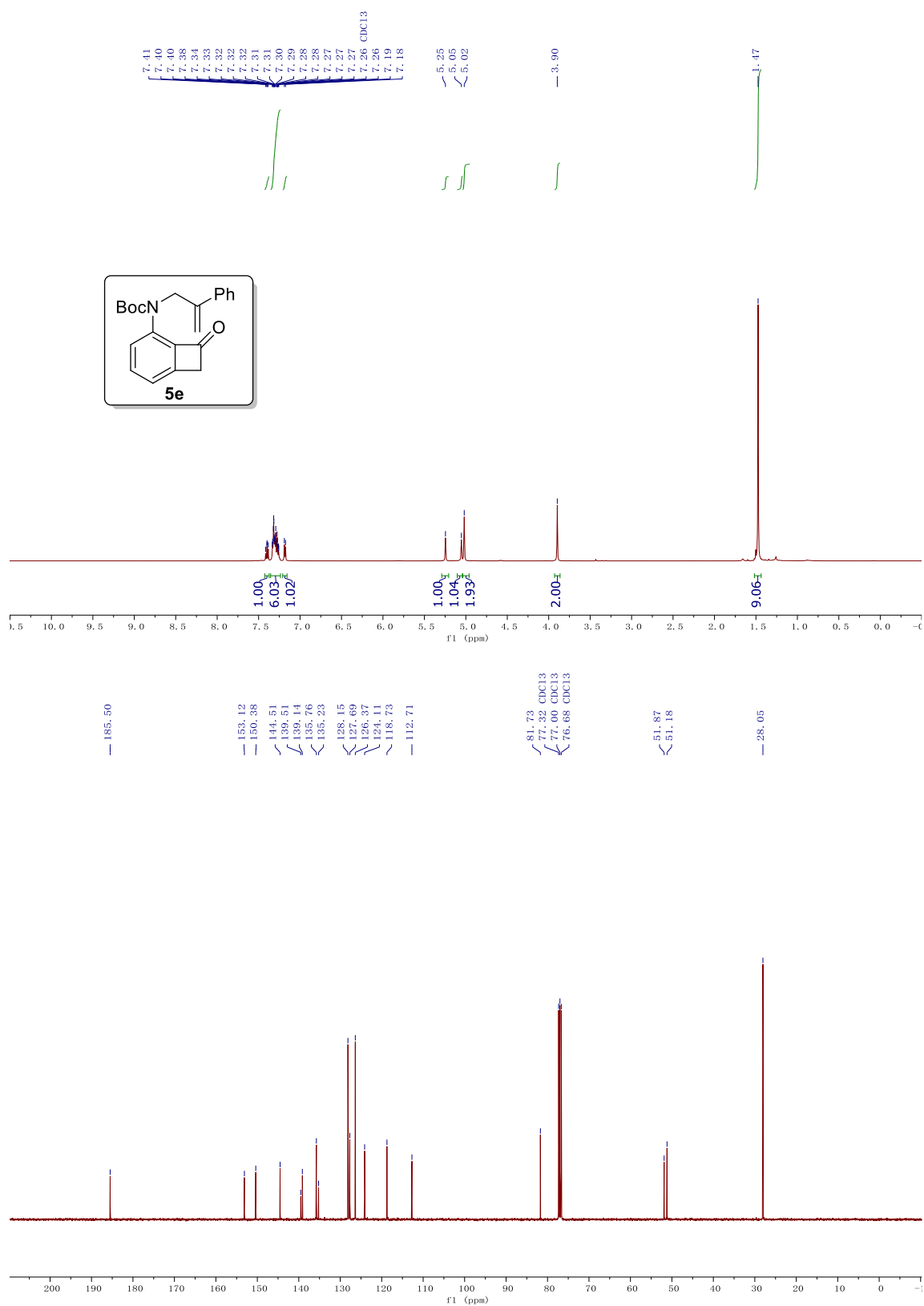


**Figure 3.8**  $^1\text{H}$ ,  $^{13}\text{C}$  NMR and  $^{19}\text{F}$ -NMR spectrum of compound **5f**

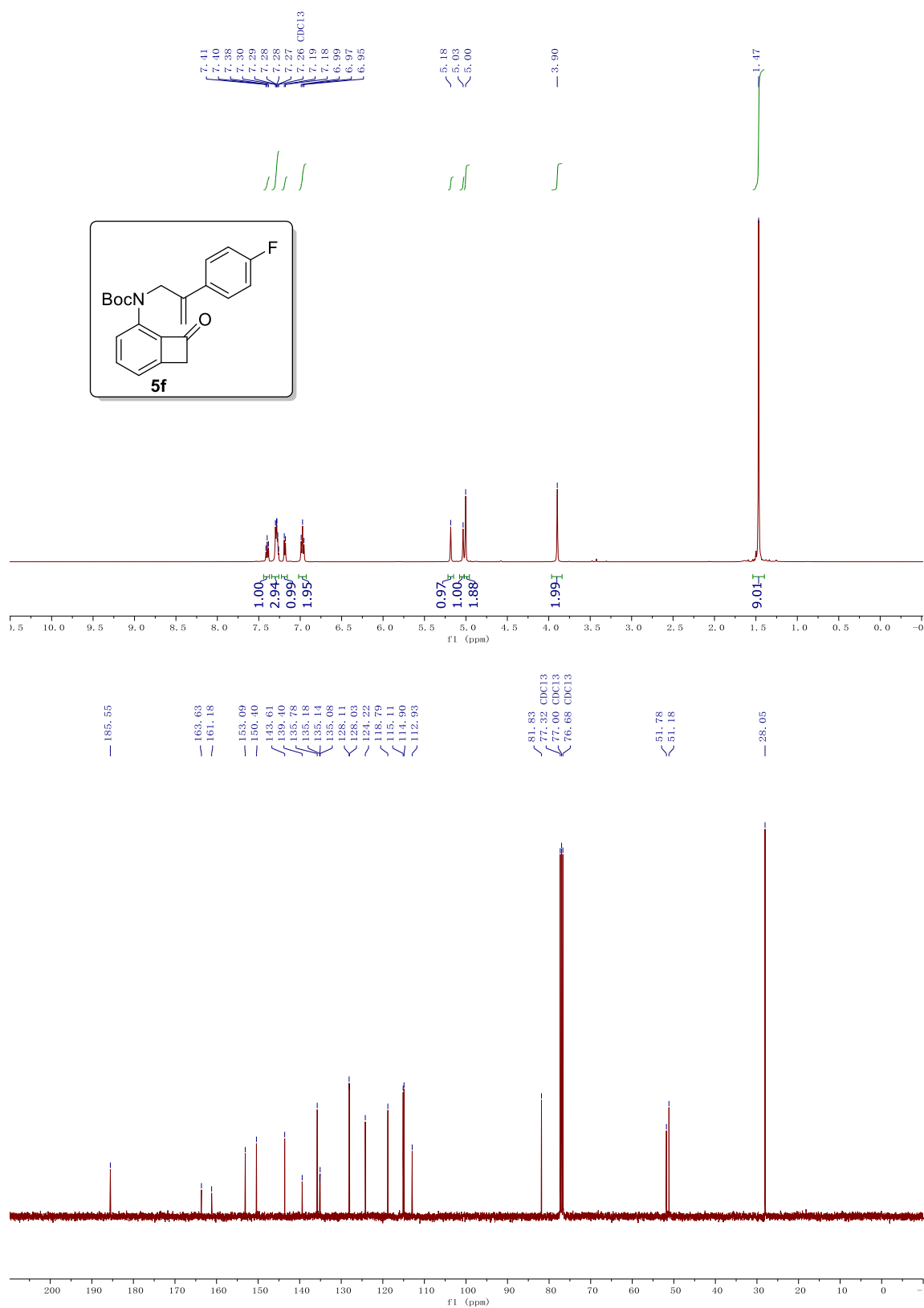


**Figure 3.8** Continued  $^1\text{H}$ ,  $^{13}\text{C}$  NMR and  $^{19}\text{F}$ -NMR spectrum of compound **5f**

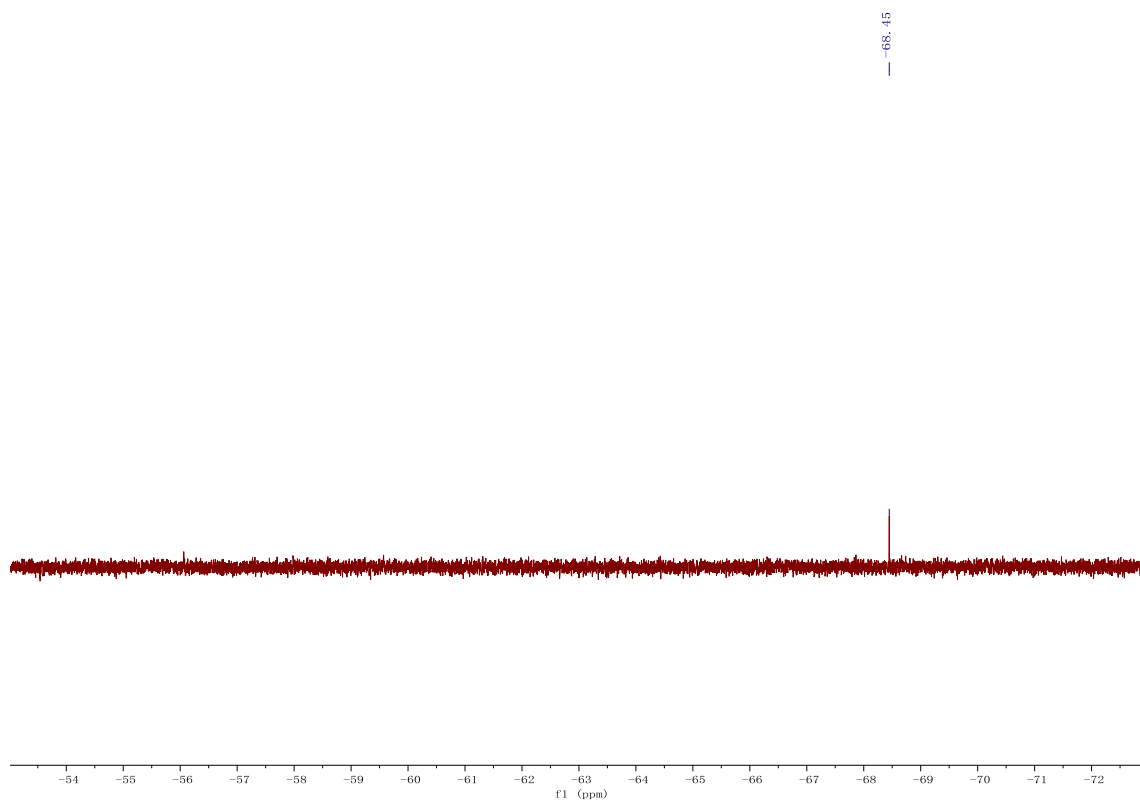


**Figure 3.9**  $^1\text{H}$  and  $^{13}\text{C}$  NMR spectrum of compound **5g**

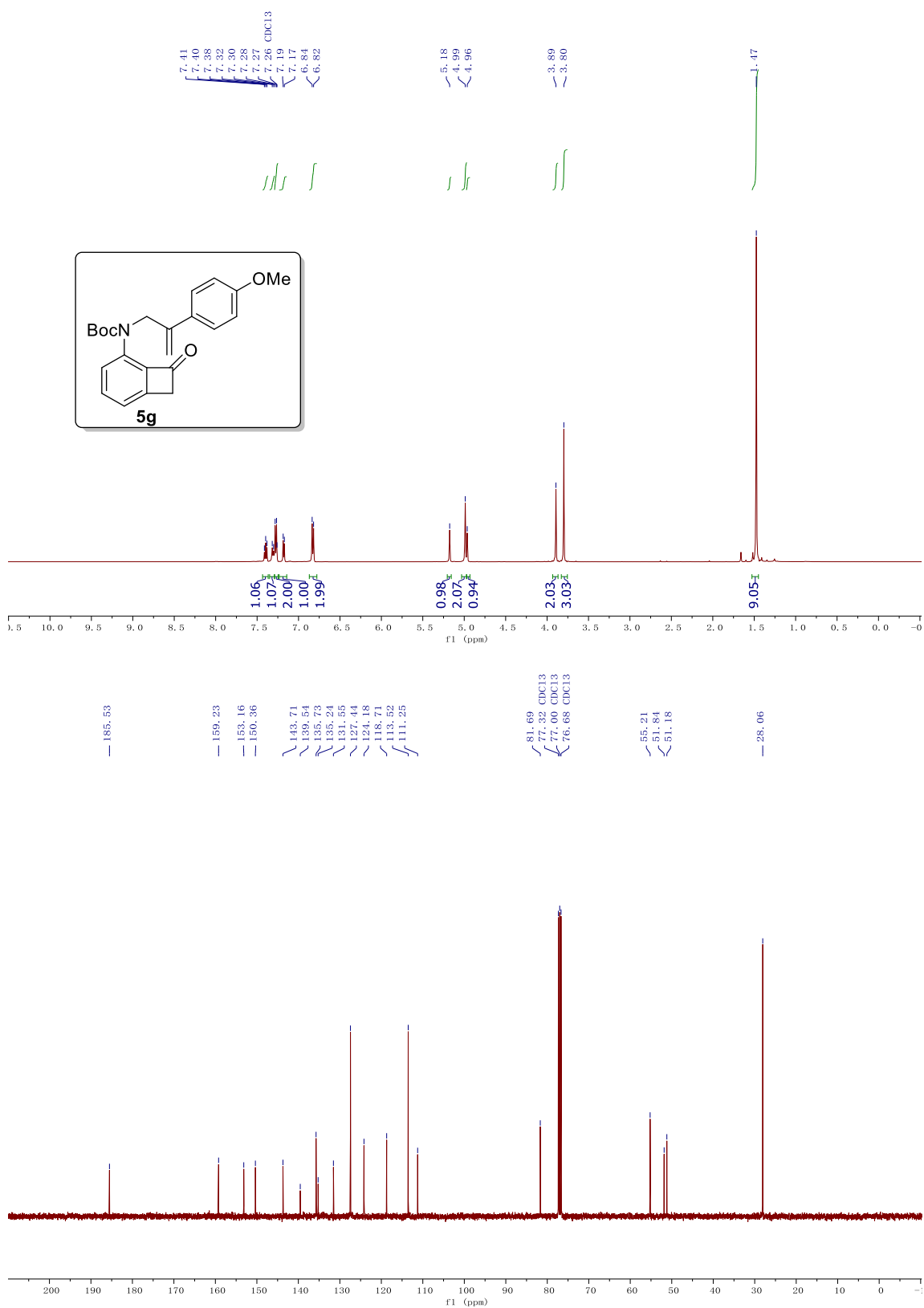


**Figure 3.10**  $^1\text{H}$  and  $^{13}\text{C}$  NMR spectrum of compound **5h**

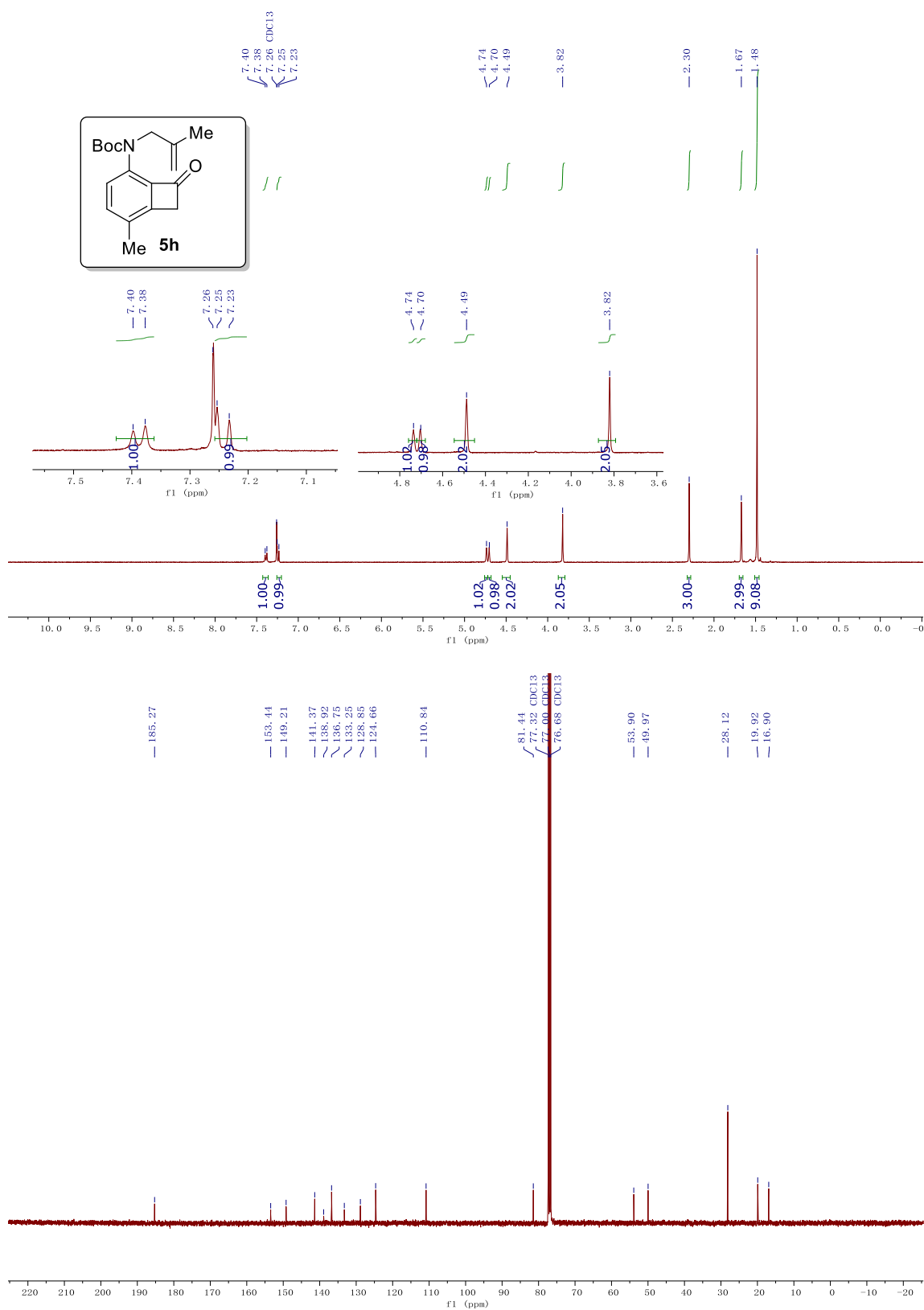


**Figure 3.11**  $^1\text{H}$  and  $^{13}\text{C}$  NMR spectrum of compound **5i**

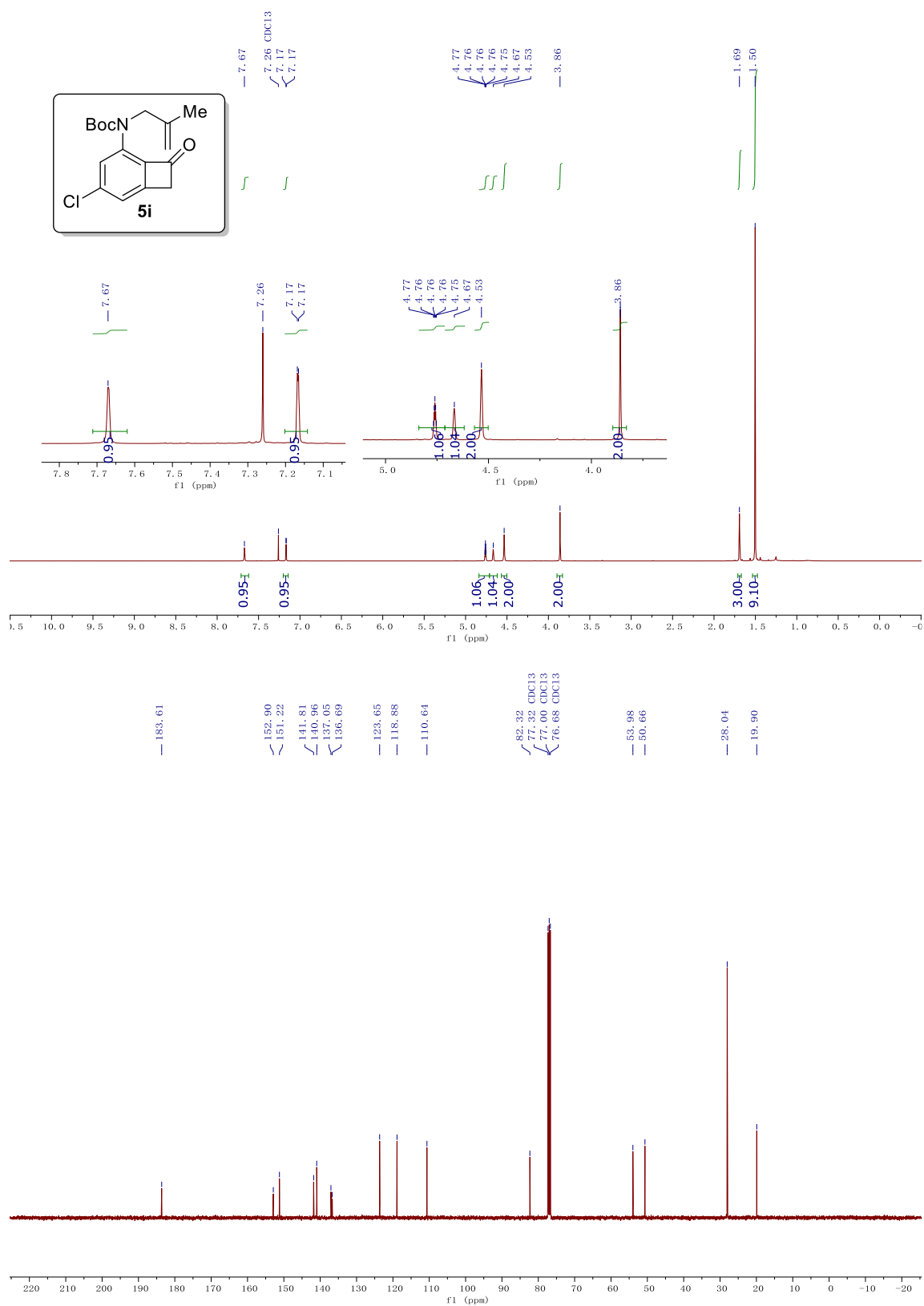




**Figure 3.12**  $^1\text{H}$  and  $^{13}\text{C}$  NMR spectrum of compound **5j**

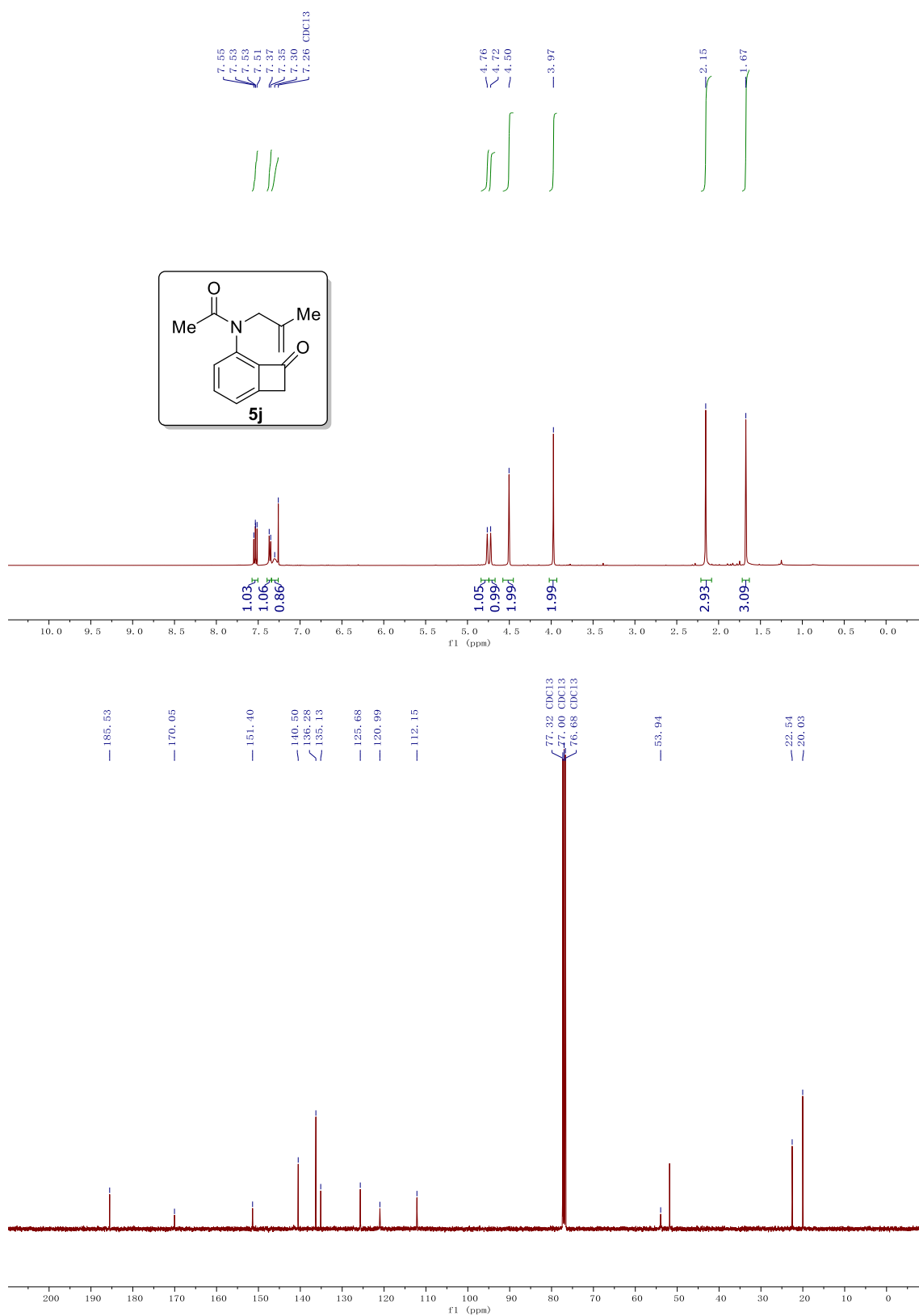


**Figure 3.13**  $^1\text{H}$  and  $^{13}\text{C}$  NMR spectrum of compound **5k**

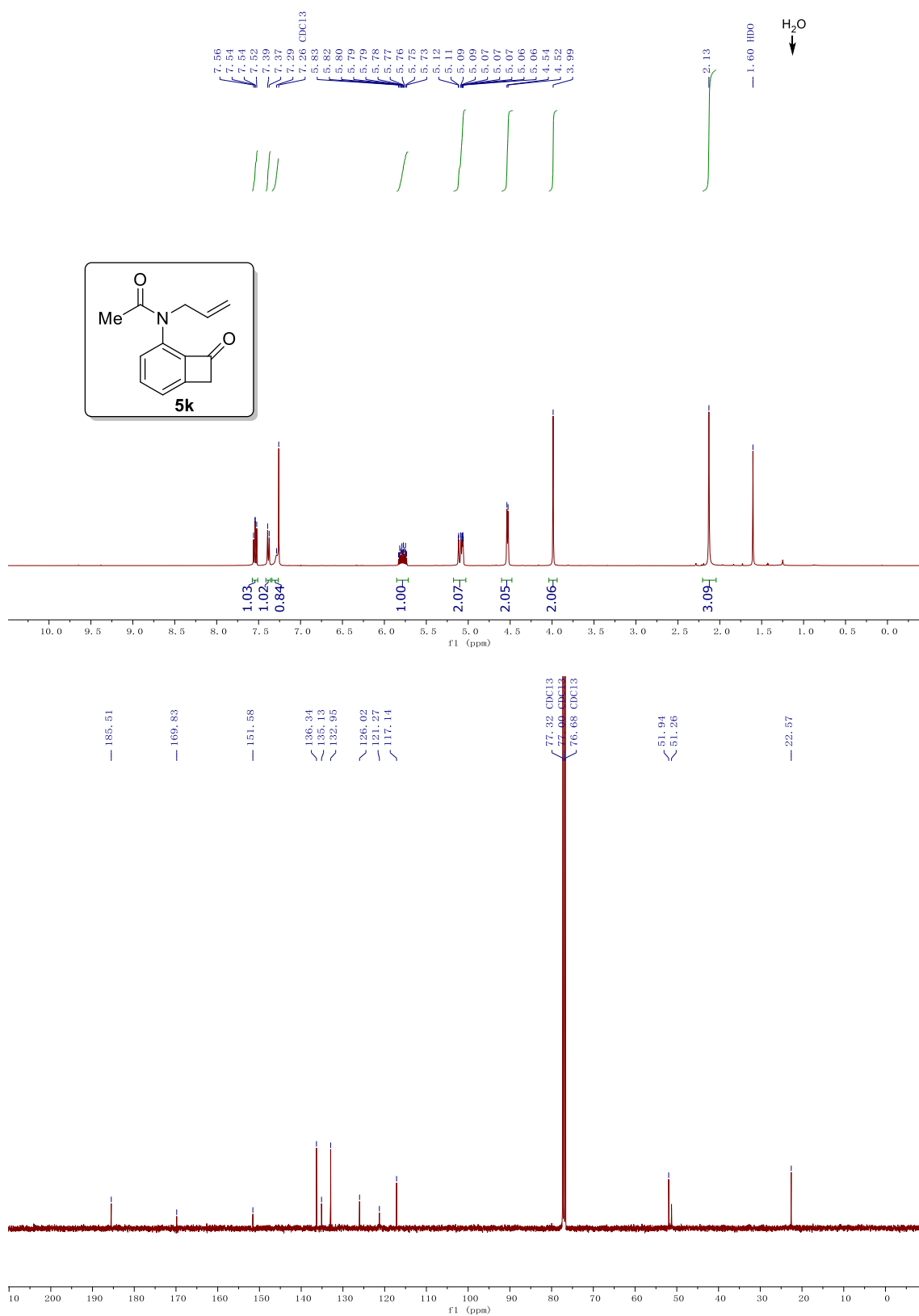


**Figure 3.14**  $^1\text{H}$  and  $^{13}\text{C}$  NMR spectrum of compound **5l-I**

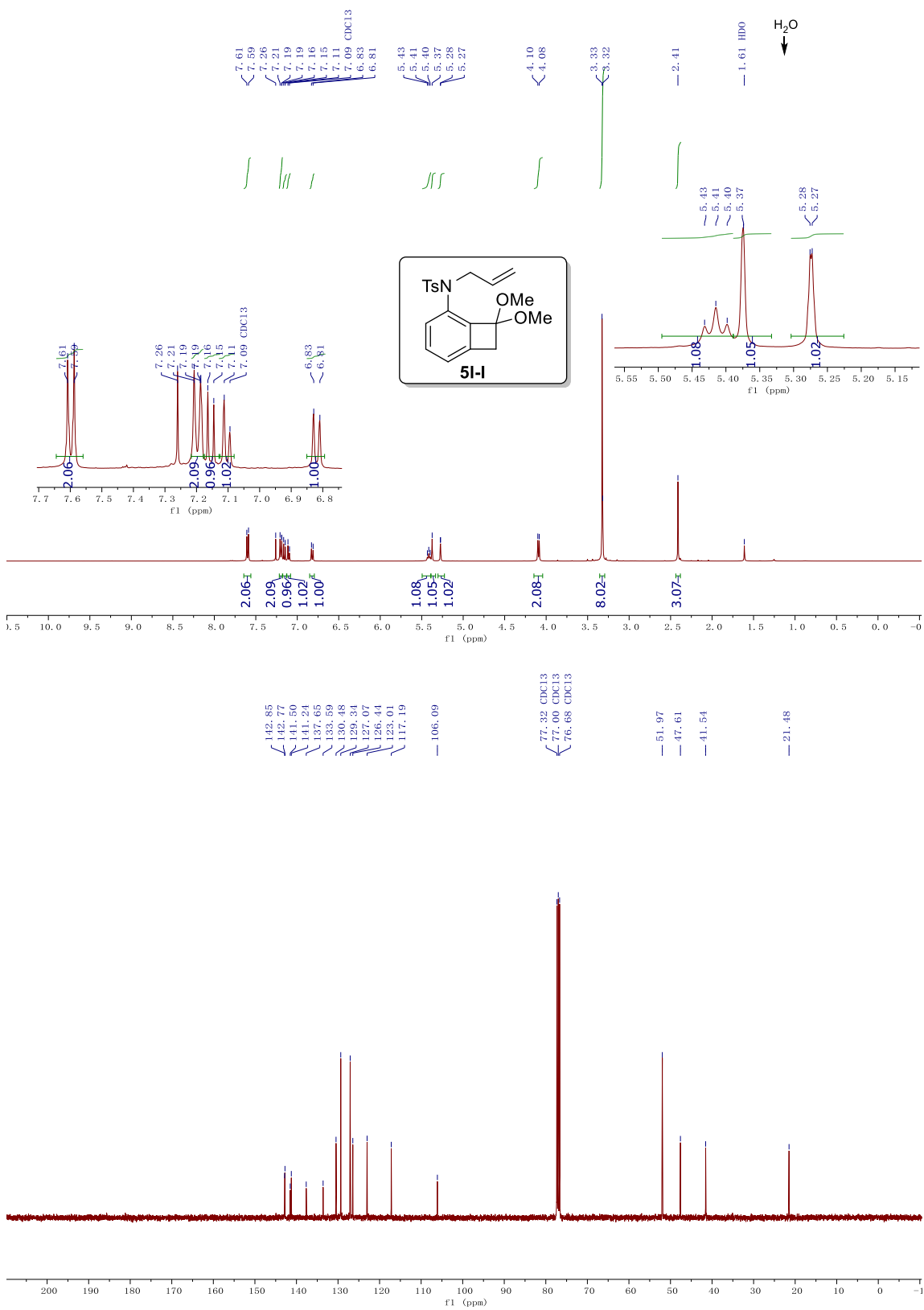


**Figure 3.15**  $^1\text{H}$  and  $^{13}\text{C}$  NMR spectrum of compound **51**

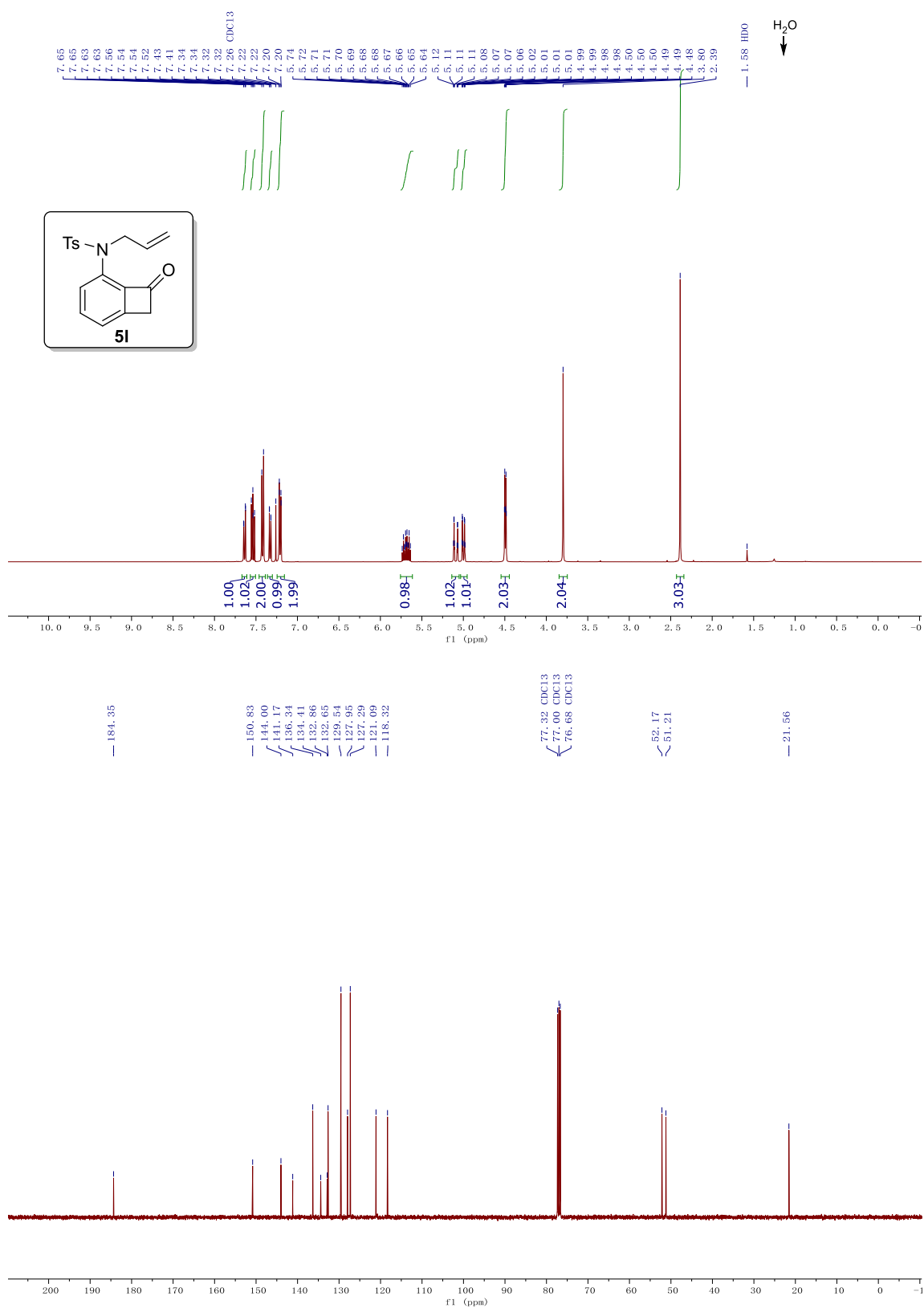


**Figure 3.16**  $^1\text{H}$  and  $^{13}\text{C}$  NMR spectrum of compound **5m**

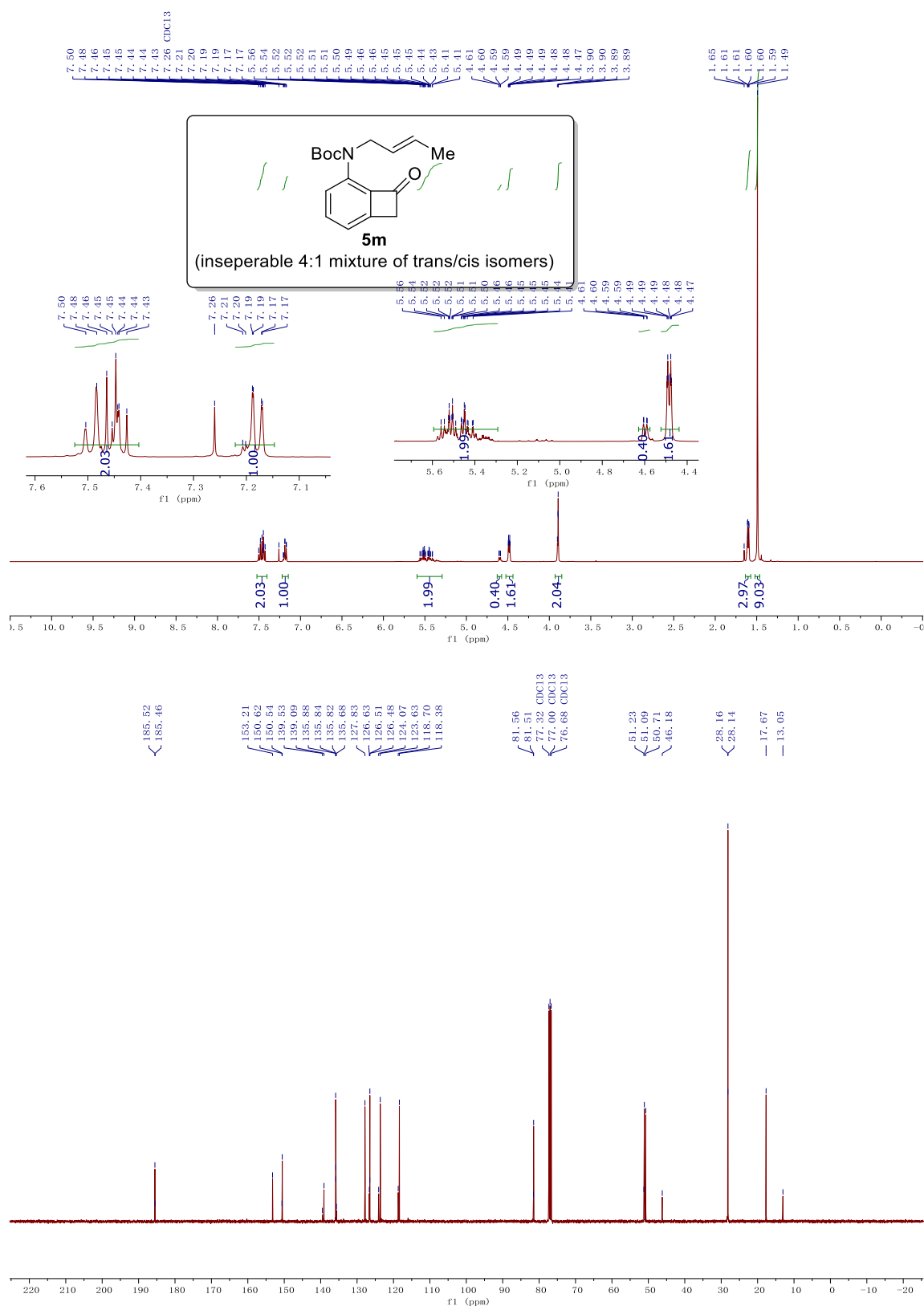


**Figure 3.17**  $^1\text{H}$  and  $^{13}\text{C}$  NMR spectrum of compound **5n**

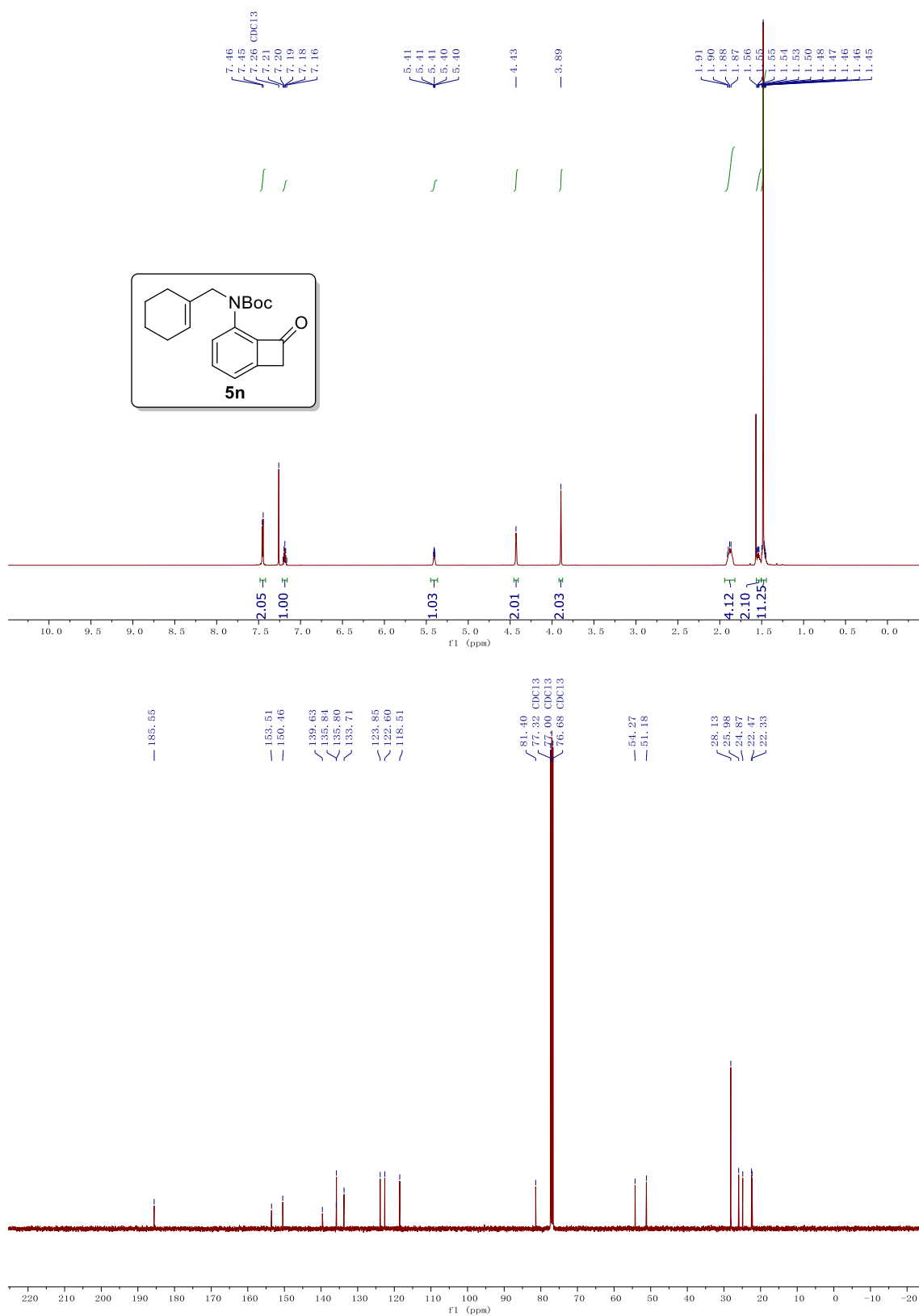


**Figure 3.18**  $^1\text{H}$  and  $^{13}\text{C}$  NMR spectrum of compound **8**

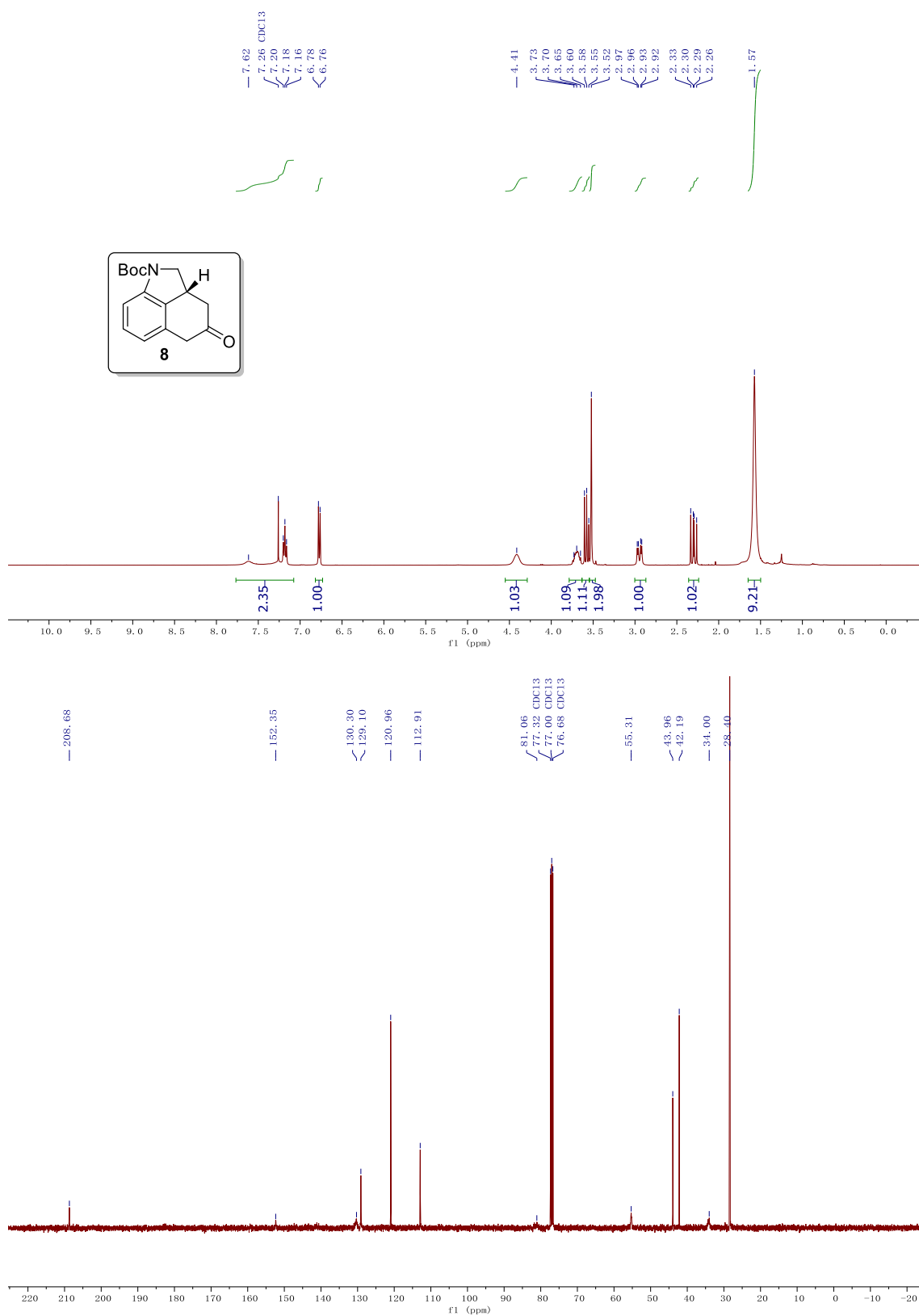


**Figure 3.19**  $^1\text{H}$  and  $^{13}\text{C}$  NMR spectrum of compound **8a**

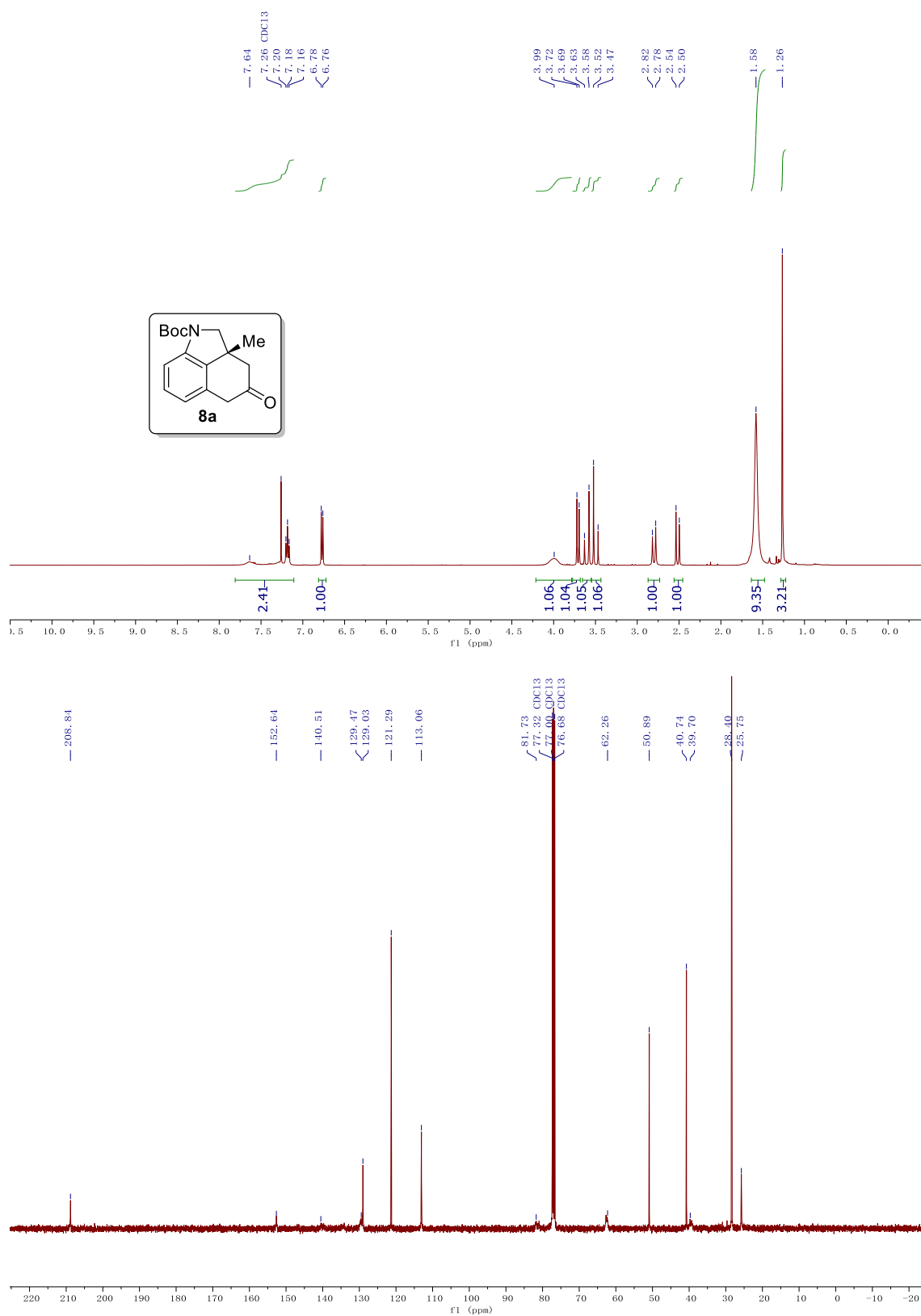




**Figure 3.20**  $^1\text{H}$  and  $^{13}\text{C}$  NMR spectrum of compound **8b**

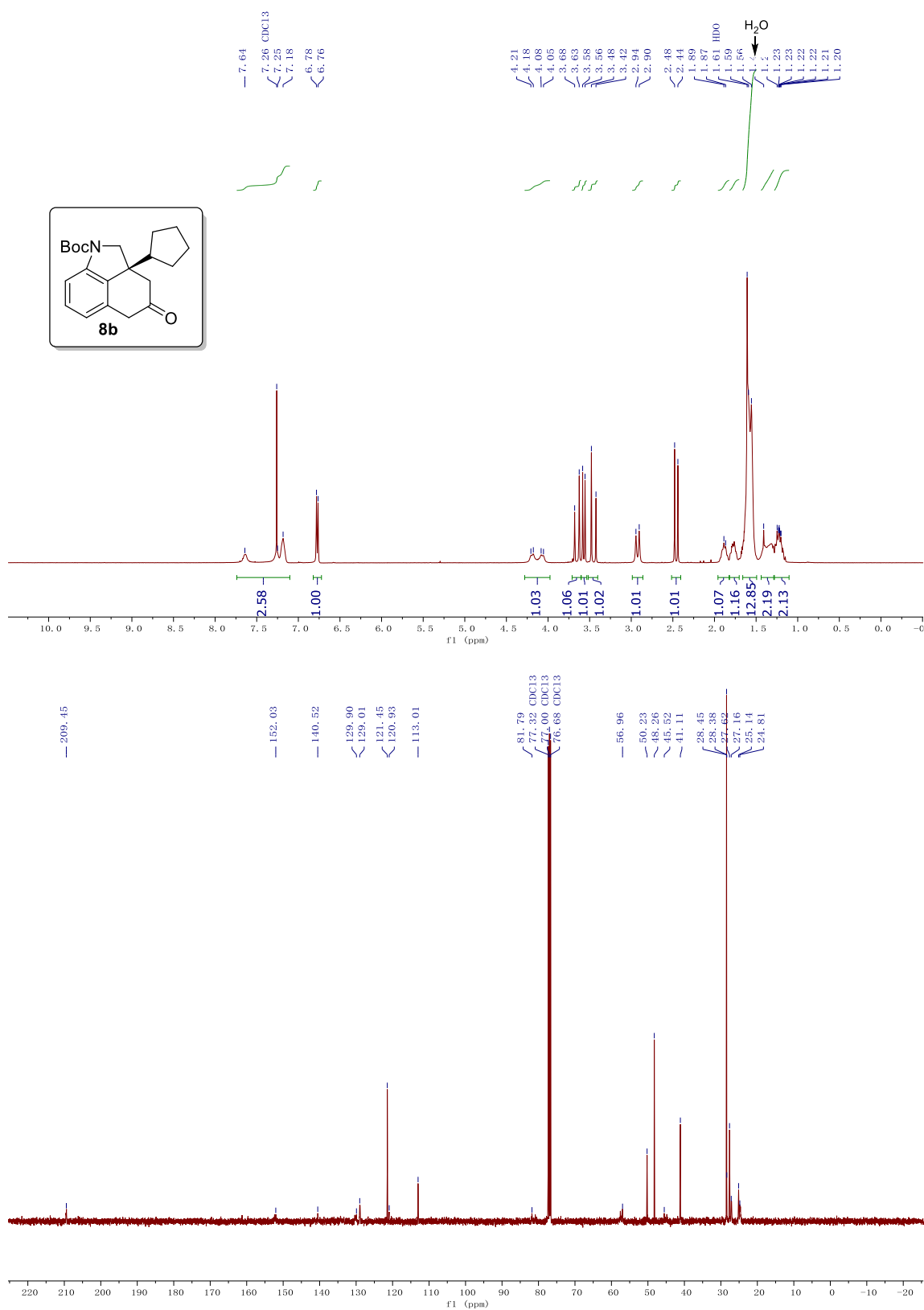


**Figure 3.21**  $^1\text{H}$  and  $^{13}\text{C}$  NMR spectrum of compound **8c**

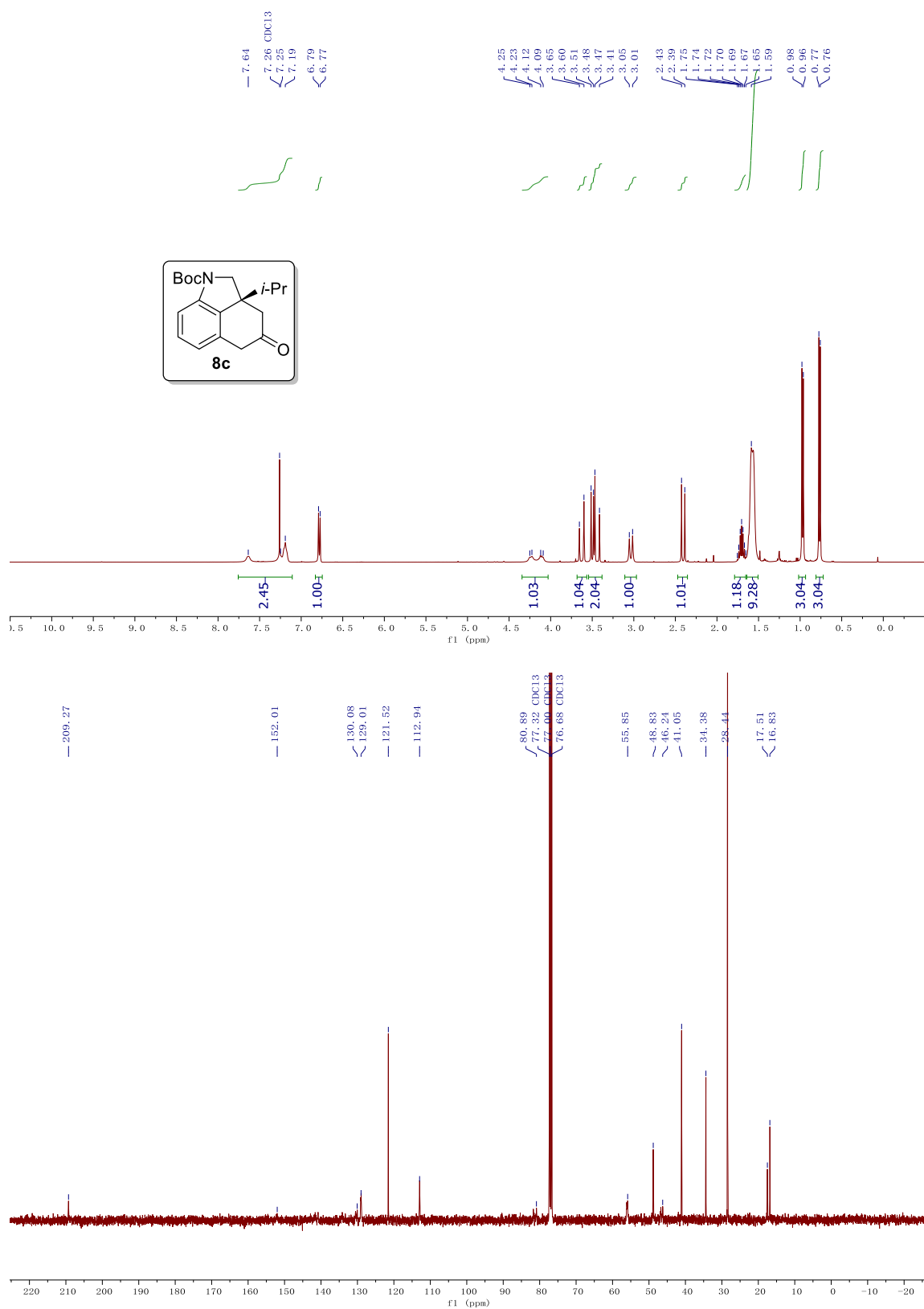


**Figure 3.22**  $^1\text{H}$  and  $^{13}\text{C}$  NMR spectrum of compound **8d**

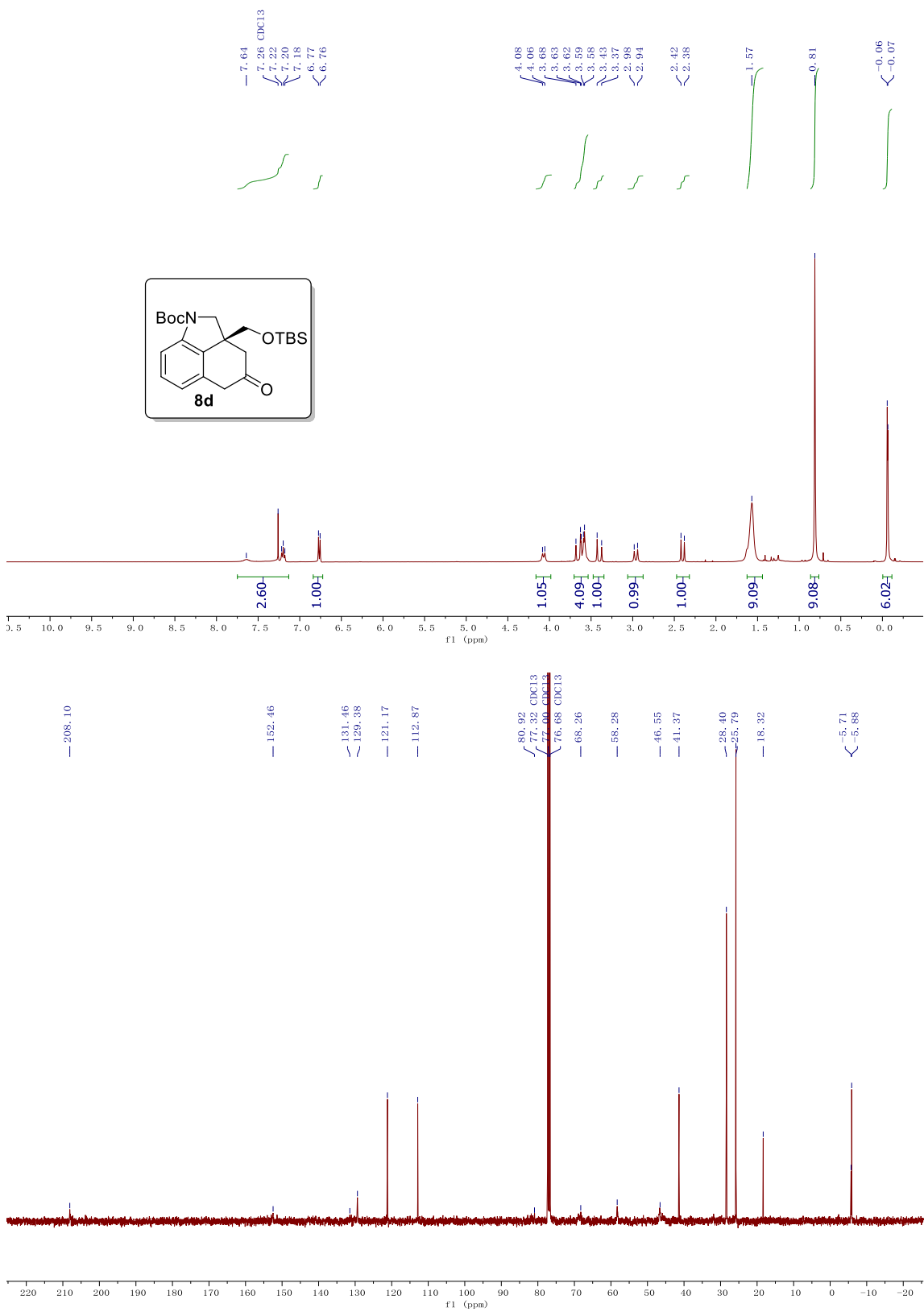


**Figure 3.23**  $^1\text{H}$  and  $^{13}\text{C}$  NMR spectrum of compound **8e**

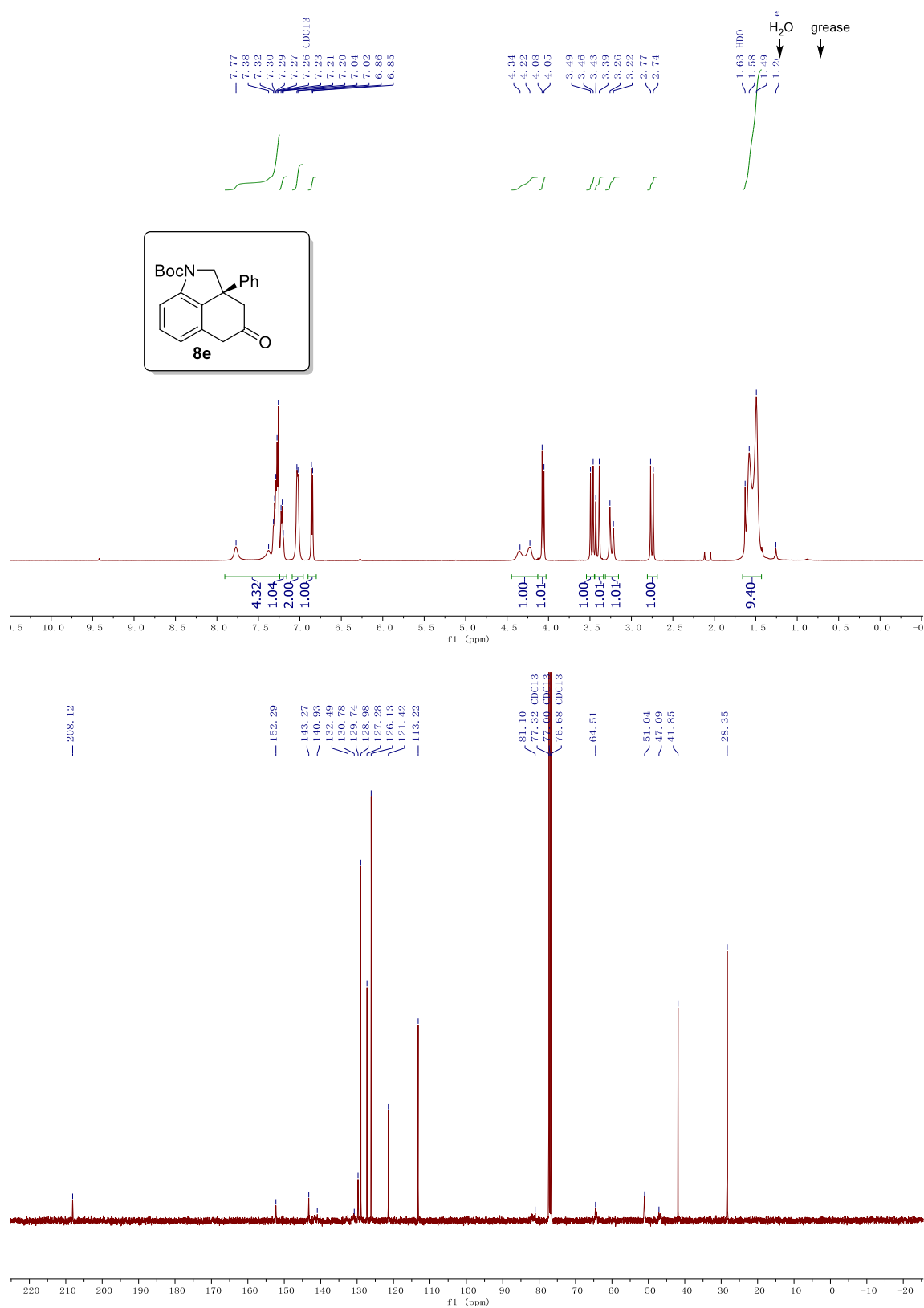


**Figure 3.24**  $^1\text{H}$ ,  $^{13}\text{C}$  NMR and  $^{19}\text{F}$  NMR spectrum of compound **8f**

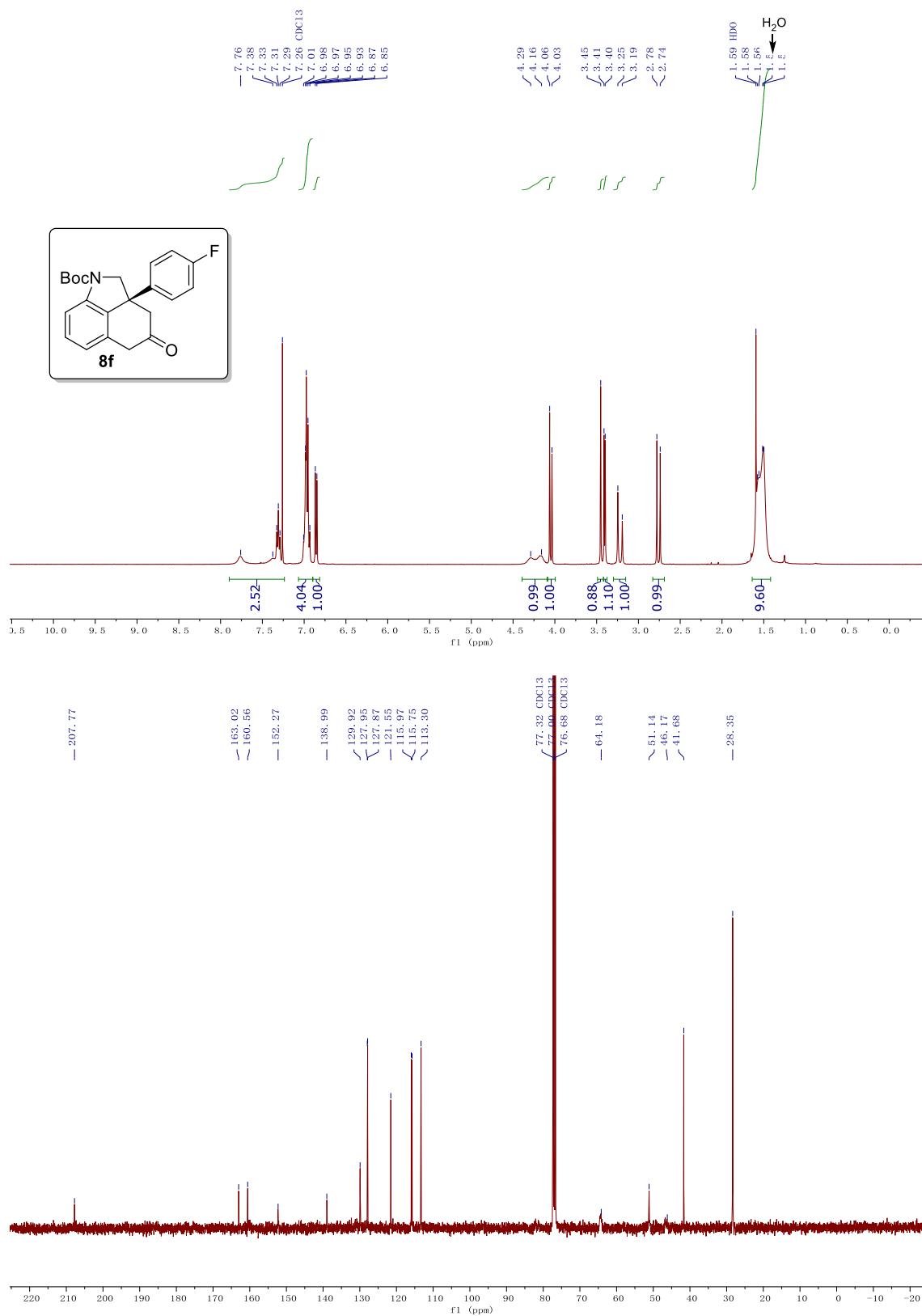


**Figure 3.24** Continued  $^1\text{H}$ ,  $^{13}\text{C}$  NMR and  $^{19}\text{F}$  NMR spectrum of compound **8f**

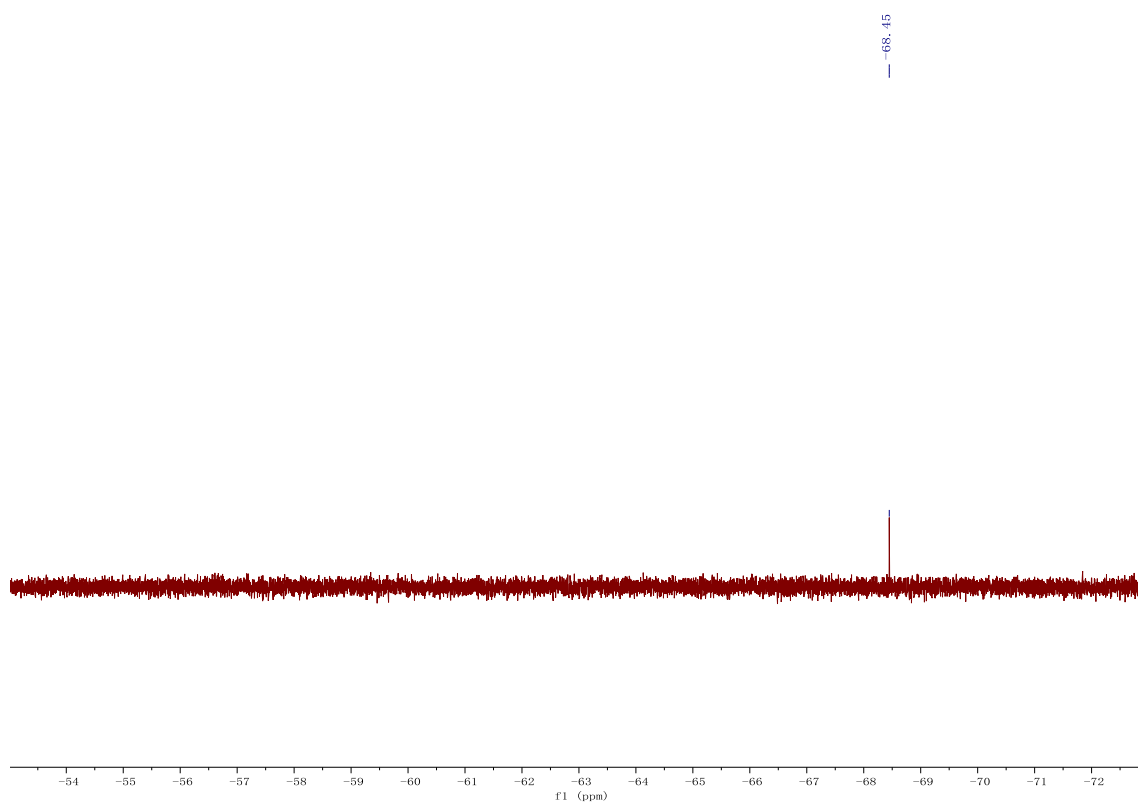


**Figure 3.25**  $^1\text{H}$  and  $^{13}\text{C}$  NMR spectrum of compound **8g**

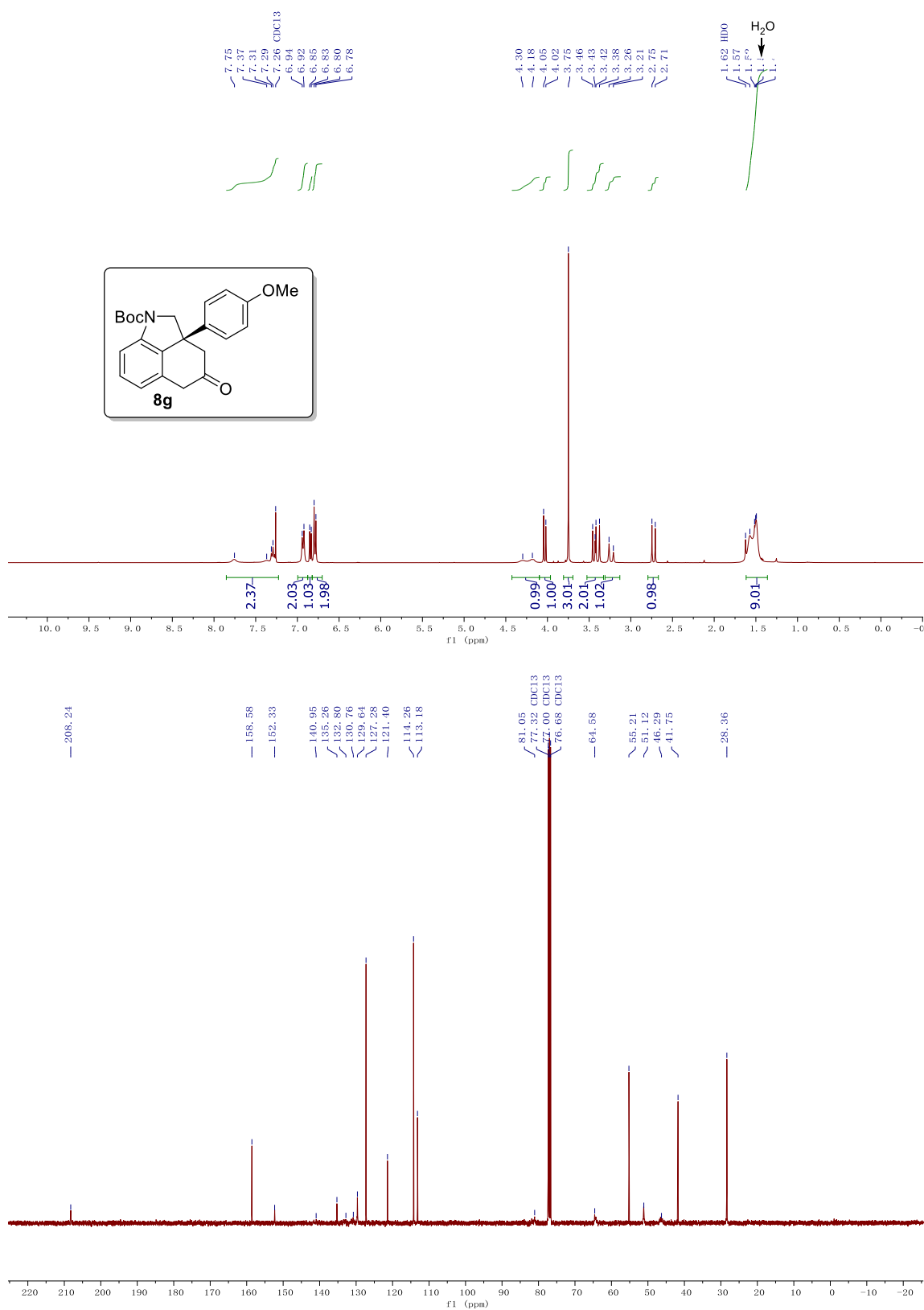


**Figure 3.26**  $^1\text{H}$  and  $^{13}\text{C}$  NMR spectrum of compound **8h**

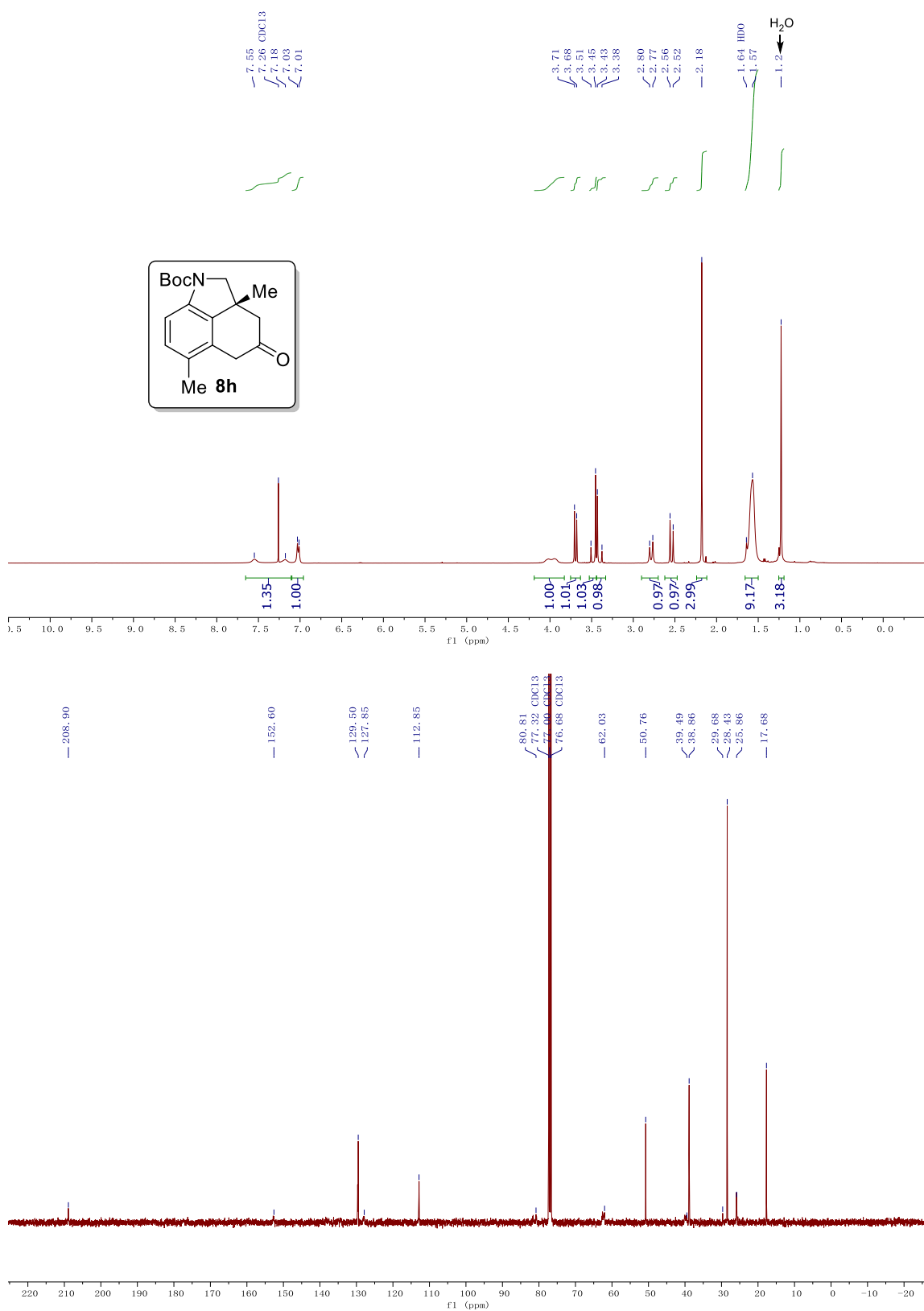




**Figure 3.27**  $^1\text{H}$  and  $^{13}\text{C}$  NMR spectrum of compound **8i**

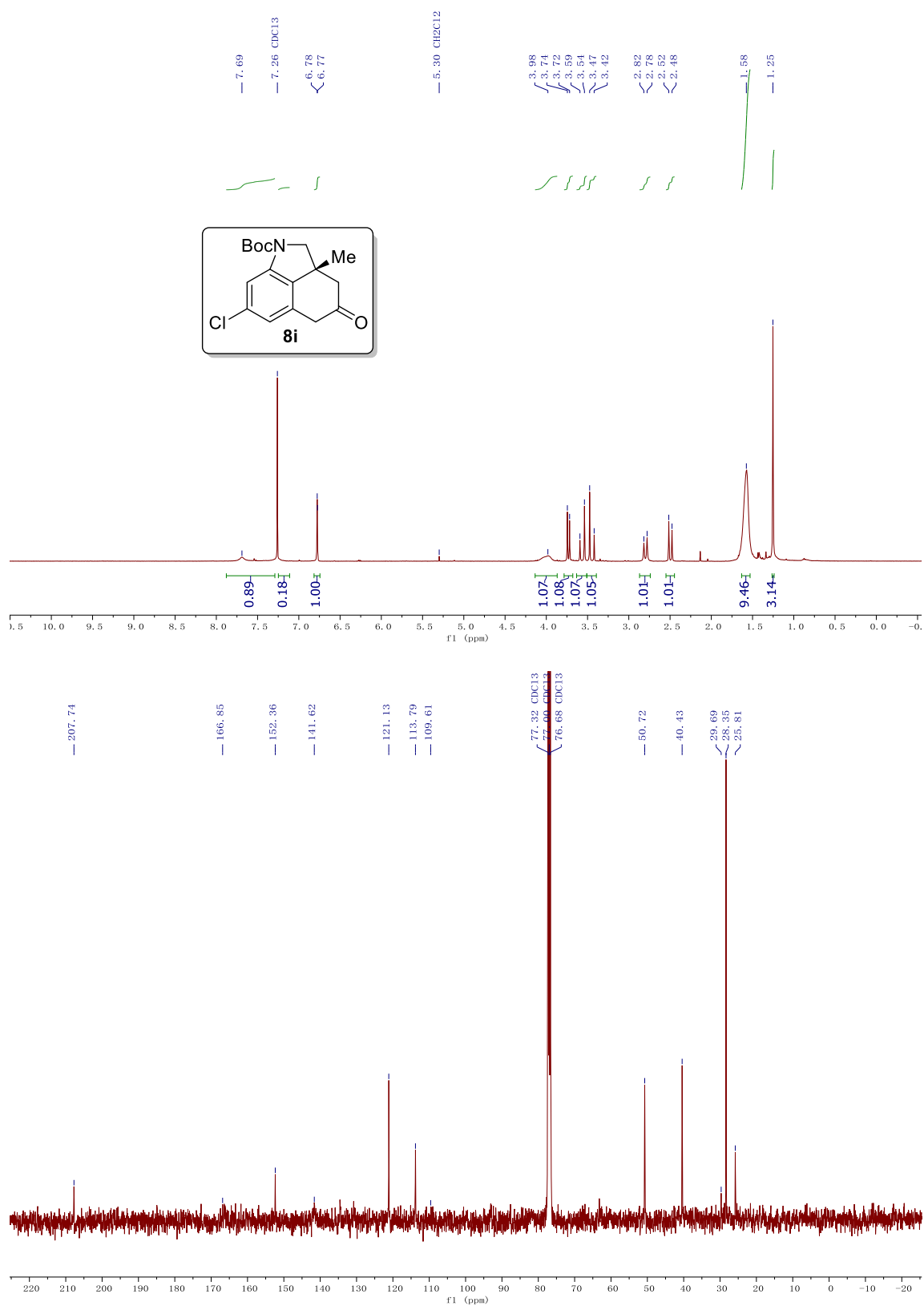


**Figure 3.28**  $^1\text{H}$  and  $^{13}\text{C}$  NMR spectrum of compound **8j**

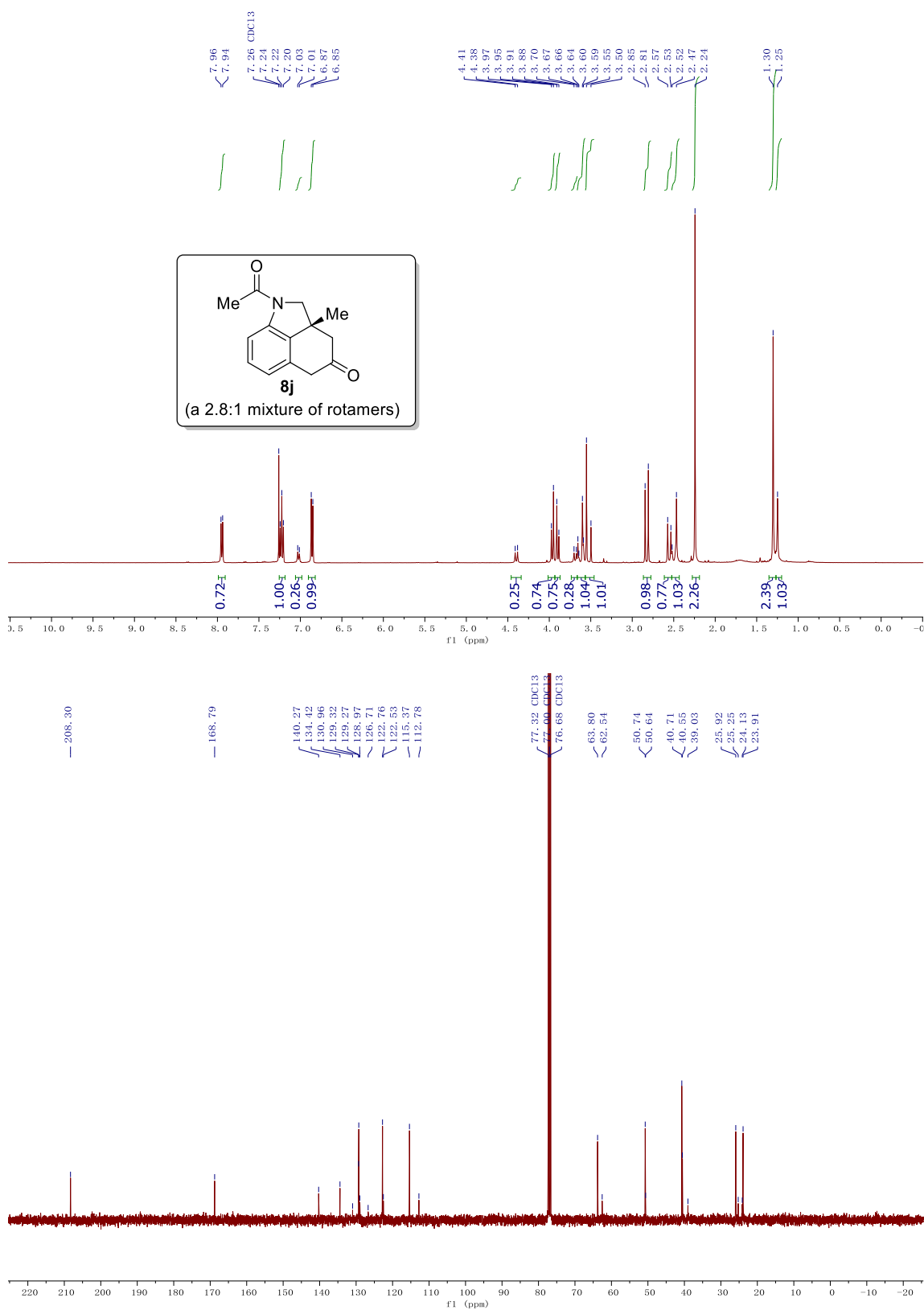


**Figure 3.29**  $^1\text{H}$  and  $^{13}\text{C}$  NMR spectrum of compound **8k**

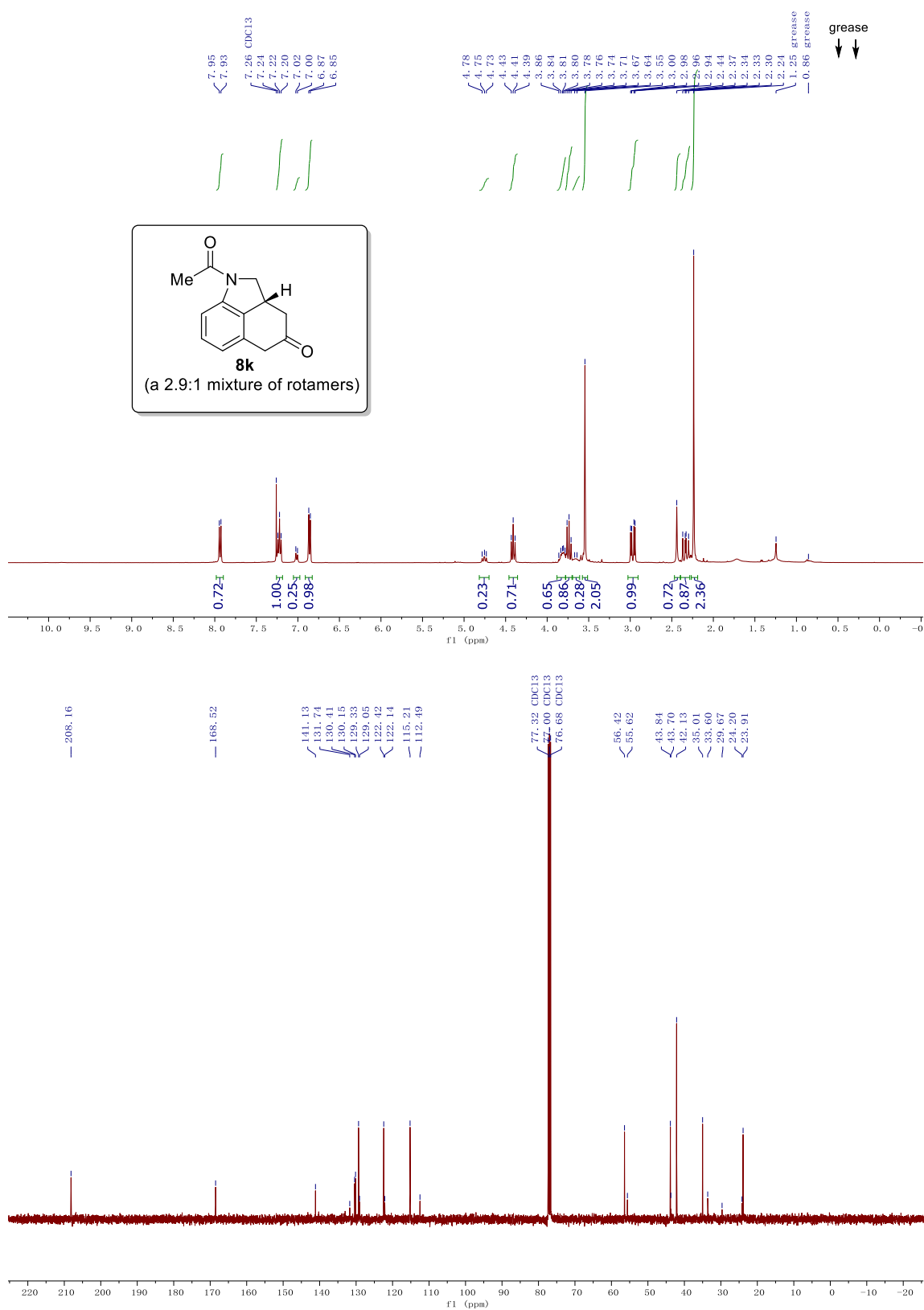


**Figure 3.30**  $^1\text{H}$  and  $^{13}\text{C}$  NMR spectrum of compound **8I**

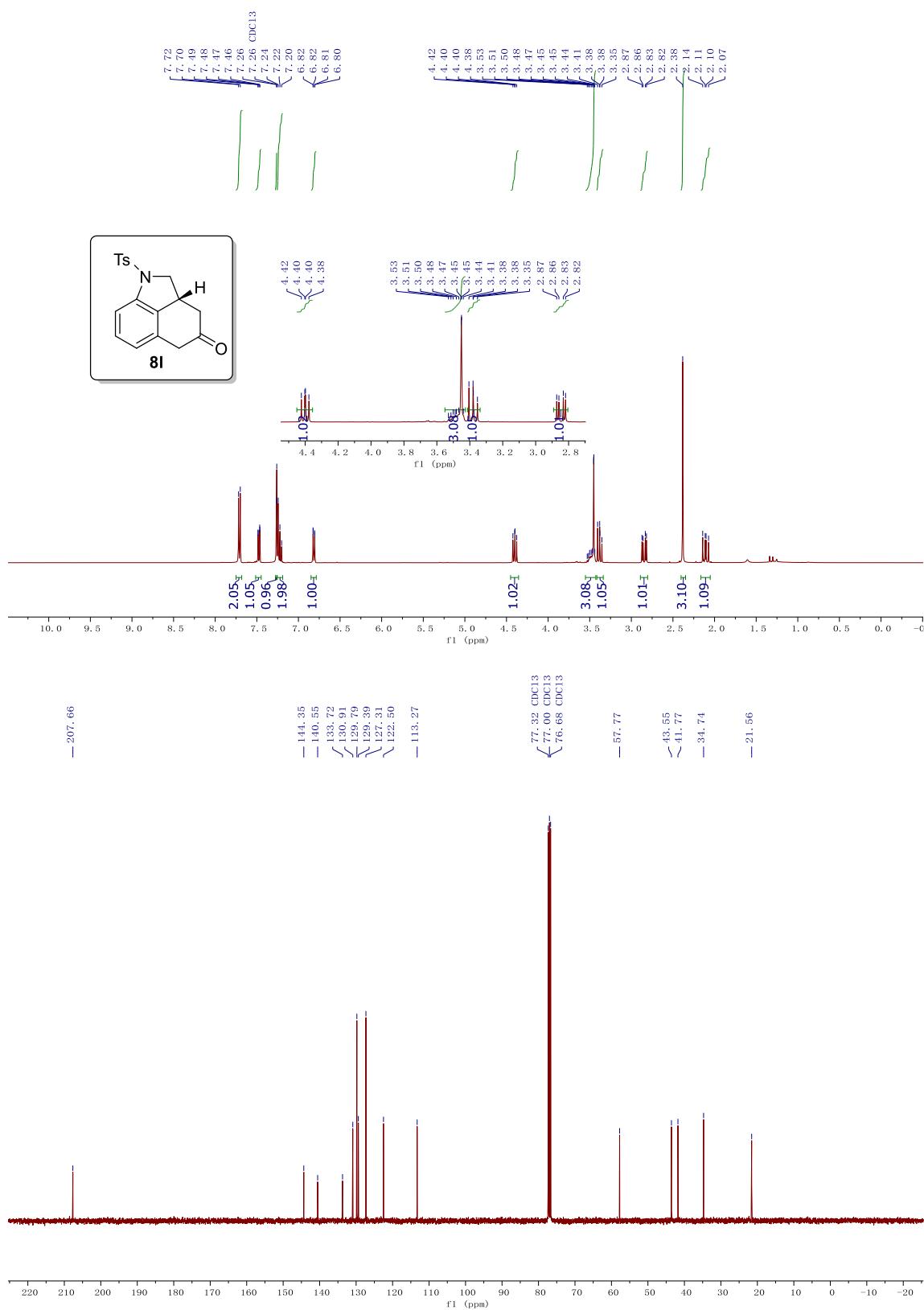


**Figure 3.31**  $^1\text{H}$  and  $^{13}\text{C}$  NMR spectrum of compound **8m**

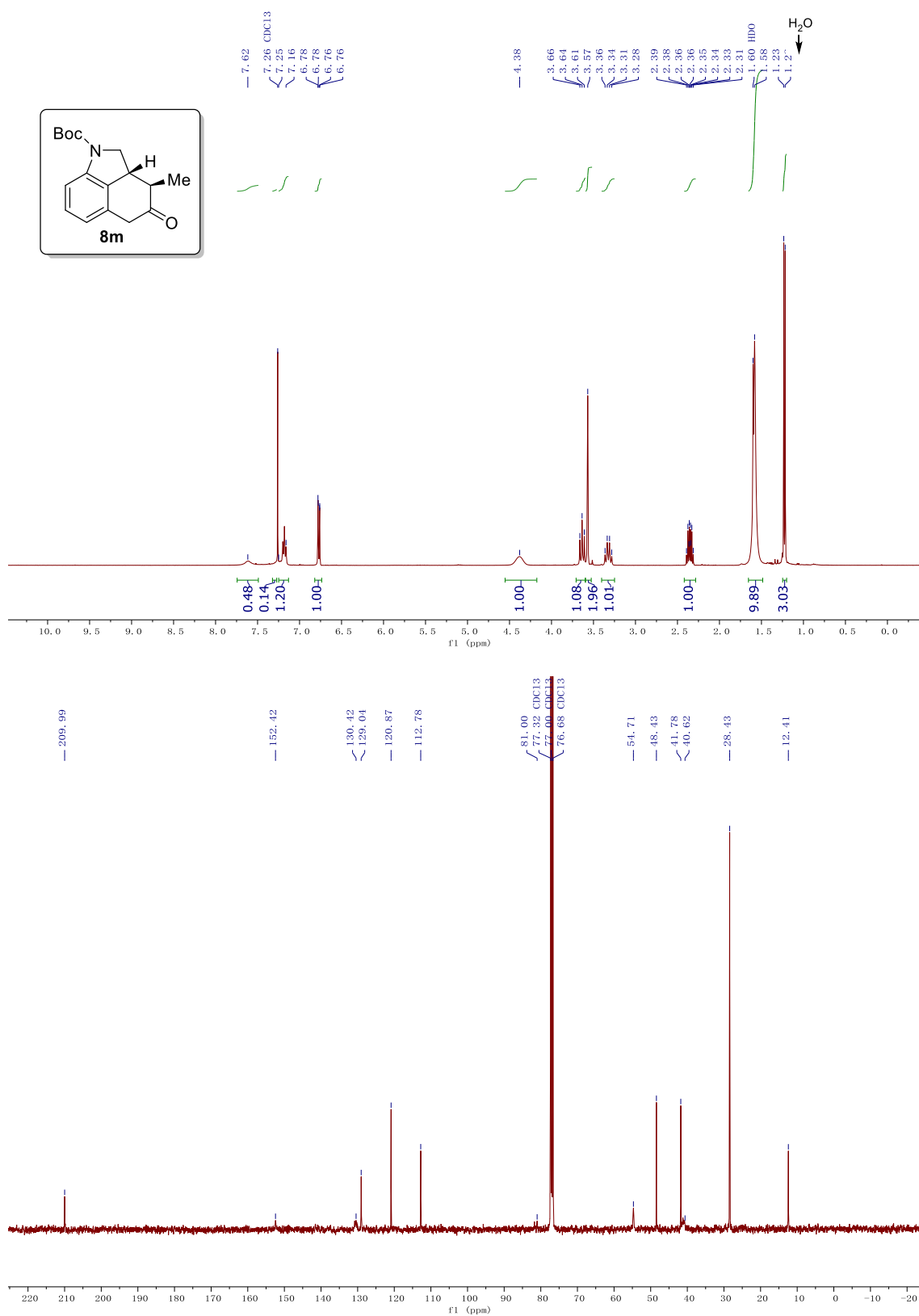


**Figure 3.32**  $^1\text{H}$  and  $^{13}\text{C}$  NMR spectrum of compound **8n**

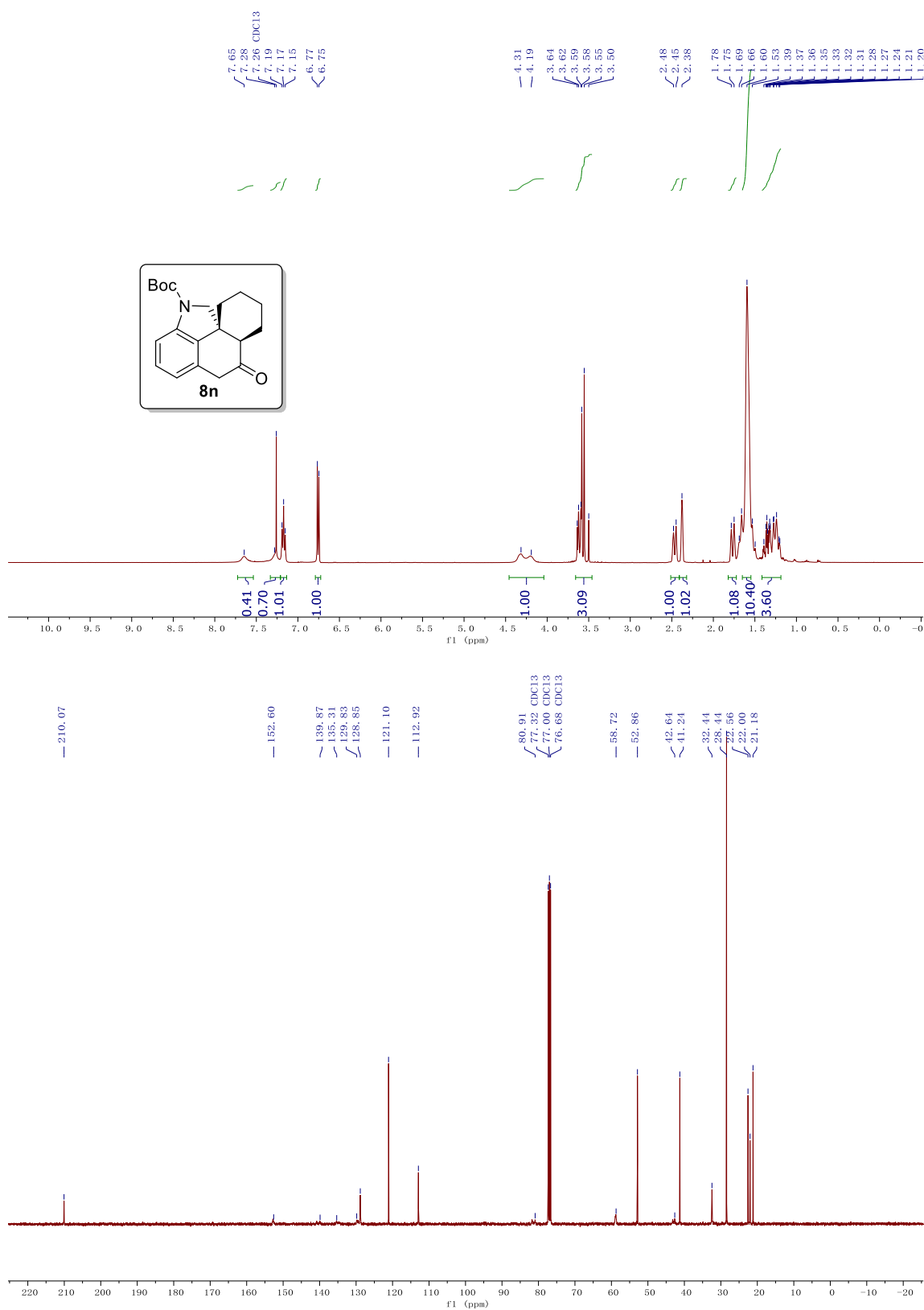


**Figure 3.33**  $^1\text{H}$  and  $^{13}\text{C}$  NMR spectrum of compound **3**

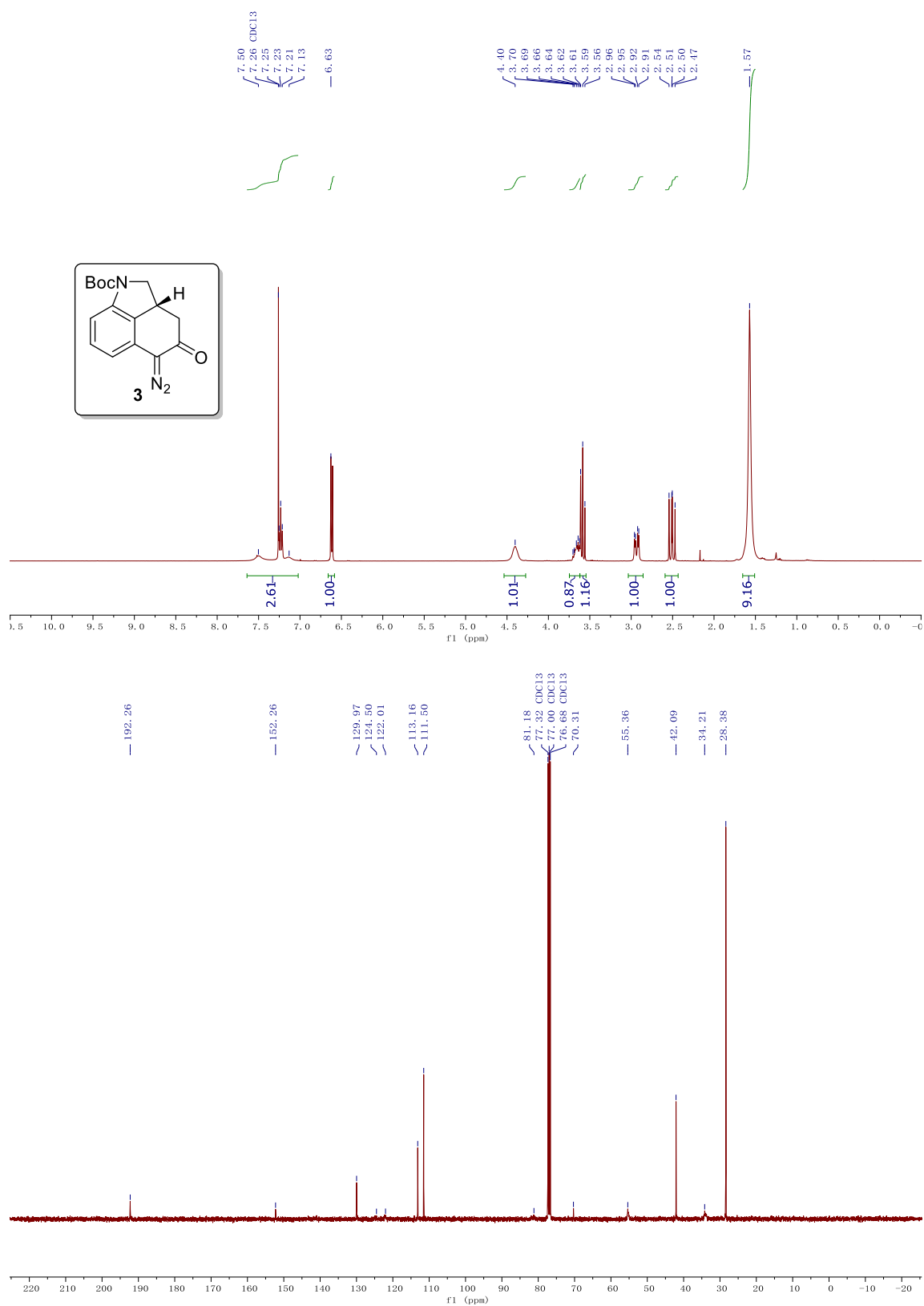


**Figure 3.34**  $^1\text{H}$  and  $^{13}\text{C}$  NMR spectrum of compound **9b** (major)

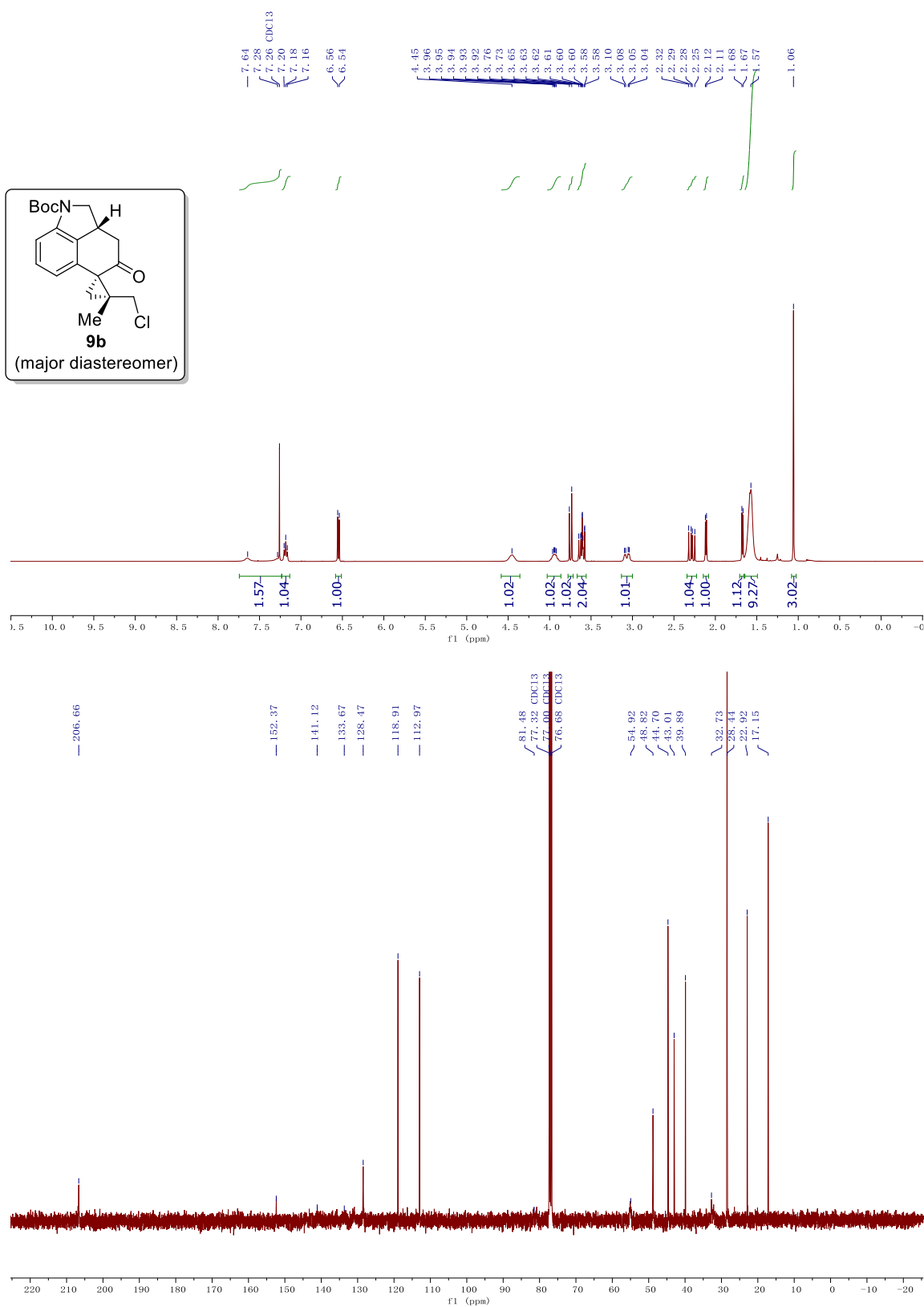




**Figure 3.35**  $^1\text{H}$  and  $^{13}\text{C}$  NMR spectrum of compound **9b** (minor)

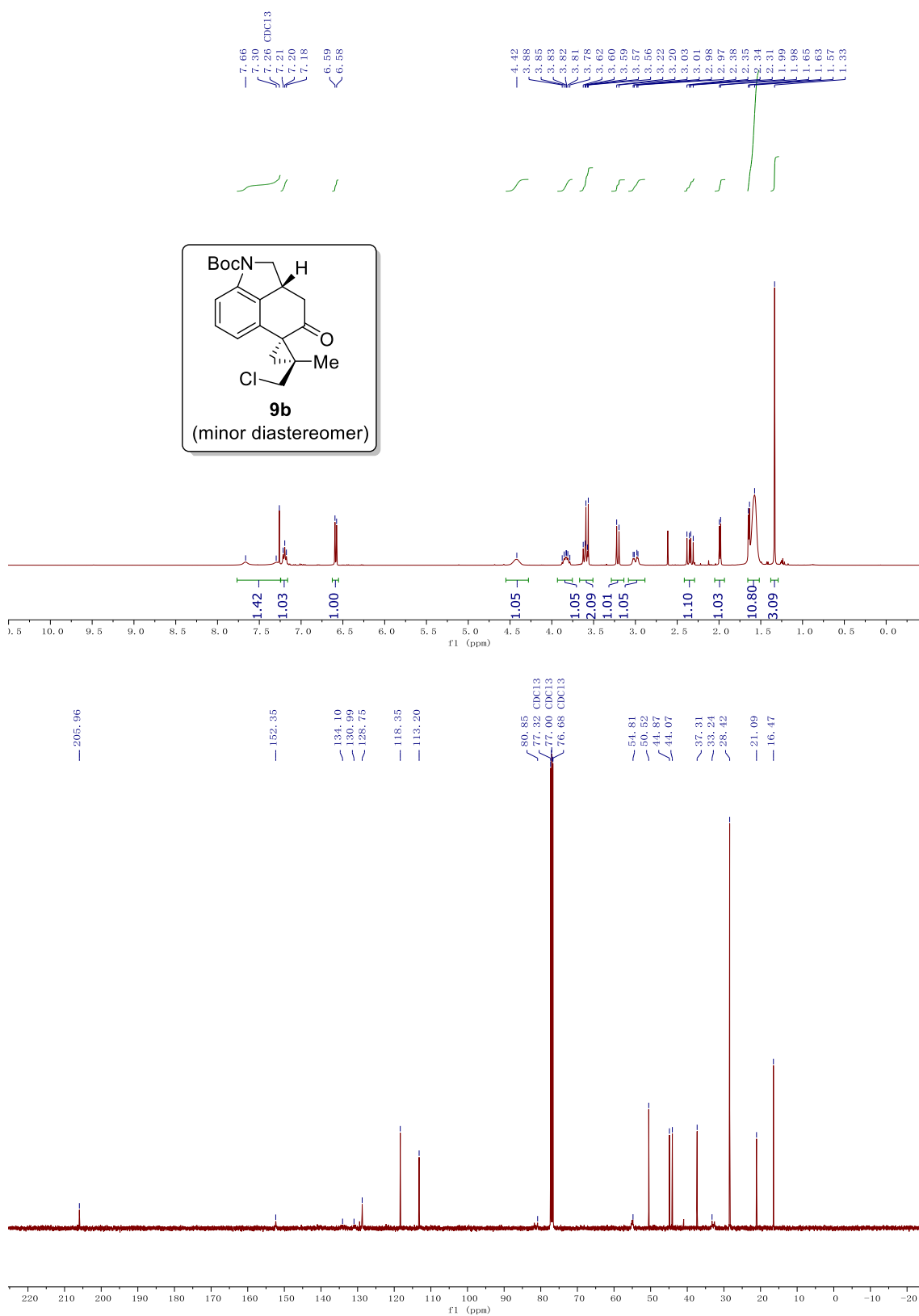


**Figure 3.36**  $^1\text{H}$  and  $^{13}\text{C}$  NMR spectrum of compound **10**

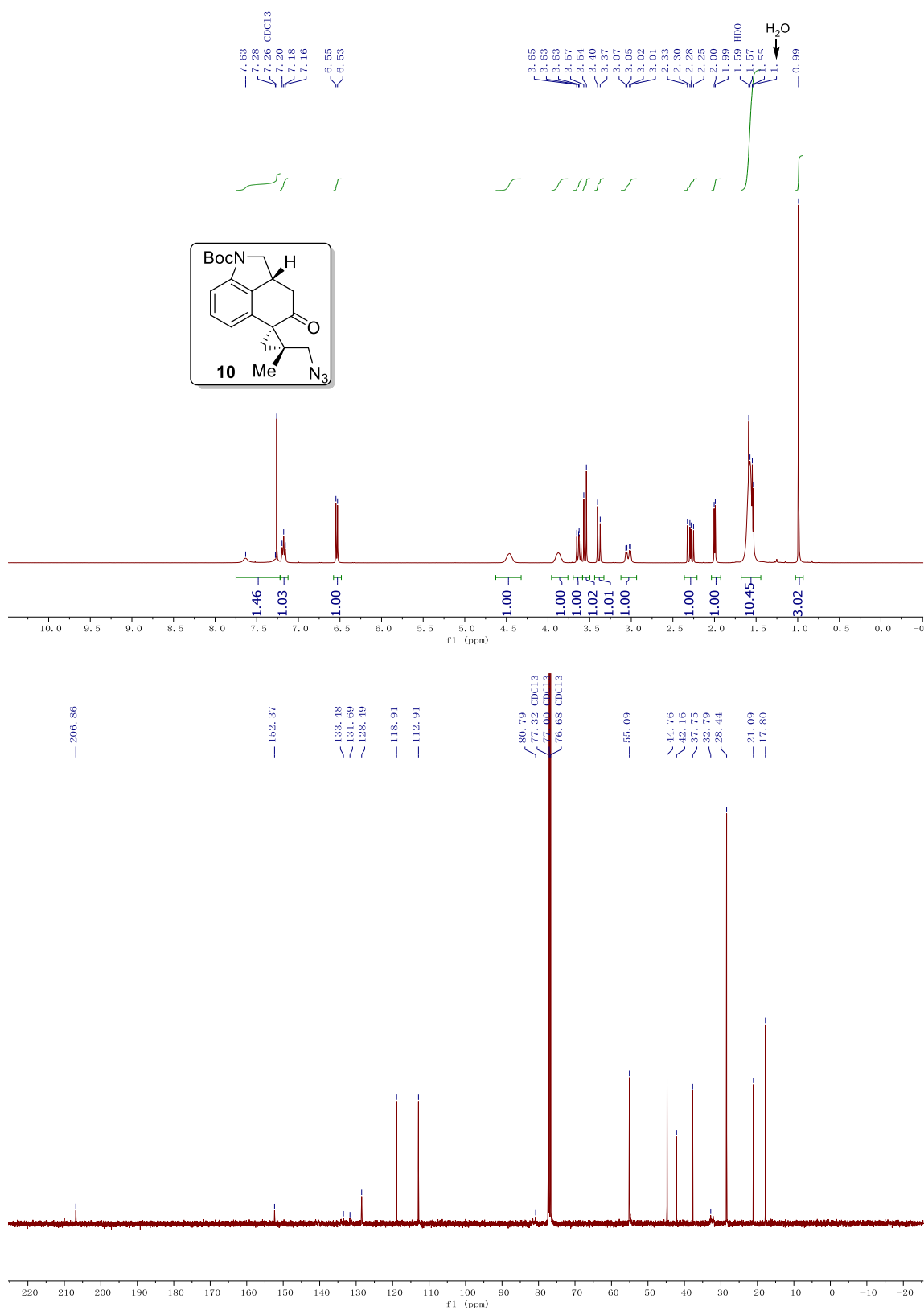


**Figure 3.37**  $^1\text{H}$  and  $^{13}\text{C}$  NMR spectrum of compound **2**

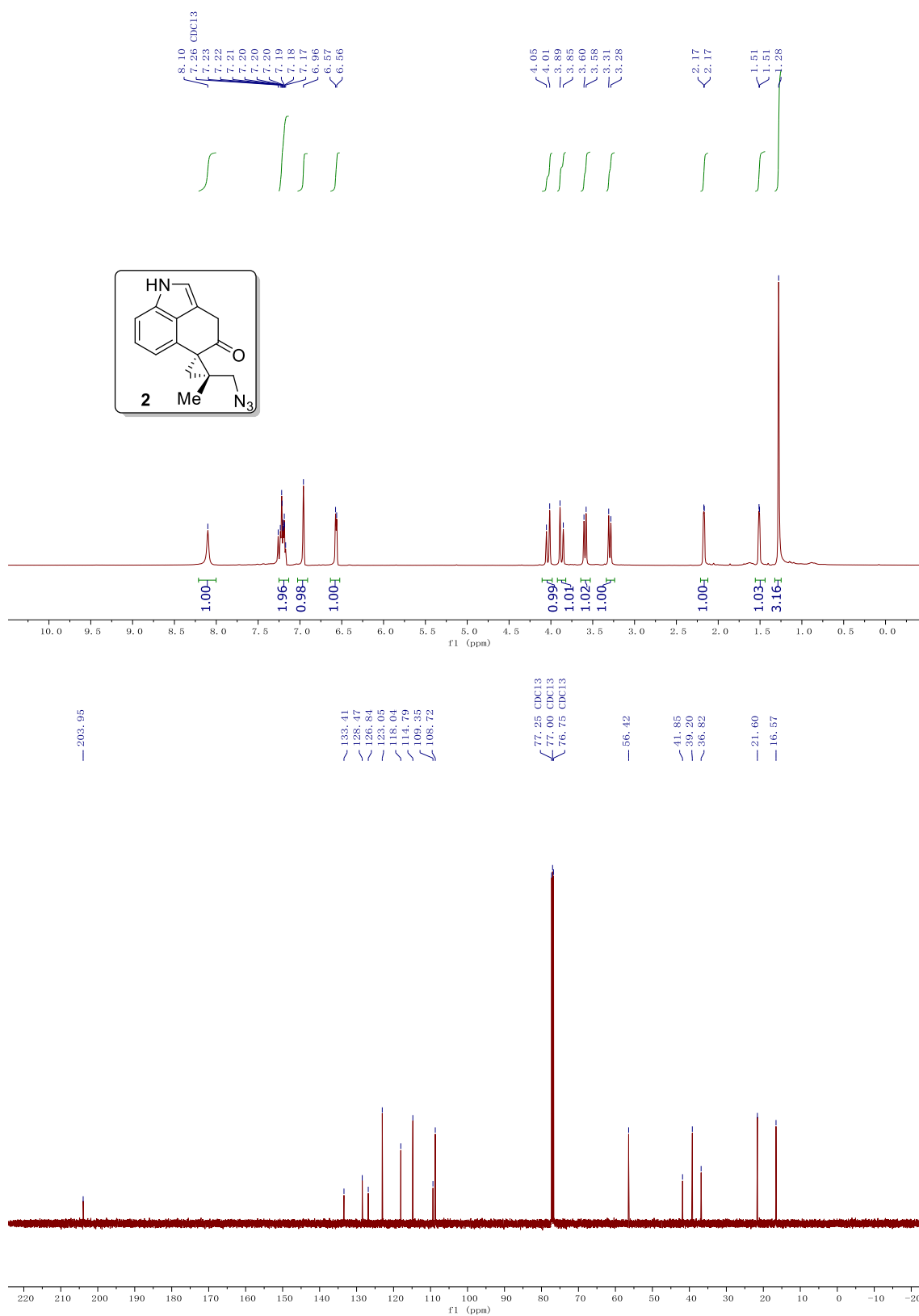


**Figure 3.38**  $^1\text{H}$  and  $^{13}\text{C}$  NMR spectrum of compound **1**

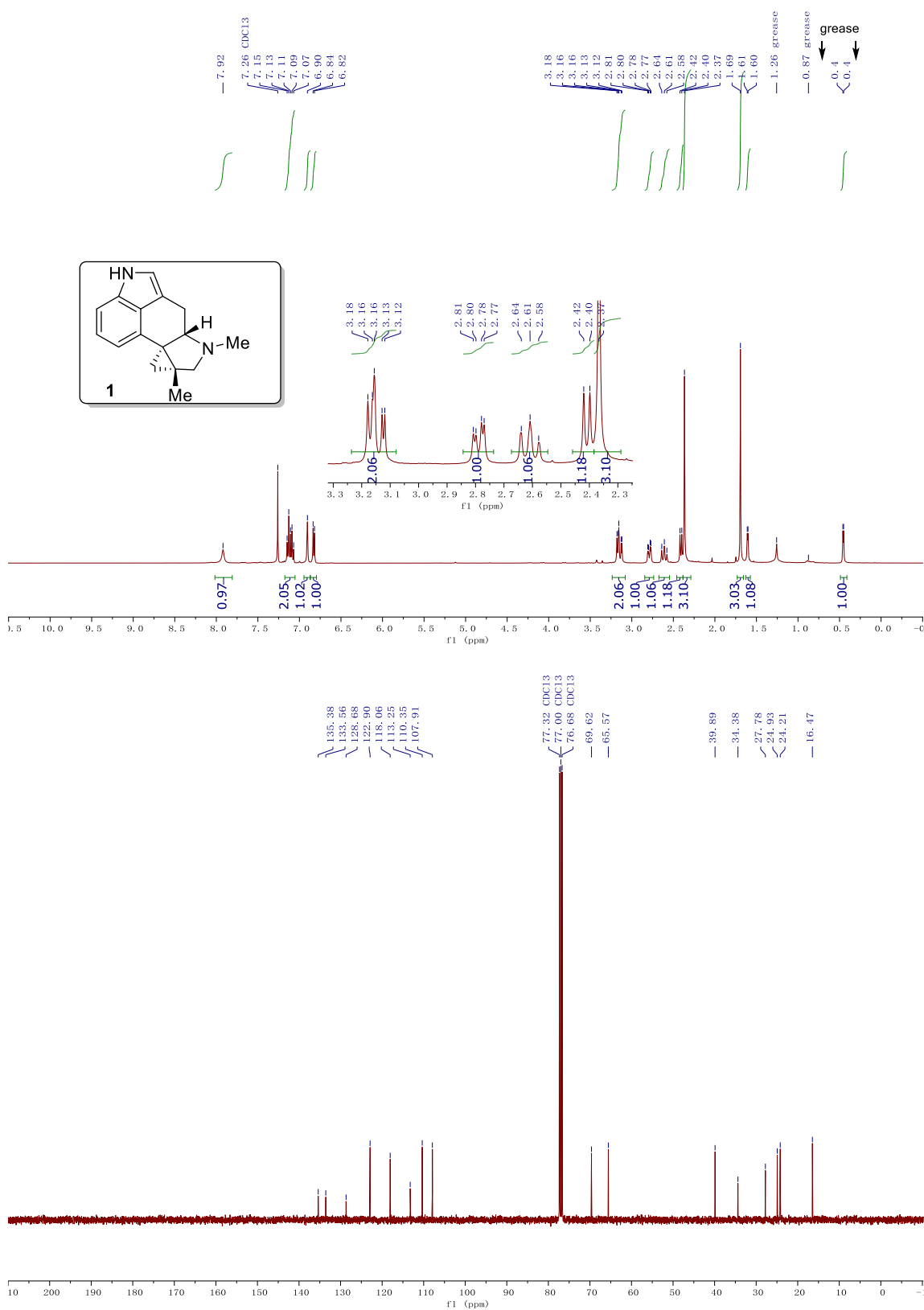


**Figure 3.39**  $^1\text{H}$  and  $^{13}\text{C}$  NMR spectrum of compound **11**

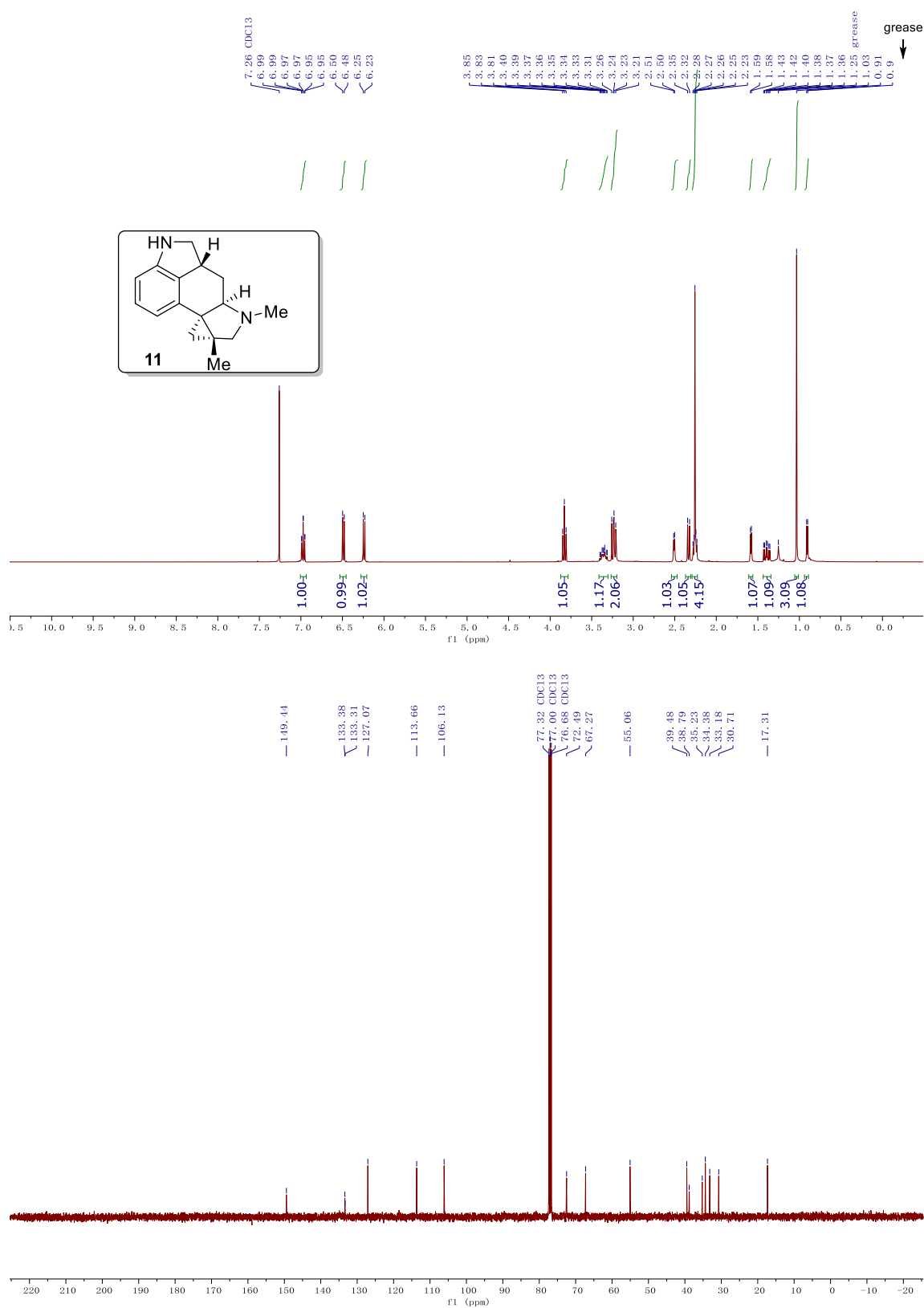


**Figure 3.40**  $^1\text{H}$  (in  $\text{CDCl}_3$  and  $\text{CD}_2\text{Cl}_2$ ) and  $^{13}\text{C}$  NMR spectrum of compound **12**

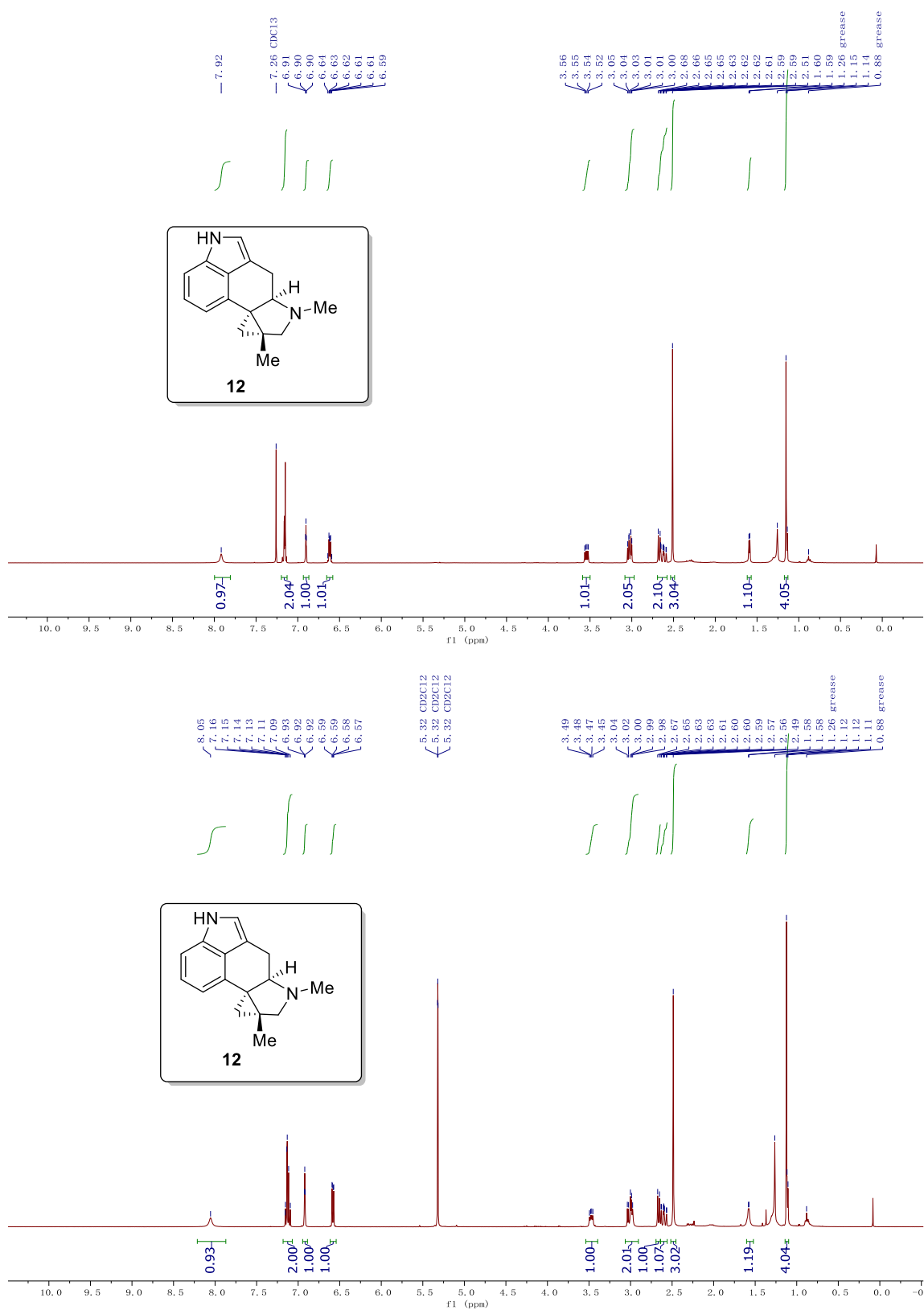
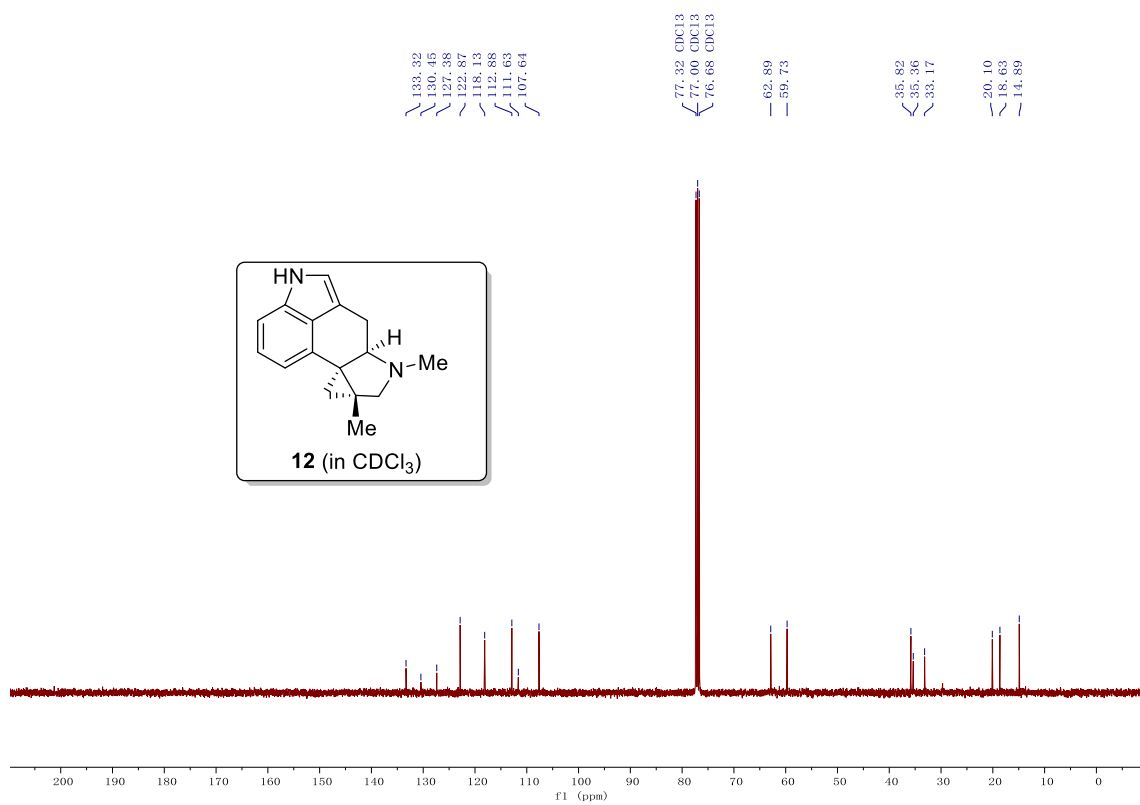


**Figure 3.40** Continued  $^1\text{H}$  (in  $\text{CDCl}_3$  and  $\text{CD}_2\text{Cl}_2$ ) and  $^{13}\text{C}$  NMR spectrum of compound **12**



## CHAPTER 4

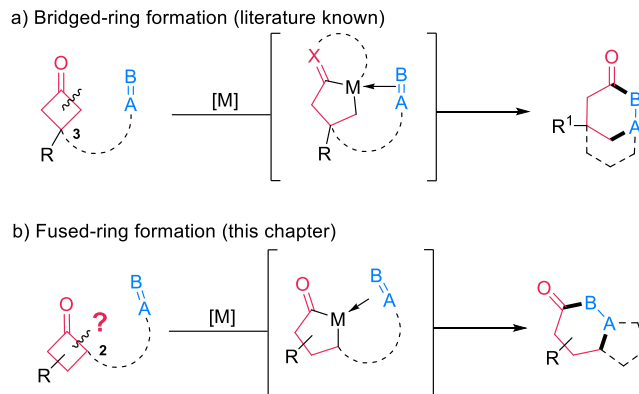
### Fused-Ring Formation via an Intramolecular “Cut-and-Sew” Reaction between Cyclobutanones and Alkynes

#### 4.1 Introduction

Among various endeavor in transition metal (TM)-catalyzed carbon–carbon bond (C–C) activation, people have explored different activation strategies to develop intriguing transformations.<sup>1</sup> In particular, oxidative addition of TM into C–C  $\sigma$  bonds followed by  $2\pi$ -insertion, namely a “cut-and-sew” process, has been demonstrated to be effective for construction of complex ring scaffolds.<sup>1r</sup> Apart from the benzocyclobutenones discussed in previous chapters, cyclobutanone derivatives are of special interest for this type of transformations due to their easy access and high reactivity towards C–C activation.<sup>1i,1n,1o,1q,1r</sup> To date, significant progress has been achieved for construction of bridged rings via intramolecular “cut-and-sew” reactions, in which cyclobutanones are coupled with an unsaturated unit tethered at the C3 position (Scheme 4.1a).<sup>2</sup> However, using such a strategy to synthesize fused-ring systems remains an unmet challenge (Scheme 4.1b).<sup>3</sup>

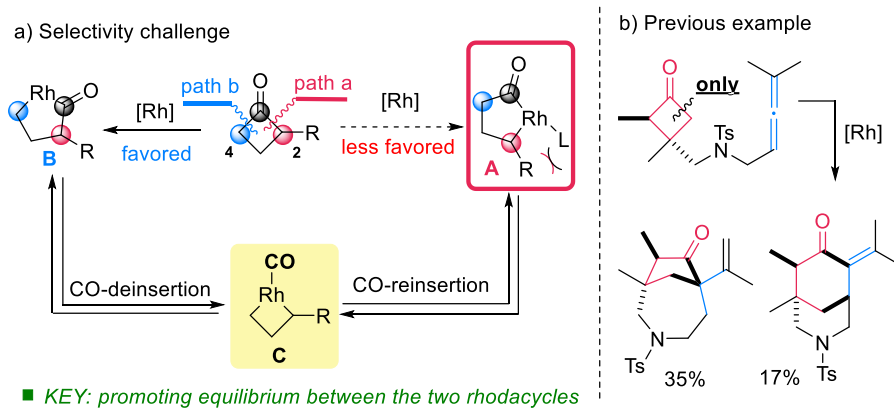


### Scheme 4.1 “Cut and Sew” Reactions with Cyclobutanones



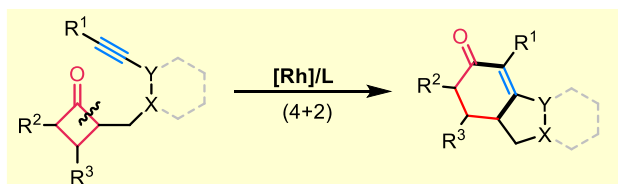
One main difficulty associated with fused-ring formation arises from the need for C–C cleavage/coupling at the more hindered C2 (proximal) position (Scheme 4.2a), as the selectivity typically favors the less hindered C4 (distal) position (Scheme 4.2b).<sup>2g</sup> In addition, decarbonylation of cyclobutanones is always a competing reaction pathway.<sup>2a,2g,2h</sup> As illustrated in Scheme 4.2a, to obtain rhodacycle **A**, which is the reactive intermediate for subsequent  $2\pi$ -insertion, *the key* would be to promote equilibrium between the two rhodacycles (**A** and **B**). Learned from our prior work on benzocyclobutenone activation, one solution is to enable a facile and reversible decarbonylation/CO-reinsertion<sup>4</sup>, in which rhodacyclopentanone **B** can be converted first to a rhodacyclobutane intermediate **C** and then to **A** via CO-reinsertion.

### Scheme 4.2 Challenge for Fused Ring Formation



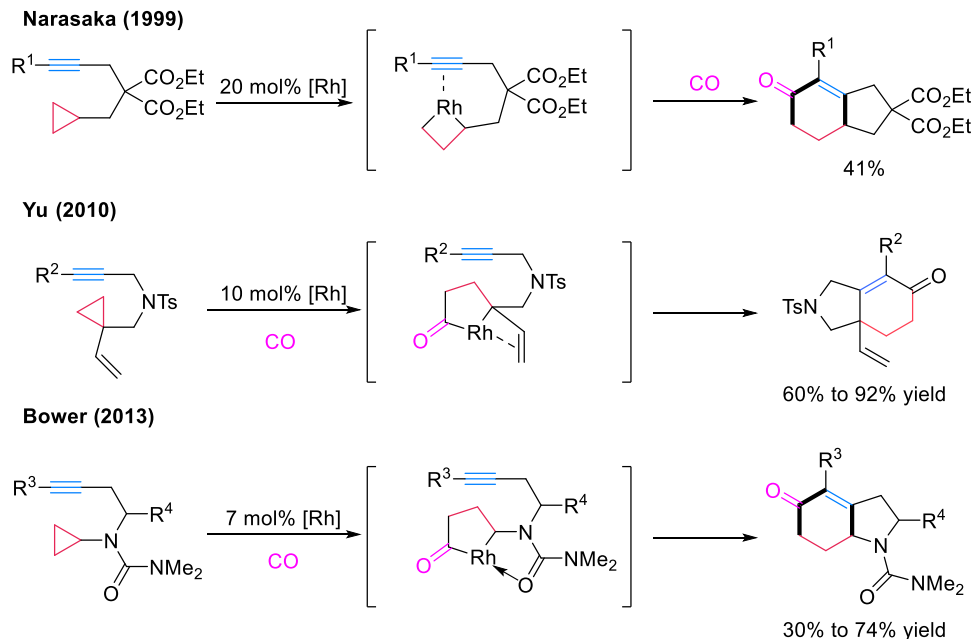
We anticipate that the choice of the ligand would be critical for this transformation, because it should promote decarbonylation/reinsertion rather than further reductive elimination of C to give cyclopropane, which represents a major difference from the benzocyclobutenone system.<sup>5</sup> In this chapter, we will discuss our development of an effective catalytic system for fused-ring formation via an intramolecular “cut and sew” reaction between cyclobutanones and alkynes (Scheme 4.3).<sup>6</sup> The transformation is enabled by use of an electron-rich, less bulky phosphine ligand, offering a rapid access to cyclohexenone-fused rings.

**Scheme 4.3** “Cut-and-Sew” with Cyclobutanones to Form Fused Rings



It should be noted that similar structures could also be obtained through a (3+2+1) cycloaddition reactions among cyclopropanes, CO and alkynes.<sup>4e,7</sup> The coupling of simple cyclopropanes, CO and alkynes was first reported by Narasaka,<sup>8</sup> albeit with a low catalyst turnover and limited substrate scope (Scheme 4.4). Use of more reactive vinyl cyclopropanes and cyclopropanes with a directing group were recently developed by Yu<sup>9</sup> and Bower<sup>10</sup> respectively, both of which exhibit excellent reactivity and selectivity (Scheme 4.4). Hence, methods that directly activate simple cyclobutanones should offer a complementary approach to the prior (3+2+1) reactions without the external CO gas or auxiliary DGs (Scheme 4.3).

## Scheme 4.4 Precedents of Cyclohexenone-Fused Ring Formation via C–C Activation



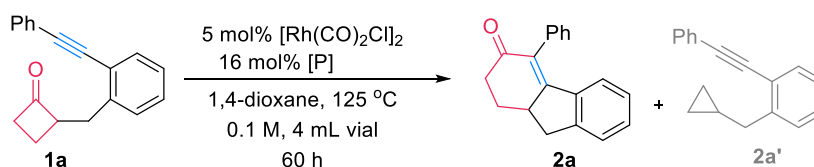
## 4.2 Results and Discussion

### 4.2.1 Condition optimization for “cut-and-sew” reactions between cyclobutanones and alkynes

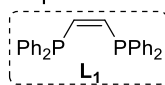
To explore the proposed “cut-and-sew” reaction, cyclobutanone **1a** was employed as the initial substrate, and the ligand effect was examined first using  $[\text{Rh}(\text{CO})_2\text{Cl}]_2$  as the pre-catalyst (Table 4.1). According to aforementioned challenges, we proposed that ligand is crucial for this transformation. First, we tested the monodentate phosphine ligands with differed electronic and steric properties (Table 4.1, entries 1-11). A range of them was found effective, and generally, higher conversion was obtained with more electron-rich ligands. For alkyl substituted phosphine ligands (Table 4.1, entries 1-4), the product **2a** was observed in all cases.  $\text{PMe}_3$  and  $\text{P}(t\text{-Bu})_3$ , which varies significantly in steric properties, gave better yields, which can be explained by that  $\text{PMe}_3$  promoted the oxidative addition step while  $\text{P}(t\text{-Bu})_3$  promoted the reductive elimination step. As the ligand became less electron-rich and more bulky from  $\text{PMe}_2\text{Ph}$  to  $\text{PPh}_3$ , the yield of **2a** decreased continuously (Table 4.1, entries 5-7) and  $\text{PMe}_2\text{Ph}$  gave the optimal yield of 82%, as well

as the conversion. Varying the electronic property of the aryl substituted phosphine ligands gave comparable yields with trialkylphosphines and there is no clear relation between the electronic property and reactivity (Table 4.1, entries 7-11). Phosphite ligands cannot yield any product (Table 4.1, entries 12 and 13). Bidentate ligands were able to facilitate this transformation, albeit with lower yield compared with  $\text{PMe}_2\text{Ph}$  (Table 4.1, entries 14-19).

**Table 4.1** Selected Ligand Screening



Entry	Ligands	Yield ( <b>2a</b> : <b>1a</b> : <b>2a'</b> )
1 <sup>a</sup>	$\text{PMe}_3$	57%: trace: 10%
2 <sup>a</sup>	$\text{PCy}_3$	37%: 23%: 18%
3 <sup>a</sup>	$\text{PBu}_3$	39%: 6%: 15%
4 <sup>a</sup>	$\text{P}(t\text{-Bu})_3$	65%: trace: 16%
5 <sup>a</sup>	<b><math>\text{PMe}_2\text{Ph}</math></b>	<b>82%: trace: 13%</b>
6 <sup>a</sup>	$\text{PMePh}_2$	50%: 22%: 8%
7 <sup>a</sup>	$\text{PPh}_3$	35%: 50%: 12%
8 <sup>a</sup>	$\text{P}(\text{tol})_3$	47%: 12%: 19%
9 <sup>a</sup>	$\text{P}(4\text{-FPh})_3$	64%: 16%: 22%
10 <sup>a</sup>	$\text{P}(4\text{-MeOPh})_3$	53%: trace: 17%
11 <sup>a</sup>	$\text{P}(3,5\text{-CF}_3\text{C}_6\text{H}_3)_3$	50%: 25%: 10%
12 <sup>b</sup>	$\text{P}(\text{OMe})_3$	0%: 0%: 0%
13 <sup>b</sup>	$\text{P}(\text{OPh})_3$	0%: 70%: trace
14 <sup>a</sup>	dppb	45%: 40%: 9%
15 <sup>a</sup>	dppe	67%: 8%: trace
16 <sup>b</sup>	dppbz	9%: 77%: 10%
17 <sup>b</sup>	binap	48%: 33%: trace
18 <sup>b</sup>	biphep	31%: 52%: trace
19 <sup>b</sup>	<b><math>\text{L}_1</math></b>	17%: 70%: trace



<sup>a</sup> Isolated yield. <sup>b</sup> NMR yield using mesitylene as internal standard

Surprisingly, one important factor was the ligand/metal ratio, with 1.6:1 being optimal (Table 4.2). When less ligand was employed ( $\text{P/Rh}=1:1$ ), the reaction still gave a complete conversion albeit with more cyclopropane side product **2a'** (Table 4.2, entry 1); however, increasing the  $\text{P/Rh}$  ratio to 2:1 completely shut down the reactivity (Table 4.2, entry 8), which

could be attributed to the generation of inactive *trans*-Rh(CO)(L)<sub>2</sub>Cl species. We reason that the active catalytic species likely contains only one phosphine ligand, but it is relatively unstable in the absence of extra PMe<sub>2</sub>Ph. This rationale was further confirmed by our mechanistic study which would be discussed later.

**Table 4.2** Screening of the [Rh]/P Ratio<sup>a</sup>

Reaction scheme: 1a (cyclobutanone with a phenyl group and a propargyl group) reacts with 5 mol% [Rh(CO)<sub>2</sub>Cl]<sub>2</sub> and y mol% PMe<sub>2</sub>Ph in 1,4-dioxane at 125 °C for 60 h to yield 2a (a bicyclic ketone) and 2a' (a cyclopropyl-substituted benzene derivative).

Entry	y	Yield (2a: 1a: 2a')
1	10 mol%	64%: trace: 24%
2	13 mol%	71%: trace: 20%
3	14 mol%	73%: trace: 20%
4	15 mol%	76%: trace: 18%
5	16 mol%	82%: trace: 13%
6	17 mol%	77%: 5%: 15%
7	18 mol%	53%: 30%: 8%
8	20 mol%	trace: 92%: trace

<sup>a</sup> All the yields are NMR yield using mesitylene as internal standard

In addition, use of the more  $\pi$ -acidic [Rh(CO)<sub>2</sub>Cl]<sub>2</sub> as a precatalyst is also crucial to generate the active species; in contrast, use of more electron-rich Rh-olefin complexes gave almost no conversions of cyclobutanone **1a** (Table 4.3, entries 2 and 3). Dioxane was found to be the best solvent (Table 4.3, entries 4-5). At lower temperature, yield decreased significantly to 67% (Table 4.3, entry 6). In the absence of precatalyst or ligand, no desired product was observed (Table 4.3, entries 7 and 8). Interestingly, when we added one equivalent of 2-amino-3-methylpyridine as a cofactor, no reaction was observed (Table 4.3, entry 9).<sup>2c</sup> This result suggests that the dynamic nature of carbonyl group in cyclobutanone could be important for this transformation.

**Table 4.3** Precatalyst/solvent Screening and Control Experiments<sup>a</sup>

Standard conditions: 5 mol%  $[\text{Rh}(\text{CO})_2\text{Cl}]_2$ , 16 mol%  $\text{PMe}_2\text{Ph}$ , 1,4-dioxane, 125 °C, 0.1 M, 4 mL vial, 60 h.

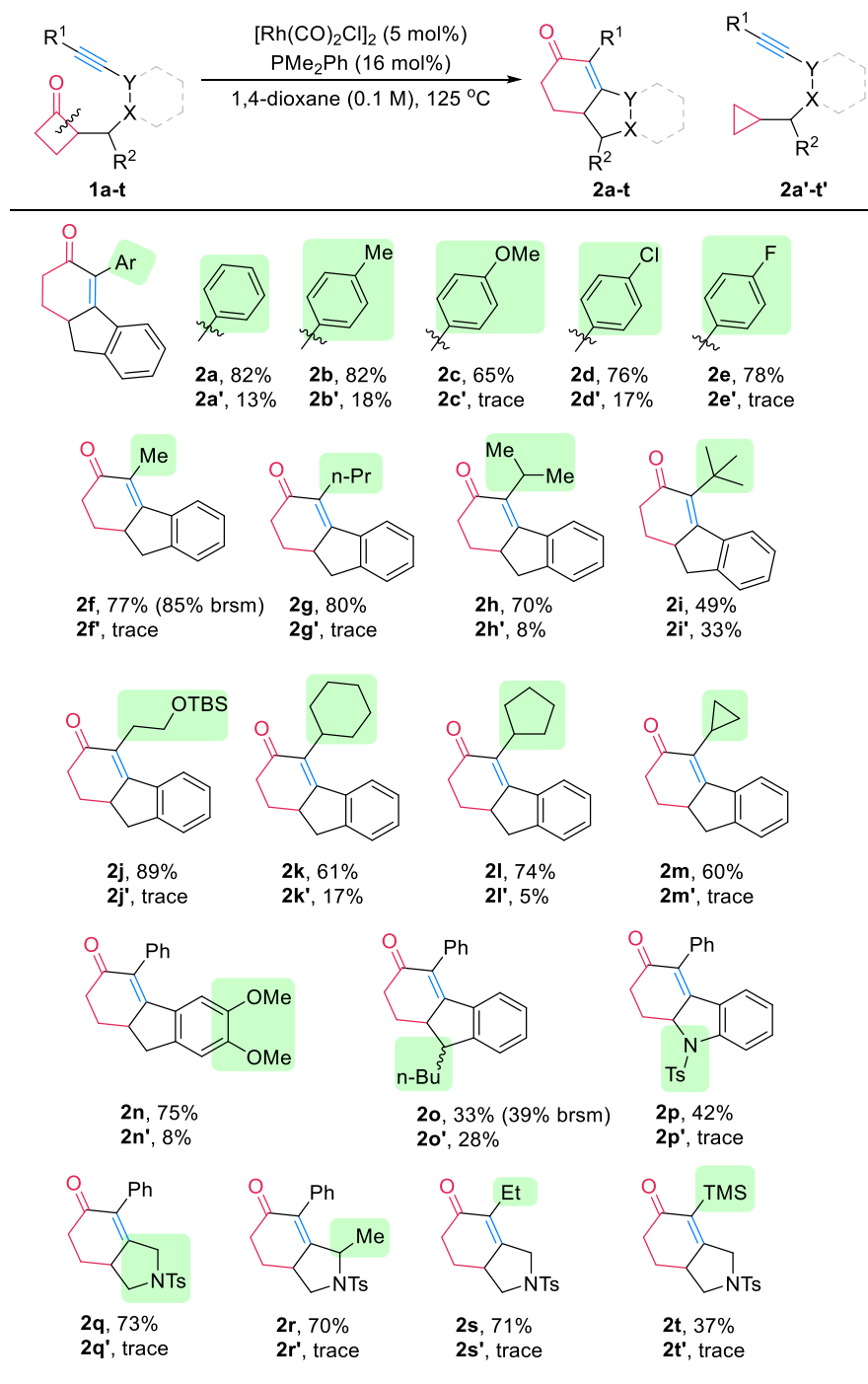
Entry	Variations from standard condition	<b>2a</b> <sup>b</sup>	Conversion <sup>b</sup>	<b>2a'</b> <sup>b</sup>
<b>1</b>	<b>none</b>	<b>82%</b>	>95%	13%
2 <sup>c</sup>	$[\text{Rh}(\text{C}_2\text{H}_4)\text{Cl}]_2$ instead of $[\text{Rh}(\text{CO})_2\text{Cl}]_2$	trace	<5%	trace
3 <sup>c</sup>	$[\text{Rh}(\text{cod})\text{Cl}]_2$ instead of $[\text{Rh}(\text{CO})_2\text{Cl}]_2$	trace	<5%	trace
4	in THF	57%	90%	11%
5	in toluene	77%	>95%	14%
6	at 115 °C	67%	>95%	18%
7 <sup>c</sup>	without $\text{PMe}_2\text{Ph}$	0%	>95%	0%
8 <sup>c</sup>	without $[\text{Rh}(\text{CO})_2\text{Cl}]_2$	0%	<5%	0%
9 <sup>c</sup>	with 100 mol% of C1	0%	<5%	0%

<sup>a</sup> Unless otherwise mentioned, the reaction was run with 10 mol % rhodium complex (based on the metal) and 16 mol % ligand (based on phosphine) on a 0.1 mmol scale at 125 °C for 60 h. <sup>b</sup> Isolated yield/conversion. <sup>c</sup> Based on crude NMR.

#### 4.2.2 Substrate scope for “cut-and-sew” reactions between cyclobutanones and alkynes

With the optimized conditions in hand, the substrate scope was next investigated (Table 4.4). First, different aryl-substituted alkynes all underwent the “cut and sew” sequence to give the corresponding tricycle products (**2a-2e**). Alkyl-substituted alkynes are also competent coupling partners; primary, secondary and tertiary alkyl substituents are all tolerated. Unsurprisingly, increasing the bulkiness on the substituent from propyl (**2g**) to isopropyl (**2h**) to *t*-butyl (**2i**) groups reduced the yield. It is noteworthy that the reaction conditions are both *pH* and *redox neutral*. The acid-labile TBS ether is compatible and 89% yield of product **2j** was isolated. In addition, cycloalkyl-substituted alkynes can be effectively coupled; the generated vinyl cyclopropane moiety (**2m**) remained intact. Moreover, substitution on the arene (**2n**) or the methylene bridge (**2o**) (between the arene and cyclobutanone) is tolerated. The reduced yield for product **2o** is due to the increasing cyclopropane formation; it is likely that the substitution hindered the migratory insertion to certain extent. Interestingly, the aniline linkage provided an indoline scaffold (**2p**).

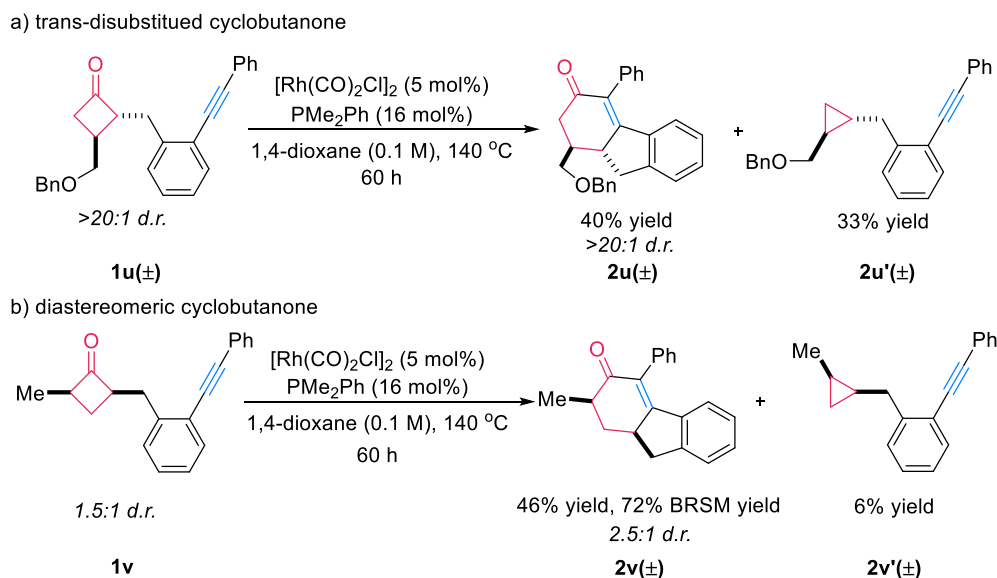
**Table 4.4 Substrate Scope<sup>a</sup>**



<sup>a</sup> all the yields of **2a-t** and **2a'-t'** are isolated yields obtained after column purification.

On the other hand, the nitrogen linker was also found efficient. With such a linker, coupling with aryl, alkyl and even silyl-substituted alkynes has been achieved, and the corresponding 6H-isoindole products (**2q-2t**) can potentially serve as valuable synthetic building blocks.<sup>10</sup>

#### Scheme 4.5 Scope for Disubstituted Cyclobutanones



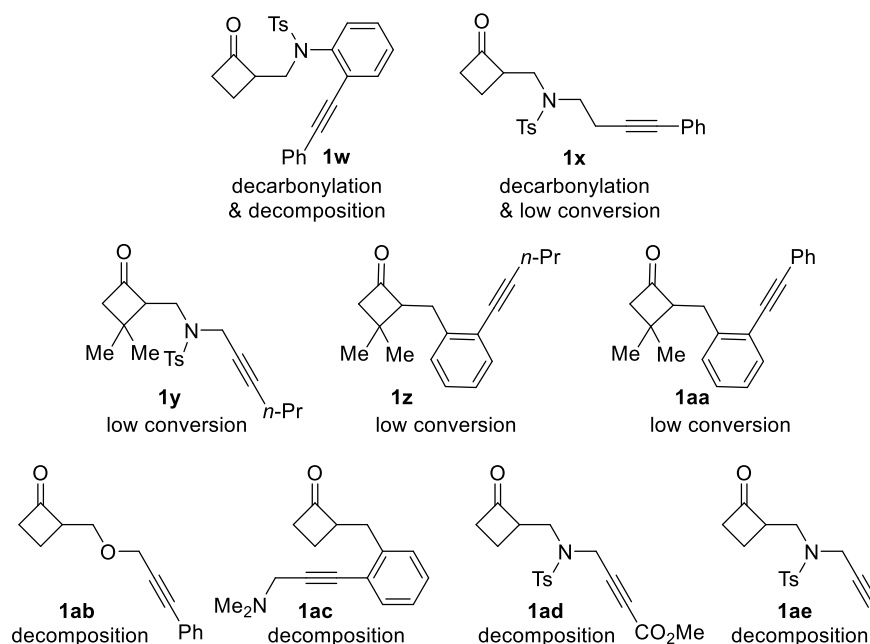
On addition, both  $\alpha$  and  $\beta$  substituted cyclobutanones can be employed albeit in moderate yields (Scheme 4.5), probably caused by the increased steric hindrance in the substrates.

Finally, there are a handful of unsuccessful substrates for this transformation under standard condition (Scheme 4.6). We screened many conditions for substrate **1w** and **1x** to generate 6,6-fused ring systems with one more carbon on the linkage. However, under those conditions, the only product we observed is the decarbonylation product **2w'** and **2x'**. The dimethyl substituents on the 3 position of cyclobutanone are not tolerated despite of different linkage and substituents on the alkyne tested, which could be attributed to the significantly increased steric bulkiness (**1y-1aa**). Oxygen linkage (**1ab**) is not viable substrate and it might be caused by the conformation flexibility of the linkage. Amine functional group (**1ac**) which can possibly coordinated to the



catalyst is not tolerated. Ester substitution on the alkyne (**1ad**) and free alkyne (**1ae**) would lead to decomposition.

**Scheme 4.6** Unsuccessful Substrates

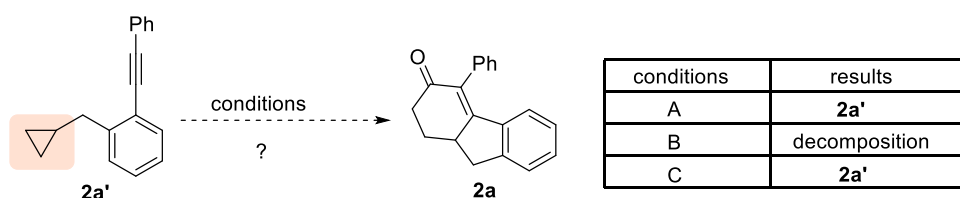


#### 4.2.3 Mechanistic study for “cut-and-sew” reactions between cyclobutanones and alkynes

With regard to the plausible reaction mechanism, there are two major questions. One is whether this (4+2) cycloaddition shares the same catalytic pathway as the (3+2+1) reaction involving cyclopropane ring opening.<sup>10</sup> The other one is whether the reaction pathway involves the cleavage of the less hindered distal C–C bond. To address the first question, control experiments with cyclopropane side product **2a'** were conducted (Scheme 4.7). Subjecting **2a'** to the standard (4+2) reaction conditions in the presence of CO gas or to the optimal conditions developed by Narasaka<sup>8</sup> or Bower<sup>10</sup> for the (3+2+1) reaction gave no desired **2a** product. This result suggests that cyclopropane formation during the (4+2) reaction is probably irreversible and **2a'** should not be an intermediate towards product formation. This observation is also consistent with the fact that coupling of unactivated cyclopropanes in the absence of DGs is rather difficult.<sup>8</sup> We then tested

the control substrate **1af** (Scheme 4.7). In the absence of alkyne group, we still observed aldehyde **1af'** as major product, which proves that alkyne did not serve as a directing group for C–C bond cleavage in our catalytic system.

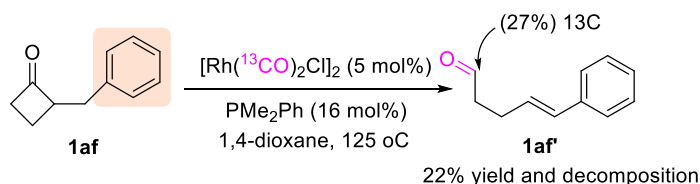
**Scheme 4.7** Control Experiments



condition A: "standard conditions" with 1 atm CO

condition B:  $[\text{Rh}(\text{CO})_2\text{Cl}]_2$ , 1,2-dichlorobenzene, 160 °C, 48 h, 1 atm CO (ref 7)

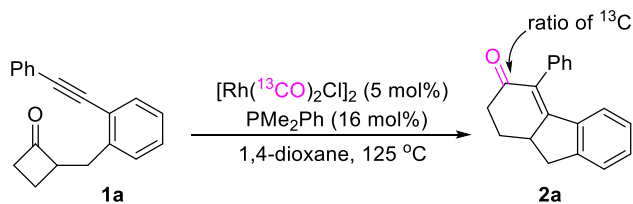
condition C:  $[\text{Rh}(\text{cod})\text{Cl}]_2$ ,  $\text{P}(\text{3,5-}\text{CF}_3\text{C}_6\text{H}_3)_3$ , PhCN,  $\text{Na}_2\text{SO}_4$ , 130 °C, 72 h, 1 atm CO (ref 9)



To explore the second question,  $^{13}\text{C}$  labeling study was conducted (Scheme 4.8). We hypothesized that, if the reaction involved cleavage of the less hindered distal C–C bond, a CO de-insertion and re-insertion into the less hindered alkyl group would have to occur (*vide supra*, Scheme 4.2). Thus, if this were the case, use of the Rh catalyst containing  $^{13}\text{CO}$  ligands would introduce  $^{13}\text{C}$ -labeled carbonyl moiety into the product. Indeed, replacement of  $[\text{Rh}(\text{CO})_2\text{Cl}]_2$  with  $[\text{Rh}(^{13}\text{CO})_2\text{Cl}]_2$  under the standard reaction conditions afforded product **2a** in 82% yield with 21%  $^{13}\text{C}$  incorporation. Give that only 5 mol%  $[\text{Rh}(^{13}\text{CO})_2\text{Cl}]_2$  was used, 86%  $^{13}\text{CO}$  from the Rh complex has been transferred into product. When we terminated the reaction at an earlier stage, there is higher  $^{13}\text{C}$  incorporation (34%) observed and no significant  $^{13}\text{C}$  incorporation was observed in starting material. We also did a series of monitoring on the  $^{13}\text{C}$  incorporation ratio at different conversion. The observation is similar to what we mentioned above, with increasing



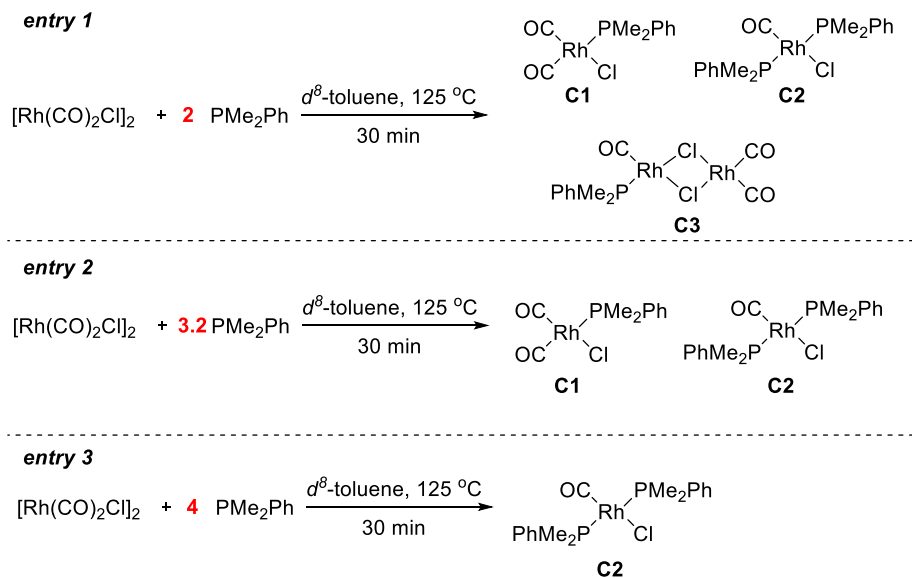
**Table 4.5** Series of  $^{13}\text{C}$  CO Exchange Experiment



conversion	10%	15%	30%	36%	52%	67%	79%	100%
yield of <b>2a</b>	9%	13%	29%	32%	46%	52%	67%	82%
$^{13}\text{C}$ incorporation	60%	53%	45%	39%	34%	28%	24%	21%

We noticed from our condition screening that the ratio between rhodium precatalyst and ligand plays an important role in this transformation. To shed some light into this observation, we want to first figure out the catalyst's resting state in this transformation at different  $[\text{Rh}]/\text{P}$  ratios (Scheme 4.9).

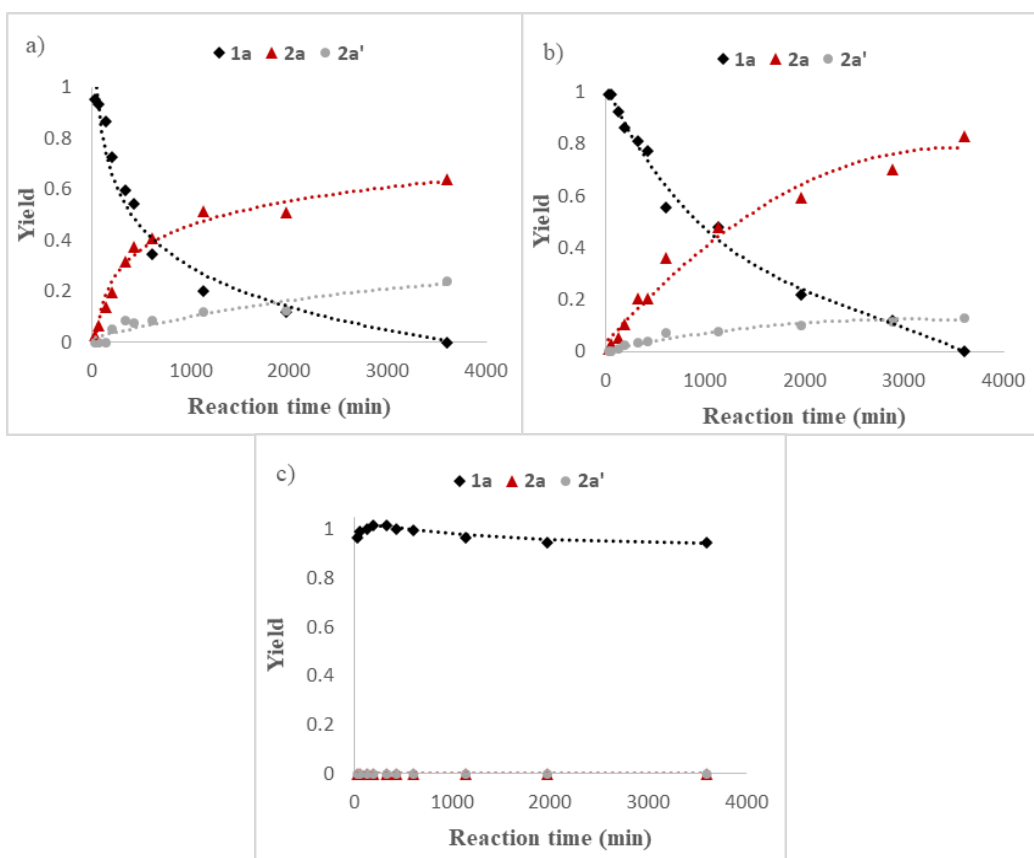
**Scheme 4.9** Resting State Study



When rhodium precatalyst and ligands were mixed in different ratios, we observed different square planar rhodium species (their structures were assigned by comparing the  $^{31}\text{P}$ -NMR with literature known spectrum)<sup>11</sup>. The mixture of entry 2 was added 3 equiv. of substrate **1a** and

kept at 125 °C for 10 h and **2a** was generated in 21% yield. The  $^{31}\text{P}$ -NMR suggested that rhodium complexes stay the same as those before the reaction. According to these results, we proposed that **C1** and **C2** are likely the resting state.

**Scheme 4.10** Kinetic Study with Different [Rh]/P Ratio



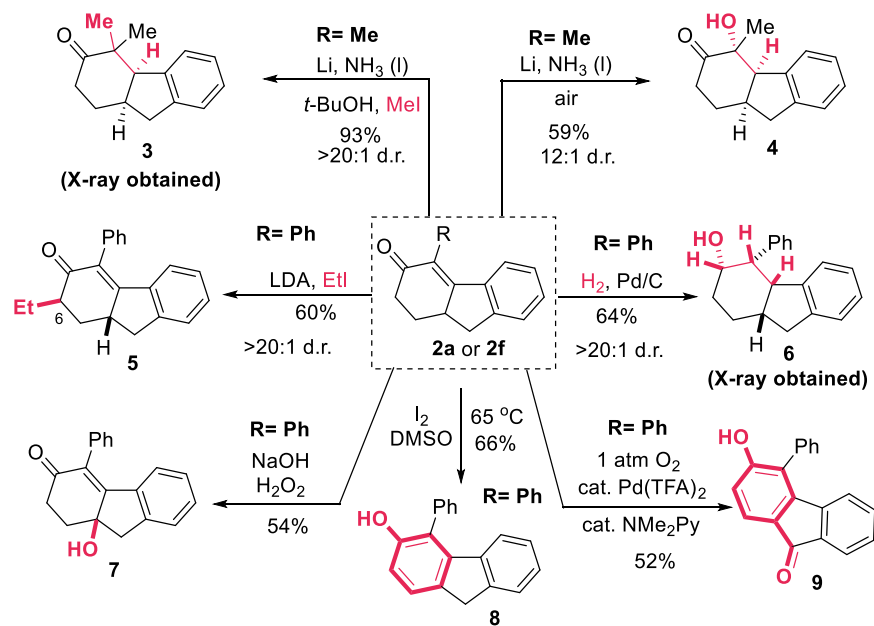
a) Rh/P=1/1. b) Rh/P=1/1.6. c) Rh/P=1/2

Following that, we did kinetic monitoring with different rhodium/phosphine ratio (Scheme 4.10). When Rh:P equals 1:1, the initial rate is significantly higher than the 1:1.6, because of higher concentration of the active catalyst. However, in this case, the catalyst died quicker than the 1:1.6 entry and led to increased yield of the **2a'** side product. When Rh:P equals 1:2, there is no **2a** or **2a'** generation, which suggests that **C2** is inactive species. From these observations, we propose **C1** to be the active catalyst for this transformation.

#### 4.2.4 Synthetic applications for “cut-and-sew” reactions between cyclobutanones and alkynes

The intriguing cyclohexanone-fused ring structures generated from this “cut-and-sew” reaction can be conveniently derivatized (Scheme 4.11). Excellent diastereoselectivity was obtained in most cases possibly driven by forming less strained 5-6 cis-fused rings. First, dissolving metal reduction, followed by alkylation or oxidation, afforded the  $\alpha$ -disubstituted cyclohexanone products **3** (X-ray structure obtained) and **4** (stereochemistry tentatively assigned), respectively.<sup>12</sup> Moreover, enolate-based alkylation occurred site- and diastereoselectively at the C6-position of the cyclohexenone moiety. Pd/C-catalyzed hydrogenation took place at the *syn* side to the methine hydrogen and directly gave the corresponding saturated alcohol. Treatment of product **2a** with base and hydrogen peroxide unexpectedly led to a  $\gamma$ -hydroxylation product (**7**).<sup>13</sup> Finally, iodine/DMSO oxidation<sup>14</sup> converted the tricycle into a functionalized fluorene, and a Pd-catalyzed aerobic oxidation<sup>15</sup> surprisingly gave 9-fluorenone **9** as the dominant product.

**Scheme 4.11** Synthetic Applications



#### 4.3 Conclusion

In summary, we have developed a novel catalyst system utilizing electron-rich phosphine with small steric hindrance, which can efficiently catalyze the C–C bond activation of cyclobutanones and enable the site-selective insertion of C≡C bond. This transformation provides the insertion product at the more hindered C–C bond and forges various fused ring scaffolds. The reaction condition is very concise, pH and redox neutral, which provides a good functional group tolerance. Through our mechanistic investigation, we found both proximal C–C bond can be readily cleaved and that led to the same intermediate through a reversible decarbonylation-reinsertion process. We foresee this discovery to open up more possibilities in diverse ring system formation through “cut-and-sew” process.

## 4.4 Experimental

### 4.4.1 General information

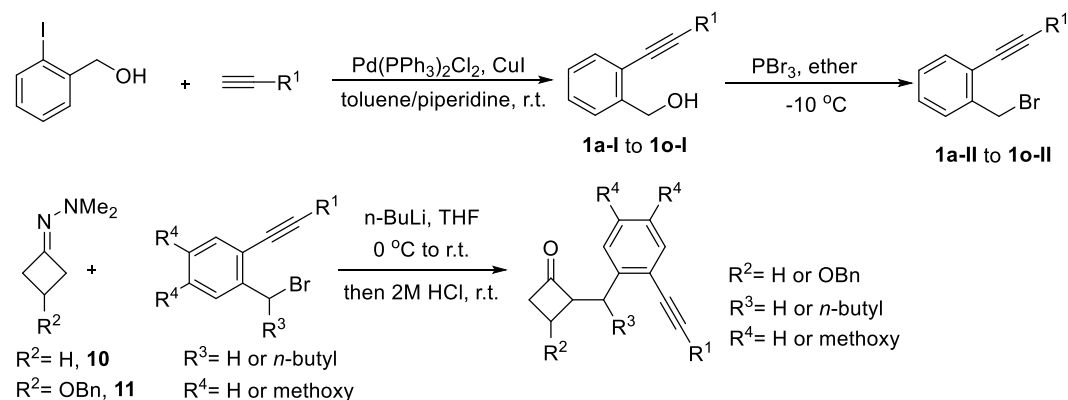
Unless noted otherwise, all solvents were dried by filtration through a Pure-Solv MD-5 Solvent Purification System (Innovative Technology). The solvents for the C–C Activation reactions were distilled freshly over sodium or calcium hydride and carefully freeze-pump-thawed. All the C–C Activation reactions were carried out under nitrogen atmosphere with a stir bar in a sealed vial. Reaction temperatures were reported as the temperatures of the bath surrounding the flasks or vials. Sensitive ligands and rhodium catalysts and solvents were transferred under nitrogen into a nitrogen-filled glovebox with standard techniques. Analytical thin-layer chromatography (TLC) was carried out using 0.2 mm commercial silica gel plates (silica gel 60, F254, EMD chemical). Vials (17 x 60 mm (7.5mL) with PTFE lined cap attached) were purchased from Qorpak and flame-dried or put in an oven overnight. High-resolution mass spectra (HRSM) were obtained on a Agilent 6224 Tof-MS and are reported as  $m/z$  (relative intensity). Accurate masses are reported for the molecular ion  $[M+Na]^+$ ,  $[M+H]^+$ . Infrared spectra were recorded on a

Nicolet 380 FTIR using neat thin film technique. Nuclear magnetic resonance spectra ( $^1\text{H}$  NMR and  $^{13}\text{C}$  NMR) were recorded with a Bruker Avance 500 instrument (500 MHz,  $^1\text{H}$  at 500 MHz,  $^{13}\text{C}$  at 126 MHz) and Bruker Avance 400 instrument (400 MHz,  $^1\text{H}$  at 400 MHz,  $^{13}\text{C}$  at 100 MHz). Unless otherwise noted, all spectra were acquired in  $\text{CDCl}_3$ . Chemical shifts are reported in parts per million (ppm,  $\delta$ ), downfield from tetramethylsilane (TMS,  $\delta=0.00\text{ppm}$ ) and are referenced to residual solvent ( $\text{CDCl}_3$ ,  $\delta=7.26$  ppm ( $^1\text{H}$ ) and 77.00 ppm ( $^{13}\text{C}$ );  $\text{CD}_2\text{Cl}_2$ ,  $\delta=5.32$  ppm ( $^1\text{H}$ ) and 53.84 ppm ( $^{13}\text{C}$ )). Coupling constants were reported in Hertz (Hz). Data for  $^1\text{H}$  NMR spectra were reported as follows: chemical shift (ppm, referenced to protium; s = singlet, d = doublet, t = triplet, q = quartet, hept=heptuplet, dd = doublet of doublets, td = triplet of doublets, ddd = doublet of doublet of doublets, m = multiplet, coupling constant (Hz), and integration).

#### 4.4.2 General information about substrate synthesis

The substrates for the C–C Activation reactions were synthesized through two different routes.

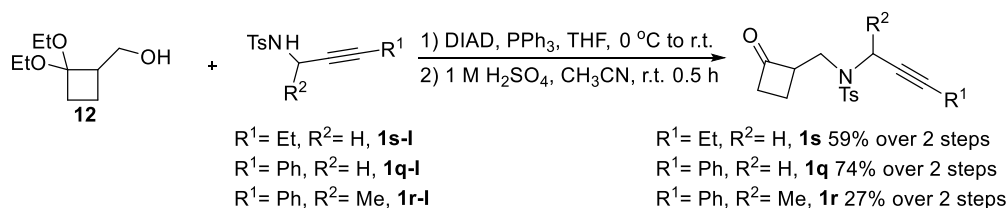
##### Synthetic route I for substrates with benzene linkage<sup>16</sup>



Substrates **1a** to **1o** and **1u** were synthesized through **Route I**.



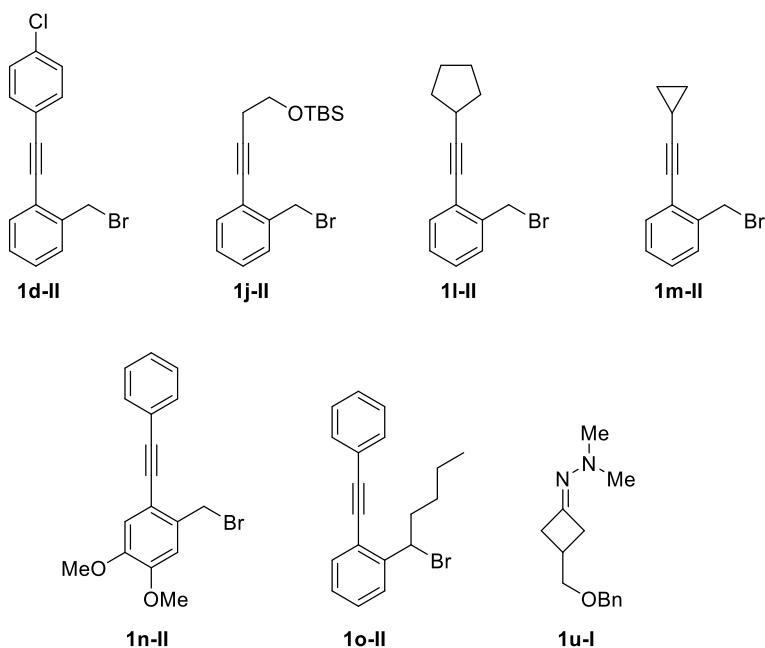
## Synthetic route II for substrates with N-Ts linkage<sup>17</sup>



Substrates **1q** to **1s** were synthesized through **route II**. **1q-I**, **1r-I** and **1s-I** are known compounds.

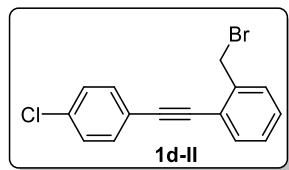
### 4.4.3 Synthesis of precursors

#### a) Synthesis of unknown precursors:

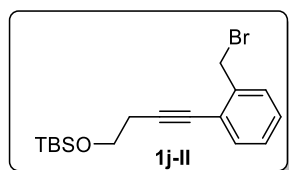


Apart from what are reported here, all other alkyl bromide precursors are known compound.<sup>18</sup> Compound **1d-II**, **1j-II**, **1l-II**, **1m-II** and **1n-II** were synthesized using the previously reported procedure as shown in route I and the alcohol precursor **1d-I**, **1j-I**, **1l-I**, **1m-I** and **1n-I** are known compounds.<sup>19</sup> Compound **1o-II** was synthesized from the corresponding alcohol **1o-I**

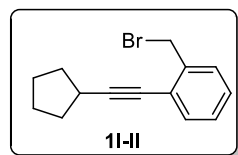
(literature known).<sup>19</sup> Because of the instability of compound **1o-II** towards column, it was subjected directly to the alkylation reaction.



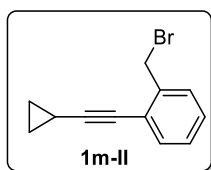
Compound **1d-II** was obtained as a white solid (M.P.: 74-75 °C) in 55% yield (1.65 g) over two steps.  $R_f = 0.8$  (EtOAc/Hexane=1/5). **<sup>1</sup>H NMR (500 MHz, CDCl<sub>3</sub>):**  $\delta$  7.56 – 7.50 (m, 3H), 7.45 (dd,  $J = 7.3, 1.6$  Hz, 1H), 7.37 – 7.28 (m, 4H), 4.72 (s, 2H). **<sup>13</sup>C NMR (126 MHz, CDCl<sub>3</sub>):**  $\delta$  139.22, 134.67, 132.81, 132.48, 129.75, 128.99, 128.80, 128.56, 122.98, 121.52, 94.06, 87.41, 31.94. **IR:**  $\nu$  3065, 3028, 1492, 1450, 1397, 1220, 1090, 1013, 949, 827, 758, 606 532, 515 cm<sup>-1</sup>; **HRMS** calcd. For [M+H]<sup>+</sup>: 304.9727. Found: 304.9707.



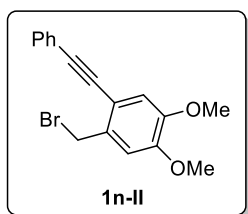
Compound **1j-II** was obtained as a colorless oil in 37% yield (1.1 g).  $R_f = 0.8$  (EtOAc/Hexane=1/5). **<sup>1</sup>H NMR (400 MHz, CDCl<sub>3</sub>):**  $\delta$  7.44 – 7.36 (m, 2H), 7.23 (td,  $J = 7.0, 1.6$  Hz, 2H), 4.66 (s, 2H), 3.86 (t,  $J = 7.1$  Hz, 2H), 2.69 (t,  $J = 7.1$  Hz, 2H), 0.92 (s, 9H), 0.10 (s, 6H). **<sup>13</sup>C NMR (101 MHz, CDCl<sub>3</sub>):**  $\delta$  139.13, 132.48, 129.61, 128.33, 128.19, 123.66, 93.31, 78.70, 61.84, 32.21, 25.92, 24.10, 18.35, -5.23. **IR:**  $\nu$  2954, 2928, 2856, 1485, 1471, 1275, 1258, 1221, 1106, 1057, 916, 837, 750 cm<sup>-1</sup>; **HRMS** calcd. For [M+H]<sup>+</sup>: 353.0931. Found: 353.0940.



Compound **1l-II** was obtained as a light yellow oil in 68% yield (1.43 g).  $R_f = 0.8$  (EtOAc/Hexane=1/5).  $^1\text{H NMR}$  (400 MHz,  $\text{CDCl}_3$ ):  $\delta$  7.40 – 7.37 (m, 2H), 7.25 – 7.21 (m, 2H), 4.65 (s, 2H), 2.90 (dt,  $J = 10.9, 7.2$  Hz, 1H), 2.05 – 1.98 (m, 2H), 1.84 – 1.76 (m, 4H), 1.67 – 1.60 (m, 2H).  $^{13}\text{C NMR}$  (100 MHz,  $\text{CDCl}_3$ ):  $\delta$  138.98, 132.33, 129.53, 128.37, 127.92, 124.16, 101.00, 77.29, 33.88, 32.44, 31.02, 25.06. **IR**:  $\nu$  2961, 2868, 1485, 1499, 1275, 1260, 1220, 750, 607  $\text{cm}^{-1}$ ; **HRMS** calcd. For  $[\text{M}+\text{H}]^+$ : 263.0430. Found: 263.0435.



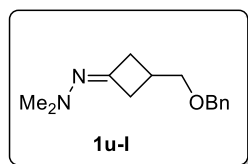
Compound **1m-II** was obtained as a light yellow oil in 36% yield (1.0 g) over two steps.  $R_f = 0.8$  (EtOAc/Hexane=1/5).  $^1\text{H NMR}$  (400 MHz,  $\text{CDCl}_3$ ):  $\delta$  7.38 (dt,  $J = 6.8, 2.2$  Hz, 2H), 7.23 (ddd,  $J = 6.1, 3.3, 1.8$  Hz, 2H), 4.63 (s, 2H), 1.55 – 1.46 (m, 1H), 0.96 – 0.86 (m, 4H).  $^{13}\text{C NMR}$  (101 MHz,  $\text{CDCl}_3$ ):  $\delta$  139.08, 132.45, 129.52, 128.34, 127.89, 123.94, 99.75, 72.78, 32.38, 8.86, 0.42. **IR**:  $\nu$  3013, 2923, 2850, 1221, 1028, 955, 842, 809, 758, 607, 542  $\text{cm}^{-1}$ ; **HRMS** calcd. For  $[\text{M}+\text{H}]^+$ : 235.0117. Found: 235.0120.



Compound **1n-II** was obtained as a white solid (M.P.: 89-92 °C) in 74% yield (2.56 g) from corresponding alcohol.  $R_f = 0.4$  (EtOAc/Hexane=1/3).  $^1\text{H NMR}$  (400 MHz,  $\text{CDCl}_3$ ):  $\delta$  7.62 – 7.53 (m, 2H), 7.42 – 7.31 (m, 3H), 7.01 (s, 1H), 6.92 (s, 1H), 3.92 (s, 3H), 3.90 (s, 3H).  $^{13}\text{C NMR}$  (101 MHz,  $\text{CDCl}_3$ ):  $\delta$  149.49, 148.93, 132.38, 131.45, 128.40, 128.36, 123.15, 115.55, 114.35, 112.30, 93.76, 86.57, 56.05, 56.00, 32.79. **IR**: 3003, 2961, 2935, 2851, 2832, 1595, 1516, 1463, 1352,

1251, 1225, 1091, 1027, 863, 756, 691, 577, 529  $\text{cm}^{-1}$ . **HRMS** calcd. For  $[\text{M}+\text{H}]^+$ : 331.0328.

Found: 331.0328.



Compound **1u-I** was obtained as a light yellow oil in 23% yield (335 g) over 5 steps.  $R_f = 0.6$  (EtOAc/Hexane=1/1).  **$^1\text{H}$  NMR (400 MHz,  $\text{CDCl}_3$ )**:  $\delta$  7.38 – 7.27 (m, 5H), 4.54 (s, 2H), 3.59 – 3.44 (m, 2H), 3.12 – 2.93 (m, 2H), 2.78 – 2.60 (m, 3H), 2.59 (s, 6H).  **$^{13}\text{C}$  NMR (101 MHz,  $\text{CDCl}_3$ )**:  $\delta$  156.90, 138.26, 128.42, 127.69, 127.67, 73.59, 73.18, 46.83, 38.22, 27.92. **IR**:  $\nu$  2955, 2855, 2776, 1782, 1682, 1453, 1364, 1097, 1027, 988, 738, 698, 606  $\text{cm}^{-1}$ ; **HRMS** calcd. For  $[\text{M}+\text{H}]^+$ : 233.1648. Found: 233.1634.

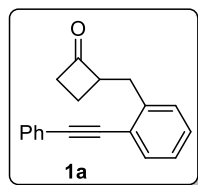
#### 4.4.4. Synthesis of substrates

##### a) Synthesis of substrates with benzene linkage (In Route I):

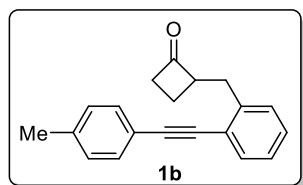
The procedure for the alkylation reaction is as follows (using substrate **1a** as an example):

*n*-BuLi (2.5 M in hexane, 0.9 mL, 1.1 equiv.) was added to a solution of known compound **10** (228.8 mg, 2.04 mmol, 1 equiv.) in freshly distilled THF (5 mL). The reaction mixture was stirred for 1 h at 0  $^\circ\text{C}$  until a yellow suspension was generated. After that, a solution of **1a-II** (608.9 mg, 2.25 mmol, 1.1 equiv.) in THF (2 mL) was added dropwise to the stirring mixture at -78  $^\circ\text{C}$ . The mixture was further stirred for 15 min at -78  $^\circ\text{C}$ , then overnight at room temperature. 2 M HCl (3.6 mL) was then added to the reaction system and the reaction was stirred vigorously for 1 h at room temperature. A mixture of diethyl ether (25 mL) and water (10 mL) was added to the reaction mixture. The aqueous phase was extracted by diethyl ether (2 $\times$ 25 mL). Then the organic phase was washed with brine (2 $\times$ 10 mL) and dried using  $\text{Na}_2\text{SO}_4$  and concentrated under reduced

pressure. The residue was purified by silica gel flash column chromatography (EtOAc/Hexane=1/10) to obtain the desired substrate **1a** (457.3 mg) as a light yellow oil in 86% yield.

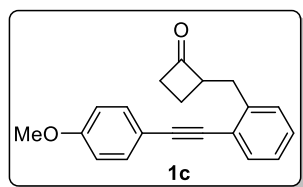


Compound **1a** was obtained as a light yellow oil in 86% yield (457.3 mg).  $R_f = 0.5$  (EtOAc/Hexane=1/5).  **$^1\text{H}$  NMR (500 MHz,  $\text{CDCl}_3$ ):**  $\delta$  7.53 (ddd,  $J = 7.2, 3.6, 1.7$  Hz, 3H), 7.41 – 7.31 (m, 3H), 7.32 – 7.18 (m, 3H), 3.79 (tdd,  $J = 9.9, 7.4, 5.8$  Hz, 1H), 3.35 (dd,  $J = 14.0, 5.7$  Hz, 1H), 3.11 – 3.01 (m, 1H), 3.05 – 2.97 (m, 1H), 2.93 (dddd,  $J = 17.6, 9.7, 5.1, 2.7$  Hz, 1H), 2.21 – 2.09 (m, 1H), 1.84 (ddt,  $J = 11.2, 9.6, 7.8$  Hz, 1H).  **$^{13}\text{C}$  NMR (100 MHz,  $\text{CDCl}_3$ ):**  $\delta$  210.70, 140.93, 132.31, 131.52, 129.24, 128.58, 128.48, 128.42, 126.43, 123.24, 122.89, 93.76, 87.91, 60.58, 44.55, 34.04, 16.80. **IR:**  $\nu$  3059, 2922, 1777, 1599, 1479, 1443, 1089, 1071, 757, 691, 553  $\text{cm}^{-1}$ ; **HRMS** calcd. For  $[\text{M}+\text{H}]^+$ : 261.1274. Found: 261.1283.

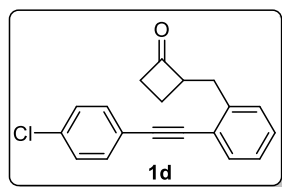


Compound **1b** was obtained as light yellow oil in 27% yield (118.9 mg).  $R_f = 0.6$  (EtOAc/Hexane=1/5).  **$^1\text{H}$  NMR (500 MHz,  $\text{CDCl}_3$ ):**  $\delta$  7.51 (dd,  $J = 7.5, 1.4$  Hz, 1H), 7.45 – 7.39 (m, 2H), 7.30 – 7.14 (m, 5H), 3.78 (dtq,  $J = 12.6, 8.2, 2.7$  Hz, 1H), 3.34 (dd,  $J = 14.0, 5.7$  Hz, 1H), 3.10 – 3.00 (m, 1H), 3.04 – 2.97 (m, 1H), 2.92 (dddd,  $J = 17.5, 9.6, 5.1, 2.7$  Hz, 1H), 2.38 (s, 3H), 2.14 (qd,  $J = 10.5, 5.1$  Hz, 1H), 1.83 (ddt,  $J = 11.2, 9.6, 7.7$  Hz, 1H).  **$^{13}\text{C}$  NMR (126 MHz,  $\text{CDCl}_3$ ):**  $\delta$  210.73, 140.80, 138.55, 132.20, 131.38, 129.20, 129.18, 128.34, 126.37, 123.11, 120.16, 93.92,

87.23, 60.60, 44.51, 34.01, 21.52, 16.76, 6.96. **IR:**  $\nu$  2922, 2853, 1778, 1510, 1448, 1393, 1073, 817, 757, 522  $\text{cm}^{-1}$ ; **HRMS** calcd. For  $[\text{M}+\text{H}]^+$ : 275.1430. Found: 275.1438.

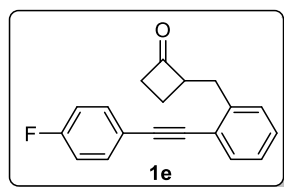


Compound **1c** was obtained as colorless oil in 68% yield (246.7 mg).  $R_f = 0.5$  (EtOAc/Hexane=1/3).  **$^1\text{H}$  NMR (400 MHz,  $\text{CDCl}_3$ ):**  $\delta$  7.53 – 7.42 (m, 3H), 7.30 – 7.16 (m, 3H), 6.93 – 6.85 (m, 2H), 3.83 (s, 3H), 3.82 – 3.73 (m, 1H), 3.35 (dd,  $J = 14.0, 5.6$  Hz, 1H), 3.12 – 2.85 (m, 3H), 2.14 (dtd,  $J = 11.3, 10.2, 5.2$  Hz, 1H), 1.90 – 1.76 (m, 1H).  **$^{13}\text{C}$  NMR (101 MHz,  $\text{CDCl}_3$ ):**  $\delta$  210.98, 159.70, 140.62, 132.94, 132.05, 129.14, 128.17, 126.36, 123.18, 115.30, 114.09, 93.76, 86.55, 60.55, 55.33, 44.51, 34.03, 16.76. **IR:**  $\nu$  3062, 2997, 2954, 2837, 1777, 1606, 1510, 1442, 1287, 1249, 1175, 1029, 832, 757, 532  $\text{cm}^{-1}$ ; **HRMS** calcd. For  $[\text{M}+\text{H}]^+$ : 291.1380. Found: 291.1384.



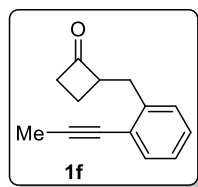
Compound **1d** was obtained as colorless oil in 48% yield (225.5 mg).  $R_f = 0.6$  (EtOAc/Hexane=1/5).  **$^1\text{H}$  NMR (400 MHz,  $\text{CDCl}_3$ ):**  $\delta$  7.51 (ddd,  $J = 7.5, 1.5, 0.6$  Hz, 1H), 7.48 – 7.43 (m, 2H), 7.37 – 7.32 (m, 2H), 7.32 – 7.26 (m, 1H), 7.26 – 7.20 (m, 2H), 3.84 – 3.69 (m, 1H), 3.35 (dd,  $J = 14.0, 5.6$  Hz, 1H), 3.13 – 2.86 (m, 3H), 2.15 (dtd,  $J = 11.3, 10.3, 5.2$  Hz, 1H), 1.82 (ddt,  $J = 11.2, 9.7, 7.8$  Hz, 1H).  **$^{13}\text{C}$  NMR (101 MHz,  $\text{CDCl}_3$ ):**  $\delta$  210.69, 140.93, 134.40, 132.69, 132.30, 129.21, 128.79, 128.76, 126.45, 122.52, 121.68, 92.57, 88.78, 60.51, 44.56, 34.02,

16.82. **IR:**  $\nu$  3059, 2923, 2852, 1778, 1492, 1447, 1397, 1090, 1014, 828, 757, 520  $\text{cm}^{-1}$ ; **HRMS** calcd. For  $[\text{M}+\text{H}]^+$ : 295.0884. Found: 295.0893.



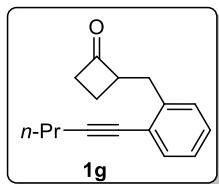
Compound **1e** was obtained as colorless oil in 67% yield (277.2mg).  $R_f$  = 0.5 (EtOAc/Hexane=1/5).

**$^1\text{H}$  NMR (400 MHz,  $\text{CDCl}_3$ ):**  $\delta$  7.54 (ddt,  $J$  = 8.5, 5.3, 3.1 Hz, 3H), 7.35 – 7.19 (m, 3H), 7.13 – 7.01 (m, 2H), 3.79 (dtq,  $J$  = 12.7, 8.1, 2.8 Hz, 1H), 3.38 (dd,  $J$  = 14.1, 5.6 Hz, 1H), 3.08 (dddd,  $J$  = 18.3, 10.6, 8.0, 2.7 Hz, 1H), 3.05 – 2.90 (m, 2H), 2.17 (ddt,  $J$  = 15.7, 10.6, 5.5 Hz, 1H), 1.85 (ddt,  $J$  = 11.3, 9.6, 7.8 Hz, 1H).  **$^{13}\text{C}$  NMR (101 MHz,  $\text{CDCl}_3$ ):**  $\delta$  210.74, 162.56 (d,  $J$  = 249.8 Hz), 140.85, 133.37 (d,  $J$  = 8.4 Hz), 132.24, 129.19, 128.60, 126.43, 122.68, 119.29 (d,  $J$  = 3.5 Hz), 115.75 (d,  $J$  = 22.1 Hz), 92.64, 87.51 (d,  $J$  = 1.5 Hz), 60.52, 44.54, 34.03, 16.82. **IR:**  $\nu$  3065, 2924, 2853, 1778, 1597, 1508, 1229, 1156, 1092, 836, 757, 525  $\text{cm}^{-1}$ ; **HRMS** calcd. For  $[\text{M}+\text{H}]^+$ : 279.1180. Found: 279.1190.



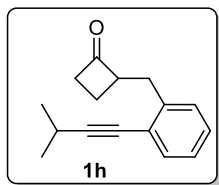
Compound **1f** was obtained as a light yellow oil in 63 % yield (850 mg).  $R_f$  = 0.6 (EtOAc/Hexane=1/5).  **$^1\text{H}$  NMR (400 MHz,  $\text{CDCl}_3$ ):**  $\delta$  7.41 – 7.35 (m, 1H), 7.23 – 7.11 (m, 3H), 3.77 – 3.65 (m, 1H), 3.24 (dd,  $J$  = 14.1, 5.7 Hz, 1H), 3.04 (dddd,  $J$  = 17.6, 10.6, 8.0, 2.7 Hz, 1H), 2.97 – 2.84 (m, 2H), 2.18 – 2.04 (m, 1H), 2.08 (s, 3H), 1.78 (ddt,  $J$  = 11.2, 9.6, 7.7 Hz, 1H).  **$^{13}\text{C}$  NMR (100 MHz,  $\text{CDCl}_3$ ):**  $\delta$  211.15, 140.61, 132.33, 128.91, 127.73, 126.23, 123.70, 90.11, 78.17,

60.47, 44.47, 33.73, 16.72, 4.50. **IR:**  $\nu$  3063, 2971, 2851, 1778, 1485, 1446, 1091, 1073, 758  $\text{cm}^{-1}$ ; **HRMS** calcd. For  $[\text{M}+\text{H}]^+$ : 199.1117. Found: 199.1122.



Compound **1g** was obtained as a colorless oil in 70% yield (420 mg).  $R_f = 0.6$  (EtOAc/Hexane=1/5).

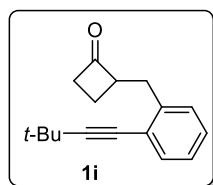
**$^1\text{H}$  NMR (500 MHz,  $\text{CDCl}_3$ ):**  $\delta$  7.38 (dd,  $J = 7.5, 1.4$  Hz, 1H), 7.23 – 7.11 (m, 3H), 3.78 – 3.67 (m, 1H), 3.24 (dd,  $J = 14.0, 5.8$  Hz, 1H), 3.10 – 2.98 (m, 1H), 2.97 – 2.85 (m, 2H), 2.42 (t,  $J = 7.0$  Hz, 2H), 2.15 – 2.06 (m, 1H), 1.79 (ddt,  $J = 11.3, 9.6, 7.7$  Hz, 1H), 1.64 (q,  $J = 7.2$  Hz, 2H), 1.06 (t,  $J = 7.4$  Hz, 3H).  **$^{13}\text{C}$  NMR (126 MHz,  $\text{CDCl}_3$ ):**  $\delta$  210.91, 140.56, 132.30, 128.96, 127.68, 126.22, 126.20, 123.74, 94.64, 79.17, 60.54, 60.54, 44.43, 33.83, 22.29, 21.55, 16.65, 13.60. **IR:**  $\nu$  3064, 2962, 2832, 1779, 1484, 1448, 1091, 1073, 758  $\text{cm}^{-1}$ ; **HRMS** calcd. For  $[\text{M}+\text{H}]^+$ : 227.1430. Found: 227.1435.



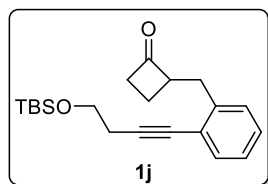
Compound **1h** was obtained as a colorless oil in 74% yield (566 mg).  $R_f = 0.5$  (EtOAc/Hexane=1/5).  **$^1\text{H}$  NMR (500 MHz,  $\text{CDCl}_3$ ):**  $\delta$  7.37 (dd,  $J = 7.5, 1.4$  Hz, 1H), 7.23 – 7.11 (m, 3H), 3.72 (dq,  $J = 8.0, 2.8$  Hz, 1H), 3.23 (dd,  $J = 13.9, 5.7$  Hz, 1H), 3.09 – 2.97 (m, 1H), 2.91 (dd,  $J = 13.8, 9.5$  Hz, 2H), 2.81 (p,  $J = 6.9$  Hz, 1H), 2.09 (dt,  $J = 10.5, 5.2$  Hz, 1H), 1.85 – 1.75 (m, 1H), 1.28 (d,  $J = 6.9$  Hz, 6H).  **$^{13}\text{C}$  NMR (126 MHz,  $\text{CDCl}_3$ ):**  $\delta$  210.92, 140.61, 132.13, 129.01, 127.70, 126.20, 123.59, 100.24, 78.26, 60.57, 44.43, 33.89, 23.09, 21.31, 16.65. **IR:**  $\nu$  2975, 2930,



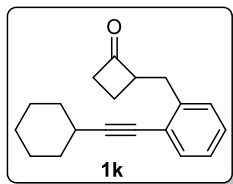
1777, 1485, 1448, 1362, 1174, 963, 912, 759  $\text{cm}^{-1}$ ; **HRMS** calcd. For  $[\text{M}+\text{Na}]^+$ : 249.1250. Found: 249.1254.



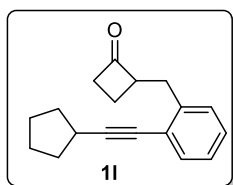
Compound **1i** was obtained as white solid (M.P.: 63-64 °C) in 77% yield (885 mg).  $R_f = 0.5$  (EtOAc/Hexane=1/5). M. P.= .  **$^1\text{H}$  NMR (500 MHz,  $\text{CDCl}_3$ )**:  $\delta$  7.39 (dd,  $J = 7.6, 1.3$  Hz, 1H), 7.26 – 7.13 (m, 3H), 3.82 – 3.68 (m, 1H), 3.25 (dd,  $J = 13.8, 5.7$  Hz, 1H), 3.11 – 3.00 (m, 1H), 3.00 – 2.88 (m, 2H), 2.12 (qd,  $J = 10.5, 5.2$  Hz, 1H), 1.84 (ddt,  $J = 11.3, 9.8, 7.7$  Hz, 1H), 1.36 (s, 9H).  **$^{13}\text{C}$  NMR (126 MHz,  $\text{CDCl}_3$ )**:  $\delta$  210.91, 140.59, 132.03, 129.05, 127.67, 126.19, 123.59, 103.03, 60.60, 44.41, 33.97, 31.04, 28.19, 16.61. **IR**:  $\nu$  3065, 2968, 2867, 1780, 1474, 1448, 1291, 1203, 1089, 1072, 757  $\text{cm}^{-1}$ ; **HRMS** calcd. For  $[\text{M}+\text{H}]^+$ : 241.1587. Found: 241.1596.



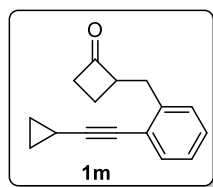
Compound **1j** was obtained as a colorless oil in 33% yield (288 mg).  $R_f = 0.6$  (EtOAc/Hexane=1/5).  **$^1\text{H}$  NMR (500 MHz,  $\text{CDCl}_3$ )**:  $\delta$  7.38 (dd,  $J = 7.5, 1.4$  Hz, 1H), 7.24 – 7.12 (m, 3H), 3.82 (t,  $J = 7.1$  Hz, 2H), 3.77 – 3.65 (m, 1H), 3.22 (dd,  $J = 14.1, 5.7$  Hz, 1H), 3.03 (dddd,  $J = 18.3, 10.5, 8.0, 2.7$  Hz, 1H), 2.97 – 2.84 (m, 2H), 2.66 (t,  $J = 7.1$  Hz, 2H), 2.10 (qd,  $J = 10.6, 5.1$  Hz, 1H), 1.84 – 1.71 (m, 1H), 0.91 (s, 9H), 0.10 (s, 6H).  **$^{13}\text{C}$  NMR (126 MHz,  $\text{CDCl}_3$ )**:  $\delta$  210.76, 140.70, 132.35, 128.96, 127.88, 126.20, 123.43, 91.47, 80.03, 61.99, 60.51, 44.46, 33.78, 25.90, 25.90, 24.00, 18.33, 16.70, -5.25, -5.48. **IR**:  $\nu$  2927, 2855, 1779, 1485, 1390, 1254, 1098, 1055, 837, 758, 668  $\text{cm}^{-1}$ ; **HRMS** calcd. For  $[\text{M}+\text{H}]^+$ : 343.2088. Found: 343.2102.



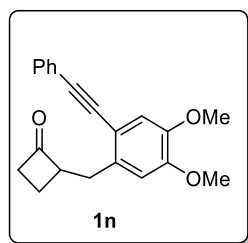
Compound **1k** was obtained as a light yellow oil in 54% yield (603 mg).  $R_f = 0.6$  (EtOAc/Hexane=1/5).  **$^1\text{H}$  NMR (500 MHz,  $\text{CDCl}_3$ ):**  $\delta$  7.41 – 7.36 (m, 1H), 7.23 – 7.10 (m, 3H), 3.81 – 3.67 (m, 1H), 3.23 (dd,  $J = 13.9, 5.8$  Hz, 1H), 3.03 (dddd,  $J = 18.4, 10.6, 8.0, 2.8$  Hz, 1H), 2.96 – 2.86 (m, 2H), 2.64 (dt,  $J = 9.7, 5.2$  Hz, 1H), 2.16 – 2.03 (m, 1H), 1.95 – 1.69 (m, 5H), 1.60 – 1.51 (m, 3H), 1.37 (s, 3H).  **$^{13}\text{C}$  NMR (100 MHz,  $\text{CDCl}_3$ ):**  $\delta$  211.04, 140.56, 132.19, 129.01, 127.64, 126.19, 123.71, 98.89, 78.97, 60.55, 44.43, 33.90, 32.73, 29.78, 25.91, 24.87, 16.61. **IR:**  $\nu$  2929, 2853, 1779, 1484, 1447, 1072, 953, 886, 757  $\text{cm}^{-1}$ ; **HRMS** calcd. For  $[\text{M}+\text{H}]^+$ : 267.1743. Found: 267.1753.



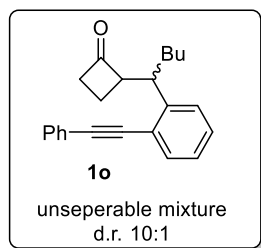
Compound **1l** was obtained as a light yellow oil in 34% yield (315 mg).  $R_f = 0.6$  (EtOAc/Hexane=1/5).  **$^1\text{H}$  NMR (400 MHz,  $\text{CDCl}_3$ ):**  $\delta$  7.37 (ddd,  $J = 7.4, 1.5, 0.7$  Hz, 1H), 7.24 – 7.09 (m, 3H), 3.79 – 3.64 (m, 1H), 3.22 (dd,  $J = 13.9, 5.7$  Hz, 1H), 3.09 – 2.98 (m, 1H), 2.96 – 2.82 (m, 3H), 2.09 (dtd,  $J = 11.3, 10.3, 5.2$  Hz, 1H), 2.04 – 1.92 (m, 2H), 1.88 – 1.56 (m, 7H).  **$^{13}\text{C}$  NMR (100 MHz,  $\text{CDCl}_3$ ):**  $\delta$  211.02, 140.55, 132.11, 129.00, 127.62, 126.19, 123.73, 99.09, 78.57, 60.55, 44.43, 34.00, 33.98, 33.90, 30.95, 24.99, 16.63. **IR:**  $\nu$  2958, 2869, 1777, 1484, 1444, 1353, 1177, 1072, 994, 919, 758  $\text{cm}^{-1}$ ; **HRMS** calcd. For  $[\text{M}+\text{H}]^+$ : 253.1587. Found: 253.1595.



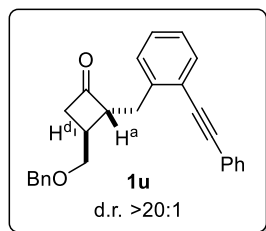
Compound **1m** was obtained as a light yellow oil in 47% yield (411.4 mg).  $R_f = 0.6$  (EtOAc/Hexane=1/5).  **$^1\text{H}$  NMR (400 MHz,  $\text{CDCl}_3$ ):**  $\delta$  7.38 – 7.34 (m, 1H), 7.22 – 7.09 (m, 3H), 3.69 (ddd,  $J = 9.5, 5.6, 2.7$  Hz, 1H), 3.21 (dd,  $J = 14.0, 5.6$  Hz, 1H), 3.10 – 2.97 (m, 1H), 2.97 – 2.83 (m, 2H), 2.10 (dtd,  $J = 11.2, 10.2, 5.2$  Hz, 1H), 1.84 – 1.72 (m, 1H), 1.47 (tt,  $J = 8.2, 5.0$  Hz, 1H), 0.93 – 0.77 (m, 4H).  **$^{13}\text{C}$  NMR (100 MHz,  $\text{CDCl}_3$ ):**  $\delta$  211.05, 140.71, 132.27, 128.94, 127.63, 126.20, 123.53, 97.93, 77.33, 74.10, 60.49, 44.45, 33.84, 16.69, 8.82, 8.78, 0.31. **IR:**  $\nu$  3010, 2923, 2852, 1778, 1485, 1447, 1392, 1178, 1087, 1072, 954, 757  $\text{cm}^{-1}$ ; **HRMS** calcd. For  $[\text{M}+\text{H}]^+$ : 225.1274. Found: 225.1285.



Compound **1n** was obtained as a light yellow solid (M.P.: 91-92  $^{\circ}\text{C}$ ) in 66% yield (695 mg).  $R_f = 0.4$  (EtOAc/Hexane=1/3).  **$^1\text{H}$  NMR (500 MHz,  $\text{CDCl}_3$ ):**  $\delta$  7.54 – 7.48 (m, 2H), 7.38 – 7.30 (m, 3H), 7.01 (s, 1H), 6.77 (s, 1H), 3.90 (d,  $J = 4.6$  Hz, 6H), 3.78 – 3.68 (m, 1H), 3.24 (dd,  $J = 14.0, 6.1$  Hz, 1H), 3.09 – 2.97 (m, 2H), 2.95 – 2.83 (m, 1H), 2.15 (qd,  $J = 10.6, 5.1$  Hz, 1H), 1.86 (ddt,  $J = 11.1, 9.5, 7.7$  Hz, 1H).  **$^{13}\text{C}$  NMR (126 MHz,  $\text{CDCl}_3$ ):**  $\delta$  210.97, 149.45, 147.26, 134.43, 131.31, 128.41, 128.10, 123.45, 114.59, 114.52, 112.45, 92.12, 88.17, 60.97, 56.00, 55.95, 44.55, 33.57, 16.48. **IR:**  $\nu$  3004, 2360, 1775, 1512, 1464, 1349, 1275, 1260, 1091, 913, 764, 750, 691  $\text{cm}^{-1}$ . **HRMS** calcd. For  $[\text{M}+\text{H}]^+$ : 321.1485. Found: 321.1485.



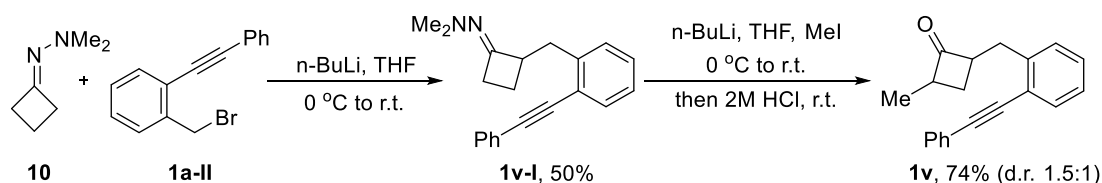
Compound **1o** was obtained as a light yellow oil in 32% yield (64 mg).  $R_f = 0.5$  (EtOAc/Hexane=1/5).  **$^1\text{H}$  NMR (500 MHz,  $\text{CDCl}_3$ ):**  $\delta$  (major) 7.57 – 7.50 (m, 3H), 7.40 – 7.32 (m, 3H), 7.32 – 7.18 (m, 3H), 3.71 (dd,  $J = 6.8, 3.6$  Hz, 2H), 2.92 (dddd,  $J = 17.8, 10.3, 7.6, 2.9$  Hz, 1H), 2.74 (dddd,  $J = 17.9, 10.0, 5.3, 2.6$  Hz, 1H), 2.19 – 2.02 (m, 1H), 1.99 – 1.83 (m, 2H), 1.78 (tdd,  $J = 13.5, 5.9, 4.4$  Hz, 1H), 1.41 – 1.08 (m, 4H), 0.84 (t,  $J = 7.2$  Hz, 3H).  **$^{13}\text{C}$  NMR (100 MHz,  $\text{CDCl}_3$ ):**  $\delta$  (major) 210.99, 144.30, 132.40, 131.47, 128.61, 128.41, 128.27, 126.75, 126.18, 123.56, 123.41, 93.61, 88.18, 65.51, 44.58, 42.50, 32.00, 29.49, 22.67, 14.60, 13.99. **IR:**  $\nu$  3059, 2956, 2928, 2859, 1777, 1599, 1493, 1443, 1072, 913, 756, 690  $\text{cm}^{-1}$ ; **HRMS** calcd. For  $[\text{M}+\text{H}]^+$ : 317.1900. Found: 317.1900.



Compound **1u** was obtained as a light yellow oil in 66% yield (361.5 mg) from **11**.  $R_f = 0.6$  (EtOAc/Hexane=1/5).  **$^1\text{H}$  NMR (400 MHz,  $\text{CDCl}_3$ ):**  $\delta$  7.54 – 7.48 (m, 3H), 7.37 – 7.31 (m, 3H), 7.31 – 7.26 (m, 2H), 7.25 – 7.14 (m, 6H), 4.34 (td,  $J = 12.4, 8.2$  Hz, 2H), 3.62 (ddd,  $J = 9.1, 7.3, 5.9$  Hz, 1H), 3.44 (dd,  $J = 9.5, 4.5$  Hz, 1H), 3.34 (dd,  $J = 13.8, 6.0$  Hz, 1H), 3.30 (dd,  $J = 9.50, 6.27$  Hz, 1H), 3.03 (dd,  $J = 13.8, 9.1$  Hz, 1H), 2.95 (d,  $J = 8.3$  Hz, 2H), 2.52 – 2.41 (m, 1H).  **$^{13}\text{C}$  NMR (101 MHz,  $\text{CDCl}_3$ ):**  $\delta$  208.85, 140.68, 138.11, 132.31, 131.49, 129.44, 128.58, 128.44, 128.39,

128.32, 127.54, 127.45, 126.44, 123.14, 122.74, 93.63, 87.88, 72.94, 71.93, 61.78, 47.42, 33.15, 30.81. **IR:**  $\nu$  3060, 3030, 2922, 2851, 1776, 1494, 1451, 1364, 1097, 914, 757, 691  $\text{cm}^{-1}$ ; **HRMS** calcd. For  $[\text{M}+\text{Na}]^+$ : 403.1669. Found: 403.1671. The diastereomer was assigned by characteristic  $J$  coupling constant (7.3) of  $\text{H}^{\text{a}}$  and  $\text{H}^{\text{d}}$  at four-membered ring<sup>17</sup>.

**b) Synthesis of substrate **1v**:**



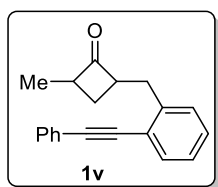
**The Procedure for the synthesis of **1v-I**:**

*n*-BuLi (2.5 M in hexane, 3.8 mL, 1.1 equiv.) was added to a solution of known compound **10** (977.7 mg, 8.7 mmol, 1 equiv.) in freshly distilled THF (10 mL). Then the reaction mixture was stirred for 1 h at 0 °C until a yellow suspension was generated. After that, a solution of **1a-II** (2.6 g, 9.6 mmol, 1.1 equiv.) in THF (10 mL) was added dropwise to the stirring mixture at -78 °C. The mixture was stirred at -78 °C for 15 min before warmed up to room temperature and stirred overnight. The reaction was quenched with a mixture of diethyl ether (25 mL) and water (10 mL) and the aqueous phase was extracted by diethyl ether (2×25 mL). Then the organic phase was washed with brine (2×10 mL) and dried over  $\text{Na}_2\text{SO}_4$  and concentrated under reduced pressure. The residue was purified by silica gel flash column chromatography (EtOAc/Hexane=1/10 to 1/5 to 1/2) to obtain the desired product **1v-I** with a small amount of impurity due to its instability. **1v-I** was subjected to the next step without further purification.

**The procedure for the synthesis of **1v**:**

*n*-BuLi (2.5 M in hexane, 0.73 mL, 1.1 equiv.) was added to a solution of compound **1v-I** (500 mg, 1.65 mmol, 1 equiv.) in freshly distilled THF (10 mL). Then the reaction mixture was stirred for 1

h at 0 °C until a yellow suspension was generated. After that, MeI (258.1 mg, 1.82 mmol, 1.1 equiv.) was added dropwise to the stirring mixture at -78 °C. The mixture was stirred at -78 °C for 15 min before warmed up to room temperature. After starting material was fully converted as shown by TLC, 2 M HCl (1 mL) was added to the reaction system and the reaction was stirred vigorously for 1 h at room temperature. A mixture of diethyl ether (10 mL) and water (10 mL) was added to the reaction mixture. The aqueous phase was extracted by diethyl ether (2×25 mL). Then the organic phase was washed with brine (2×20 mL) and dried over Na<sub>2</sub>SO<sub>4</sub> and concentrated under reduced pressure. The residue was purified by silica gel flash column chromatography (EtOAc/Hexane=1/10) to obtain the desired substrate **1v** (335 mg) as a light yellow oil in 74% yield.



3:2 mixture of diastereomers

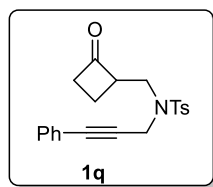
Compound **1v** was obtained as a yellow oil in 74% yield (335 mg).  $R_f = 0.6$  (EtOAc/Hexane=1/5). **<sup>1</sup>H NMR (500 MHz, CDCl<sub>3</sub>):**  $\delta$  7.53 (ddt,  $J = 9.2, 4.5, 2.6$  Hz, 3H), 7.36 (td,  $J = 4.9, 2.9$  Hz, 3H), 7.31 – 7.26 (m, 1H), 7.26 – 7.17 (m, 2H), 3.73 (ddd,  $J = 9.4, 6.3, 3.2$  Hz, 1H), 3.34 (ddd,  $J = 14.0, 12.4, 5.8$  Hz, 1H), 3.30 – 3.17 (m, 1H), 3.05 (dd,  $J = 14.0, 9.5$  Hz, 0.6H), 2.97 (dd,  $J = 14.0, 9.1$  Hz, 0.4H), 2.38 (d,  $J = 10.5$  Hz, 0.4H), 2.10 (ddd,  $J = 11.5, 10.0, 6.1$  Hz, 0.6H), 1.73 (ddd,  $J = 11.4, 9.7, 6.3$  Hz, 0.6H), 1.41 (dt,  $J = 10.7, 8.4$  Hz, 0.4H), 1.19 (d,  $J = 7.6$  Hz, 1.8H), 1.12 (d,  $J = 7.3$  Hz, 1.2H). **<sup>13</sup>C NMR (126 MHz, CDCl<sub>3</sub>):**  $\delta$  214.63, 212.92, 141.25, 140.95, 132.32, 132.25, 131.50, 131.48, 129.28, 129.16, 128.53, 128.44, 128.37, 128.35, 126.43, 126.30, 123.26, 122.98, 122.83, 93.69, 93.62, 87.97, 87.90, 57.88, 57.81, 52.11, 51.57, 34.46, 33.78, 25.91, 25.19, 24.93,

14.86, 13.51. **IR:**  $\nu$  3059, 2960, 2867, 1772, 1599, 1493, 1443, 1372, 1101, 1070, 914, 756, 690  $\text{cm}^{-1}$ ; **HRMS** calcd. For  $[\text{M}+\text{Na}]^+$ : 297.1250. Found: 297.1258.

c) Synthesis of substrates with NTs linkage (In Route II):

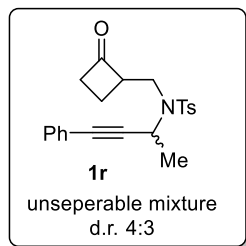
The procedure for Mitsunobu reaction and deprotection cascade is as follows (using substrate **1q** as an example):

A solution of **12** (174.2 mg, 1.0 mmol, 1 equiv.) and DIAD (208.3 mg, 1.03 mmol, 1.03 equiv.) in THF (5 mL) was added to a solution of known<sup>5</sup> compound **1q-I** (313.9 mg, 1.1 mmol, 1.1 equiv.) and triphenylphosphine (270.0 mg, 1.03 mmol, 1.03 equiv.) in THF (5 mL) at 0 °C. Then the reaction mixture was warmed up to room temperature and stirred overnight. After the reaction finished, solvent was removed by rotavap and the residue was dissolved in 5 mL acetonitrile and 3 mL 1M  $\text{H}_2\text{SO}_4$  was added to the solution. The resulting mixture was stirred at room temperature for 0.5 h and the progress of the reaction was monitored by TLC. When the starting material was fully consumed, the reaction mixture was diluted with ether and washed by water, saturated  $\text{NaHCO}_3$  solution and brine successively. Then the organic phase was dried over magnesium sulfate, then filtered and concentrated. The residue was purified by silica gel flash column chromatography (EtOAc/Hexane=1/10 to 1/5) to obtain the desired substrate **1q** (258.3 mg) as a white solid in 74% yield.

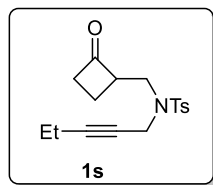


Compound **1q** was obtained as a white solid (M.P.: 102-104 °C) in 74% yield (258.3 mg).  $R_f$  = 0.4 (EtOAc/Hexane=1/5).  **$^1\text{H}$  NMR (400 MHz,  $\text{CDCl}_3$ ):**  $\delta$  7.76 (d,  $J$  = 8.3 Hz, 2H), 7.31 – 7.20 (m, 5H), 7.05 (dd,  $J$  = 8.2, 1.5 Hz, 2H), 4.44 (dd,  $J$  = 18.7, 0.8 Hz, 1H), 4.31 (dd,  $J$  = 18.7, 0.6 Hz, 1H),

3.72 – 3.61 (m, 1H), 3.58 – 3.40 (m, 2H), 3.19 – 3.06 (m, 1H), 3.05 – 2.93 (m, 1H), 2.33 (s, 3H), 2.32 – 2.22 (m, 1H), 2.02 (ddt,  $J = 11.5, 9.7, 7.9$  Hz, 1H).  **$^{13}\text{C}$  NMR (100 MHz,  $\text{CDCl}_3$ ):**  $\delta$  208.48, 143.71, 135.59, 131.50, 129.59, 128.48, 128.12, 127.80, 121.99, 85.90, 81.58, 59.13, 45.39, 45.06, 38.31, 21.42, 15.49. **IR:**  $\nu$  2960, 2923, 2858, 1778, 1597, 1490, 1442, 1348, 1162, 1090, 1024, 903, 815, 758, 658, 571, 544  $\text{cm}^{-1}$ ; **HRMS** calcd. For  $[\text{M}+\text{H}]^+$ : 368.1315. Found: 368.1319.



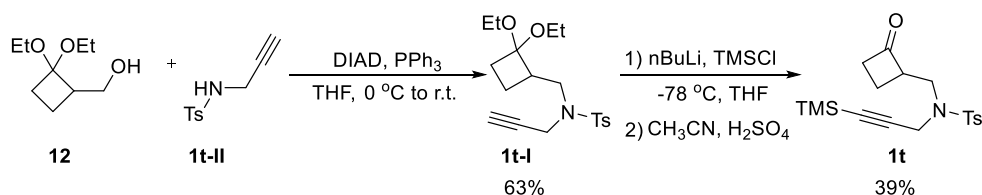
Compound **1r** was obtained as an oil in 79% yield (53.1 mg).  $R_f = 0.4$  (EtOAc/Hexane=1/3).  **$^1\text{H}$  NMR (400 MHz,  $\text{CDCl}_3$ ):**  $\delta$  7.76 (dd,  $J = 9.8, 8.1$  Hz, 2H), 7.27 (dd,  $J = 7.5, 3.6$  Hz, 3H), 7.26 – 7.20 (m, 2H), 7.09 – 7.02 (m, 2H), 5.10 – 4.98 (m, 1H), 4.01 (s, 0.42H), 3.77 – 3.63 (m, 0.56H), 3.55 – 3.37 (m, 1.58H), 3.28 (dd,  $J = 15.5, 9.6$  Hz, 0.44H), 3.14 – 3.00 (m, 1H), 3.01 – 2.85 (m, 1H), 2.35 (d,  $J = 3.3$  Hz, 3H), 2.34 – 2.26 (m, 1H), 2.24 – 2.10 (m, 0.60H), 1.99 – 1.85 (m, 0.43H), 1.52 (d,  $J = 7.1$  Hz, 1.77H), 1.47 (d,  $J = 7.0$  Hz, 1.32H).  **$^{13}\text{C}$  NMR (100 MHz,  $\text{CDCl}_3$ ):**  $\delta$  208.71, 208.53, 143.75, 143.67, 135.47, 135.23, 131.51, 131.49, 129.63, 129.61, 128.50, 128.18, 128.16, 127.88, 127.79, 121.98, 86.25, 86.00, 85.25, 84.96, 61.34, 61.15, 47.27, 46.58, 44.50, 43.53, 43.40, 22.50, 22.04, 21.48, 21.47, 16.95, 16.28. **IR:**  $\nu$  2968, 2863, 1777, 1275, 1165, 1121, 913, 748, 658  $\text{cm}^{-1}$ ; **HRMS** calcd. For  $[\text{M}+\text{H}]^+$ : 382.1471. Found: 382.1472.





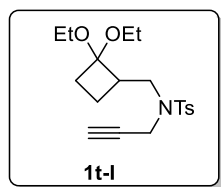
Compound **1s** was obtained as a colorless oil in 59% yield (396.7 mg).  $R_f = 0.3$  (EtOAc/Hexane=1/3).  **$^1\text{H}$  NMR (400 MHz,  $\text{CDCl}_3$ ):**  $\delta$  7.75 – 7.69 (m, 2H), 7.29 (dq,  $J = 8.0, 0.6$  Hz, 2H), 4.24 – 4.12 (m, 1H), 4.02 (dtd,  $J = 18.3, 2.2, 0.6$  Hz, 1H), 3.72 – 3.55 (m, 1H), 3.50 – 3.30 (m, 2H), 3.10 (dddd,  $J = 18.6, 10.6, 8.2, 2.5$  Hz, 1H), 2.98 (dddd,  $J = 17.7, 9.7, 5.2, 2.6$  Hz, 1H), 2.24 (dtd,  $J = 11.5, 10.3, 5.2$  Hz, 1H), 1.99 (ddt,  $J = 11.5, 9.7, 7.9$  Hz, 1H), 1.90 (qt,  $J = 7.5, 2.3$  Hz, 2H), 0.94 – 0.82 (m, 3H).  **$^{13}\text{C}$  NMR (100 MHz,  $\text{CDCl}_3$ ):**  $\delta$  208.67, 143.47, 135.75, 129.38, 127.83, 87.89, 71.61, 59.03, 45.07, 45.02, 37.81, 21.50, 15.52, 13.42, 12.10. **IR:**  $\nu$  2977, 2923, 1778, 1597, 1442, 1347, 1161, 1089, 1014, 903, 815, 750, 656, 569, 544  $\text{cm}^{-1}$ ; **HRMS** calcd. For  $[\text{M}+\text{H}]^+$ : 342.1134. Found: 342.1151.

### **Synthesis of substrate 1t**



### **The procedures for synthesis of 1t-I:**

A solution of **6** (261.3 mg, 1.5 mmol, 1 equiv.) and DIAD (313.4 mg, 1.55 mmol, 1.03 equiv.) in THF (5 mL) was added to a solution of known<sup>20a</sup> compound **1t-II** (345.3 mg, 1.65 mmol, 1.1 equiv.) and triphenylphosphine (406.2 mg, 1.55 mmol, 1.03 equiv.) in THF (5 mL) at 0 °C. Then the reaction mixture was warmed up to room temperature and stirred overnight. After the reaction finished, solvent was removed by rotavap and the residue was purified by silica gel flash column chromatography (EtOAc/Hexane=1/15 to 1/10) to obtain the desired compound **1t-I** (346 mg) as a colorless oil in 63% yield.

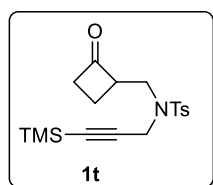


Compound **1t-I** was obtained as a colorless oil in 63% yield (346 mg).  $R_f = 0.6$  (EtOAc/Hexane=1/5).  **$^1\text{H}$  NMR (400 MHz,  $\text{CDCl}_3$ ):**  $\delta$  7.74 (d,  $J = 8.3$  Hz, 2H), 7.29 (dt,  $J = 8.0$ , 0.7 Hz, 2H), 4.27 (ddd,  $J = 18.4$ , 2.5, 1.0 Hz, 1H), 4.09 (dd,  $J = 18.4$ , 2.5 Hz, 1H), 3.48 – 3.31 (m, 5H), 3.24 (dd,  $J = 14.2$ , 6.7 Hz, 1H), 2.74 (ddd,  $J = 8.7$ , 6.8, 1.4 Hz, 1H), 2.42 (s, 3H), 2.19 (dddd,  $J = 12.2$ , 10.0, 4.6, 1.0 Hz, 1H), 2.04 – 1.94 (m, 2H), 1.91 – 1.80 (m, 1H), 1.46 (ddt,  $J = 11.3$ , 10.2, 7.7 Hz, 1H), 1.18 (td,  $J = 7.1$ , 1.2 Hz, 6H).  **$^{13}\text{C}$  NMR (100 MHz,  $\text{CDCl}_3$ ):**  $\delta$  143.35, 135.97, 129.38, 127.81, 102.10, 77.11, 73.33, 56.62, 56.28, 46.76, 43.71, 37.19, 29.42, 21.54, 16.76, 15.28, 15.24. **IR:**  $\nu$  3271, 2976, 1930, 2883, 1598, 1445, 1348, 1260, 1162, 1049, 911, 749, 660, 580, 545  $\text{cm}^{-1}$ ; **HRMS** calcd. For  $[\text{M}+\text{Na}]^+$ : 388.1553. Found: 388.1560.

#### The procedures for synthesis of **1t**:

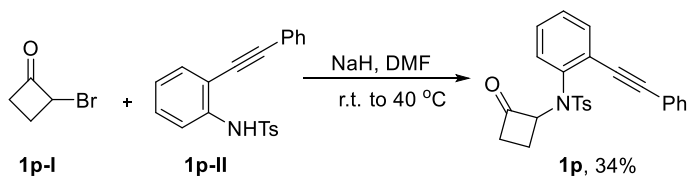
A 10 mL Schlenk flask charged with solution of **1t-I** (185 mg, 0.51 mmol, 1 equiv.) in THF (5 mL) was cooled to  $-78^\circ\text{C}$  by acetone-dry ice bath, then  $n\text{-BuLi}$  (2.5 M, 0.34 mL, 1.05 equiv.) was added to the mixture. The mixture was stirred at  $-78^\circ\text{C}$  for 1.5 h before  $\text{TMSCl}$  (60.5 mg, 0.56 mmol, 1.1 equiv.) was added to the reaction. The mixture was further stirred for 15 min at  $-78^\circ\text{C}$ , then overnight at room temperature. The reaction was quenched with a mixture of diethyl ether (15 mL) and water (10 mL) and the aqueous phase was extracted by diethyl ether ( $2 \times 15$  mL). Then the organic phase was washed with brine ( $2 \times 10$  mL) and dried over  $\text{Na}_2\text{SO}_4$  and concentrated under reduced pressure. The residue was dissolved in 5 mL acetonitrile and 3 mL 1M  $\text{H}_2\text{SO}_4$  was added to the solution. The resulting mixture was stirred at room temperature for 0.5 h and the progress of the reaction was monitored by TLC. When the starting material was fully consumed,

reaction mixture was diluted with ether and washed with water, saturated  $\text{NaHCO}_3$  solution and brine successively. Then the organic phase was dried over  $\text{MgSO}_4$ , then filtered and concentrated. The residue was purified by silica gel flash column chromatography ( $\text{EtOAc/Hexane}=1/10$  to  $1/5$ ) to obtain the desired substrate **1t** (258.3 mg) as a white solid in 60% yield (70 mg).



Compound **1t** was obtained as a light yellow oil in 60% yield (70 mg) from **1t-I**.  $R_f = 0.5$  ( $\text{EtOAc/Hexane}=1/5$ ).  **$^1\text{H}$  NMR (500 MHz,  $\text{CDCl}_3$ ):**  $\delta$  7.77 – 7.70 (m, 2H), 7.30 (d,  $J = 8.1$  Hz, 2H), 4.30 – 4.20 (m, 1H), 4.10 (d,  $J = 18.7$  Hz, 1H), 3.71 – 3.57 (m, 1H), 3.46 (dd,  $J = 14.0, 8.8$  Hz, 1H), 3.38 (dd,  $J = 14.0, 5.9$  Hz, 1H), 3.12 (dddd,  $J = 18.7, 10.6, 8.2, 2.5$  Hz, 1H), 3.00 (dddd,  $J = 17.7, 9.7, 5.1, 2.7$  Hz, 1H), 2.43 (s, 3H), 2.32 – 2.19 (m, 1H), 2.06 – 1.93 (m, 1H), -0.00 (s, 9H).  **$^{13}\text{C}$  NMR (100 MHz,  $\text{CDCl}_3$ ):**  $\delta$  208.35, 143.54, 135.53, 129.53, 127.72, 97.63, 91.23, 58.96, 45.08, 44.96, 38.22, 21.48, 15.46, -0.50. **IR:**  $\nu$  2959, 2923, 2853, 1780, 1598, 1445, 1349, 1250, 1162, 1090, 1027, 991, 845, 759, 665, 546  $\text{cm}^{-1}$ ; **HRMS** calcd. For  $[\text{M}+\text{Na}]^+$ : 386.1217. Found: 386.1217.

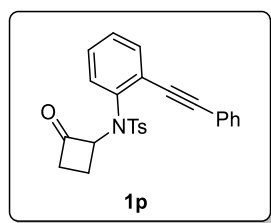
#### d) Synthesis of substrate **1p**:



Substrates **1p** were synthesized through alkylation of **1p-II** as shown above. **1p-I** and **1p-II** are known compounds.<sup>21</sup>

#### Procedure:

NaH (86.4 mg, 3.6 mmol, 1.2 equiv.) was added to a 20 mL vial with solution of known compound **1p-II** (978.6 mg, 3 mmol, 1 equiv.) in DMF (10 mL) at room temperature. After the mixture was stirred for 30 min at room temperature, **1p-I** (536.4 mg, 3.6 mmol, 1.2 equiv.) in DMF (2 mL) was added. Then the reaction mixture was heated to 40 °C for 5 h. The progress of the reaction was monitored by TLC. When the starting material was fully consumed, reaction mixture was diluted with ether and water was added slowly to the vial. The organic phase was dried over MgSO<sub>4</sub>, filtered and concentrated. The residue was purified by silica gel flash column chromatography (EtOAc/Hexane=1/10 to 1/5) to obtain the desired substrate **1p** (400 mg) as an orange oil in 34% yield.

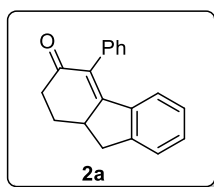


Compound **1p** was obtained as a light yellow oil in 34% yield (400 g) from known compound.  $R_f$  = 0.4 (EtOAc/Hexane=1/3). **<sup>1</sup>H NMR (400 MHz, CDCl<sub>3</sub>):**  $\delta$  7.69 (d,  $J$  = 8.3 Hz, 2H), 7.54 (d,  $J$  = 7.4 Hz, 1H), 7.52 – 7.45 (m, 2H), 7.39 – 7.26 (m, 6H), 7.15 (d,  $J$  = 8.5 Hz, 2H), 5.34 (s, 1H), 2.82 – 2.70 (m, 1H), 2.70 – 2.56 (m, 1H), 2.48 (qd,  $J$  = 10.5, 4.6 Hz, 1H), 2.30 (m, 1H), 2.30 (s, 3H). **<sup>13</sup>C NMR (101 MHz, CDCl<sub>3</sub>):**  $\delta$  204.65, 143.53, 138.24, 137.43, 133.25, 132.27, 131.78, 129.38, 129.07, 128.91, 128.58, 128.28, 127.83, 125.95, 122.91, 94.43, 86.08, 72.63, 40.23, 21.52, 19.40. **IR:**  $\nu$  3063, 2968, 2255, 2219, 1793, 1598, 1494, 1444, 1346, 1161, 1091, 912, 758, 669, 544 cm<sup>-1</sup>; **HRMS** calcd. For [M+H]<sup>+</sup>: 416.1315. Found: 416.1316.

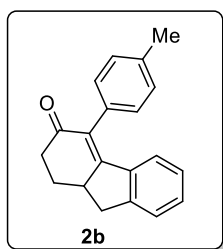
#### *4.4.5 Rh-catalyzed intramolecular coupling between cyclobutanones and alkynes*

##### General procedure:

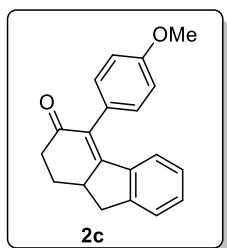
In a nitrogen-filled glove box, a 4 mL vial was charged with the cyclobutanone substrates (0.1 mmol), followed by 800  $\mu$ L 1,4-dioxane. 100  $\mu$ L of  $\text{PMe}_2\text{Ph}$  stock solution (22.1 mg/1000  $\mu$ L, 2.21 mg, 0.016 mmol, 16 mol%) and 100  $\mu$ L of  $[\text{Rh}(\text{CO})_2\text{Cl}]_2$  stock solution (19.4 mg/1000  $\mu$ L, 1.94 mg, 0.005 mmol, 5 mol%) were added sequentially to the vial. After stirring to a homogeneous solution, the vial was capped and the reaction was maintained at 125  $^\circ\text{C}$  (**1a** to **1t**) and 140  $^\circ\text{C}$  (**1u** and **1v**) for 60 h. After the reaction was complete, solvent was removed by rotavap and the residue was directly purified by silica gel flash chromatography.



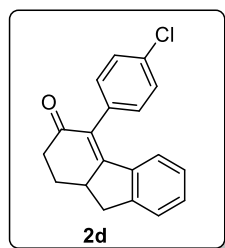
Compound **2a** was isolated as a white solid (M.P.: 118-120  $^\circ\text{C}$ ) in 82% yield.  $R_f = 0.4$  (EtOAc/Hexane=1/2).  **$^1\text{H}$  NMR (500 MHz,  $\text{CDCl}_3$ ):**  $\delta$  7.39 (q,  $J = 9.9, 7.2$  Hz, 3H), 7.31 (d,  $J = 7.6$  Hz, 1H), 7.28 – 7.21 (m, 1H), 7.15 (s, 2H), 6.91 (t,  $J = 7.6$  Hz, 1H), 6.41 (d,  $J = 7.9$  Hz, 1H), 3.37 – 3.22 (m, 2H), 2.86 – 2.73 (m, 2H), 2.61 (ddd,  $J = 17.3, 14.3, 5.0$  Hz, 1H), 2.43 (dtd,  $J = 12.0, 4.7, 2.2$  Hz, 1H), 2.06 (dtd,  $J = 16.4, 12.5, 4.2$  Hz, 1H).  **$^{13}\text{C}$  NMR (100 MHz,  $\text{CDCl}_3$ ):**  $\delta$  198.28, 162.69, 148.84, 138.46, 135.34, 132.51, 130.72, 129.67, 128.70, 127.66, 126.62, 125.14, 43.13, 38.44, 37.31, 29.14. **IR:**  $\nu$  3057, 2938, 2860, 1654, 1620, 1593, 1463, 1359, 1326, 1182, 1002, 910, 829, 732, 699, 578  $\text{cm}^{-1}$ ; **HRMS** calcd. For  $[\text{M}+\text{Na}]^+$ : 283.1093. Found: 283.1094.



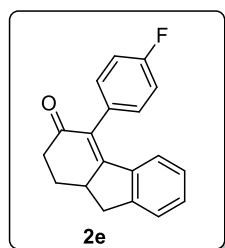
Compound **2b** was isolated as a white solid (M.P.: 168-172 °C) in 82% yield.  $R_f = 0.4$  (EtOAc/Hexane=1/2).  **$^1\text{H}$  NMR (400 MHz,  $\text{CDCl}_3$ ):**  $\delta$  7.30 (d,  $J = 7.5$  Hz, 1H), 7.28 – 7.18 (m, 3H), 7.04 (s, 2H), 6.98 – 6.89 (m, 1H), 6.50 (d,  $J = 8.0$  Hz, 1H), 3.38 – 3.21 (m, 2H), 2.87 – 2.72 (m, 2H), 2.59 (ddd,  $J = 17.1, 14.2, 5.0$  Hz, 1H), 2.41 (m, 4H), 2.11 – 1.98 (m, 1H).  **$^{13}\text{C}$  NMR (100 MHz,  $\text{CDCl}_3$ ):**  $\delta$  198.47, 162.51, 148.78, 138.58, 137.25, 132.46, 132.19, 130.63, 129.47, 129.35, 126.65, 126.59, 125.10, 43.10, 38.46, 37.30, 29.15, 21.40. **IR:**  $\nu$  3023, 2922, 2859, 1657, 1597, 1510, 1462, 1358, 1335, 1206, 1092, 980, 811, 773, 734, 678, 518  $\text{cm}^{-1}$ ; **HRMS** calcd. For  $[\text{M}+\text{H}]^+$ : 297.1250. Found: 297.1255.



Compound **2c** was isolated as a white solid (M.P.: 132-135 °C) in 65% yield.  $R_f = 0.4$  (EtOAc/Hexane=1/3).  **$^1\text{H}$  NMR (400 MHz,  $\text{CDCl}_3$ ):**  $\delta$  7.34 – 7.29 (m, 1H), 7.28 – 7.23 (m, 1H), 7.21 – 6.89 (m, 5H), 6.56 – 6.50 (m, 1H), 3.86 (s, 3H), 3.36 – 3.20 (m, 2H), 2.87 – 2.71 (m, 2H), 2.60 (ddd,  $J = 17.2, 14.2, 5.0$  Hz, 1H), 2.47 – 2.36 (m, 1H), 2.12 – 1.96 (m, 1H).  **$^{13}\text{C}$  NMR (100 MHz,  $\text{CDCl}_3$ ):**  $\delta$  198.71, 162.84, 159.05, 148.81, 138.59, 132.02, 130.84, 130.66, 127.37, 126.63, 126.62, 125.13, 114.23, 55.24, 43.16, 38.45, 37.32, 29.11. **IR:**  $\nu$  2934, 1655, 1603, 1509, 1463, 1334, 1245, 1174, 1030, 979, 823, 774, 734, 578  $\text{cm}^{-1}$ ; **HRMS** calcd. For  $[\text{M}+\text{H}]^+$ : 291.1380. Found: 291.1395.

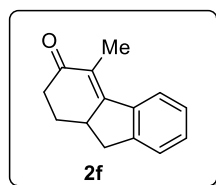


Compound **2d** was isolated as a white solid (M.P.: 145-147 °C) in 76% yield.  $R_f = 0.4$  (EtOAc/Hexane=1/3).  **$^1\text{H}$  NMR (400 MHz,  $\text{CDCl}_3$ ):**  $\delta$  7.40 (d,  $J = 7.8$  Hz, 2H), 7.35 – 7.26 (m, 2H), 7.11 (s, 2H), 7.00 – 6.93 (m, 1H), 6.50 (d,  $J = 8.0$  Hz, 1H), 3.38 – 3.21 (m, 2H), 2.87 – 2.72 (m, 2H), 2.60 (ddd,  $J = 17.2, 14.2, 5.0$  Hz, 1H), 2.48 – 2.38 (m, 1H), 2.12 – 1.98 (m, 1H).  **$^{13}\text{C}$  NMR (100 MHz,  $\text{CDCl}_3$ ):**  $\delta$  198.04, 163.20, 149.02, 138.12, 133.76, 133.65, 131.27, 131.16, 131.03, 128.99, 126.76, 126.51, 125.31, 43.26, 38.35, 37.29, 29.01. **IR:**  $\nu$  3010, 2922, 1657, 1588, 1489, 1335, 1183, 1069, 816, 734, 578  $\text{cm}^{-1}$ ; **HRMS** calcd. For  $[\text{M}+\text{Na}]^+$ : 317.0704. Found: 317.0710.

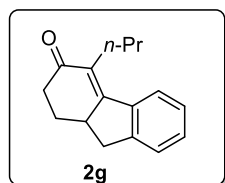


Compound **2e** was isolated as a white solid (M.P.: 120-121 °C) in 78% yield.  $R_f = 0.3$  (EtOAc/Hexane=1/3).  **$^1\text{H}$  NMR (400 MHz,  $\text{CDCl}_3$ ):**  $\delta$  7.38 – 7.33 (m, 1H), 7.33 – 7.27 (m, 1H), 7.15 (s, 4H), 6.98 (dd,  $J = 8.2, 7.0$  Hz, 1H), 6.49 (d,  $J = 7.9$  Hz, 1H), 3.40 – 3.23 (m, 2H), 2.90 – 2.75 (m, 2H), 2.63 (ddd,  $J = 17.2, 14.2, 4.9$  Hz, 1H), 2.46 (ddt,  $J = 12.6, 5.1, 2.1$  Hz, 1H), 2.07 (dddd,  $J = 14.3, 12.8, 11.9, 4.3$  Hz, 1H).  **$^{13}\text{C}$  NMR (100 MHz,  $\text{CDCl}_3$ ):**  $\delta$  198.36, 163.32, 162.39 (d,  $J = 246.2$  Hz), 148.98, 138.23, 131.33, 131.08 (d,  $J = 3.5$  Hz), 130.94, 126.58 (d,  $J = 21.6$  Hz),

125.28, 115.76 (d,  $J = 21.3$  Hz), 43.21, 38.35, 37.29, 29.02. **IR:**  $\nu$  2943, 1656, 1597, 1507, 1335, 1223, 1182, 911, 826, 773, 733, 584  $\text{cm}^{-1}$ ; **HRMS** calcd. For  $[\text{M}+\text{Na}]^+$ : 301.0999. Found: 301.1000.

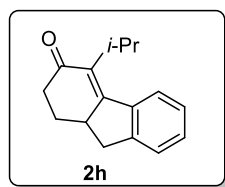


Compound **2f** was isolated as a colorless oil in 77% yield.  $R_f = 0.5$  (EtOAc/Hexane=1/5).  **$^1\text{H}$  NMR (400 MHz,  $\text{CDCl}_3$ ):**  $\delta$  7.74 (d,  $J = 7.4$  Hz, 1H), 7.39 – 7.34 (m, 2H), 7.34 – 7.29 (m, 1H), 3.25 – 3.11 (m, 2H), 2.79 – 2.69 (m, 1H), 2.66 (ddd,  $J = 17.1, 4.2, 2.3$  Hz, 1H), 2.46 (ddd,  $J = 17.1, 14.4, 4.9$  Hz, 1H), 2.32 (dtd,  $J = 12.5, 4.5, 2.3$  Hz, 1H), 2.13 (d,  $J = 2.2$  Hz, 3H), 1.88 (dddd,  $J = 14.4, 12.5, 11.7, 4.2$  Hz, 1H).  **$^{13}\text{C}$  NMR (100 MHz,  $\text{CDCl}_3$ ):**  $\delta$  199.76, 161.02, 148.55, 139.71, 130.24, 127.10, 126.92, 126.78, 125.32, 43.26, 37.95, 37.64, 29.27, 11.12. **IR:**  $\nu$  3304, 2954, 1720, 1632, 1463, 1330, 1276, 1205, 1070, 925, 849, 749, 580  $\text{cm}^{-1}$ ; **HRMS** calcd. For  $[\text{M}+\text{H}]^+$ : 199.1117. Found: 199.1121.

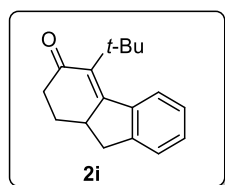


Compound **2g** was isolated as a colorless oil in 80% yield.  $R_f = 0.5$  (EtOAc/Hexane=1/3).  **$^1\text{H}$  NMR (500 MHz,  $\text{CDCl}_3$ ):**  $\delta$  7.64 (d,  $J = 7.6$  Hz, 1H), 7.39 – 7.27 (m, 3H), 3.26 – 3.09 (m, 2H), 2.77 – 2.59 (m, 3H), 2.52 – 2.38 (m, 2H), 2.37 – 2.26 (m, 1H), 1.87 (dd,  $J = 14.5, 4.1$  Hz, 1H), 1.59 (dd,  $J = 9.4, 3.8$  Hz, 1H), 1.50 – 1.38 (m, 1H), 1.03 (t,  $J = 7.3$  Hz, 3H).  **$^{13}\text{C}$  NMR (100 MHz,  $\text{CDCl}_3$ ):**  $\delta$  199.49, 160.65, 148.53, 139.18, 132.50, 130.23, 127.08, 126.29, 125.35, 43.28, 38.15, 37.69, 29.40, 27.00, 22.08, 14.33. **IR:**  $\nu$  2956, 2868, 1665, 1598, 1462, 1362, 1327, 1183, 1114, 770, 733  $\text{cm}^{-1}$ ; **HRMS** calcd. For  $[\text{M}+\text{H}]^+$ : 227.1430. Found: 227.1442.

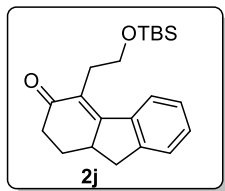




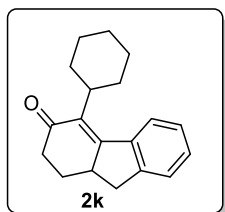
Compound **2h** was isolated as an oily solid (M.P.: 63-65 °C) in 70% yield.  $R_f = 0.6$  (EtOAc/Hexane=1/3).  **$^1\text{H}$  NMR (500 MHz,  $\text{CDCl}_3$ ):**  $\delta$  7.69 – 7.64 (m, 1H), 7.35 (dd,  $J = 5.6, 1.1$  Hz, 2H), 7.31 – 7.26 (m, 1H), 3.31 (hept,  $J = 6.9$  Hz, 1H), 3.19 – 3.01 (m, 2H), 2.74 (dd,  $J = 14.9, 7.3$  Hz, 1H), 2.55 (ddd,  $J = 17.6, 4.4, 2.2$  Hz, 1H), 2.35 (ddd,  $J = 17.6, 14.4, 4.9$  Hz, 1H), 2.27 – 2.18 (m, 1H), 1.82 (dddd,  $J = 14.4, 12.5, 11.7, 4.4$  Hz, 1H), 1.43 (d,  $J = 7.1$  Hz, 3H), 1.25 (d,  $J = 6.8$  Hz, 3H).  **$^{13}\text{C}$  NMR (100 MHz,  $\text{CDCl}_3$ ):**  $\delta$  199.39, 159.77, 148.41, 139.27, 137.11, 130.09, 126.73, 126.46, 125.31, 44.32, 38.90, 37.88, 28.47, 28.01, 20.80, 20.70. **IR:**  $\nu$  2952, 2869, 1658, 1598, 1461, 1357, 1325, 995, 771, 733  $\text{cm}^{-1}$ ; **HRMS** calcd. For  $[\text{M}+\text{H}]^+$ : 227.1430. Found: 227.1444.



Compound **2i** was isolated as a light yellow oil in 49% yield.  $R_f = 0.6$  (EtOAc/Hexane=1/3).  **$^1\text{H}$  NMR (400 MHz,  $\text{CDCl}_3$ ):**  $\delta$  7.67 (d,  $J = 7.5$  Hz, 1H), 7.30 – 7.26 (m, 2H), 7.26 – 7.19 (m, 1H), 3.11 – 2.93 (m, 2H), 2.76 (dd,  $J = 14.4, 7.9$  Hz, 1H), 2.51 (ddd,  $J = 18.7, 5.7, 1.6$  Hz, 1H), 2.31 (ddd,  $J = 18.7, 13.8, 5.6$  Hz, 1H), 2.15 – 2.06 (m, 1H), 1.84 – 1.71 (m, 1H), 1.38 (s, 9H).  **$^{13}\text{C}$  NMR (100 MHz,  $\text{CDCl}_3$ ):**  $\delta$  201.70, 157.81, 148.62, 143.12, 140.15, 129.41, 129.28, 125.58, 124.62, 48.19, 38.49, 38.34, 34.91, 30.61, 27.23. **IR:**  $\nu$  2957, 2863, 1660, 1576, 1461, 1362, 1318, 1203, 991, 768, 737  $\text{cm}^{-1}$ ; **HRMS** calcd. For  $[\text{M}+\text{H}]^+$ : 241.1587. Found: 241.1601.

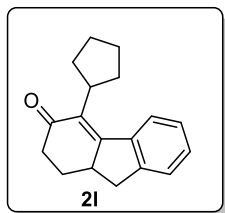


Compound **2j** was isolated as a colorless oil in 89% yield.  $R_f = 0.6$  (EtOAc/Hexane=1/3).  **$^1\text{H NMR}$  (400 MHz,  $\text{CDCl}_3$ ):**  $\delta$  8.00 (d,  $J = 7.7$  Hz, 1H), 7.39 – 7.26 (m, 3H), 3.85 (ddd,  $J = 9.9, 8.0, 5.2$  Hz, 1H), 3.72 (dt,  $J = 9.9, 7.5$  Hz, 1H), 3.24 – 3.12 (m, 2H), 2.99 – 2.80 (m, 2H), 2.72 (d,  $J = 8.3$  Hz, 1H), 2.63 (ddd,  $J = 16.9, 4.1, 2.4$  Hz, 1H), 2.44 (ddd,  $J = 16.9, 14.4, 4.9$  Hz, 1H), 2.37 – 2.26 (m, 1H), 1.96 – 1.80 (m, 1H), 0.84 (s, 9H), 0.03 (d,  $J = 0.3$  Hz, 3H), 0.00 (d,  $J = 0.7$  Hz, 3H).  **$^{13}\text{C NMR}$  (100 MHz,  $\text{CDCl}_3$ ):**  $\delta$  199.57, 162.98, 148.38, 139.05, 130.51, 128.36, 127.05, 126.90, 125.14, 61.97, 43.56, 38.07, 37.74, 29.29, 28.78, 25.94, 18.32, -5.28, -5.31. **IR:**  $\nu$  2882, 1659, 1600, 1471, 1360, 1337, 1254, 1100, 1076, 928, 836, 774, 732  $\text{cm}^{-1}$ ; **HRMS** calcd. For  $[\text{M}+\text{Na}]^+$ : 365.1907. Found: 365.1909.

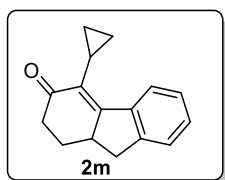


Compound **2k** was isolated as a white solid (M.P.: 103-105  $^{\circ}\text{C}$ ) in 61% yield.  $R_f = 0.6$  (EtOAc/Hexane=1/3).  **$^1\text{H NMR}$  (400 MHz,  $\text{CDCl}_3$ ):**  $\delta$  7.60 (d,  $J = 7.6$  Hz, 1H), 7.32 (dd,  $J = 26.6, 4.0$  Hz, 3H), 3.14 (dd,  $J = 15.2, 8.0$  Hz, 1H), 3.06 (ddt,  $J = 11.7, 7.8, 3.8$  Hz, 1H), 2.88 (td,  $J = 10.3, 8.6, 6.0$  Hz, 1H), 2.74 (dd,  $J = 15.2, 7.6$  Hz, 1H), 2.59 – 2.49 (m, 1H), 2.41 – 2.29 (m, 1H), 2.29 – 2.17 (m, 2H), 2.17 – 2.03 (m, 1H), 1.92 – 1.66 (m, 5H), 1.49 – 1.31 (m, 3H), 1.24 – 1.09 (m, 1H).  **$^{13}\text{C NMR}$  (100 MHz,  $\text{CDCl}_3$ ):**  $\delta$  199.55, 160.23, 148.49, 139.38, 136.71, 130.07, 126.78, 126.42, 125.30, 44.36, 39.18, 38.87, 37.90, 30.41, 29.92, 28.43, 27.27, 26.90, 25.97. **IR:**  $\nu$  2933,

2862, 1655, 1598, 1450, 1325, 1276, 1181, 986, 769, 733  $\text{cm}^{-1}$ ; **HRMS** calcd. For  $[\text{M}+\text{Na}]^+$ : 289.1563. Found: 289.15774.

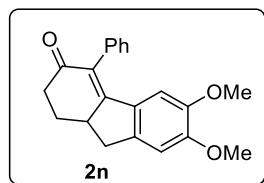


Compound **2l** was isolated as a colorless oil in 74% yield.  $R_f = 0.6$  (EtOAc/Hexane=1/3).  **$^1\text{H}$  NMR (400 MHz,  $\text{CDCl}_3$ ):**  $\delta$  7.66 (dd,  $J = 7.8, 1.0$  Hz, 1H), 7.37 – 7.31 (m, 2H), 7.31 – 7.24 (m, 1H), 3.45 – 3.31 (m, 1H), 3.19 – 3.02 (m, 2H), 2.80 – 2.71 (m, 1H), 2.56 (ddd,  $J = 17.5, 4.3, 2.3$  Hz, 1H), 2.42 – 2.31 (m, 1H), 2.23 (ddt,  $J = 10.1, 4.3, 2.3$  Hz, 1H), 2.03 – 1.88 (m, 5H), 1.71 – 1.52 (m, 4H).  **$^{13}\text{C}$  NMR (100 MHz,  $\text{CDCl}_3$ ):**  $\delta$  199.12, 160.93, 148.41, 139.53, 134.75, 130.09, 126.69, 126.20, 125.30, 44.58, 38.93, 38.52, 37.94, 31.24, 30.79, 28.35, 27.05, 26.91. **IR:**  $\nu$  2938, 2863, 1658, 1597, 1462, 1326, 1274, 1153, 943, 769, 733  $\text{cm}^{-1}$ ; **HRMS** calcd. For  $[\text{M}+\text{H}]^+$ : 253.1587. Found: 253.1602.

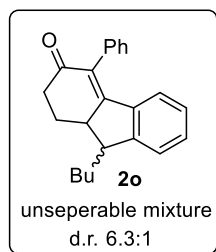


Compound **2m** was isolated as a colorless oil in 58% yield.  $R_f = 0.6$  (EtOAc/Hexane=1/3).  **$^1\text{H}$  NMR (400 MHz,  $\text{CDCl}_3$ ):**  $\delta$  8.02 (d,  $J = 7.8$  Hz, 1H), 7.40 – 7.26 (m, 3H), 3.22 – 3.08 (m, 2H), 2.78 – 2.66 (m, 1H), 2.58 (ddd,  $J = 17.6, 4.4, 2.3$  Hz, 1H), 2.41 (ddd,  $J = 17.6, 14.2, 5.0$  Hz, 1H), 2.29 – 2.21 (m, 1H), 1.79 (dddd,  $J = 14.2, 12.6, 11.8, 4.5$  Hz, 1H), 1.61 (ddt,  $J = 8.5, 5.6, 2.9$  Hz, 1H), 1.13 – 1.02 (m, 1H), 0.86 (dddd,  $J = 9.1, 7.9, 6.1, 4.5$  Hz, 1H), 0.49 – 0.42 (m, 1H), 0.35 – 0.26 (m, 1H).  **$^{13}\text{C}$  NMR (100 MHz,  $\text{CDCl}_3$ ):**  $\delta$  199.80, 164.00, 148.67, 138.66, 131.93, 130.47,

127.91, 126.35, 124.94, 43.98, 38.41, 37.56, 28.54, 9.59, 8.05, 7.91. **IR:**  $\nu$  2925, 2855, 1657, 1597, 1462, 1306, 1204, 1027, 997, 770, 734  $\text{cm}^{-1}$ ; **HRMS** calcd. For  $[\text{M}+\text{H}]^+$ : 225.1274. Found: 225.1290.

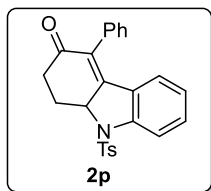


Compound **2n** was isolated as a colorless oil in 75% yield.  $R_f = 0.3$  (EtOAc/Hexane=1/3).  **$^1\text{H}$  NMR (400 MHz,  $\text{CDCl}_3$ ):**  $\delta$  7.57 – 7.27 (m, 4H), 7.05 (s, 1H), 6.78 (s, 1H), 5.85 (s, 1H), 3.87 (s, 3H), 3.38 – 3.26 (m, 1H), 3.31 (s, 3H), 3.20 (dd,  $J = 15.8, 7.9$  Hz, 1H), 2.78 (dd,  $J = 6.5, 2.3$  Hz, 1H), 2.74 (dd,  $J = 4.4, 2.2$  Hz, 1H), 2.60 (ddd,  $J = 17.2, 14.0, 4.9$  Hz, 1H), 2.39 (dtd,  $J = 12.0, 4.7, 2.4$  Hz, 1H), 2.02 (dtd,  $J = 13.7, 12.4, 4.4$  Hz, 1H).  **$^{13}\text{C}$  NMR (100 MHz,  $\text{CDCl}_3$ ):**  $\delta$  198.05, 163.76, 152.01, 147.88, 142.99, 135.74, 130.55, 130.36, 129.74, 128.70, 127.50, 108.16, 106.92, 55.96, 55.17, 43.42, 38.42, 37.04, 29.12. **IR:**  $\nu$  2937, 2835, 2250, 1647, 1590, 1490, 1464, 1322, 1293, 1220, 1189, 977, 750, 701  $\text{cm}^{-1}$ ; **HRMS** calcd. For  $[\text{M}+\text{H}]^+$ : 321.1485. Found: 321.1487.

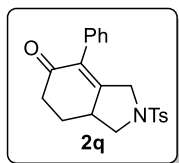


Compound **2o** was isolated as a colorless oil in 33% yield.  $R_f = 0.5$  (EtOAc/Hexane=1/5).  **$^1\text{H}$  NMR (500 MHz,  $\text{CDCl}_3$ ):**  $\delta$  7.50 – 7.34 (m, 3H), 7.28 (dd,  $J = 13.8, 7.4$  Hz, 2H), 7.14 (s, 2H), 6.90 (t,  $J = 7.5$  Hz, 1H), 6.38 (d,  $J = 7.8$  Hz, 1H), 3.45 – 3.24 (m, 0.21H), 3.04 – 2.84 (m, 1.87H), 2.82 – 2.69 (m, 1H), 2.59 (ddd,  $J = 17.4, 14.2, 4.9$  Hz, 1H), 2.52 – 2.36 (m, 1H), 2.26 – 2.14 (m, 0.23H), 2.11 – 1.92 (m, 1.88H), 1.80 – 1.63 (m, 1H), 1.54 – 1.35 (m, 3.94H), 1.35 – 1.18 (m,

0.83H), 0.96 (t,  $J = 7.1$  Hz, 2.78H), 0.88 (t,  $J = 6.9$  Hz, 0.41H).  **$^{13}\text{C}$  NMR (100 MHz,  $\text{CDCl}_3$ ):**  $\delta$  (major) 198.46, 161.95, 152.42, 137.91, 135.41, 132.23, 130.80, 129.75, 128.75, 127.67, 126.68, 126.45, 123.97, 49.41, 48.05, 38.49, 33.19, 29.23, 28.97, 23.20, 14.09. **IR:**  $\nu$  2928, 2858, 1661, 1594, 1463, 1330, 1274, 1179, 750, 700  $\text{cm}^{-1}$ ; **HRMS** calcd. For  $[\text{M}+\text{H}]^+$ : 317.1900. Found: 317.1900.

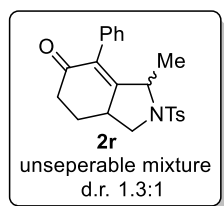


Compound **2p** was isolated as a light yellow oil in 42% yield.  $R_f = 0.5$  (EtOAc/Hexane=1/5).  **$^1\text{H}$  NMR (400 MHz,  $\text{CDCl}_3$ ):**  $\delta$  8.20 (dt,  $J = 8.5, 0.8$  Hz, 1H), 7.73 – 7.65 (m, 2H), 7.29 (ddd,  $J = 8.4, 7.2, 1.2$  Hz, 1H), 7.26 – 7.22 (m, 5H), 7.15 – 7.11 (m, 2H), 7.09 (ddd,  $J = 8.2, 7.3, 1.0$  Hz, 1H), 6.93 – 6.84 (m, 1H), 4.74 – 4.69 (m, 1H), 3.77 (dddd,  $J = 17.6, 7.5, 3.5, 0.8$  Hz, 1H), 3.34 (dddd,  $J = 18.1, 10.0, 6.5, 1.9$  Hz, 1H), 2.89 (ddd,  $J = 13.9, 10.0, 7.8$  Hz, 1H), 2.55 (dddd,  $J = 13.9, 6.5, 3.5, 1.1$  Hz, 1H), 2.38 (s, 3H).  **$^{13}\text{C}$  NMR (100 MHz,  $\text{CDCl}_3$ ):**  $\delta$  207.24, 145.18, 137.45, 136.74, 135.72, 134.49, 130.06, 128.85, 128.42, 128.01, 127.65, 126.40, 124.93, 123.72, 119.22, 118.58, 114.82, 53.23, 35.14, 24.64, 21.65. **IR:**  $\nu$  3028, 2921, 1718, 1597, 1451, 1371, 1247, 1170, 1149, 1090, 910, 746, 707, 659, 576, 541  $\text{cm}^{-1}$ ; **HRMS** calcd. For  $[\text{M}+\text{H}]^+$ : 416.1315. Found: 416.1315.

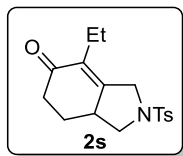


Compound **2q** was isolated as a white solid (M.P.: 158-160  $^{\circ}\text{C}$ ) in 73% yield.  $R_f = 0.3$  (EtOAc/Hexane=1/3).  **$^1\text{H}$  NMR (400 MHz,  $\text{CDCl}_3$ ):**  $\delta$  7.65 (d,  $J = 8.2$  Hz, 2H), 7.39 – 7.29 (m, 5H), 7.03 (d,  $J = 8.1$  Hz, 2H), 4.32 (dd,  $J = 17.6, 1.6$  Hz, 1H), 3.95 (dd,  $J = 9.5, 8.2$  Hz, 1H), 3.65

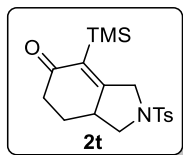
(dd,  $J = 17.6, 2.2$  Hz, 1H), 3.19 – 3.05 (m, 1H), 2.71 (dd,  $J = 10.5, 9.5$  Hz, 1H), 2.65 (ddd,  $J = 17.3, 4.4, 2.5$  Hz, 1H), 2.52 – 2.43 (m, 4H), 2.43 (s, 4H), 2.24 (ddt,  $J = 12.8, 4.9, 2.5$  Hz, 1H), 1.72 (dddd,  $J = 14.7, 12.9, 11.6, 4.4$  Hz, 1H).  **$^{13}\text{C}$  NMR (100 MHz,  $\text{CDCl}_3$ ):**  $\delta$  195.98, 158.93, 144.05, 134.48, 133.32, 132.91, 129.91, 129.01, 128.34, 128.11, 127.64, 127.35, 53.12, 51.13, 40.86, 36.93, 26.37, 21.59. **IR:**  $\nu$  3056, 2950, 2869, 1674, 1598, 1493, 1443, 1346, 1272, 1163, 1094, 1038, 912, 816, 733, 701, 679, 596, 550  $\text{cm}^{-1}$ ; **HRMS** calcd. For  $[\text{M}+\text{Na}]^+$ : 390.1134. Found: 390.1143.



Compound **2r** was isolated as a colorless oil in 70% yield.  $R_f = 0.5$  (EtOAc/Hexane=1/5).  **$^1\text{H}$  NMR (400 MHz,  $\text{CDCl}_3$ ):**  $\delta$  (major) 7.65 (d,  $J = 8.3$  Hz, 2H), 7.39 – 7.34 (m, 5H), 6.83 – 6.74 (m, 2H), 4.24 (qd,  $J = 6.6, 1.9$  Hz, 1H), 3.92 (dd,  $J = 9.2, 8.3$  Hz, 1H), 3.24 (ddd,  $J = 8.1, 4.8, 2.5$  Hz, 1H), 2.73 (dd,  $J = 10.4, 9.3$  Hz, 1H), 2.60 – 2.49 (m, 2H), 2.48 (s, 3H), 2.30 – 2.22 (m, 1H), 1.64 – 1.48 (m, 1H), 1.23 (d,  $J = 6.6$  Hz, 3H).  $\delta$  (minor)  **$^1\text{H}$  NMR (400 MHz, Chloroform- $d$ )**  $\delta$  7.80 – 7.73 (m, 2H), 7.41 – 7.29 (m, 5H), 7.07 – 6.99 (m, 2H), 4.97 (q,  $J = 6.8$  Hz, 1H), 3.98 (dd,  $J = 12.1, 8.3$  Hz, 1H), 3.05 (t,  $J = 11.8$  Hz, 1H), 2.65 (ddd,  $J = 17.7, 4.5, 2.2$  Hz, 1H), 2.45 (s, 3H), 2.44 – 2.30 (m, 2H), 2.13 (dtd,  $J = 12.1, 5.0, 2.2$  Hz, 1H), 1.71 (dtd,  $J = 14.5, 12.4, 4.5$  Hz, 1H), 0.87 (d,  $J = 6.8$  Hz, 3H).  **$^{13}\text{C}$  NMR (100 MHz,  $\text{CDCl}_3$ ):**  $\delta$  (mixture) 196.74, 196.67, 165.85, 162.51, 144.10, 143.90, 136.56, 134.72, 133.97, 133.68, 133.18, 132.94, 130.07, 129.78, 129.18, 129.00, 128.49, 128.48, 128.05, 128.01, 127.82, 127.02, 58.52, 58.48, 54.11, 50.55, 42.07, 37.84, 36.97, 36.61, 26.56, 26.45, 22.19, 21.63, 21.60, 18.89. **IR:**  $\nu$  2931, 2869, 1675, 1597, 1493, 1344, 1275, 1162, 1093, 915, 817, 751, 701, 659, 575, 550  $\text{cm}^{-1}$ ; **HRMS** calcd. For  $[\text{M}+\text{H}]^+$ : 382.1471. Found: 382.1475.

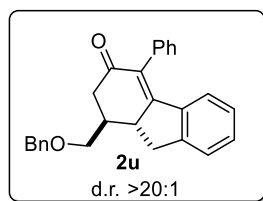


Compound **2s** was isolated as a colorless oil in 71% yield.  $R_f = 0.3$  (EtOAc/Hexane=1/3).  **$^1\text{H}$  NMR (400 MHz,  $\text{CDCl}_3$ ):**  $\delta$  7.74 (d,  $J = 8.3$  Hz, 2H), 7.37 (d,  $J = 7.9$  Hz, 2H), 4.26 (d,  $J = 16.6$  Hz, 1H), 3.89 (dd,  $J = 9.2, 7.9$  Hz, 1H), 3.82 (dd,  $J = 16.9, 2.5$  Hz, 1H), 2.96 (q,  $J = 11.7$  Hz, 1H), 2.59 (dd,  $J = 10.9, 9.2$  Hz, 1H), 2.49 (ddd,  $J = 17.1, 4.3, 2.3$  Hz, 5H), 2.45 (s, 4H), 2.30 (ddd,  $J = 17.2, 14.6, 4.9$  Hz, 1H), 2.23 – 2.08 (m, 2H), 2.03 (qd,  $J = 7.5, 6.1$  Hz, 1H), 1.55 (dddd,  $J = 14.5, 12.6, 11.7, 4.4$  Hz, 1H), 0.91 (t,  $J = 7.5$  Hz, 3H).  **$^{13}\text{C}$  NMR (100 MHz,  $\text{CDCl}_3$ ):**  $\delta$  196.95, 156.63, 144.11, 134.63, 132.56, 129.92, 127.73, 53.42, 50.11, 40.57, 36.73, 26.54, 21.60, 19.58, 12.89. **IR:**  $\nu$  2965, 2872, 1667, 1598, 1453, 1346, 1164, 1094, 1041, 913, 815, 732, 675, 593, 550  $\text{cm}^{-1}$ ; **HRMS** calcd. For  $[\text{M}+\text{Na}]^+$ : 320.1315. Found: 320.1308.

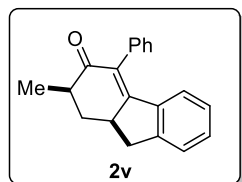


Compound **2t** was isolated as a white solid (M.P.: 138-140  $^{\circ}\text{C}$ ) in 37% yield.  $R_f = 0.4$  (EtOAc/Hexane=1/5).  **$^1\text{H}$  NMR (400 MHz,  $\text{CDCl}_3$ ):**  $\delta$  7.72 (d,  $J = 8.2$  Hz, 2H), 7.37 (dd,  $J = 8.6, 0.7$  Hz, 2H), 4.30 (dd,  $J = 17.3, 1.3$  Hz, 1H), 3.87 (dd,  $J = 9.0, 8.1$  Hz, 1H), 3.81 (dd,  $J = 17.3, 2.4$  Hz, 1H), 2.86 (dd,  $J = 12.3, 6.6$  Hz, 1H), 2.51 (dd,  $J = 11.0, 9.3$  Hz, 1H), 2.46 (s, 3H), 2.45 – 2.40 (m, 1H), 2.27 (ddd,  $J = 17.2, 14.4, 5.2$  Hz, 1H), 2.12 (dtd,  $J = 12.4, 5.0, 2.3$  Hz, 1H), 1.54 (dtd,  $J = 14.4, 12.3, 4.6$  Hz, 1H), 0.15 (s, 9H).  **$^{13}\text{C}$  NMR (100 MHz,  $\text{CDCl}_3$ ):**  $\delta$  201.09, 170.41, 144.14, 134.08, 132.34, 129.92, 127.80, 52.42, 52.22, 42.05, 36.75, 25.99, 21.61, 0.39. **IR:**  $\nu$  2924, 2852,

1659, 1600, 1453, 1349, 1262, 1165, 1094, 875, 841, 665, 597, 550  $\text{cm}^{-1}$ ; **HRMS** calcd. For  $[\text{M}+\text{Na}]^+$ : 364.1397. Found: 364.1400.



Compound **2u** was isolated as a colorless oil in 40% yield (d.r. >20:1).  $R_f = 0.3$  (EtOAc/Hexane=1/4).  **$^1\text{H}$  NMR (500 MHz,  $\text{CDCl}_3$ )**:  $\delta$  7.55 – 7.27 (m, 9H), 7.23 (m, 3H), 6.91 (t,  $J = 7.6$  Hz, 1H), 6.41 (d,  $J = 7.9$  Hz, 1H), 4.62 (d,  $J = 12.0$  Hz, 1H), 4.57 (d,  $J = 12.1$  Hz, 1H), 3.69 – 3.58 (m, 2H), 3.27 (ddt,  $J = 30.5, 15.5, 7.9$  Hz, 2H), 2.84 (ddd,  $J = 21.2, 16.2, 5.4$  Hz, 2H), 2.64 (dd,  $J = 16.9, 13.3$  Hz, 1H), 2.52 – 2.39 (m, 1H).  **$^{13}\text{C}$  NMR (100 MHz,  $\text{CDCl}_3$ )**:  $\delta$  198.40, 162.04, 148.43, 138.26, 138.23, 135.23, 132.40, 130.75, 129.62, 128.72, 128.45, 127.69, 127.52, 126.60, 125.14, 73.32, 72.20, 45.31, 41.76, 41.62, 35.86. **IR**:  $\nu$  3060, 2856, 1657, 1594, 1463, 1313, 1108, 1073, 776, 737, 699  $\text{cm}^{-1}$ ; **HRMS** calcd. For  $[\text{M}+\text{H}]^+$ : 381.1849. Found: 381.1848. The stereochemistry was tentatively assigned according to the stereochemistry of starting material **1v**.



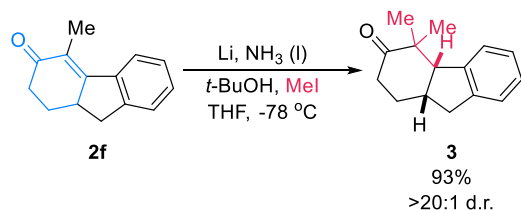
Compound **2v** (major) was isolated as a white solid (M.P.: 123-125  $^{\circ}\text{C}$ ) in 33% yield and **2v** (minor) was isolated as a white solid in 13% (d.r. =2.5:1 based on isolated yield).  $R_f = 0.4$  (EtOAc/Hexane=1/4).  **$^1\text{H}$  NMR (500 MHz,  $\text{CDCl}_3$ )**:  $\delta$  (major) 7.49 – 7.33 (m, 3H), 7.30 (d,  $J = 7.6$  Hz, 1H), 7.25 – 6.96 (m, 3H), 6.91 (t,  $J = 7.6$  Hz, 1H), 6.44 (d,  $J = 7.9$  Hz, 1H), 3.41 – 3.32 (m, 1H), 3.24 (dd,  $J = 15.8, 8.1$  Hz, 1H), 2.80 (dd,  $J = 15.8, 7.3$  Hz, 1H), 2.59 (dq,  $J = 13.5, 6.7$ ,



4.3 Hz, 1H), 2.44 (dt,  $J = 12.5, 4.4$  Hz, 1H), 1.85 (q,  $J = 12.6$  Hz, 1H), 1.27 (d,  $J = 6.8$  Hz, 3H).  $\delta$  (minor) 7.48 – 7.35 (m, 3H), 7.34 – 7.27 (m, 2H), 7.25 – 7.08 (m, 2H), 6.91 (t,  $J = 7.6$  Hz, 1H), 6.40 (d,  $J = 7.9$  Hz, 1H), 3.56 – 3.42 (m, 1H), 3.24 (dd,  $J = 15.8, 8.0$  Hz, 1H), 2.85 – 2.71 (m, 2H), 2.35 – 2.15 (m, 2H), 1.38 (d,  $J = 7.6$  Hz, 3H).  **$^{13}\text{C}$  NMR (100 MHz,  $\text{CDCl}_3$ ):**  $\delta$  (major) 200.66, 161.82, 148.52, 138.56, 135.61, 132.05, 130.54, 129.73, 128.59, 127.50, 126.55, 126.46, 125.10, 43.03, 42.25, 37.66, 37.34, 16.20. **IR:**  $\nu$  3020, 2928, 2852, 1658, 1595, 1462, 1372, 1330, 1179, 1093, 774, 731, 699  $\text{cm}^{-1}$ ; **HRMS** calcd. For  $[\text{M}+\text{Na}]^+$ : 297.1250. Found: 297.1253. The major diastereomer's stereochemistry was assigned according to 2-D NMR (see in **2-D NMR spectra**).

#### 4.4.6 Procedures and data for synthetic applications

##### a) Dissolving metal reduction followed by alkylation of **2f**: synthesis of **3**



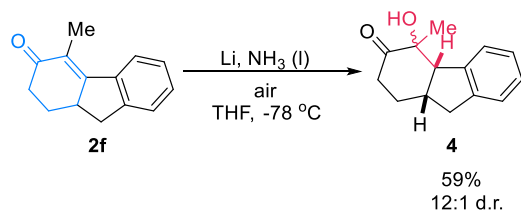
##### Procedure:<sup>22</sup>

1 mL liquid ammonia was condensed in a 10 mL Schlenk flask at  $-78\text{ }^\circ\text{C}$  and nitrogen atmosphere was introduced after condensation. A solution of **2f** (20.0 mg, 0.1 mmol, 1 equiv.) and  $t\text{-BuOH}$  (8.2 mg, 0.11 mmol, 1.1 equiv.) in anhydrous tetrahydrofuran (1 mL) was added dropwise to the stirring liquid ammonia at  $-78\text{ }^\circ\text{C}$ . Under  $\text{N}_2$  flow, the rubber stopper of Schlenk flask was removed and pieces of lithium (6.9 mg, 1.0 mmol, 10 equiv.) was added to the stirring mixture. After stirring at  $-78\text{ }^\circ\text{C}$  for 3 h, iodomethane (851.3 mg, 6 mmol, 60 equiv.) was injected into the flask and stirred for another 3 h. 1 mL of saturated aqueous ammonia chloride solution was injected to the flask and the system was opened and slowly warmed up to room temperature. After the ammonia was removed, the reaction was diluted with ether (10 mL) and washed with sat.  $\text{NH}_4\text{Cl}$  (aq.) solution

(20 mL) and brine (20 mL). The combined organic extract was dried by  $\text{MgSO}_4$  and concentrated under reduced pressure. The crude product was purified with silica gel flash column chromatography (EtOAc/Hexane= 1/10 to 1/5) to afford compound **3** as a white solid in 93% yield (20.0 mg).

Compound **3** was isolated as a white solid (M.P.: 70-72 °C) in 93% yield (d.r. >20:1).  $R_f$  = 0.6 (EtOAc/Hexane=1/5).  **$^1\text{H}$  NMR (500 MHz,  $\text{CDCl}_3$ ):**  $\delta$  7.30 – 7.26 (m, 1H), 7.25 – 7.14 (m, 3H), 3.30 (d,  $J$  = 8.7 Hz, 1H), 3.16 – 3.02 (m, 1H), 2.98 – 2.81 (m, 2H), 2.60 (ddd,  $J$  = 15.7, 6.2, 4.4 Hz, 1H), 2.41 (ddd,  $J$  = 15.7, 11.4, 5.2 Hz, 1H), 2.26 (dddd,  $J$  = 13.7, 7.4, 6.1, 5.1 Hz, 1H), 1.98 (dddd,  $J$  = 14.0, 11.5, 7.9, 4.4 Hz, 1H), 1.28 (s, 3H), 0.81 (s, 3H).  **$^{13}\text{C}$  NMR (100 MHz,  $\text{CDCl}_3$ ):**  $\delta$  217.10, 144.29, 143.28, 127.11, 126.13, 125.74, 124.78, 53.78, 48.12, 39.59, 38.03, 36.68, 26.37, 24.90, 22.63. **IR:**  $\nu$  2969, 2932, 1707, 1458, 1378, 1319, 1224, 1177, 1098, 940, 754, 735  $\text{cm}^{-1}$ ; **HRMS** calcd. For  $[\text{M}+\text{H}]^+$ : 215.1430. Found: 215.1430.

#### b) Dissolving metal reduction followed by oxidation of **2f**: synthesis of **4**



#### Procedure:<sup>23</sup>

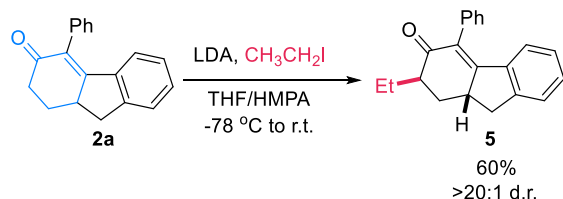
1 mL liquid ammonia was condensed in a 10 mL Schlenk flask at -78 °C and nitrogen atmosphere was introduced after condensation. A solution of **2f** (12.0 mg, 0.06 mmol, 1 equiv.) in anhydrous tetrahydrofuran (1 mL) was added dropwise to the stirring liquid ammonia at -78 °C. Under  $\text{N}_2$  flow, the rubber stopper of Schlenk flask was removed and pieces of lithium (1.8 mg, 0.27 mmol, 4.4 equiv.) was added to the stirring mixture. After stirring at -78 °C for 3 h, 1 mL of saturated aqueous ammonia chloride solution was injected to the flask and the system was opened and slowly

warmed up to room temperature. After the ammonia was removed, the reaction was diluted with ether (10 mL) and washed with sat.  $\text{NH}_4\text{Cl}$  (aq.) solution (20 mL) and brine (20 mL). The combined organic extract was dried by  $\text{MgSO}_4$  and concentrated under reduced pressure. The crude product was purified with silica gel flash column chromatography (EtOAc/Hexane= 1/10 to 1/5) to afford compound **4** as a colorless oil in 59% yield (7.7 mg). (note: The d.r. of **4** decreased if being kept in chloroform).

Compound **4** was isolated as a colorless oil in 59% yield (d.r.=12:1).  $R_f$ = 0.4 (EtOAc/Hexane=1/5).

**$^1\text{H}$  NMR (400 MHz,  $\text{CDCl}_3$ ):**  $\delta$  9.37 – 9.22 (m, 1H), 7.44 – 7.38 (m, 1H), 7.26 – 7.19 (m, 3H), 4.00 (d,  $J$  = 9.6 Hz, 1H), 3.18 (dd,  $J$  = 15.7, 8.7 Hz, 1H), 3.07 – 2.94 (m, 1H), 2.87 (dd,  $J$  = 15.7, 8.9 Hz, 1H), 2.68 (ddd,  $J$  = 16.8, 6.6, 5.1 Hz, 1H), 2.49 (ddd,  $J$  = 16.7, 10.2, 5.4 Hz, 1H), 2.23 (ddd,  $J$  = 13.8, 6.8, 1.4 Hz, 1H), 2.02 (ddd,  $J$  = 10.3, 8.5, 5.0 Hz, 1H), 1.02 (s, 3H).  **$^{13}\text{C}$  NMR (100 MHz,  $\text{CDCl}_3$ ):**  $\delta$  214.20, 143.31, 141.09, 127.50, 126.72, 126.61, 124.51, 88.91, 48.99, 38.87, 37.11, 36.74, 26.43, 18.25. **IR:**  $\nu$  3300, 2934, 1717, 1458, 1275, 1260, 913, 764, 749  $\text{cm}^{-1}$ ; **HRMS** calcd. For  $[\text{M}+\text{H}-(\text{H}_2\text{O})]^+$ : 199.1117. Found: 199.1114.

### c) $\alpha$ -alkylation of **2a**: synthesis of **5**



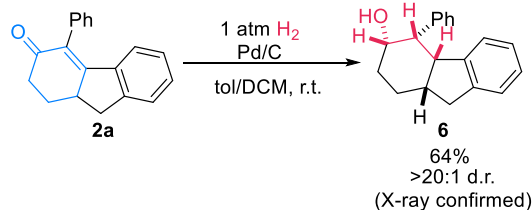
#### Procedure:

To a 10 mL flamed-dried Schlenk flask equipped with a nitrogen-filled balloon was added THF (2.3 mL) and freshly distilled  $i\text{-Pr}_2\text{NH}$  (506.0 mg, 0.7 mL, 5.0 mmol, 1 equiv.). The reaction mixture was cooled to  $-78\text{ }^\circ\text{C}$  with an acetone-dry ice bath and  $n\text{-BuLi}$  (2.5 M in hexane, 2.0 mL, 5 mmol, 1 equiv.) was added dropwise. Upon completion, the system was warmed to  $0\text{ }^\circ\text{C}$  and

stirred for 0.5 h under nitrogen atmosphere. Meanwhile, to another 10 mL flamed-dried flask equipped with a nitrogen-filled balloon were added compound **2a** (26 mg, 0.1 mmol, 1 equiv.) and THF (5 mL). After cooling to -78 °C with an acetone-dry ice bath, the newly made LDA solution as indicated above (1 M in THF/Hexane, 2.0 mL, 2.00 mmol, 20 equiv.) was added dropwise and the reaction was warmed up to -20 °C for 0.5 h. After that, the reaction was cooled to -78 °C again and EtI (779.9 mg, 0.4 mL, 5 mmol, 50 equiv.) was added dropwise. The reaction was gradually warmed up to room temperature for 3 h and was quenched by adding NH<sub>4</sub>Cl (sat.) 5 mL. The mixture was extracted with diethyl ether (10 mL×3), washed with brine, and dried with Na<sub>2</sub>SO<sub>4</sub>. The combined organic extract was concentrated under reduced pressure and purified by silica gel flash column chromatography (EtOAc/Hexane=1/10) on silica gel to afford compound **5** as a colorless oil in 60% yield (d.r. >20:1). The relative stereochemistry was determined by 2-D NMR (see in **2-D NMR spectra**).

Compound **5** was isolated as a colorless oil in 60% yield (d.r. >20:1).  $R_f$  = 0.6 (EtOAc/Hexane=1/5). **<sup>1</sup>H NMR (400 MHz, CDCl<sub>3</sub>)**: δ 7.48 – 7.34 (m, 3H), 7.33 – 7.29 (m, 1H), 7.23 (td,  $J$  = 7.5, 1.2 Hz, 1H), 7.14 (s, 2H), 6.95 – 6.88 (m, 1H), 6.41 (dt,  $J$  = 8.0, 0.9 Hz, 1H), 3.43 (ddt,  $J$  = 12.3, 7.7, 3.9 Hz, 1H), 3.22 (dd,  $J$  = 15.7, 8.0 Hz, 1H), 2.80 (dd,  $J$  = 15.7, 7.5 Hz, 1H), 2.51 (dtt,  $J$  = 6.7, 4.9, 2.5 Hz, 1H), 2.38 (ddd,  $J$  = 13.1, 4.6, 2.0 Hz, 1H), 2.26 – 2.12 (m, 1H), 1.93 – 1.68 (m, 2H), 1.09 (t,  $J$  = 7.4 Hz, 3H). **<sup>13</sup>C NMR (100 MHz, CDCl<sub>3</sub>)**: δ 201.10, 161.14, 148.74, 138.54, 135.64, 131.73, 130.53, 129.82, 128.65, 127.56, 126.57, 126.56, 125.08, 47.45, 38.38, 37.54, 32.18, 23.05, 12.39. **IR**: ν 2930, 1654, 1462, 1337, 1275, 1260, 1177, 764, 749, 699 cm<sup>-1</sup>; **HRMS** calcd. For [M+H]<sup>+</sup>: 289.1587. Found: 289.1589.

d) H<sub>2</sub>/ (Pd/C) reduction of **2a**: synthesis of **6**

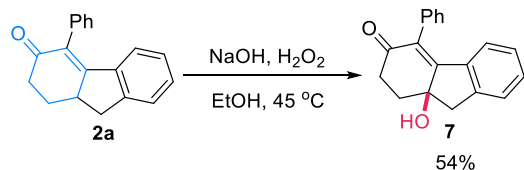


#### Procedure:

A 10 mL Schlenk flask was charged with **2a** (26 mg, 0.1 mmol, 1 equiv.) and Pd/C (26.0 mg, 0.24 mmol, 2.4 equiv.) before it was degassed and backfilled with hydrogen three times. After that, toluene (1 mL) and dichloromethane (1 mL) were injected into the flask. A balloon of hydrogen was kept on top of the flask. After stirring at room temperature overnight, the reaction was diluted with dichloromethane (10 mL) and filtered through a filtration paper. The resulting solution was concentrated under reduced pressure and purified by silica gel flash column chromatography (EtOAc/Hexane= 1/10 to 1/5) to afford compound **6** as a bright yellow oil in 64% yield (17.0 mg). The stereochemistry was determined by X-ray crystallography.

Compound **6** was isolated as a white solid (M.P.: 110-112 °C) in 64% yield (d.r.>20:1).  $R_f$  = 0.6 (EtOAc/Hexane=1/5).  **$^1\text{H}$  NMR (400 MHz,  $\text{CDCl}_3$ ):**  $\delta$  7.77 (dt,  $J$  = 8.4, 1.1 Hz, 2H), 7.42 (dd,  $J$  = 8.4, 7.0 Hz, 2H), 7.30 (td,  $J$  = 7.5, 1.0 Hz, 1H), 7.20 (t,  $J$  = 6.6 Hz, 1H), 7.08 – 7.02 (m, 1H), 6.88 – 6.82 (m, 1H), 6.48 (d,  $J$  = 7.6 Hz, 1H), 4.72 – 4.62 (m, 1H), 3.97 (t,  $J$  = 5.7 Hz, 1H), 3.34 (d,  $J$  = 4.3 Hz, 1H), 3.08 – 2.77 (m, 1H), 2.69 – 2.57 (m, 1H), 2.59 (d,  $J$  = 15.5 Hz, 1H), 1.95 (dq,  $J$  = 13.6, 3.5 Hz, 1H), 1.65 (tdd,  $J$  = 13.5, 4.6, 2.2 Hz, 1H), 1.56 – 1.42 (m, 3H).  **$^{13}\text{C}$  NMR (100 MHz,  $\text{CDCl}_3$ ):**  $\delta$  144.16, 143.77, 142.35, 128.58, 127.66, 126.48, 126.16, 126.14, 125.74, 125.46, 68.36, 47.01, 45.13, 40.95, 38.60, 32.89, 21.50. **IR:**  $\nu$  3580, 3022, 2926, 2854, 1456, 1275, 973, 913, 763, 748, 698  $\text{cm}^{-1}$ ; **HRMS** calcd. For  $[\text{M}+\text{H}-(\text{H}_2\text{O})]^+$ :247.1481. Found: 247.1484.

#### e) Epoxidation of **2a**: synthesis of **7**



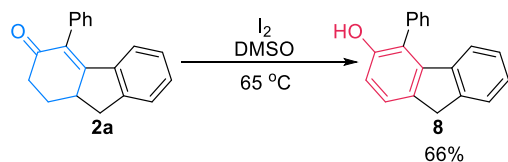
#### Procedure:

A 20 mL vial was charged with **2a** (26 mg, 0.1 mmol, 1 equiv.) in 10 mL anhydrous ethanol, NaOH (12 mg, 0.3 mmol, 3.0 equiv.) and H<sub>2</sub>O<sub>2</sub> (28 L, 1 mmol, 10 equiv.). After stirring at 45 °C overnight, the reaction was diluted with dichloromethane and filtered through a pad of silica gel and MgSO<sub>4</sub>. The combined organic extract was concentrated under reduced pressure and purified by silica gel flash column chromatography (EtOAc/Hexane=1/5 to 1/1) to afford compound **7** as a colorless oil in 54% yield.

Compound **7** was isolated as a colorless oil in 54% yield (14.9 mg). *R<sub>f</sub>* = 0.2 (EtOAc/Hexane=1/1).

**<sup>1</sup>H NMR (400 MHz, CDCl<sub>3</sub>):** δ 7.52 – 7.37 (m, 3H), 7.38 – 7.23 (m, 2H), 7.16 (s, 2H), 7.00 – 6.92 (m, 1H), 6.47 (d, *J* = 7.9 Hz, 1H), 3.24 (d, *J* = 16.6 Hz, 1H), 3.18 (d, *J* = 16.6 Hz, 1H), 3.09 (ddd, *J* = 17.7, 13.3, 5.4 Hz, 1H), 2.66 (ddd, *J* = 17.7, 4.9, 1.9 Hz, 1H), 2.55 (ddd, *J* = 13.6, 5.4, 1.9 Hz, 1H), 2.36 (td, *J* = 13.4, 4.9 Hz, 1H), 2.29 – 2.09 (m, 1H). **<sup>13</sup>C NMR (100 MHz, CDCl<sub>3</sub>):** δ 198.30, 158.52, 146.11, 136.32, 134.40, 133.35, 131.36, 129.30, 128.80, 128.05, 127.56, 127.17, 125.95, 77.21, 46.43, 33.65, 33.53. **IR:** ν 3404, 3058, 2924, 2245, 1647, 1595, 1463, 1442, 1331, 1275, 1192, 1064, 1004, 960, 906, 750, 733, 699 cm<sup>-1</sup>; **HRMS** calcd. For [M+H]<sup>+</sup>: 277.1223. Found: 277.1225.

#### f) Oxidation of **2a**: synthesis of **8**



#### Procedure:<sup>14</sup>

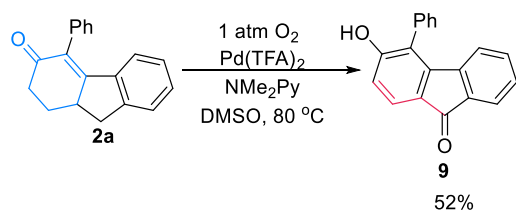
A 4 mL vial was charged with **2a** (20 mg, 0.077 mmol, 1 equiv.) in 0.5 mL anhydrous DMSO and I<sub>2</sub> (4.9 mg, 0.038 mmol, 0.5 equiv.) under nitrogen atmosphere. After stirring at 65 °C overnight, the reaction was diluted with ethyl acetate (10 mL) and washed with saturated Na<sub>2</sub>S<sub>2</sub>O<sub>3</sub> aqueous solution (10 mL). Then the organic phase was washed with brine (10 mL) and dried by a pad of MgSO<sub>4</sub>. The combined organic extract was concentrated under reduced pressure and purified by silica gel flash column chromatography (EtOAc/Hexane=1/10 to 1/5) to afford compound **8** as a light yellow oil in 66% yield (13.2 mg).

Compound **8** was isolated as a colorless oil in 66% yield (13.2 mg). *R<sub>f</sub>* = 0.6 (EtOAc/Hexane=1/5).

**<sup>1</sup>H NMR (400 MHz, CDCl<sub>3</sub>):** δ 7.65 – 7.53 (m, 3H), 7.52 – 7.41 (m, 4H), 7.19 (td, *J* = 7.4, 1.1 Hz, 1H), 7.03 – 6.96 (m, 2H), 6.51 (dt, *J* = 7.9, 0.9 Hz, 1H), 4.82 (t, *J* = 0.8 Hz, 1H), 3.88 (s, 2H).

**<sup>13</sup>C NMR (100 MHz, CDCl<sub>3</sub>):** δ 152.04, 144.71, 141.52, 140.03, 135.52, 134.44, 130.45, 129.90, 128.88, 126.33, 126.23, 125.11, 124.84, 122.92, 122.33, 113.66, 36.22. **IR:** ν 3511, 3050, 2887, 1595, 1478, 1444, 1424, 1276, 1231, 1170, 912, 763, 747, 701 cm<sup>-1</sup>; **HRMS** calcd. For [M+H]<sup>+</sup>: 259.1117. Found: 259.1117.

#### g) Aerobic Oxidation of **2a**: synthesis of **9**



#### Procedure:<sup>15</sup>

A 8 mL rubber-head test tube was charged with **2a** (26 mg, 0.1 mmol, 1 equiv.) in 0.5 mL anhydrous DMSO, Pd(TFA)<sub>2</sub> (1.7 mg, 0.005 mmol, 5 mol%), 2-Me<sub>2</sub>NPy (1.2 mg, 0.01 mmol, 10 mol%) and TsOH (3.8 mg, 0.02 mmol, 20 mol%) before purging oxygen through the solution for

5 min. A balloon of oxygen was kept on top of the test tube through the rubber. After stirring at 80 °C overnight, the reaction was diluted with ethyl acetate (10 mL) and washed with brine (10 mL) and dried by a pad of MgSO<sub>4</sub>. The combined organic extract was concentrated under reduced pressure and purified by silica gel flash column chromatography (EtOAc/Hexane= 1/5) to afford compound **9** as a bright yellow oil in 52% yield (13.5 mg).

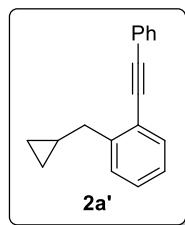
Compound **9** was isolated as a yellow oil in 52% yield (13.5 mg).  $R_f = 0.3$  (EtOAc/Hexane=1/5).

**<sup>1</sup>H NMR (400 MHz, CDCl<sub>3</sub>):**  $\delta$  7.68 – 7.57 (m, 5H), 7.45 (dd,  $J = 7.7, 1.7$  Hz, 2H), 7.17 (td,  $J = 7.4, 1.1$  Hz, 1H), 7.10 (td,  $J = 7.6, 1.3$  Hz, 1H), 6.88 (d,  $J = 8.1$  Hz, 1H), 6.27 (dt,  $J = 7.5, 0.9$  Hz, 1H), 5.53 (s, 1H). **<sup>13</sup>C NMR (100 MHz, CDCl<sub>3</sub>):**  $\delta$  192.61, 159.14, 144.11, 143.32, 135.55, 133.86, 132.63, 130.16, 130.11, 129.57, 128.86, 127.30, 125.90, 124.28, 123.80, 122.60, 114.91. **IR:**  $\nu$  3246, 1685, 1603, 1575, 1420, 1380, 1275, 1184, 1097, 942, 903, 834, 763, 749, 699 cm<sup>-1</sup>; **HRMS** calcd. For [M+H]<sup>+</sup>: 273.0910. Found: 273.0914.

#### 4.4.7 Mechanistic study

##### I. Subjecting **2a'** to carbonylative (3+2+1) conditions

**2a'** was obtained as a side product from the key reaction of **1a**.

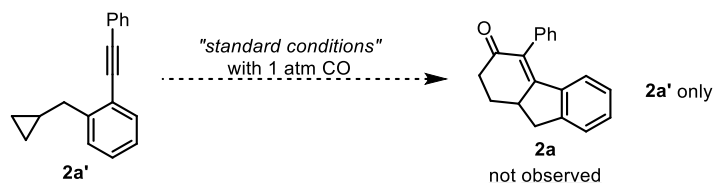


Compound **2a'** was isolated as a colorless oil.  $R_f = 0.8$  (EtOAc/Hexane=1/5). **<sup>1</sup>H NMR (400 MHz, CDCl<sub>3</sub>):**  $\delta$  7.53 (ddd,  $J = 6.6, 5.2, 1.9$  Hz, 3H), 7.40 – 7.33 (m, 4H), 7.32 – 7.27 (m, 1H), 7.21 (dd,  $J = 7.5, 1.4$  Hz, 1H), 2.81 (d,  $J = 6.9$  Hz, 2H), 1.20 – 1.07 (m, 1H), 0.58 – 0.49 (m, 2H), 0.29 (dt,  $J = 6.0, 4.5$  Hz, 2H). **<sup>13</sup>C NMR (100 MHz, CDCl<sub>3</sub>):**  $\delta$  <sup>13</sup>C NMR (101 MHz, Chloroform-*d*)  $\delta$



144.19, 132.06, 131.46, 128.55, 128.40, 128.36, 128.16, 125.81, 123.56, 122.54, 92.91, 88.45, 38.79, 11.27, 4.67. **IR:**  $\nu$  3060, 3000, 2923, 1599, 1492, 1442, 1016, 754, 689  $\text{cm}^{-1}$ ; **HRMS** calcd. For  $[\text{M}+\text{H}]^+$ : 233.1325. Found: 233.1311.

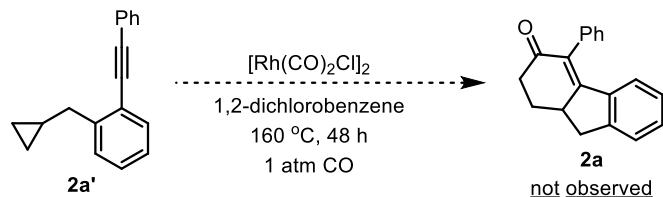
a) Utilizing “standard conditions” with 1 atm CO



#### Procedure:

In a nitrogen-filled glovebox, a flame dried reaction tube, containing a magnetic stirrer, was charged with **2a'** (19.0 mg, 0.082 mmol, 1 equiv.) in FPT 1,4-dioxane (0.8 mL).  $\text{PMe}_2\text{Ph}$  (1.81 mg, 0.0131 mmol, 16 mol%) and  $[\text{Rh}(\text{CO})_2\text{Cl}]_2$  (1.6 mg, 0.0041 mmol, 5 mol%) were added as a stock solution to the system. The tube was sealed with a rubber septum and the reaction mixture was sparged with CO for 2 minutes, then heated at 125 °C under a CO atmosphere (1 atm.) for 60 h. The mixture was cooled to room temperature and filtered through a pad of silica gel to afford >90% recovery of **2a'** indicated by crude  $^1\text{H}$ -NMR.

b) Narasaka's (3+2+1) condition

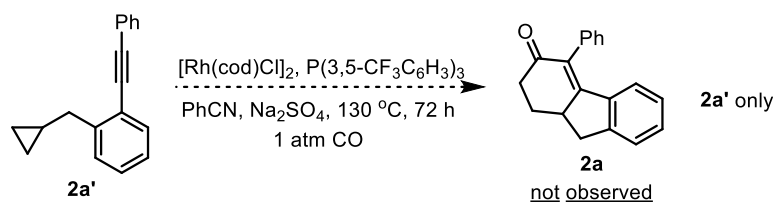


#### Procedure:<sup>8</sup>

A flame-dried reaction tube, fitted with a magnetic stirrer, was charged with  $[\text{Rh}(\text{CO})_2\text{Cl}]_2$  (3.0 mg, 0.0075 mmol, 10 mol%) in a nitrogen-filled glovebox. Compound **2a'** (18.0 mg, 0.077 mmol,

1 equiv.) in a nitrogen sparged anhydrous 1,2-dichlorobenzene (300  $\mu$ L) was added via syringe. The reaction mixture was sparged with CO for 2 minutes, and then heated at 160  $^{\circ}$ C under a CO atmosphere (1 atm.) for 48 h. The mixture was cooled to r.t. and filtered through a pad of silica gel to afford a crude mixture which has no NMR signal from **2a'** or **2a** indicated by crude NMR.

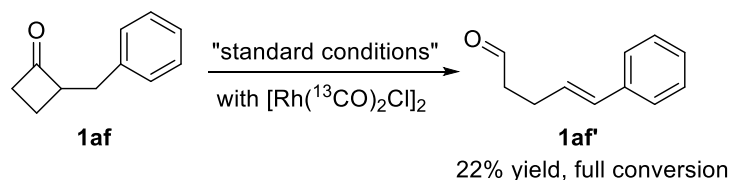
c) Bower's (3+2+1) condition



#### Procedure:<sup>10</sup>

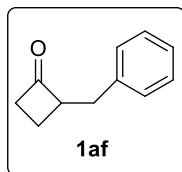
An oven-dried reaction tube, fitted with a magnetic stirrer, was charged with  $[\text{Rh}(\text{cod})\text{Cl}]_2$  (1.0 mg, 0.002 mmol, 3.75 mol%),  $\text{P}(3,5\text{-(CF}_3)_2\text{Ph})_3$  (5.5 mg, 0.0082 mmol, 15 mol%) and  $\text{Na}_2\text{SO}_4$  (1.6 mg, 0.011, 20 mol%). The tube was fitted with a rubber septum and purged with nitrogen. Compound **2a'** (12.8 mg, 0.055 mmol, 1 equiv.) in a nitrogen sparged anhydrous benzonitrile solution (0.07 M) was added via syringe. The reaction mixture was sparged with CO for 2 minutes, and then heated at 130  $^{\circ}$ C under a CO atmosphere (1 atm.) for 72 h. The mixture was cooled to r.t. and filtered through a pad of silica gel to afford >90% recovery of **2a'** indicated by crude NMR.

#### *II. Subjecting **1w** to standard conditions*

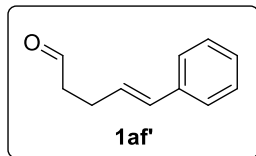


Compound **1af** was synthesized according to literature known procedure and matched the reported characterization data<sup>24</sup>. Adopting the aforementioned standard procedure for C-C activation

reaction, **1af'** was isolated as the only characterizable product and its spectra matched the reported data<sup>25</sup>.



Compound **1af** was isolated as a colorless oil in 56% yield from compound **10** and benzyl bromide.  $R_f = 0.7$  (EtOAc/Hexane=1/5). **<sup>1</sup>H NMR (500 MHz, CDCl<sub>3</sub>):**  $\delta$  7.29 (dd,  $J = 8.2, 6.8$  Hz, 2H), 7.22 (s, 1H), 7.20 – 7.16 (m, 2H), 3.71 – 3.53 (m, 1H), 3.11 – 2.98 (m, 2H), 2.89 (ddd,  $J = 9.7, 5.1, 2.8$  Hz, 1H), 2.81 (dd,  $J = 14.4, 9.0$  Hz, 1H), 2.23 – 2.10 (m, 1H), 1.75 (ddt,  $J = 11.2, 9.6, 7.6$  Hz, 1H).

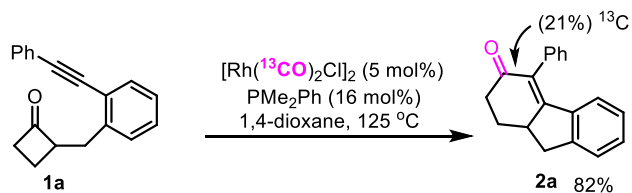


Compound **1af'** was isolated as a colorless oil in 22% yield from **1af**.  $R_f = 0.5$  (EtOAc/Hexane=1/5). **<sup>1</sup>H NMR (400 MHz, CDCl<sub>3</sub>):**  $\delta$  9.83 (s, 1H), 7.38 – 7.28 (m, 3H), 7.21 (t,  $J = 8.7$  Hz, 2H), 6.44 (d,  $J = 15.9$  Hz, 2H), 6.21 (dt,  $J = 15.4, 6.4$  Hz, 2H), 2.70 – 2.60 (t,  $J = 7.1$  Hz, 2H), 2.61 – 2.53 (t,  $J = 7.0$  Hz, 2H).

### III. <sup>13</sup>CO labeling study

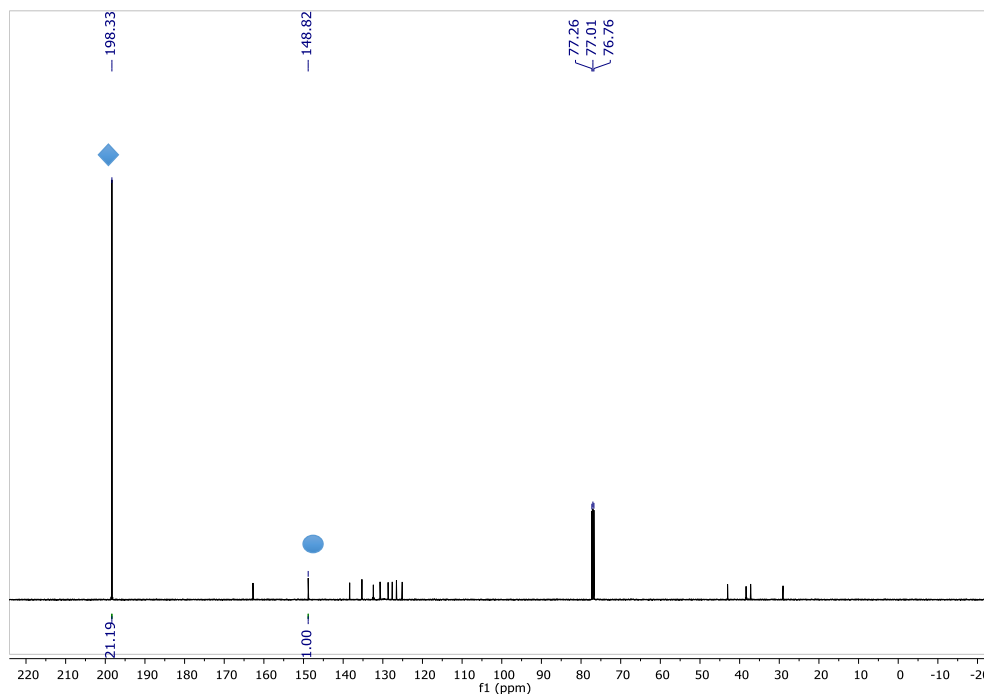
[Rh(<sup>13</sup>CO)<sub>2</sub>Cl]<sub>2</sub> was prepared according to literature procedure (using <sup>13</sup>CO atmosphere instead of CO) and its characterization matched the reported data.<sup>26</sup>

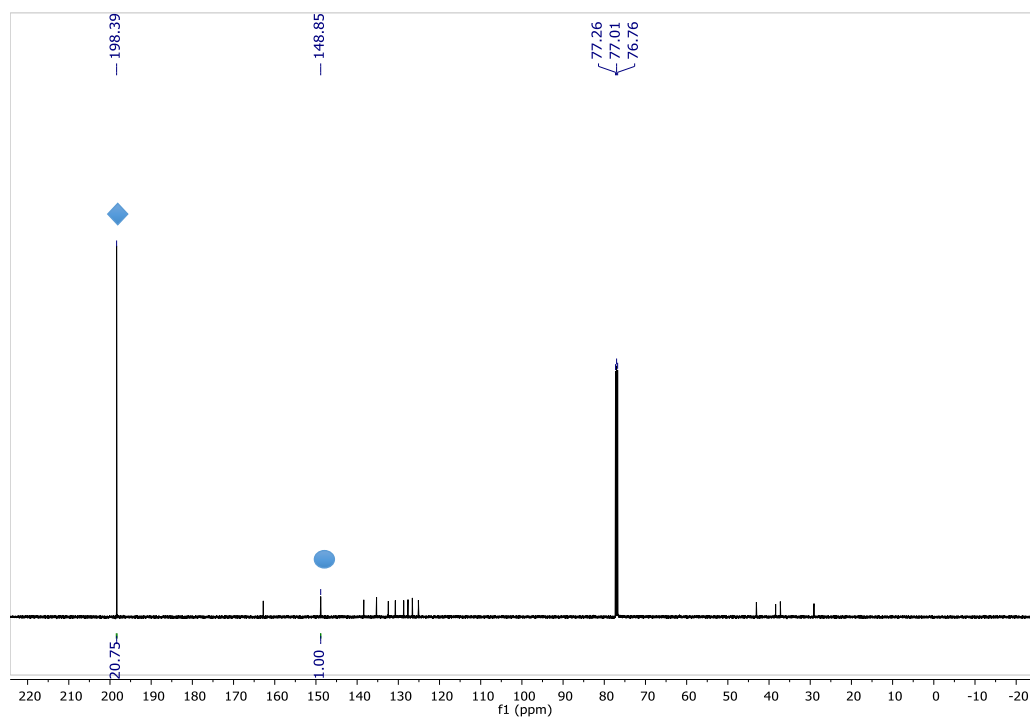
The reaction below adopted the standard procedure of C–C activation and **2a** (<sup>13</sup>CO incorporated) was isolated in 82% yield. Using this entry as an example to demonstrate how we measure the <sup>13</sup>CO incorporation ratio.



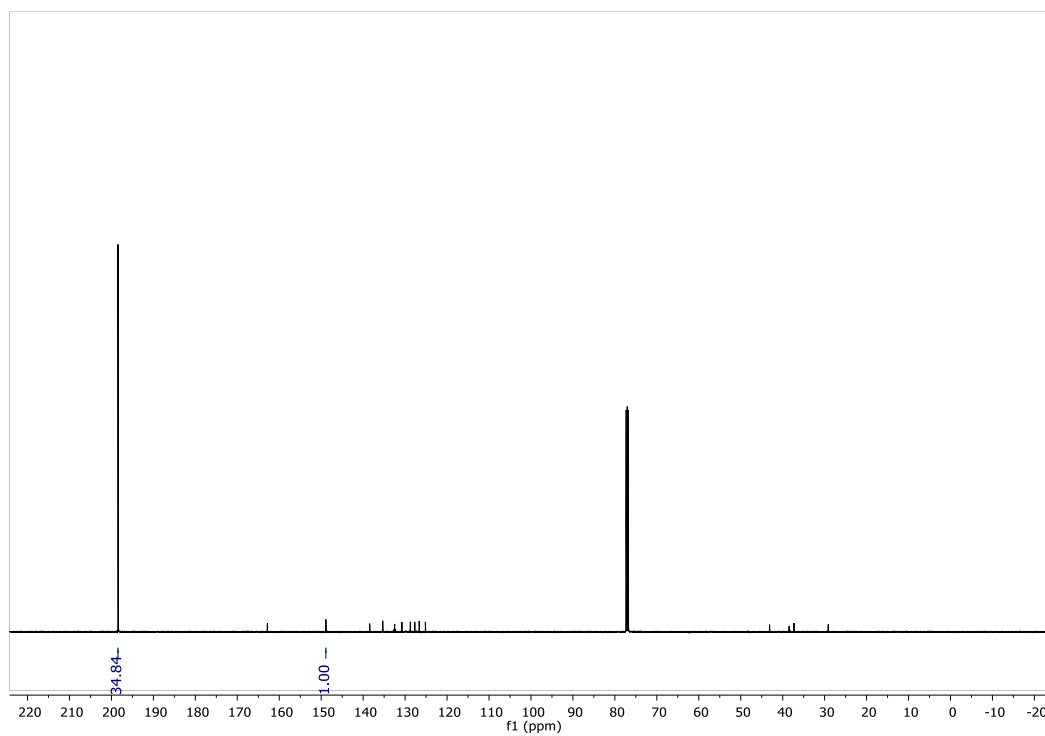
**Method A:** Quantitative  $^{13}\text{C}$ -NMR experiment:<sup>27</sup>

The  $^{13}\text{C}$  NMR spectra were acquired on a Bruker AVANCE III HD 500 MHz; 11.7 Tesla NMR spectrometer (126 MHz for  $^{13}\text{C}$ ,  $\text{CDCl}_3$ ) at 295 K with inverse-gated decoupling.  $T_1$  values of enriched carbon (marked with diamond shape in the spectra below) and the reference carbon (marked with oval shape in the spectra below) were determined to be 5.7 second and 8.7 second prior to the acquisitions, and delays of 50 s ( $50 \text{ s} > 5 \times T_1$ ) were utilized between scans. The reaction was repeated twice and the spectra are shown below. 21%  $^{13}\text{C}$  was found to be incorporated as an average of two experiments (Exp 1 and Exp 2).





at 52% conversion:

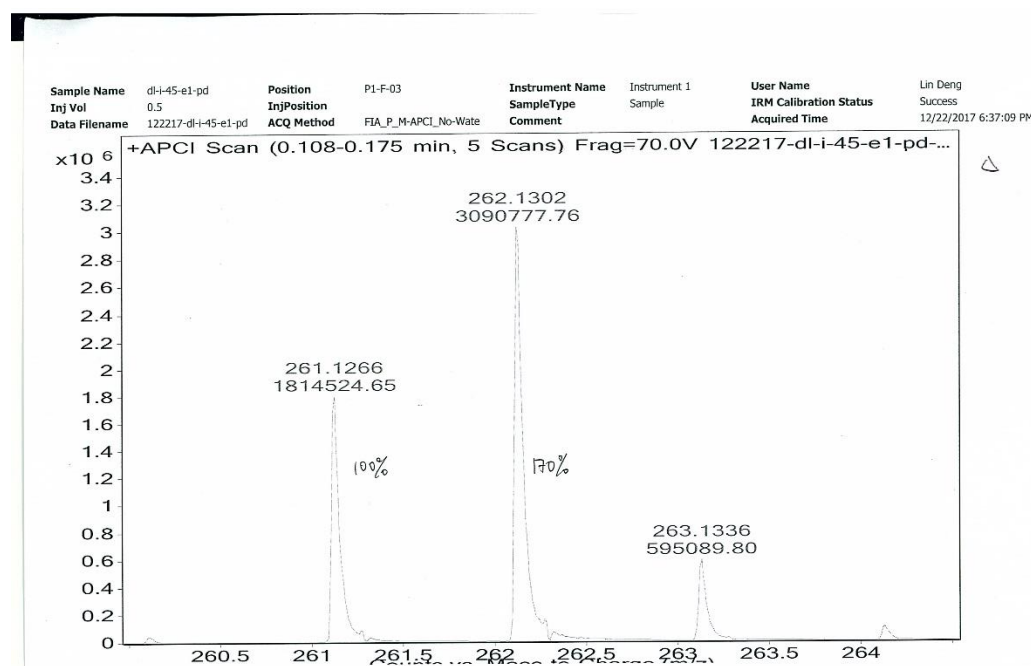


**Method B:** Using high resolution mass spectroscopy to determine the incorporation ratio of  $^{13}\text{C}$

For compound 2a without  $^{13}\text{C}$  incorporation, the native isotope peak can be calculated according to the natural abundance of  $^{13}\text{C}$ . We obtained this ratio from chemdraw as  $[\text{M}+\text{H}+1]^+$  (262.1307) equals 20.5% when setting the  $[\text{M}+\text{H}]^+$  (261.1274) as 100%. From this ratio, we can derive a function between the experimental  $[\text{M}+\text{H}+1]^+$  (y) and incorporation ratio (x). The function is  $y = (20.5 + 0.795x)/(100 - x) \times 100$

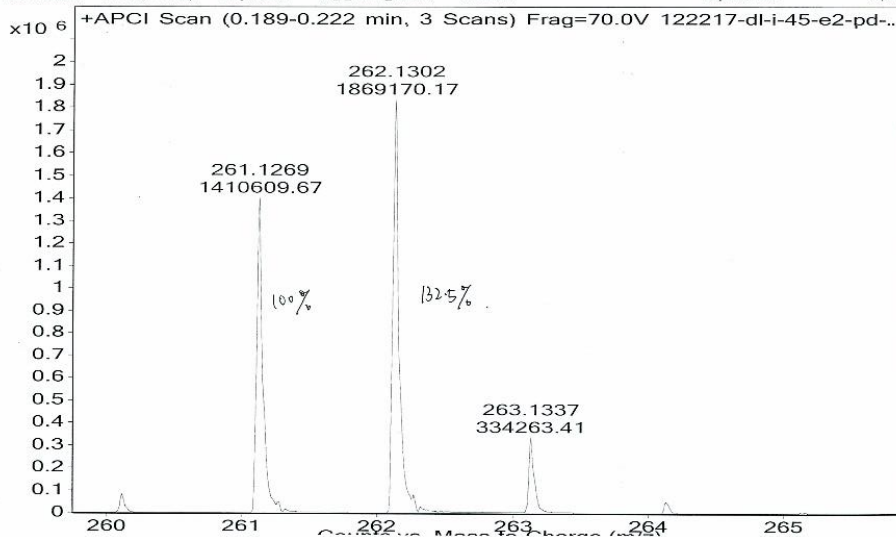
Using Agilent TOF LCMS, we acquired the mass spectrum of column purified product 2a at different conversion and obtained the experimental  $[\text{M}+\text{H}+1]^+$  (y), then the incorporation ratio can be calculated accordingly.

10% conversion:



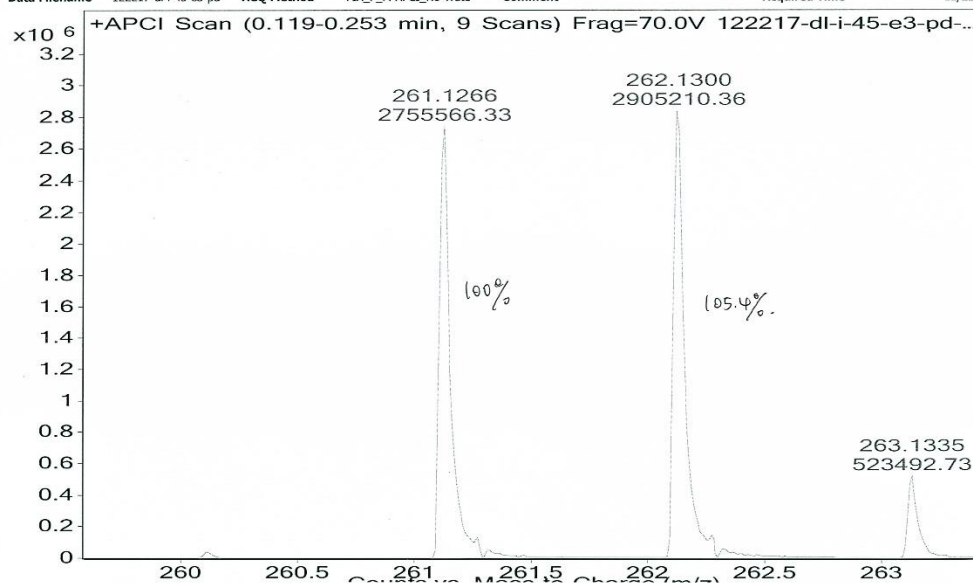
15% conversion:

Sample Name	dl-i-45-e2-pd	Position	P1-F-04	Instrument Name	Instrument 1	User Name	Lin Deng
Inj Vol	0.5	InjPosition		SampleType	Sample	IRM Calibration Status	Success
Data Filename	122217-dl-i-45-e2-pd	ACQ Method	FIA_P_M-APCI_No-Wate	Comment		Acquired Time	12/22/2017 6:41:27 PM



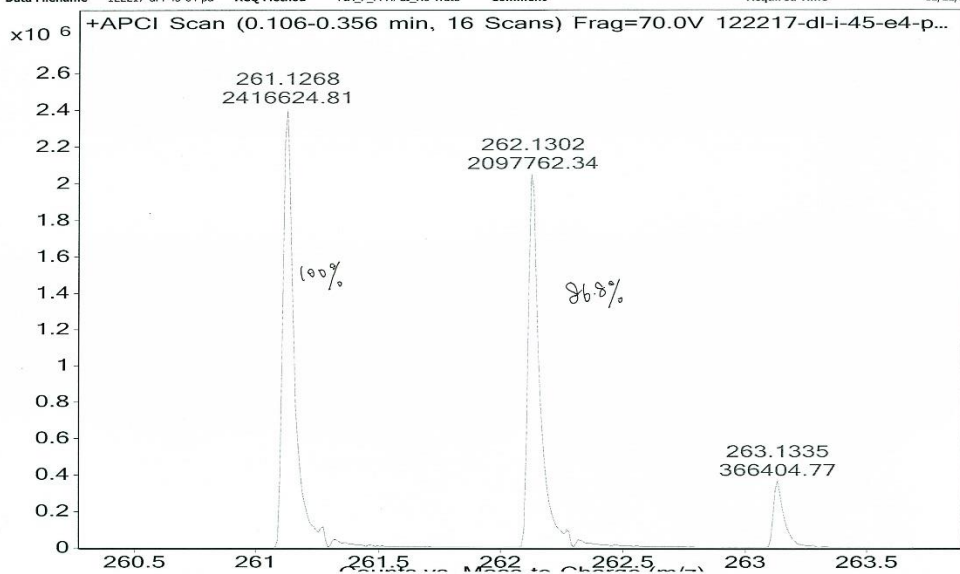
30% conversion:

Sample Name	dl-i-45-e3-pd	Position	P1-F-05	Instrument Name	Instrument 1	User Name	Lin Deng
Inj Vol	0.5	InjPosition		SampleType	Sample	IRM Calibration Status	Success
Data Filename	122217-dl-i-45-e3-pd	ACQ Method	FIA_P_M-APCI_No-Wate	Comment		Acquired Time	12/22/2017 6:42:53 PM



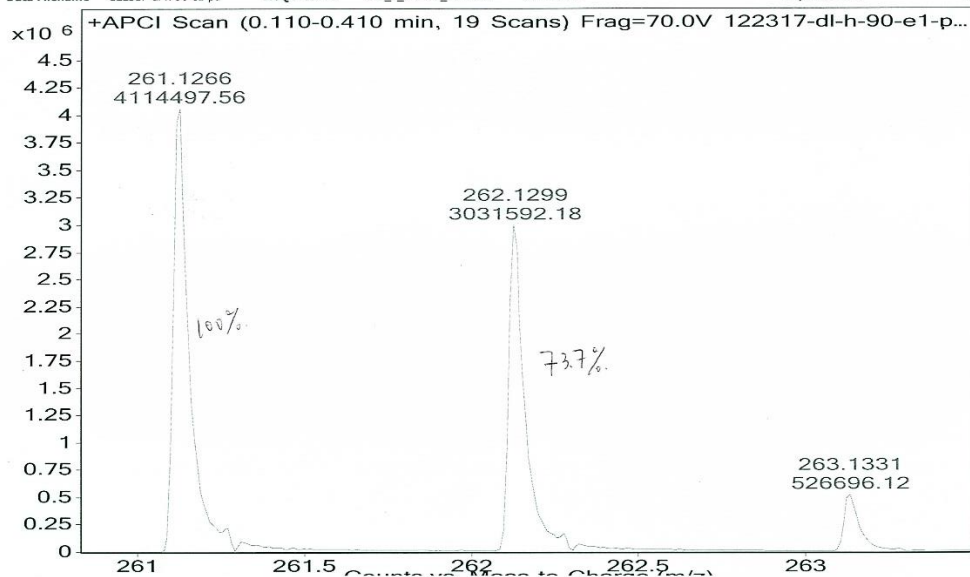
36% conversion:

Sample Name	dl-i-45-e4-pd	Position	P1-F-06	Instrument Name	Instrument 1	User Name	Lin Deng
Inj Vol	0.5	InjPosition		SampleType	Sample	IRM Calibration Status	Success
Data Filename	122217-dl-i-45-e4-pd	ACQ Method	FIA_P_M-APCI_No-Wate	Comment		Acquired Time	12/22/2017 6:45:45 PM



52% conversion:

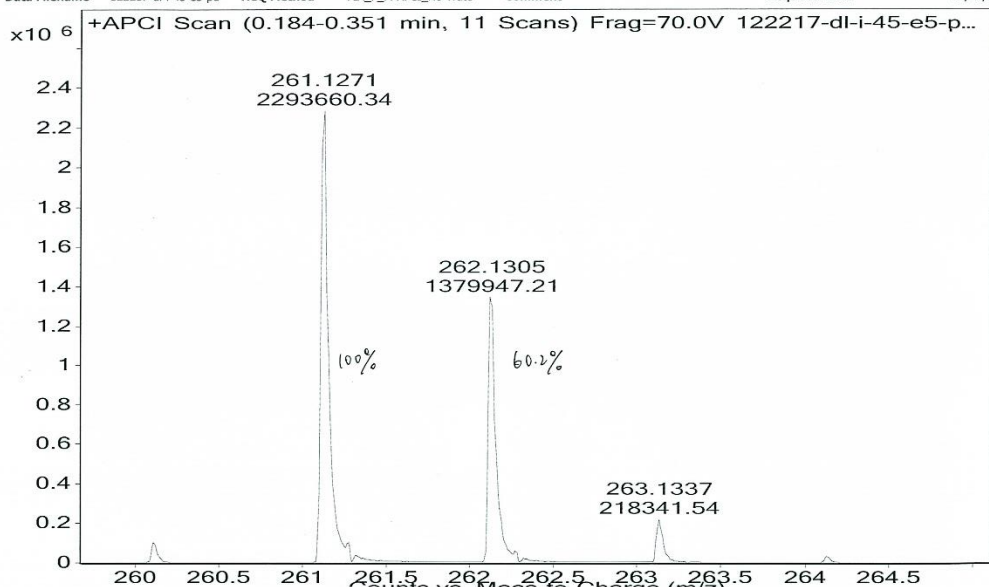
Sample Name	dl-h-90-e1-pd	Position	P2-A-04	Instrument Name	Instrument 1	User Name	Lin Deng
Inj Vol	0.5	InjPosition		SampleType	Sample	IRM Calibration Status	Success
Data Filename	122317-dl-h-90-e1-pd	ACQ Method	FIA_P_M-APCI_No-Wate	Comment		Acquired Time	12/23/2017 3:34:14



67% conversion:

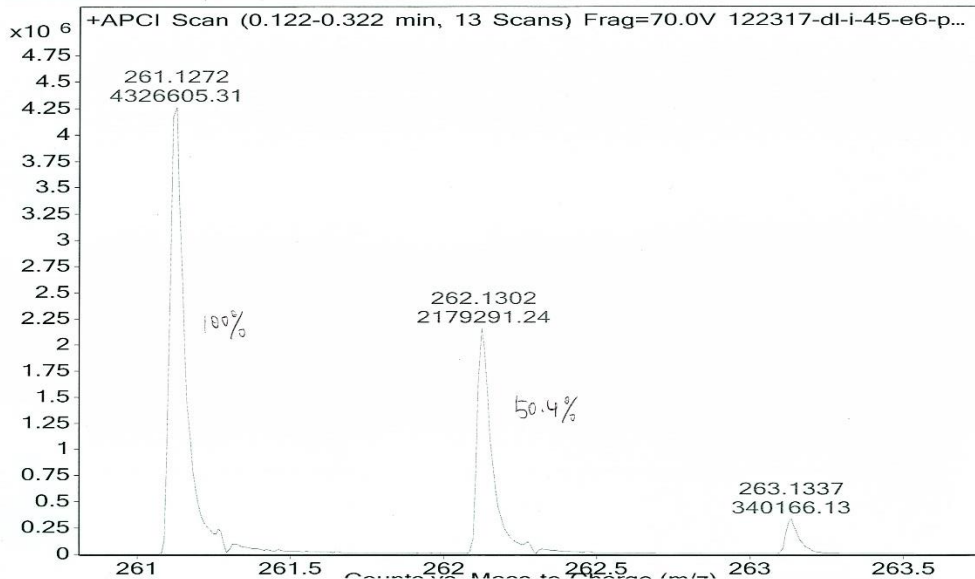


Sample Name	dl-i-45-e5-pd	Position	P1-F-07	Instrument Name	Instrument 1	User Name	Lin Deng
Inj Vol	0.5	InjPosition		SampleType	Sample	IRM Calibration Status	Success
Data Filename	122217-dl-i-45-e5-pd	ACQ Method	FIA_P_M-APCI-No-Wate	Comment		Acquired Time	12/22/2017 6:50:06 PM



79% conversion:

Sample Name	dl-i-45-e6-pd	Position	P2-A-03	Instrument Name	Instrument 1	User Name	Lin Deng
Inj Vol	0.5	InjPosition		SampleType	Sample	IRM Calibration Status	Success
Data Filename	122317-dl-i-45-e6-pd	ACQ Method	FIA_P_M-APCI-No-Wate	Comment		Acquired Time	12/23/2017 3:31:20 PM

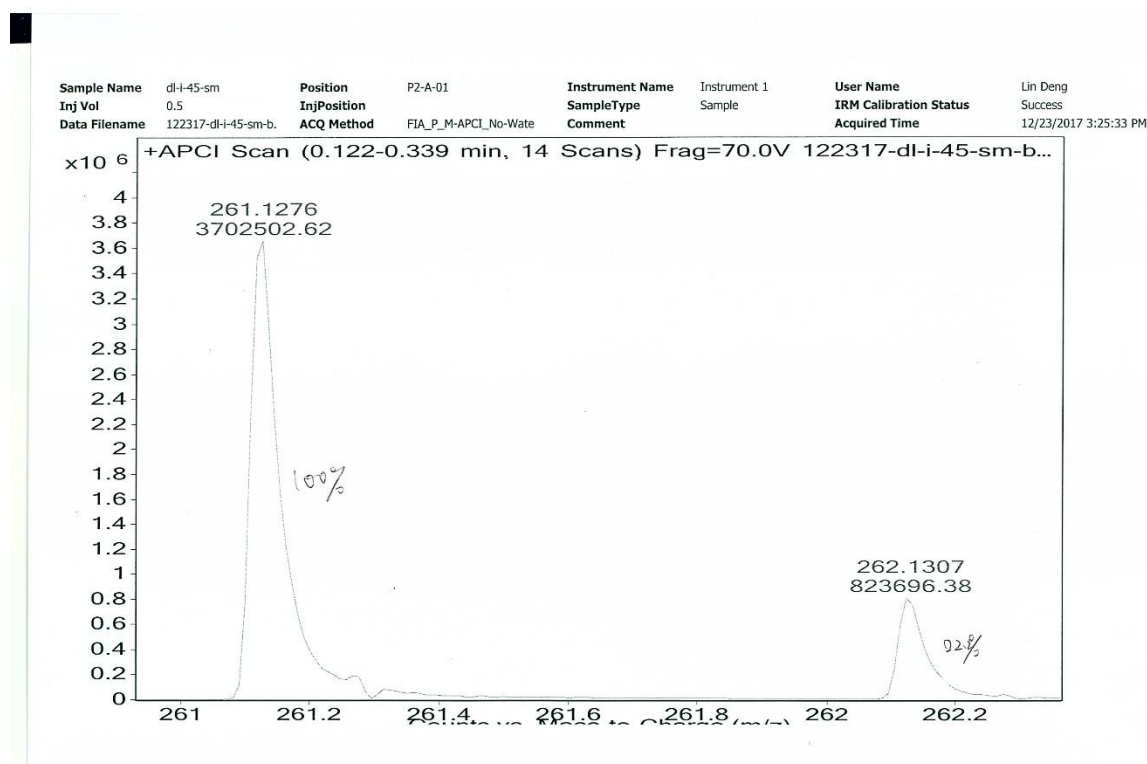


Shown below are the calculated incorporation ratio we obtained from this study.

conversion	10%	15%	30%	36%	52%	67%	79%	100%
yield of <b>2a</b>	9%	13%	29%	32%	46%	52%	67%	82%
<sup>13</sup> C incorporation	60%	53%	45%	39%	34%	28%	24%	21%

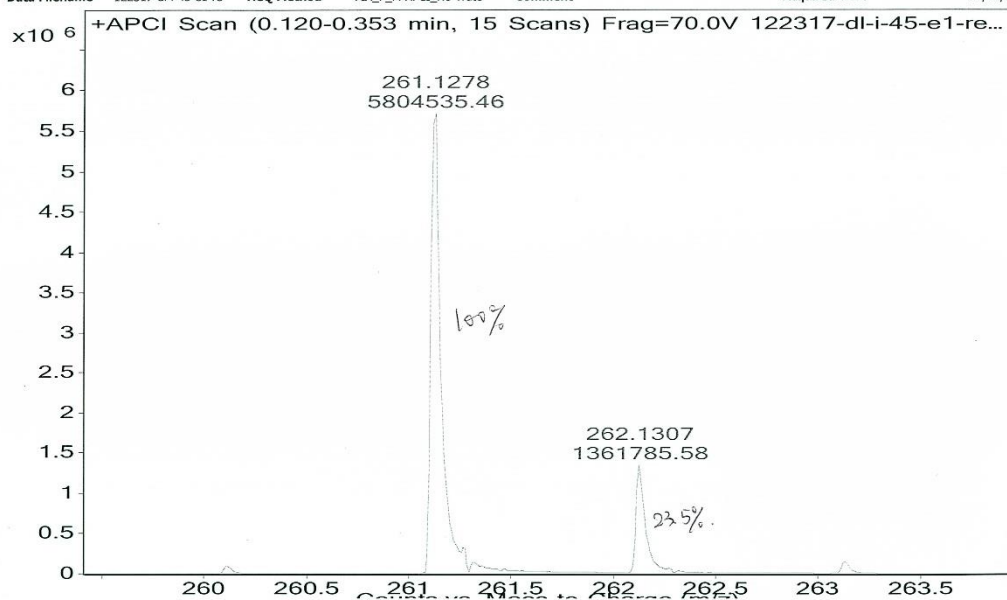
Starting material was also recycled at 10% and 52% conversion. Both of them did not show significant <sup>13</sup>C incorporation compared with the original starting material from comparing their isotope peaks in mass spectroscopy.

Original starting material:



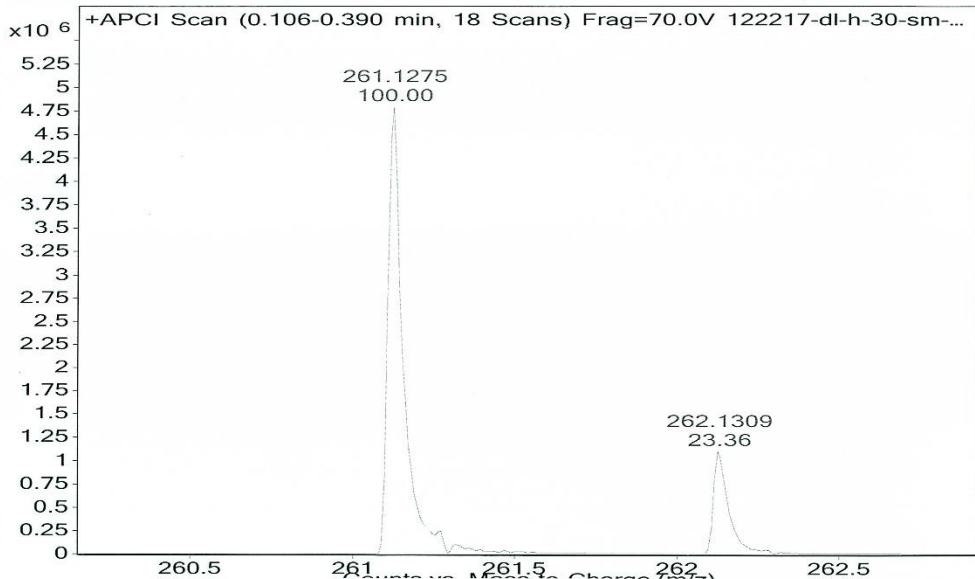
Recycled starting material at 10% conversion:

Sample Name	dl-i-45-e1-resm	Position	P2-A-02	Instrument Name	Instrument 1	User Name	Lin Deng
Inj Vol	0.5	InjPosition		SampleType	Sample	IRM Calibration Status	Success
Data Filename	122317-dl-i-45-e1-re	ACQ Method	FIA_P_M-APCI_No-Wate	Comment		Acquired Time	12/23/2017 3:28:28 PM

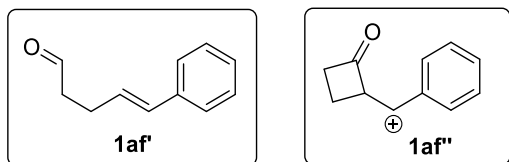


Recycled starting material at 52% conversion:

Sample Name	dl-h-30-sm	Position	P1-F-02	Instrument Name	Instrument 1	User Name	Lin Deng
Inj Vol	0.5	InjPosition		SampleType	Sample	IRM Calibration Status	Success
Data Filename	122217-dl-h-30-sm-a	ACQ Method	FIA_P_M-APCI_No-Wate	Comment		Acquired Time	12/22/2017 6:34:15

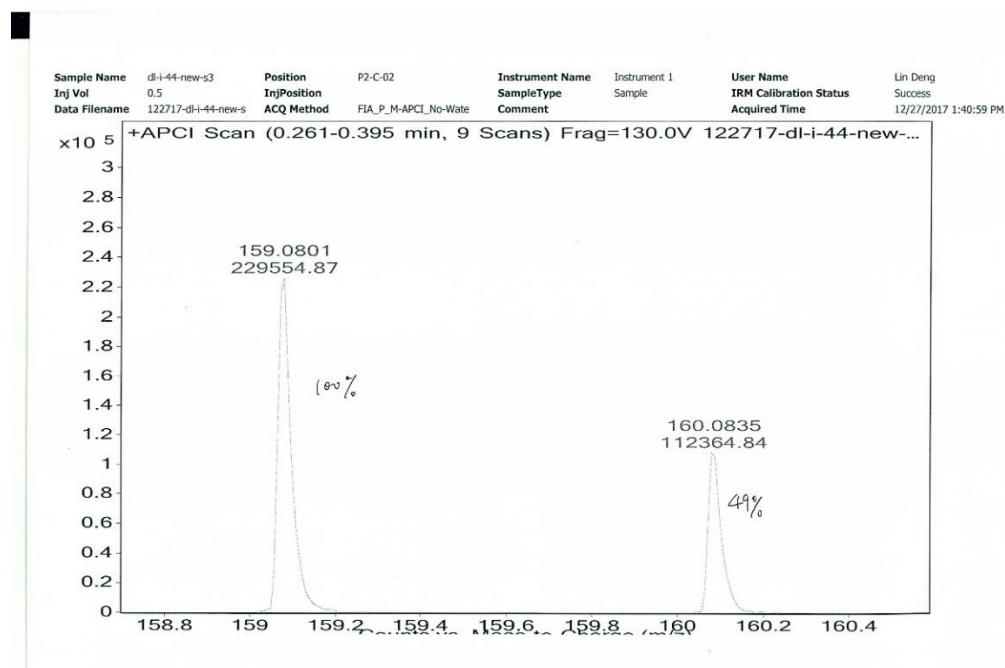


### Measurement of $^{13}\text{C}$ incorporation in **1af'**:



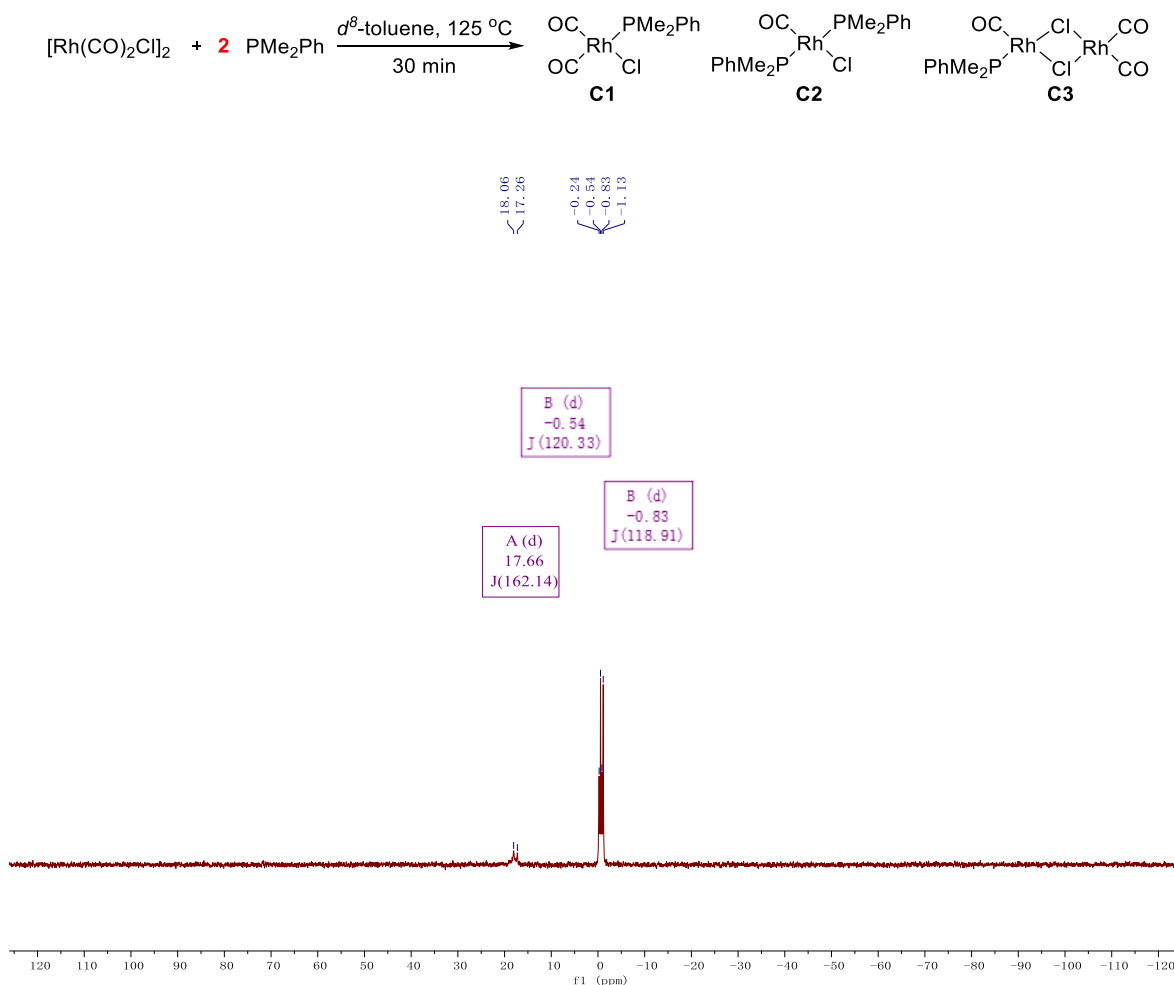
For compound **1af'** without  $^{13}\text{C}$  incorporation, the native isotope peak can be calculated according to the natural abundance of  $^{13}\text{C}$ . Because of the weak aldehyde C-H bond under the mass spectroscopy condition, **1af'** will cyclize to form carbocation **1af''** as shown. In mass spectrum, the  $m/z$  we observed is **1af''** ( $m/z=159.0804$ ). We obtained the ratio for **1af''** from chemdraw as  $[\text{M}+1]^+$  equals 11.9% when setting the  $[\text{M}]^+$  as 100%. From this ratio, we can derive a function between the experimental  $[\text{M}+1]^+$  (y) and incorporation ratio (x). The function is  $y = (11.9 + 0.88x)/(100 - x) \times 100$

Using Agilent TOF LCMS, we acquired the mass spectrum of column purified product **1w'** and obtained the experimental  $[\text{M}+1]^+$  (y) equals 49%, then the incorporation ratio can be calculated as 27%.

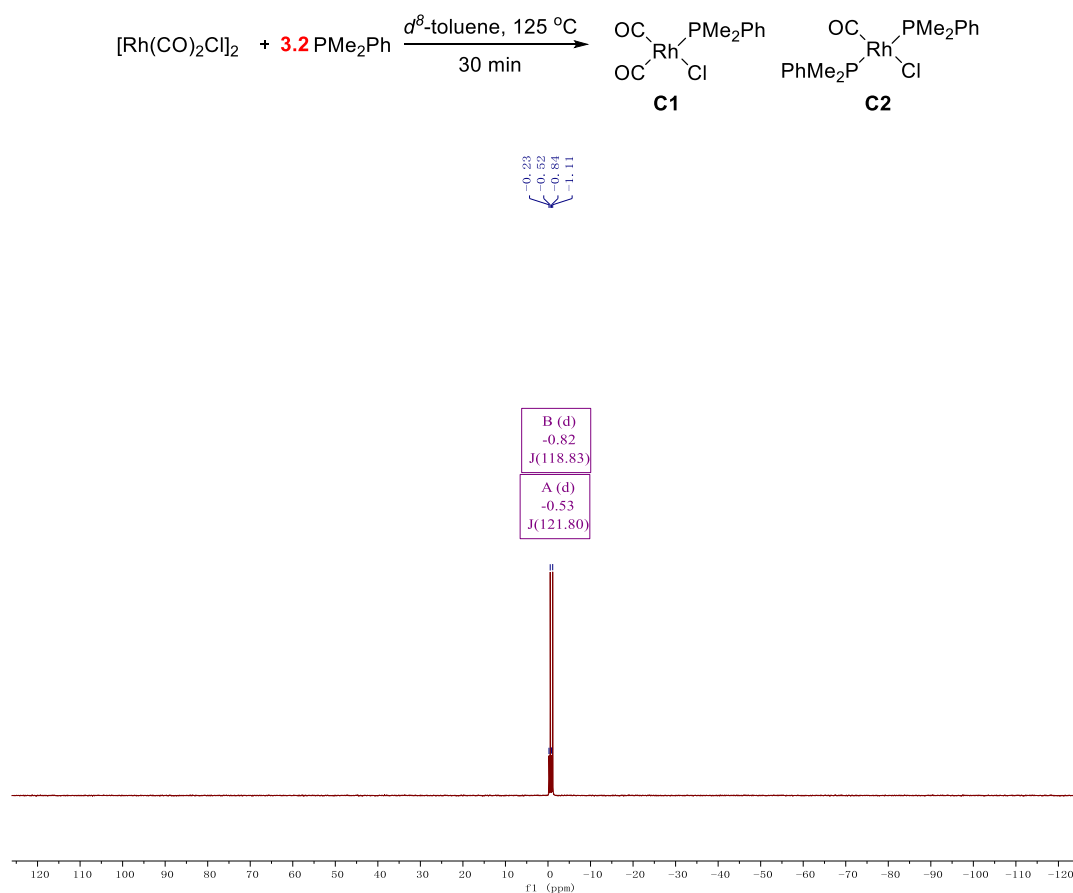


#### IV. Resting state study

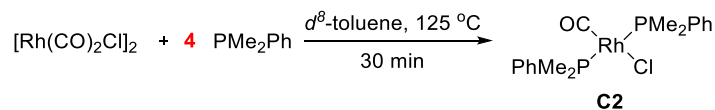
a) When catalyst  $[\text{Rh}(\text{CO})_2\text{Cl}]_2$  (10 mg, 0.0257 mmol, 1 eq) was mixed with  $\text{PMe}_2\text{Ph}$  (7.1 mg, 0.0514 mmol, 2 eq) at 1:1 ratio in  $d^8$ -toluene at 125 °C for 30 min, the  $^{31}\text{P}$ -NMR spectrum (at 294 K) is shown below. The three sets of signals are assigned to be **C1** ( $\delta$  -0.54 (d,  $J$  = 120.3 Hz)), **C2** ( $\delta$  -0.83 (d,  $J$  = 118.9 Hz)) and **C3** ( $\delta$  17.66 (d,  $J$  = 162.1 Hz)) according to literature.<sup>11</sup>

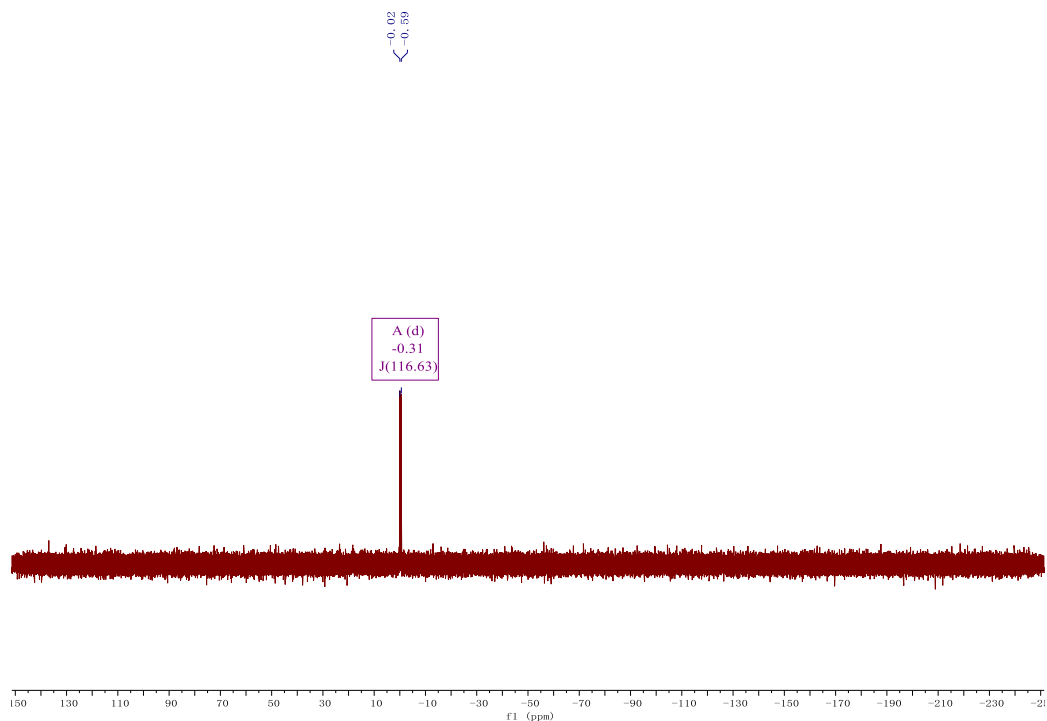


b) When catalyst  $[\text{Rh}(\text{CO})_2\text{Cl}]_2$  (10 mg, 0.0257 mmol, 1 eq) was mixed with  $\text{PMe}_2\text{Ph}$  (11.4 mg, 0.0822 mmol, 3.2 eq) at 1:1.6 ratio in  $d^8$ -toluene at 125 °C for 30 min, the  $^{31}\text{P}$ -NMR spectrum (at 294 K) is shown below. The two sets of signals are assigned to be **C1** ( $\delta$  -0.53 (d,  $J$  = 121.8 Hz)), **C2** ( $\delta$  -0.82 (d,  $J$  = 118.8 Hz)) according to literature.<sup>11</sup>

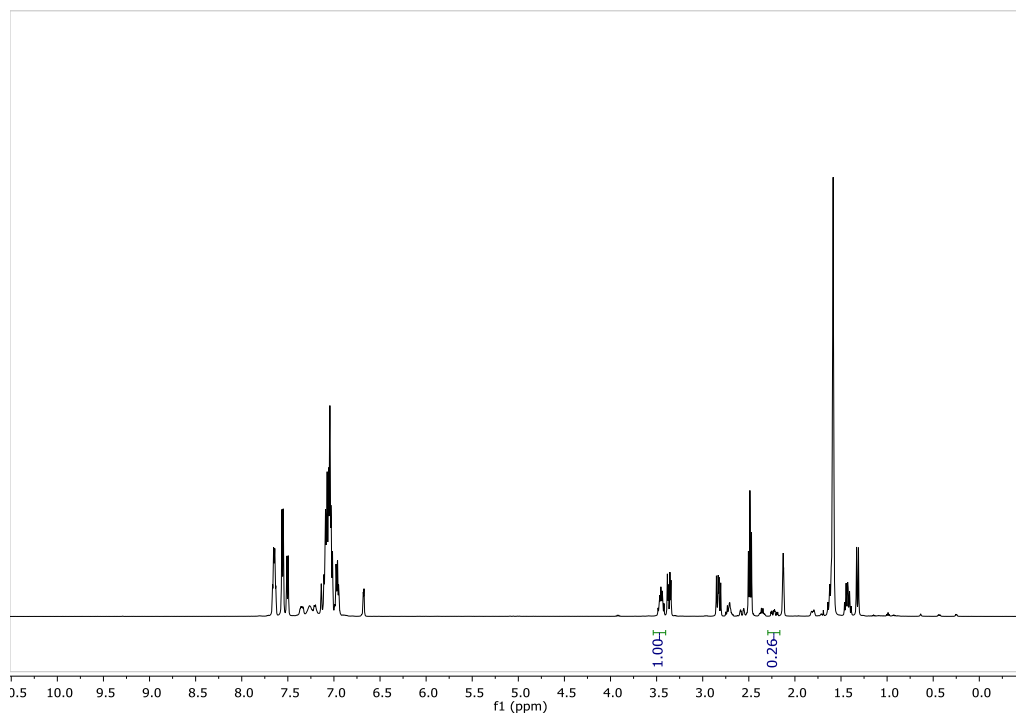


c) When catalyst  $[\text{Rh}(\text{CO})_2\text{Cl}]_2$  (10 mg, 0.0257 mmol, 1 eq) was mixed with  $\text{PMe}_2\text{Ph}$  (14.2 mg, 0.103 mmol, 4 eq) at 1:2 ratio in  $d^8$ -toluene at  $125^\circ\text{C}$  for 30 min, the  $^{31}\text{P}$ -NMR spectrum (at 200 K) is shown below. The one set of signal are assigned to be **C2** ( $\delta$  -0.31 (d,  $J = 116.6$  Hz)) according to literature.<sup>11</sup>





d) The NMR tube in b) was added 3 equivalent of substrate **1a** and heated to 125 °C for 12 h. The crude H-NMR was shown below. The two peaks integrated in the H-NMR belong to starting material **1a** and product **2a**. So the estimated yield of **2a** is  $0.26/(1+0.26)$  equals to 20%.



#### 4.4.8 X-ray data

##### a) X-ray data for **2a**

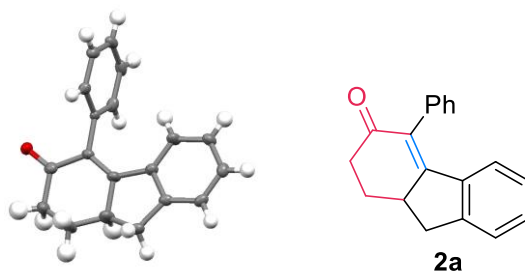


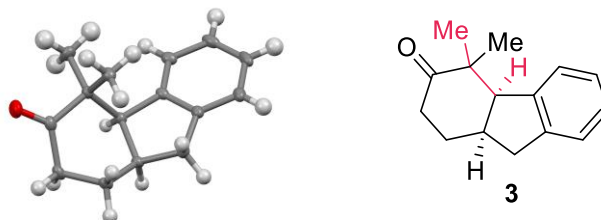
**Table 4.6** Crystal Data and Structure Refinement for **2a**

Identification code	Complex
Empirical formula	C <sub>19</sub> H <sub>16</sub> O
Formula weight	260.32
Temperature/K	100.0
Crystal system	monoclinic
Space group	P2 <sub>1</sub> /n
a/Å	10.6293(4)
b/Å	7.8160(3)
c/Å	16.5040(6)
$\alpha$ /°	90
$\beta$ /°	91.724(2)
$\gamma$ /°	90
Volume/Å <sup>3</sup>	1370.51(9)
Z	4
$\rho_{\text{calc}}$ /cm <sup>3</sup>	1.262
$\mu$ /mm <sup>-1</sup>	0.076



**Table 4.6** Continued Crystal Data and Structure Refinement for **2a**

F(000)	552.0
Crystal size/mm <sup>3</sup>	0.03 × 0.02 × 0.02
Radiation	MoK $\alpha$ ( $\lambda$ = 0.71073)
2 $\Theta$ range for data collection/°	4.498 to 48.88
Index ranges	-12 ≤ h ≤ 12, -9 ≤ k ≤ 9, -19 ≤ l ≤ 19
Reflections collected	13330
Independent reflections	2261 [ $R_{\text{int}}$ = 0.0495, $R_{\text{sigma}}$ = 0.0306]
Data/restraints/parameters	2261/57/209
Goodness-of-fit on $F^2$	1.161
Final R indexes [ $I \geq 2\sigma(I)$ ]	$R_1$ = 0.0624, $wR_2$ = 0.1612
Final R indexes [all data]	$R_1$ = 0.0808, $wR_2$ = 0.1708
Largest diff. peak/hole / e $\text{\AA}^{-3}$	0.36/-0.32

b) X-ray data for **3****Table 4.7** Crystal Data and Structure Refinement for **3**

Identification code	DL-h-116
Empirical formula	C <sub>15</sub> H <sub>18</sub> O

**Table 4.7** Continued Crystal Data and Structure Refinement for **3**

Formula weight	214.29
Temperature/K	100
Crystal system	monoclinic
Space group	P2 <sub>1</sub> /c
a/Å	7.9732(5)
b/Å	7.5678(5)
c/Å	19.3603(13)
$\alpha$ /°	90
$\beta$ /°	92.343(2)
$\gamma$ /°	90
Volume/Å <sup>3</sup>	1167.22(13)
Z	4
$\rho_{\text{calc}}$ /cm <sup>3</sup>	1.219
$\mu$ /mm <sup>-1</sup>	0.074
F(000)	464.0
Crystal size/mm <sup>3</sup>	0.1 × 0.08 × 0.05
Radiation	MoK $\alpha$ ( $\lambda$ = 0.71073)
2 $\Theta$ range for data collection/° 5.114 to 60.214	
Index ranges	-11 ≤ h ≤ 11, -10 ≤ k ≤ 10, -27 ≤ l ≤ 27
Reflections collected	24376
Independent reflections	3431 [R <sub>int</sub> = 0.0447, R <sub>sigma</sub> = 0.0342]

**Table 4.7** Continued Crystal Data and Structure Refinement for **3**

Data/restraints/parameters	3431/0/147
Goodness-of-fit on $F^2$	1.014
Final R indexes [ $I \geq 2\sigma(I)$ ]	$R_1 = 0.0474$ , $wR_2 = 0.1055$
Final R indexes [all data]	$R_1 = 0.0729$ , $wR_2 = 0.1166$
Largest diff. peak/hole / $e \text{ \AA}^{-3}$	0.47/-0.18

c) X-ray data for **6**

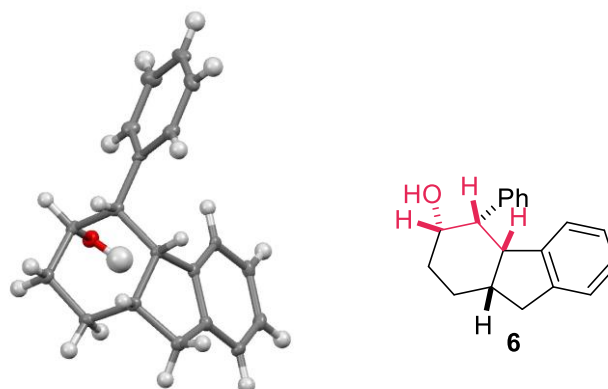


**Table 4.8** Crystal Data and Structure Refinement for **6**.

Identification code	DL-h-59
Empirical formula	$C_{19}H_{20}O$
Formula weight	264.35
Temperature/K	100.0
Crystal system	monoclinic
Space group	$P2_1$
$a/\text{\AA}$	5.8407(4)
$b/\text{\AA}$	22.3977(15)

**Table 4.8** Continued Crystal Data and Structure Refinement for **6**

$c/\text{\AA}$	10.7014(7)
$\alpha/^\circ$	90
$\beta/^\circ$	97.123(2)
$\gamma/^\circ$	90
Volume/ $\text{\AA}^3$	1389.13(16)
Z	4
$\rho_{\text{calc}}/\text{g/cm}^3$	1.264
$\mu/\text{mm}^{-1}$	0.076
F(000)	568.0
Crystal size/ $\text{mm}^3$	$0.02 \times 0.02 \times 0.01$
Radiation	MoK $\alpha$ ( $\lambda = 0.71073$ )
2 $\Theta$ range for data collection/ $^\circ$	4.246 to 54.354
Index ranges	$-7 \leq h \leq 7$ , $-28 \leq k \leq 28$ , $-13 \leq l \leq 13$
Reflections collected	18648
Independent reflections	6167 [ $R_{\text{int}} = 0.0417$ , $R_{\text{sigma}} = 0.0592$ ]
Data/restraints/parameters	6167/1/369
Goodness-of-fit on $F^2$	1.015
Final R indexes [ $I \geq 2\sigma(I)$ ]	$R_1 = 0.0468$ , $wR_2 = 0.0988$
Final R indexes [all data]	$R_1 = 0.0749$ , $wR_2 = 0.1096$
Largest diff. peak/hole / $e \text{\AA}^{-3}$	0.28/-0.21
Flack parameter	0.2(7)

## 4.5 References

- (1) For selected reviews, see: (a) Crabtree, R. H. *Chem. Rev.* **1985**, 85, 245. (b) Jones, W. D. *Nature* **1993**, 364, 676. (c) Murakami, M.; Ito, Y., *Cleavage of Carbon–Carbon Single Bonds by Transition Metals*. In *Top. Organomet. Chem.*, 1999; Vol. 3, pp 97. (d) Rybtchinski, B.; Milstein, D. *Angew. Chem. Int. Ed.* **1999**, 38, 870. (e) Jun, C.-H. *Chem. Soc. Rev.* **2004**, 33, 610. (f) Miura, M.; Satoh, T., *Catalytic Processes Involving  $\beta$ -Carbon Elimination*. In *Top. Organomet. Chem.*, 2005; Vol. 14, pp 1. (g) Necas, D.; Kotorá, M. *Curr. Org. Chem.* **2007**, 11, 1566. (h) Murakami, M.; Matsuda, T. *Chem. Comm.* **2011**, 47, 1100. (i) Seiser, T.; Saget, T.; Tran, D. N.; Cramer, N. *Angew. Chem. Int. Ed.* **2011**, 50, 7740. (j) Korotvicka, A.; Necas, D.; Kotorá, M. *Curr. Org. Chem.* **2012**, 16, 1170. (k) Ruhland, K. *Eur. J. Org. Chem.* **2012**, 2012, 2683. (l) Chen, F.; Wang, T.; Jiao, N. *Chem. Rev.* **2014**, 114, 8613. (m) Dermenci, A.; Coe, J. W.; Dong, G. *Org. Chem. Front.* **2014**, 1, 567. (n) Dong, G., *C–C bond activation*. Springer-Verlag: Berlin, 2014; Vol. 346. (o) Murakami, M.; Ishida, N., *Fundamental Reactions to Cleave Carbon–Carbon  $\sigma$ -Bonds with Transition Metal Complexes*. In *Cleavage of Carbon-Carbon Single Bonds by Transition Metals*, Wiley-VCH Verlag GmbH & Co. KGaA: 2015; pp 1. (p) Souillart, L.; Cramer, N. *Chem. Rev.* **2015**, 115, 9410. (q) Chen, P.-h.; Dong, G. *Chem. Eur. J.* **2016**, 22, 18290. (r) Chen, P.-h.; Billett, B. A.; Tsukamoto, T.; Dong, G. *ACS Cat.* **2017**, 7, 1340. (s) Fumagalli, G.; Stanton, S.; Bower, J. F. *Chem. Rev.* **2017**, 117, 9404.
- (2) For representative examples, see: (a) Murakami, M.; Itahashi, T.; Ito, Y. *J. Am. Chem. Soc.* **2002**, 124, 13976. (b) Ko, H. M.; Dong, G. *Nat. Chem.* **2014**, 6, 739. (c) Parker, E.; Cramer, N. *Organometallics* **2014**, 33, 780. (d) Souillart, L.; Cramer, N. *Angew. Chem. Int. Ed.* **2014**, 53, 9640. (e) Souillart, L.; Parker, E.; Cramer, N. *Angew. Chem. Int. Ed.* **2014**, 53, 3001. (f) Souillart, L.; Cramer, N. *Chem. Eur. J.* **2015**, 21, 1863. (g) Zhou, X.; Dong, G. *J. Am. Chem. Soc.* **2015**, 137, 13715. (h) Zhou, X.; Ko, H. M.; Dong, G. *Angew. Chem. Int. Ed.* **2016**, 55, 13867.
- (3) For the (6+2) coupling of 2-vinyl cyclobutanones with olefins, see: (a) Wender, P. A.; Correa, A. G.; Sato, Y.; Sun, R. *J. Am. Chem. Soc.* **2000**, 122, 7815. (b) Matsuda, T.; Fujimoto, A.; Ishibashi, M.; Murakami, M. *Chem. Lett.* **2004**, 33, 876. (c) Matsuda, T.; Makino, M.; Murakami, M. *Angew. Chem. Int. Ed.* **2005**, 44, 4608.
- (4) (a) Roundhill, D. M.; Lawson, D. N.; Wilkinson, G. *J. Chem. Soc. (A)* **1968**, 845. (b) McQuillin, F. J.; Powell, K. G. *J. Chem. Soc., Dalton Trans.* **1972**, 2123. (c) Murakami, M.; Amii, H.; Ito, Y. *Nature* **1994**, 370, 540. (d) Murakami, M.; Amii, H.; Shigeto, K.; Ito, Y. *J. Am. Chem. Soc.* **1996**, 118, 8285. (e) Wang, G.-W.; McCreanor, N. G.; Shaw, M. H.; Whittingham, W. G.; Bower, J. F. *J. Am. Chem. Soc.* **2016**, 138, 13501.
- (5) (a) Xu, T.; Dong, G. *Angew. Chem. Int. Ed.* **2012**, 51, 7567. (b) Xu, T.; Ko, H. M.; Savage, N. A.; Dong, G. *J. Am. Chem. Soc.* **2012**, 134, 20005. (c) Chen, P.-h.; Xu, T.; Dong, G. *Angew. Chem. Int. Ed.* **2014**, 53, 1674. (d) Xu, T.; Dong, G. *Angew. Chem. Int. Ed.* **2014**, 53, 10733. (e) Deng, L.; Xu, T.; Li, H.; Dong, G. *J. Am. Chem. Soc.* **2016**, 138, 369. (f) Lu, G.; Fang, C.; Xu, T.; Dong, G.; Liu, P. *J. Am. Chem. Soc.* **2015**, 137, 8274.

- (6) For representative examples of intermolecular cyclobutanone/alkyne couplings catalyzed by nickel, see: (a) Murakami, M.; Ashida, S.; Matsuda, T. *J. Am. Chem. Soc.* **2005**, *127*, 6932. (b) Murakami, M.; Ashida, S.; Matsuda, T. *Tetrahedron* **2006**, *62*, 7540. (c) Kumar, P.; Louie, J. *Org. Lett.* **2012**, *14*, 2026. (d) Ishida, N.; Yuhki, T.; Murakami, M. *Org. Lett.* **2012**, *14*, 3898. (e) Ho, K. Y. T.; Aïssa, C. *Chem. Eur. J.* **2012**, *18*, 3486. (f) Li, Y.; Lin, Z. *Organometallics* **2013**, *32*, 3003. (g) Thakur, A.; Evangelista, J. L.; Kumar, P.; Louie, J. *J. Org. Chem.* **2015**, *80*, 9951. (h) Barday, M.; Ho, K. Y. T.; Halsall, C. T.; Aïssa, C. *Org. Lett.* **2016**, *18*, 1756.
- (7) For representative examples of (3+2+1) reactions involving cyclopropanes, see: (a) Mazumder, S.; Shang, D.; Negru, D. E.; Baik, M.-H.; Evans, P. A. *J. Am. Chem. Soc.* **2012**, *134*, 20569. (b) Kim, S.; Chung, Y. K. *Org. Lett.* **2014**, *16*, 4352. (c) Feng, Y.; Yu, Z.-X. *J. Org. Chem.* **2015**, *80*, 1952. (d) Shaw, M. H.; Croft, R. A.; Whittingham, W. G.; Bower, J. F. *J. Am. Chem. Soc.* **2015**, *137*, 8054. (e) Shaw, M. H.; McCreanor, N. G.; Whittingham, W. G.; Bower, J. F. *J. Am. Chem. Soc.* **2015**, *137*, 463. (f) Bose, S.; Yang, J.; Yu, Z.-X. *J. Org. Chem.* **2016**, *81*, 6757. (g) Shaw, M. H.; Whittingham, W. G.; Bower, J. F. *Tetrahedron* **2016**, *72*, 2731.
- (8) Koga, Y.; Narasaka, K. *Chem. Lett.* **1999**, 28, 705.
- (9) Jiao, L.; Lin, M.; Zhuo, L.-G.; Yu, Z.-X. *Org. Lett.* **2010**, *12*, 2528.
- (10) Shaw, M. H.; Melikhova, E. Y.; Kloer, D. P.; Whittingham, W. G.; Bower, J. F. *J. Am. Chem. Soc.* **2013**, *135*, 4992.
- (11) Rotondo, E.; Battaglia, G.; Giordano, G.; Cusmano, F. P. *J. Organomet. Chem.* **1993**, *450*, 245.
- (12) Jiang, X.; Covey, D. F. *J. Org. Chem.* **2002**, *67*, 4893.
- (13) Garcia-Cabeza, A.; Marin-Barrios, R.; Azarken, R.; Moreno-Dorado, F. J.; Ortega, M. J.; Vidal, H.; Gatica, J. M.; Massanet, G. M.; Guerra, F. M. *Eur. J. Org. Chem.* **2013**, 8307 and references therein.
- (14) Wang, S.-K.; Chen, M.-T.; Zhao, D.-Y.; You, X.; Luo, Q.-L. *Adv. Synth. Catal.* **2016**, 358, 4093.
- (15) Pun, D.; Diao, T.; Stahl, S. S. *J. Am. Chem. Soc.* **2013**, *135*, 8213.
- (16) Liniger, M.; VanderVelde, D. G.; Takase, M. K.; Shahgholi, M.; Stoltz, B. M. *J. Am. Chem. Soc.* **2016**, *138*, 969.
- (17) Wender, P. A.; Correa, A. G.; Sato, Y.; Sun, R. *J. Am. Chem. Soc.* **2000**, *122*, 7815.
- (18) a) Tadross, P. M.; Bugga, P.; Stoltz, B. M. *Organic & Biomolecular Chemistry* **2011**, *9*, 5354. b) Salezadeh-Asl, R.; Lee-Ruff, E. *Tetrahedron: Asymmetry* **2005**, *16*, 3986. c) Suarez, L. L.; Greaney, M. F. *Chem. Commun.* **2011**, 47, 7992. d) Sashida, H.; Ohyanagi, K.; Minoura, M.; Akiba, K.-y. *J. Chem. Soc., Perkin Trans. 1* **2002**, 606. e) Obata, T.; Suzuki, S.; Nakagawa,

- A.; Kajihara, R.; Noguchi, K.; Saito, A. *Org. Lett.* **2016**, *18*, 4136. f) Trost, B. M.; Vladuchick, W. C.; Bridges, A. J. *J. Am. Chem. Soc.* **1980**, *102*, 3548. g) Xu, L.; Liu, Z.; Dong, W.; Song, J.; Miao, M.; Xu, J.; Ren, H. *Org. Bio. Chem.* **2015**, *13*, 6333.
- (19) Li, D. Y.; Shi, K. J.; Mao, X. F.; Zhao, Z. L.; Wu, X. Y.; Liu, P. N. *Tetrahedron* **2014**, *70*, 7022.
- (20) a) Vinoth, P.; Nagarajan, S.; Maheswari, C. U.; Sudalai, A.; Pace, V.; Sridharan, V. *Org. Lett.* **2016**, *18*, 3442. b) Yukiteru, I.; Mitsuhiro, Y. *Chem. Lett.* **2014**, *43*, 1758.
- (21) a) Ishii, S.; Niwa, Y.; Watanabe, S. *J. Fluorine Chem.* **2016**, *182*, 41. b) Yu, L.-Z.; Wei, Y.; Shi, M. *Chem. Commun.* **2017**, *53*, 8980.
- (22) Kaplan, H. Z.; Rendina, V. L.; Kingsbury, J. S. *J. Org. Chem.* **2013**, *78*, 4620.
- (23) Yamashita, S.; Iso, K.; Kitajima, K.; Himuro, M.; Hirama, M. *J. Org. Chem.* **2011**, *76*, 2408.
- (24) Nordvik, T.; Brinker, U. H. *J. Org. Chem.* **2003**, *68*, 9394.
- (25) Musacchio, A. J.; Nguyen, L. Q.; Beard, G. H.; Knowles, R. R. *J. Am. Chem. Soc.* **2014**, *136*, 12217.
- (26) Montag, M.; Schwartsburd, L.; Cohen, R.; Leitun, G.; Ben-David, Y.; Martin, J. M. L.; Milstein, D. *Angew. Chem. Int. Ed.* **2007**, *46*, 1901.
- (27) Rathbun, C. M.; Johnson, J. B. *J. Am. Chem. Soc.* **2011**, *133*, 2031.

## 4.6 NMR Spectra

**Figure 4.1**  $^1\text{H}$  and  $^{13}\text{C}$  NMR spectrum of compound **1d-II**

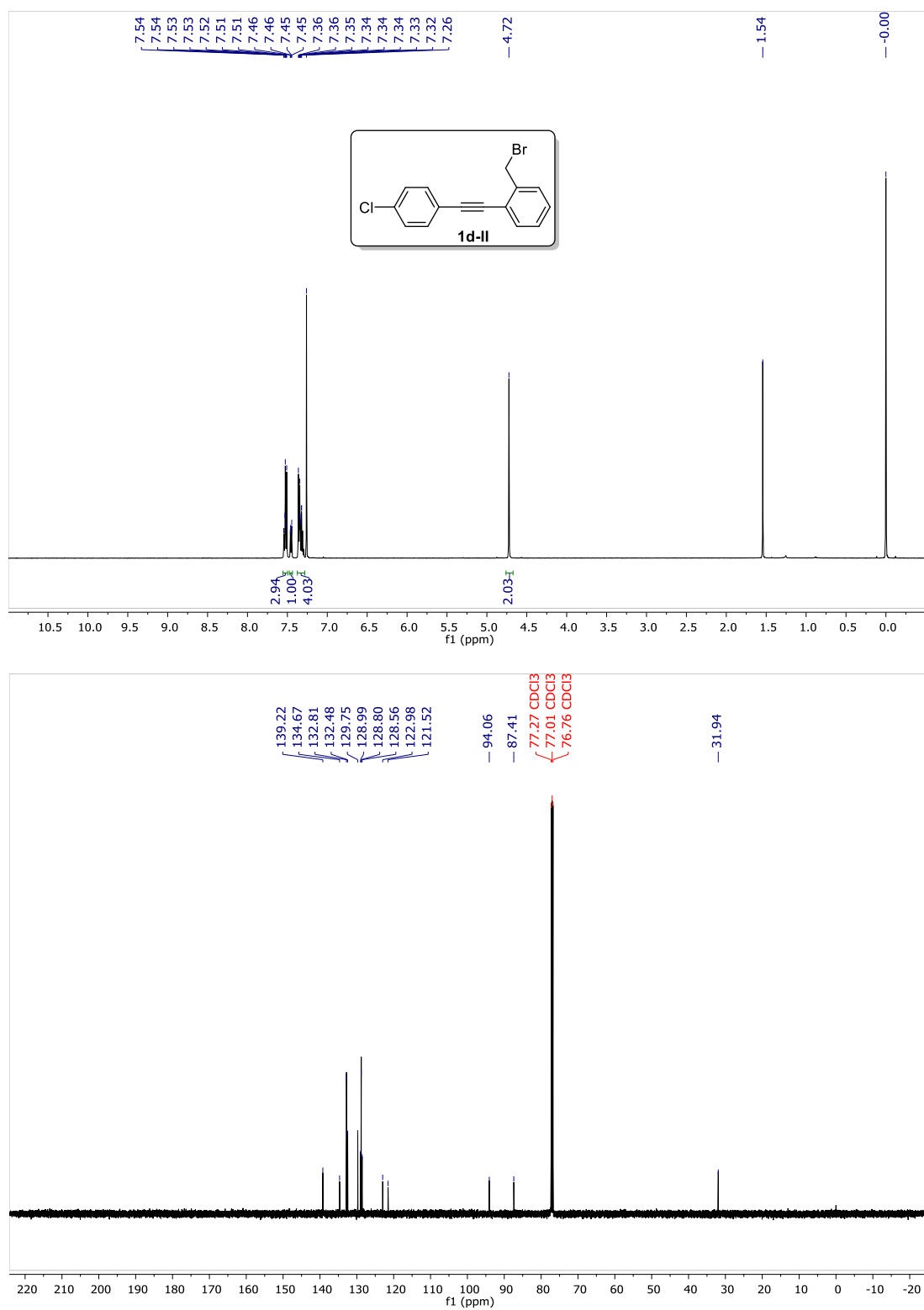




**Figure 4.2**  $^1\text{H}$  and  $^{13}\text{C}$  NMR spectrum of compound **1j-II**

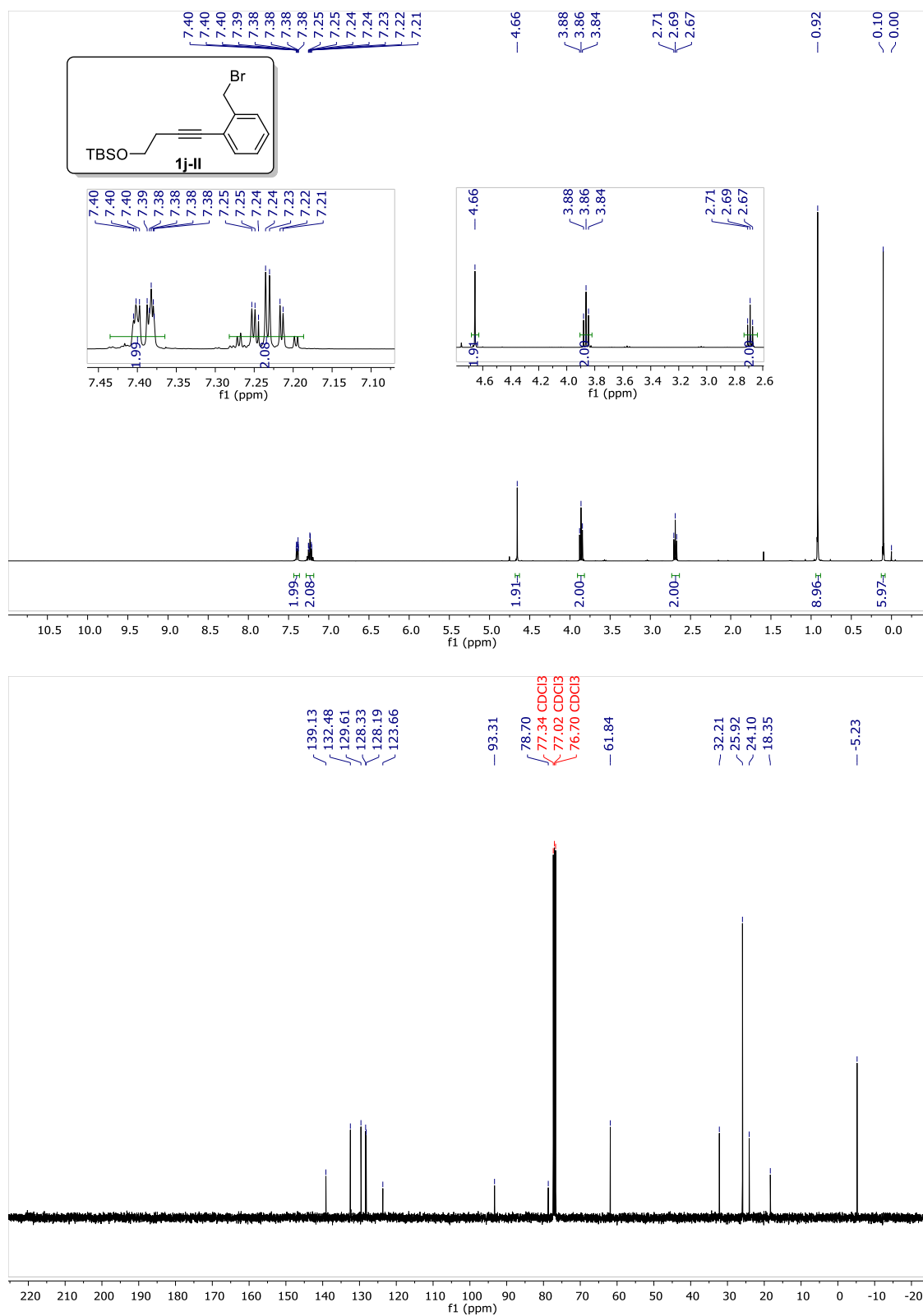


**Figure 4.3**  $^1\text{H}$  and  $^{13}\text{C}$  NMR spectrum of compound **11-II**

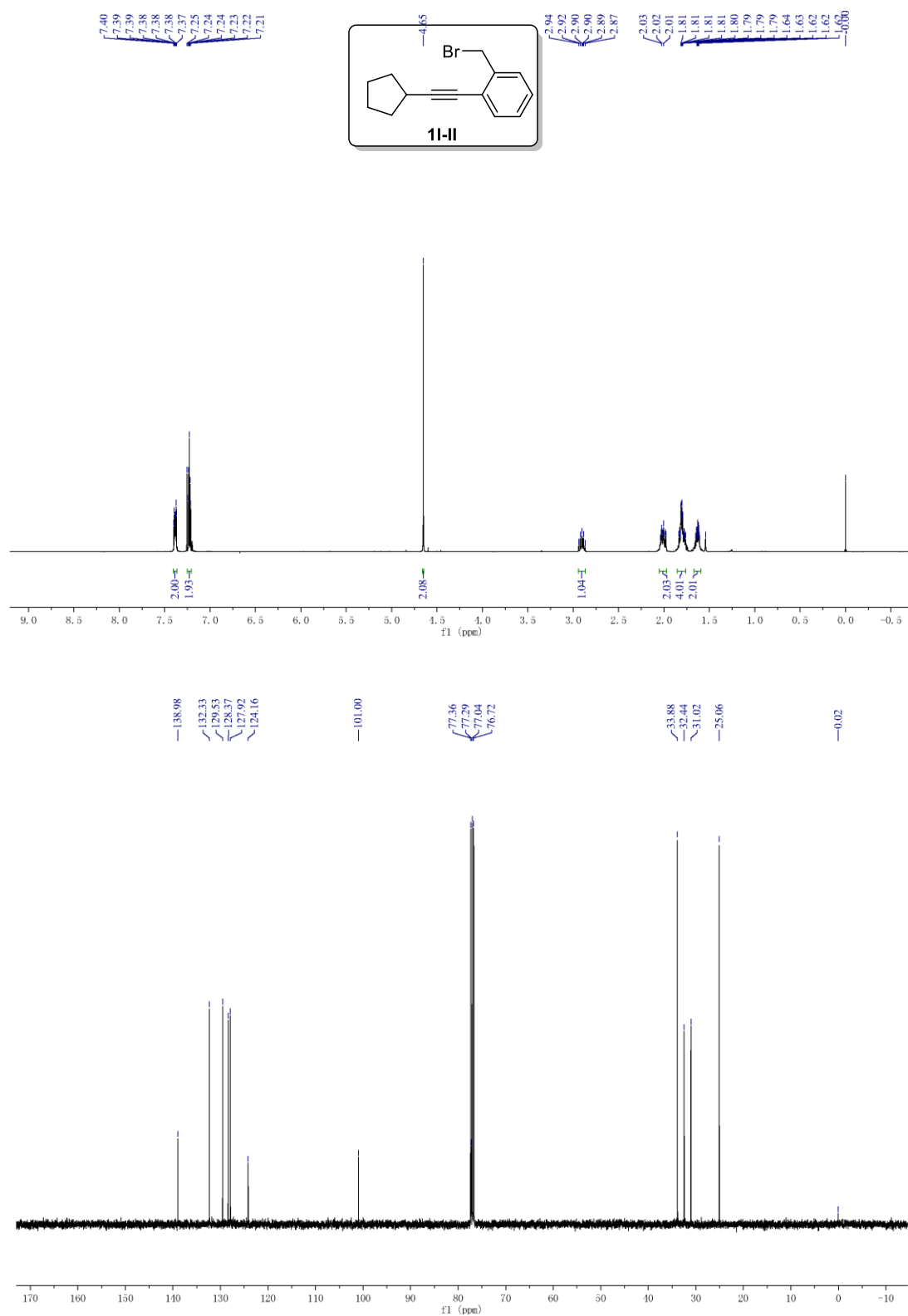


**Figure 4.4**  $^1\text{H}$  and  $^{13}\text{C}$  NMR spectrum of compound **1m-II**

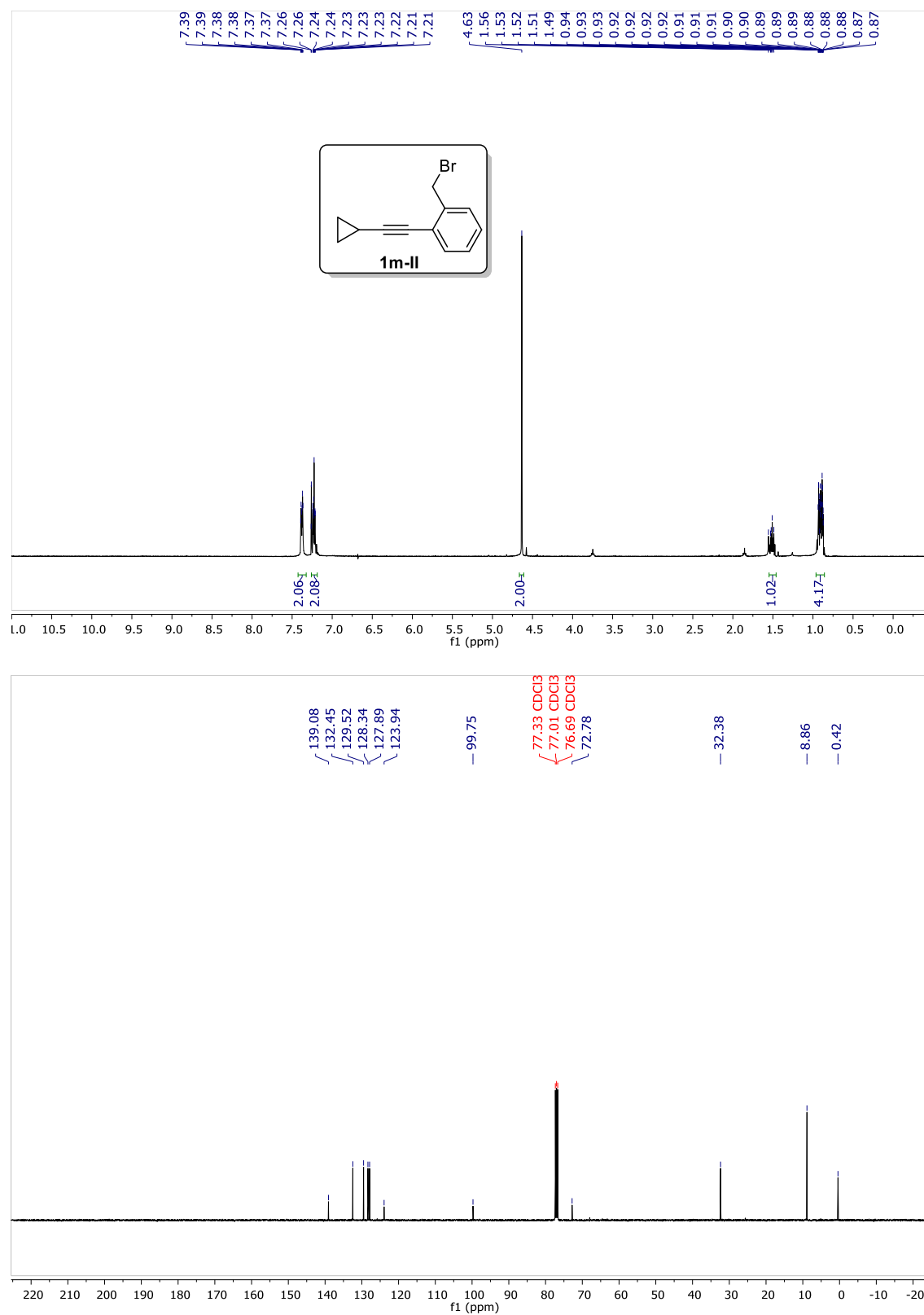


**Figure 4.5**  $^1\text{H}$  and  $^{13}\text{C}$  NMR spectrum of compound **1n-I**

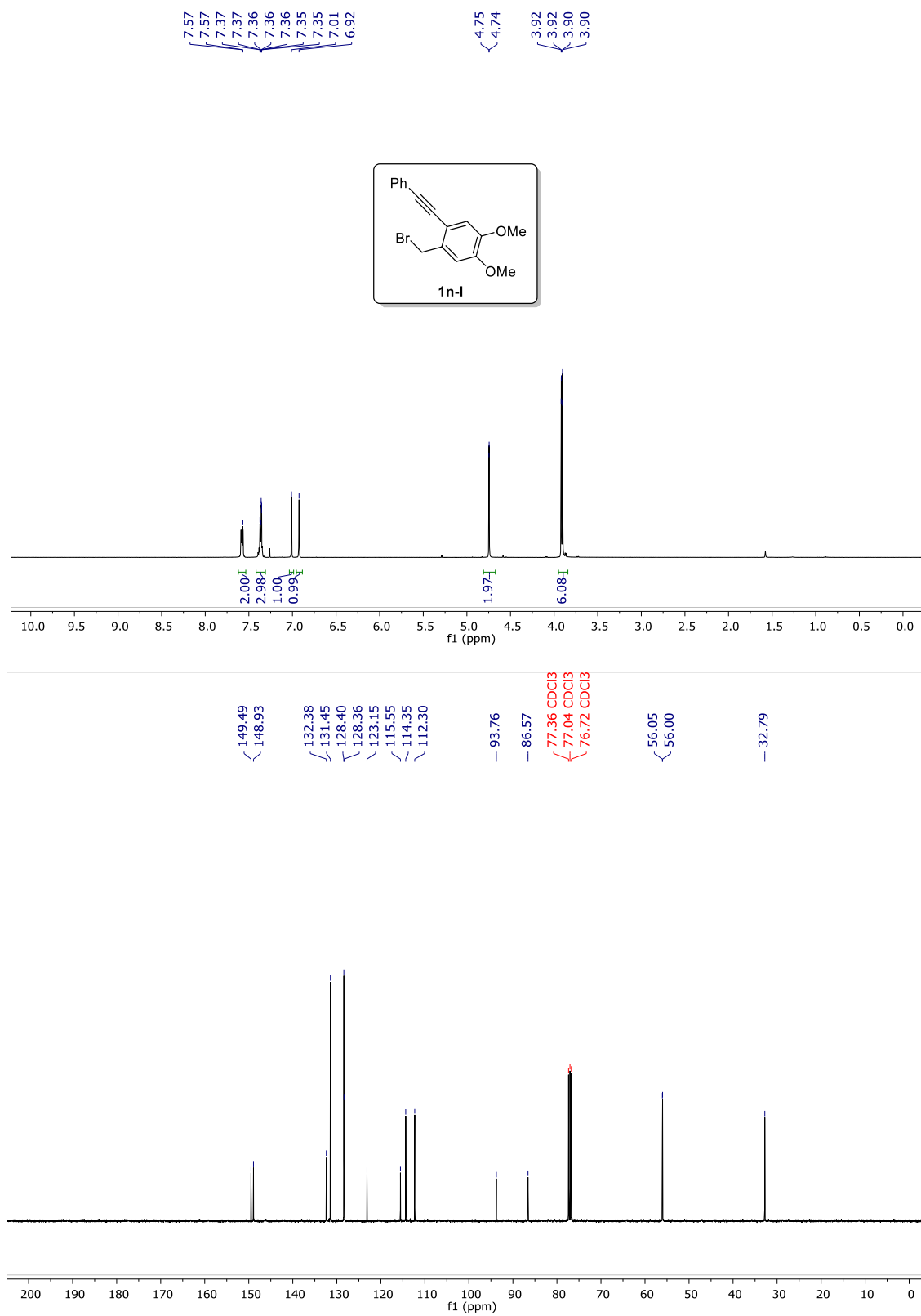


**Figure 4.6**  $^1\text{H}$  and  $^{13}\text{C}$  NMR spectrum of compound **1u-I**

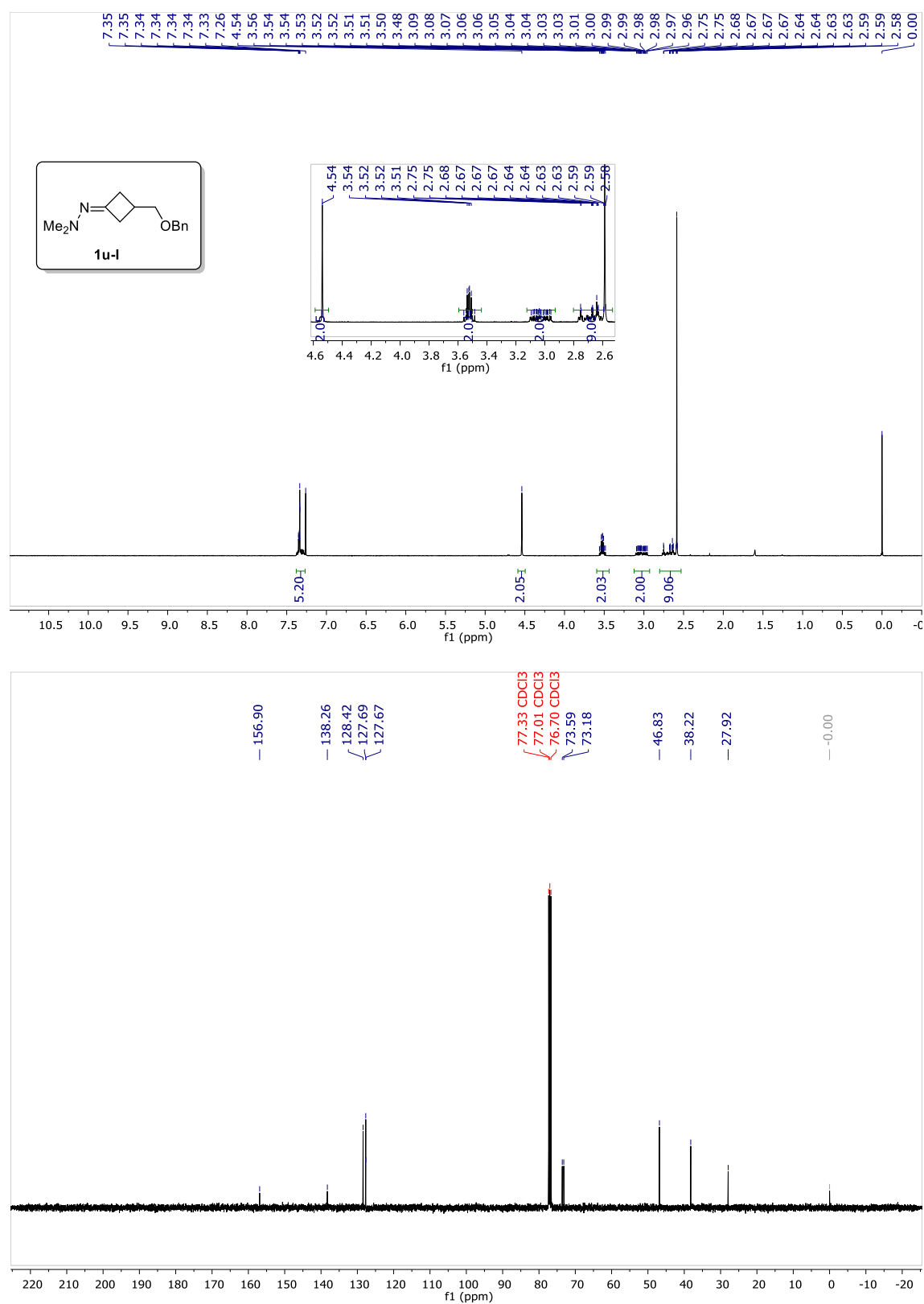


**Figure 4.7**  $^1\text{H}$  and  $^{13}\text{C}$  NMR spectrum of compound **1t-I**

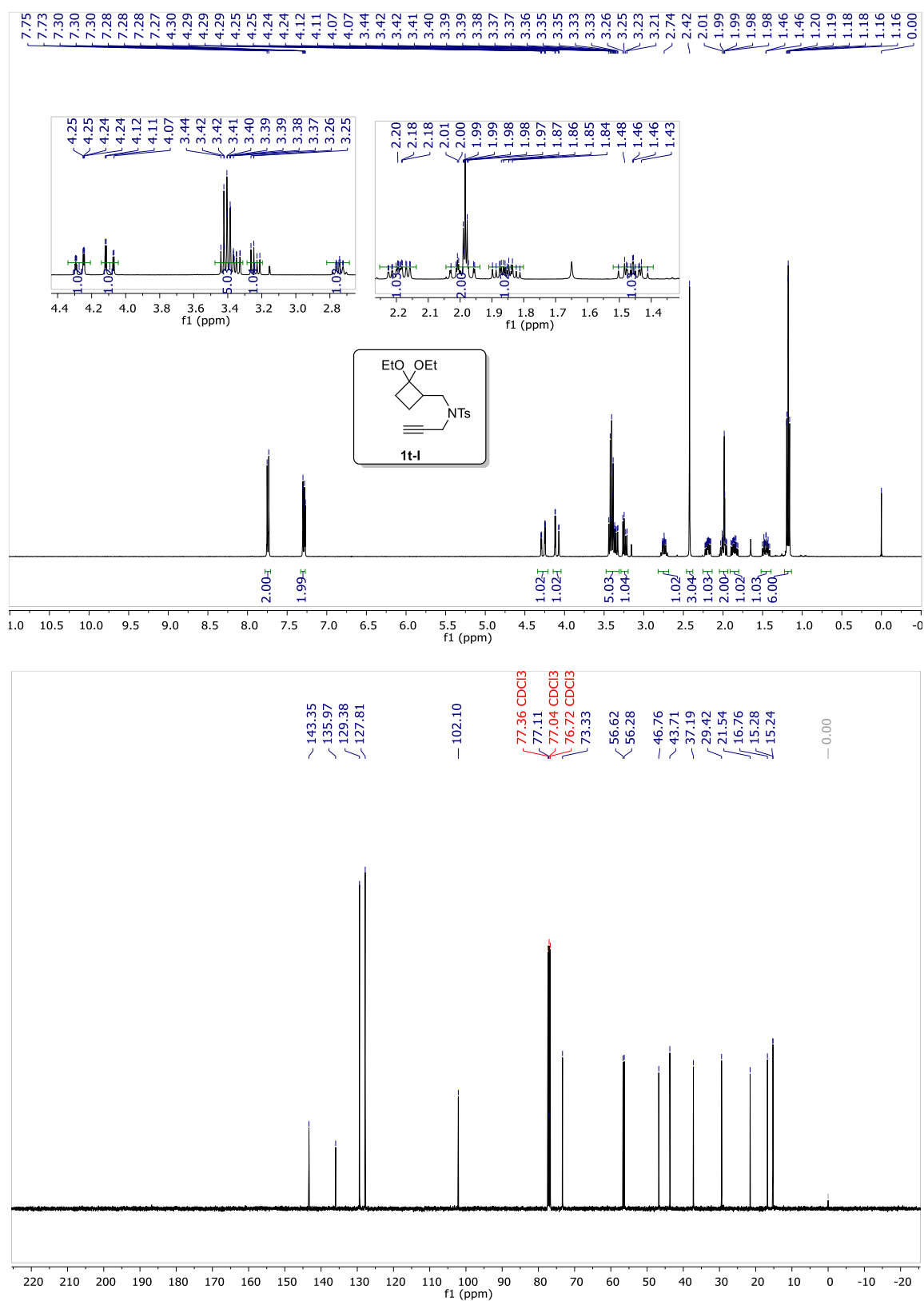


**Figure 4.8**  $^1\text{H}$  and  $^{13}\text{C}$  NMR spectrum of compound **1a**

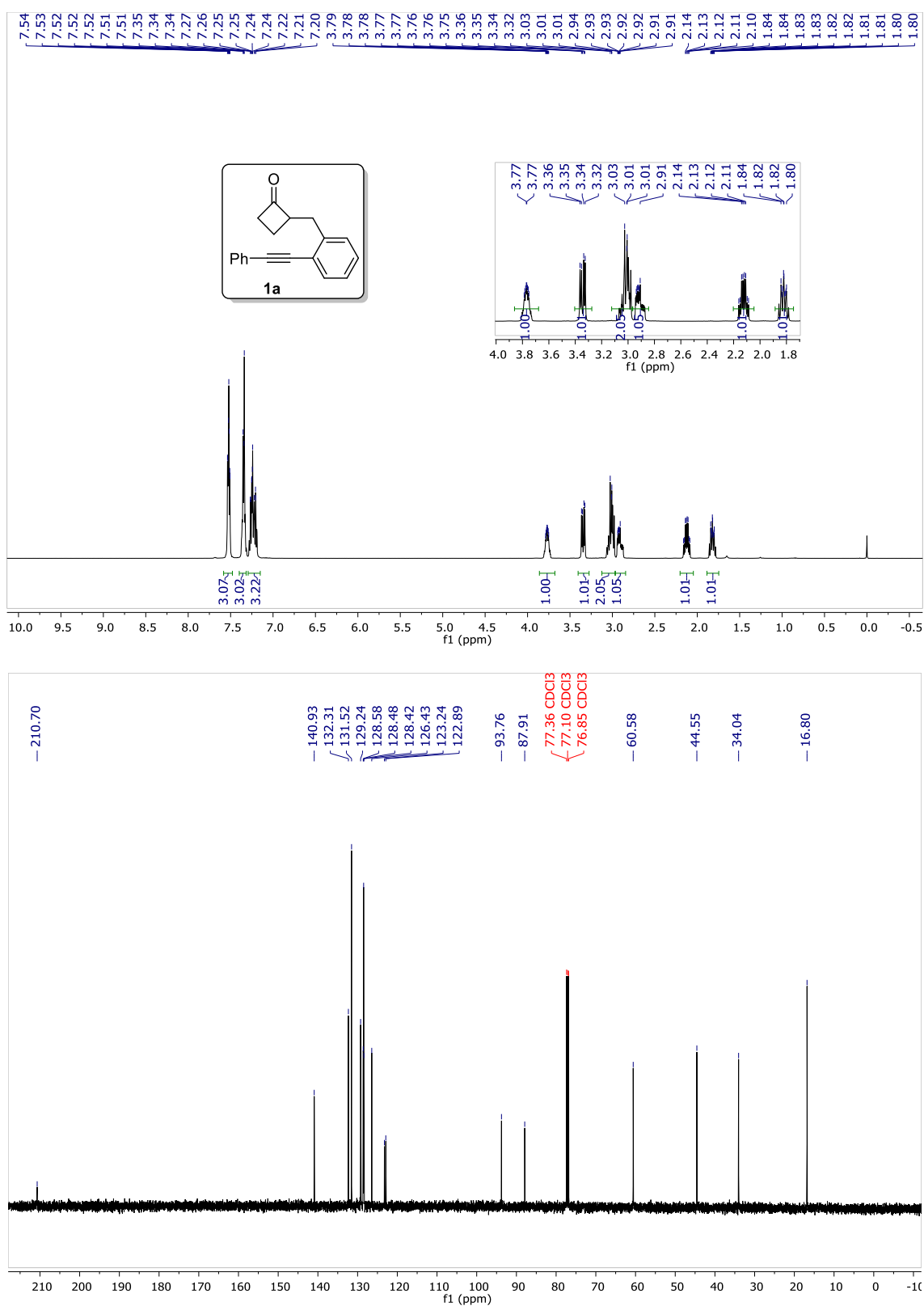


**Figure 4.9**  $^1\text{H}$  and  $^{13}\text{C}$  NMR spectrum of compound **1b**

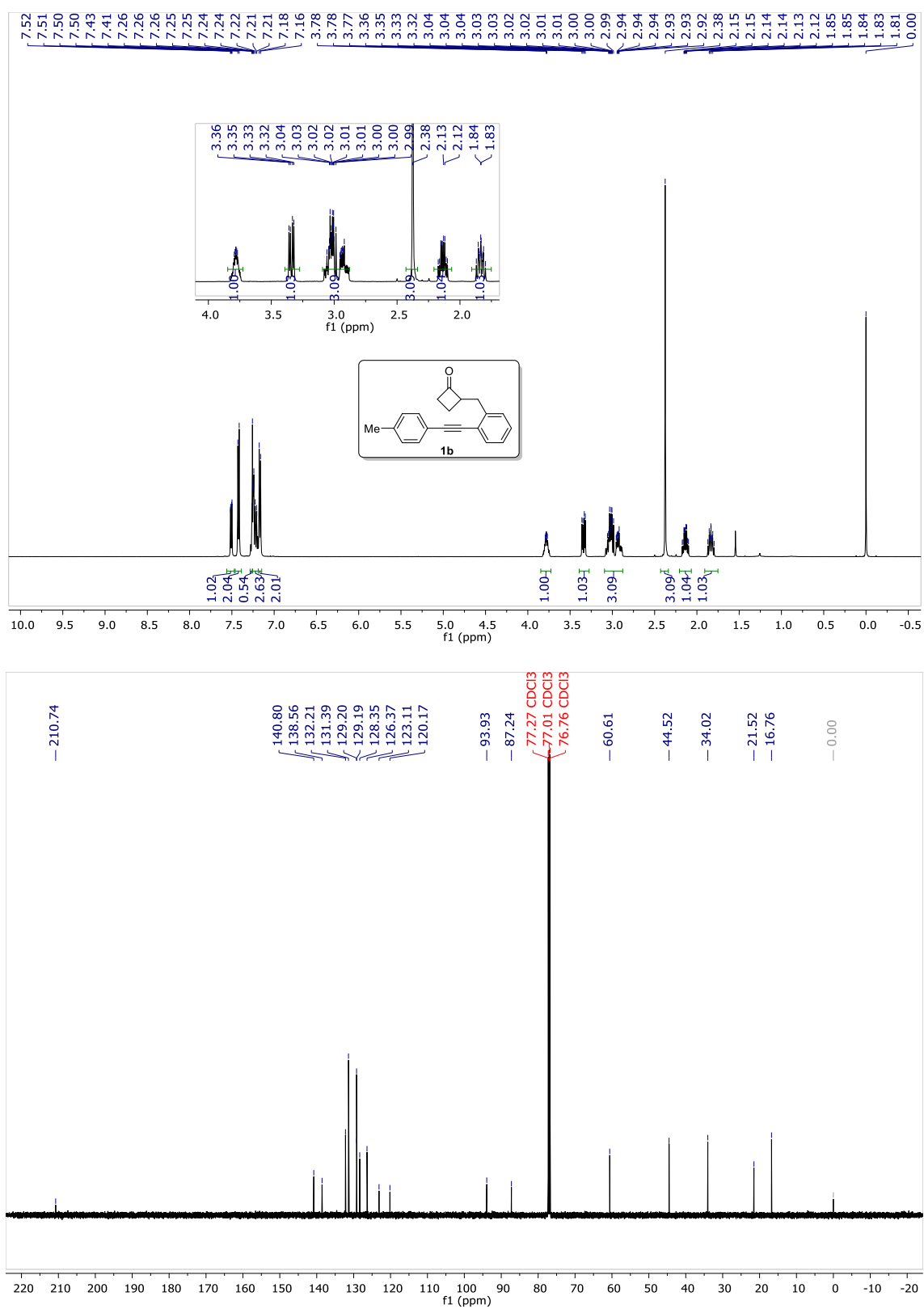




**Figure 4.10**  $^1\text{H}$  and  $^{13}\text{C}$  NMR spectrum of compound **1c**

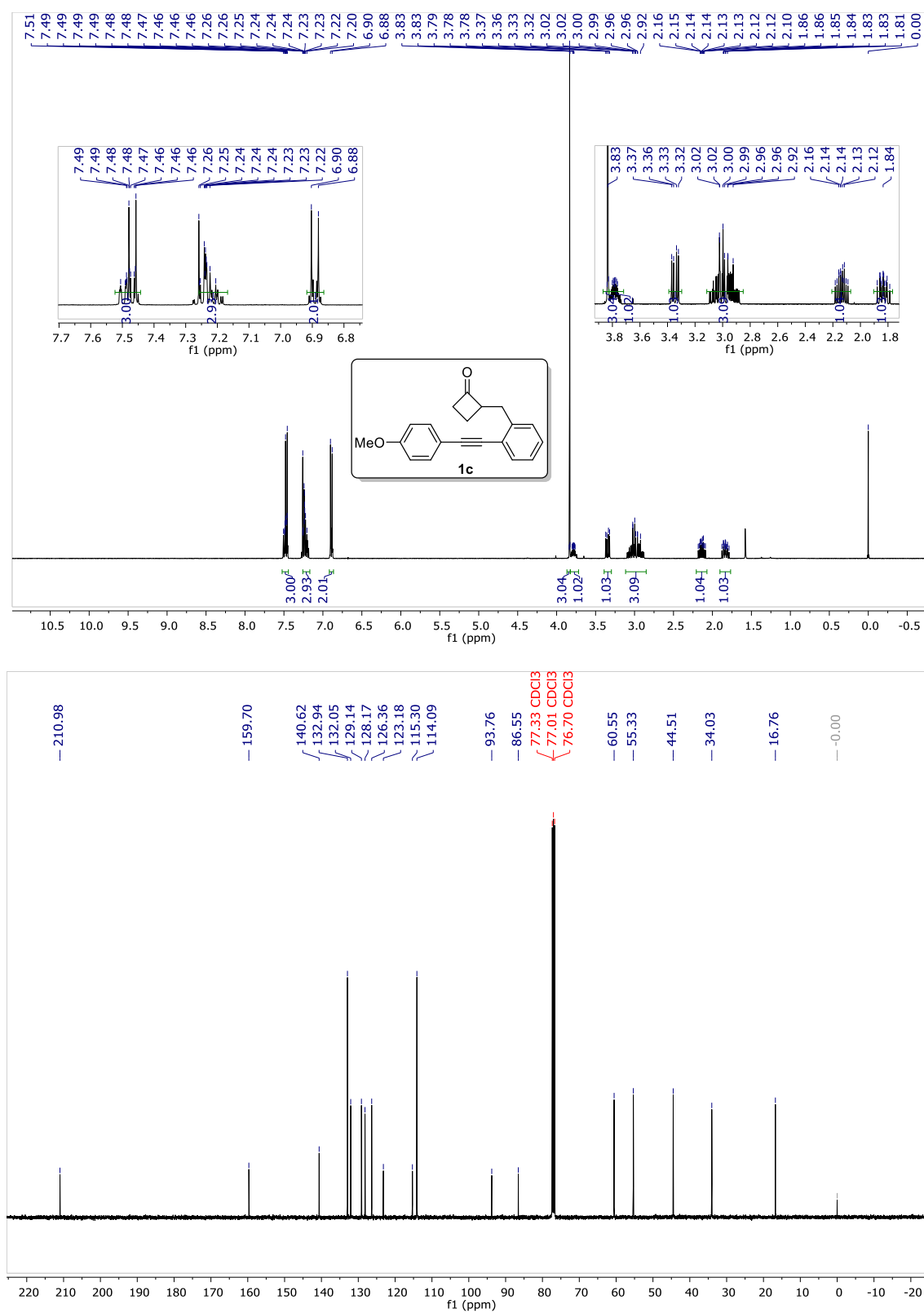


**Figure 4.11**  $^1\text{H}$  and  $^{13}\text{C}$  NMR spectrum of compound **1d**

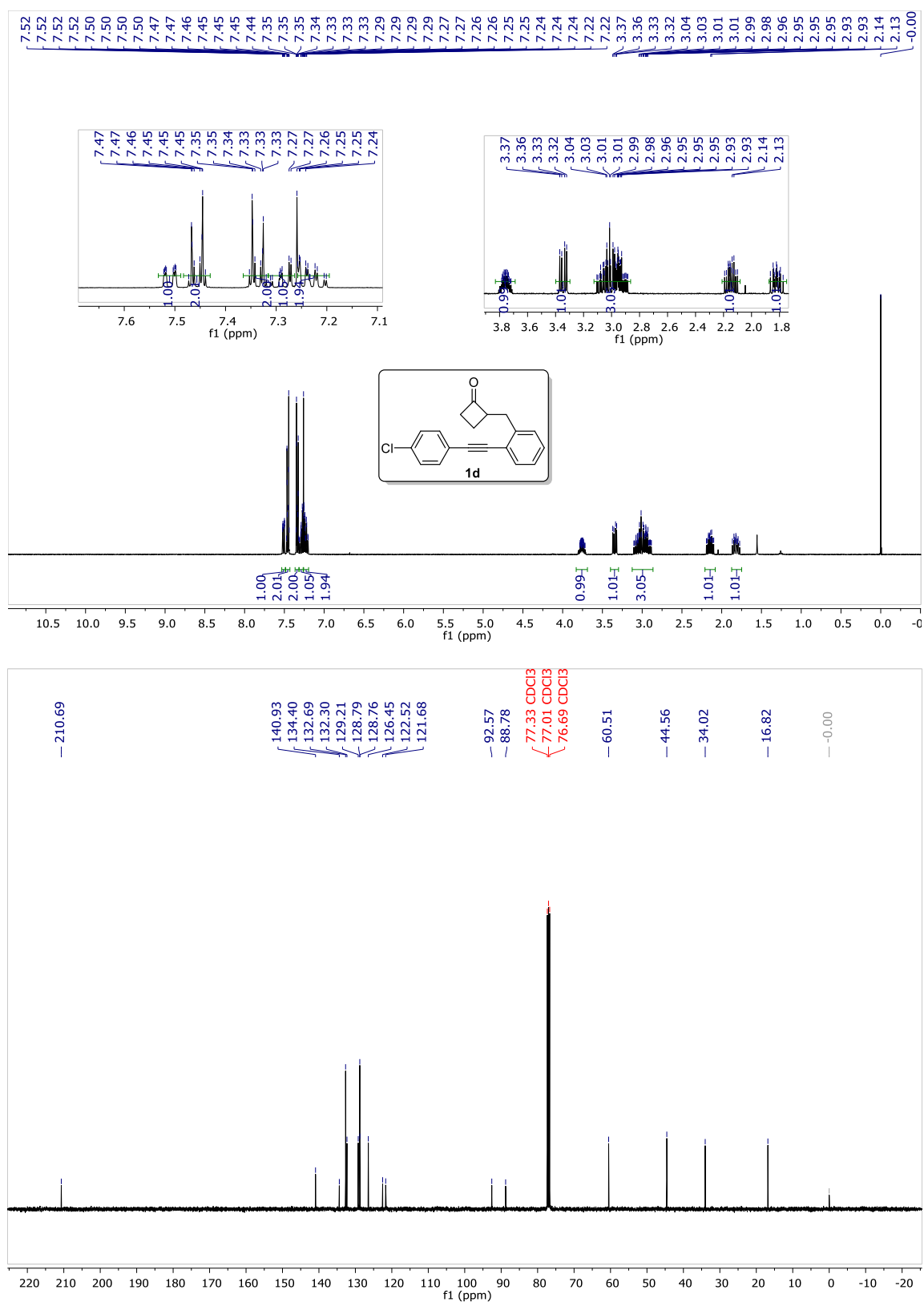


**Figure 4.12**  $^1\text{H}$  and  $^{13}\text{C}$  NMR spectrum of compound **1e**

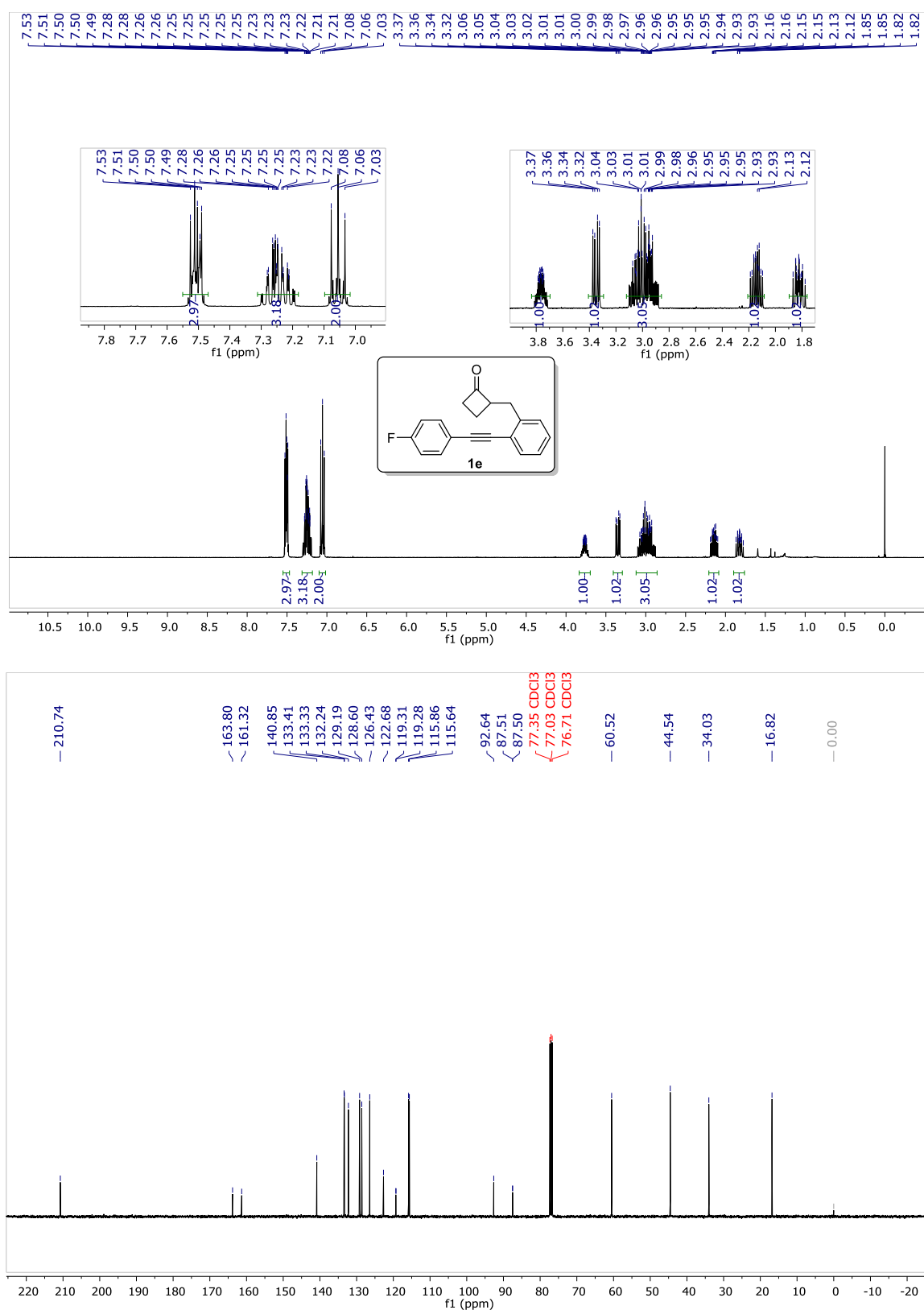


**Figure 4.13**  $^1\text{H}$  and  $^{13}\text{C}$  NMR spectrum of compound **1f**

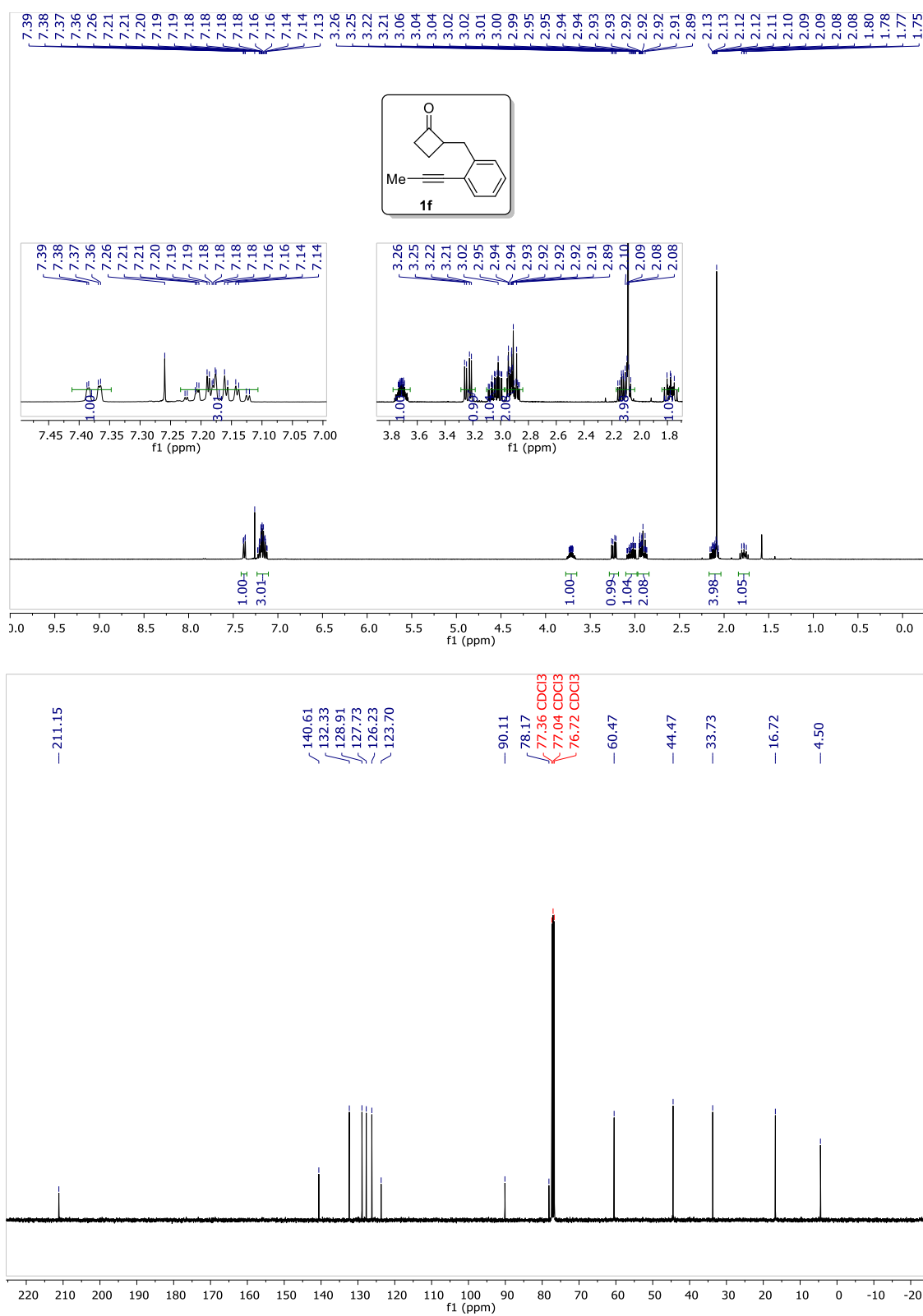


**Figure 4.14**  $^1\text{H}$  and  $^{13}\text{C}$  NMR spectrum of compound **1g**

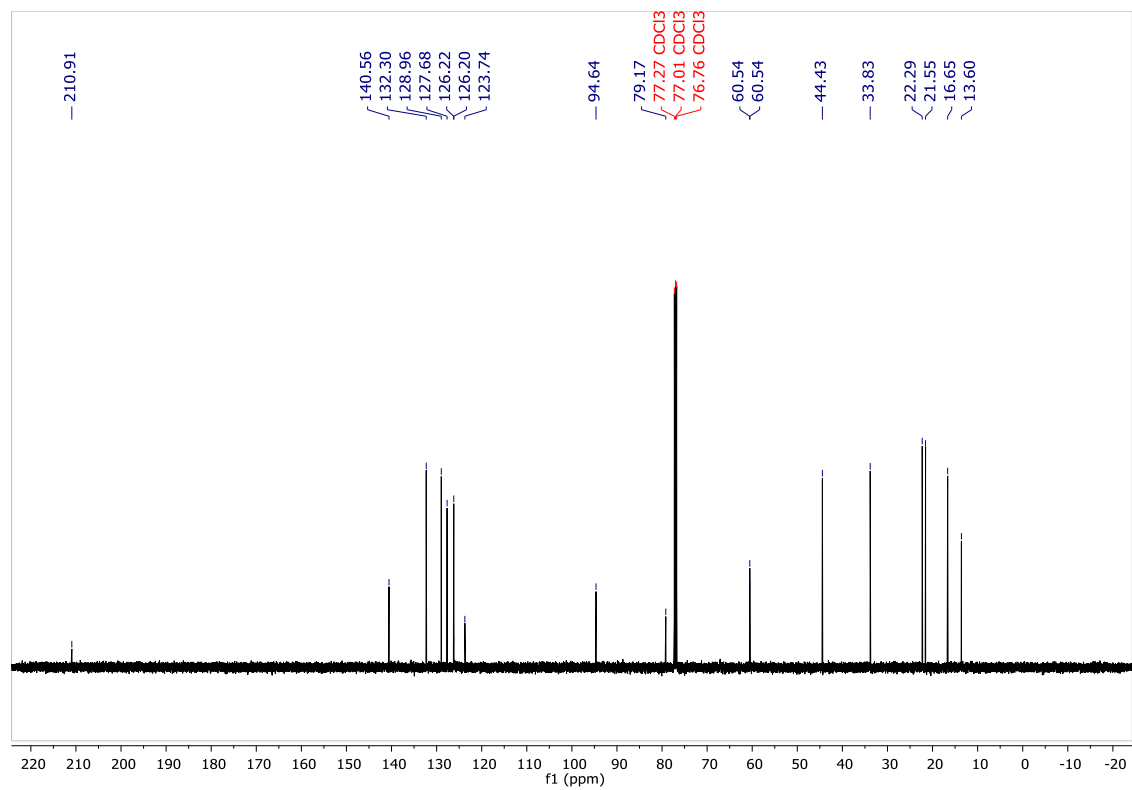
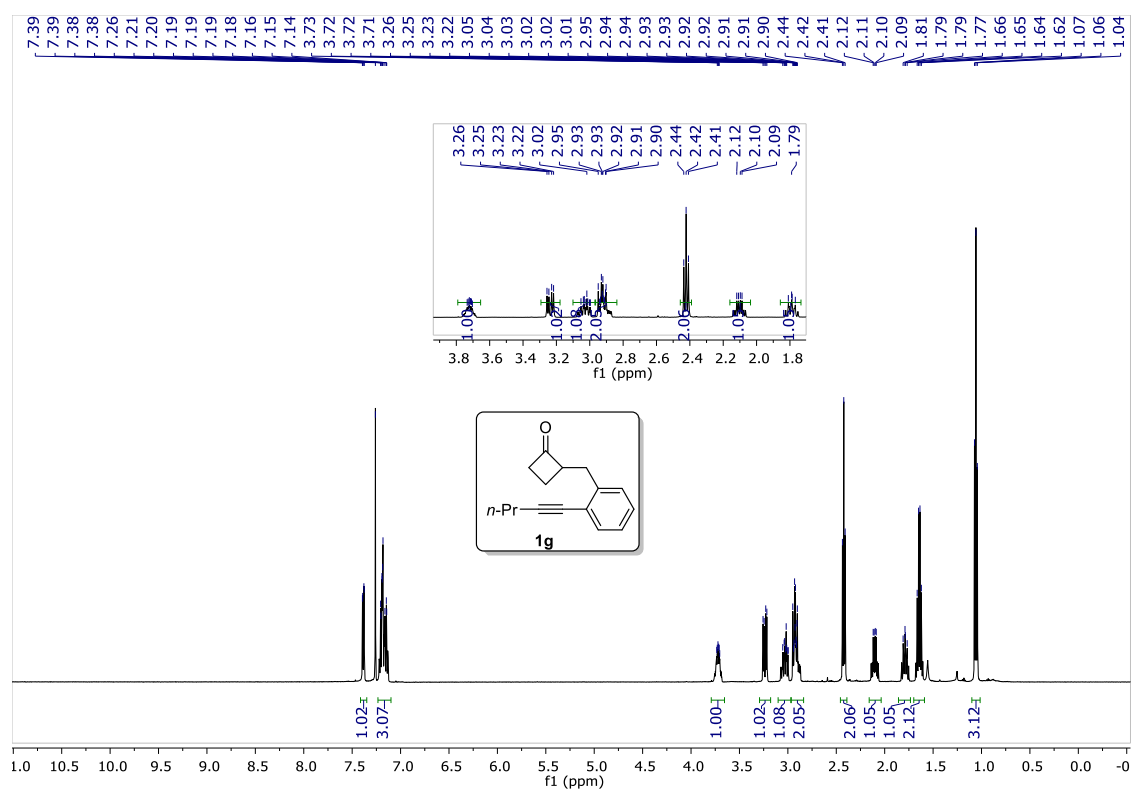


**Figure 4.15**  $^1\text{H}$  and  $^{13}\text{C}$  NMR spectrum of compound **1h**

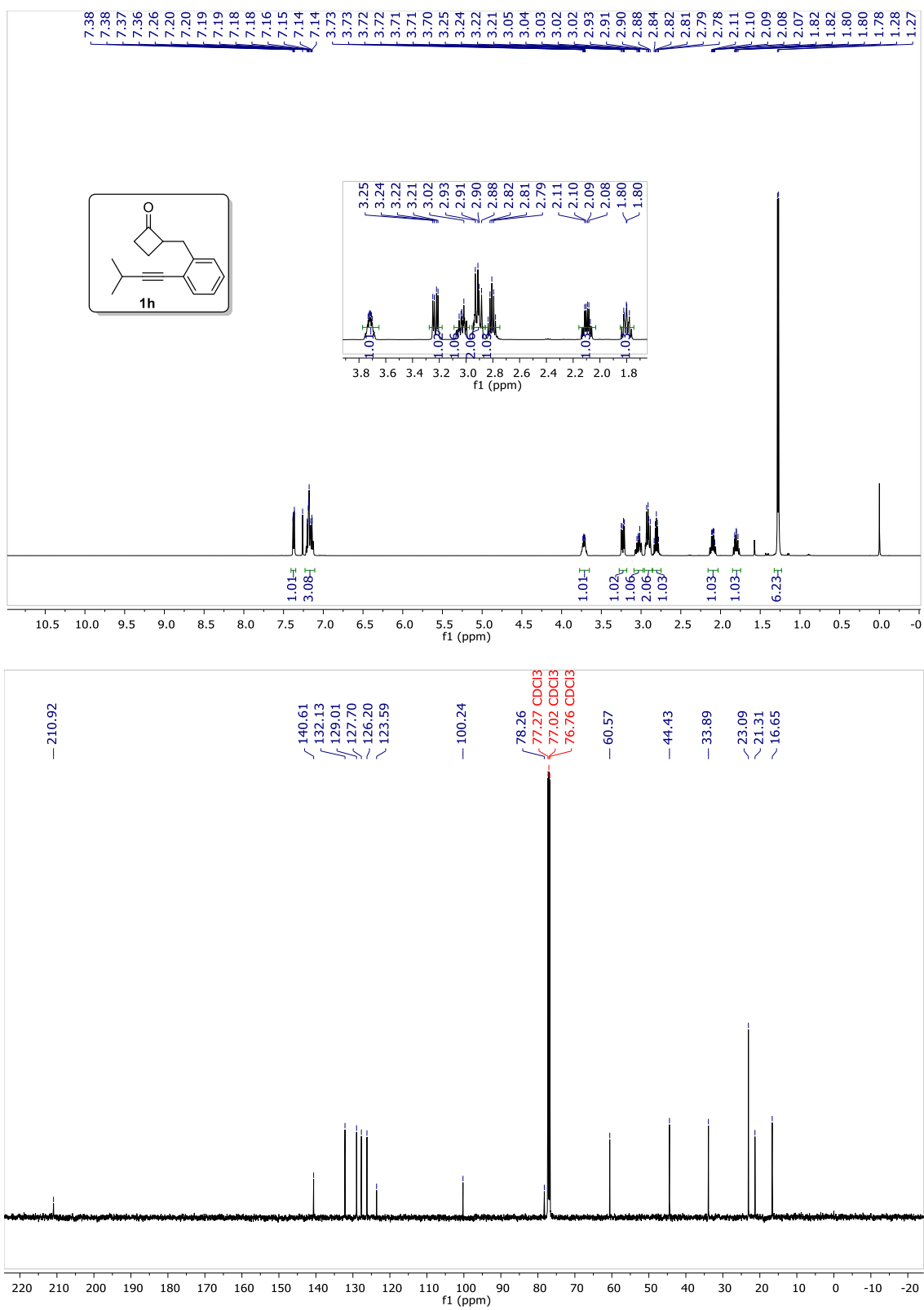


**Figure 4.16**  $^1\text{H}$  and  $^{13}\text{C}$  NMR spectrum of compound **1i**

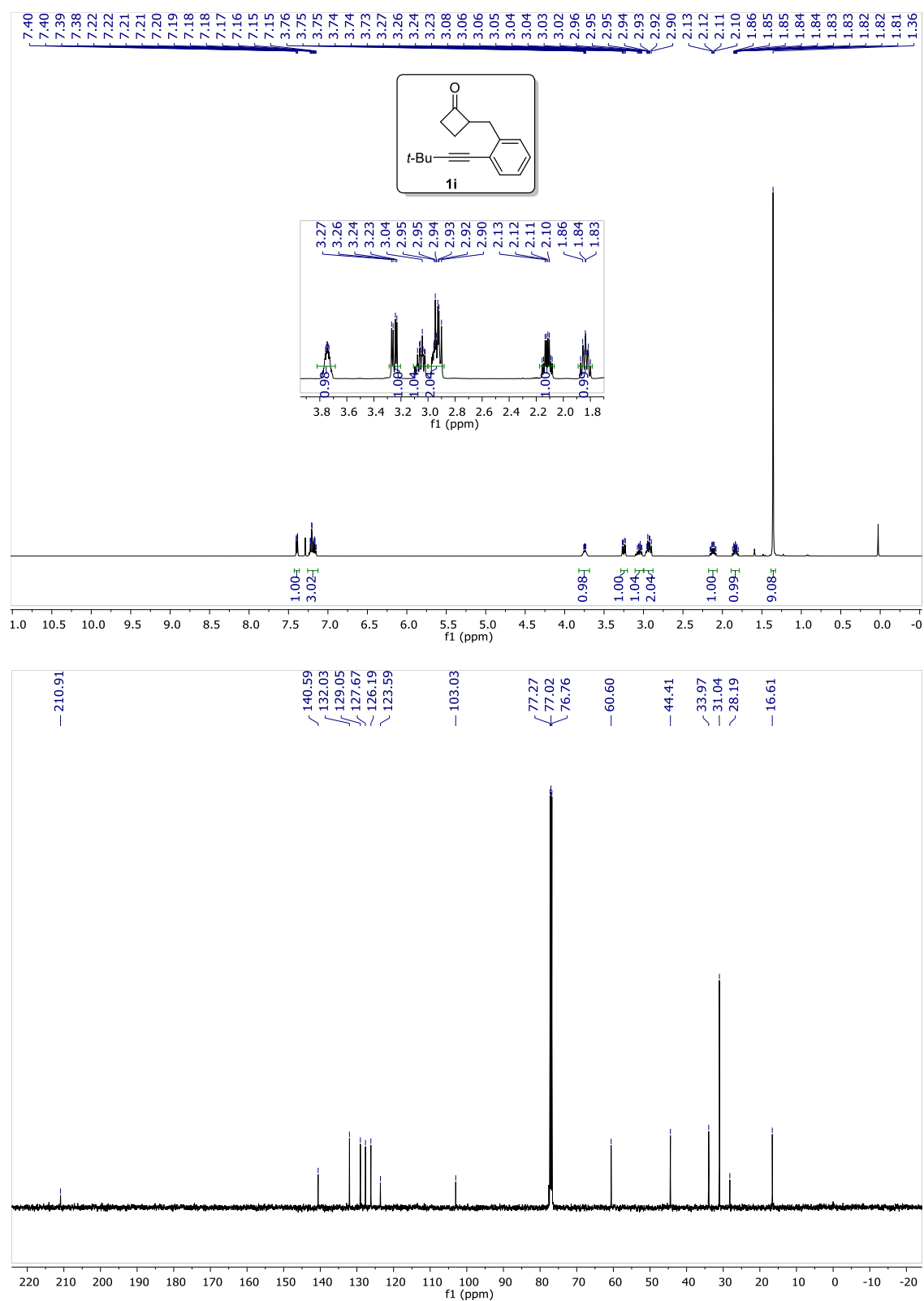


**Figure 4.17**  $^1\text{H}$  and  $^{13}\text{C}$  NMR spectrum of compound **1j**

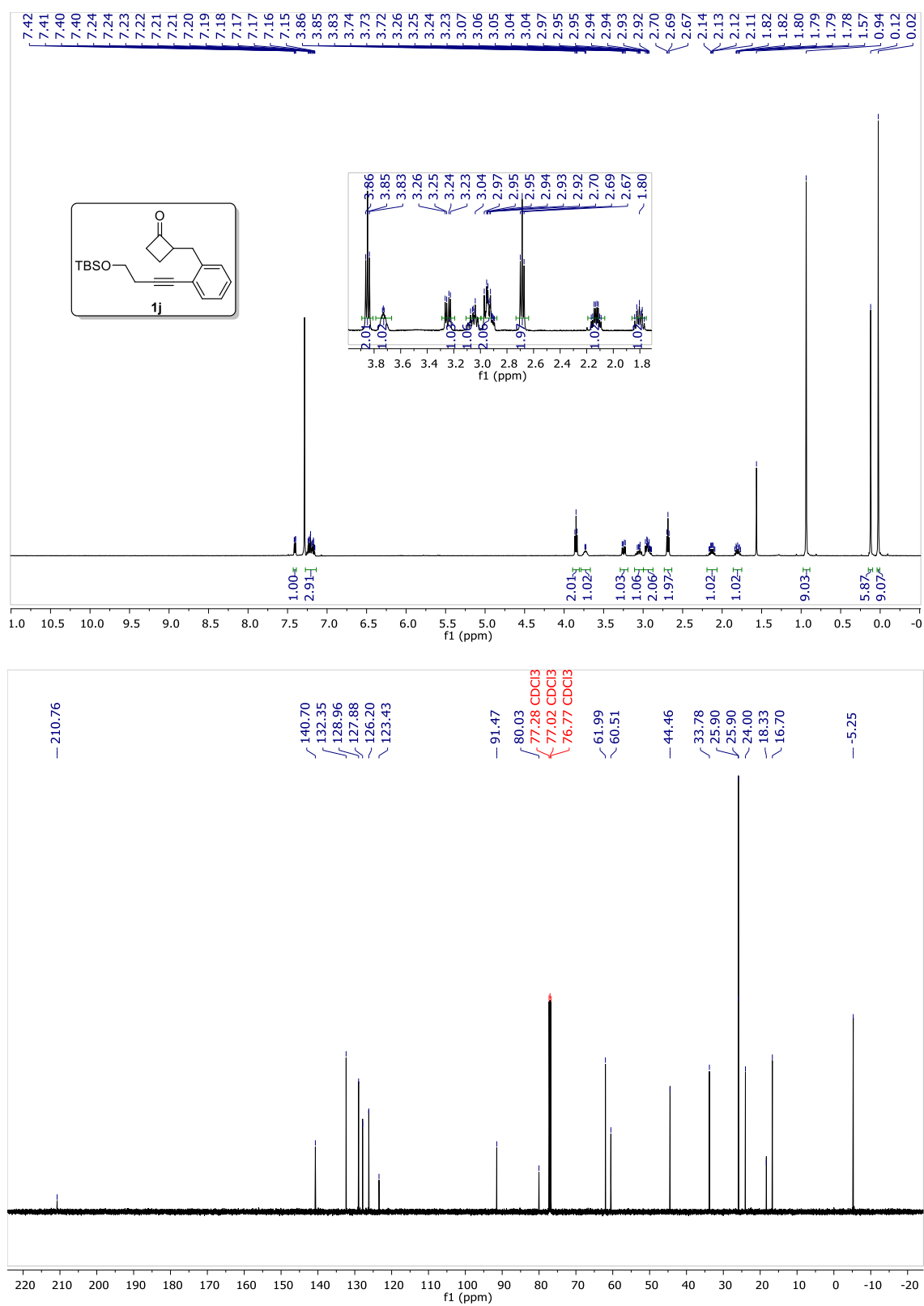




**Figure 4.18**  $^1\text{H}$  and  $^{13}\text{C}$  NMR spectrum of compound **1k**

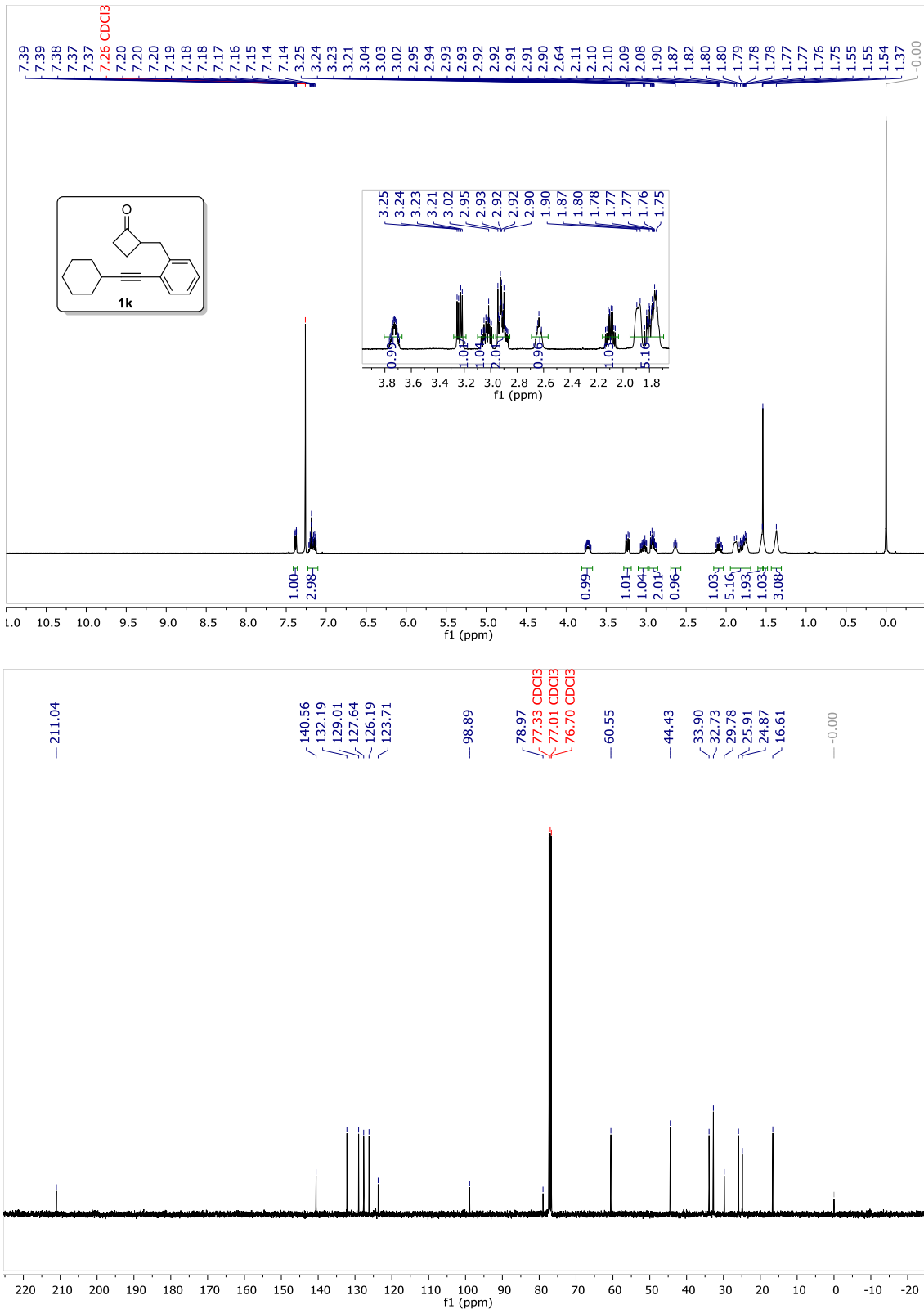


**Figure 4.19**  $^1\text{H}$  and  $^{13}\text{C}$  NMR spectrum of compound **11**

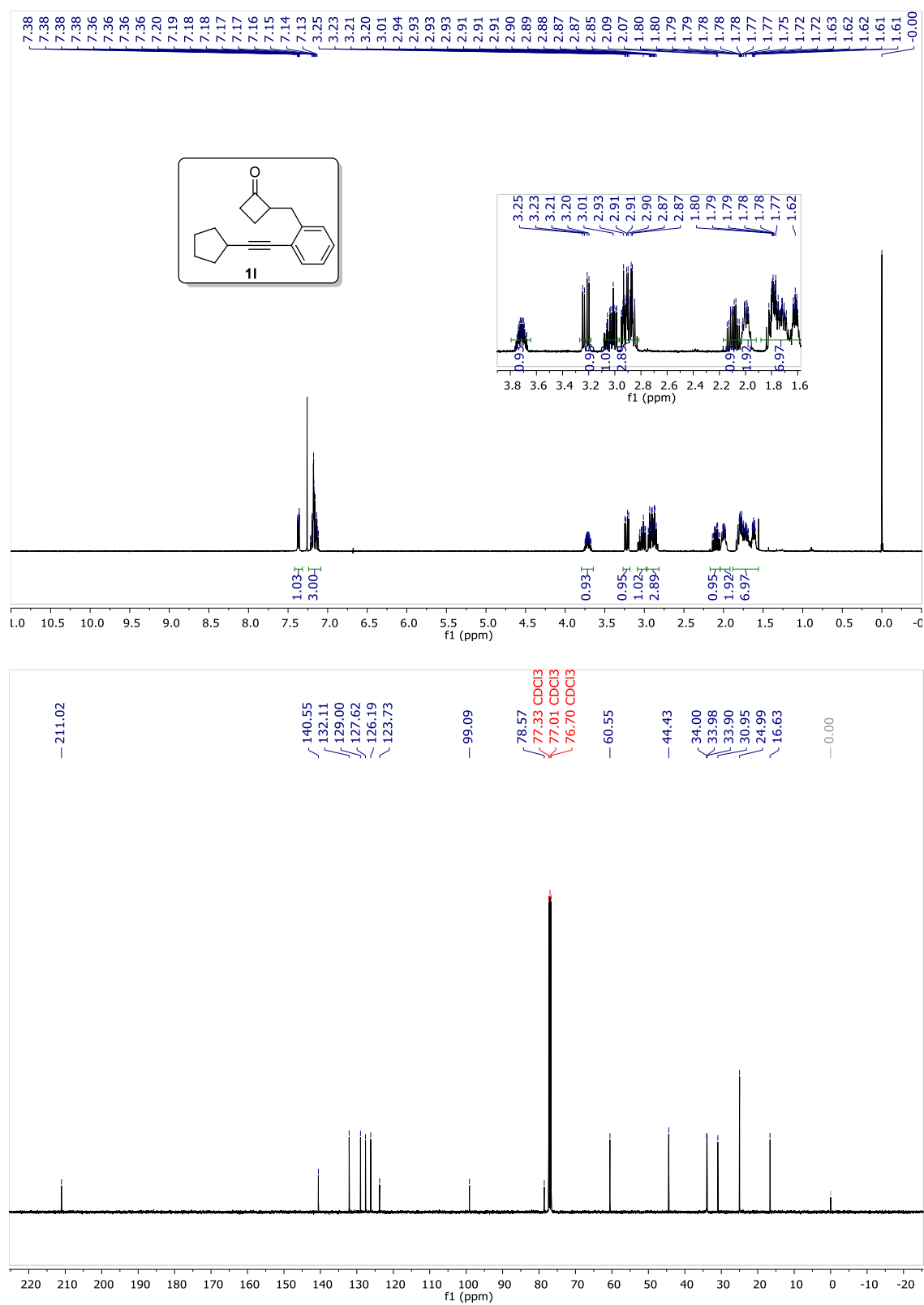


**Figure 4.20**  $^1\text{H}$  and  $^{13}\text{C}$  NMR spectrum of compound **1m**

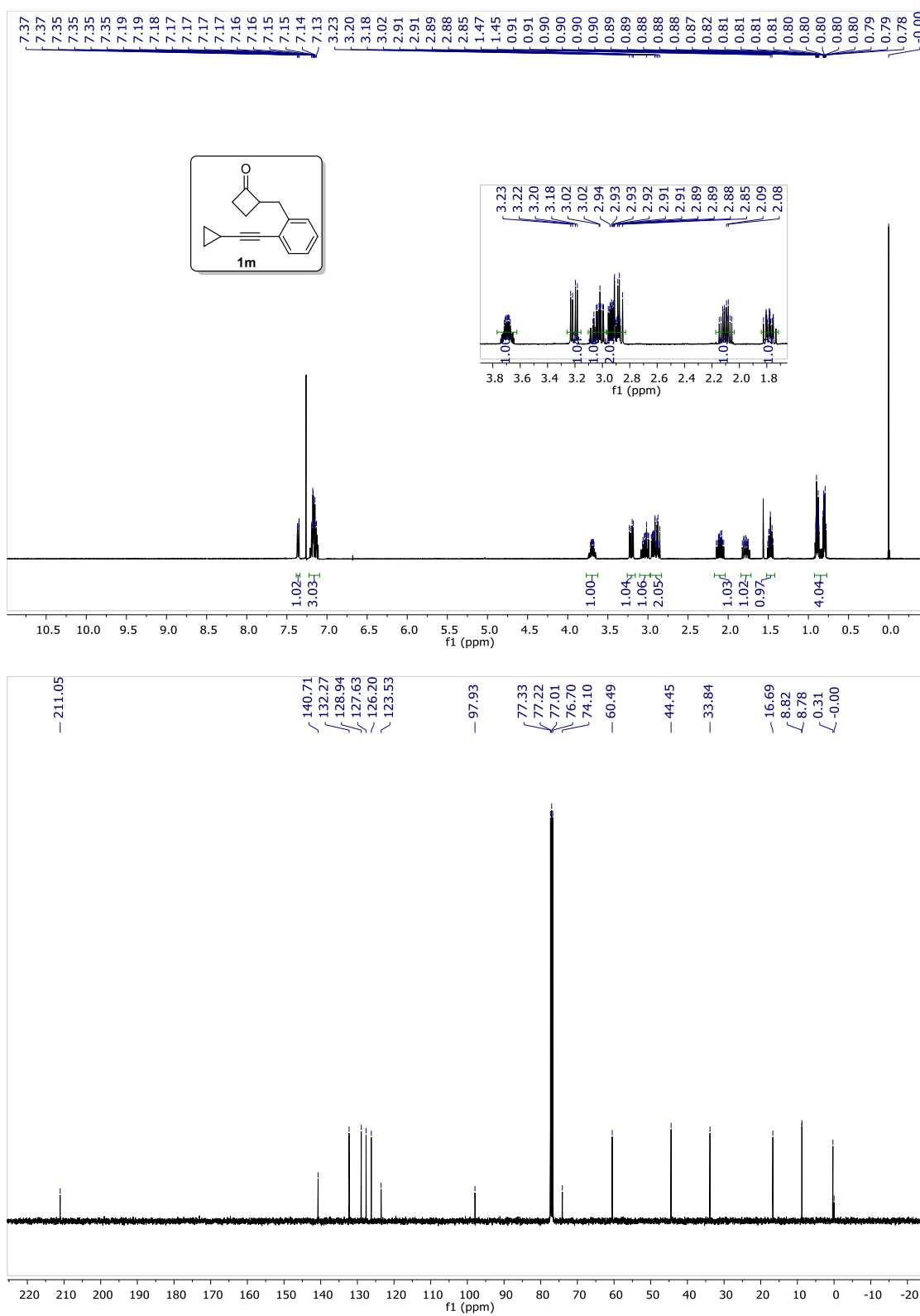


**Figure 4.21**  $^1\text{H}$  and  $^{13}\text{C}$  NMR spectrum of compound **1n**

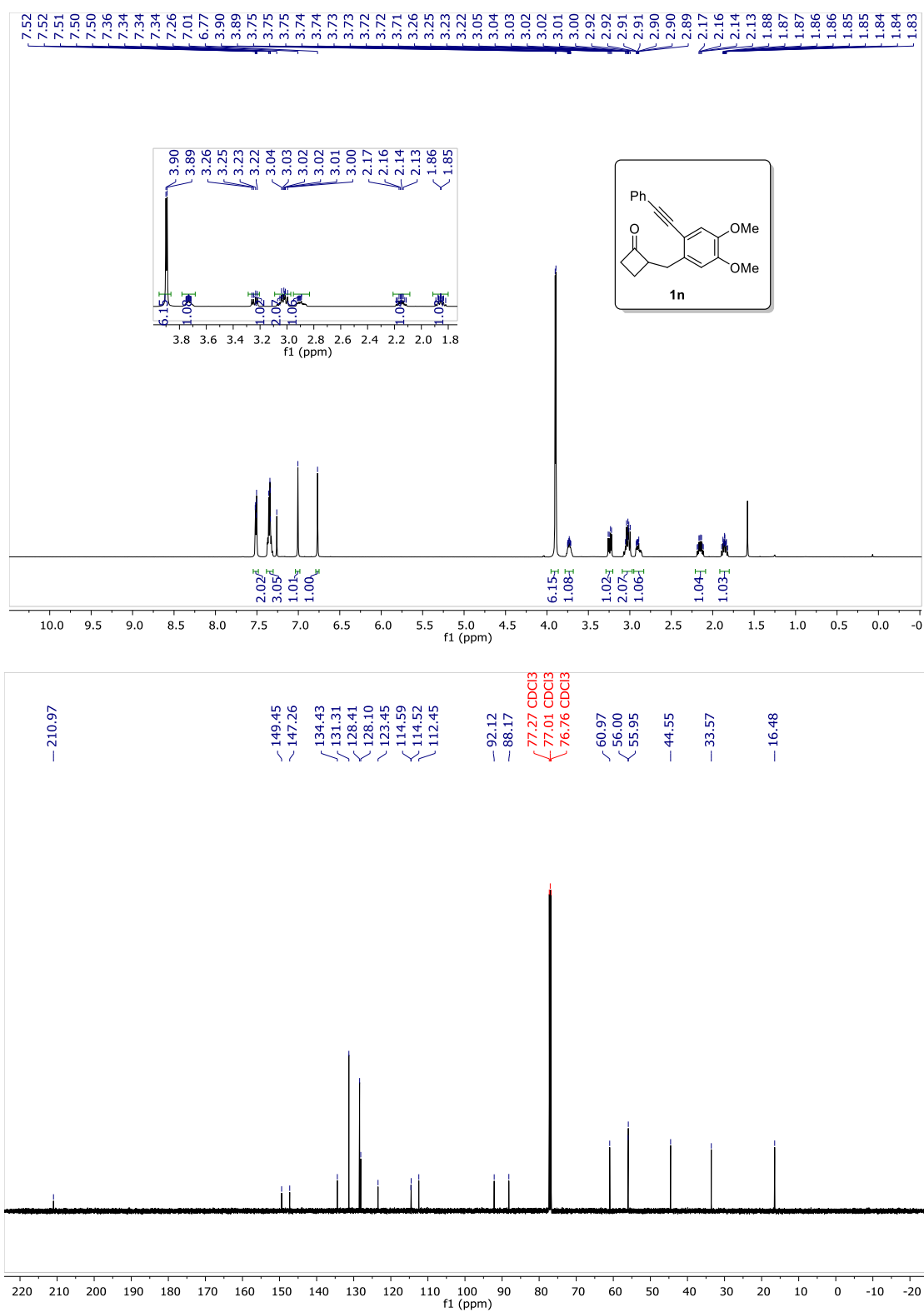
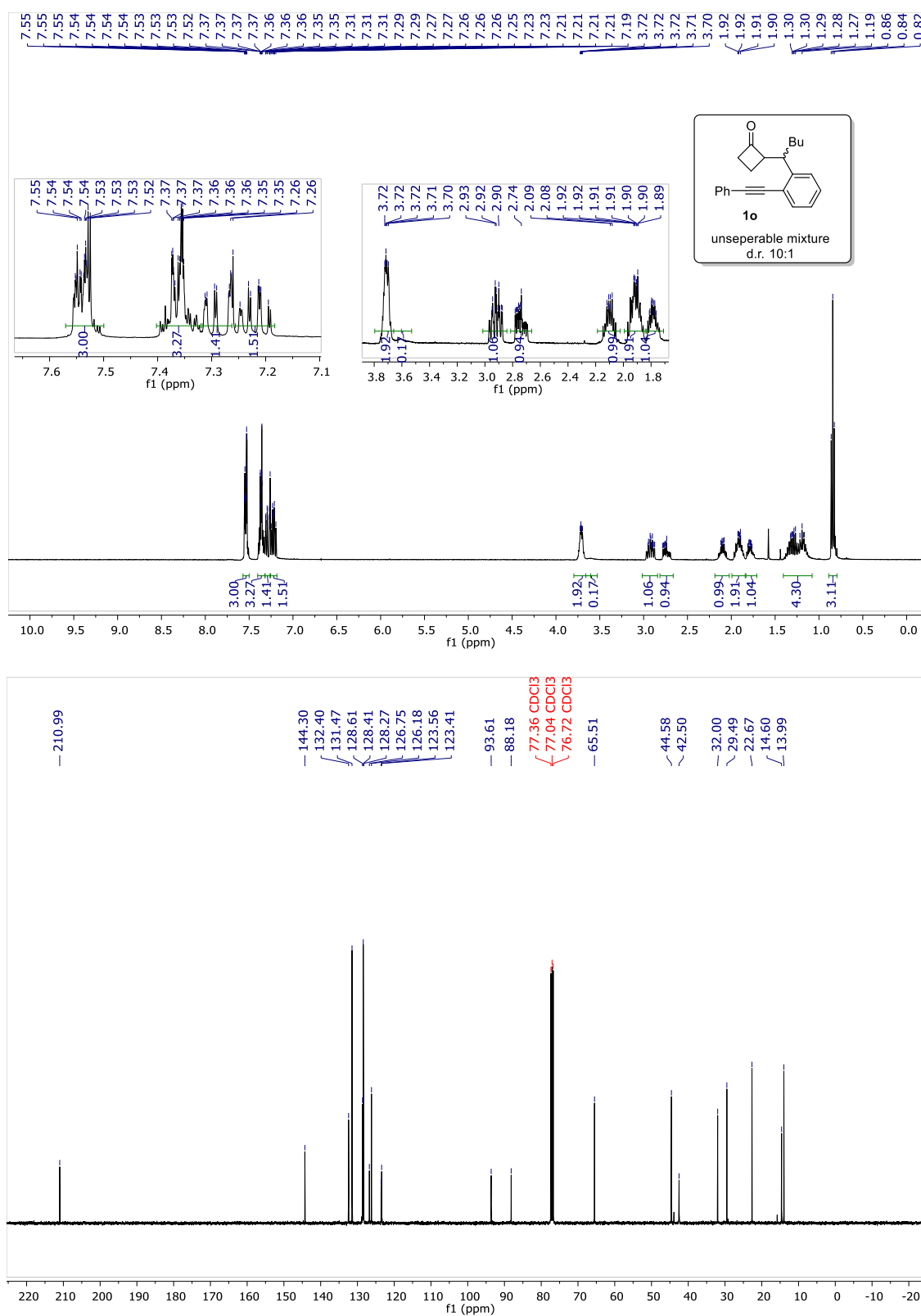
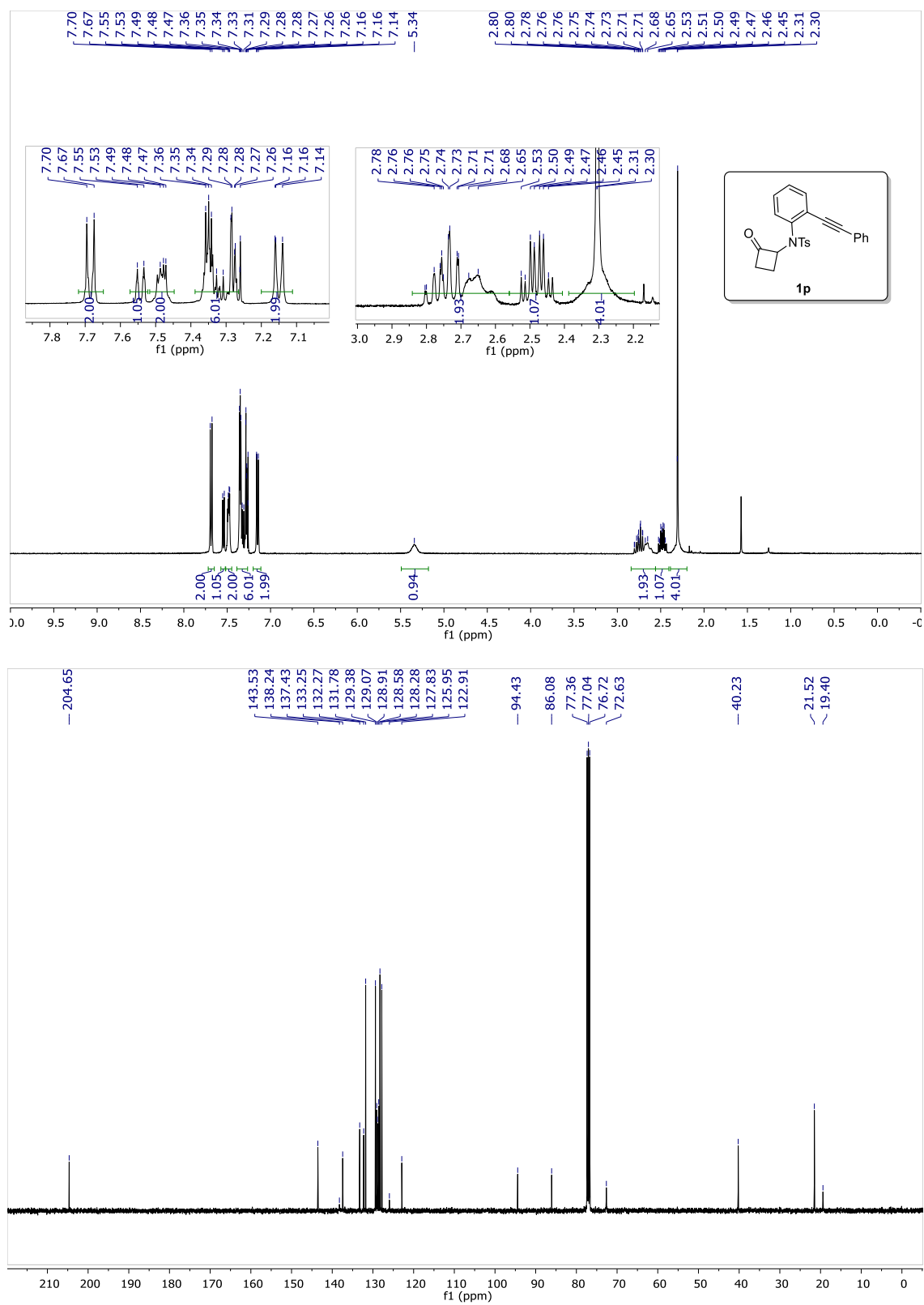


Figure 4.22  $^1\text{H}$  and  $^{13}\text{C}$  NMR spectrum of compound **1o**



**Figure 4.23**  $^1\text{H}$  and  $^{13}\text{C}$  NMR spectrum of compound **1p**



**Figure 4.24**  $^1\text{H}$  and  $^{13}\text{C}$  NMR spectrum of compound **1q**

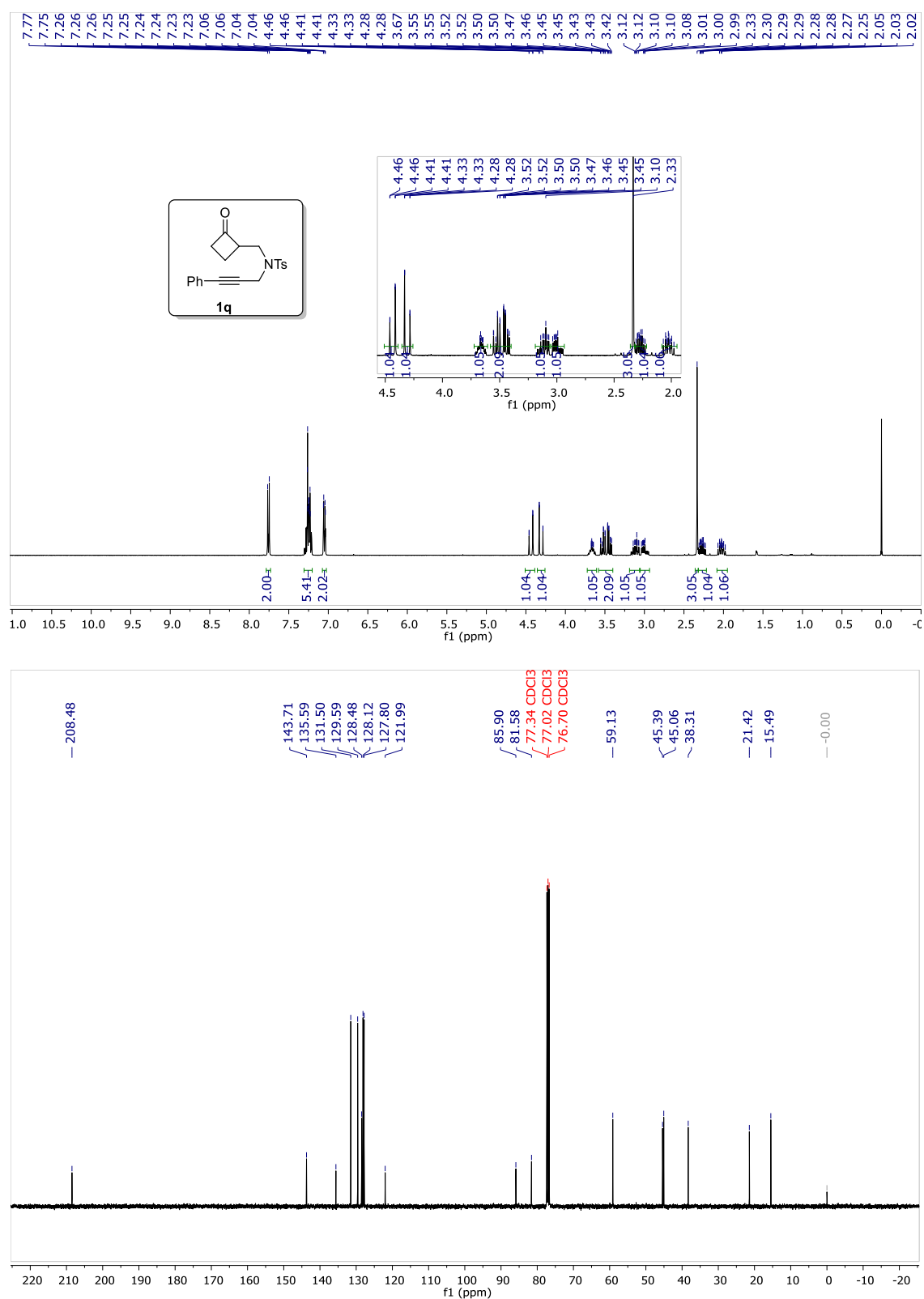
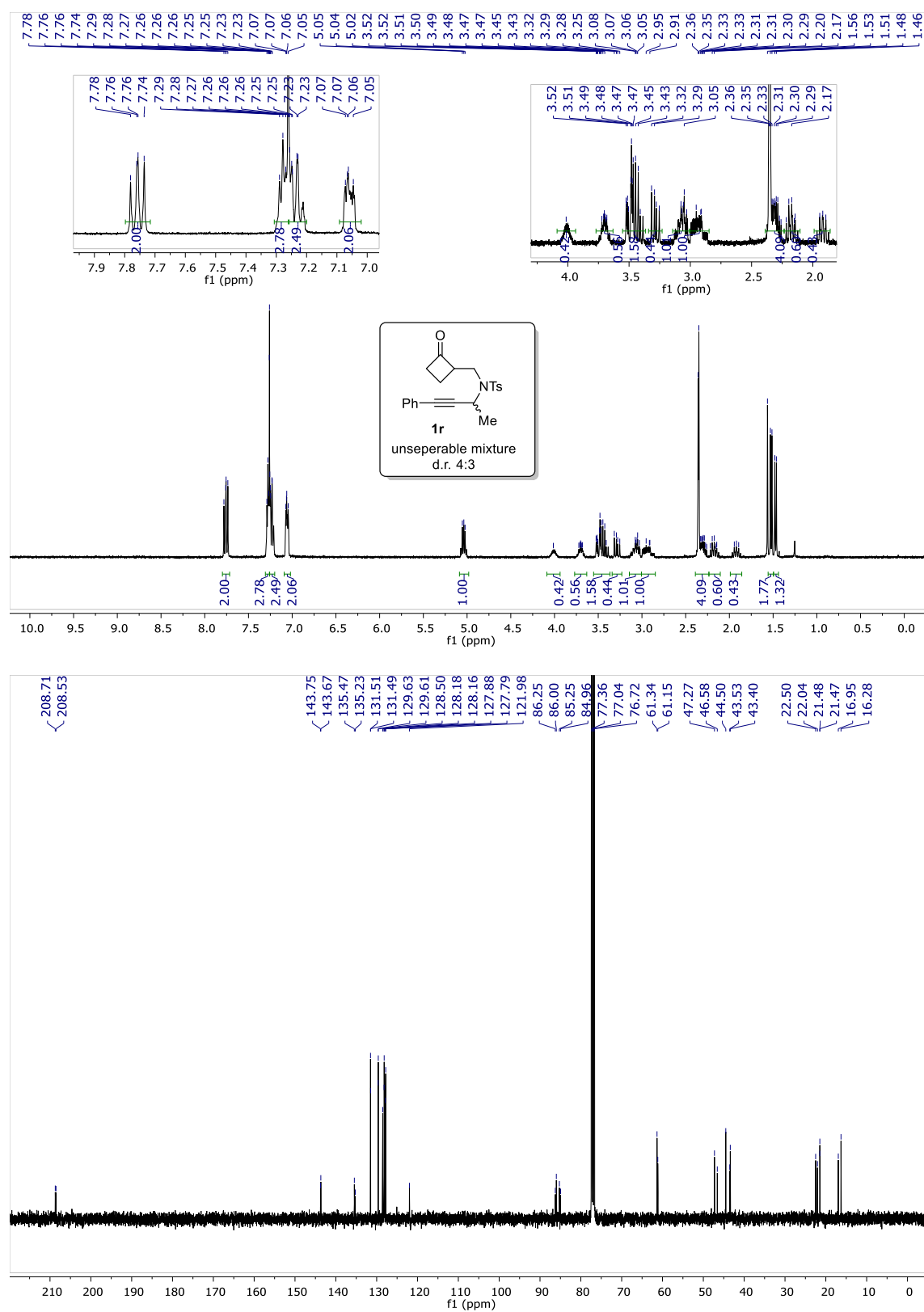
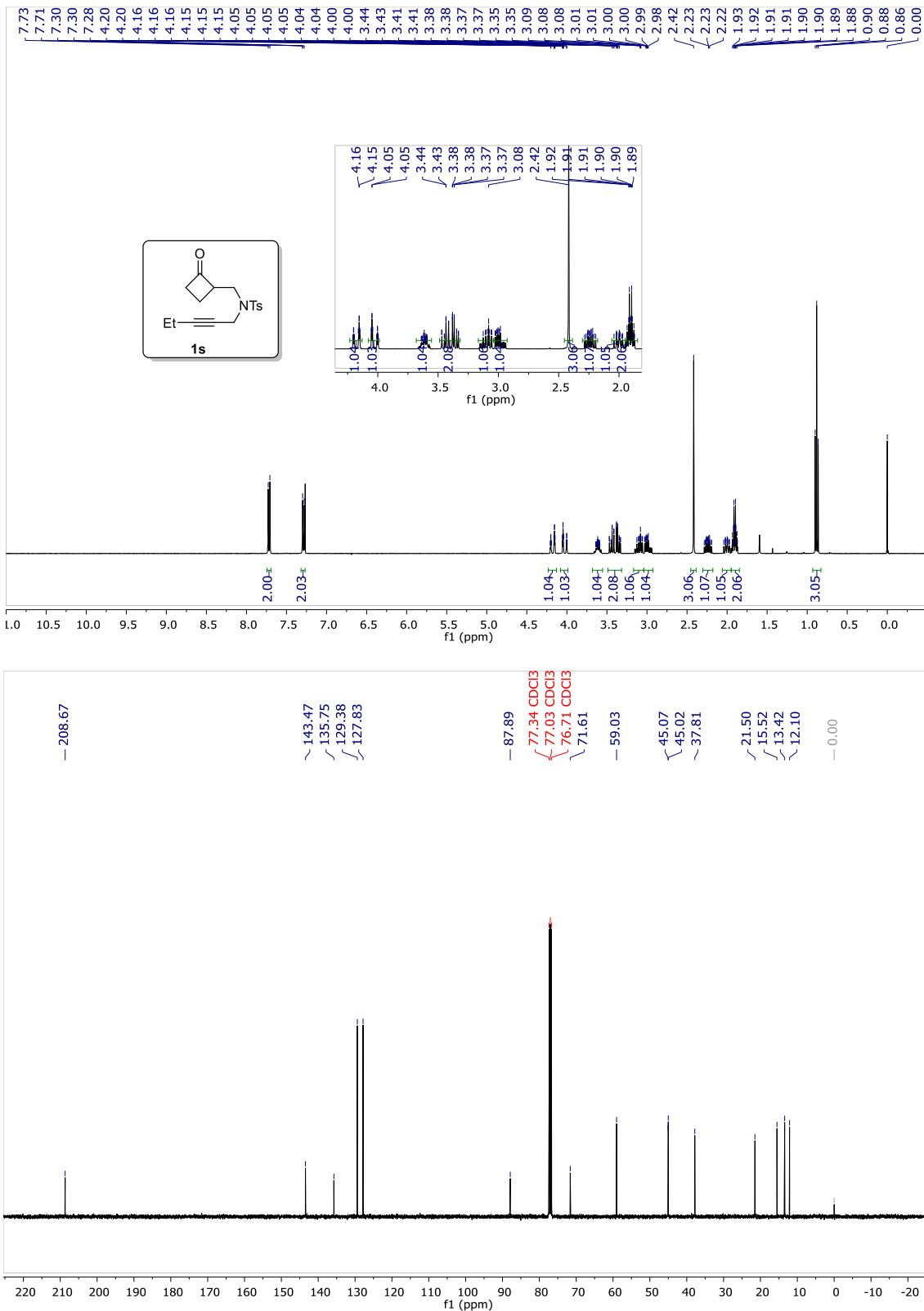


Figure 4.25  $^1\text{H}$  and  $^{13}\text{C}$  NMR spectrum of compound **1r**





**Figure 4.26**  $^1\text{H}$  and  $^{13}\text{C}$  NMR spectrum of compound **1s**



**Figure 4.27**  $^1\text{H}$  and  $^{13}\text{C}$  NMR spectrum of compound **1t**

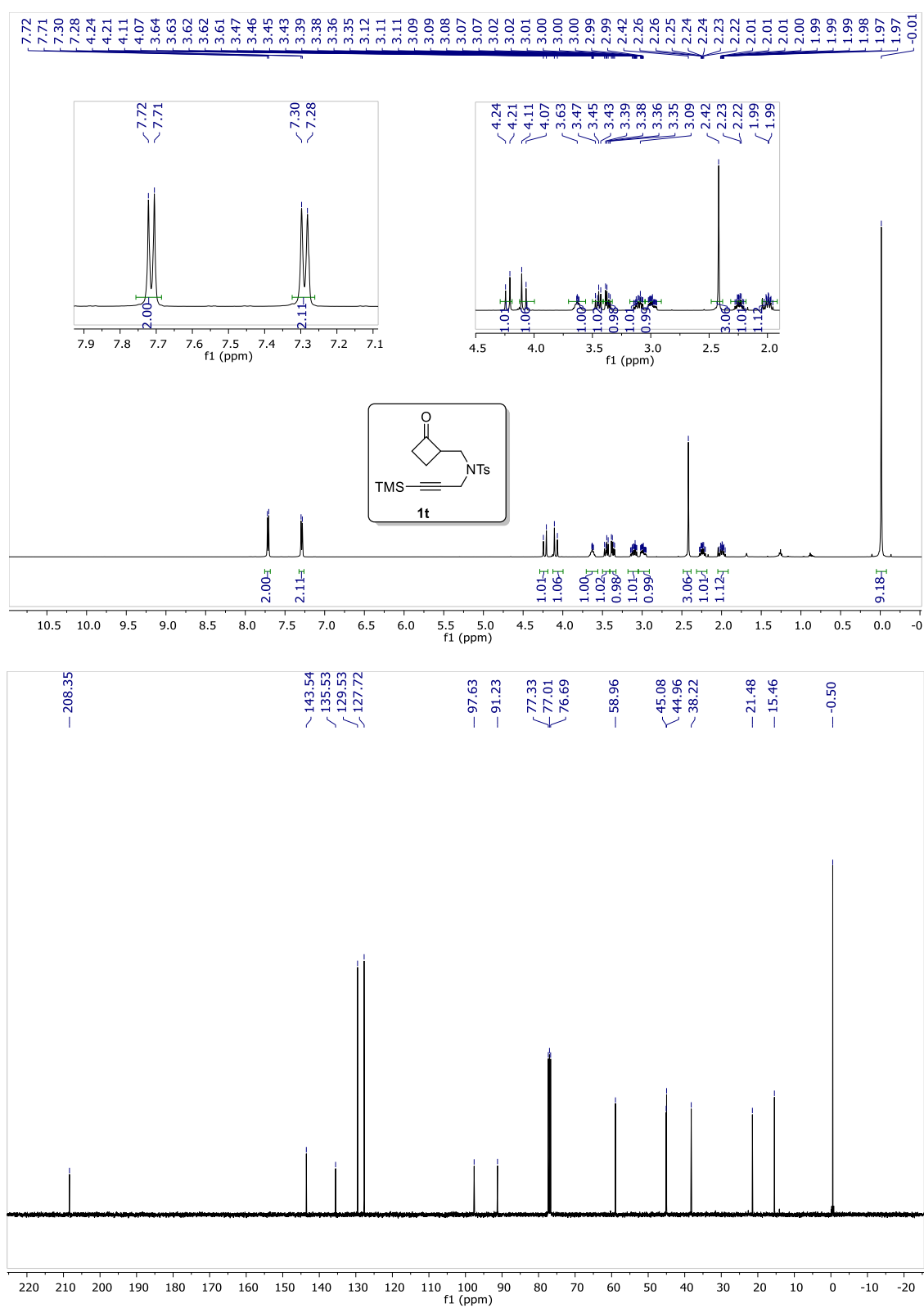


**Figure 4.28**  $^1\text{H}$  and  $^{13}\text{C}$  NMR spectrum of compound **1u**

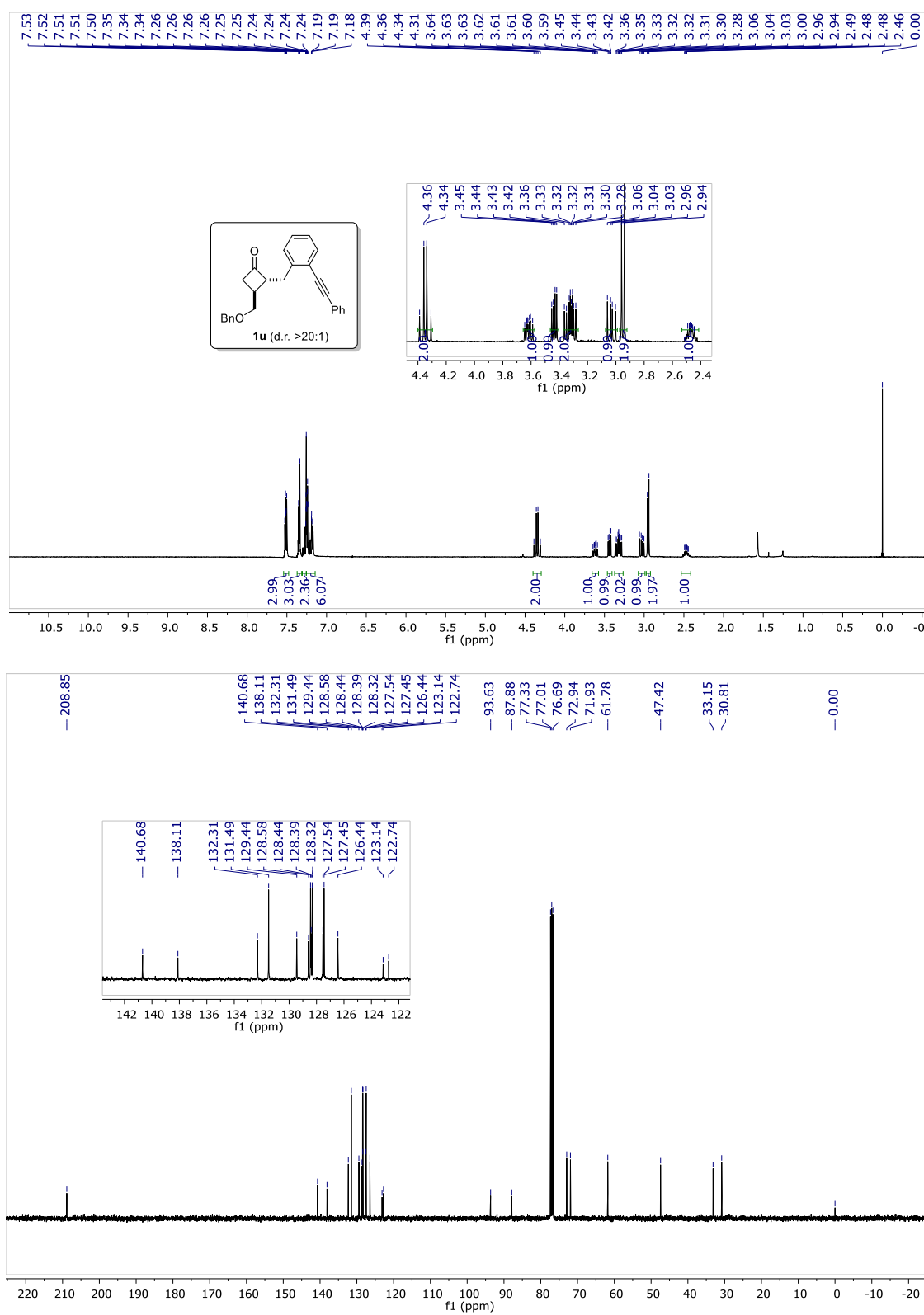


**Figure 4.29**  $^1\text{H}$  and  $^{13}\text{C}$  NMR spectrum of compound **1v**

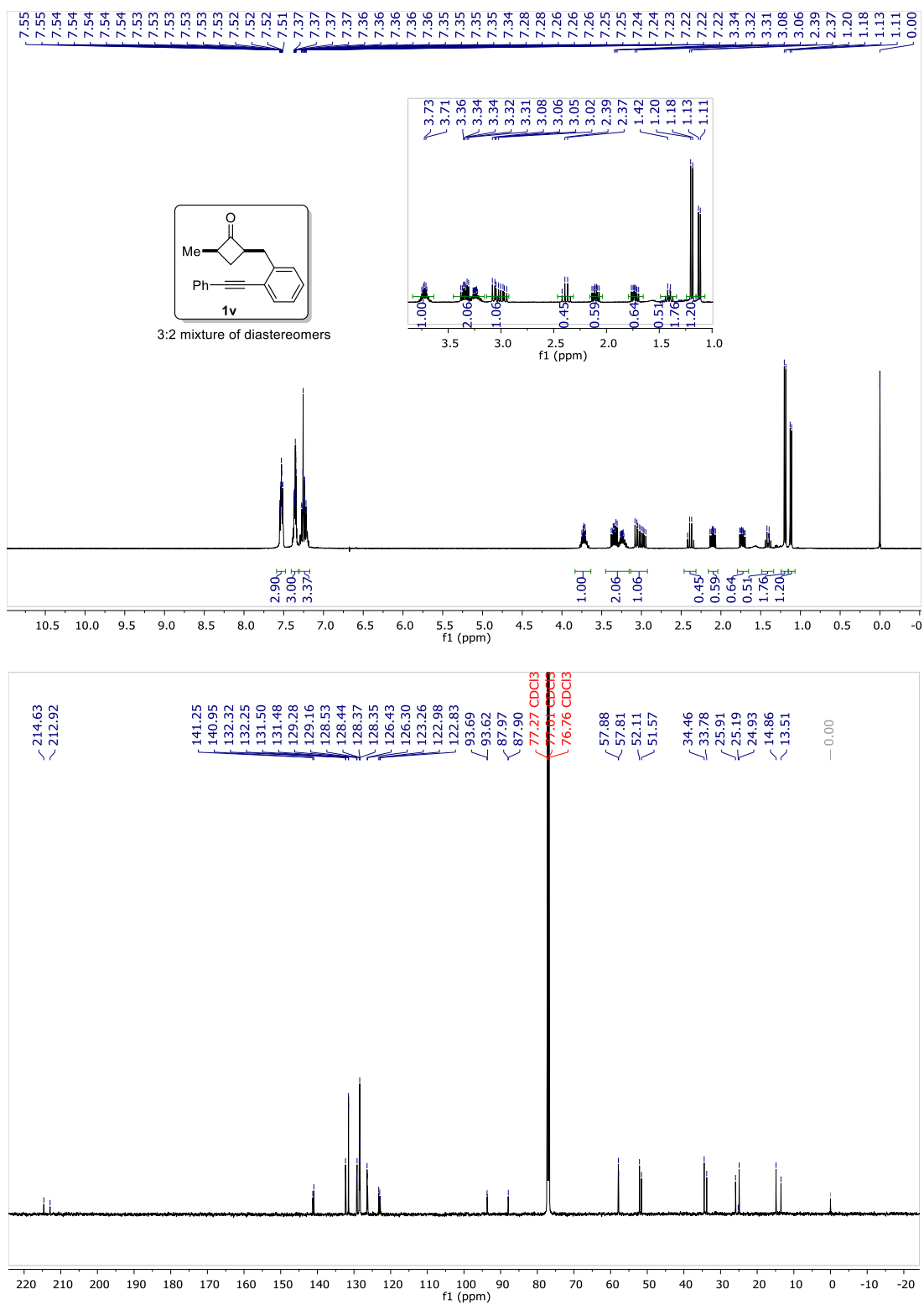


**Figure 4.30**  $^1\text{H}$  and  $^{13}\text{C}$  NMR spectrum of compound **2a**

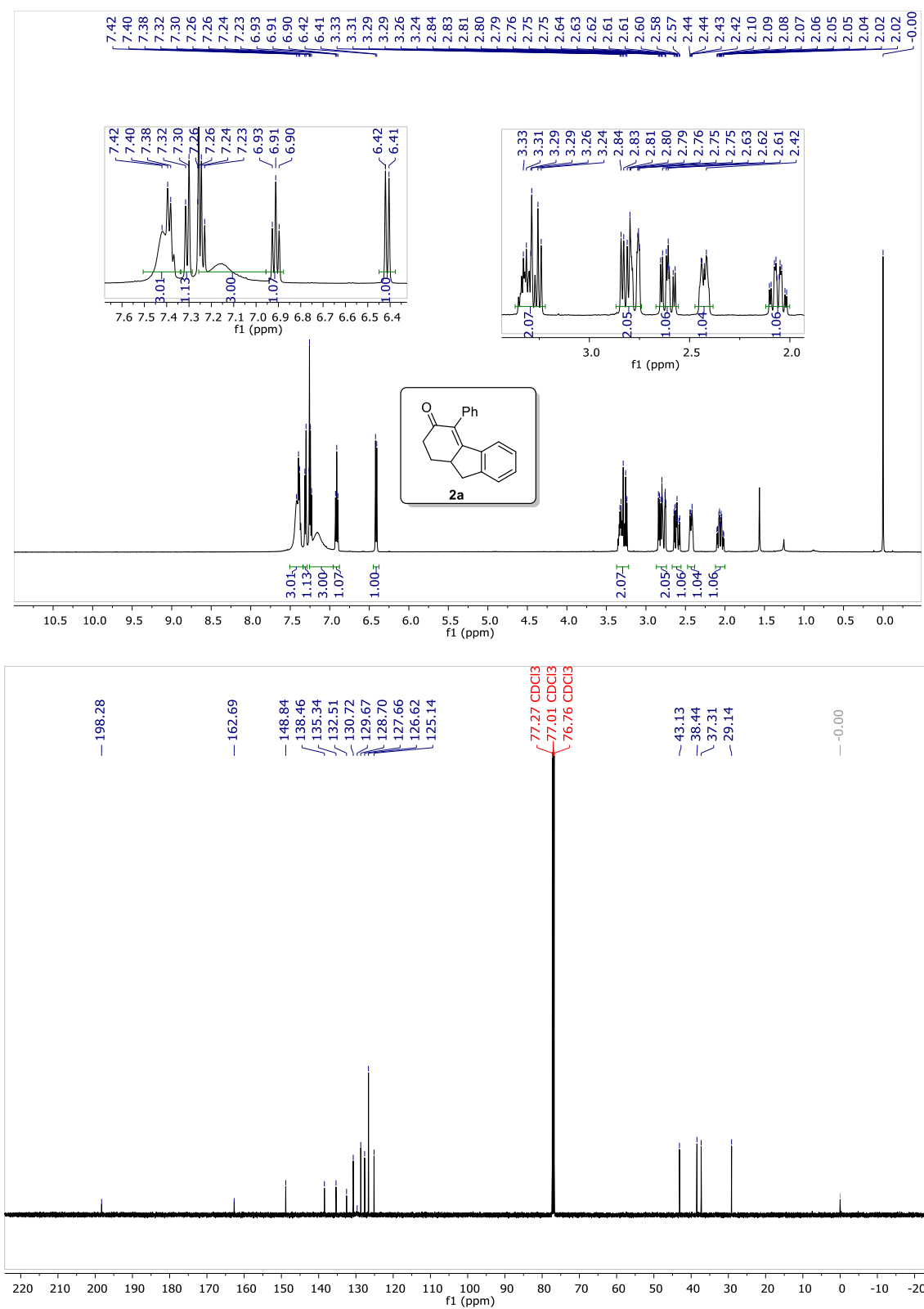


**Figure 4.31**  $^1\text{H}$  and  $^{13}\text{C}$  NMR spectrum of compound **2b**

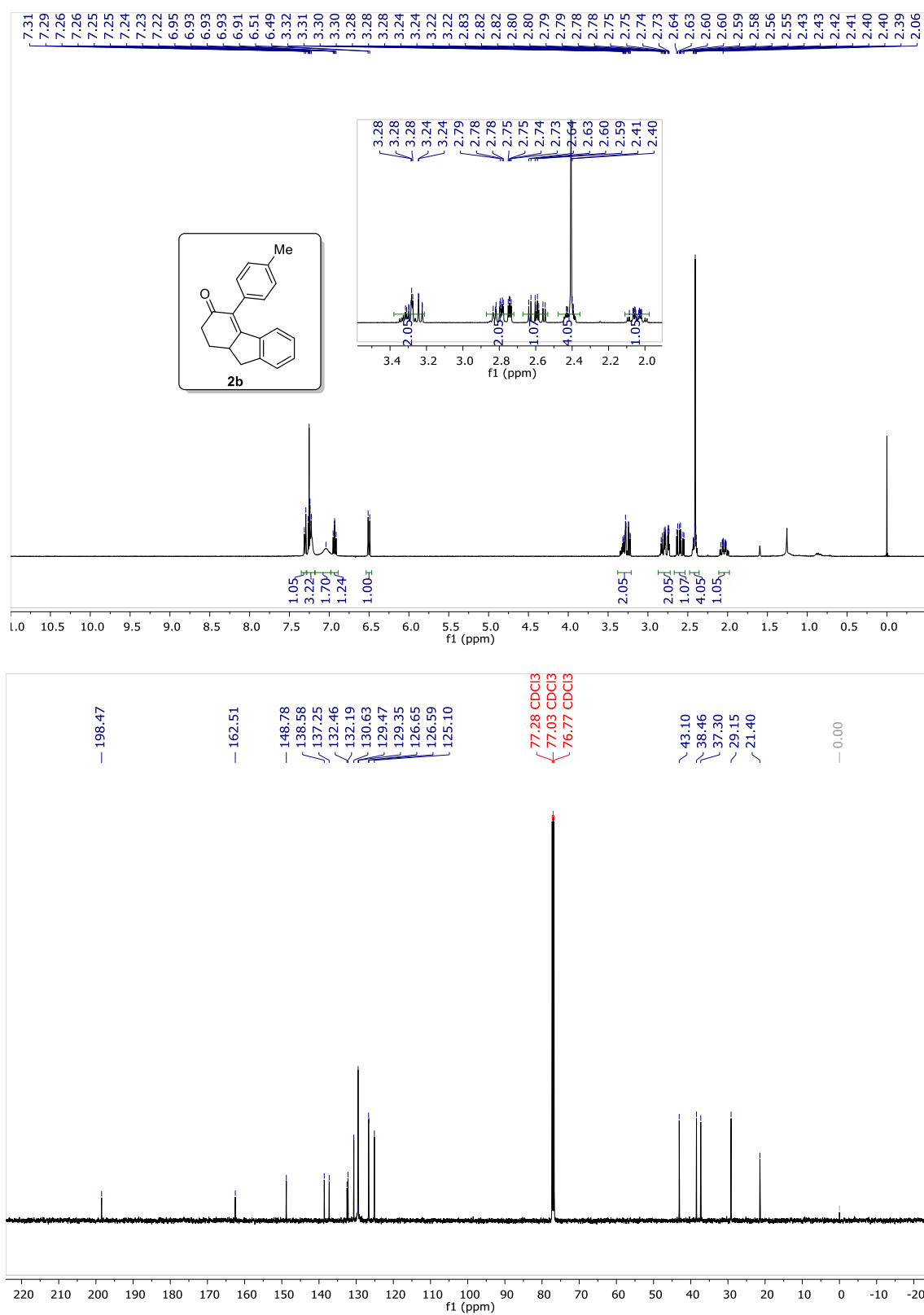


Figure 4.32  $^1\text{H}$  and  $^{13}\text{C}$  NMR spectrum of compound **2c**

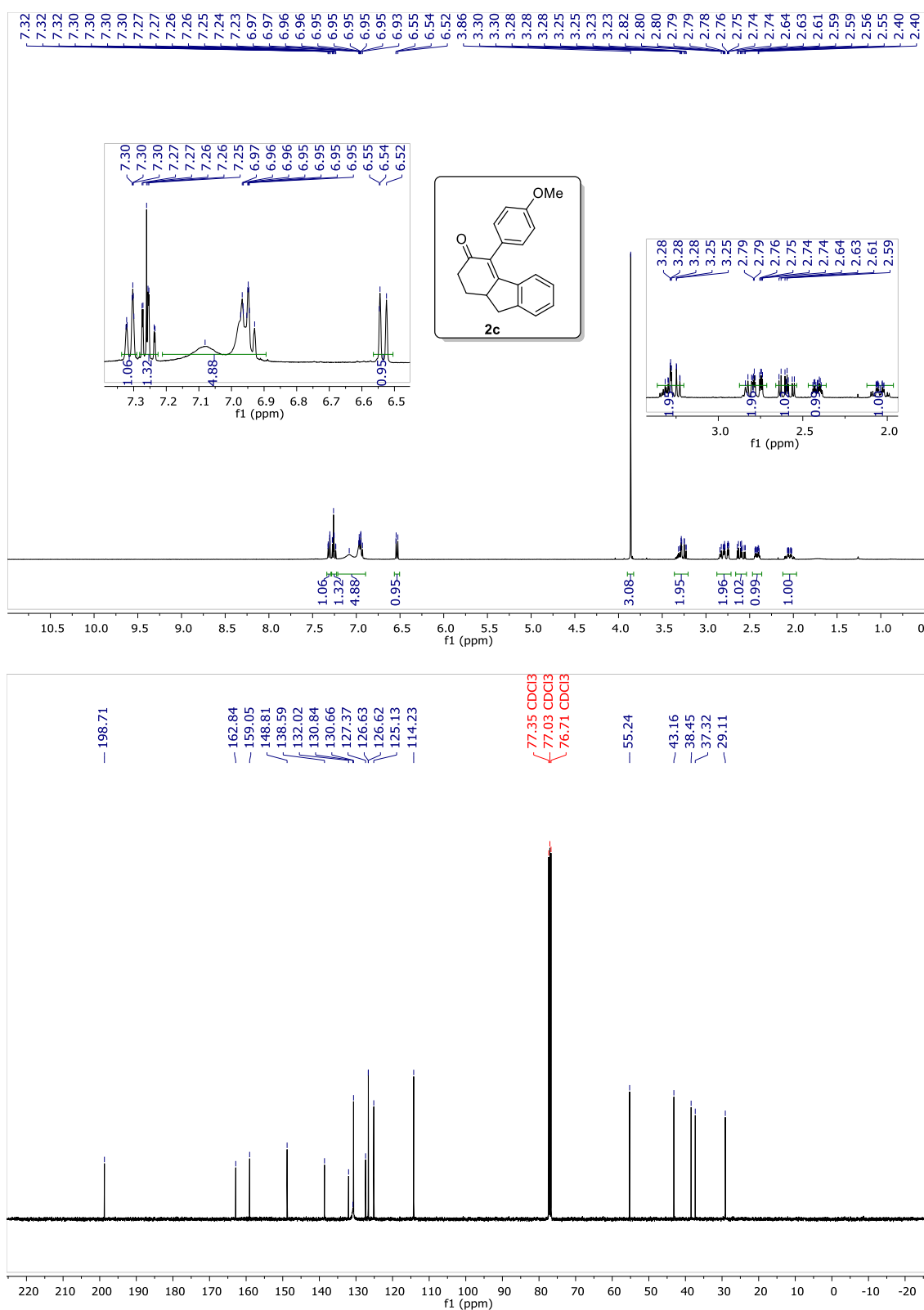


Figure 4.33  $^1\text{H}$  and  $^{13}\text{C}$  NMR spectrum of compound **2d**

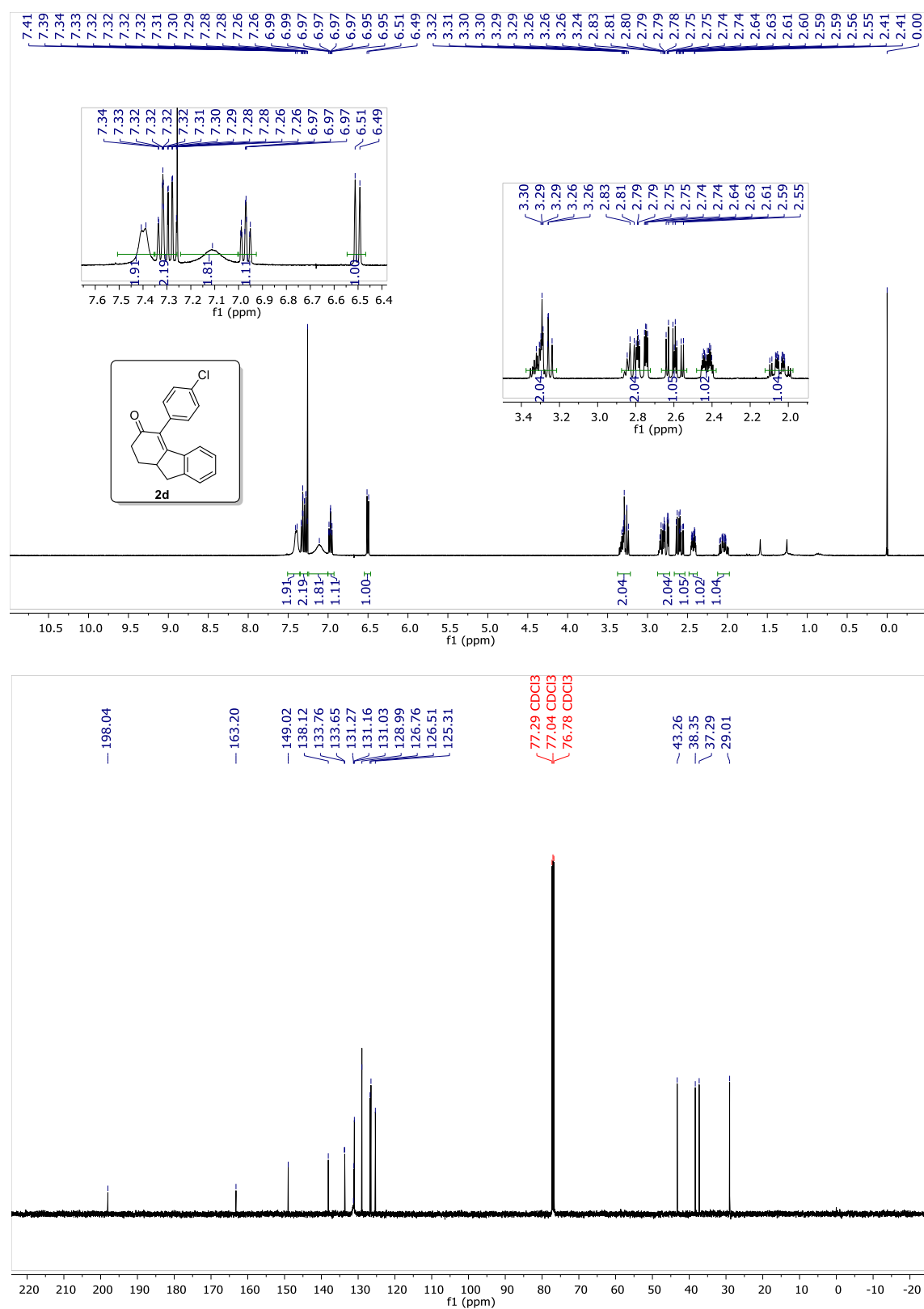
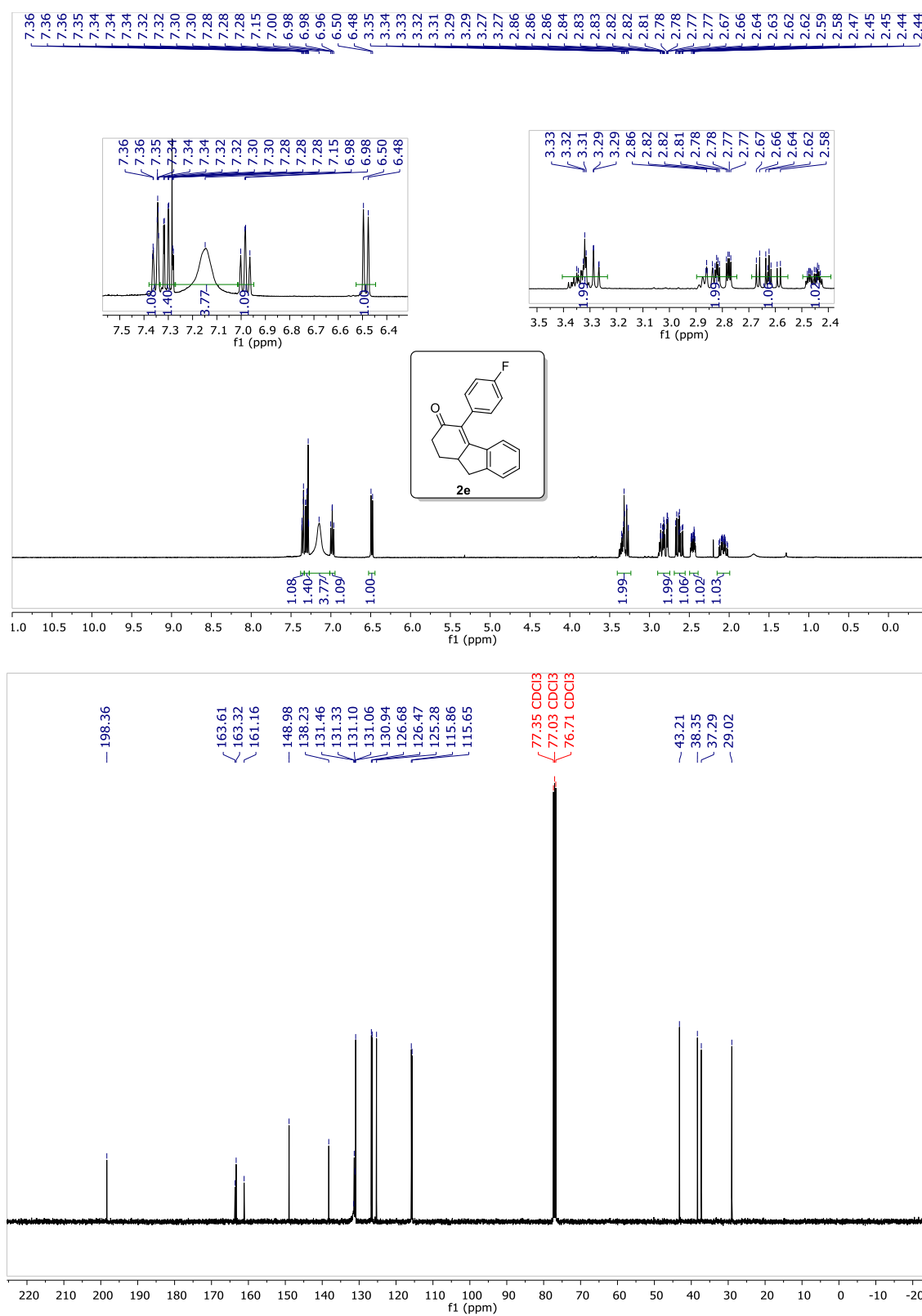




Figure 4.34  $^1\text{H}$  and  $^{13}\text{C}$  NMR spectrum of compound **2e**



**Figure 4.35**  $^1\text{H}$  and  $^{13}\text{C}$  NMR spectrum of compound **2f**

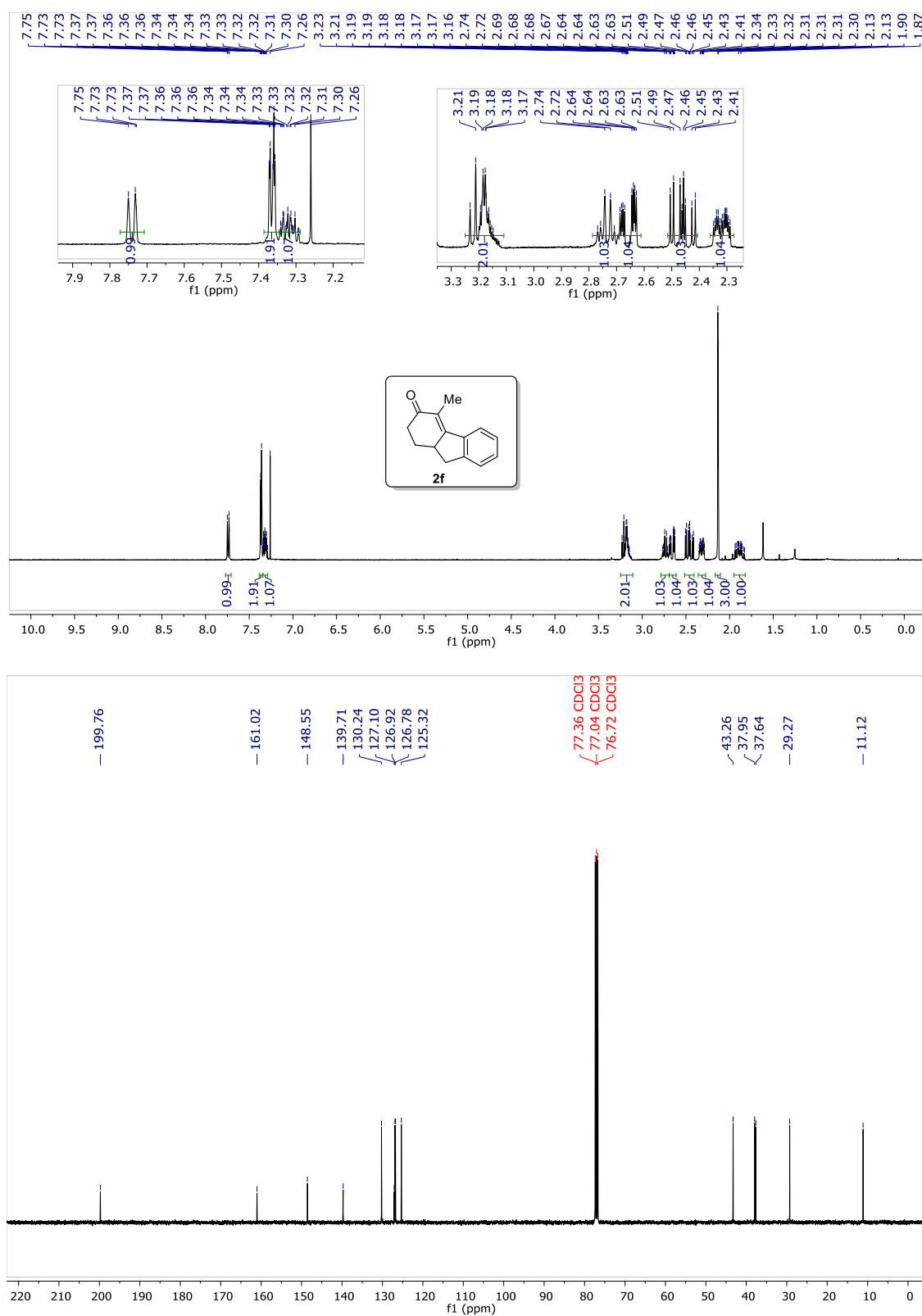
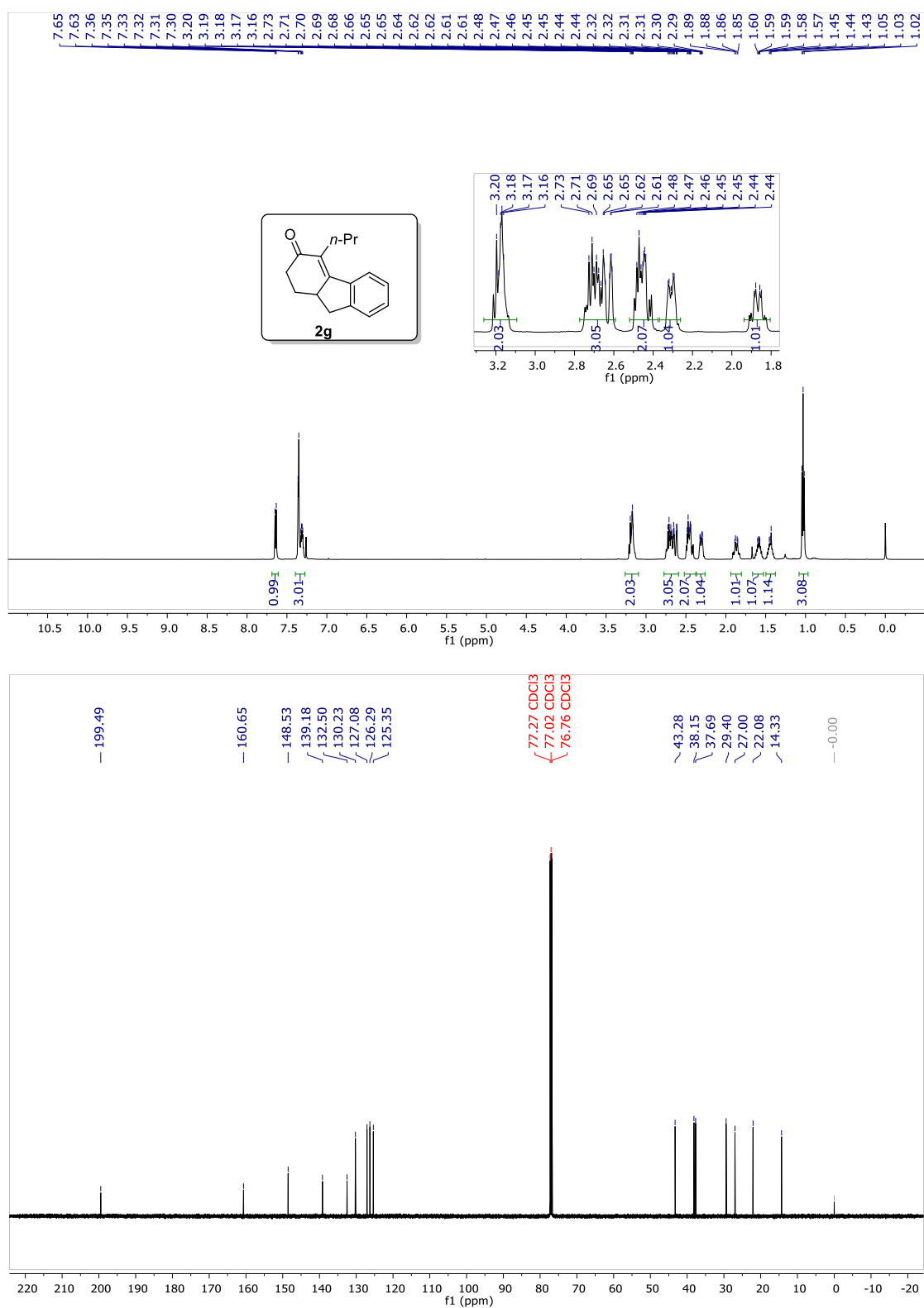
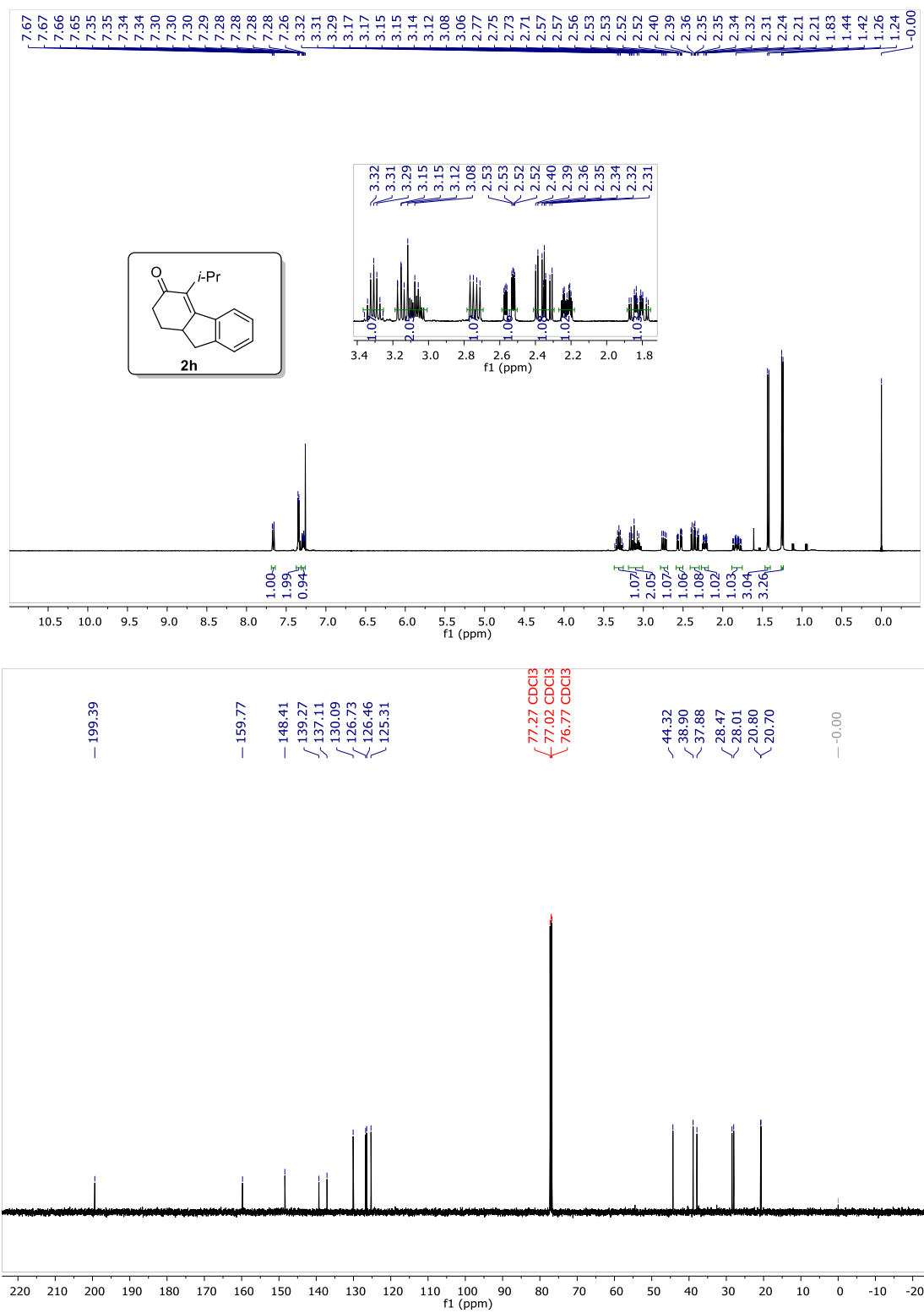


Figure 4.36  $^1\text{H}$  and  $^{13}\text{C}$  NMR spectrum of compound **2g**



**Figure 4.37**  $^1\text{H}$  and  $^{13}\text{C}$  NMR spectrum of compound **2h**



**Figure 4.38**  $^1\text{H}$  and  $^{13}\text{C}$  NMR spectrum of compound **2i**

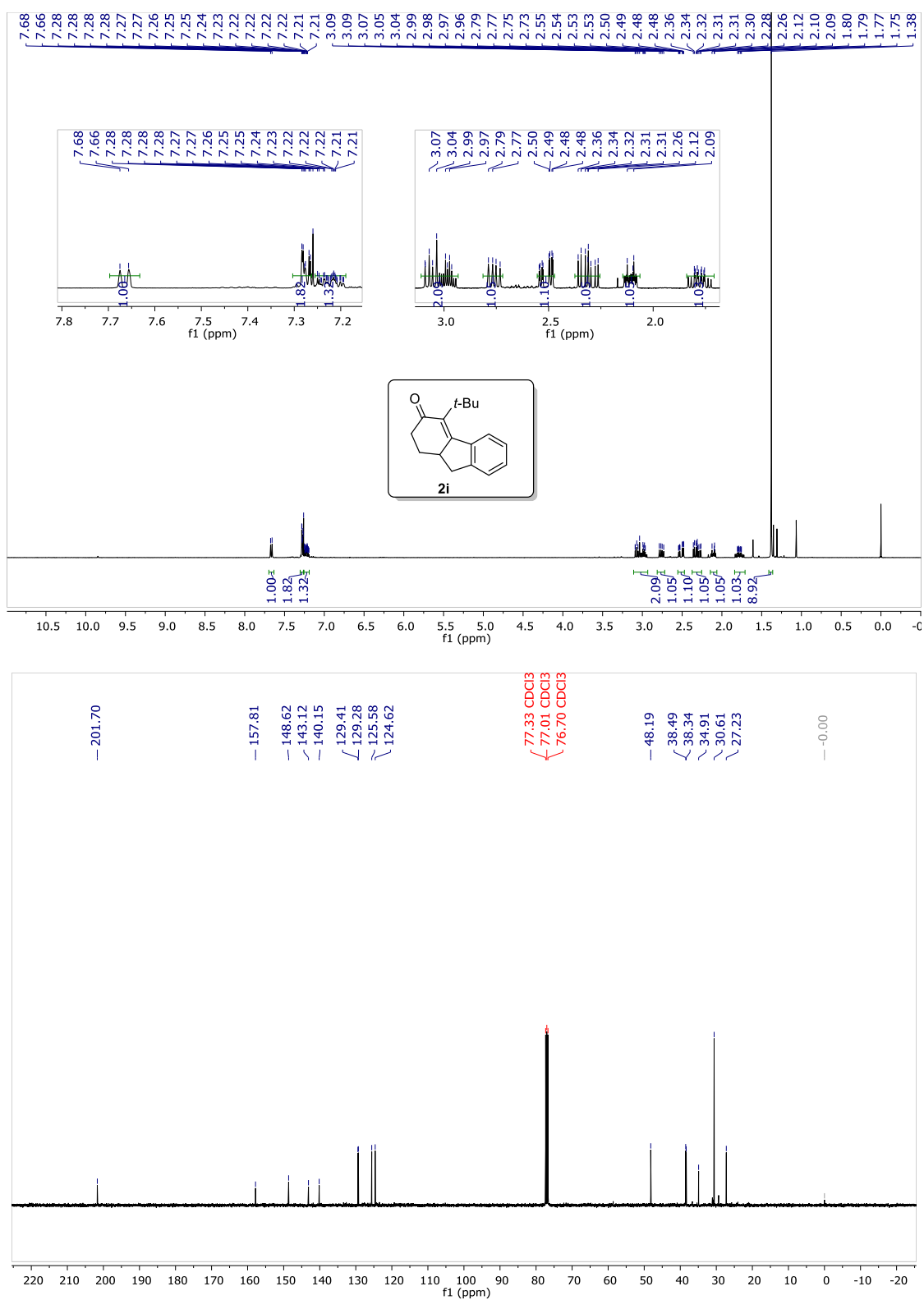


**Figure 4.39**  $^1\text{H}$  and  $^{13}\text{C}$  NMR spectrum of compound **2j**

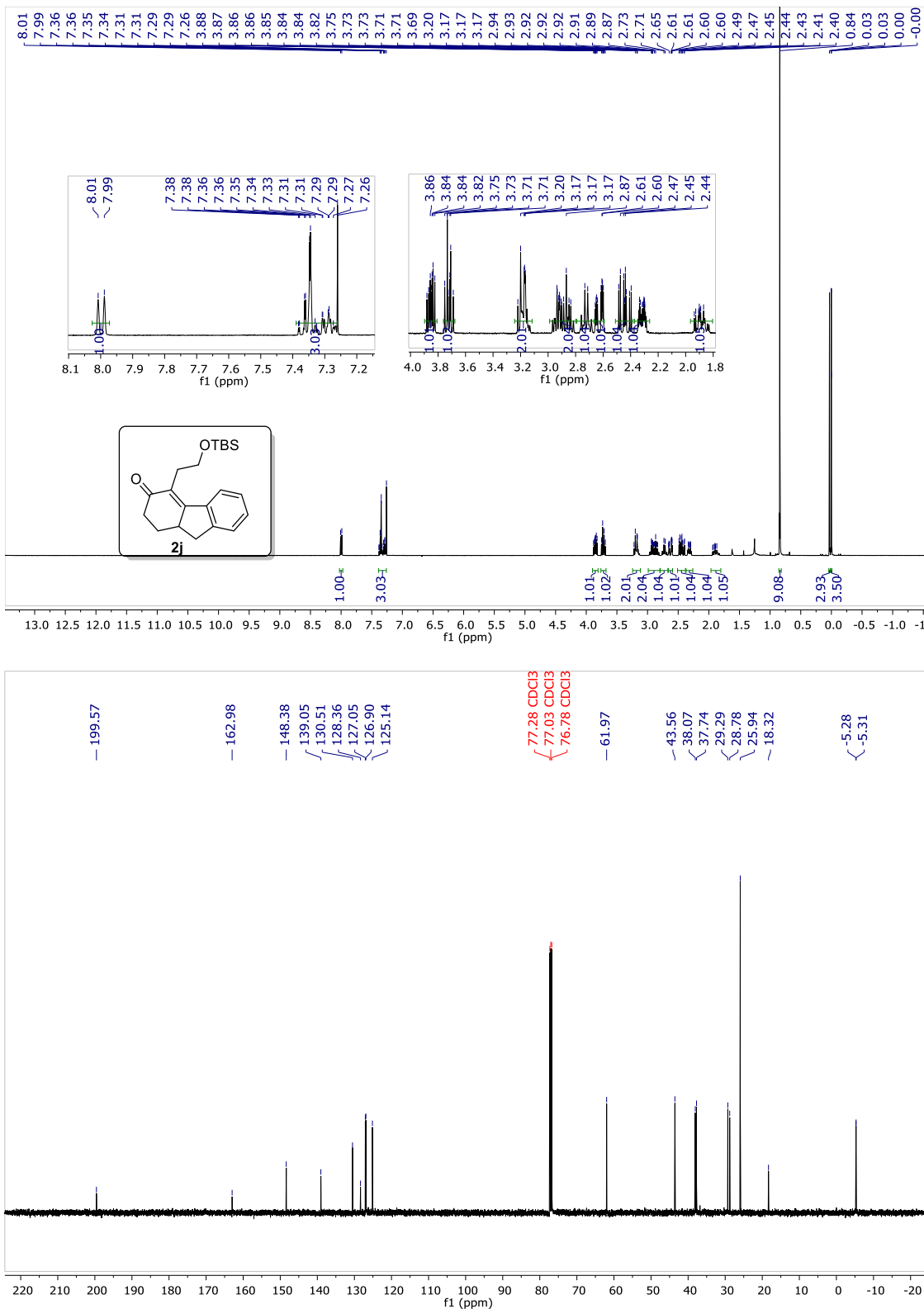


**Figure 4.40**  $^1\text{H}$  and  $^{13}\text{C}$  NMR spectrum of compound **2k**

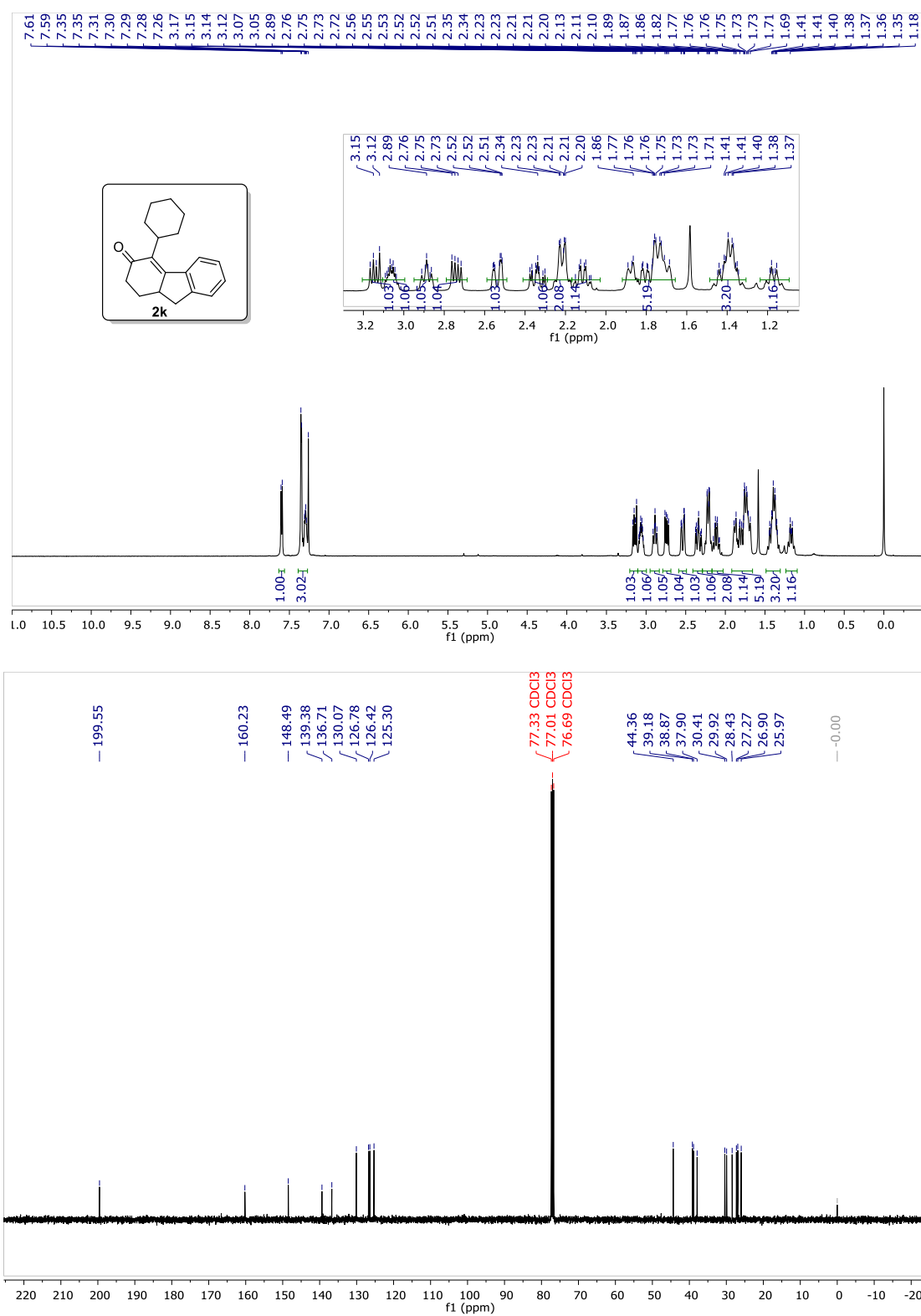


**Figure 4.41**  $^1\text{H}$  and  $^{13}\text{C}$  NMR spectrum of compound **21**

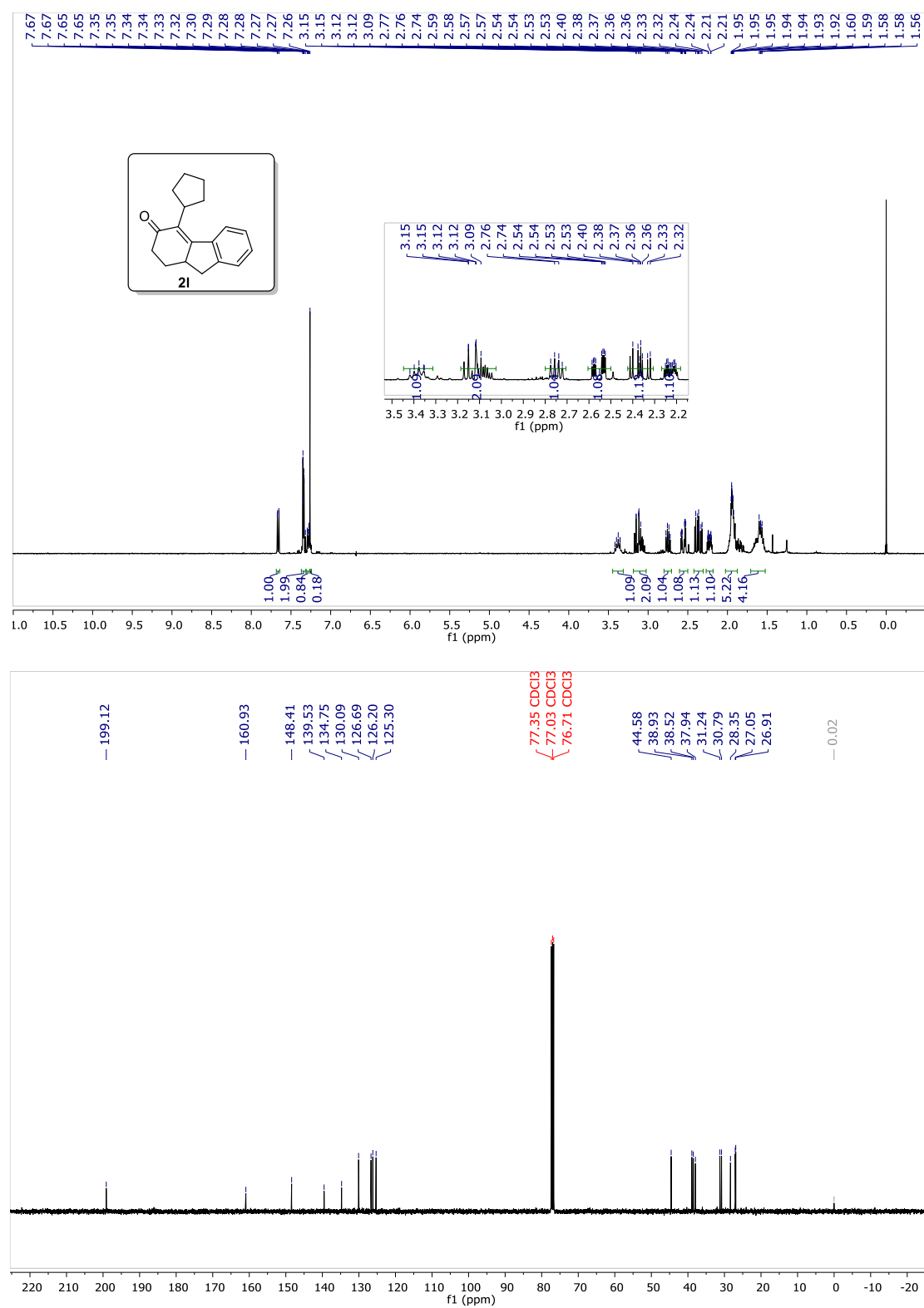




**Figure 4.42**  $^1\text{H}$  and  $^{13}\text{C}$  NMR spectrum of compound **2m**

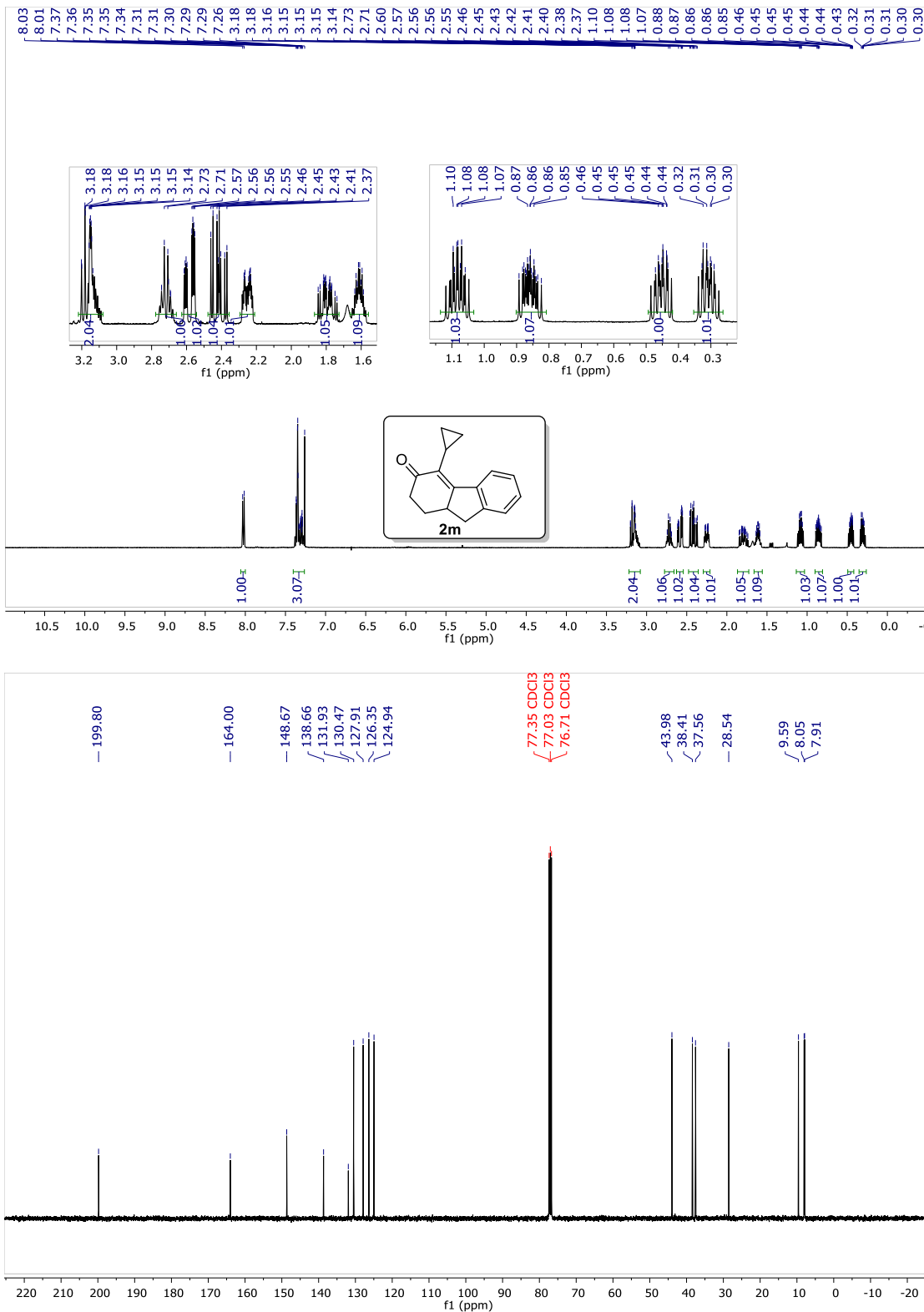


**Figure 4.43**  $^1\text{H}$  and  $^{13}\text{C}$  NMR spectrum of compound **2n**

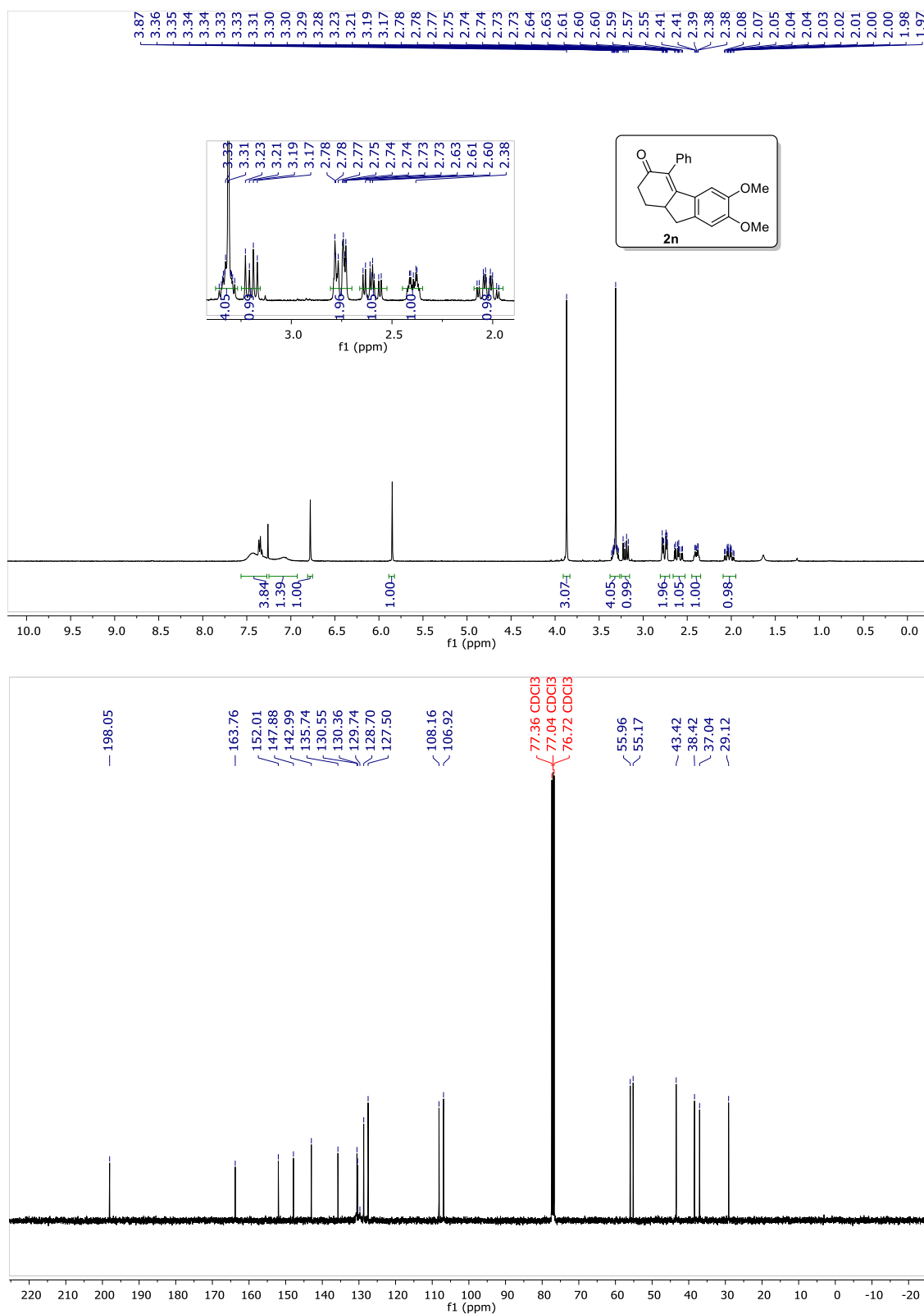


**Figure 4.44**  $^1\text{H}$  and  $^{13}\text{C}$  NMR spectrum of compound **2o**

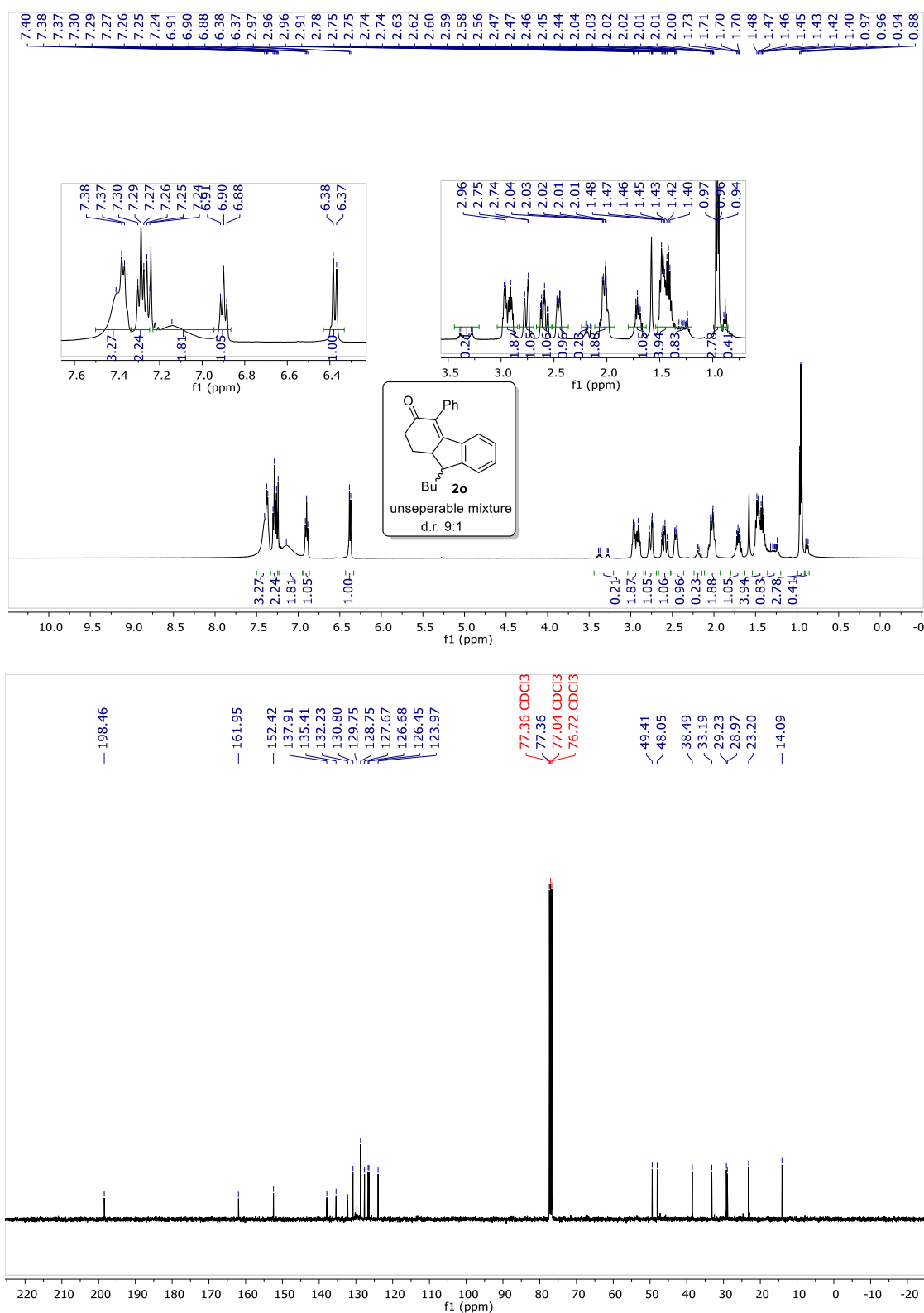
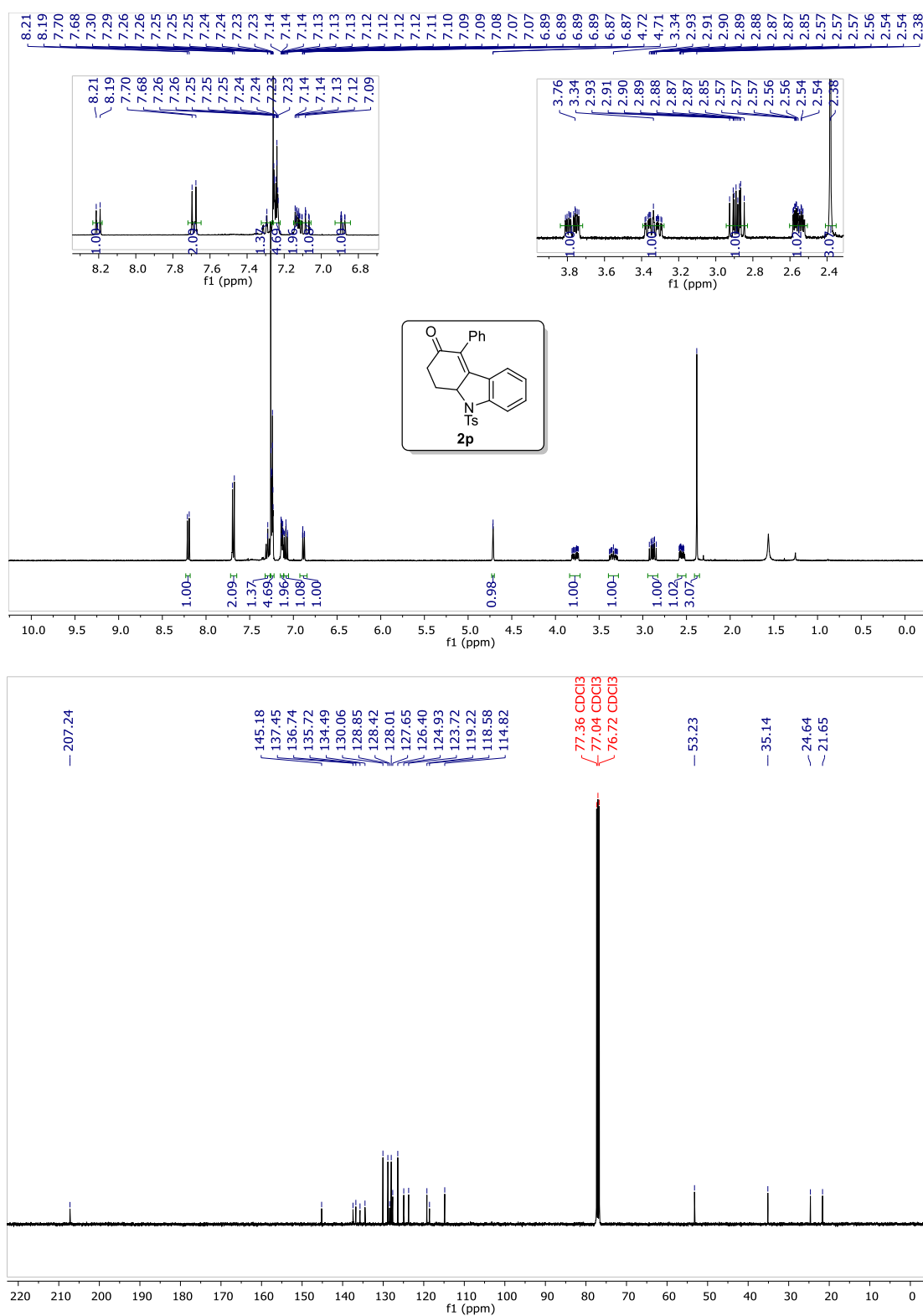


Figure 4.45  $^1\text{H}$  and  $^{13}\text{C}$  NMR spectrum of compound **2p**



**Figure 4.46**  $^1\text{H}$  and  $^{13}\text{C}$  NMR spectrum of compound **2q**

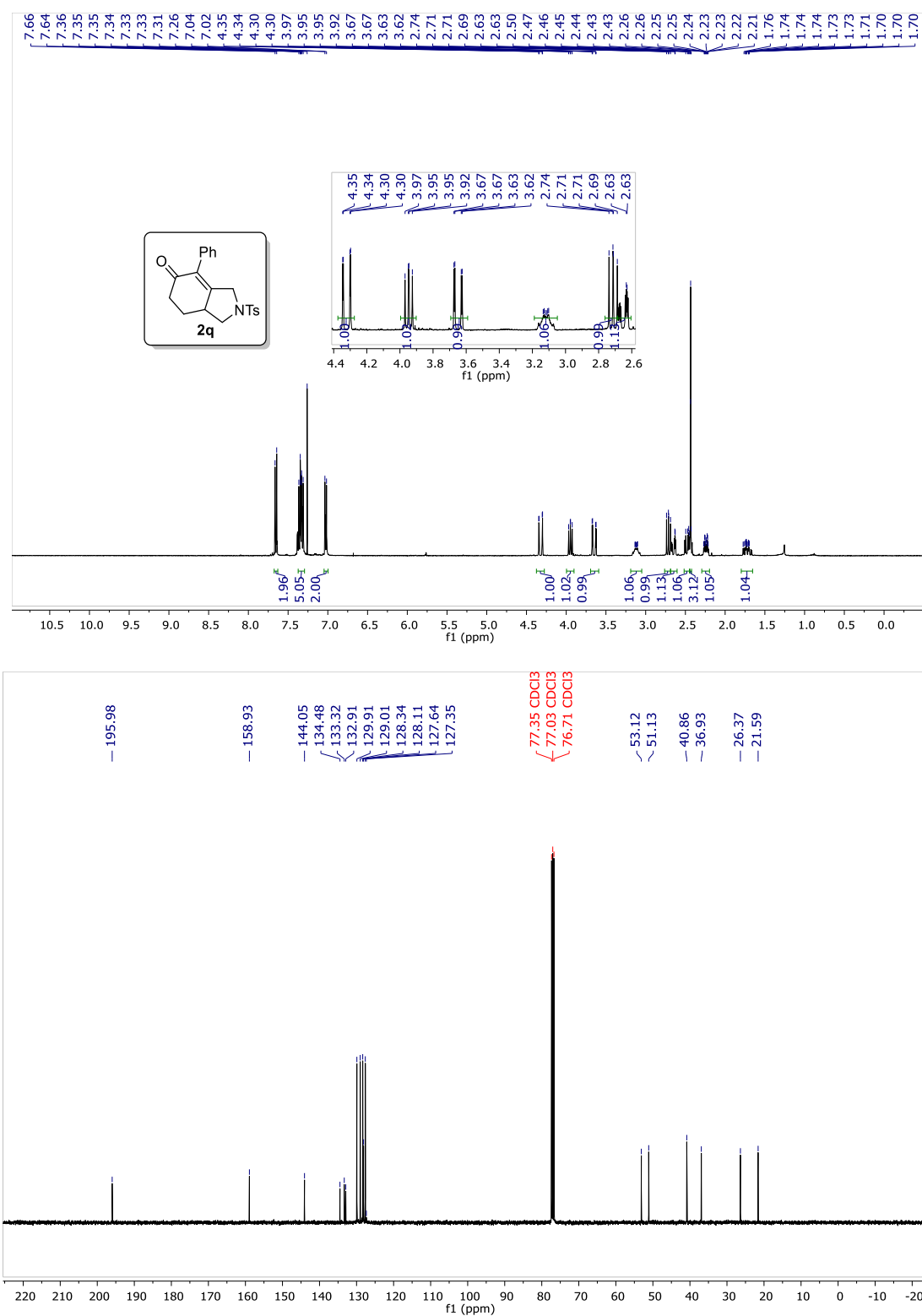
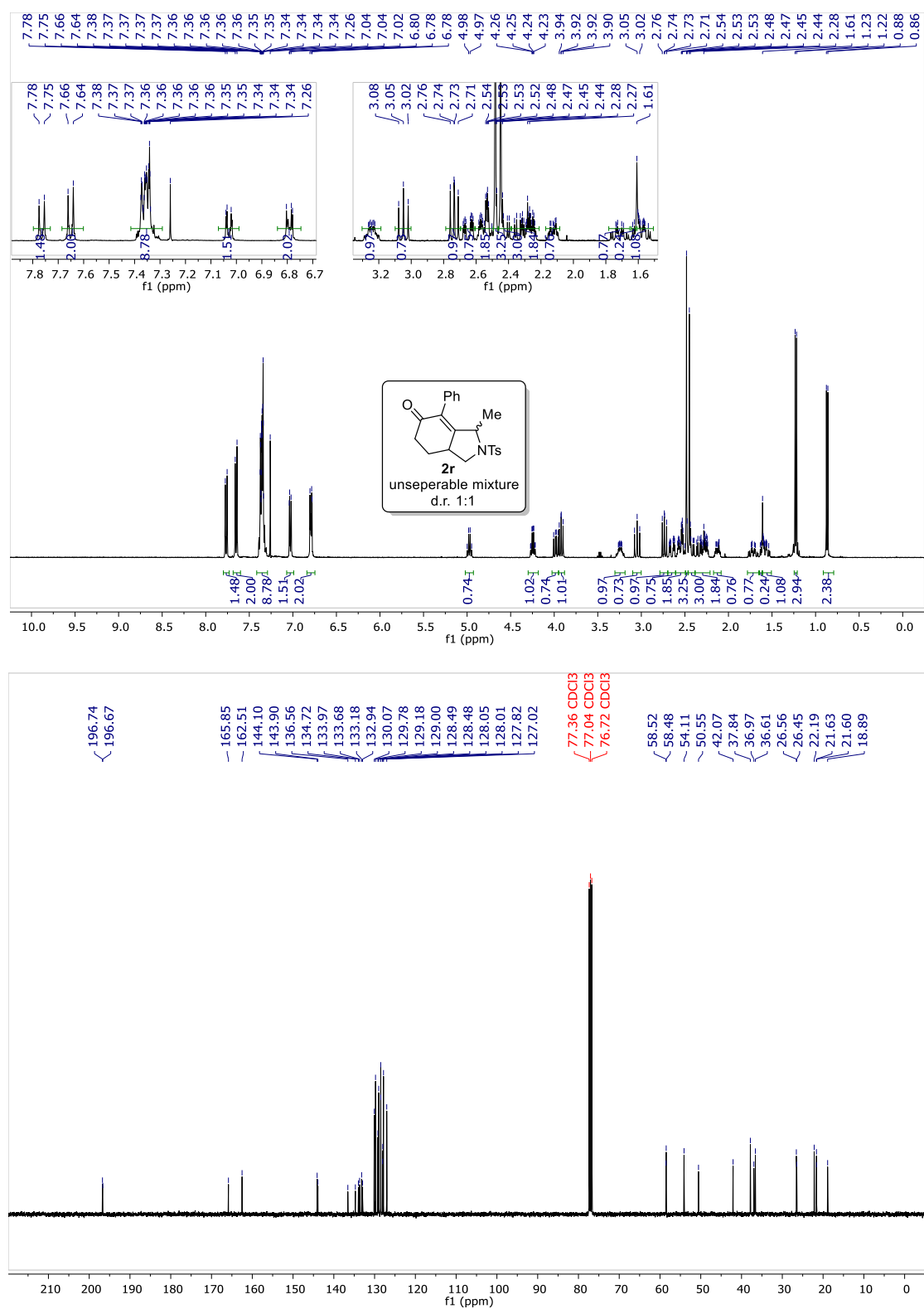
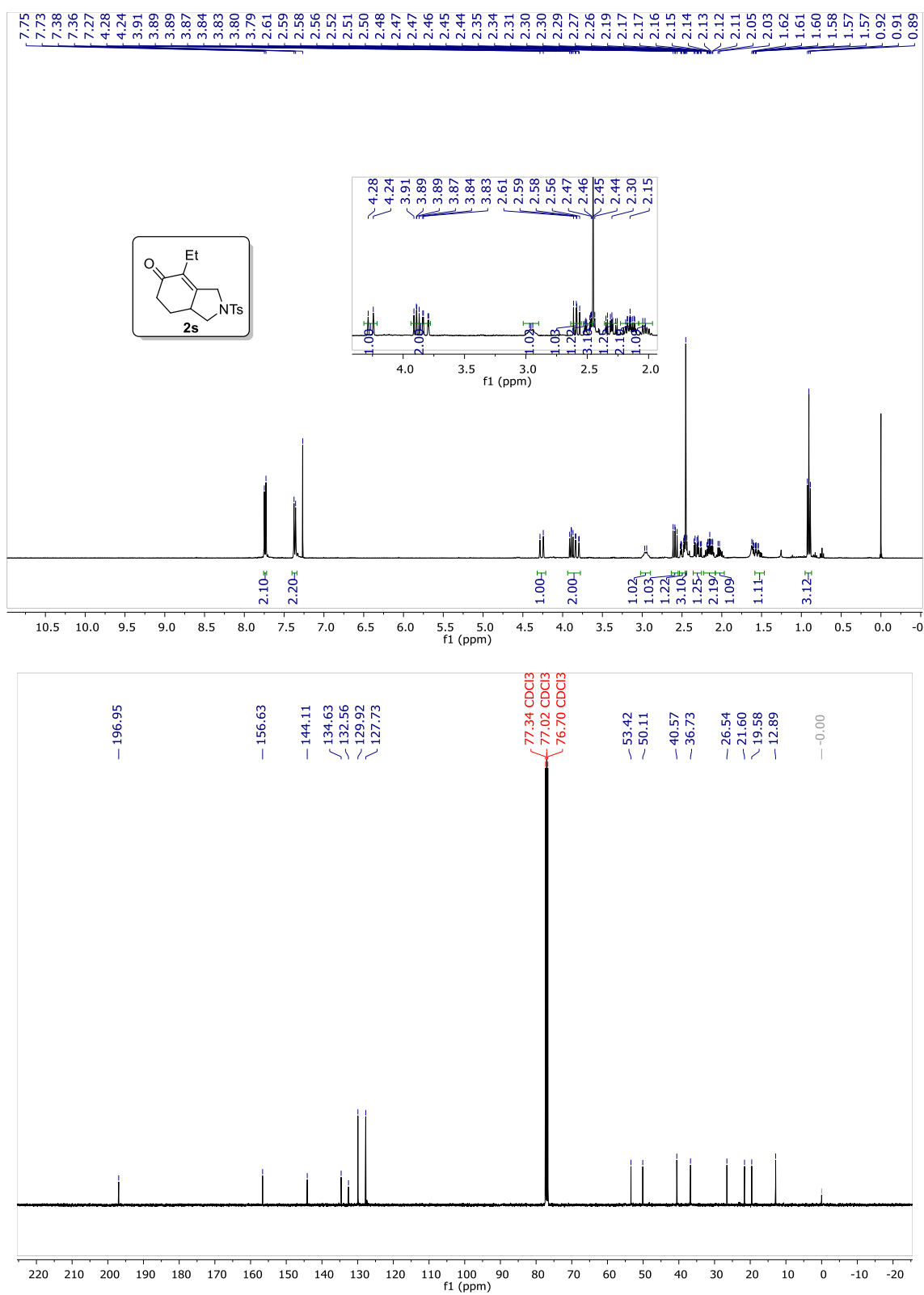


Figure 4.47  $^1\text{H}$  and  $^{13}\text{C}$  NMR spectrum of compound **2r**



**Figure 4.48**  $^1\text{H}$  and  $^{13}\text{C}$  NMR spectrum of compound **2s**



**Figure 4.49**  $^1\text{H}$  and  $^{13}\text{C}$  NMR spectrum of compound **2t**

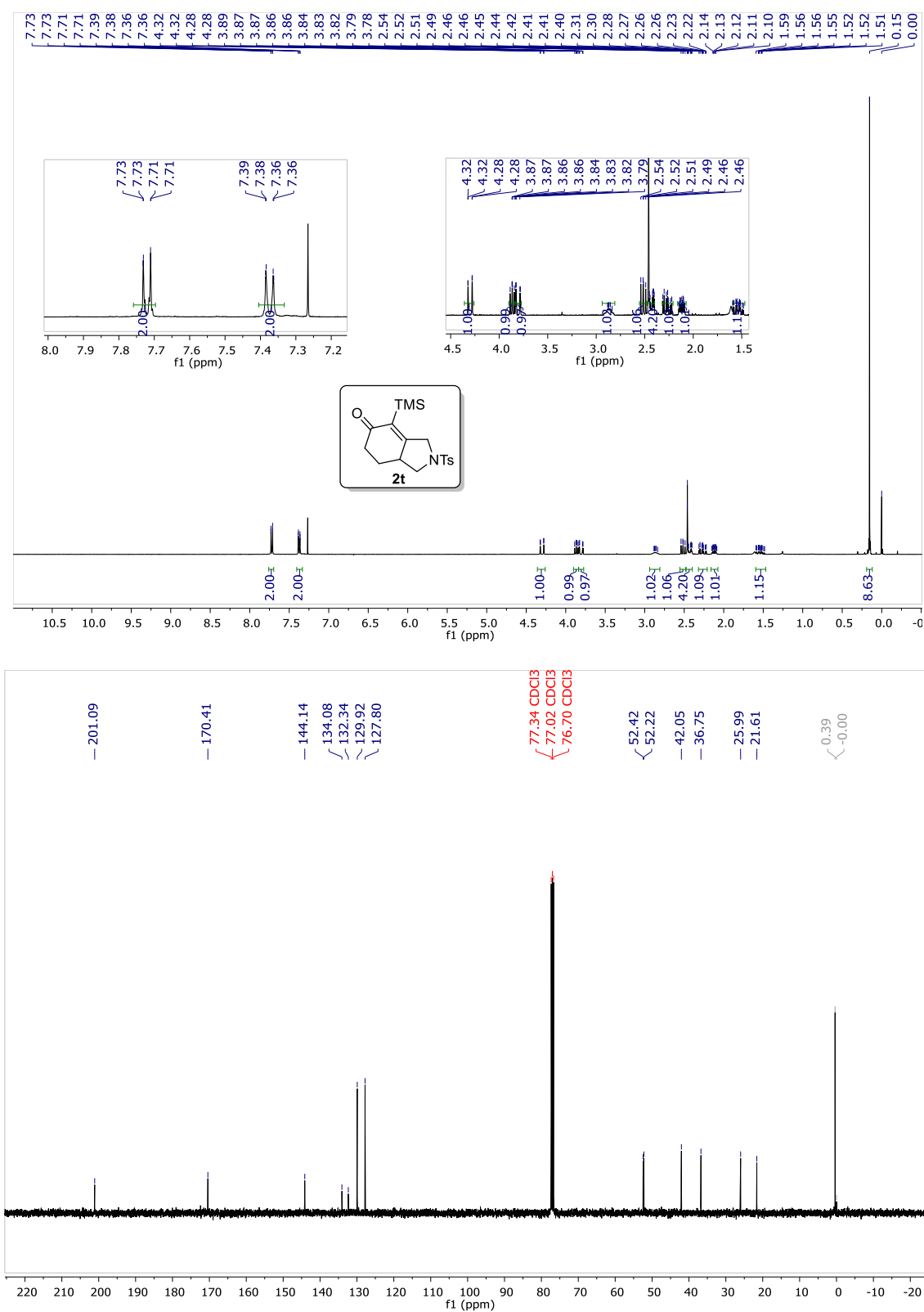




**Figure 4.50**  $^1\text{H}$  and  $^{13}\text{C}$  NMR spectrum of compound **2u**

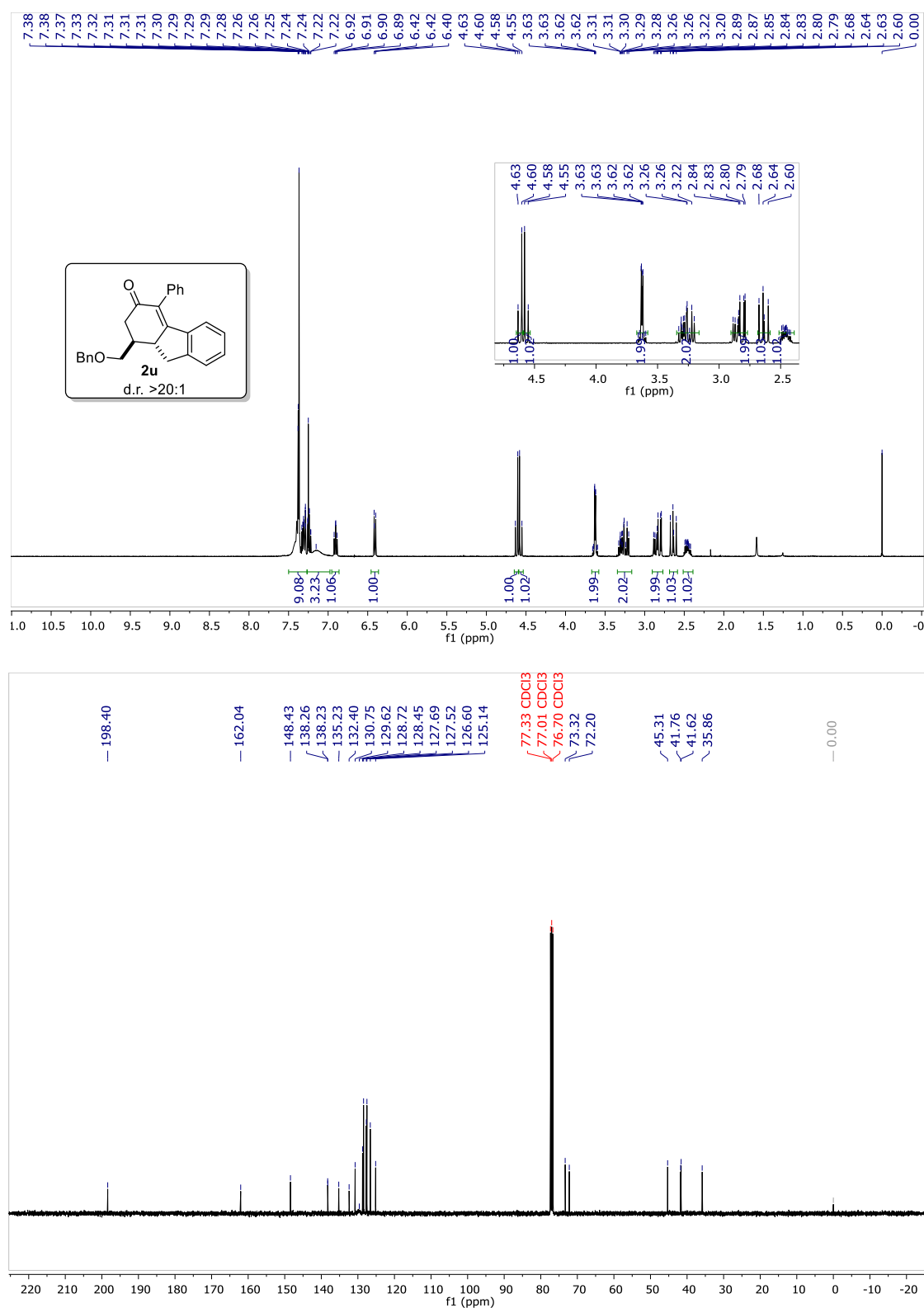


**Figure 4.51**  $^1\text{H}$  and  $^{13}\text{C}$  NMR spectrum of compound **2v** (major)

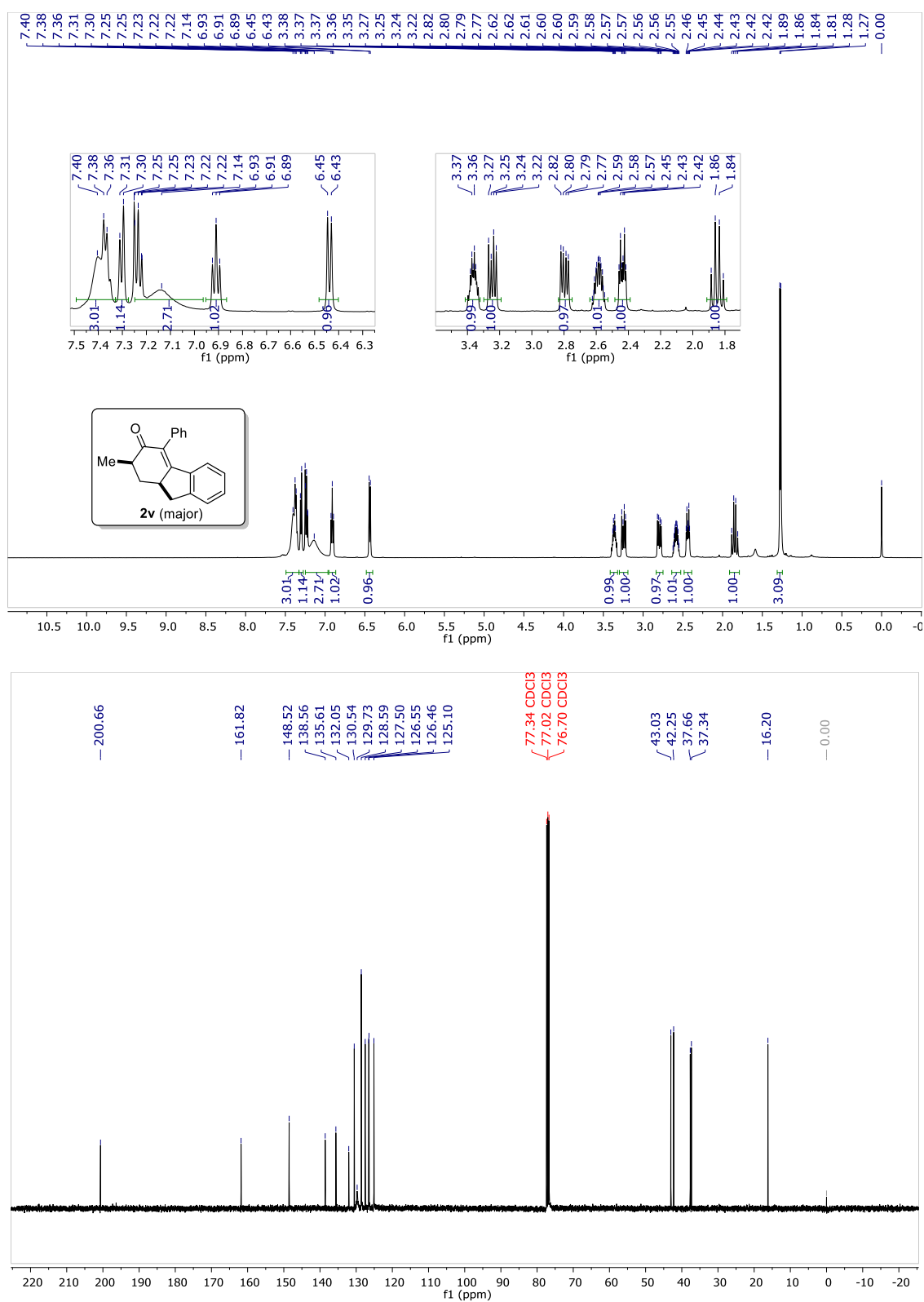


**Figure 4.52**  $^1\text{H}$  and  $^{13}\text{C}$  NMR spectrum of compound **3**

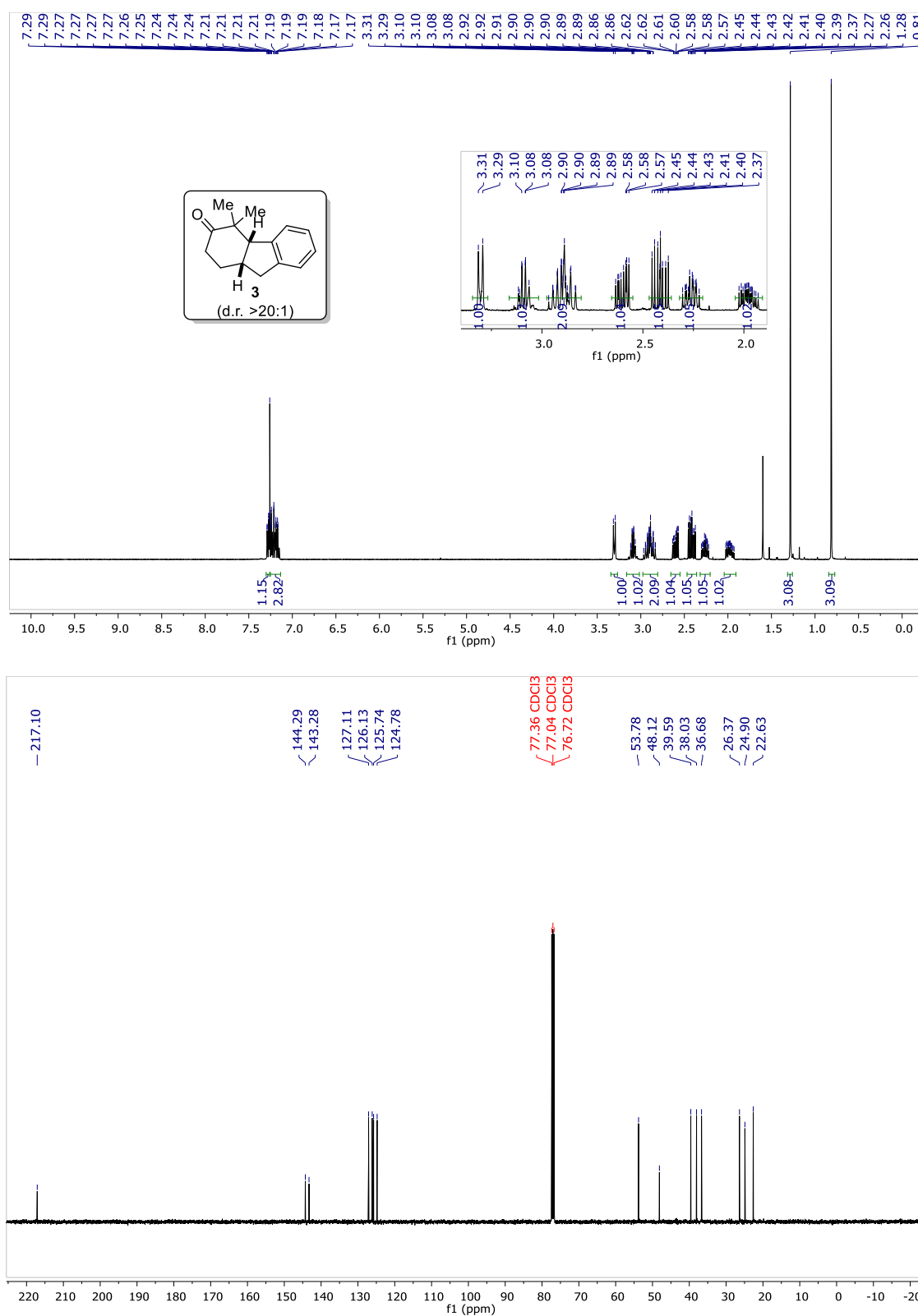


**Figure 4.53**  $^1\text{H}$  and  $^{13}\text{C}$  NMR spectrum of compound **4**

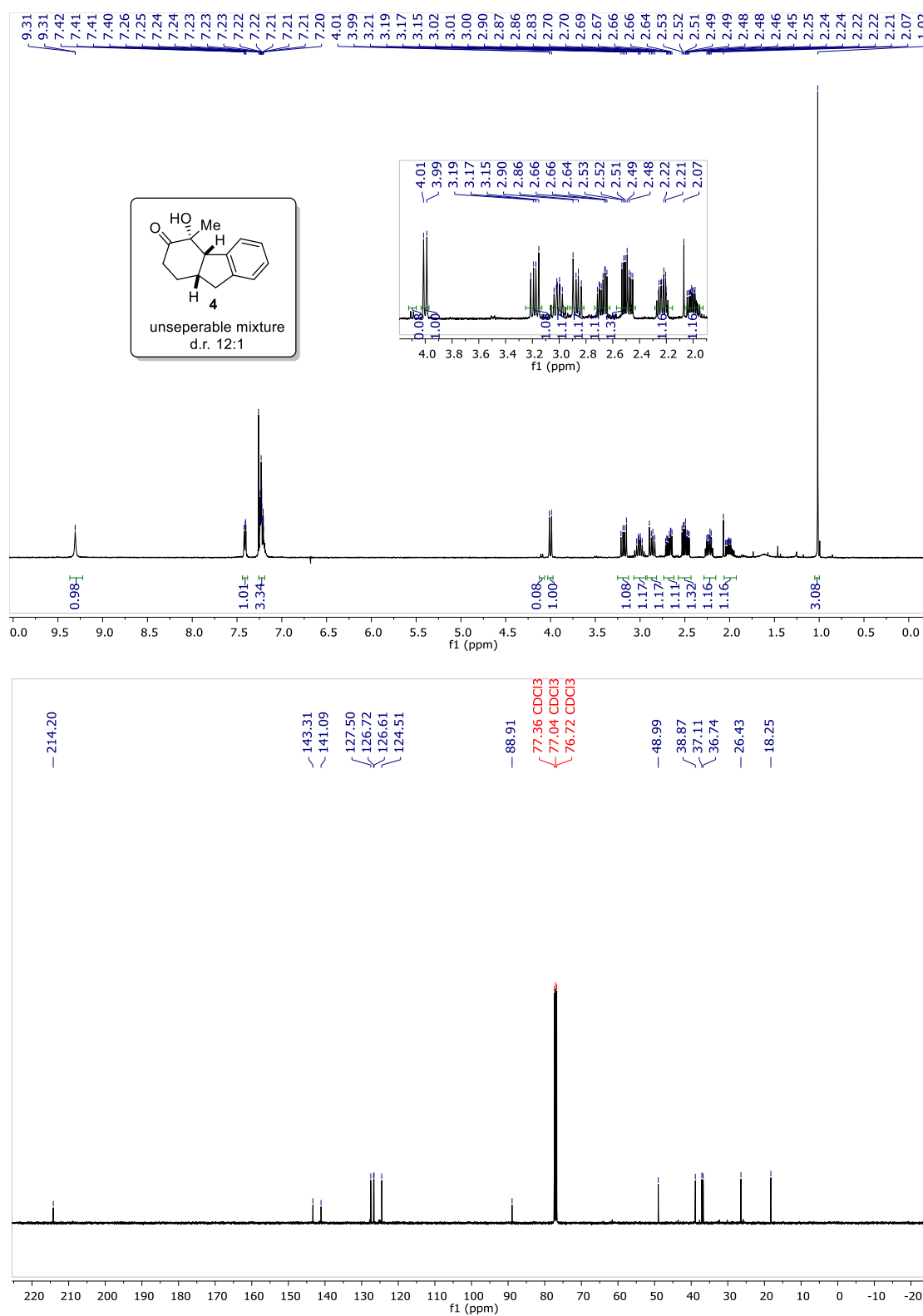


**Figure 4.54**  $^1\text{H}$  and  $^{13}\text{C}$  NMR spectrum of compound **5**

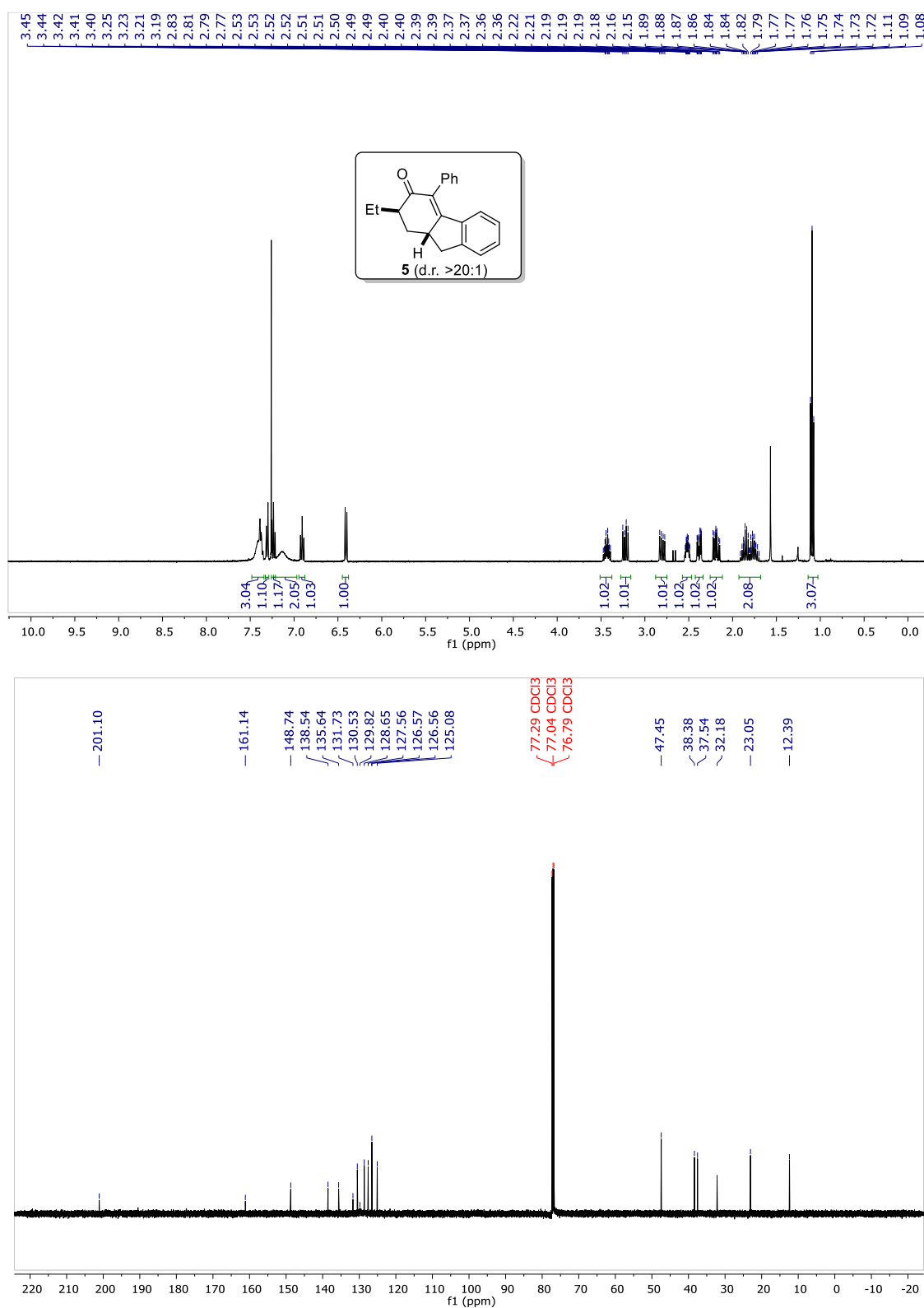


**Figure 4.55**  $^1\text{H}$  and  $^{13}\text{C}$  NMR spectrum of compound **6**

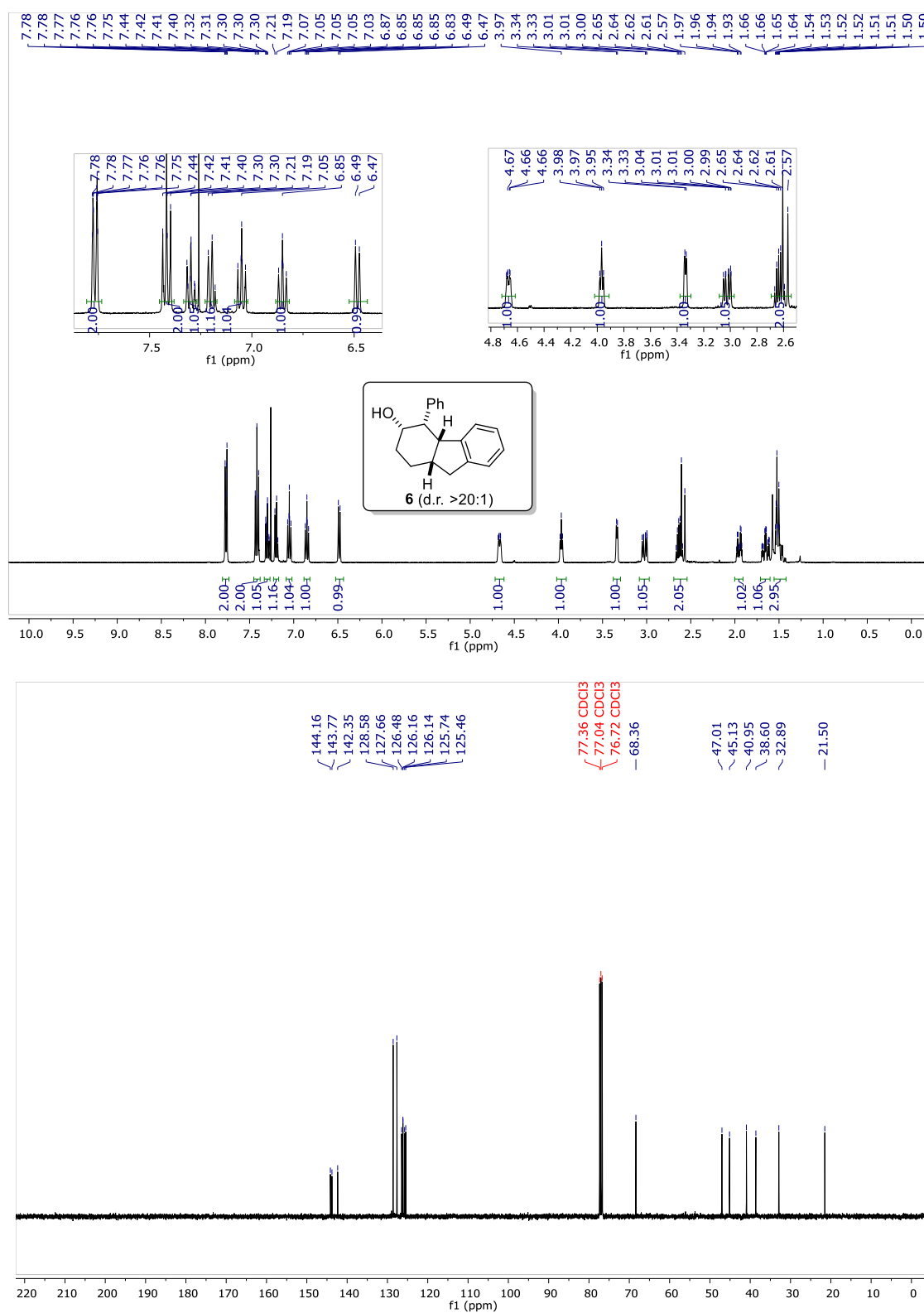
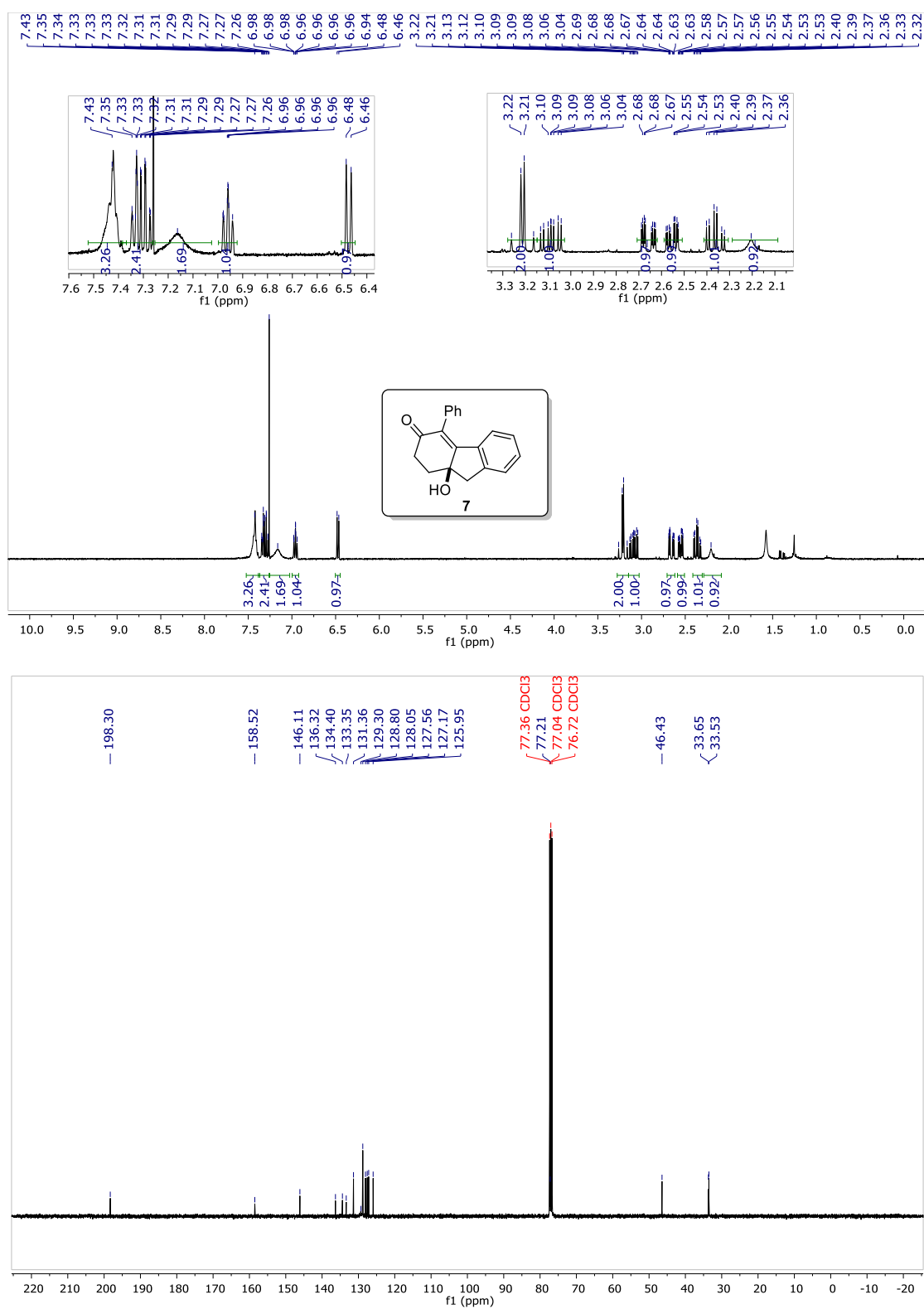
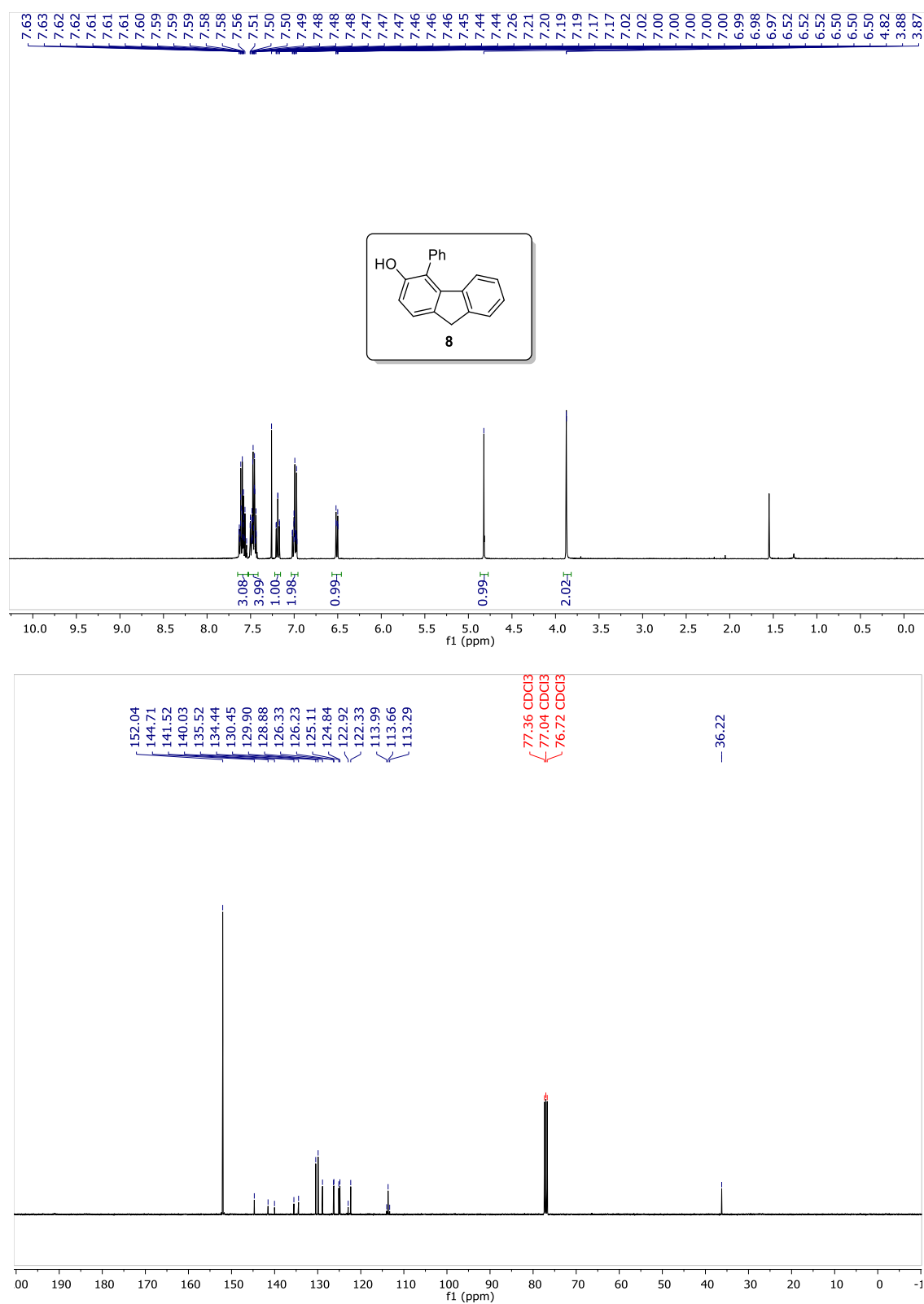


Figure 4.56  $^1\text{H}$  and  $^{13}\text{C}$  NMR spectrum of compound 7

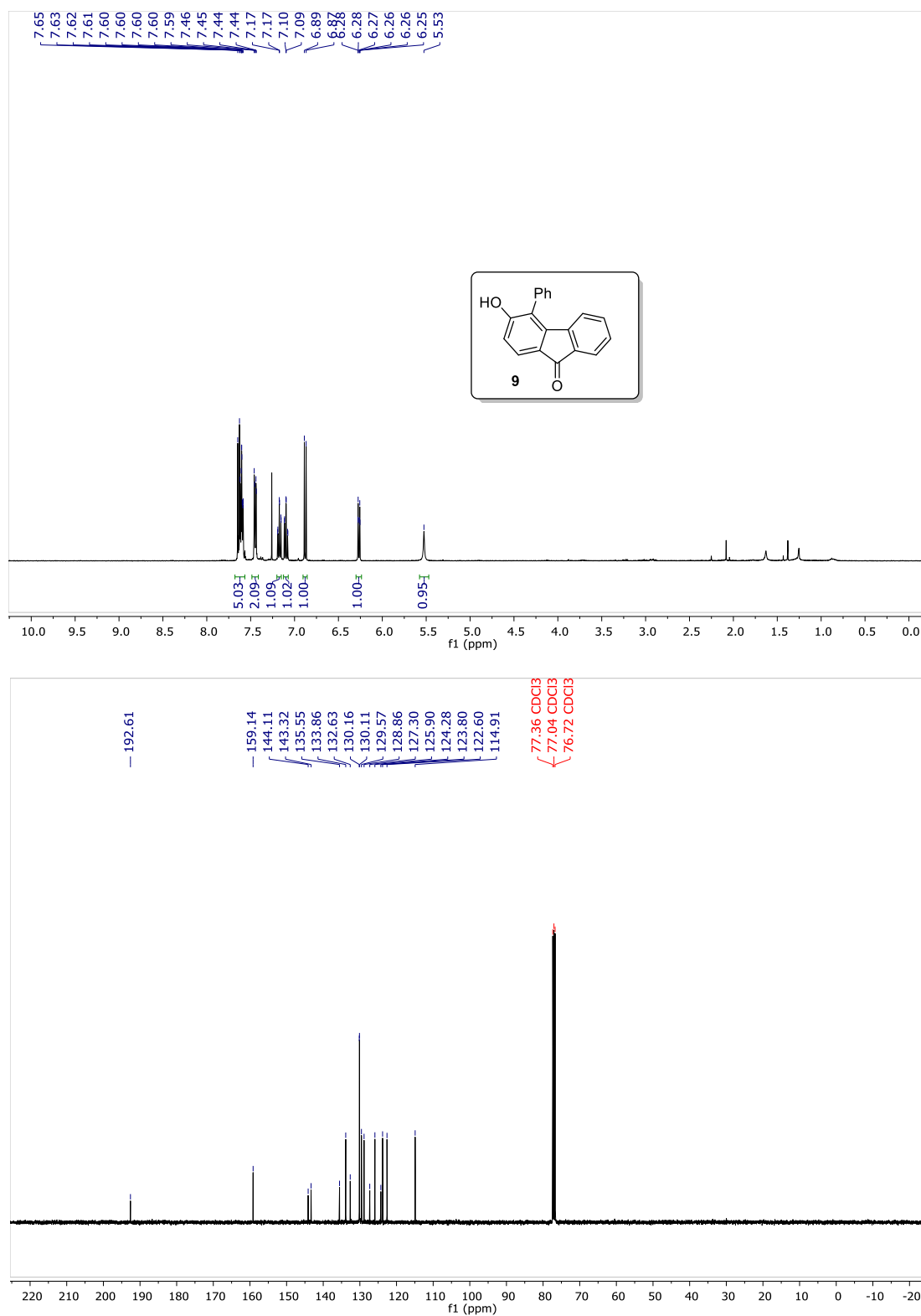


**Figure 4.57**  $^1\text{H}$  and  $^{13}\text{C}$  NMR spectrum of compound **8**

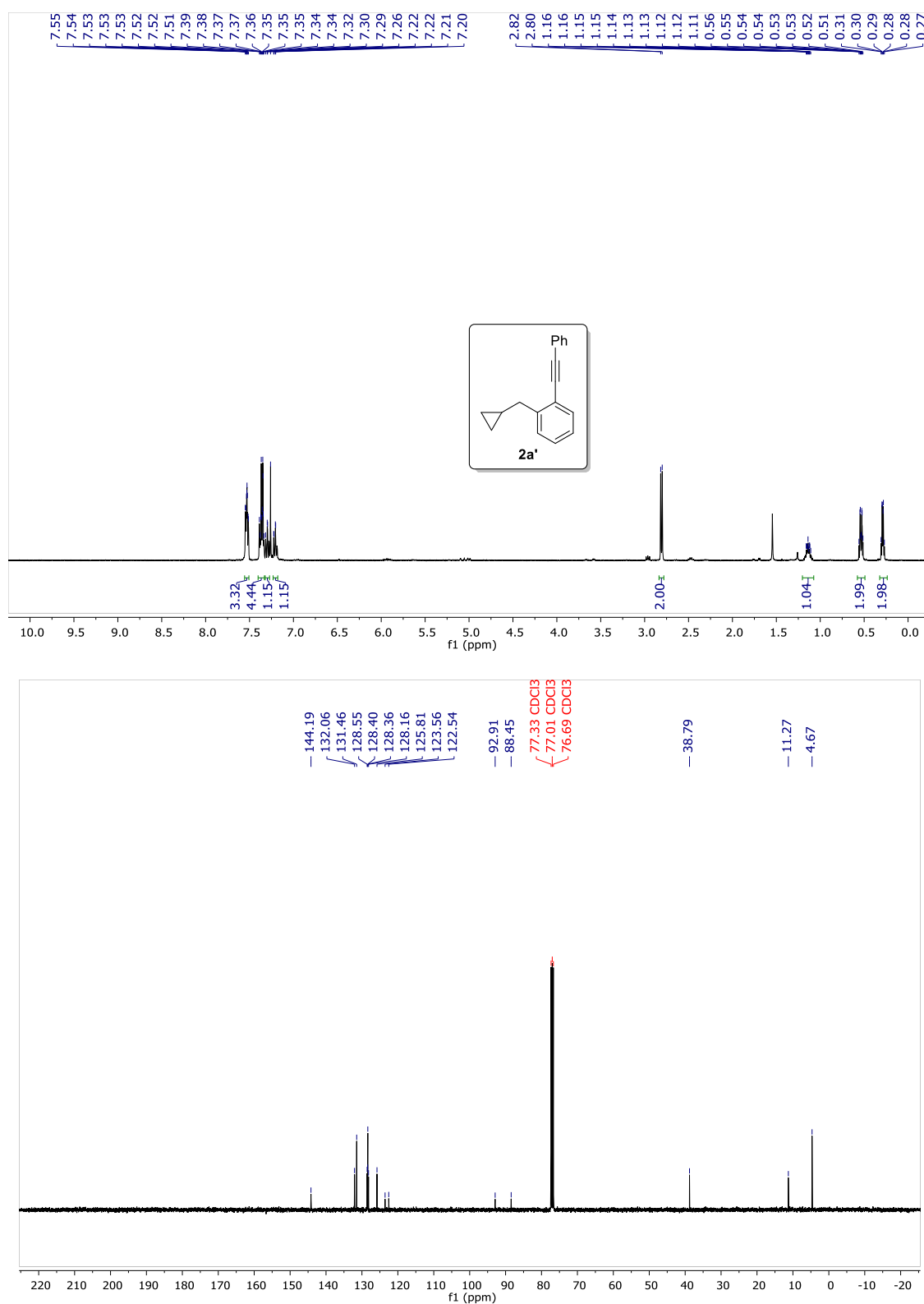




**Figure 4.58**  $^1\text{H}$  and  $^{13}\text{C}$  NMR spectrum of compound **9**



**Figure 4.59**  $^1\text{H}$  and  $^{13}\text{C}$  NMR spectrum of compound **2a'**



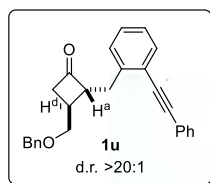
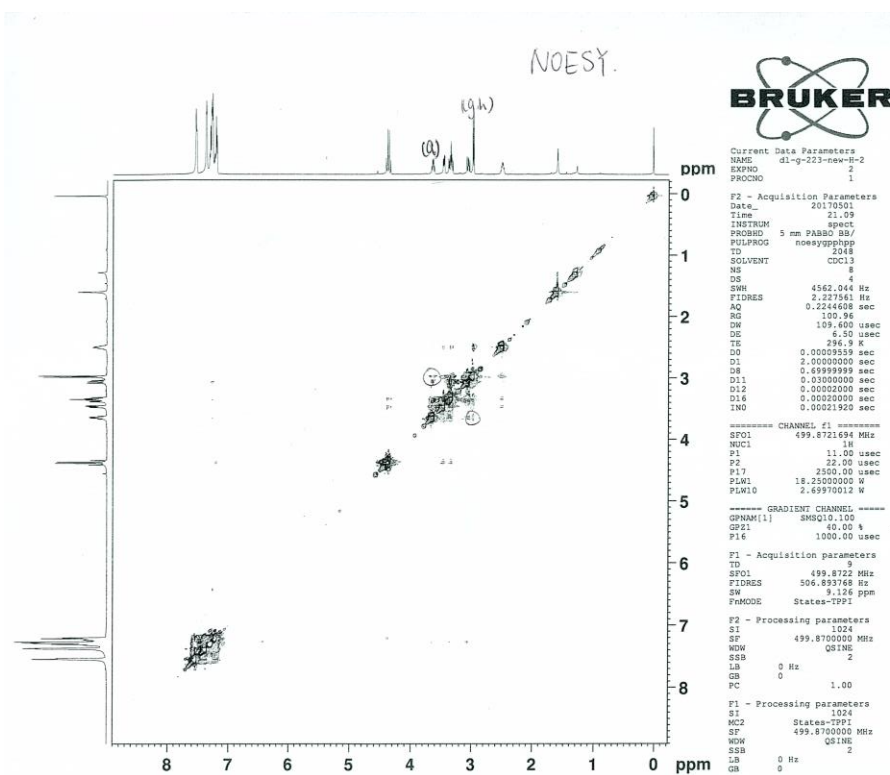
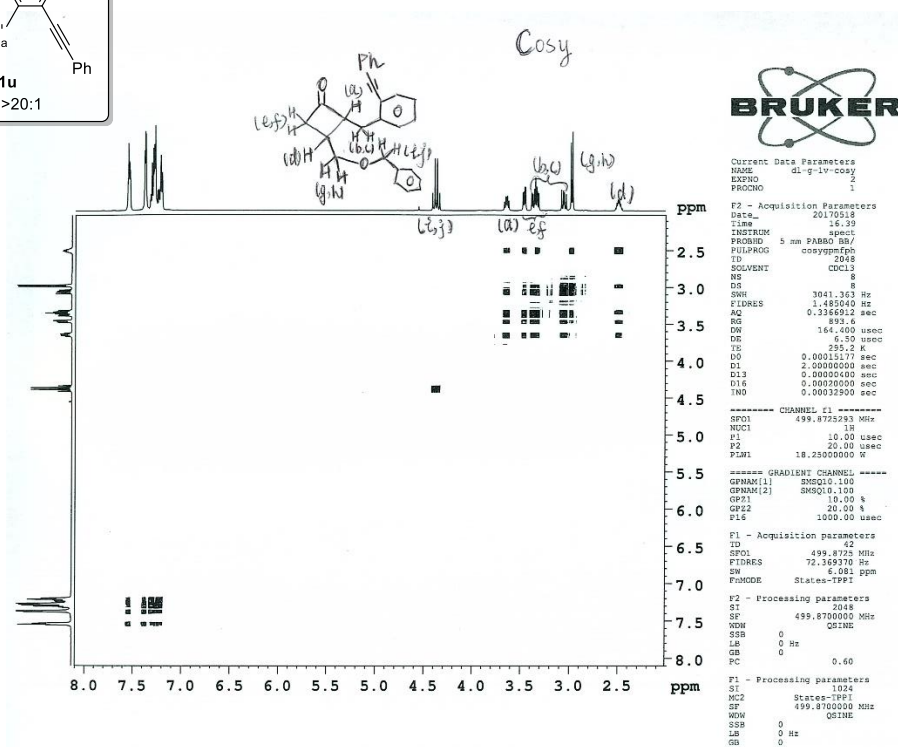


Figure 4.60 2D-NMR spectrum of compound **1u**



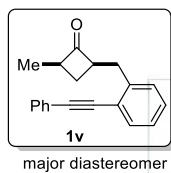
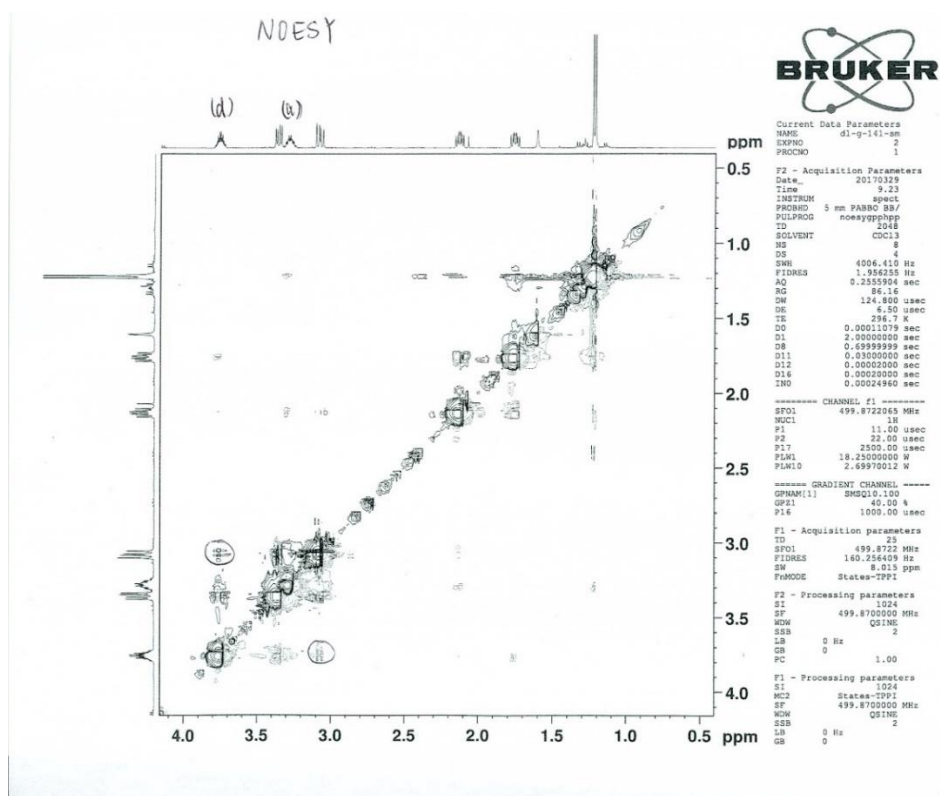
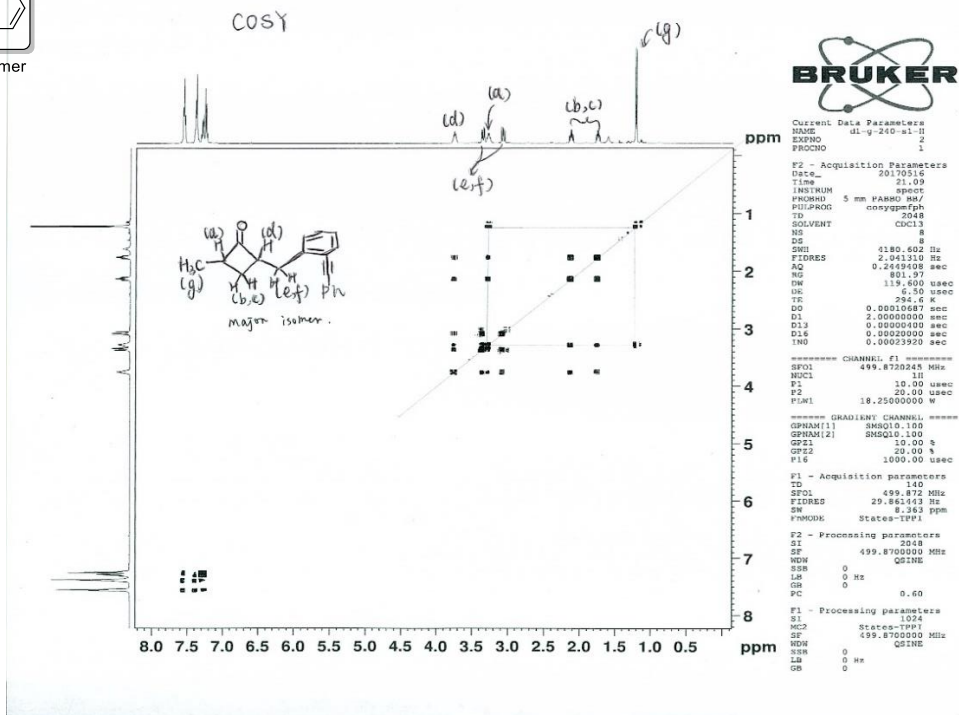


Figure 4.61 2D-NMR spectrum of compound 1v



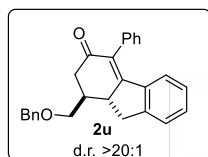
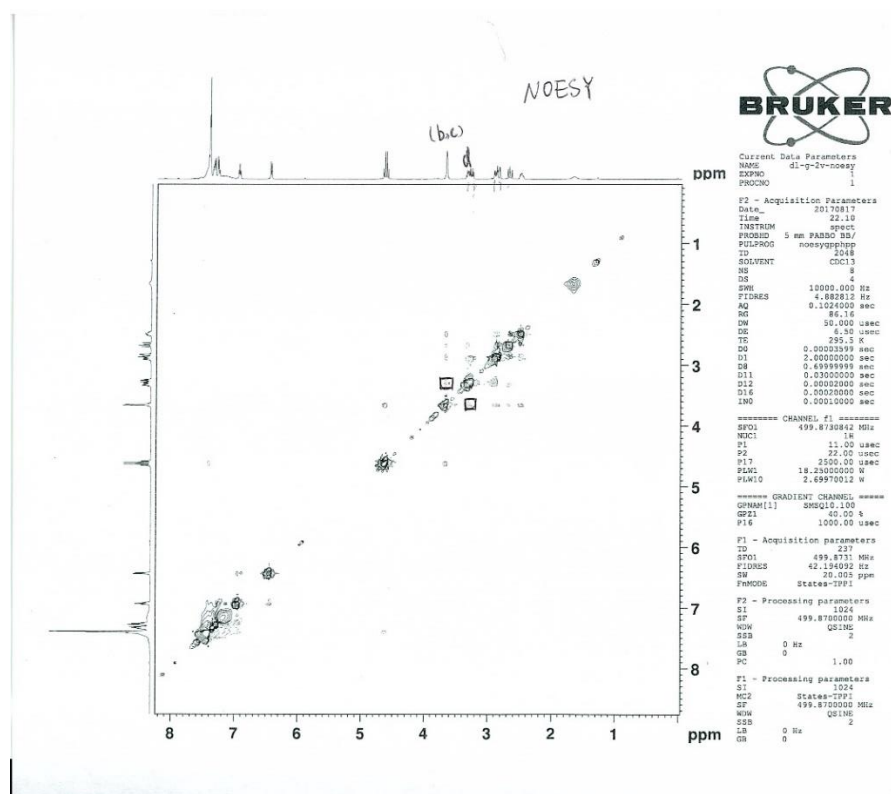
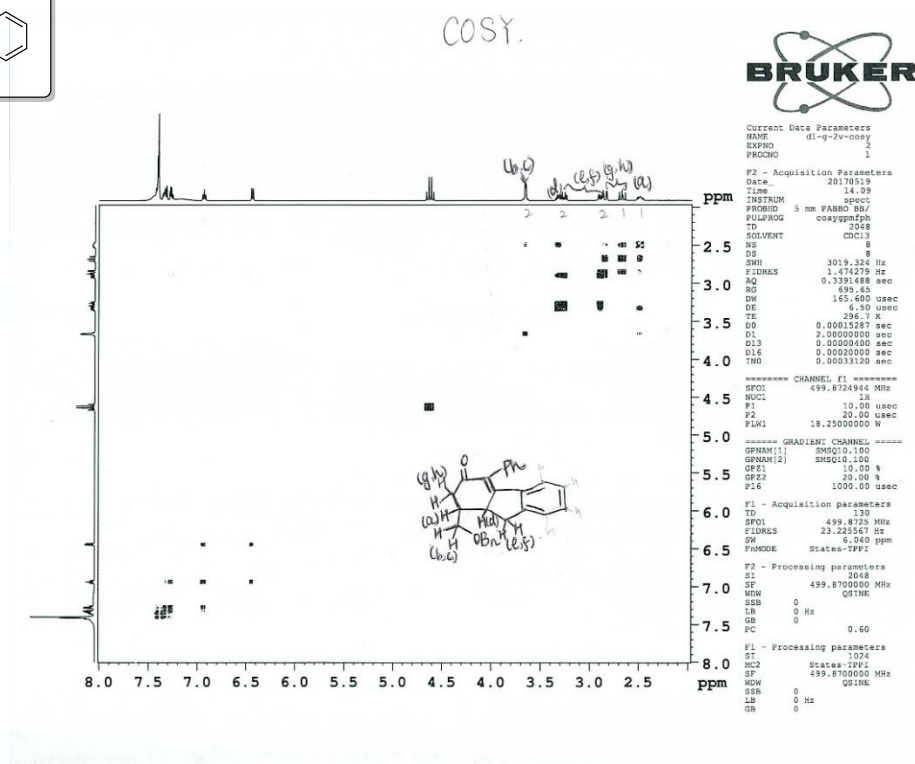


Figure 4.62 2D-NMR spectrum of compound **2u**



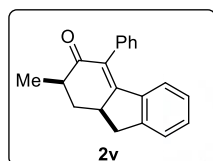
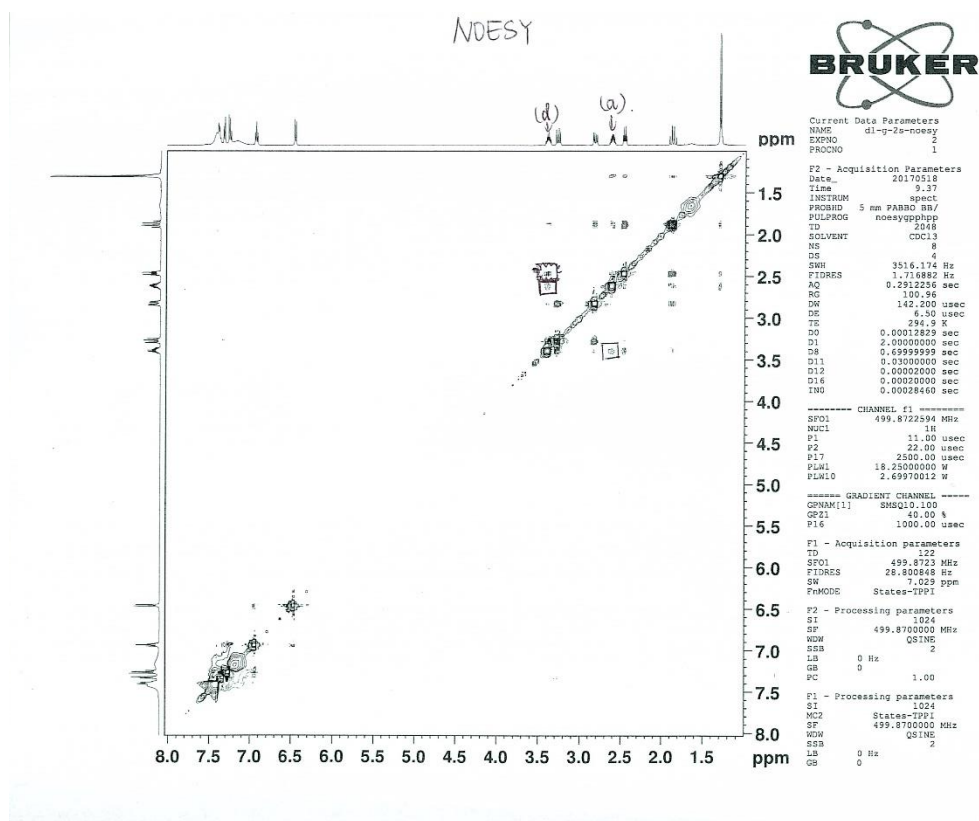
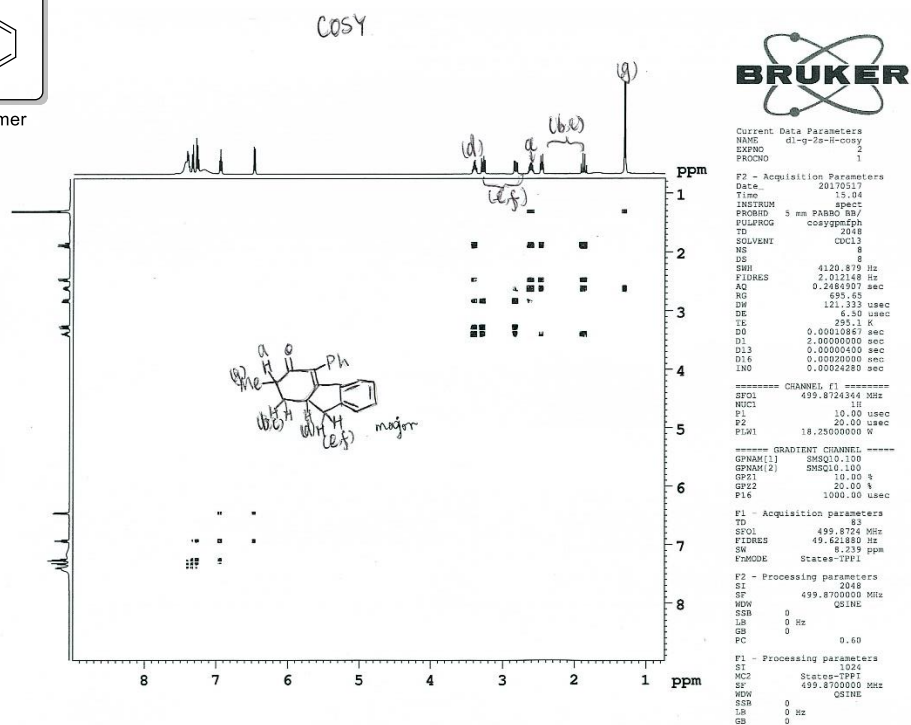


Figure 4.63 2D-NMR spectrum of compound 2v



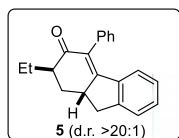
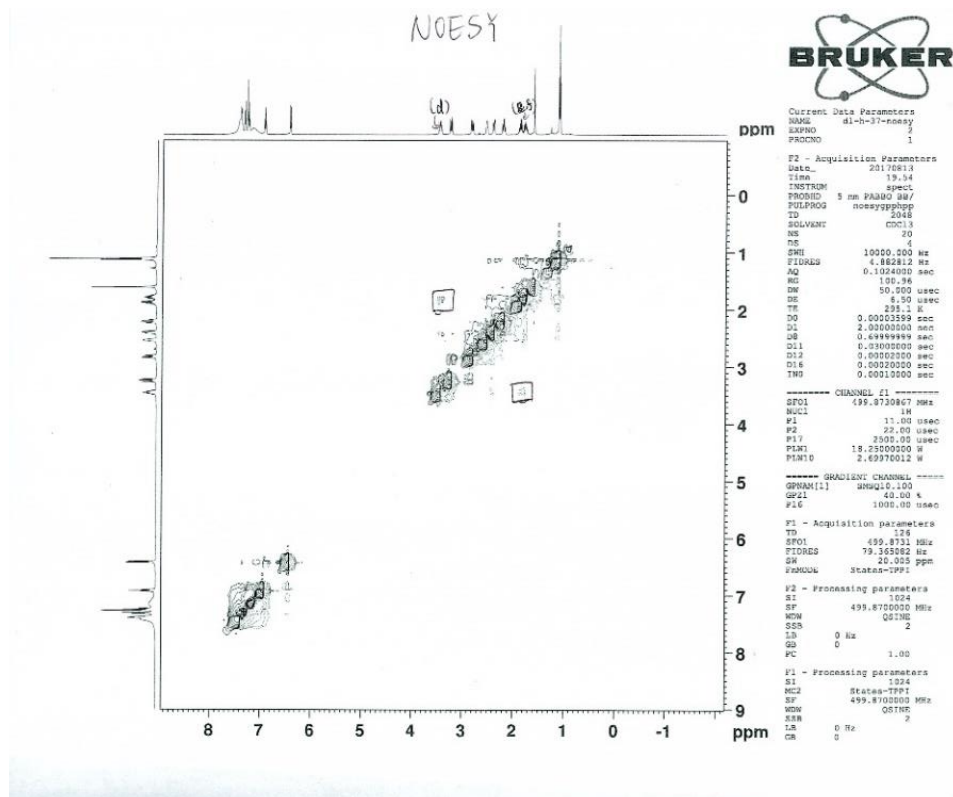
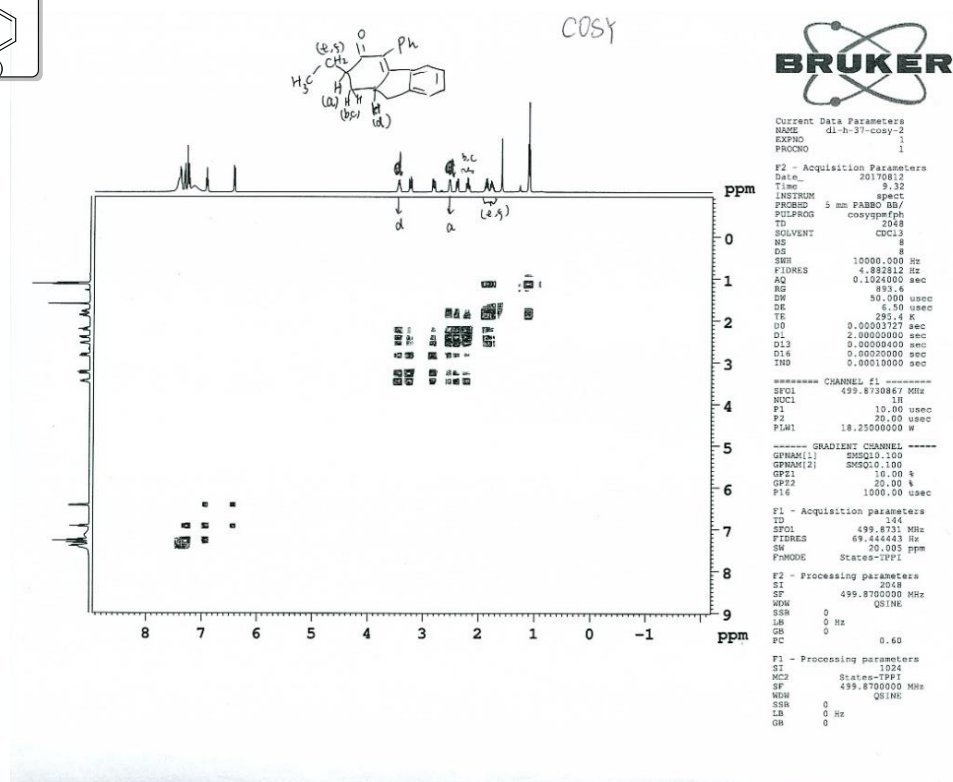


Figure 4.64 2D-NMR spectrum of compound 5



## CHAPTER 5

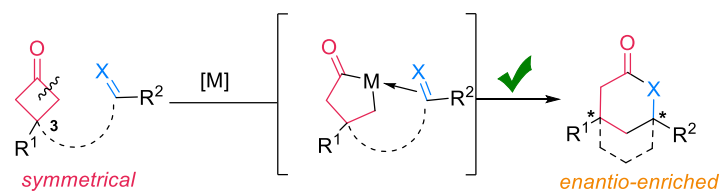
### (Dynamic) Kinetic Resolution of Cyclobutanones through “Cut-and-Sew” Approach

#### 5.1 Introduction

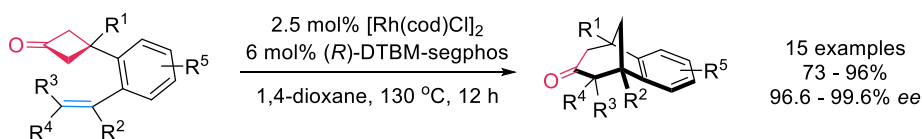
As discussed in Chapter 1, in the past decade, significant progress has been made for the “cut-and-sew” reactions between 3-substituted cyclobutanones and unsaturated units.<sup>1</sup> Starting from restricted types of substrates<sup>1a,1d,1e</sup> then to general substrates<sup>1b,1f,1g</sup>, several bridged ring systems were synthesized through this approach. The 3-substituted cyclobutanones are symmetrical, so it is possible to realize enantioselective transformations through desymmetrization. In 2014, Cramer reported an enantioselective intramolecular carboacylation of olefins through C–C activation of 3-substituted cyclobutanones to generate [3.2.1] bridged ring systems with excellent enantioselectivity.<sup>1e</sup> Later in 2015, our group disclosed an enantioselective [4+1] intramolecular addition between 3-substituted cyclobutanones and allenes, which extended the scope of this strategy to more general substrates (Scheme 5.1).<sup>1f</sup>



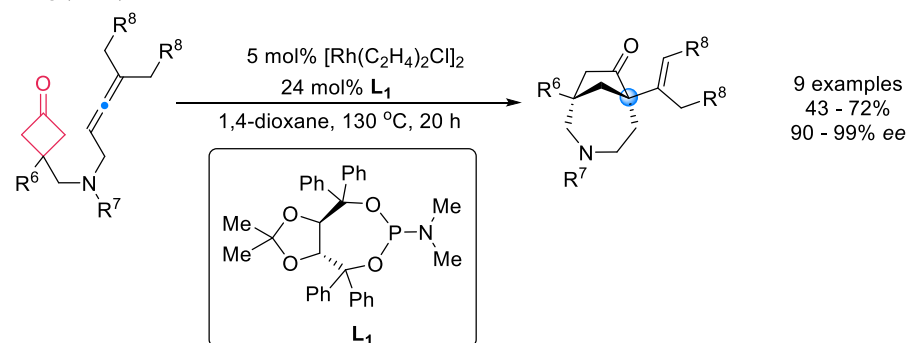
### Scheme 5.1 Asymmetric Cyclohexenone-Bridged Ring Formation via C–C Activation



Cramer (2014)



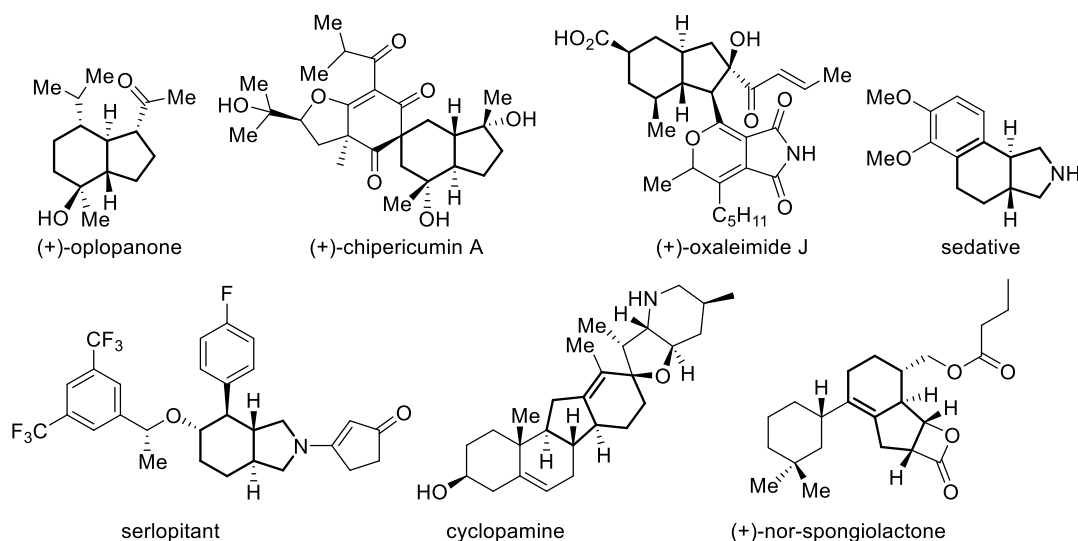
Dong (2015)



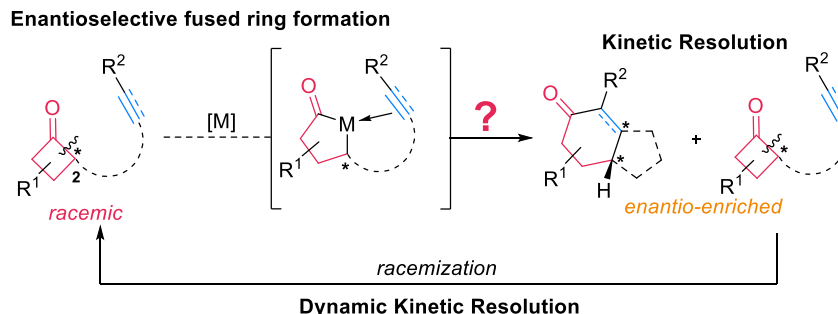
Fused ring systems can also be accessed through C–C bond activation approach when 2-substituted cyclobutanones are used as the starting materials. In particular, 5,6-fused ring systems are widely found in natural products and pharmaceuticals, and many of them have shown attractive bioactivity towards different bacteria or cancer cell lines (Scheme 5.2).<sup>2</sup> However, there has only been a few reports on the construction of fused ring systems using C–C bond activation, and only restricted substrates have been employed.<sup>3</sup> The transformation we developed in Chapter 4 serves as a unique example utilizing “cut-and-sew” strategy,<sup>3b,4</sup> and the enantioselective version using this strategy has not been disclosed yet. The difficulty of realizing such asymmetric transformations attributes to the intrinsic structural feature of 2-substituted cyclohexanones. Comparing with 3-substituted cyclobutanones, they are not symmetrical as they possess an existing chiral center. Therefore, in order to access enantioenriched fused ring systems from racemic

cyclobutanones with high efficiency, approaches other than asymmetric catalysis are required, such as dynamic kinetic resolution (Scheme 5.3).

**Scheme 5.2** Representative Natural Products with the Fused Ring Systems Generated



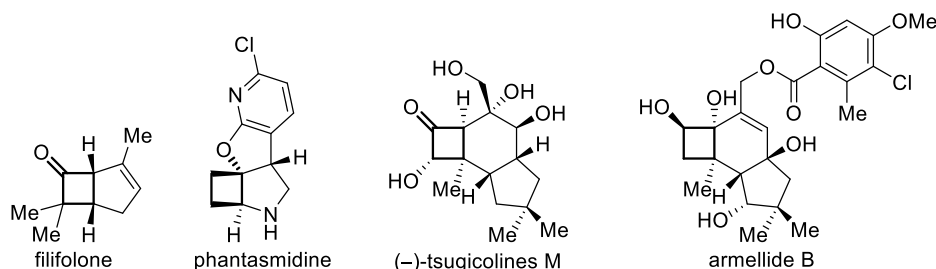
**Scheme 5.3** Asymmetric Cyclohexenone-Fused or Bridged Ring Formation via C–C Activation



On the other hand, chiral cyclobutanones are valuable building blocks for organic synthesis and widely found in natural products and bioactive compounds (Scheme 5.4),<sup>5</sup> yet it still remains challenging to access such structural motifs with satisfactory enantioselectivity.<sup>6</sup> In contrast, a variety of mature synthetic methods have been developed and extensively utilized to synthesize racemic cyclobutanones. Therefore, it would be appealing if enantioenriched cyclobutanones can be accessed from their easily available racemic mixtures. We foresaw that the kinetic resolution

of 2-substituted cyclobutanones would be of special interest as it provides an efficient way to obtain both enantioenriched cyclobutanones and fused ring systems (Scheme 5.3).

**Scheme 5.4** Representative Natural Products with Four-membered Ring



The challenge for this proposal is three-fold: 1) the potential CO extrusion and re-insertion equilibrium would increase the complexity of the reaction pathway, which might lead to various side reactions and diminished enantioselectivity; 2) “cut-and-sew” reaction normally demands relatively high temperature (100 – 150 °C), which would increase the difficulty for efficient enantio-control; 3) for dynamic kinetic resolution, a fast racemization is necessary before the enantio-determining step.

## 5.2 Results and Discussion

### 5.2.1 Condition optimization for kinetic resolution of cyclobutanones

Based on our previous optimal conditions of “cut-and-sew” reactions between cyclobutanones and alkynes<sup>4</sup>, we initiated the condition screening of the proposed transformation employing cyclobutanone **1a** as the substrate. The ligand effect was first examined using  $[\text{Rh}(\text{CO})_2\text{Cl}]_2$  as the precatalyst at 125 °C (Table 5.1). Gratifyingly, under the same conditions for the alkyne insertion, **2a** was obtained in 75% yield with excellent diastereoselectivity (Table 5.1, entry 1). However, apart from DTBM-segphos which delivered **2a** in 35% yield, most chiral phosphine ligands tested were not able to yield the insertion product **2a** (Table 5.1, entries 2-8). To our disappointment, the product obtained using DTBM-segphos is completely racemic. According

to our mechanistic studies in Chapter 4, fast CO extrusion and re-insertion happened during the reaction, which could be related to the lack of enantio-control when  $[\text{Rh}(\text{CO})_2\text{Cl}]_2$  was used as the precatalyst, though the exact reason is unclear.

**Table 5.1** Initial Condition Screening<sup>a</sup>

1a  $\xrightarrow[125\text{ }^\circ\text{C, 1,4-dioxane}]{5\text{ mol\% } [\text{Rh}(\text{CO})_2\text{Cl}]_2}$  2a

Entry	Ligand	Yield <sup>b</sup>	dr	ee <sup>c</sup>
1	16 mol% $\text{PMe}_2\text{Ph}$	75%	>20:1	N/A
2	8 mol% ( <i>R</i> )-BINAP	0%	N/A	N/A
3	8 mol% ( <i>R</i> )-tol-BINAP	0%	N/A	N/A
4	8 mol% ( <i>R</i> )-MeO-BIPHEP	0%	N/A	N/A
5	8 mol% ( <i>S,S</i> )-DIOP	0%	N/A	N/A
6	8 mol% ( <i>R</i> )-DTBM-segphos	35%	>20:1	0%
7	15 mol% ( <i>S</i> )-monophos	0%	N/A	N/A
8	15 mol% <b>L<sub>1</sub></b>	0%	N/A	N/A

<sup>a</sup> The reactions were run at 0.1 mmol scale, 0.1 mol/L concentration for 12 to 36 h. <sup>b</sup> Isolation yield. <sup>c</sup> ee was determined by HPLC.

**L<sub>1</sub>**

**Table 5.2** Selected Condition Screening with Different Precatalysts<sup>a</sup>

1a  $\xrightarrow[100\text{ }^\circ\text{C, 1,4-dioxane}]{10\text{ mol\% } [\text{Rh}], 6\text{ mol\% } (\text{R})\text{-DTBM-segphos}}$  2a + 1a

Entry	[Rh]	2a	ee of 2a <sup>d</sup>	1a	ee of 1a <sup>d</sup>
1 <sup>b</sup>	$\text{Rh}(\text{cod})_2\text{BF}_4$	27%	90%	27%	2%
2 <sup>c</sup>	$\text{Rh}(\text{nbd})_2\text{BF}_4$	17%	N/D	46%	N/D
3 <sup>c</sup>	$\text{Rh}(\text{cod})_2\text{NTf}_2$	26%	N/D	17%	N/D
4 <sup>c</sup>	$[\text{Rh}(\text{cod})(\text{CH}_3\text{CN})_2]\text{BF}_4$	16%	N/D	35%	N/D
5 <sup>c</sup>	$[\text{Rh}(\text{cod})\text{OH}]_2$	0%	N/D	83%	N/D
6 <sup>c</sup>	$\text{Rh}(\text{cod})(\text{acac})$	0%	N/D	61%	N/D
7 <sup>c</sup>	$\text{Rh}(\text{CH}_2=\text{CH}_2)_2(\text{acac})$	0%	N/D	74%	N/D
8 <sup>c</sup>	$\text{Rh}(\text{CO})_2(\text{acac})$	0%	N/D	82%	N/D

<sup>a</sup> The reactions were run at 0.1 mmol scale, 0.1 mol/L concentration for 12 to 36 h. <sup>b</sup> Isolation yield. <sup>c</sup> NMR yield using 1,1,2,2-tetrachloroethane as the internal standard. <sup>d</sup> ee was determined by HPLC.

To address this concern, we did further screening with different precatalysts (Table 5.2). Among the tested precatalysts, only cationic rhodium precatalysts gave moderate yield of the product (Table 5.2, entries 1-4). Gratifyingly, we observed 90% ee when Rh(cod)<sub>2</sub>BF<sub>4</sub> was used, and the recycled starting material was close to racemic, which suggested that the process is possibly a dynamic kinetic resolution.

**Table 5.3** Selected Condition Screening with Different Ligands<sup>a</sup>

10 mol% Rh(cod)<sub>2</sub>BF<sub>4</sub>  
6 mol% (*R*)-DTBM-segphos  
100 °C, 1,4-dioxane

Entry	Modification on the Condition	<b>2a</b> <sup>c</sup>	ee of <b>2a</b> <sup>d</sup>	<b>1a</b> <sup>c</sup>	ee of <b>1a</b> <sup>d</sup>	<b>3a</b> <sup>c</sup>
1 <sup>b</sup>	none	27%	90%	27%	2%	0%
2	10 mol% ( <i>R</i> )-DM-segphos	7%	N/D	20%	N/D	32%
3	( <i>R</i> )-xyl-sdp	0%	N/D	60%	N/D	21%
4	( <i>R</i> )-xyl-binap	0%	N/D	30%	N/D	15%
5	10 mol% ( <i>R</i> )-H8-binap	4%	N/D	8%	N/D	30%
6	10 mol% ( <i>R</i> )-synphos	8%	N/D	69%	N/D	5%
7	10 mol% ( <i>R</i> )-MeO-biphep	5%	N/D	25%	N/D	37%
8	( <i>R</i> )-C3-tunephos	0%	N/D	>90%	N/D	0%
9	10 mol% ( <i>R</i> )-difluorpos	8%	N/D	37%	N/D	34%
10	( <i>R,R</i> )- <i>i</i> -Pr-Duphos, 90 °C	0%	N/D	0%	N/D	83%
11	12 mol% P(cyclohexyl) <sub>3</sub> , 90 °C	12%	N/A	65%	N/A	0%
12	15 mol% P(DTBM) <sub>3</sub>	16%	N/A	17%	N/A	0%

<sup>a</sup> The reactions were run at 0.05 mmol scale, 0.1 mol/L concentration for 12 to 36 h. <sup>b</sup> Isolation yield. <sup>c</sup> NMR yield using 1,1,2,2-tetrachloroethane as the internal standard. <sup>d</sup> ee was determined by HPLC.

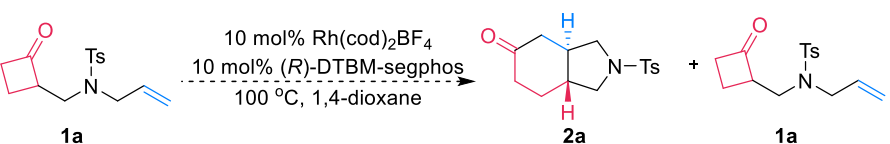
**3a**

With the expectation that the ligands would significantly influence the reactivity and enantioselectivity, we did further screening with different bidentate and monodentate ligands (Table 5.3). We found that DTBM-segphos is the privileged ligand for this transformation among bidentate chiral phosphine ligands possessing different backbond structures tested (Table 5.3, entries 1-10). Notably, side product **3a** could be observed in considerable yields when these ligands were used, while the desired product is often generated in very low yields. The current results

suggest that an electron-rich phosphine ligand is necessary for the high efficiency of this transformation.

We further tested different basic and acidic additives which could potentially promote the racemization of the starting material via enolization of the ketone (Table 5.4). For inorganic bases or amines, we did not observe improvements on the yield of **2a** (Table 5.4, entries 1-5). When sodium bicarbonate was added, the product generated was found to be racemic (Table 5.4, entry 2). When 2,6-di(*t*-butyl)pyridine was introduced, the mass balance of the reaction was improved, but the yield and ee of **2a** were not influenced (Table 5.4, entry 6). Lewis acids were also tested, but no improvement was observed (Table 5.4, entries 7 and 8).

**Table 5.4** Selected Condition Screening with Different Additives<sup>a</sup>



Entry	Additives	<b>2a</b> <sup>c</sup>	ee of <b>2a</b> <sup>d</sup>	<b>1a</b> <sup>c</sup>	ee of <b>1a</b> <sup>d</sup>
1	10 mol% Na <sub>2</sub> CO <sub>3</sub> , 90 °C	19%	N/D	65%	N/D
2 <sup>b</sup>	10 mol% NaHCO <sub>3</sub> , 90 °C	20%	0%	72%	N/D
3	10 mol% NaOAc, 90 °C	23%	N/D	58%	N/D
4	10 mol% DIPEA, 90 °C	20%	N/D	53%	N/D
5	20 mol% Na <sub>2</sub> CO <sub>3</sub> , 120 °C	19%	N/D	50%	N/D
6 <sup>b</sup>	20 mol% <b>A</b> <sub>1</sub> , 120 °C	24%	90%	35%	N/D
7	20mol% ZnCl <sub>2</sub> , 100 °C	11%	N/D	55%	N/D
8	20mol% BPh <sub>3</sub> , 100 °C	0%	N/D	0 %	N/D

**A**<sub>1</sub>: 2,6-di(*t*-butyl)pyridine

<sup>a</sup> The reactions were run at 0.05 mmol scale, 0.1 mol/L concentration for 12 to 36 h. <sup>b</sup> Isolation yield. <sup>c</sup> NMR yield using 1,1,2,2-tetrachloroethane as the internal standard. <sup>d</sup> ee was determined by HPLC.

Following that, different pre-coordinating groups on rhodium precatalysts and counter-ions were examined (Table 5.5). It is obvious that when the cationic rhodium catalysts were generated in situ, [Rh(CH<sub>2</sub>=CH<sub>2</sub>)<sub>2</sub>Cl]<sub>2</sub> is the optimal precursor which might be attributed to the complete exchange of the ethylene ligand in the precatalyst with the chiral ligand (Table 5.5, entries 1-4). Among the counter-ions tested in the reaction, SbF<sub>6</sub> anion was found to give the highest reactivity

and enantioselectivity (Table 5.5, entries 5-9). The reason might be that  $\text{SbF}_6^-$  anion is weakly associated to the rhodium cation, which would lead to faster migratory insertion.

**Table 5.5** Selected Condition Screening with In-Situ Generated Cationic Rhodium Catalysts<sup>a</sup>

Entry	Precatalyst	<b>2a</b> <sup>b</sup>	ee of <b>2a</b> <sup>d</sup>	<b>1a</b> <sup>b</sup>	ee of <b>1a</b> <sup>d</sup>
1	$[\text{Rh}(\text{coe})_2\text{Cl}]_2 / \text{AgBF}_4$	28%	54%	40%	N/D
2 <sup>c</sup>	$[\text{Rh}(\text{CO})_2\text{Cl}]_2 / \text{AgBF}_4$	26%	N/D	0%	N/D
3 <sup>c</sup>	$[\text{Rh}(\text{hexadiene})_2\text{Cl}]_2 / \text{AgBF}_4$	28%	N/D	31%	N/D
4	$[\text{Rh}(\text{CH}_2=\text{CH}_2)_2\text{Cl}]_2 / \text{AgBF}_4$	37%	56%	21%	N/D
5 <sup>c</sup>	$[\text{Rh}(\text{cod})\text{Cl}]_2 / \text{AgOTf}$	9%	N/D	70%	N/D
6	$[\text{Rh}(\text{cod})\text{Cl}]_2 / \text{AgBF}_4$	24%	90%	33%	N/D
7	$[\text{Rh}(\text{cod})\text{Cl}]_2 / \text{AgPF}_6$	29%	92%	36%	N/D
8	$[\text{Rh}(\text{cod})\text{Cl}]_2 / \text{AgSbF}_6$	29%	84%	29%	N/D
9	$[\text{Rh}(\text{CH}_2=\text{CH}_2)_2\text{Cl}]_2 / \text{AgSbF}_6$ , 90 °C	36%	98%	29%	0%

<sup>a</sup> The reactions were run at 0.05 mmol scale, 0.1 mol/L concentration for 12 to 36 h.

<sup>b</sup> Isolation yield. <sup>c</sup> NMR yield using 1,1,2,2-tetrachloroethane as the internal standard.

<sup>d</sup> ee was determined by HPLC.

The relatively low mass balance suggests that lower temperature might be beneficial for the reaction. A series of different temperatures was then tested for this transformation using the optimal precatalyst/ligand combination (Table 5.6). Distinct from all the known “cut-and-sew” reactions,<sup>7</sup> this transformation can happen smoothly even at room temperature with excellent yield and ee (Table 5.6, entries 5 and 6). As the temperature of reaction decreases, the ee of the recycled starting material increased accordingly, which suggests that the racemization process requires higher temperature (Table 5.6, entries 1-5). The conditions shown in entry 6 are optimal for a kinetic resolution process, as both **2a** and **1a** can be obtained in excellent yield and ee, and the calculated selectivity factor is very high.

**Table 5.6** Selected Condition Screening at Different Temperatures<sup>a</sup>

Entry	Modifications on the Condition	<b>2a<sup>b</sup></b>	ee of <b>2a<sup>c</sup></b>	<b>1a<sup>b</sup></b>	ee of <b>1a<sup>c</sup></b>	<i>s<sup>d</sup></i>
1	90 °C, with 20 mol% (R)-DTBM-segphos	36%	98%	29%	0%	--
2	75 °C, with 20 mol% (R)-DTBM-segphos	34%	98%	50%	28%	130
3	65 °C, with 20 mol% (R)-DTBM-segphos	33%	98%	47%	71%	211
4	45 °C, with 20 mol% (R)-DTBM-segphos	47%	95%	40%	94%	139
5	r.t., with 20 mol% (R)-DTBM-segphos	43%	98%	44%	99%	525
<b>6</b>	<b>None</b>	<b>46%</b>	<b>98%</b>	<b>47%</b>	<b>98%</b>	<b>458</b>

<sup>a</sup> The reactions were run at 0.1 mmol scale, 0.1 mol/L concentration for 12 h. <sup>b</sup> Isolation yield. <sup>c</sup> ee was determined by HPLC. <sup>d</sup> Selectivity (*s*) = ln[(1 - *C*)(1 - ee<sub>SM</sub>)]/ln[(1 - *C*)(1 + ee<sub>SM</sub>)]; calculated conversion (*C*) = ee<sub>SM</sub>/(ee<sub>SM</sub> + ee<sub>PD</sub>).

Interestingly, when we purify the reaction mixture using prep TLC, the recycled **1a** is completely racemized at room temperature. Considering that the prep TLC silica gel is very acidic, we proposed that strong acids might help the racemization process. Further screening of the acidic additives were conducted, but none of them can improve the result for the dynamic kinetic resolution (Table 5.7, entries 3-5).

**Table 5.7** Selected Condition Screening for Acidic Additives<sup>a</sup>

Entry	Modifications on the Condition	<b>2a</b>	ee of <b>2a<sup>c</sup></b>	<b>1a</b>	ee of <b>1a<sup>c</sup></b>
<b>1<sup>b</sup></b>	None, column purification	43%	98%	44%	99%
<b>2<sup>b</sup></b>	None, prep TLC purification	45%	98%	42%	0%
<b>3<sup>d</sup></b>	50 wt% silica gel	15%	N/D	66%	N/D
<b>4<sup>d</sup></b>	20 mol% p-TsOH	41%	N/D	40%	N/D
<b>5<sup>d</sup></b>	20 mol% AcOH	36%	N/D	43%	N/D

<sup>a</sup> The reactions were run at 0.1 mmol scale, 0.1 mol/L concentration for 12 h. <sup>b</sup> Isolation yield. <sup>c</sup> ee was determined by HPLC. <sup>d</sup> The reactions were run at 0.05 mmol scale with NMR yield using 1,1,2,2-tetrachloroethane as the internal standard.

Selected control experiments are shown below. When racemic DTBM-segphos was used in the reaction, 90% yield was obtained, which further supports that the reaction is a kinetic



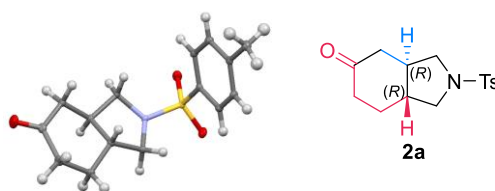
resolution (Table 5.8, entry 1). Currently, 1,4-dioxane is found to be the optimal solvent and 0.1 M is the optimal concentration (Table 5.8, entries 2-5). Both precatalyst and ligand are essential for this transformation (Table 5.8, entries 6-7). The absolute stereochemistry of **2a** was confirmed by X-ray crystallography (Scheme 5.5).

**Table 5.8** Selected Control Experiments<sup>a</sup>

Entry	Modifications on the Condition	<b>2a</b> <sup>b</sup>	ee of <b>2a</b> <sup>c</sup>	<b>1a</b> <sup>b</sup>	ee of <b>1a</b> <sup>c</sup>
1 <sup>d</sup>	45 °C, 20 mol% (R/S)-DTBM-segphos	90%	N/A	0%	N/A
2	24 h, toluene	44%	N/D	42%	N/D
3	24 h, MeTHF	0	N/D	90%	N/D
4	12 h, 0.2 M	49%	N/D	40%	N/D
5	12 h, 0.4 M	49%	N/D	30%	N/D
6	w/o [Rh(=)Cl] <sub>2</sub> / AgSbF <sub>6</sub>	0%	N/A	99%	N/A
7	w/o (R)-DTBM-segphos, with Rh(cod) <sub>2</sub> BF <sub>4</sub>	0%	N/A	94%	N/A

<sup>a</sup> The reactions were run at 0.05 mmol scale, 0.1 mol/L concentration for 12 h. <sup>b</sup> NMR yield using 1,1,2,2-tetrachloroethane as the internal standard. <sup>c</sup> ee was determined by HPLC. <sup>d</sup> The reactions were run at 0.1 mmol scale with isolation yield.

**Scheme 5.5** X-ray Structure of **2a**

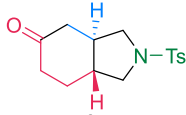
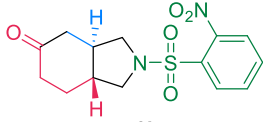
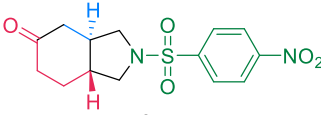
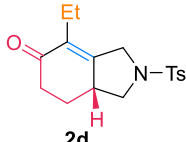
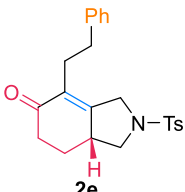
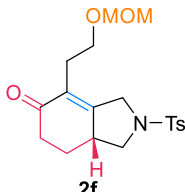
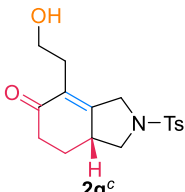
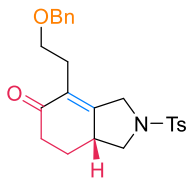
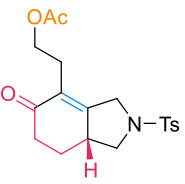
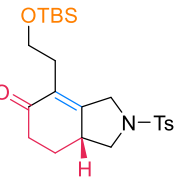
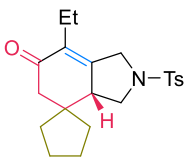


### 5.2.2 Substrate scope for kinetic resolution of cyclobutanones

With the optimized conditions for kinetic resolution in hand, we next investigated the substrate scope (Table 5.9). The protecting group on the nitrogen linkage can be changed to 2-nosyl and 4-nosyl groups with good yield and ee maintained (Table 5.9, **2b** and **2c**). Gratifyingly, alkyne-tethered substrates can be engaged in this transformation smoothly (**2d** to **2k**). The reaction

condition is very mild, so many labile groups are well tolerated under the standard conditions, such as MOM, benzyl, acyl and TBS-protected alcohols. The free-alcohol-containing substrate can also yield the product with excellent yield and ee. Substituent on the 3-position of the cyclobutanone would reduce the reactivity, but the kinetic resolution happened with good reactivity and selectivity at slightly elevated temperature (**2k**).

**Table 5.9** Substrate Scope<sup>a,b</sup>

 <p><b>2a</b> <b>2a</b>: 46% yield, 98% ee <b>1a</b>: 47% yield, 98% ee C = 0.50, s = 458</p>	 <p><b>2b</b> <b>2b</b>: 44% yield, 95% ee <b>1b</b>: 47% yield, 90% ee C = 0.49, s = 120</p>	 <p><b>2c</b> <b>2c</b>: 50% yield, 94% ee <b>1c</b>: 42% yield, 96% ee C = 0.51, s = 127</p>	
 <p><b>2d</b> <b>2d</b>: 48% yield, 98% ee <b>1d</b>: 40% yield, 98% ee C = 0.50, s = 458</p>	 <p><b>2e</b> <b>2e</b>: 42% yield, 96% ee <b>1e</b>: 45% yield, 90% ee C = 0.48, s = 152</p>	 <p><b>2f</b> <b>2f</b>: 48% yield, 98% ee <b>1f</b>: 50% yield, 98% ee C = 0.50, s = 458</p>	 <p><b>2g<sup>c</sup></b> <b>2g</b>: 46% yield, 98% ee <b>1g</b>: 48% yield, 88% ee C = 0.47, s = 290</p>
 <p><b>2h</b> <b>2h</b>: 38% yield, 98% ee <b>1h</b>: 45% yield, 98% ee C = 0.50, s = 458</p>	 <p><b>2i</b> <b>2i</b>: 46% yield, 96% ee <b>1i</b>: 50% yield, 98% ee C = 0.51, s = 226</p>	 <p><b>2j</b> <b>2j</b>: 43% yield, 94% ee <b>1j</b>: 40% yield, 99% ee C = 0.51, s = 170</p>	 <p><b>2k<sup>d</sup></b> <b>2k</b>: 32% yield, 99.5% ee <b>1k</b>: 43% yield, 65% ee C = 0.40, s = 785</p>

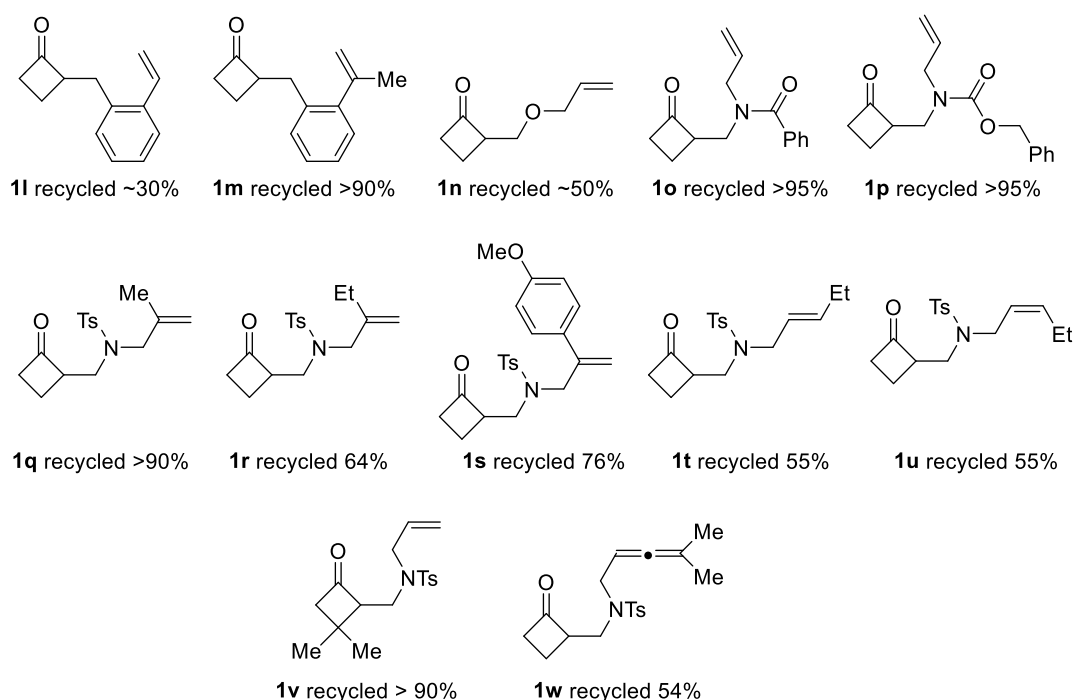
<sup>a</sup> Reaction conditions: at 0.1 mmol scale, [Rh(CH<sub>2</sub>=CH<sub>2</sub>)<sub>2</sub>Cl]<sub>2</sub> (5 mol %), (*R*)-DTBM-segphos (10 mol %), AgSbF<sub>6</sub> (10 mol %), 1,4-dioxane (1 mL), r.t., 12-13 h. <sup>b</sup> Isolation yield; ee is determined by chiral HPLC; selectivity (s) = ln[(1 - C)(1 - ee<sub>SM</sub>)]/ln[(1 - C)(1 + ee<sub>SM</sub>)], calculated conversion (C) = ee<sub>SM</sub>/(ee<sub>SM</sub> + ee<sub>PD</sub>).

<sup>c</sup> THF is used as the solvent. <sup>d</sup> Reaction temperature is 40 °C.

Apart from the successful examples shown in table 5.9, we have synthesized and tested many other substrates, but unfortunately, they cannot give satisfying results for the kinetic resolution. Different linkages other than *N*-Ts were tested, such as benzene (**1l** and **1m**), oxygen

(**1n**) or *N*-acyl (**1o** and **1p**), but none of them can yield any product, which could be explained by the flexibility of the linkage or the stronger coordination from the acyl group. The reaction is sensitive to the steric hindrance of the olefin moiety (**1q** to **1u**). Substrates with 1,1- or 1,2-disubstituted olefins are not viable under the current conditions. Gem-dimethyl substituents on the 3-position of the cyclobutanone are not tolerated (**1v**) and allene is not a feasible coupling partner due to severe isomerization (**1w**).

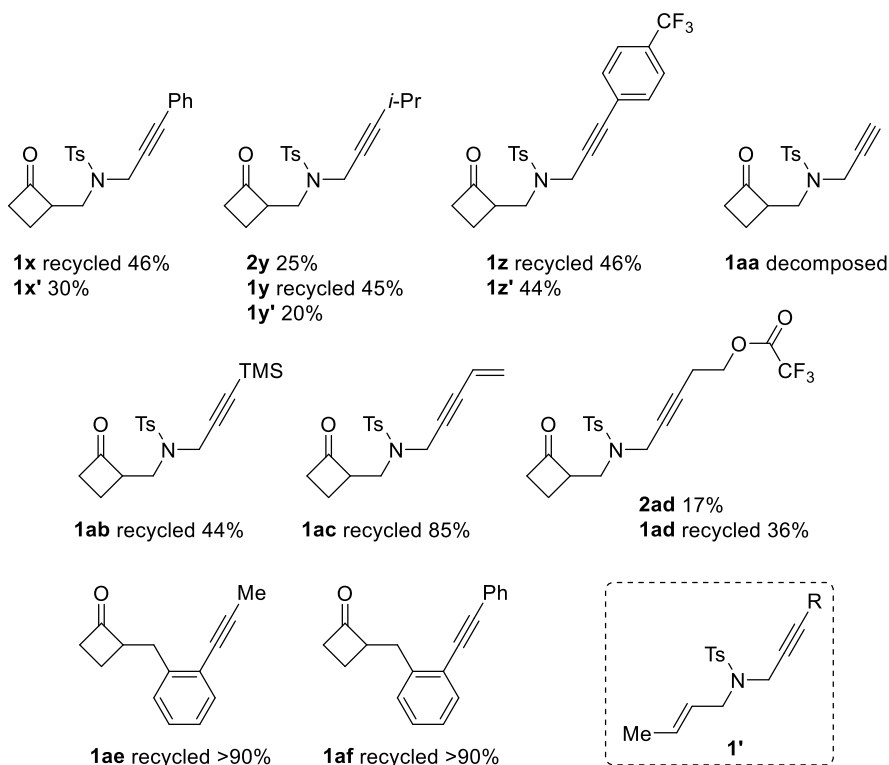
**Scheme 5.6** Unsuccessful Substrates on Olefin- or Allene-Tethered Substrates



For different substituents on the alkyne moiety, similar sensitivity to steric hindrance was observed (Scheme 5.7). Aryl substituents are not tolerated (**1x** and **1z**). Simply switching the ethyl group to a bulkier isopropyl group (**1y**) caused significant decrease of the yield. Additionally, **1x**, **1y** and **1z** decomposed to olefins (**1x'**, **1y'** and **1z'**, the general structure is shown as **1'**) via decarbonylation followed by  $\beta$ -hydrogen elimination. Terminal alkyne (**1aa**) leads to severe decomposition. TMS and vinyl substituted alkynes are not viable substrates (**1ab** and **1ac**).

Benzene linkage cannot facilitate the desired transformation in the alkyne-tethered substrates as well (**1ae** and **1af**).

**Scheme 5.7** Unsuccessful Substrates on Alkyne-Tethered Substrates



### 5.3 Conclusion and Outlook

In summary, we have developed a highly selective kinetic resolution process for intramolecular addition between 2-substituted cyclobutanones and olefins or alkynes. Impressive selectivity was observed with a selectivity factor ranging from 120 to 785. In addition, the kinetic resolution is highly efficient at room temperature, at which catalytic C–C activation through oxidative addition of cyclobutanones has not been achieved. Given the mild reaction conditions, various functional groups are well tolerated. We envision that the newly developed kinetic resolution process would provide access to a wide variety of chiral 5,6-fused ring systems and

chiral substituted cyclobutanones and cyclobutanols, which are often found to be important building blocks for bioactive natural products and pharmaceuticals.

At current stage, we are still focusing on understanding the enantio-determining step and the reason why this reaction can happen at low temperature through collaboration with computational chemists. Meanwhile, exploration on different olefin-tethered substrates and the synthetic utility of this method is ongoing in our laboratory. With the encouraging preliminary results on dynamic kinetic resolution, further screening to realize a high efficiency is also currently being explored.

It is encouraging to see how far we have gone in terms of activating these inert C–C bonds, from more strained cyclobutenones to cyclobutanones, from high temperature to room temperature, and from racemic to highly enantioselective transformations. In the near future, we foresee that the “cut-and-sew” chemistry of various ketones will be a widely adopted approach for synthetic chemists to forge the backbones of complex molecules with all the past, current and ongoing efforts in this area.

## 5.4 Experimental

### 5.4.1 General information

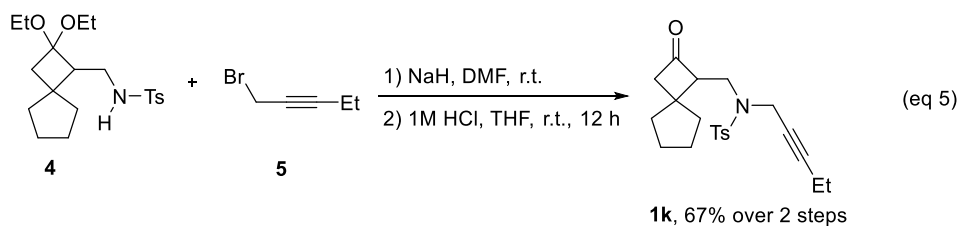
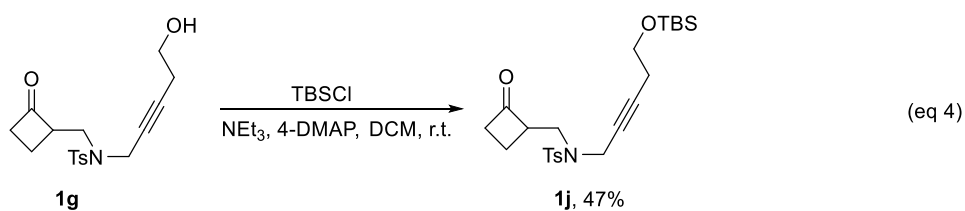
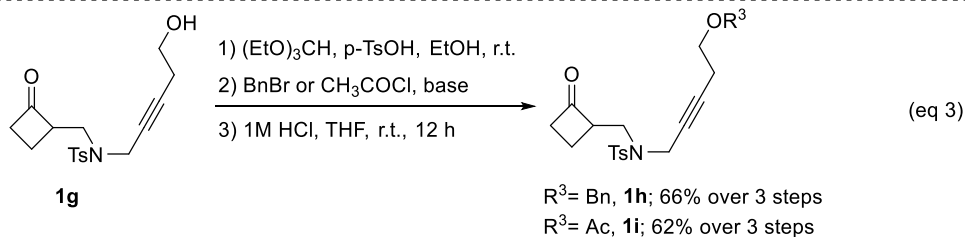
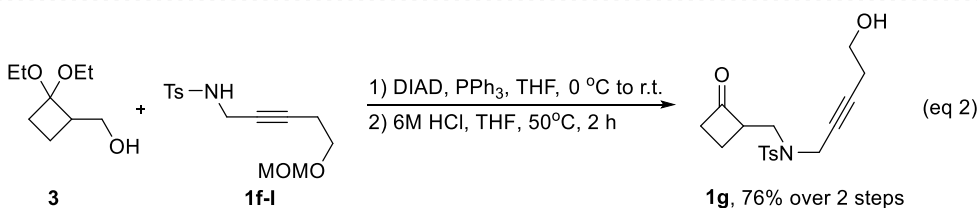
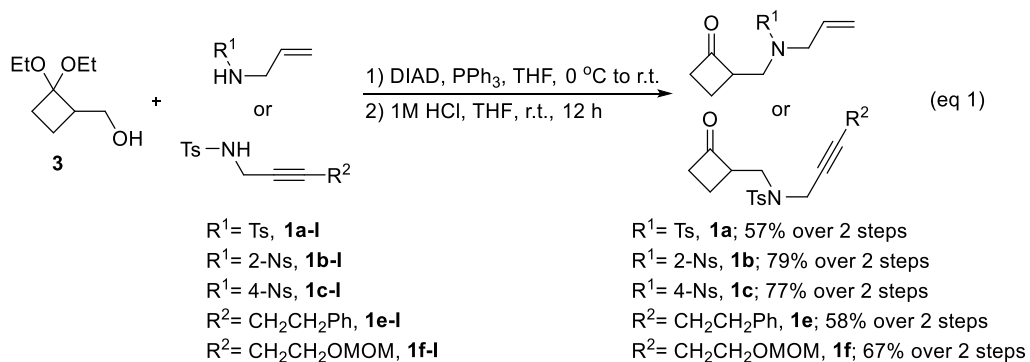
Unless noted otherwise, all solvents were dried by filtration through a Pure-Solv MD-5 Solvent Purification System (Innovative Technology). The solvents for the C–C Activation reactions were distilled freshly over sodium or calcium hydride and carefully freeze-pump-thawed. All the C–C Activation reactions were carried out under nitrogen atmosphere with a stir bar in a sealed vial. Reaction temperatures were reported as the temperatures of the bath surrounding the flasks or vials. Sensitive ligands and rhodium catalysts and solvents were transferred under nitrogen into a nitrogen-filled glovebox with standard techniques. Analytical thin-layer chromatography (TLC)

was carried out using 0.2 mm commercial silica gel plates (silica gel 60, F254, EMD chemical). Vials (17 x 60 mm (7.5mL) with PTFE lined cap attached) were purchased from Qorpak and flame-dried or put in an oven overnight. High-resolution mass spectra (HRSM) were obtained on a Agilent 6224 Tof-MS and are reported as  $m/z$  (relative intensity). Accurate masses are reported for the molecular ion  $[M+Na]^+$ ,  $[M+H]^+$ . Infrared spectra were recorded on a Nicolet 380 FTIR using neat thin film technique. Nuclear magnetic resonance spectra ( $^1H$  NMR and  $^{13}C$  NMR) were recorded with a Bruker Avance 500 instrument (500 MHz,  $^1H$  at 500 MHz,  $^{13}C$  at 126 MHz) and Bruker Avance 400 instrument (400 MHz,  $^1H$  at 400 MHz,  $^{13}C$  at 100 MHz). Unless otherwise noted, all spectra were acquired in  $CDCl_3$ . Chemical shifts are reported in parts per million (ppm,  $\delta$ ), downfield from tetramethylsilane (TMS,  $\delta=0.00$ ppm) and are referenced to residual solvent ( $CDCl_3$ ,  $\delta=7.26$  ppm ( $^1H$ ) and 77.00 ppm ( $^{13}C$ );  $CD_2Cl_2$ ,  $\delta=5.32$  ppm ( $^1H$ ) and 53.84 ppm ( $^{13}C$ )). Coupling constants were reported in Hertz (Hz). Data for  $^1H$  NMR spectra were reported as follows: chemical shift (ppm, referenced to protium; s = singlet, d = doublet, t = triplet, q = quartet, hept=heptuplet, dd = doublet of doublets, td = triplet of doublets, ddd = doublet of doublet of doublets, m = multiplet, coupling constant (Hz), and integration). Analytical HPLC was carried out on an Angilent 1260 infinity HPLC with DAD, Chiralpak IA-IF, served as columns, and mixtures of *n*-hexane and *i*-PrOH were used for elution.

#### 5.4.2 Substrate synthesis

Substrates **1a** to **1f** were synthesized through Mitsunobu reaction followed by deprotection of the ketal (eq 1). **1a-I** to **1f-I** and **1d** are literature known compounds, and their characterization data match the reported data.<sup>4,8a-e</sup> Substrate **1g** was synthesized from **3** and **1f-I** using stronger deprotection condition (eq 2). Substrate **1h** and **1i** were synthesized from **1g** through a three-step one-column procedure (eq 3). Substrate **1h** was synthesized from **1g** after TBS protection (eq 4).

Substrate **1k** was synthesized from **4** and **5** (commercial available) through substitution reaction followed by deprotection (eq 5). The ketal protected cyclobutanone **3** is a known compounds.<sup>9</sup>



The procedure for Mitsunobu reaction and deprotection cascade is as follows (using substrate **1a** as an example):

A solution of **3** (574.9 mg, 3.3 mmol, 1.1 equiv.) and DIAD (727.9 mg, 3.6 mmol, 1.2 equiv.) in THF (5 mL) was added to a solution of known compound **1a-I** (633.9 mg, 3 mmol, 1.0 equiv.) and triphenylphosphine (943.6 mg, 3.6 mmol, 1.2 equiv.) in THF (5 mL) at 0 °C. Then the reaction mixture was warmed up to room temperature and stirred overnight. After the reaction was finished, the solvent was removed by rotavap and the residue was dissolved in 6 mL THF, and then 2 mL 1M HCl was added to the solution. The resulting mixture was stirred at room temperature overnight. After the starting material was fully consumed, the reaction mixture was diluted with ethyl acetate and washed with water, saturated NaHCO<sub>3</sub> solution and brine successively. The organic phase was dried over magnesium sulfate, filtered and concentrated. The residue was purified by silica gel flash column chromatography (EtOAc/Hexane=1/10 to 1/5) to obtain the desired substrate **1a** (506 mg) as a colorless oil in 57% yield.

The procedure for synthesis of substrate **1g**:

A solution of **3** (514.5 mg, 2.95 mmol, 1.2 equiv.) and DIAD (552.5 mg, 2.73 mmol, 1.1 equiv.) in THF (5 mL) was added to a solution of known compound **1f-I** (735.0 mg, 2.47 mmol, 1.0 equiv.) and triphenylphosphine (715.7 mg, 2.73 mmol, 1.1 equiv.) in THF (5 mL) at 0 °C. Then the reaction mixture was warmed up to room temperature and stirred overnight. After the reaction was finished, the solvent was removed by rotavap and the residue was dissolved in 6 mL THF, then 2 mL 6M HCl was added to the solution. The resulting mixture was stirred at 50 °C for 2 h. After the starting material was fully consumed, the reaction mixture was diluted with ethyl acetate and washed with water, saturated NaHCO<sub>3</sub> solution and brine successively. The organic phase was dried over magnesium sulfate, filtered and concentrated. The residue was purified by silica gel flash column chromatography (EtOAc/Hexane=1/1 to 2/1) to obtain the desired substrate **1g** (627 mg) as a colorless oil in 76% yield over 2 steps.



The procedure for synthesis of substrate **1h**:

**1g** (185.0 mg, 0.55 mmol, 1.0 equiv.) was dissolved in EtOH (5 mL) before (EtO)<sub>3</sub>CH (274  $\mu$ L, 1.65 mmol, 3.0 equiv.) and *p*-TsOH (18.9 mg, 0.11 mmol, 0.2 equiv.) were added to the stirring solution. The reaction was stirred at room temperature overnight before quenched by saturated aqueous NaHCO<sub>3</sub> solution (20 mL) and the mixture was extracted with ethyl acetate (3 $\times$ 20 mL), washed with brine, and dried over Na<sub>2</sub>SO<sub>4</sub>. The crude product was dissolved in DMF (5 mL) and NaH (44 mg, 1.1 mmol, 2.0 equiv.) was added to the stirring solution. After the reaction mixture was stirred for 10 min, BnBr (67.1  $\mu$ L, 0.565 mmol, 1.02 equiv.) was added and the mixture was stirred at room temperature overnight before quenched by water. The resulting mixture was extracted with ethyl acetate (3 $\times$ 20 mL), washed with brine, and dried over Na<sub>2</sub>SO<sub>4</sub>. Then solvent was removed by rotavap and the residue was dissolved in 6 mL THF, then 2 mL 1M HCl was added to the solution. The resulting mixture was stirred at room temperature overnight. After the starting material was fully consumed, the reaction mixture was diluted with ethyl acetate and washed by water, saturated NaHCO<sub>3</sub> solution and brine successively. Then the organic phase was dried over magnesium sulfate, then filtered and concentrated. The residue was purified by silica gel flash column chromatography (EtOAc/Hexane=1/10 to 1/4) to obtain the desired substrate **1h** (154 mg) as a colorless oil in 66% yield over 3 steps.

The procedure for synthesis of substrate **1i**:

**1g** (143.0 mg, 0.43 mmol, 1.0 equiv.) was dissolved in EtOH (5 mL) before (EtO)<sub>3</sub>CH (213  $\mu$ L, 1.28 mmol, 3.0 equiv.) and *p*-TsOH (14.8 mg, 0.086 mmol, 0.2 equiv.) were added to the stirring solution. The reaction was stirred at room temperature overnight before quenched by saturated aqueous NaHCO<sub>3</sub> solution (20 mL) and the mixture was extracted with ethyl acetate (3 $\times$ 20 mL), washed with brine, and dried over Na<sub>2</sub>SO<sub>4</sub>. The crude product was dissolved in DCM (5 mL) and

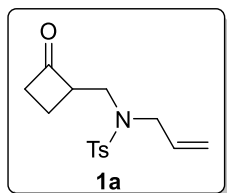
pyridine (104  $\mu$ L, 1.29 mmol, 3.0 equiv.) was added to the stirring solution. After the reaction mixture was stirred for 10 min, acetyl chloride (61  $\mu$ L, 0.86 mmol, 2.0 equiv.) was added and the mixture was stirred at room temperature overnight before quenched by water. The resulting mixture was extracted with ethyl acetate (3 $\times$ 20 mL), washed with brine, and dried over Na<sub>2</sub>SO<sub>4</sub>. Then solvent was removed by rotavap and the residue was dissolved in 6 mL THF, then 2 mL 1M HCl was added to the solution. The resulting mixture was stirred at room temperature overnight. After the starting material was fully consumed, the reaction mixture was diluted with ethyl acetate and washed by water, saturated NaHCO<sub>3</sub> solution and brine successively. Then the organic phase was dried over magnesium sulfate, then filtered and concentrated. The residue was purified by silica gel flash column chromatography (EtOAc/Hexane=1/10 to 1/2) to obtain the desired substrate **1i** (100 mg) as a colorless oil in 62% yield over 3 steps.

The procedure for synthesis of substrate **1j**:

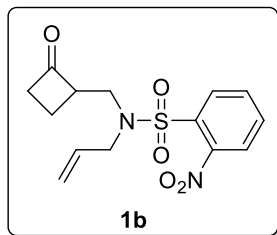
**1g** (167.7 mg, 0.5 mmol, 1.0 equiv.) and 4-DMAP (6.1 mg, 0.05 mmol, 0.1 equiv.) was dissolved in DCM (5 mL) before injected into a flame-dried Schlenk flask, and the flask was cooled to 0 °C and NEt<sub>3</sub> (210  $\mu$ L, 1.5 mmol, 3 equiv) was added into the stirring solution. Then TBSCl (113.0 mg, 0.75 mmol, 1.5 equiv.) was dissolved in DCM (3 mL) and added to the reaction mixture. The reaction was warmed to room temperature and stirred overnight before quenched by saturated aqueous NH<sub>4</sub>Cl solution (20 mL) and the mixture was extracted with ethyl acetate (3 $\times$ 20 mL), washed with brine, and dried over Na<sub>2</sub>SO<sub>4</sub>. After the solvent was removed, the residue was purified by silica gel flash column chromatography (EtOAc/Hexane=1/10 to 1/5) to obtain the desired substrate **1j** (106 mg) as a colorless oil in 47% yield.

The procedure for synthesis of substrate **1k**:

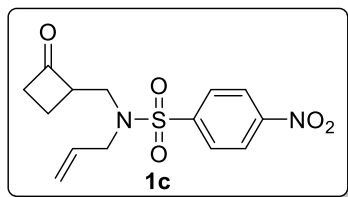
**4** (381.5 mg, 1.0 mmol, 1.0 equiv.) was dissolved in DMF (5 mL) and NaH (80 mg, 2.0 mmol, 2.0 equiv.) was added to the stirring solution. After the reaction mixture was stirred for 10 min, **5** (310  $\mu$ L, 3.0 mmol, 3.0 equiv.) was added and the mixture was stirred at room temperature overnight before quenched by water. The resulting mixture was extracted with ethyl acetate (3 $\times$ 20 mL), washed with brine, and dried over Na<sub>2</sub>SO<sub>4</sub>. Then solvent was removed by rotavap and the residue was dissolved in 6 mL THF, then 2 mL 1M HCl was added to the solution. The resulting mixture was stirred at room temperature overnight. After the starting material was fully consumed, the reaction mixture was diluted with ethyl acetate and washed by water, saturated NaHCO<sub>3</sub> solution and brine successively. Then the organic phase was dried over magnesium sulfate, then filtered and concentrated. The residue was purified by silica gel flash column chromatography (EtOAc/Hexane=1/10 to 1/5) to obtain the desired substrate **1k** (250 mg) as a colorless oil in 67% yield over 2 steps.



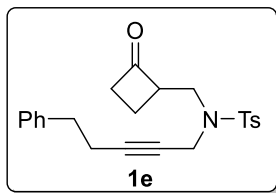
Compound **1a** was isolated as a colorless oil in 57% yield over 2 steps.  $R_f$  = 0.4 (EtOAc/Hexane=1/3). **<sup>1</sup>H NMR (400 MHz, CDCl<sub>3</sub>)**:  $\delta$  7.75 – 7.62 (m, 2H), 7.34 – 7.28 (m, 2H), 5.57 (ddt,  $J$  = 17.2, 10.1, 6.4 Hz, 1H), 5.28 – 5.05 (m, 2H), 3.91 – 3.73 (m, 2H), 3.67 – 3.52 (m, 1H), 3.43 (dd,  $J$  = 14.5, 8.6 Hz, 1H), 3.25 (dd,  $J$  = 14.5, 5.8 Hz, 1H), 3.06 (dddd,  $J$  = 17.8, 10.6, 8.2, 2.5 Hz, 1H), 2.93 (dddd,  $J$  = 17.7, 9.8, 5.1, 2.6 Hz, 1H), 2.43 (s, 3H), 2.21 (dtd,  $J$  = 11.5, 10.3, 5.1 Hz, 1H), 2.01 – 1.83 (m, 1H). **<sup>13</sup>C NMR (101 MHz, CDCl<sub>3</sub>)**: 208.76, 143.49, 136.56, 132.77, 129.77, 127.16, 119.32, 59.52, 51.22, 45.92, 44.75, 21.52, 15.72. **IR**:  $\nu$  2925, 1778, 1598, 1447, 1343, 1160, 1091, 934 cm<sup>-1</sup>; **HRMS** calcd. For [M+H]<sup>+</sup>: 294.1158 Found: 294.1163.



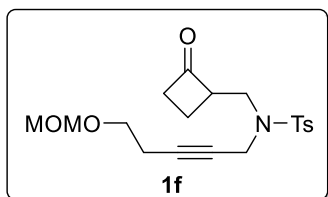
Compound **1b** was isolated as a colorless oil in 79% yield over 2 steps.  $R_f = 0.3$  (EtOAc/Hexane=1/2).  **$^1\text{H}$  NMR (400 MHz,  $\text{CDCl}_3$ )**:  $\delta$  8.08 – 8.01 (m, 1H), 7.76 – 7.62 (m, 3H), 5.64 (ddt,  $J = 17.2, 10.1, 6.3$  Hz, 1H), 5.39 – 5.01 (m, 2H), 4.08 – 3.91 (m, 2H), 3.71 – 3.42 (m, 3H), 3.07 (dddd,  $J = 17.7, 10.4, 8.2, 2.2$  Hz, 1H), 2.94 (dddd,  $J = 17.8, 9.8, 5.1, 2.4$  Hz, 1H), 2.22 (dddd,  $J = 11.5, 10.5, 9.7, 5.1$  Hz, 1H), 1.97 – 1.77 (m, 1H).  **$^{13}\text{C}$  NMR (101 MHz,  $\text{CDCl}_3$ )**:  $\delta$  208.22, 147.91, 133.63, 133.41, 132.17, 131.76, 131.03, 124.26, 119.77, 59.25, 50.40, 45.59, 44.82, 15.68. **IR**:  $\nu$  2926, 1778, 1545, 1373, 1163, 1084, 775  $\text{cm}^{-1}$ ; **HRMS** calcd. For  $[\text{M}+\text{Na}]^+$ : 347.0672 Found: 347.0684.



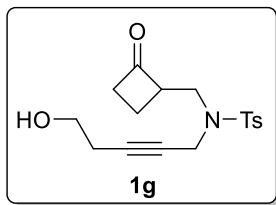
Compound **1c** was isolated as a white solid in 77% yield over 2 steps. Melting Point: 85-87  $^{\circ}\text{C}$ .  $R_f = 0.3$  (EtOAc/Hexane=1/2).  **$^1\text{H}$  NMR (400 MHz,  $\text{CDCl}_3$ )**:  $\delta$  8.40 – 8.30 (m, 2H), 8.07 – 7.92 (m, 2H), 5.55 (ddt,  $J = 16.6, 10.1, 6.3$  Hz, 1H), 5.32 – 5.07 (m, 2H), 4.00 – 3.84 (m, 2H), 3.67 – 3.54 (m, 1H), 3.49 (dd,  $J = 14.5, 7.9$  Hz, 1H), 3.34 (dd,  $J = 14.5, 6.2$  Hz, 1H), 3.10 (dddd,  $J = 17.9, 10.6, 8.3, 2.4$  Hz, 1H), 2.96 (dddd,  $J = 17.8, 9.7, 5.0, 2.6$  Hz, 1H), 2.34 – 2.18 (m, 1H), 2.05 – 1.74 (m, 1H).  **$^{13}\text{C}$  NMR (101 MHz,  $\text{CDCl}_3$ )**:  $\delta$  207.94, 150.03, 145.67, 131.73, 128.34, 124.45, 120.15, 59.21, 51.04, 45.89, 44.88, 15.66. **IR**:  $\nu$  2925, 1778, 1530, 1351, 1163, 1088, 772  $\text{cm}^{-1}$ ; **HRMS** calcd. For  $[\text{M}+\text{Na}]^+$ : 347.0672 Found: 347.0677.



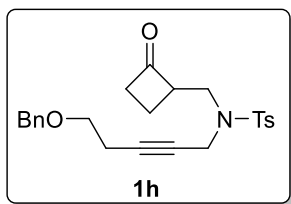
Compound **1e** was isolated as a light yellow solid in 58% yield over 2 steps. Melting Point: 98–100 °C.  $R_f$  = 0.4 (EtOAc/Hexane=1/3).  **$^1\text{H}$  NMR (400 MHz,  $\text{CDCl}_3$ )**:  $\delta$  7.72 – 7.65 (m, 2H), 7.30 – 7.23 (m, 4H), 7.23 – 7.17 (m, 1H), 7.11 – 7.02 (m, 2H), 4.15 (dtd,  $J$  = 18.4, 2.2, 0.8 Hz, 1H), 4.04 (dt,  $J$  = 18.4, 2.2 Hz, 1H), 3.61 – 3.48 (m, 1H), 3.44 – 3.24 (m, 2H), 3.07 (dddd,  $J$  = 17.8, 10.6, 8.2, 2.5 Hz, 1H), 2.94 (dddd,  $J$  = 17.7, 9.8, 5.1, 2.7 Hz, 1H), 2.54 (t,  $J$  = 7.4 Hz, 2H), 2.40 (s, 3H), 2.28 – 2.11 (m, 3H), 1.90 (ddt,  $J$  = 11.4, 9.7, 7.9 Hz, 1H).  **$^{13}\text{C}$  NMR (101 MHz,  $\text{CDCl}_3$ )**:  $\delta$  208.48, 143.44, 140.22, 135.73, 129.36, 128.37, 128.22, 127.83, 126.36, 85.66, 73.11, 59.02, 45.01, 37.79, 34.49, 21.52, 20.47, 15.47. **IR**:  $\nu$  2925, 1778, 1598, 1454, 1348, 1162, 1090, 750  $\text{cm}^{-1}$ ; **HRMS** calcd. For  $[\text{M}+\text{Na}]^+$ : 418.1447 Found: 418.1451.



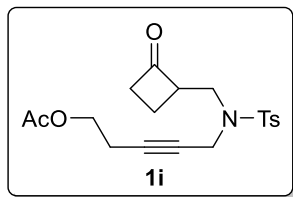
Compound **1f** was isolated as a colorless oil in 67% yield over 2 steps.  $R_f$  = 0.4 (EtOAc/Hexane=1/3).  **$^1\text{H}$  NMR (400 MHz,  $\text{CDCl}_3$ )**:  $\delta$  7.80 – 7.66 (m, 2H), 7.32 – 7.27 (m, 2H), 4.57 (s, 2H), 4.19 (dtd,  $J$  = 18.4, 2.2, 0.9 Hz, 1H), 4.09 – 4.00 (m, 1H), 3.68 – 3.54 (m, 1H), 3.44 (ddd,  $J$  = 14.0, 8.7, 0.9 Hz, 1H), 3.39 – 3.31 (m, 6H), 3.10 (dddd,  $J$  = 17.8, 10.6, 8.3, 2.5 Hz, 1H), 2.98 (dddd,  $J$  = 17.7, 9.8, 5.2, 2.6 Hz, 1H), 2.43 (s, 3H), 2.32 – 2.17 (m, 3H), 1.99 (ddt,  $J$  = 11.5, 9.7, 7.9 Hz, 1H).  **$^{13}\text{C}$  NMR (101 MHz,  $\text{CDCl}_3$ )**:  $\delta$  208.56, 143.54, 135.69, 129.40, 127.83, 96.33, 83.08, 73.54, 65.58, 59.00, 55.27, 45.11, 45.00, 37.79, 21.49, 19.93, 15.47. **IR**:  $\nu$  2925, 1778, 1598, 1443, 1348, 1162, 1028, 918  $\text{cm}^{-1}$ ; **HRMS** calcd. For  $[\text{M}+\text{H}]^+$ : 380.1526 Found: 380.1539.



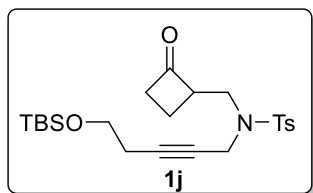
Compound **1g** was isolated as a colorless oil in 76% yield over 2 steps.  $R_f = 0.4$  (EtOAc/Hexane=2/1).  **$^1\text{H}$  NMR (400 MHz,  $\text{CDCl}_3$ )**:  $\delta$  7.76 – 7.67 (m, 2H), 7.36 – 7.28 (m, 2H), 4.18 (dtd,  $J = 18.4, 2.2, 0.9$  Hz, 1H), 4.13 – 3.99 (m, 1H), 3.70 – 3.55 (m, 1H), 3.53 – 3.43 (m, 3H), 3.37 (dd,  $J = 14.0, 5.9$  Hz, 1H), 3.11 (dddd,  $J = 17.9, 10.6, 8.2, 2.5$  Hz, 1H), 2.98 (dddd,  $J = 17.8, 9.8, 5.2, 2.6$  Hz, 1H), 2.43 (s, 3H), 2.32 – 2.15 (m, 3H), 1.99 (dtd,  $J = 11.5, 9.8, 8.0$  Hz, 1H), 1.65 (br, 1H).  **$^{13}\text{C}$  NMR (101 MHz,  $\text{CDCl}_3$ )**:  $\delta$  208.89, 143.77, 135.67, 129.46, 127.75, 83.24, 74.44, 60.68, 58.99, 45.10, 45.00, 37.76, 22.89, 21.51, 15.36. **IR**:  $\nu$  3531, 2925, 1777, 1598, 1346, 1161, 1090, 750  $\text{cm}^{-1}$ ; **HRMS** calcd. For  $[\text{M}+\text{H}]^+$ : 336.1264 Found: 336.1271.



Compound **1h** was isolated as a colorless oil in 66% yield over 3 steps.  $R_f = 0.4$  (EtOAc/Hexane=1/3).  **$^1\text{H}$  NMR (400 MHz,  $\text{CDCl}_3$ )**:  $\delta$  7.78 – 7.66 (m, 2H), 7.40 – 7.33 (m, 2H), 7.33 – 7.28 (m, 3H), 7.25 – 7.22 (m, 2H), 4.46 (s, 2H), 4.18 (dtd,  $J = 18.3, 2.3, 0.8$  Hz, 1H), 4.11 – 3.98 (m, 1H), 3.72 – 3.52 (m, 1H), 3.42 (ddd,  $J = 14.1, 8.6, 0.8$  Hz, 1H), 3.38 – 3.27 (m, 3H), 3.07 (dddd,  $J = 17.8, 10.6, 8.2, 2.5$  Hz, 1H), 2.95 (dddd,  $J = 17.8, 9.7, 5.2, 2.6$  Hz, 1H), 2.39 (s, 3H), 2.29 – 2.14 (m, 3H), 2.05 – 1.86 (m, 1H).  **$^{13}\text{C}$  NMR (101 MHz,  $\text{CDCl}_3$ )**:  $\delta$  208.58, 143.45, 137.86, 135.68, 129.37, 128.45, 127.82, 127.79, 127.64, 83.16, 73.51, 72.94, 67.99, 59.02, 45.15, 44.99, 37.84, 21.51, 19.86, 15.48. **IR**:  $\nu$  2923, 1777, 1597, 1453, 1348, 1161, 1092, 746  $\text{cm}^{-1}$ ; **HRMS** calcd. For  $[\text{M}+\text{H}]^+$ : 426.1734 Found: 426.1744.

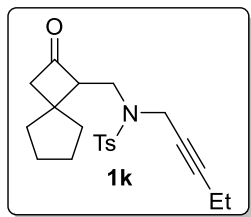


Compound **1i** was isolated as a colorless oil in 62% yield over 3 steps.  $R_f = 0.3$  (EtOAc/Hexane=1/3).  **$^1\text{H}$  NMR (400 MHz,  $\text{CDCl}_3$ )**:  $\delta$  7.86 – 7.59 (m, 2H), 7.35 – 7.28 (m, 2H), 4.20 (dtd,  $J = 18.4, 2.2, 0.9$  Hz, 1H), 4.06 (dtd,  $J = 18.5, 2.2, 0.6$  Hz, 1H), 3.93 – 3.79 (m, 2H), 3.72 – 3.55 (m, 1H), 3.44 (ddd,  $J = 14.0, 8.5, 0.9$  Hz, 1H), 3.34 (ddd,  $J = 14.0, 6.0, 0.6$  Hz, 1H), 3.11 (dddd,  $J = 17.9, 10.6, 8.2, 2.5$  Hz, 1H), 2.98 (dddd,  $J = 17.7, 9.8, 5.2, 2.6$  Hz, 1H), 2.43 (s, 3H), 2.34 – 2.17 (m, 3H), 2.03 (s, 3H), 2.02 – 1.92 (m, 1H).  **$^{13}\text{C}$  NMR (101 MHz,  $\text{CDCl}_3$ )**:  $\delta$  208.52, 170.59, 143.71, 135.65, 129.43, 127.78, 81.91, 74.12, 61.83, 58.99, 45.08, 45.01, 37.70, 21.49, 20.79, 18.88, 15.43. **IR**:  $\nu$  2925, 1778, 1739, 1597, 1348, 1240, 1162, 816  $\text{cm}^{-1}$ ; **HRMS** calcd. For  $[\text{M}+\text{Na}]^+$ : 400.1189 Found: 400.1186.



Compound **1j** was isolated as a colorless oil in 47% yield.  $R_f = 0.4$  (EtOAc/Hexane=1/4).  **$^1\text{H}$  NMR (400 MHz,  $\text{CDCl}_3$ )**:  $\delta$  7.82 – 7.63 (m, 2H), 7.32 – 7.27 (m, 2H), 4.32 – 4.14 (m, 1H), 4.05 (dt,  $J = 18.3, 2.2$  Hz, 1H), 3.69 – 3.56 (m, 1H), 3.51 – 3.40 (m, 3H), 3.34 (dd,  $J = 14.1, 6.0$  Hz, 1H), 3.10 (dddd,  $J = 17.8, 10.6, 8.2, 2.5$  Hz, 1H), 2.98 (dddd,  $J = 17.8, 9.7, 5.2, 2.6$  Hz, 1H), 2.42 (s, 3H), 2.24 (dtd,  $J = 11.5, 10.3, 5.2$  Hz, 1H), 2.11 (tt,  $J = 7.3, 2.2$  Hz, 2H), 1.98 (ddt,  $J = 11.5, 9.8, 8.0$  Hz, 1H), 0.87 (s, 9H), 0.04 (s, 6H).  **$^{13}\text{C}$  NMR (101 MHz,  $\text{CDCl}_3$ )**:  $\delta$  208.50, 143.46, 135.72, 129.35, 127.82, 83.31, 73.49, 61.45, 59.05, 45.09, 44.99, 37.81, 25.81, 22.84, 21.52, 18.23, 15.48,

-5.33. **IR:**  $\nu$  2929, 1780, 1598, 1350, 1163, 1095, 838  $\text{cm}^{-1}$ ; **HRMS** calcd. For  $[\text{M}+\text{Na}]^+$ : 472.1948 Found: 472.1956.



Compound **1k** was isolated as a white solid in 67% yield over 2 steps. Melting Point: 58-59 °C.  $R_f$  = 0.4 (EtOAc/Hexane=1/5).  **$^1\text{H}$  NMR (400 MHz,  $\text{CDCl}_3$ ):**  $\delta$  7.83 – 7.64 (m, 2H), 7.32 – 7.27 (m, 2H), 4.29 (dtd,  $J$  = 18.5, 2.3, 0.8 Hz, 1H), 4.01 (dt,  $J$  = 18.4, 2.2 Hz, 1H), 3.65 – 3.42 (m, 2H), 3.34 – 3.11 (m, 1H), 3.03 – 2.83 (m, 1H), 2.69 (dd,  $J$  = 16.8, 1.7 Hz, 1H), 2.42 (s, 3H), 2.05 – 1.62 (m, 9H), 1.51 (dddd,  $J$  = 12.5, 7.6, 3.4, 1.3 Hz, 1H), 0.86 (t,  $J$  = 7.5 Hz, 3H).  **$^{13}\text{C}$  NMR (101 MHz,  $\text{CDCl}_3$ ):**  $\delta$  207.03, 143.44, 135.33, 129.34, 127.93, 88.04, 71.36, 62.29, 57.86, 42.28, 40.66, 39.72, 37.27, 32.21, 23.92, 23.84, 21.49, 13.40, 12.08. **IR:**  $\nu$  2940, 1775, 1598, 1451, 1349, 1162, 906  $\text{cm}^{-1}$ ; **HRMS** calcd. For  $[\text{M}+\text{Na}]^+$ : 396.1604 Found: 396.1603.

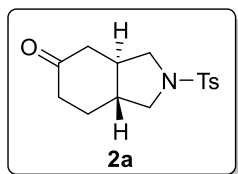
#### 5.4.3 Rh-catalyzed kinetic resolutions between cyclobutanones and alkynes

##### General procedure:

In a nitrogen-filled glove box, a 4 mL vial was charged with the cyclobutanone substrates (0.1 mmol),  $[\text{Rh}(\text{CH}_2=\text{CH}_2)_2\text{Cl}]_2$  (1.9 mg, 0.005 mmol, 5 mol%), (*R*)-DTBM-segphos (11.8 mg, 0.01 mmol, 10 mol%) and  $\text{AgSbF}_6$  (3.4 mg, 0.01 mmol, 10 mol%), followed by 1000  $\mu\text{L}$  1,4-dioxane. After a homogeneous solution was formed, the vial was capped and the reaction was maintained at room temperature (**1a** to **1j**) and 40 °C (**1k**) for 12-13 h. After the reaction was complete, solvent was removed by rotavap and the residue was directly purified by silica gel flash chromatography.



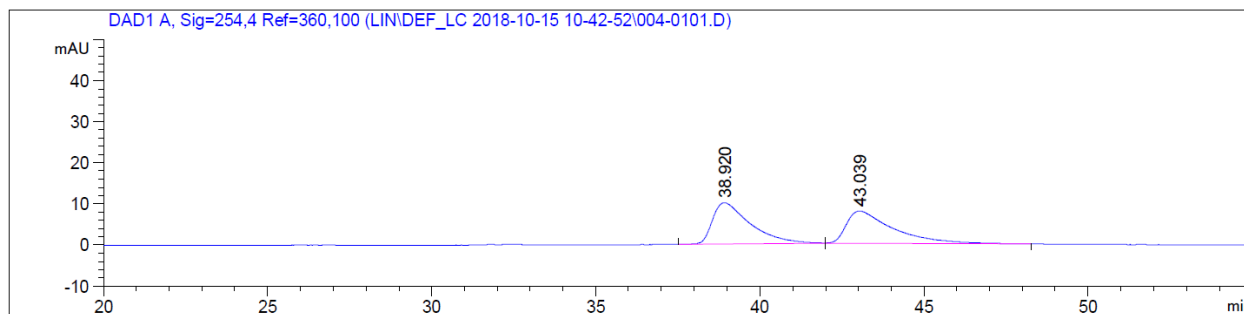
Both **2a** to **2k** and recycled **1a** to **1k** were collected and measured the yield. The H-NMR spectrum of recycled **1a** to **1k** are identical with the original spectrum. The HPLC data and optical rotation data was collected and shown in following session.



**2a** (13.5 mg) was isolated as a white solid in 46% yield. Melting Point: 186-188 °C.  $R_f = 0.2$  (EtOAc/Hexane=1/3).  **$^1\text{H}$  NMR (400 MHz,  $\text{CDCl}_3$ )**:  $\delta$  7.81 – 7.68 (m, 2H), 7.39 – 7.30 (m, 2H), 3.68 (dd,  $J = 9.6, 7.1$  Hz, 1H), 3.59 (dd,  $J = 9.7, 7.0$  Hz, 1H), 2.96 (dd,  $J = 10.7, 9.7$  Hz, 1H), 2.86 (dd,  $J = 10.7, 9.6$  Hz, 1H), 2.53 (ddd,  $J = 14.3, 4.0, 1.9$  Hz, 1H), 2.48 – 2.40 (m, 4H), 2.26 (dddd,  $J = 15.4, 13.1, 6.7, 0.9$  Hz, 1H), 2.19 – 2.07 (m, 2H), 1.96 – 1.84 (m, 1H), 1.81 – 1.68 (m, 1H), 1.44 (tdd,  $J = 14.7, 12.7, 5.7$  Hz, 1H).  **$^{13}\text{C}$  NMR (101 MHz,  $\text{CDCl}_3$ )**:  $\delta$  208.27, 143.56, 134.35, 129.80, 127.28, 52.61, 51.90, 44.17, 43.88, 42.75, 39.81, 26.47, 21.55. **IR**:  $\nu$  2937, 1705, 1598, 1343, 1160, 1027, 816  $\text{cm}^{-1}$ ; **HRMS** calcd. For  $[\text{M}+\text{Na}]^+$ : 316.0978. Found: 316.0977.

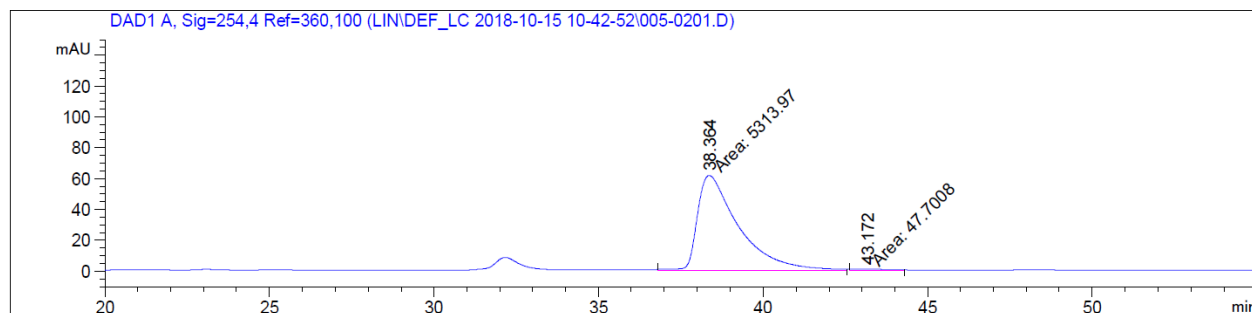
Chiral HPLC for **2a** (Chiralpak IA, hexane:isopropanol = 90:10, 1 mL/min, 254 nm),  $t_{\text{minor}} = 43.2$  min,  $t_{\text{major}} = 38.4$  min.  $[\alpha]_D^{22.6} = 72.6$  ( $c = 1.79$ ,  $\text{CH}_2\text{Cl}_2$ ) at 98 % ee.

### Racemic Sample 2a



Peak #	RetTime [min]	Type	Width [min]	Area [mAU*s]	Height [mAU]	Area %
1	38.920	BB	1.1182	794.42914	10.00704	50.8163
2	43.039	BB	1.3591	768.90729	7.80643	49.1837

### **Enantiomeric Sample 2a**



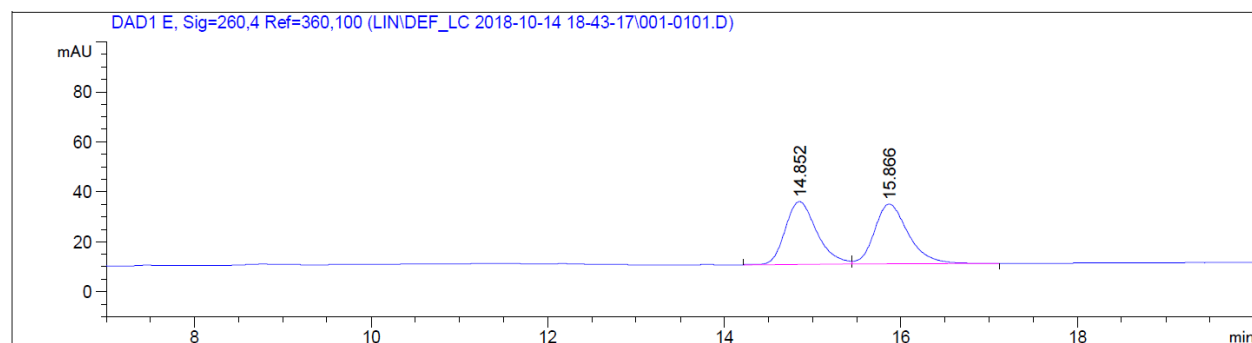
Peak #	RetTime [min]	Type	Width [min]	Area [mAU*s]	Height [mAU]	Area %
1	38.364	MM	1.4433	5313.96729	61.36508	99.1103
2	43.172	MM	1.2534	47.70079	6.34297e-1	0.8897

**1a** (13.8 mg) was recycled as a colorless oil in 47% yield.

Chiral HPLC for **1a** (Chiralpak IA, hexane:isopropanol = 90:10, 1 mL/min, 260 nm),  $t_{\text{minor}} = 15.0$

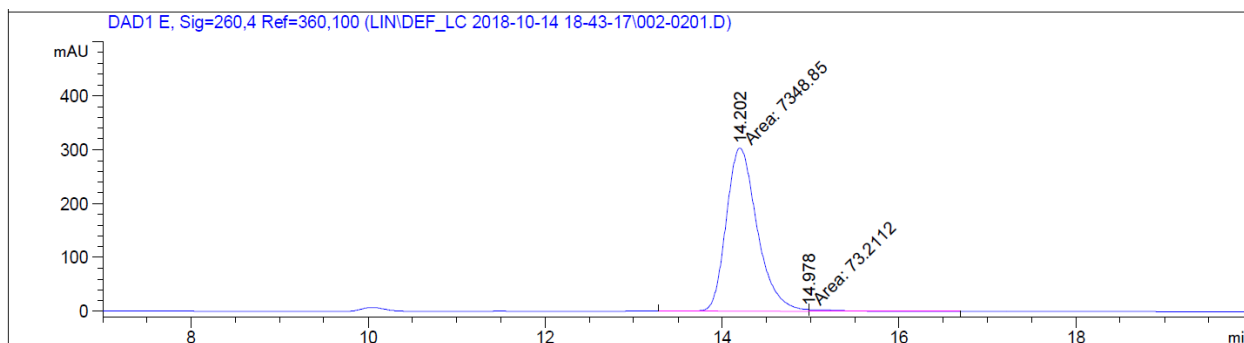
min,  $t_{\text{major}} = 14.2$  min.  $[\alpha]_{\text{D}}^{22.6} = -30.4$  ( $c = 1.38$ ,  $\text{CH}_2\text{Cl}_2$ ) at 98 % ee.

### **Racemic Sample 1a**

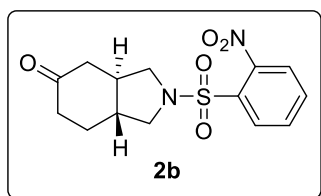


Peak #	RetTime [min]	Type	Width [min]	Area [mAU*s]	Height [mAU]	Area %
1	14.852	BV	0.3820	626.01959	25.18777	49.4295
2	15.866	VB	0.4058	640.47095	23.96771	50.5705

### Enantiomeric Sample 1a



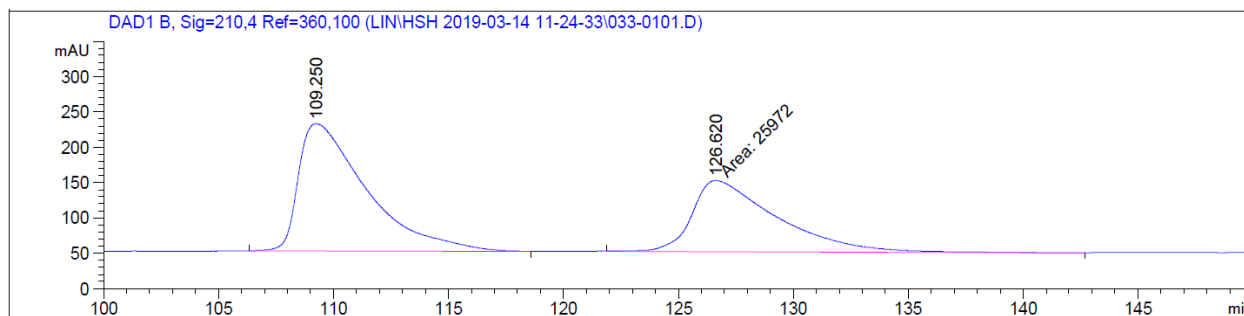
Peak #	RetTime [min]	Type	Width [min]	Area [mAU*s]	Height [mAU]	Area %
1	14.202	MF	0.4050	7348.84521	302.39944	99.0136
2	14.978	FM	0.3892	73.21117	3.13483	0.9864



**2b** (14.3 mg) was isolated as a light yellow solid in 44% yield. Melting Point: 187-189 °C.  $R_f$  = 0.3 (EtOAc/Hexane=1/1).  **$^1\text{H}$  NMR (400 MHz,  $\text{CDCl}_3$ )**:  $\delta$  8.14 – 7.99 (m, 1H), 7.76 – 7.67 (m, 2H), 7.66 – 7.61 (m, 1H), 3.81 (dd,  $J$  = 9.3, 6.8 Hz, 1H), 3.73 (dd,  $J$  = 9.3, 6.7 Hz, 1H), 3.17 – 3.01 (m, 2H), 2.61 (ddd,  $J$  = 14.2, 3.8, 1.9 Hz, 1H), 2.51 (ddt,  $J$  = 15.5, 4.9, 1.9 Hz, 1H), 2.34 (dddd,  $J$  = 15.5, 13.1, 6.6, 0.9 Hz, 1H), 2.27 – 1.97 (m, 4H), 1.63 – 1.49 (m, 1H).  **$^{13}\text{C}$  NMR (101 MHz,  $\text{CDCl}_3$ )**:  $\delta$  208.06, 133.57, 132.46, 131.62, 130.84, 124.01, 52.56, 51.96, 44.40, 43.81, 42.97, 39.81, 26.39. **IR**:  $\nu$  2925, 1714, 1544, 1373, 1349, 1164, 779  $\text{cm}^{-1}$ ; **HRMS** calcd. For  $[\text{M}+\text{Na}]^+$ : 347.0672. Found: 347.0675.

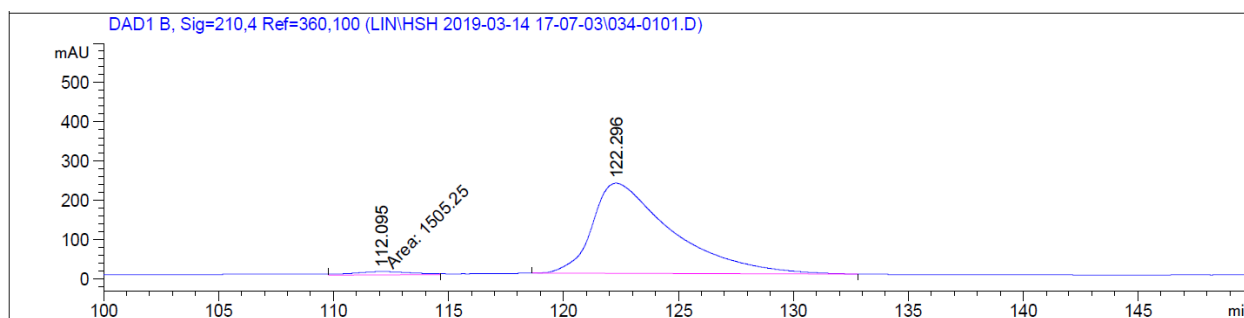
Chiral HPLC for **2b** (Chiralpak ID, hexane:isopropanol = 75:25, 1 mL/min, 210 nm),  $t_{\text{minor}} = 112.1$  min,  $t_{\text{major}} = 122.3$  min.  $[\alpha]_{\text{D}}^{22.6} = -278.2$  ( $c = 0.87$ ,  $\text{CH}_2\text{Cl}_2$ ) at 95 % ee.

### Racemic Sample 2b



Peak #	RetTime [min]	Type	Width [min]	Area [mAU*s]	Height [mAU]	Area %
1	109.250	BB	2.7723	3.69506e4	180.19525	58.7239
2	126.620	MM	4.2934	2.59720e4	100.82098	41.2761

### Enantiomeric Sample 2b

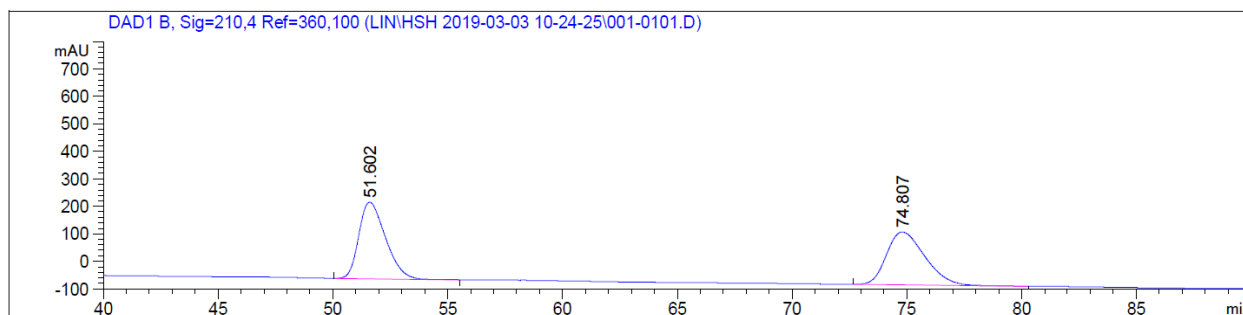


Peak #	RetTime [min]	Type	Width [min]	Area [mAU*s]	Height [mAU]	Area %
1	112.095	MM	2.9839	1505.25464	8.40771	2.6500
2	122.296	BB	3.2182	5.52972e4	229.56522	97.3500

**1b** (15.2 mg) was recycled as a colorless oil in 47% yield.

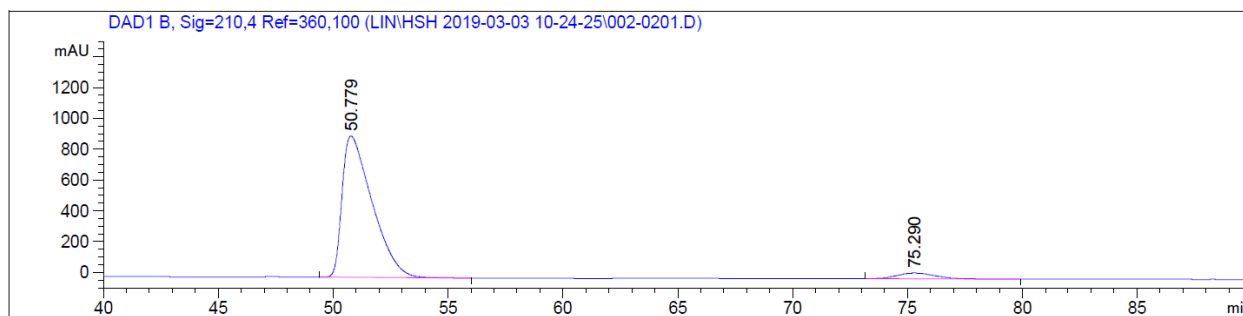
Chiral HPLC for **1b** (Chiralpak IC, hexane:isopropanol = 80:20, 1 mL/min, 210 nm),  $t_{\text{minor}} = 75.3$  min,  $t_{\text{major}} = 50.8$  min.  $[\alpha]_{\text{D}}^{22.6} = -11.4$  ( $c = 0.35$ ,  $\text{CH}_2\text{Cl}_2$ ) at 90 % ee.

### Racemic Sample 1b

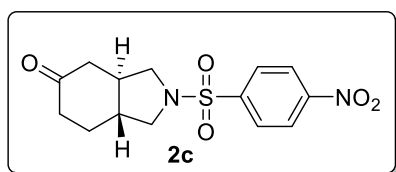


Peak #	RetTime [min]	Type	Width [min]	Area [mAU*s]	Height [mAU]	Area %
1	51.602	BB	1.2512	2.24296e4	278.62781	50.0578
2	74.807	BB	1.7533	2.23778e4	192.91267	49.9422

### Enantiomeric Sample 1b



Peak #	RetTime [min]	Type	Width [min]	Area [mAU*s]	Height [mAU]	Area %
1	50.779	BB	1.3107	8.34725e4	918.11938	95.1164
2	75.290	BB	1.5053	4285.75098	36.89252	4.8836

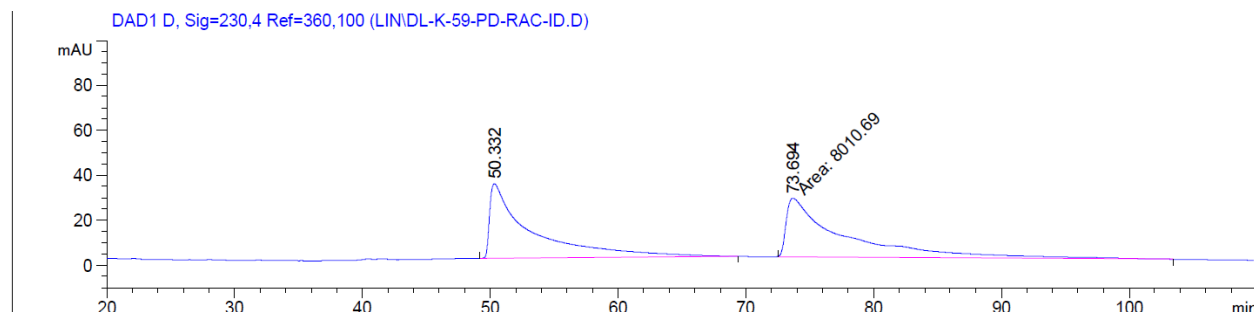


**2c** (16.2 mg) was isolated as a white solid in 50% yield. Melting Point: 210 °C (decomposed).  $R_f$  = 0.3 (EtOAc/Hexane=1/1). **<sup>1</sup>H NMR (400 MHz, DMSO-*d*<sub>6</sub>)**: δ 8.46 – 8.40 (m, 2H), 8.19 – 8.04 (m, 2H), 3.62 (dd,  $J$  = 9.5, 7.0 Hz, 1H), 3.55 (dd,  $J$  = 9.4, 6.8 Hz, 1H), 2.90 (dd,  $J$  = 10.6, 9.5 Hz, 1H), 2.83 (dd,  $J$  = 10.7, 9.5 Hz, 1H), 2.36 – 2.22 (m, 3H), 2.18 (ddt,  $J$  = 15.3, 4.9, 1.8 Hz, 1H), 2.04 – 1.70 (m, 3H), 1.53 – 1.32 (m, 1H). **<sup>13</sup>C NMR (101 MHz, DMSO-*d*<sub>6</sub>)**: δ 209.05, 150.35, 2.04 – 1.70 (m, 3H), 1.53 – 1.32 (m, 1H).

142.75, 129.14, 125.21, 52.90, 52.27, 43.59, 43.42, 41.94, 39.71, 25.94. **IR:**  $\nu$  2923, 1704, 1528, 1461, 1347, 1161, 855  $\text{cm}^{-1}$ ; **HRMS** calcd. For  $[\text{M}+\text{H}]^+$ : 325.0853. Found: 325.0852.

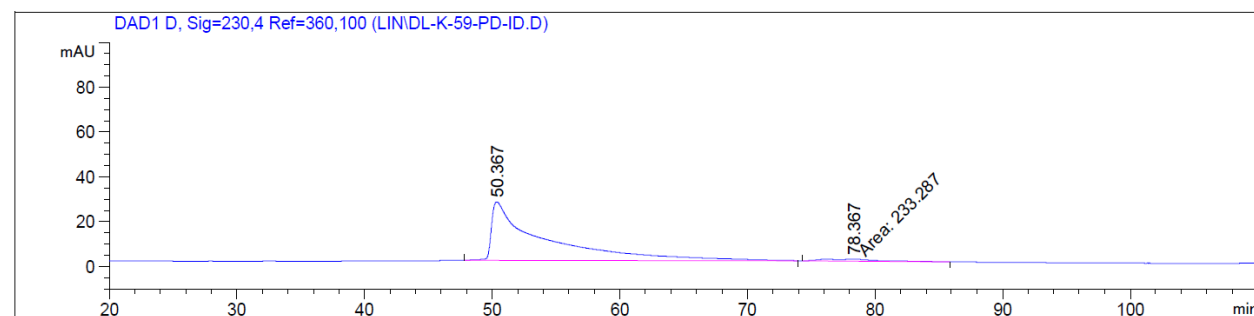
Chiral HPLC of **2c** (Chiralpak ID, hexane:isopropanol = 75:25, 1 mL/min, 230 nm),  $t_{\text{minor}} = 78.4$  min,  $t_{\text{major}} = 50.4$  min.  $[\alpha]_{\text{D}}^{22.6} = -33.3$  ( $c = 0.75$ ,  $\text{CH}_2\text{Cl}_2$ ) at 94 % ee.

### Racemic Sample 2c



Peak #	RetTime [min]	Type	Width [min]	Area [mAU*s]	Height [mAU]	Area %
1	50.332	BB	2.8479	7471.58105	33.12019	48.2589
2	73.694	MM	5.1135	8010.69189	26.10973	51.7411

### Enantiomeric Sample 2c

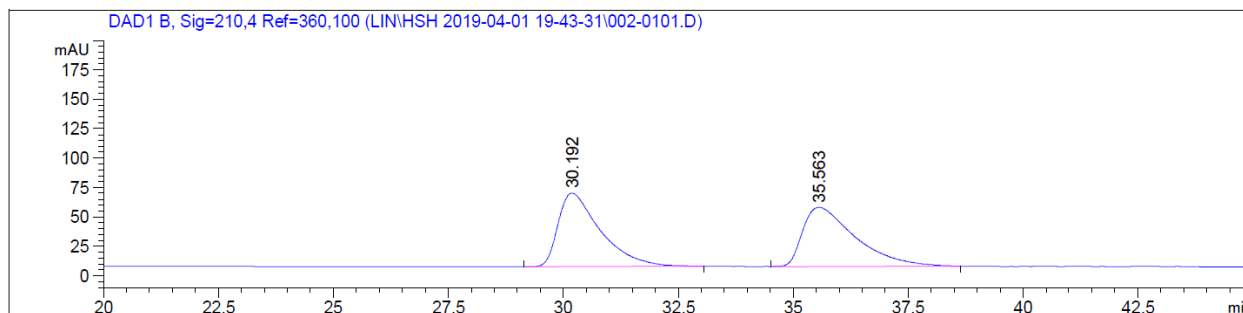


Peak #	RetTime [min]	Type	Width [min]	Area [mAU*s]	Height [mAU]	Area %
1	50.367	BB	3.4522	7271.30029	26.08440	96.8914
2	78.367	MM	4.6921	233.28732	8.28652e-1	3.1086

**1c** (13.6 mg) was recycled as a white solid in 42% yield.

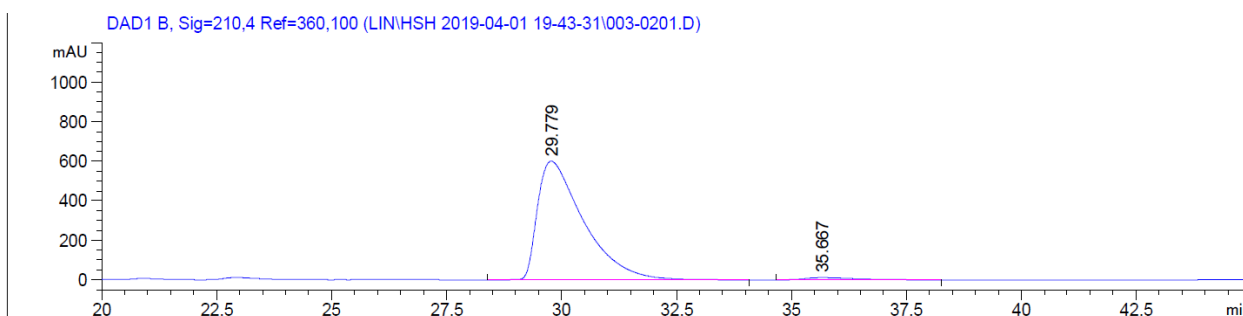
Chiral HPLC for **1c** (Chiralpak IA, hexane:isopropanol = 90:10, 1 mL/min, 210 nm),  $t_{\text{minor}} = 35.7$  min,  $t_{\text{major}} = 29.8$  min.  $[\alpha]_{\text{D}}^{22.6} = -82.4$  ( $c = 0.74$ ,  $\text{CH}_2\text{Cl}_2$ ) at 96 % ee.

### Racemic Sample 1c

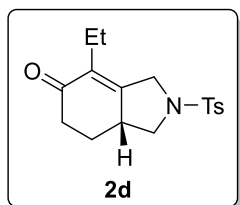


Peak #	RetTime [min]	Type	Width [min]	Area [mAU*s]	Height [mAU]	Area %
1	30.192	BB	0.9501	4013.14819	62.58150	50.2500
2	35.563	BB	1.1437	3973.21191	50.18191	49.7500

### Enantiomeric Sample 1c



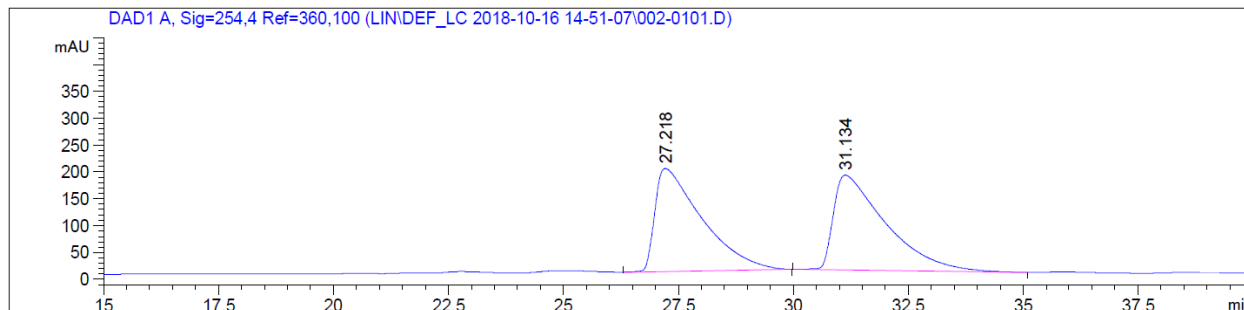
Peak #	RetTime [min]	Type	Width [min]	Area [mAU*s]	Height [mAU]	Area %
1	29.779	BB	1.0360	4.17410e4	599.75763	97.9710
2	35.667	BB	1.0209	864.47595	11.74302	2.0290



**2d** (15.2 mg) was isolated as a colorless oil in 48% yield. The characterization data of **2d** is identical as the reported data.<sup>3</sup> The HPLC data of **1d** and **2d** is shown below.

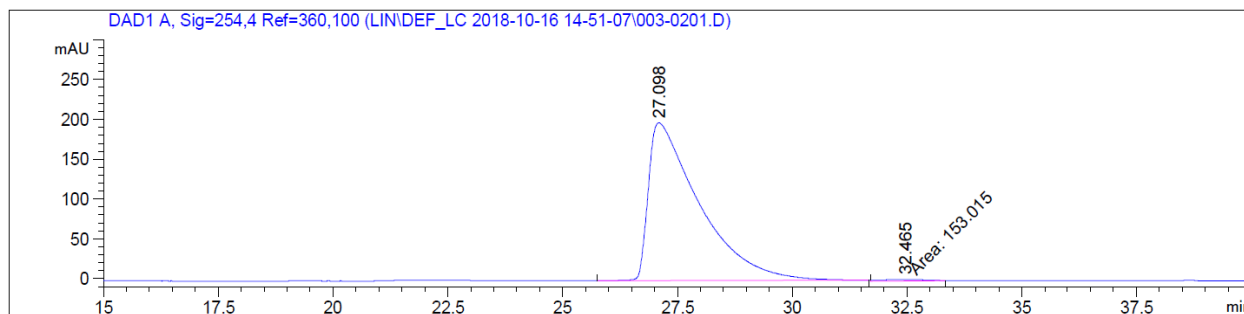
Chiral HPLC of **2d** (Chiralpak IB, hexane:isopropanol = 92:8, 1 mL/min, 254 nm),  $t_{\text{minor}} = 32.5$  min,  $t_{\text{major}} = 27.1$  min.  $[\alpha]_{\text{D}}^{22.6} = -205.0$  ( $c = 1.00$ ,  $\text{CH}_2\text{Cl}_2$ ) at 98 % ee.

### **Racemic Sample 2d**



Peak #	RetTime [min]	Type	Width [min]	Area [mAU*s]	Height [mAU]	Area %
1	27.218	BB	0.9983	1.35299e4	191.49348	49.2997
2	31.134	BB	1.1400	1.39142e4	176.07523	50.7003

### **Enantiomeric Sample 2d**



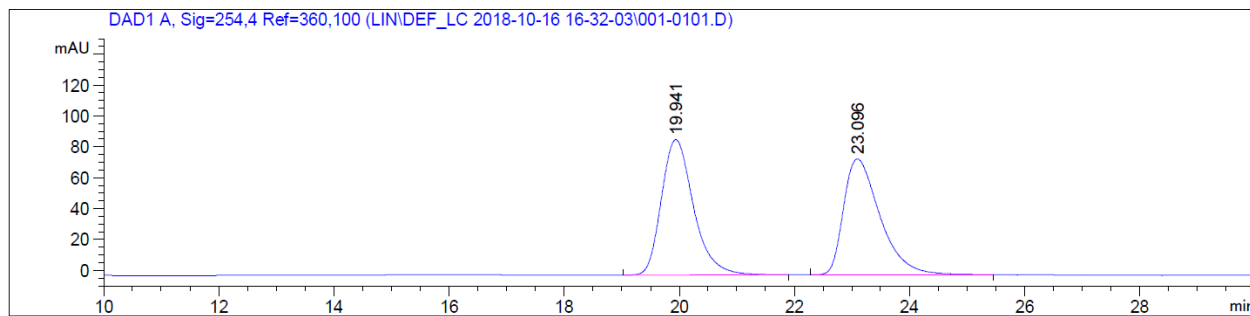
Peak #	RetTime [min]	Type	Width [min]	Area [mAU*s]	Height [mAU]	Area %
1	27.098	BB	1.0934	1.52927e4	197.93497	99.0093
2	32.465	MM	0.8101	153.01463	2.24809	0.9907

**1d** (12.6 mg) was recycled as a colorless oil in 40% yield.



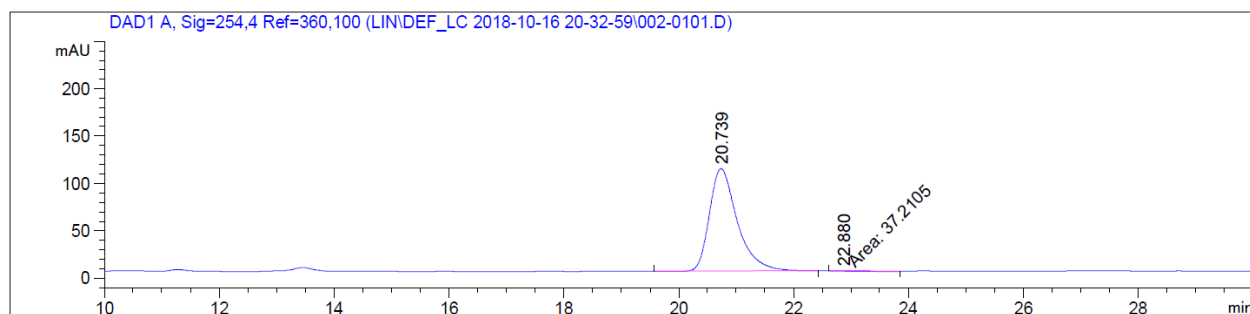
Chiral HPLC for **1d** (Chiralpak IA, hexane:isopropanol = 95:5, 1 mL/min, 254 nm),  $t_{\text{minor}} = 22.9$  min,  $t_{\text{major}} = 20.7$  min.  $[\alpha]_{\text{D}}^{22.6} = -12.7$  ( $c = 0.79$ ,  $\text{CH}_2\text{Cl}_2$ ) at 98 % ee.

### Racemic Sample 1d

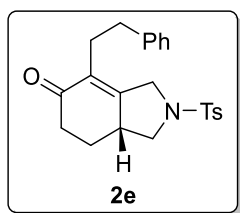


Peak #	RetTime [min]	Type	Width [min]	Area [mAU*s]	Height [mAU]	Area %
1	19.941	BB	0.5996	3409.07446	87.68116	50.8446
2	23.096	BB	0.6652	3295.82153	74.92858	49.1554

### Enantiomeric Sample 1d

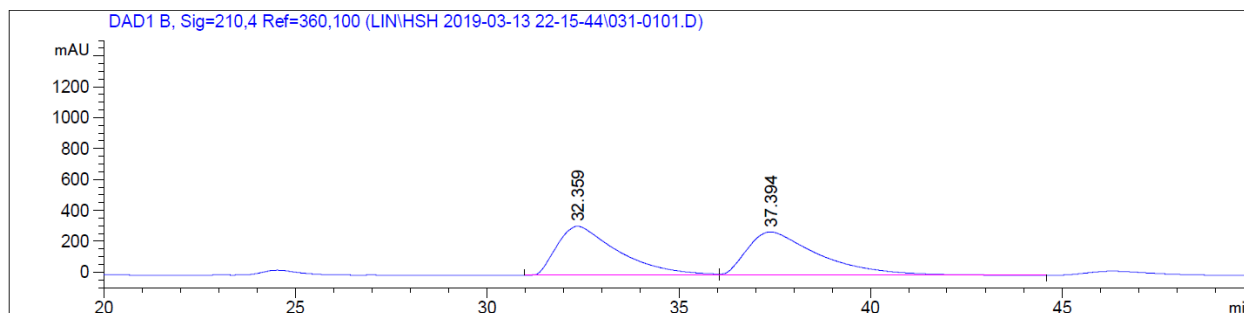


Peak #	RetTime [min]	Type	Width [min]	Area [mAU*s]	Height [mAU]	Area %
1	20.739	BB	0.5111	3663.22852	108.16530	98.9944
2	22.880	MM	0.8522	37.21054	7.27732e-1	1.0056



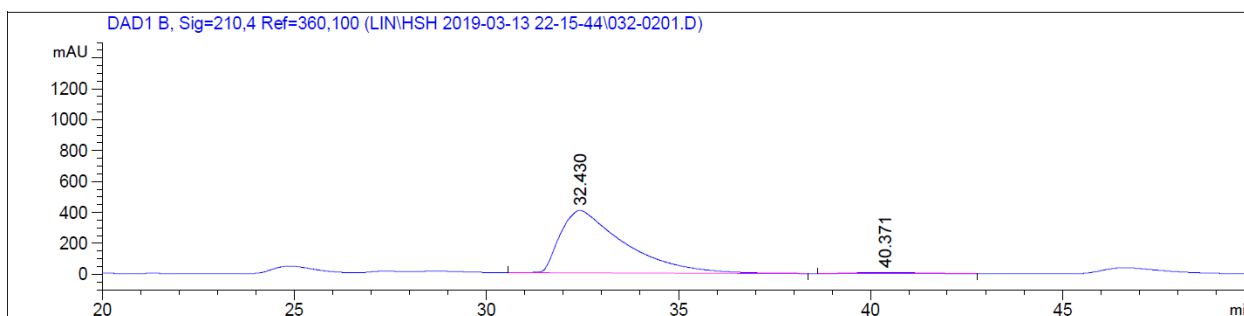
**2e** (16.6 mg) was isolated as a colorless oil in 42% yield.  $R_f = 0.3$  (EtOAc/Hexane=1/4).  $^1\text{H}$  NMR (400 MHz,  $\text{CDCl}_3$ ):  $\delta$  7.79 – 7.60 (m, 2H), 7.41 – 7.32 (m, 2H), 7.24 – 7.17 (m, 2H), 7.15 – 7.01 (m, 3H), 3.90 – 3.72 (m, 2H), 3.45 (dd,  $J = 17.0, 2.4$  Hz, 1H), 2.92 – 2.77 (m, 1H), 2.72 – 2.54 (m, 2H), 2.55 – 2.39 (m, 6H), 2.36 – 2.24 (m, 2H), 2.10 (dtd,  $J = 12.3, 4.8, 2.4$  Hz, 1H), 1.58 – 1.45 (m, 1H).  $^{13}\text{C}$  NMR (101 MHz,  $\text{CDCl}_3$ ):  $\delta$  197.00, 158.41, 143.95, 141.24, 132.81, 131.89, 129.87, 128.59, 128.22, 127.67, 126.09, 53.19, 50.13, 40.63, 36.77, 34.16, 28.88, 26.41, 21.60. IR:  $\nu$  2925, 1666, 1453, 1346, 1164, 1094, 816  $\text{cm}^{-1}$ ; HRMS calcd. For  $[\text{M}+\text{H}]^+$ : 396.1628. Found: 396.1627. Chiral HPLC of **2e** (Chiralpak IB, hexane:isopropanol = 92:8, 1 mL/min, 210 nm),  $t_{\text{minor}} = 40.4$  min,  $t_{\text{major}} = 32.4$  min.  $[\alpha]_D^{22.6} = -115.7$  ( $c = 1.59$ ,  $\text{CH}_2\text{Cl}_2$ ) at 96 % ee.

### Racemic Sample 2e



Peak #	RetTime [min]	Type	Width [min]	Area [mAU*s]	Height [mAU]	Area %
1	32.359	BV	1.6295	3.49792e4	316.47583	49.1240
2	37.394	VB	1.8760	3.62267e4	279.89749	50.8760

### Enantiomeric Sample 2e

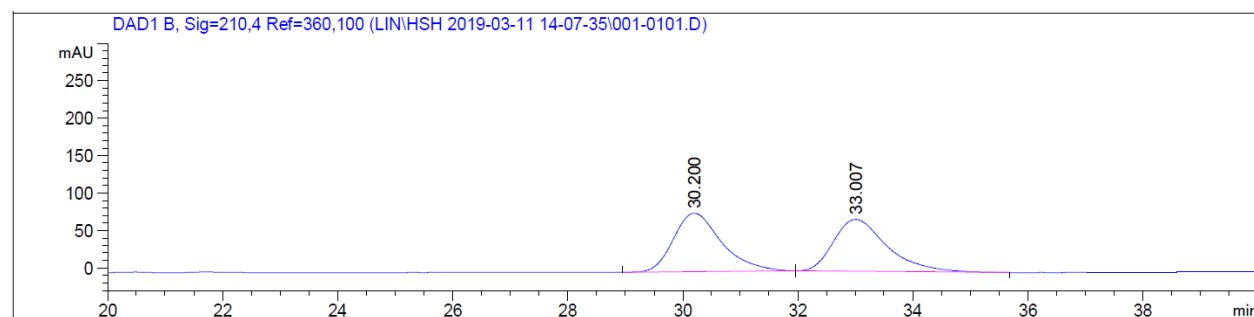


Peak #	RetTime [min]	Type	Width [min]	Area [mAU*s]	Height [mAU]	Area %
1	32.430	BB	1.6659	4.66369e4	404.27081	98.1967
2	40.371	BB	1.3748	856.43756	7.63441	1.8033

**1e** (17.7 mg) was recycled as a colorless oil in 45% yield.

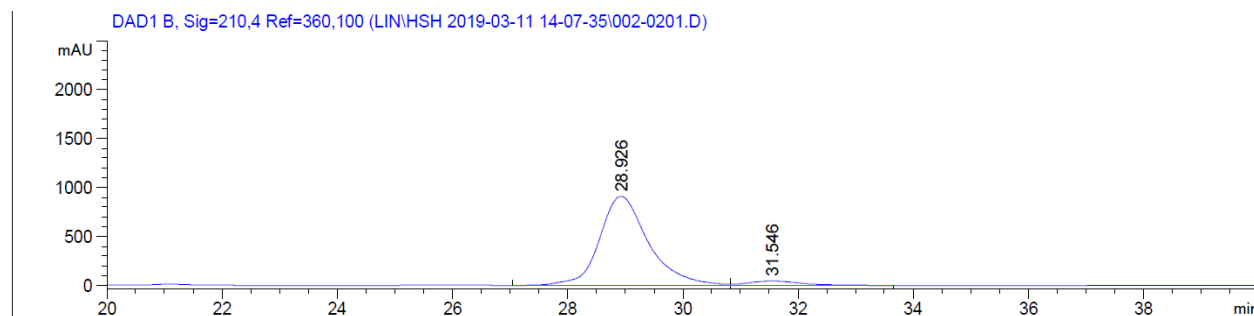
Chiral HPLC for **1e** (Chiralpak IA, hexane:isopropanol = 95:5, 1 mL/min, 210 nm),  $t_{\text{minor}} = 31.5$  min,  $t_{\text{major}} = 28.9$  min.  $[\alpha]_{\text{D}}^{22.6} = -109.6$  (c = 1.35, CH<sub>2</sub>Cl<sub>2</sub>) at 90 % ee.

### Racemic Sample 1e

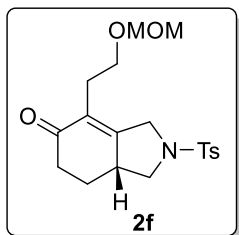


Peak #	RetTime [min]	Type	Width [min]	Area [mAU*s]	Height [mAU]	Area %
1	30.200	BB	0.8791	4529.69287	78.05059	50.2543
2	33.007	BB	0.9803	4483.84424	69.35200	49.7457

### Enantiomeric Sample 1e



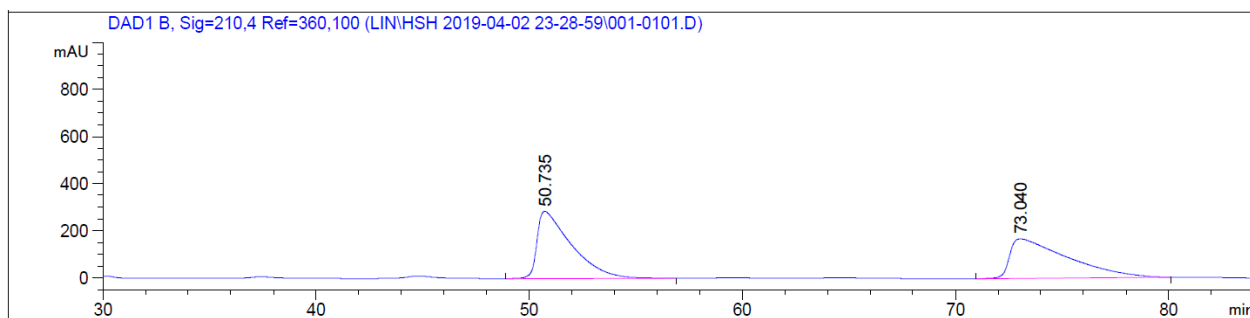
Peak #	RetTime [min]	Type	Width [min]	Area [mAU*s]	Height [mAU]	Area %
1	28.926	BV	0.8862	5.36689e4	909.85333	94.8979
2	31.546	VB	0.9372	2885.44653	45.91332	5.1021



**2f** (18.2 mg) was isolated as a colorless oil in 48% yield.  $R_f = 0.3$  (EtOAc/Hexane=1/2).  **$^1\text{H}$  NMR** (400 MHz,  $\text{CDCl}_3$ ):  $\delta$  7.76 – 7.69 (m, 2H), 7.42 – 7.33 (m, 2H), 4.48 – 4.42 (m, 2H), 4.40 – 4.31 (m, 1H), 4.02 – 3.83 (m, 2H), 3.57 – 3.43 (m, 2H), 3.22 (s, 3H), 3.09 – 2.90 (m, 1H), 2.57 (dd,  $J = 10.9, 9.3$  Hz, 1H), 2.54 – 2.40 (m, 5H), 2.38 – 2.25 (m, 2H), 2.15 (dtd,  $J = 12.3, 4.8, 2.4$  Hz, 1H), 1.55 (dddd,  $J = 14.6, 12.7, 11.6, 4.4$  Hz, 1H).  **$^{13}\text{C}$  NMR** (101 MHz,  $\text{CDCl}_3$ ):  $\delta$  196.88, 159.93, 144.02, 132.44, 129.92, 129.84, 127.81, 96.14, 66.05, 55.01, 53.51, 50.82, 40.74, 36.60, 27.01, 26.46, 21.57. **IR**:  $\nu$  2923, 1666, 1468, 1346, 1164, 1041, 816  $\text{cm}^{-1}$ ; **HRMS** calcd. For  $[\text{M}+\text{H}]^+$ : 380.1526. Found: 380.1516.

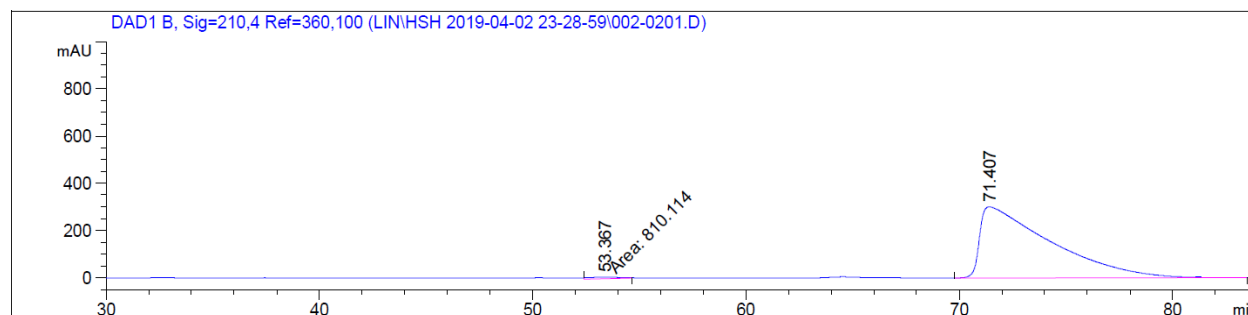
Chiral HPLC of **2f** (Chiralpak IF, hexane:isopropanol = 85:15, 1 mL/min, 210 nm),  $t_{\text{minor}} = 53.4$  min,  $t_{\text{major}} = 71.4$  min.  $[\alpha]_D^{22.6} = -461.1$  ( $c = 0.95$ ,  $\text{CH}_2\text{Cl}_2$ ) 98 % ee.

### Racemic Sample 2f



Peak #	RetTime [min]	Type	Width [min]	Area [mAU*s]	Height [mAU]	Area %
1	50.735	BB	1.5793	3.20088e4	285.22900	50.4156
2	73.040	BB	2.4590	3.14812e4	167.47899	49.5844

### Enantiomeric Sample 2f

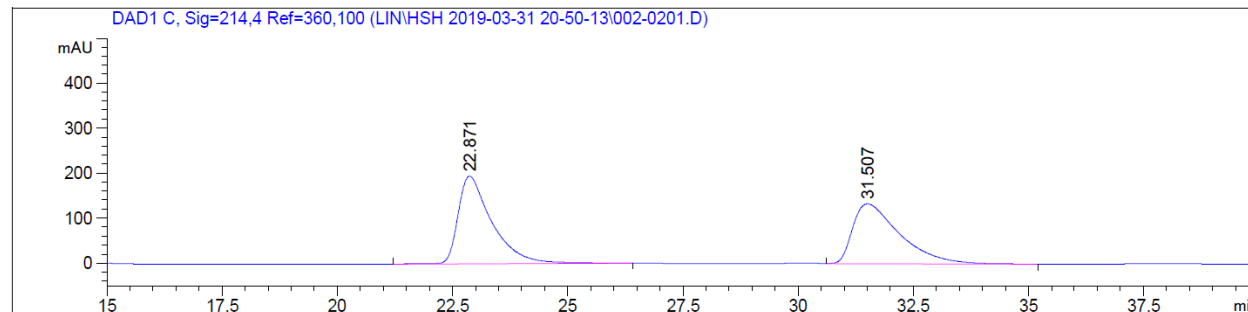


Peak #	RetTime [min]	Type	Width [min]	Area [mAU*s]	Height [mAU]	Area %
1	53.367	MM	1.1920	810.11365	8.17228	1.1493
2	71.407	BB	2.9724	6.96760e4	301.02255	98.8507

**1f** (19.0 mg) was recycled as a colorless oil in 50% yield.

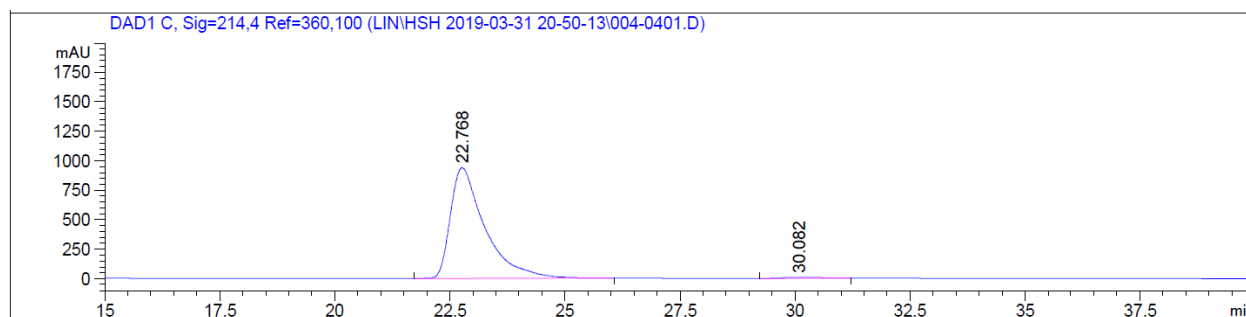
Chiral HPLC for **1f** (Chiralpak IA, hexane:isopropanol = 92:8, 1 mL/min, 214 nm),  $t_{\text{minor}} = 30.1$  min,  $t_{\text{major}} = 22.8$  min.  $[\alpha]_{\text{D}}^{22.6} = -22.7$  ( $c = 2.42$ ,  $\text{CH}_2\text{Cl}_2$ ) at 98 % ee.

### Racemic Sample 1f

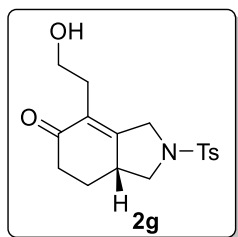


Peak #	RetTime [min]	Type	Width [min]	Area [mAU*s]	Height [mAU]	Area %
1	22.871	BB	0.7378	9914.95898	194.80487	51.3800
2	31.507	BB	1.0453	9382.36133	132.95697	48.6200

### Enantiomeric Sample 1f



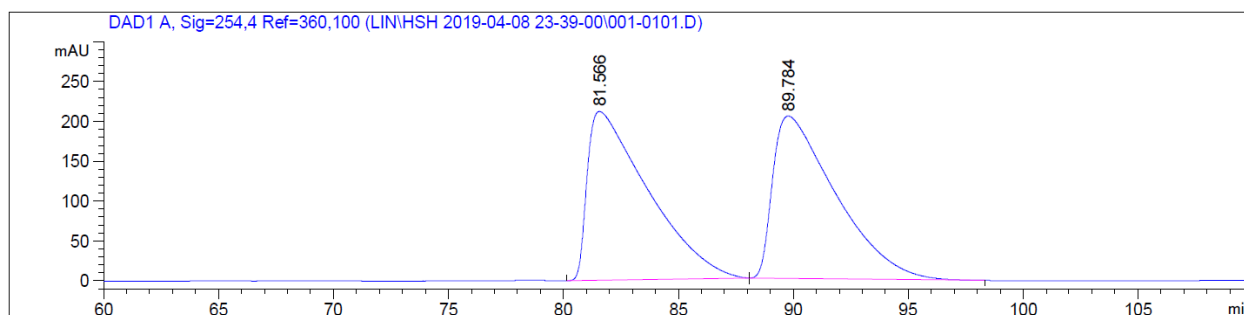
Peak #	RetTime [min]	Type	Width [min]	Area [mAU*s]	Height [mAU]	Area %
1	22.768	BB	0.7530	4.88321e4	938.55890	99.1581
2	30.082	BB	0.8286	414.61984	7.34519	0.8419



**2g** (15.4 mg) was isolated as a white solid in 46% yield. Melting Point: 110-113 °C.  $R_f = 0.2$  (EtOAc/Hexane=1/1).  **$^1\text{H}$  NMR (400 MHz,  $\text{CDCl}_3$ )**:  $\delta$  7.82 – 7.64 (m, 2H), 7.46 – 7.34 (m, 2H), 4.33 (d,  $J = 17.2$  Hz, 1H), 4.02 – 3.84 (m, 2H), 3.62 (q,  $J = 5.3$  Hz, 2H), 3.22 – 2.87 (m, 1H), 2.61 (dd,  $J = 10.9, 9.3$  Hz, 1H), 2.53 (ddd,  $J = 17.5, 4.5, 2.5$  Hz, 1H), 2.49 – 2.41 (m, 4H), 2.41 – 2.25 (m, 2H), 2.21 – 2.11 (m, 1H), 1.98 (br, 1H), 1.60 (dddd,  $J = 14.5, 12.7, 11.6, 4.4$  Hz, 1H).  **$^{13}\text{C}$  NMR (101 MHz,  $\text{CDCl}_3$ )**:  $\delta$  198.34, 160.23, 144.16, 132.44, 130.34, 129.92, 127.75, 61.44, 53.36, 50.67, 40.79, 36.58, 29.95, 26.39, 21.59. **IR**:  $\nu$  3449, 2927, 1664, 1597, 1344, 1163, 1043, 816  $\text{cm}^{-1}$ ; **HRMS** calcd. For  $[\text{M}+\text{Na}]^+$ : 358.1083. Found: 358.1084.

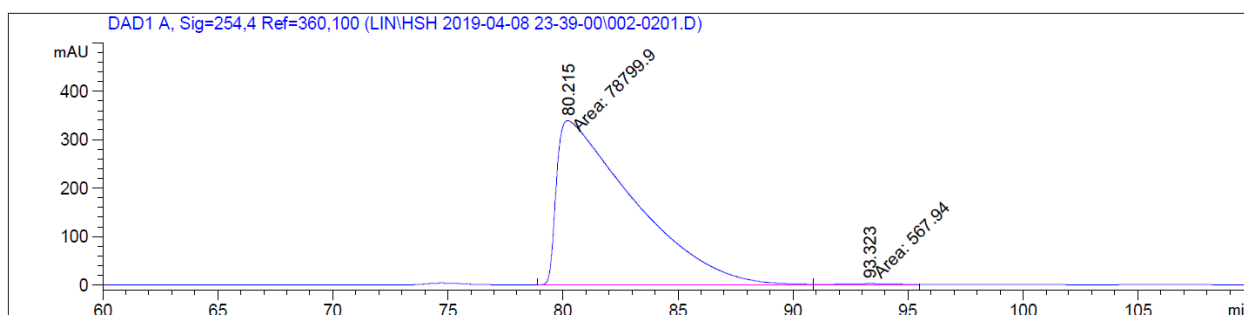
Chiral HPLC of **2g** (Chiralpak ID, hexane:isopropanol = 80:20, 1 mL/min, 254 nm),  $t_{\text{minor}} = 93.3$  min,  $t_{\text{major}} = 80.2$  min.  $[\alpha]_{\text{D}}^{22.6} = -440.1$  ( $c = 1.67$ ,  $\text{CH}_2\text{Cl}_2$ ) at 98 % ee.

### Racemic Sample 2g



Peak #	RetTime [min]	Type	Width [min]	Area [mAU*s]	Height [mAU]	Area %
1	81.566	BB	2.5356	3.88361e4	211.56149	50.0374
2	89.784	BB	2.7116	3.87781e4	203.64401	49.9626

### Enantiomeric Sample 2g

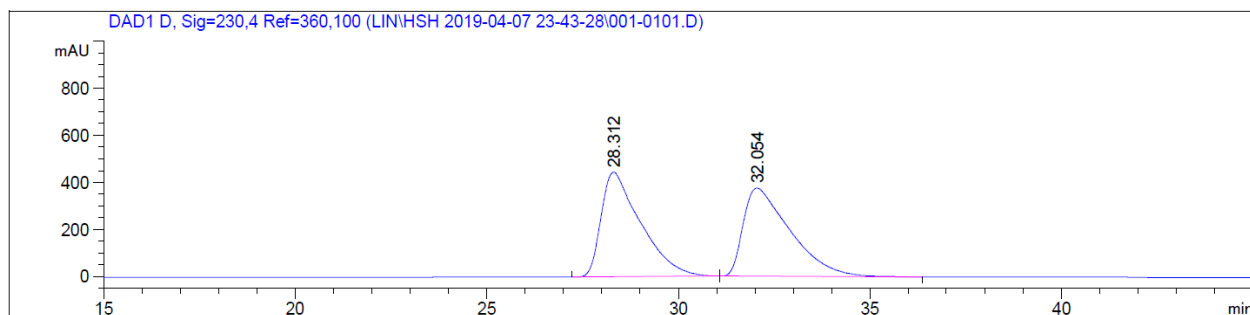


Peak #	RetTime [min]	Type	Width [min]	Area [mAU*s]	Height [mAU]	Area %
1	80.215	MM	3.8759	7.87999e4	338.84863	99.2844
2	93.323	MM	3.3607	567.94049	2.81659	0.7156

**1g** (16.0 mg) was recycled as a colorless oil in 48% yield.

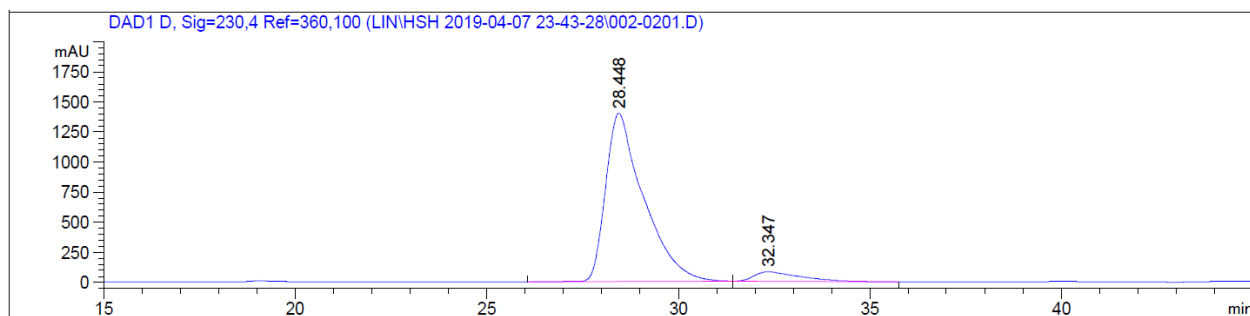
Chiral HPLC for **1g** (Chiralpak IA, hexane:isopropanol = 90:10, 1 mL/min, 230 nm),  $t_{\text{minor}} = 32.3$  min,  $t_{\text{major}} = 28.4$  min.  $[\alpha]_{\text{D}}^{22.6} = -38.1$  ( $c = 1.89$ ,  $\text{CH}_2\text{Cl}_2$ ) at 88 % ee.

### Racemic Sample 1g

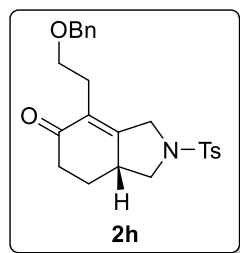


Peak #	RetTime [min]	Type	Width [min]	Area [mAU*s]	Height [mAU]	Area %
1	28.312	BB	1.0146	3.18558e4	444.21750	50.0000
2	32.054	BB	1.2101	3.18558e4	374.60620	50.0000

### Enantiomeric Sample 1g



Peak #	RetTime [min]	Type	Width [min]	Area [mAU*s]	Height [mAU]	Area %
1	28.448	BB	0.9778	9.64094e4	1399.38074	93.7091
2	32.347	BB	1.1552	6472.22217	78.88539	6.2909



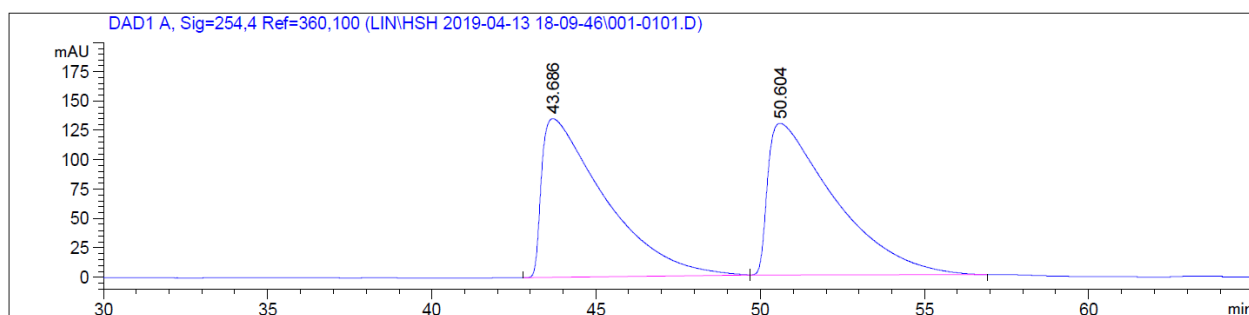
**2h** (16.1 mg) was isolated as a colorless oil in 38% yield.  $R_f = 0.4$  (EtOAc/Hexane=1/3).  $^1\text{H}$  NMR (400 MHz,  $\text{CDCl}_3$ ):  $\delta$  7.75 – 7.64 (m, 2H), 7.37 – 7.24 (m, 5H), 7.22 – 7.16 (m, 2H), 4.47 – 4.24 (m, 3H), 3.97 (dd,  $J = 17.3, 2.4$  Hz, 1H), 3.89 (dd,  $J = 9.3, 8.0$  Hz, 1H), 3.48 – 3.39 (m, 2H), 3.00 – 2.86 (m, 1H), 2.59 (dd,  $J = 10.9, 9.3$  Hz, 1H), 2.52 – 2.42 (m, 2H), 2.41 – 2.21 (m, 5H), 2.11



(dtd,  $J = 12.3, 4.9, 2.4$  Hz, 1H), 1.52 (dddd,  $J = 14.5, 12.7, 11.6, 4.4$  Hz, 1H).  $^{13}\text{C}$  NMR (101 MHz,  $\text{CDCl}_3$ ):  $\delta$  196.96, 159.92, 143.97, 138.31, 132.56, 130.00, 129.82, 128.35, 127.74, 127.53, 127.39, 72.74, 68.54, 53.45, 50.93, 40.71, 36.58, 27.14, 26.42, 21.53. IR:  $\nu$  2925, 1667, 1598, 1453, 1347, 1164, 1095, 816  $\text{cm}^{-1}$ ; HRMS calcd. For  $[\text{M}+\text{H}]^+$ : 426.1734. Found: 426.1734.

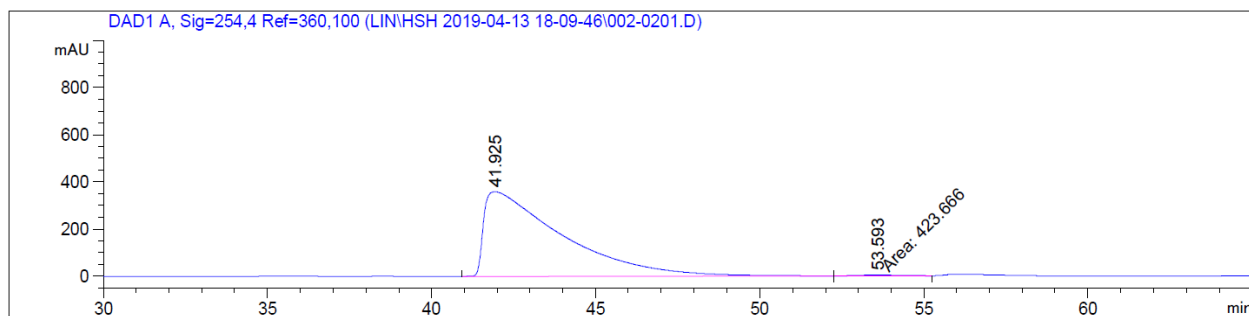
Chiral HPLC of **2h** (Chiralpak IB, hexane:isopropanol = 92:8, 1 mL/min, 254 nm),  $t_{\text{minor}} = 53.6$  min,  $t_{\text{major}} = 41.9$  min.  $[\alpha]_{\text{D}}^{22.6} = -299.0$  ( $c = 1.94$ ,  $\text{CH}_2\text{Cl}_2$ ) at 98 % ee.

### Racemic Sample 2h



Peak #	RetTime [min]	Type	Width [min]	Area [mAU*s]	Height [mAU]	Area %
1	43.686	BB	1.8622	1.80186e4	135.25679	49.7106
2	50.604	BB	1.9752	1.82283e4	129.10634	50.2894

### Enantiomeric Sample 2h



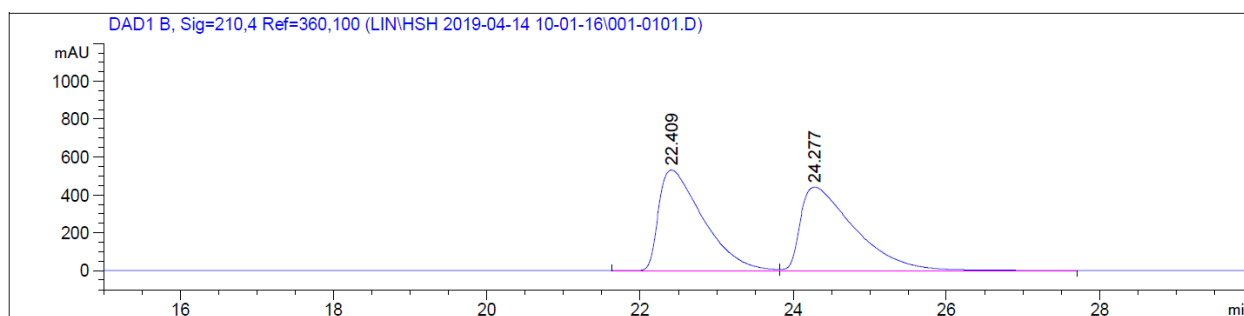
Peak #	RetTime [min]	Type	Width [min]	Area [mAU*s]	Height [mAU]	Area %
1	41.925	BB	2.2364	5.90058e4	358.84818	99.2871
2	53.593	MM	1.7877	423.66602	3.94976	0.7129

**1h** (19.0 mg) was recycled as a colorless oil in 45% yield.

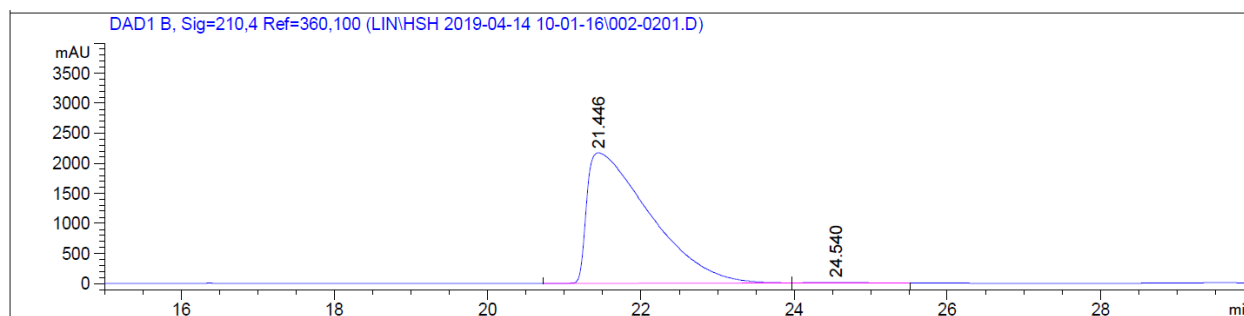
Chiral HPLC for **1h** (Chiralpak IB, hexane:isopropanol = 92:8, 1 mL/min, 210 nm),  $t_{\text{minor}} = 24.5$

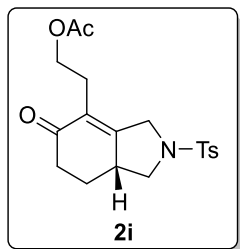
min,  $t_{\text{major}} = 21.4$  min.  $[\alpha]_{\text{D}}^{22.6} = -77.2$  ( $c = 2.06$ ,  $\text{CH}_2\text{Cl}_2$ ) at 98 % ee.

### Racemic Sample 1h



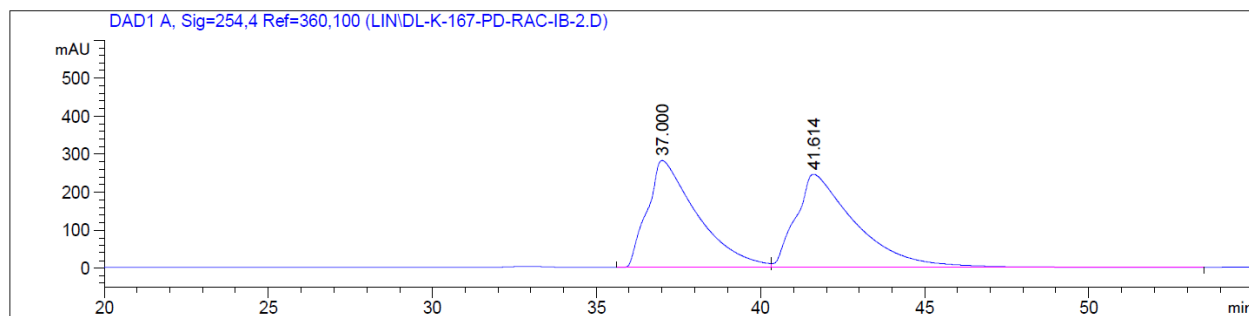
### Enantiomeric Sample 1h





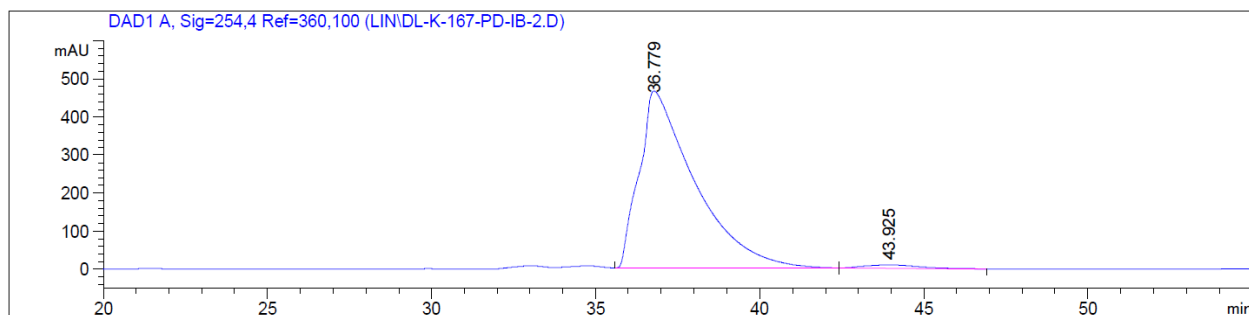
**2i** (17.5 mg) was isolated as a colorless oil in 46% yield.  $R_f = 0.3$  (EtOAc/Hexane=1/2).  **$^1\text{H}$  NMR** (400 MHz,  $\text{CDCl}_3$ ):  $\delta$  7.81 – 7.69 (m, 2H), 7.46 – 7.33 (m, 2H), 4.30 (d,  $J = 17.2$  Hz, 1H), 4.09 (ddd,  $J = 10.8, 6.7, 6.0$  Hz, 1H), 4.00 (ddd,  $J = 10.9, 6.9, 6.0$  Hz, 1H), 3.92 (dd,  $J = 9.3, 7.9$  Hz, 1H), 3.86 (dd,  $J = 17.1, 2.4$  Hz, 1H), 3.07 – 2.94 (m, 1H), 2.60 (dd,  $J = 10.9, 9.3$  Hz, 1H), 2.57 – 2.42 (m, 5H), 2.42 – 2.27 (m, 2H), 2.15 (dtd,  $J = 12.3, 4.9, 2.4$  Hz, 1H), 1.90 (s, 3H), 1.65 – 1.51 (m, 1H).  **$^{13}\text{C}$  NMR** (101 MHz,  $\text{CDCl}_3$ ):  $\delta$  196.63, 170.71, 159.80, 144.17, 132.51, 129.94, 129.16, 127.77, 62.55, 53.39, 50.49, 40.81, 36.47, 26.33, 26.20, 21.56, 20.78. **IR**:  $\nu$  2953, 1738, 1668, 1598, 1347, 1241, 1164, 1043, 817  $\text{cm}^{-1}$ ; **HRMS** calcd. For  $[\text{M}+\text{H}]^+$ : 378.1370. Found: 378.1368. Chiral HPLC of **2i** (Chiralpak IB, hexane:isopropanol = 80:20, 0.7 mL/min, 254 nm),  $t_{\text{minor}} = 43.9$  min,  $t_{\text{major}} = 36.8$  min.  $[\alpha]_D^{22.6} = -271.3$  ( $c = 1.74$ ,  $\text{CH}_2\text{Cl}_2$ ) at 96 % ee.

### Racemic Sample 2i



Peak #	RetTime [min]	Type	Width [min]	Area [mAU*s]	Height [mAU]	Area %
1	37.000	BV	1.4381	2.98068e4	281.78027	48.8373
2	41.614	VB	1.6972	3.12261e4	245.61517	51.1627

### Enantiomeric Sample 2i

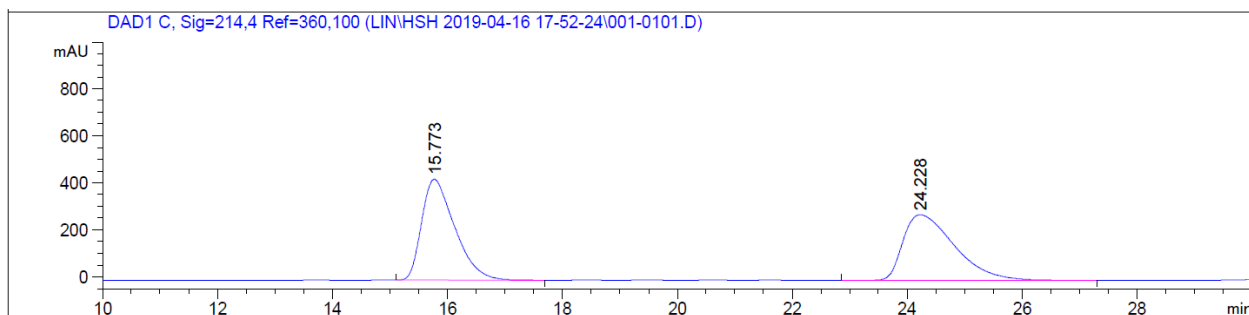


Peak #	RetTime [min]	Type	Width [min]	Area [mAU*s]	Height [mAU]	Area %
1	36.779	BB	1.6022	5.47271e4	464.62576	98.2376
2	43.925	BB	1.4614	981.81592	9.18286	1.7624

**1i** (19.0 mg) was recycled as a colorless oil in 50% yield.

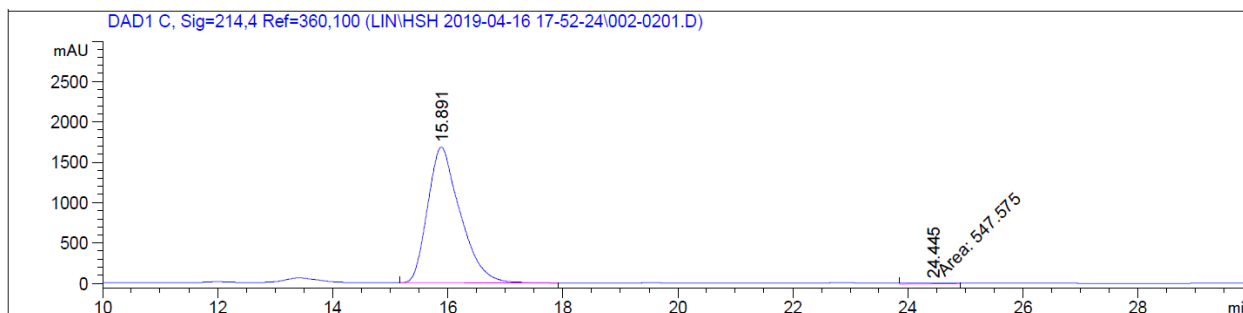
Chiral HPLC for **1i** (Chiralpak IA, hexane:isopropanol = 85:15, 1 mL/min, 214 nm),  $t_{\text{minor}} = 24.4$  min,  $t_{\text{major}} = 15.9$  min.  $[\alpha]_{\text{D}}^{22.6} = -76.6$  ( $c = 1.97$ ,  $\text{CH}_2\text{Cl}_2$ ) at 98 % ee.

### Racemic Sample 1i

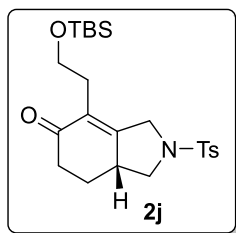


Peak #	RetTime [min]	Type	Width [min]	Area [mAU*s]	Height [mAU]	Area %
1	15.773	BB	0.5999	1.71289e4	428.94064	49.7365
2	24.228	BB	0.9731	1.73103e4	279.27560	50.2635

### Enantiomeric Sample 1i



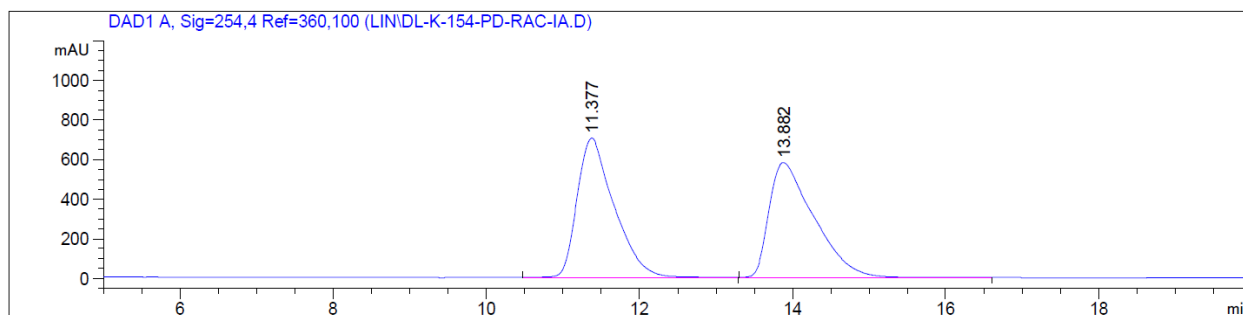
Peak #	RetTime [min]	Type	Width [min]	Area [mAU*s]	Height [mAU]	Area %
1	15.891	VB	0.5757	6.58570e4	1678.60291	99.1754
2	24.445	MM	0.7602	547.57501	9.23121	0.8246



**2j** (19.0 mg) was isolated as a colorless oil in 43% yield.  $R_f = 0.4$  (EtOAc/Hexane=1/3).  **$^1\text{H}$  NMR (400 MHz,  $\text{CDCl}_3$ )**:  $\delta$  7.89 – 7.64 (m, 2H), 7.49 – 7.31 (m, 2H), 4.33 (dt,  $J = 17.0, 1.2$  Hz, 1H), 4.01 – 3.81 (m, 2H), 3.71 – 3.53 (m, 2H), 3.09 – 2.88 (m, 1H), 2.61 (dd,  $J = 10.9, 9.3$  Hz, 1H), 2.50 (ddd,  $J = 17.2, 4.3, 2.4$  Hz, 1H), 2.44 (s, 3H), 2.42 – 2.21 (m, 3H), 2.14 (dtd,  $J = 12.4, 4.8, 2.4$  Hz, 1H), 1.57 (dddd,  $J = 14.5, 12.6, 11.6, 4.4$  Hz, 1H), 0.79 (s, 9H), -0.06 (s, 3H), -0.08 (s, 3H).  **$^{13}\text{C}$  NMR (101 MHz,  $\text{CDCl}_3$ )**:  $\delta$  197.02, 160.02, 143.93, 132.79, 130.00, 129.89, 127.73, 61.41, 53.32, 50.85, 40.87, 36.69, 30.10, 26.41, 25.86, 21.55, 18.24, -5.40, -5.51. **IR**:  $\nu$  2928, 1669, 1472, 1350, 1256, 1165, 1096, 837  $\text{cm}^{-1}$ ; **HRMS** calcd. For  $[\text{M}+\text{Na}]^+$ : 472.1948. Found: 472.1959.

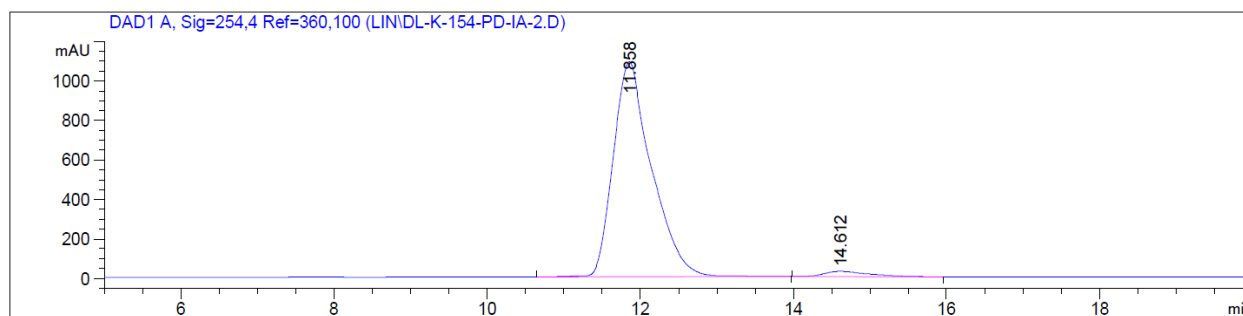
Chiral HPLC of **2j** (Chiralpak IA, hexane:isopropanol = 90:10, 1 mL/min, 254 nm),  $t_{\text{minor}} = 14.6$  min,  $t_{\text{major}} = 11.9$  min.  $[\alpha]_D^{22.6} = -125.5$  ( $c = 1.45$ ,  $\text{CH}_2\text{Cl}_2$ ) at 94 % ee.

### Racemic Sample 2j



Peak #	RetTime [min]	Type	Width [min]	Area [mAU*s]	Height [mAU]	Area %
1	11.377	BB	0.4897	2.35040e4	703.69000	50.0046
2	13.882	BB	0.5848	2.34997e4	579.81519	49.9954

### Enantiomeric Sample 2j

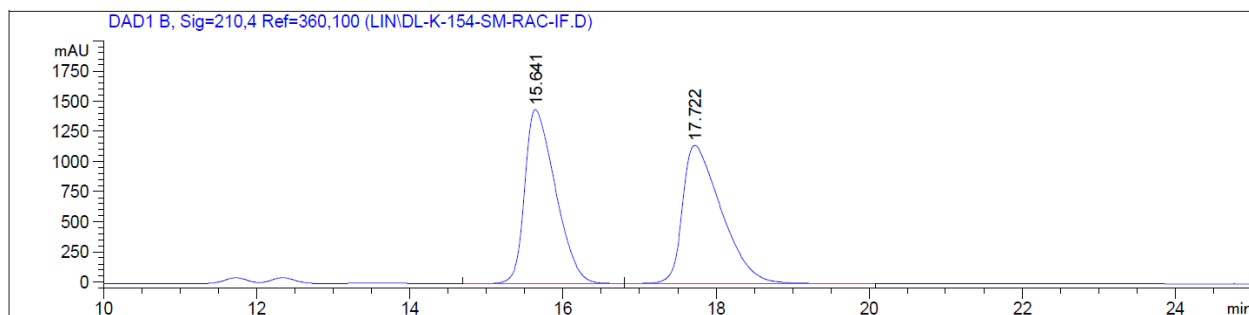


Peak #	RetTime [min]	Type	Width [min]	Area [mAU*s]	Height [mAU]	Area %
1	11.858	BB	0.5090	3.78350e4	1089.98828	97.2285
2	14.612	BB	0.5789	1078.47021	26.94623	2.7715

**1j** (17.8 mg) was recycled as a colorless oil in 40% yield.

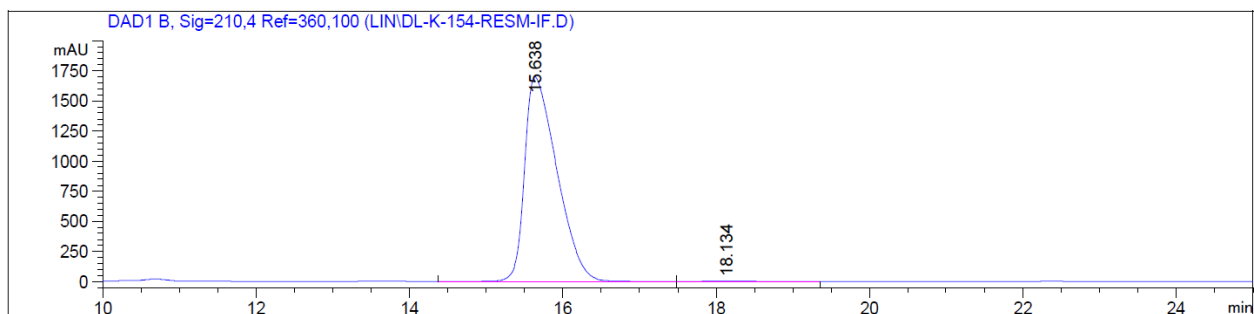
Chiral HPLC for **1j** (Chiralpak IF, hexane:isopropanol = 90:10, 1 mL/min, 210 nm),  $t_{\text{minor}} = 18.1$  min,  $t_{\text{major}} = 15.6$  min.  $[\alpha]_{\text{D}}^{22.6} = -63.4$  ( $c = 1.72$ ,  $\text{CH}_2\text{Cl}_2$ ) at 99 % ee.

### Racemic Sample 1j

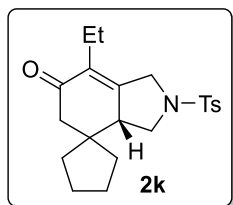


Peak #	RetTime [min]	Type	Width [min]	Area [mAU*s]	Height [mAU]	Area %
1	15.641	BB	0.4297	4.00821e4	1444.53015	49.7845
2	17.722	BB	0.5360	4.04290e4	1144.77795	50.2155

### Enantiomeric Sample 1j



Peak #	RetTime [min]	Type	Width [min]	Area [mAU*s]	Height [mAU]	Area %
1	15.638	BB	0.4537	4.98079e4	1700.44434	99.5962
2	18.134	BB	0.5668	201.95364	5.13556	0.4038



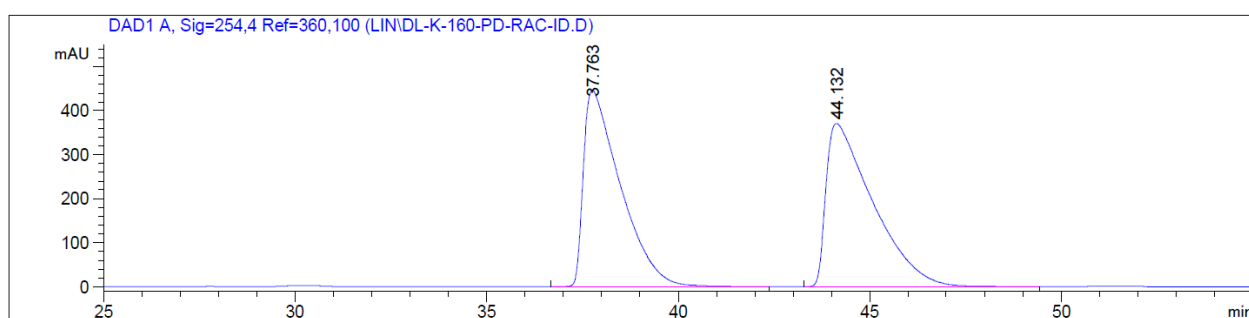
**2k** (11.9 mg) was isolated as a colorless oil in 32% yield.  $R_f = 0.4$  (EtOAc/Hexane=1/3).  $^1\text{H NMR}$  (400 MHz,  $\text{CDCl}_3$ ):  $\delta$  7.80 – 7.66 (m, 2H), 7.44 – 7.34 (m, 2H), 4.22 (d,  $J = 16.9$  Hz, 1H), 3.93 – 3.68 (m, 2H), 3.26 – 3.07 (m, 1H), 2.85 (dd,  $J = 10.6, 9.3$  Hz, 1H), 2.49 – 2.41 (m, 4H), 2.26 (d,  $J = 16.0$  Hz, 1H), 2.15 (dq,  $J = 14.9, 7.6$  Hz, 1H), 2.09 – 1.98 (m, 1H), 1.71 – 1.54 (m, 3H), 1.52 –

1.39 (m, 3H), 1.32 – 1.23 (m, 1H), 1.18 (ddd,  $J = 13.7, 8.1, 6.4$  Hz, 1H), 0.89 (t,  $J = 7.5$  Hz, 3H).

$^{13}\text{C}$  NMR (101 MHz,  $\text{CDCl}_3$ ):  $\delta$  197.57, 155.24, 144.13, 134.29, 132.65, 129.90, 127.69, 51.69, 50.44, 49.72, 48.88, 46.80, 38.94, 30.17, 25.56, 24.68, 21.61, 19.51, 12.75. **IR**:  $\nu$  2954, 1668, 1598, 1452, 1348, 1165, 1093, 816  $\text{cm}^{-1}$ ; **HRMS** calcd. For  $[\text{M}+\text{Na}]^+$ : 396.1604. Found: 396.1613.

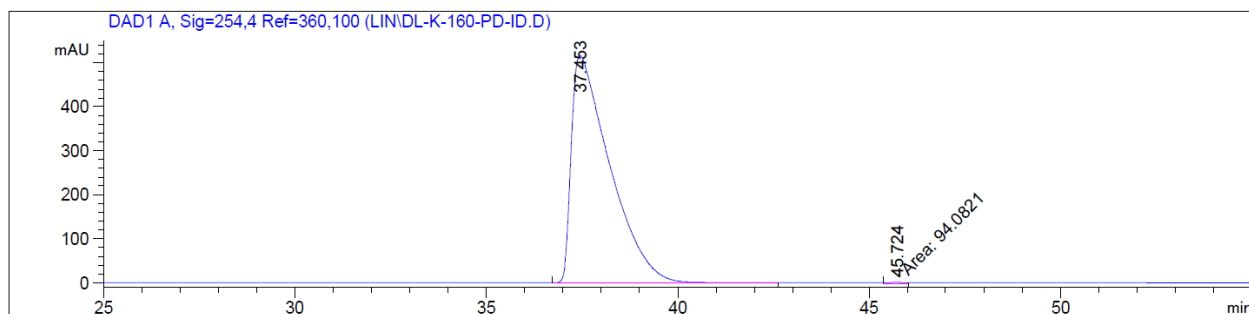
Chiral HPLC of **2k** (Chiralpak ID, hexane:isopropanol = 90:10, 1 mL/min, 254 nm),  $t_{\text{minor}} = 45.7$  min,  $t_{\text{major}} = 37.4$  min.  $[\alpha]_{\text{D}}^{22.6} = 294.4$  ( $c = 0.72$ ,  $\text{CH}_2\text{Cl}_2$ ) at 99.5 % ee.

### Racemic Sample 2k



Peak #	RetTime [min]	Type	Width [min]	Area [mAU*s]	Height [mAU]	Area %
1	37.763	BB	0.9745	2.99144e4	446.01627	48.7265
2	44.132	BB	1.2227	3.14780e4	370.70117	51.2735

### Enantiomeric Sample 2k



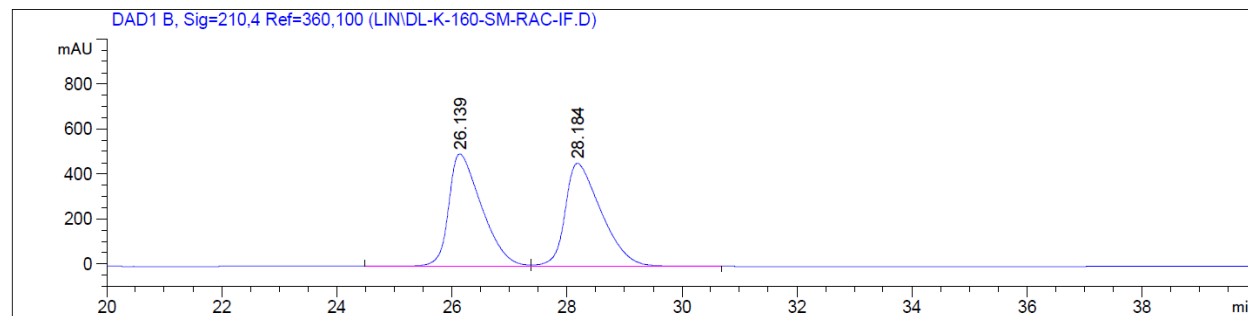
Peak #	RetTime [min]	Type	Width [min]	Area [mAU*s]	Height [mAU]	Area %
1	37.453	BB	1.0162	3.59899e4	515.68945	99.7393
2	45.724	MM	0.6383	94.08212	2.45648	0.2607

**1k** (16.0 mg) was recycled as a colorless oil in 43% yield.



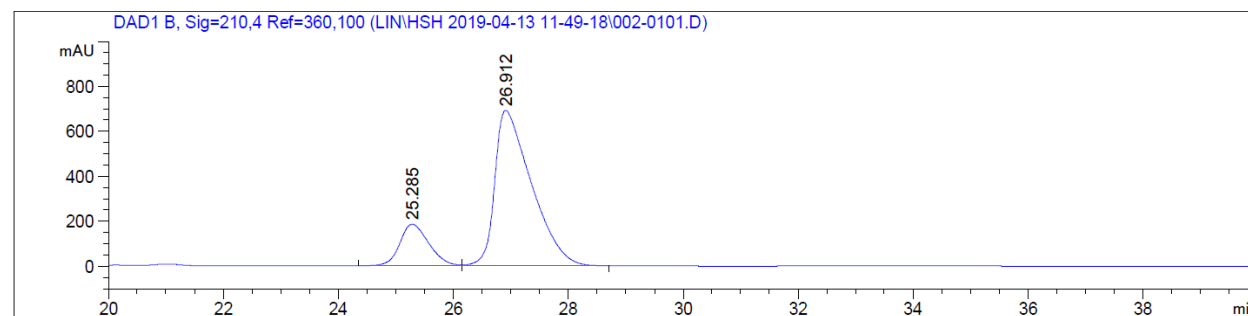
Chiral HPLC for **1k** (Chiralpak IF, hexane:isopropanol = 92:8, 1 mL/min, 210 nm),  $t_{\text{minor}} = 25.3$  min,  $t_{\text{major}} = 26.9$  min.  $[\alpha]_{\text{D}}^{22.6} = -443.6$  ( $c = 0.78$ ,  $\text{CH}_2\text{Cl}_2$ ) at 65 % ee.

### Racemic Sample 1k



Peak #	RetTime [min]	Type	Width [min]	Area [mAU*s]	Height [mAU]	Area %
1	26.139	BV	0.5970	1.98359e4	499.83862	49.7800
2	28.184	VB	0.6537	2.00112e4	458.07532	50.2200

### Enantiomeric Sample 1k



Peak #	RetTime [min]	Type	Width [min]	Area [mAU*s]	Height [mAU]	Area %
1	25.285	BV	0.5393	6468.58789	184.35934	17.4563
2	26.912	VB	0.6545	3.05873e4	690.84247	82.5437

### 5.4.4 X-ray data

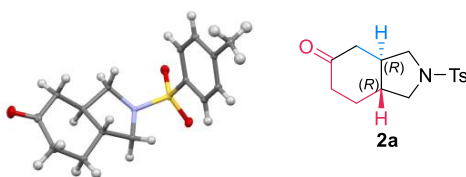


**Table 5.10** Crystal Data and Structure Refinement for **2a**

Identification code	cu_0767
Empirical formula	C <sub>15</sub> H <sub>19</sub> NO <sub>3</sub> S
Formula weight	293.37
Temperature/K	100(2)
Crystal system	monoclinic
Space group	P2 <sub>1</sub>
a/Å	8.6148(2)
b/Å	14.8424(4)
c/Å	10.8526(3)
α/°	90
β/°	95.3830(10)
γ/°	90
Volume/Å <sup>3</sup>	1381.54(6)
Z	4
ρ <sub>calc</sub> /g/cm <sup>3</sup>	1.410
μ/mm <sup>-1</sup>	2.147
F(000)	624.0
Crystal size/mm <sup>3</sup>	0.17 × 0.15 × 0.1
Radiation	CuKα (λ = 1.54178)
2Θ range for data collection/°	8.182 to 144.758
Index ranges	-10 ≤ h ≤ 10, -18 ≤ k ≤ 18, -13 ≤ l ≤ 13
Reflections collected	18690
Independent reflections	5193 [R <sub>int</sub> = 0.0371, R <sub>sigma</sub> = 0.0440]
Data/restraints/parameters	5193/1/363
Goodness-of-fit on F <sup>2</sup>	1.047
Final R indexes [I ≥ 2σ (I)]	R <sub>1</sub> = 0.0319, wR <sub>2</sub> = 0.0786
Final R indexes [all data]	R <sub>1</sub> = 0.0339, wR <sub>2</sub> = 0.0798
Largest diff. peak/hole / e Å <sup>-3</sup>	0.35/-0.27
Flack parameter	0.066(8)

## 5.5 References

- (1) (a) Murakami, M.; Itahashi, T.; Ito, Y. *J. Am. Chem. Soc.* **2002**, *124*, 13976. (b) Ko, H. M.; Dong, G. *Nat. Chem.* **2014**, *6*, 739. (c) Parker, E.; Cramer, N. *Organometallics* **2014**, *33*, 780. (d) Souillart, L.; Cramer, N. *Angew. Chem. Int. Ed.* **2014**, *53*, 9640. (e) Souillart, L.; Parker, E.; Cramer, N. *Angew. Chem. Int. Ed.* **2014**, *53*, 3001. (f) Zhou, X.; Dong, G. *J. Am. Chem.*

- Soc.* **2015**, *137*, 13715. (g) Zhou, X.; Ko, H. M.; Dong, G. *Angew. Chem. Int. Ed.* **2016**, *55*, 13867.
- (2) (a) Ioannou, E.; Nappo, M.; Avila, C.; Vagias, C.; Roussis, V. *J. Nat. Prod.* **2009**, *72*, 1716. (b) Rateb, M. E.; Houssen, W. E.; Schumacher, M.; Harrison, W. T. A.; Diederich, M.; Ebel, R.; Jaspars, M. *J. Nat. Prod.* **2009**, *72*, 1471. (c) Abe, S.; Tanaka, N.; Kobayashi, J. i. *J. Nat. Prod.* **2012**, *75*, 484. (d) Wang, G.-W.; McCreanor, N. G.; Shaw, M. H.; Whittingham, W. G.; Bower, J. F. *J. Am. Chem. Soc.* **2016**, *138*, 13501.
- (3) (a) Wender, P. A.; Correa, A. G.; Sato, Y.; Sun, R. *J. Am. Chem. Soc.* **2000**, *122*, 7815. (b) Matsuda, T.; Fujimoto, A.; Ishibashi, M.; Murakami, M. *Chem. Lett.* **2004**, *33*, 876. (c) Matsuda, T.; Makino, M.; Murakami, M. *Angew. Chem. Int. Ed.* **2005**, *44*, 4608.
- (4) Deng, L.; Jin, L.; Dong, G. *Angew. Chem. Int. Ed.* **2018**, *57*, 2702.
- (5) (a) Asfaw, N.; Storesund, H. J.; Skattebøl, L.; Aasen, A. J. *Phytochemistry* **1999**, *52*, 1491. (b) Sinninghe Damsté, J. S.; Strous, M.; Rijpstra, W. I. C.; Hopmans, E. C.; Genevasen, J. A. J.; van Duin, A. C. T.; van Niftrik, L. A.; Jetten, M. S. M. *Nature* **2002**, *419*, 708. (c) Yang, P.-S.; Cheng, M.-J.; Peng, C.-F.; Chen, J.-J.; Chen, I.-S. *J. Nat. Prod.* **2009**, *72*, 53. (d) Zheng, Y.; Shen, Y. *Org. Lett.* **2009**, *11*, 109. (e) Blakemore, D. C.; Bryans, J. S.; Carnell, P.; Carr, C. L.; Chessum, N. E. A.; Field, M. J.; Kinsella, N.; Osborne, S. A.; Warren, A. N.; Williams, S. C. *Bioorg. Med. Chem. Lett.* **2010**, *20*, 461. (f) Bohnert, M.; Miethbauer, S.; Dahse, H.-M.; Ziemen, J.; Nett, M.; Hoffmeister, D. *Bioorg. Med. Chem. Lett.* **2011**, *21*, 2003.
- (6) (a) Belluš, D.; Ernst, B. *Angew. Chem. Int. Ed.* **1988**, *27*, 797. (b) Lee-Ruff, E.; Mladenova, G. *Chem. Rev.* **2003**, *103*, 1449. (c) Namyslo, J. C.; Kaufmann, D. E. *Chem. Rev.* **2003**, *103*, 1485. (d) Seiser, T.; Saget, T.; Tran, D. N.; Cramer, N. *Angew. Chem. Int. Ed.* **2011**, *50*, 7740. (e) Carreira, E. M.; Fessard, T. C. *Chem. Rev.* **2014**, *114*, 8257. (f) Xu, Y.; Conner, M. L.; Brown, M. K. *Angew. Chem. Int. Ed.* **2015**, *54*, 11918. (g) Chen, P.-h.; Dong, G. *Chem. Eur. J.* **2016**, *22*, 18290.
- (7) For selected reviews on "cut-and-sew" chemistry: (a) Chen, P.-h.; Billett, B. A.; Tsukamoto, T.; Dong, G. *ACS Cat.* **2017**, *7*, 1340. (b) Souillart, L.; Cramer, N. *Chem. Rev.* **2015**, *115*, 9410. (c) Fumagalli, G.; Stanton, S.; Bower, J. F. *Chem. Rev.* **2017**, *117*, 9404. For selected examples: see ref 1, 3, 4, and (d) Xu, T.; Dong, G. *Angew. Chem. Int. Ed.* **2012**, *51*, 7567. (e) Xu, T.; Ko, H. M.; Savage, N. A.; Dong, G. *J. Am. Chem. Soc.* **2012**, *134*, 20005. (f) Chen, P.-h.; Xu, T.; Dong, G. *Angew. Chem. Int. Ed.* **2014**, *53*, 1674. (g) Zhu, Z.; Li, X.; Chen, S.; Chen, P.-h.; Billett, B. A.; Huang, Z.; Dong, G. *ACS Cat.* **2018**, *8*, 845.
- (8) (a) Torres, Ò.; Roglans, A.; Pla-Quintana, A. *Adv. Synth. Catal.* **2016**, *358*, 3512. (b) Cassú, D.; Parella, T.; Solà, M.; Pla-Quintana, A.; Roglans, A. *Chem. Eur. J.* **2017**, *23*, 14889. (c) Crespín, L. N. S.; Greb, A.; Blakemore, D. C.; Ley, S. V. *J. Org. Chem.* **2017**, *82*, 13093. (d) Kim-Lee, S.-H.; Alonso, I.; Mauleón, P.; Arrayás, R. G.; Carretero, J. C. *ACS Cat.* **2018**, *8*, 8993. (e) Yudasaka, M.; Shimbo, D.; Maruyama, T.; Tada, N.; Itoh, A. *Org. Lett.* **2019**, *21*, 1098.
- (9) Venneri, P. C.; Warkentin, J. *Can. J. Chem.* **2000**, *78*, 1194.

## 5.6 NMR Spectra

**Figure 5.1**  $^1\text{H}$  and  $^{13}\text{C}$  NMR spectrum of compound **1a**

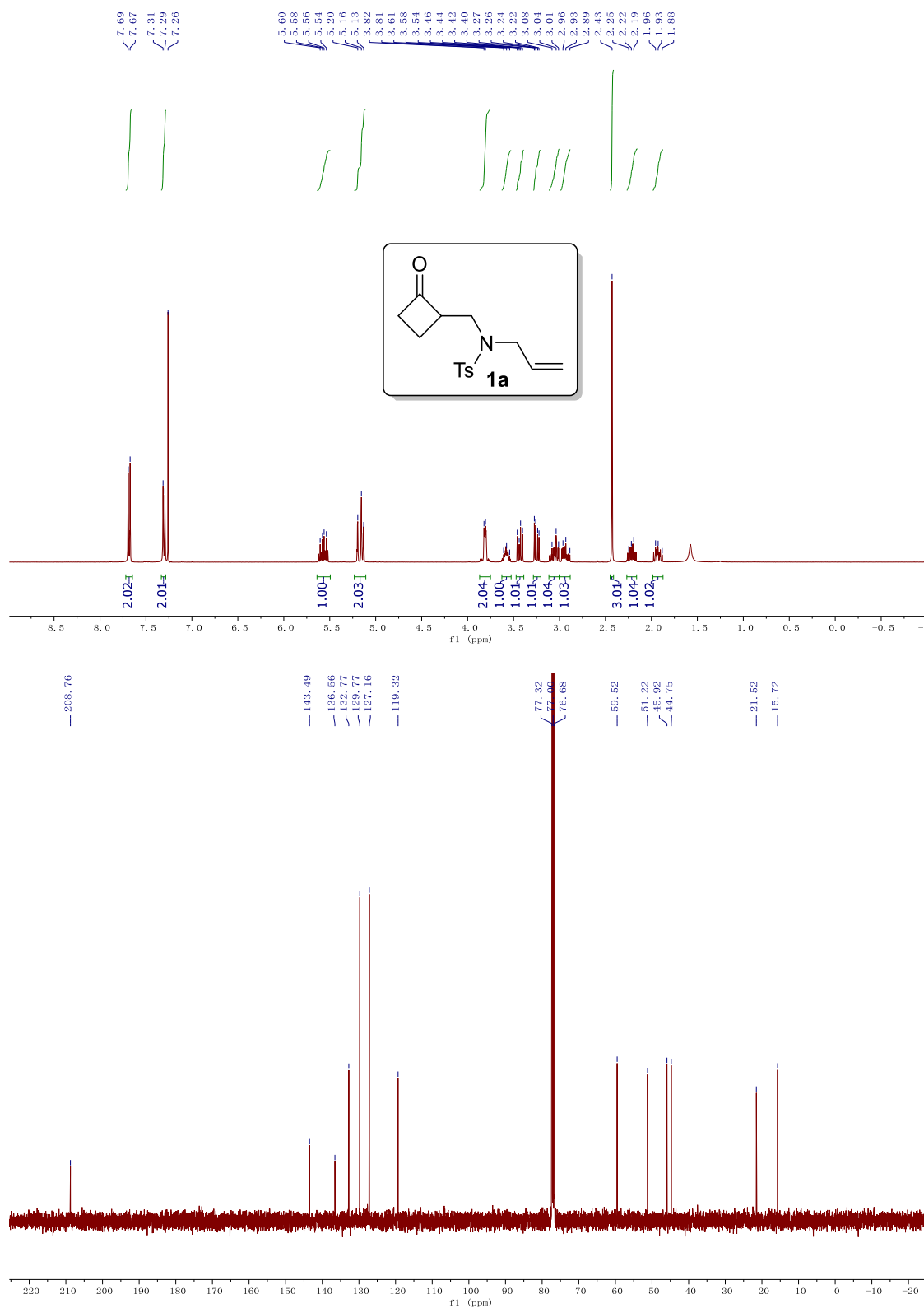


**Figure 5.2**  $^1\text{H}$  and  $^{13}\text{C}$  NMR spectrum of compound **1b**

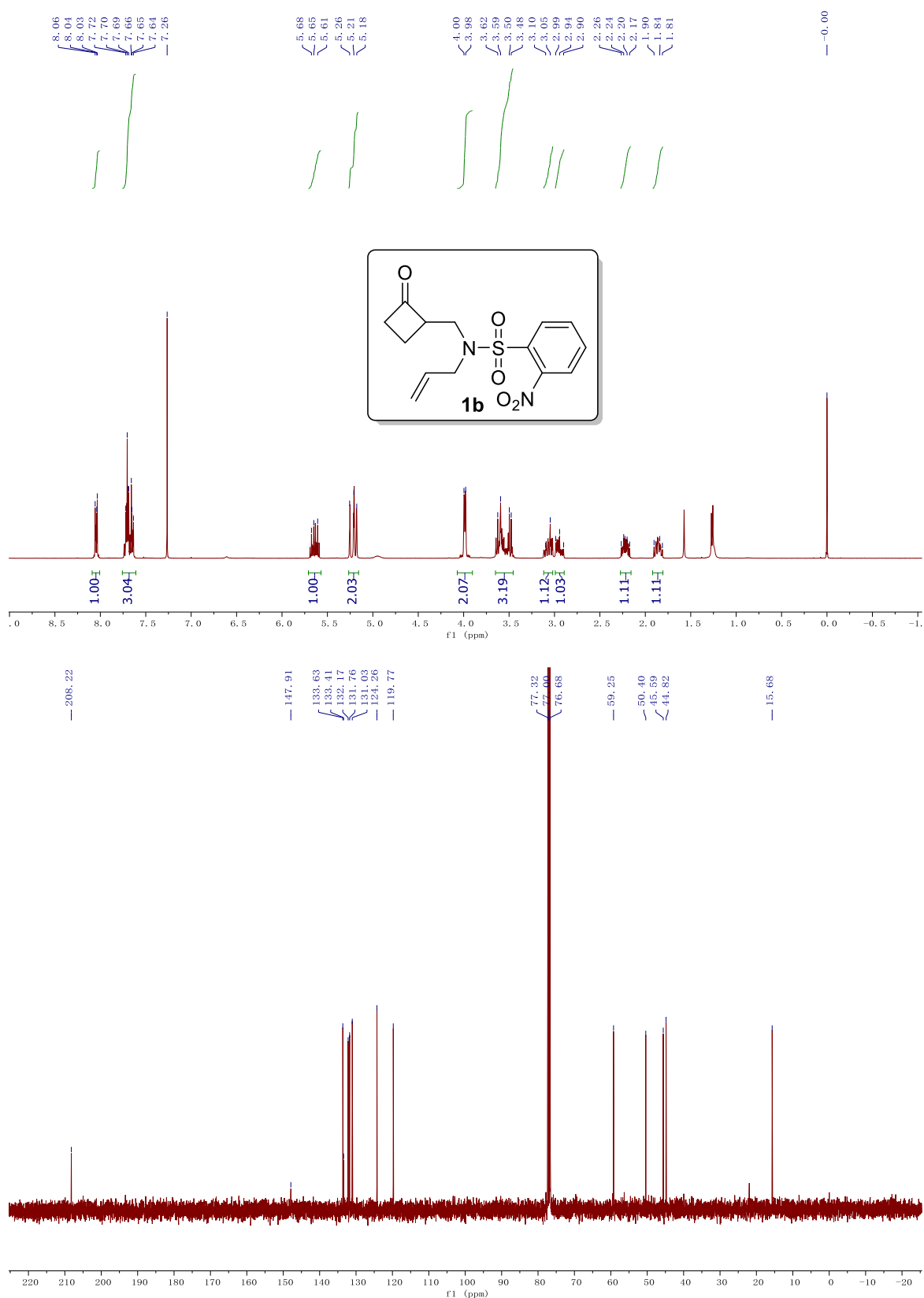


**Figure 5.3**  $^1\text{H}$  and  $^{13}\text{C}$  NMR spectrum of compound **1c**

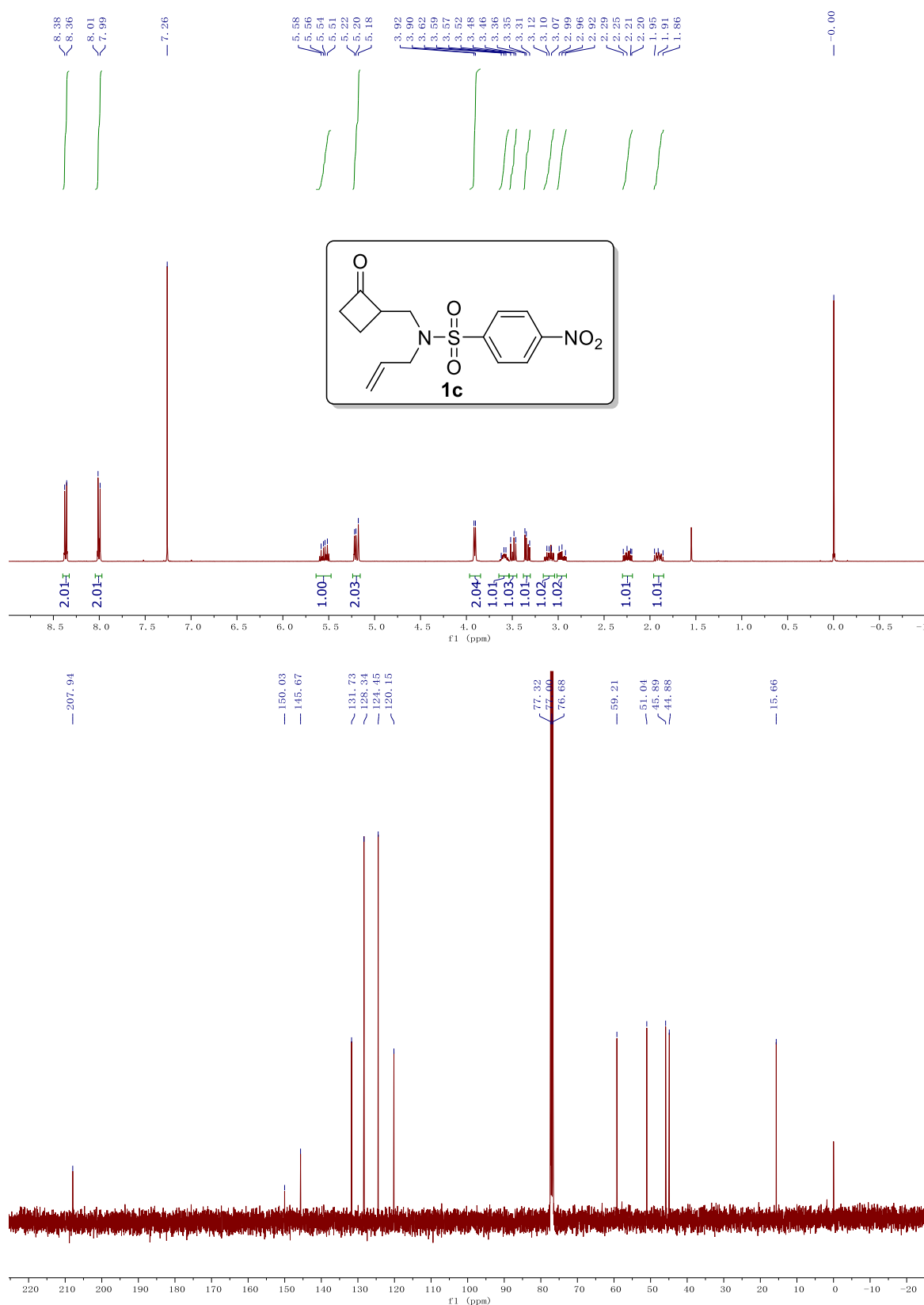


**Figure 5.4**  $^1\text{H}$  and  $^{13}\text{C}$  NMR spectrum of compound **1e**

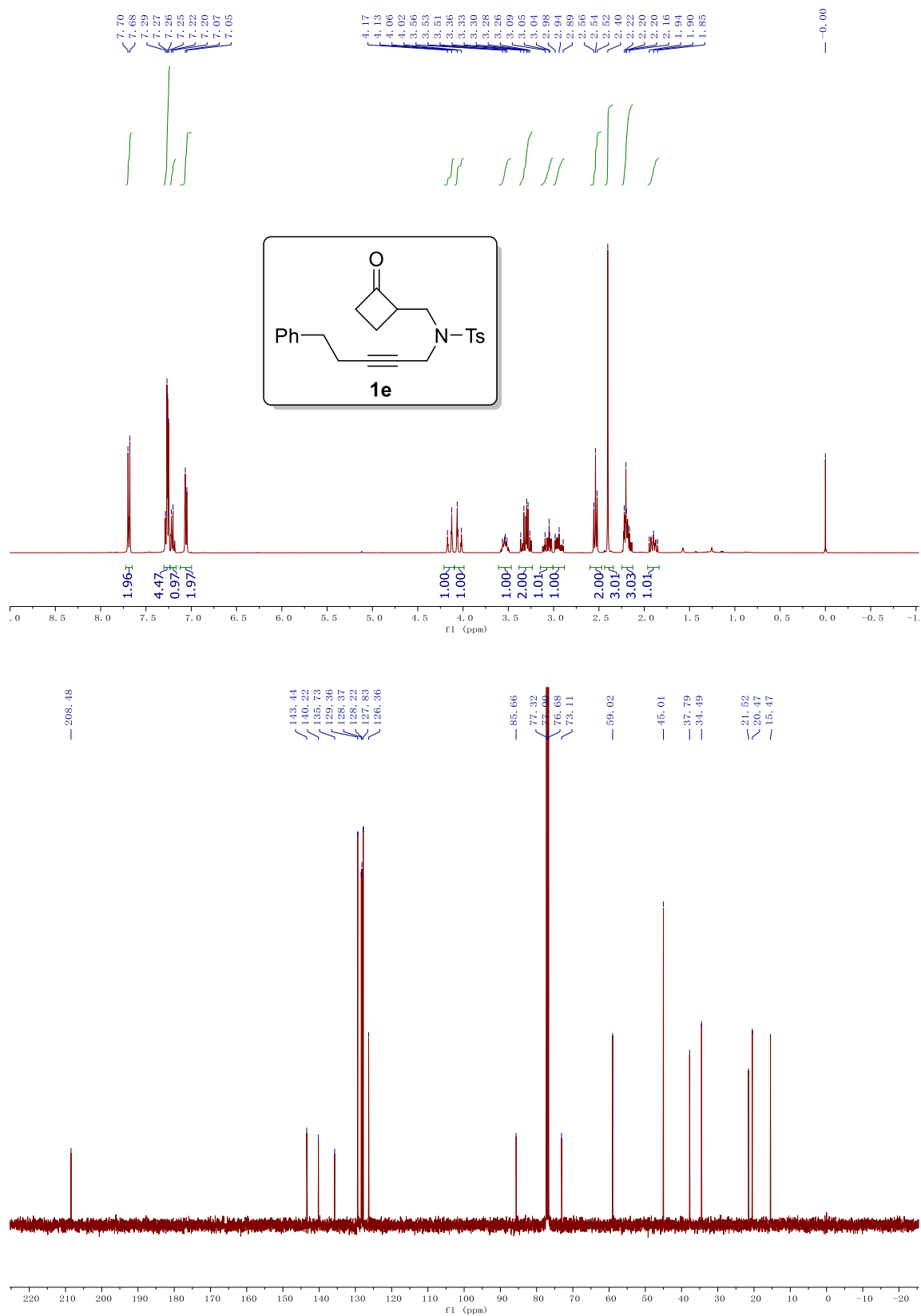


**Figure 5.5**  $^1\text{H}$  and  $^{13}\text{C}$  NMR spectrum of compound **1f**

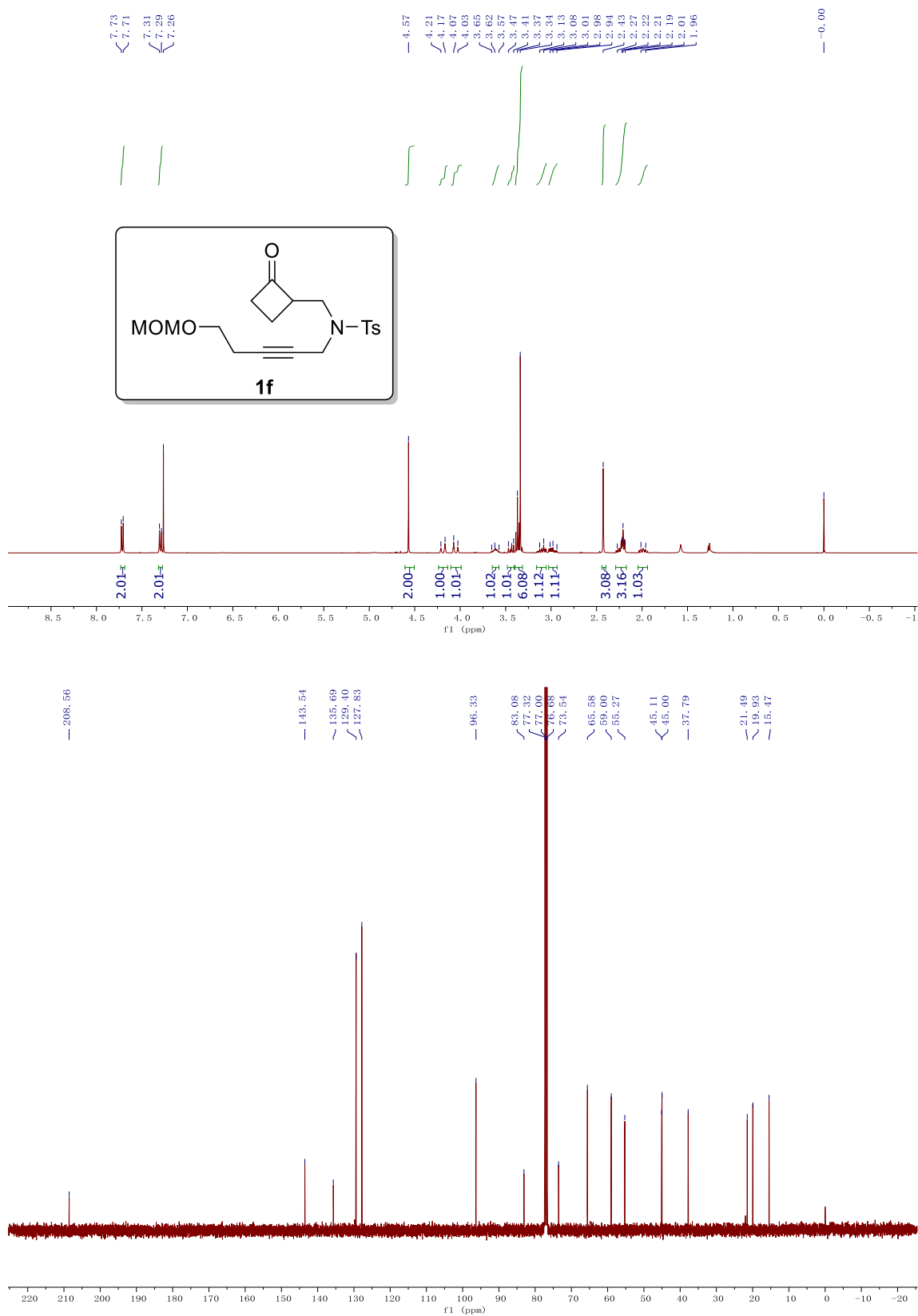




**Figure 5.6**  $^1\text{H}$  and  $^{13}\text{C}$  NMR spectrum of compound **1g**

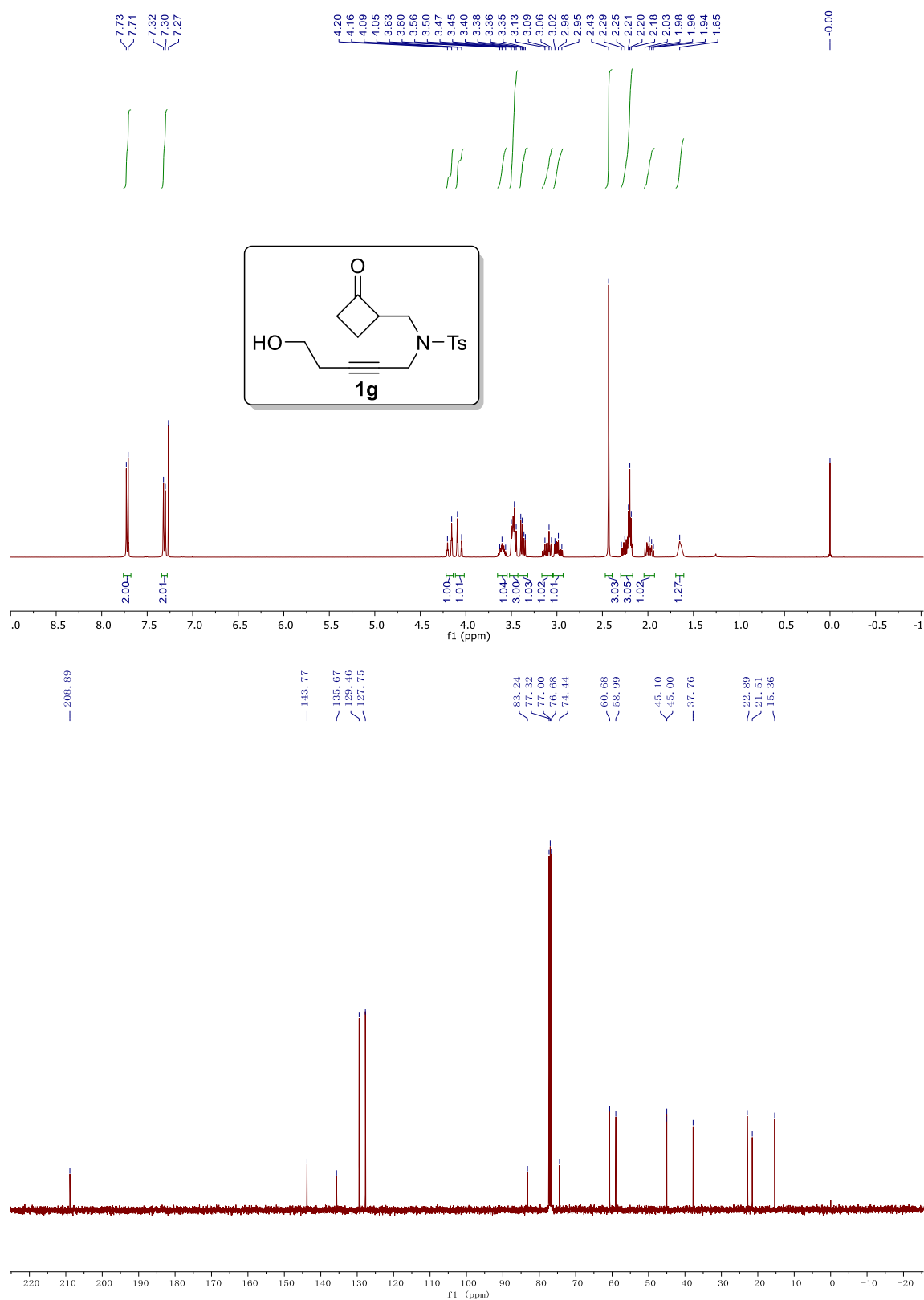


**Figure 5.7**  $^1\text{H}$  and  $^{13}\text{C}$  NMR spectrum of compound **1h**

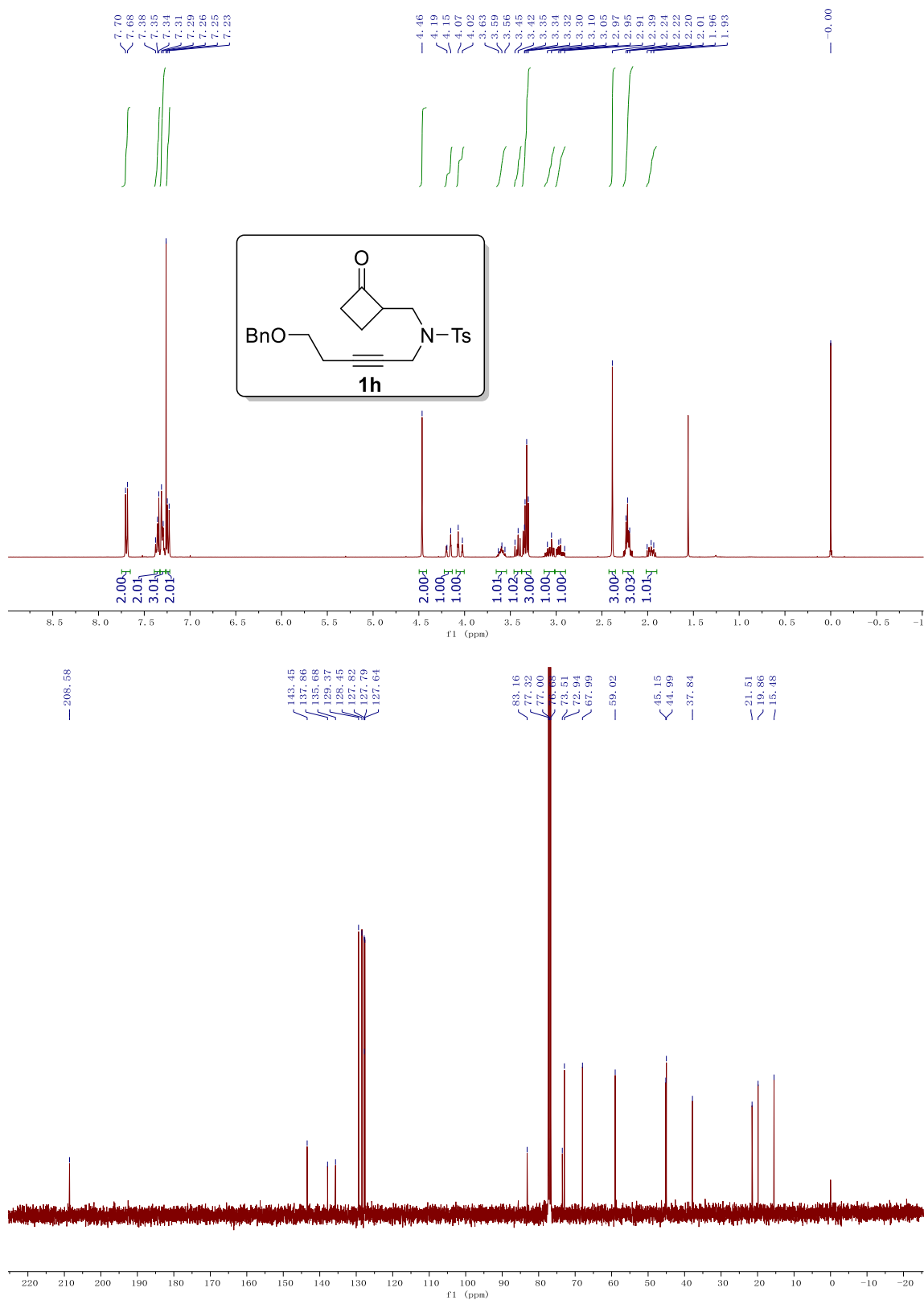


**Figure 5.8**  $^1\text{H}$  and  $^{13}\text{C}$  NMR spectrum of compound **1i**

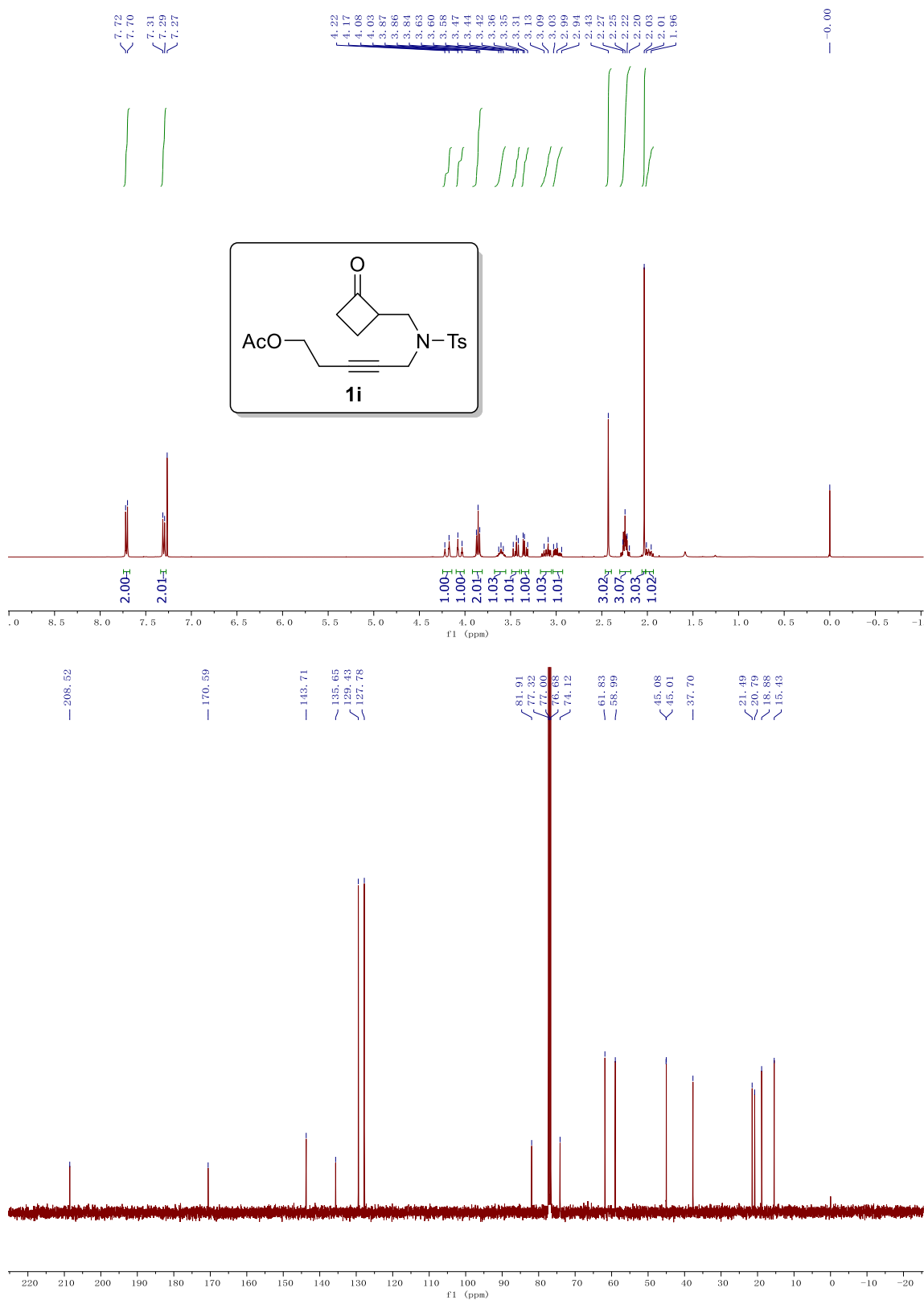


**Figure 5.9**  $^1\text{H}$  and  $^{13}\text{C}$  NMR spectrum of compound **1j**

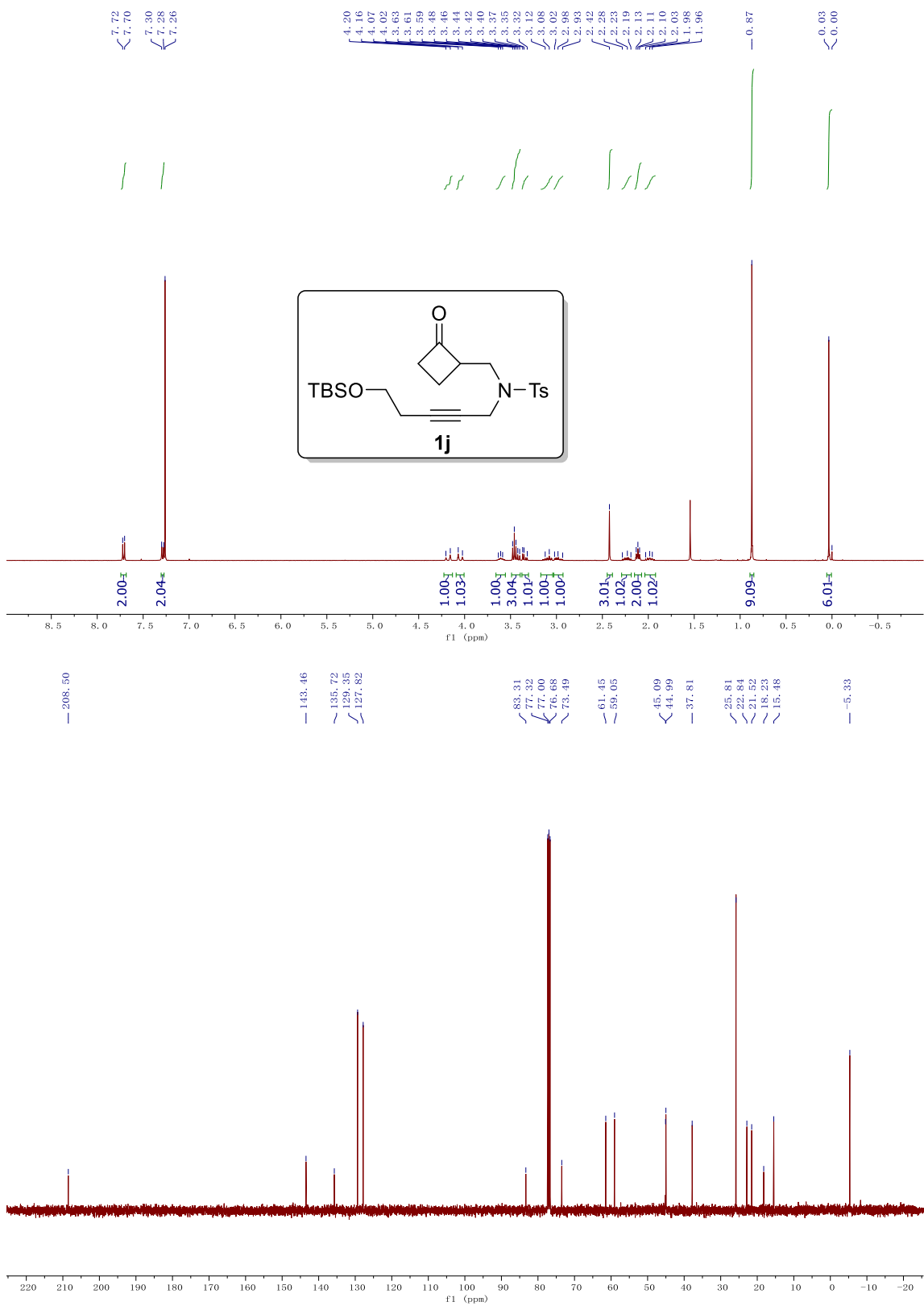


**Figure 5.10**  $^1\text{H}$  and  $^{13}\text{C}$  NMR spectrum of compound **1k**

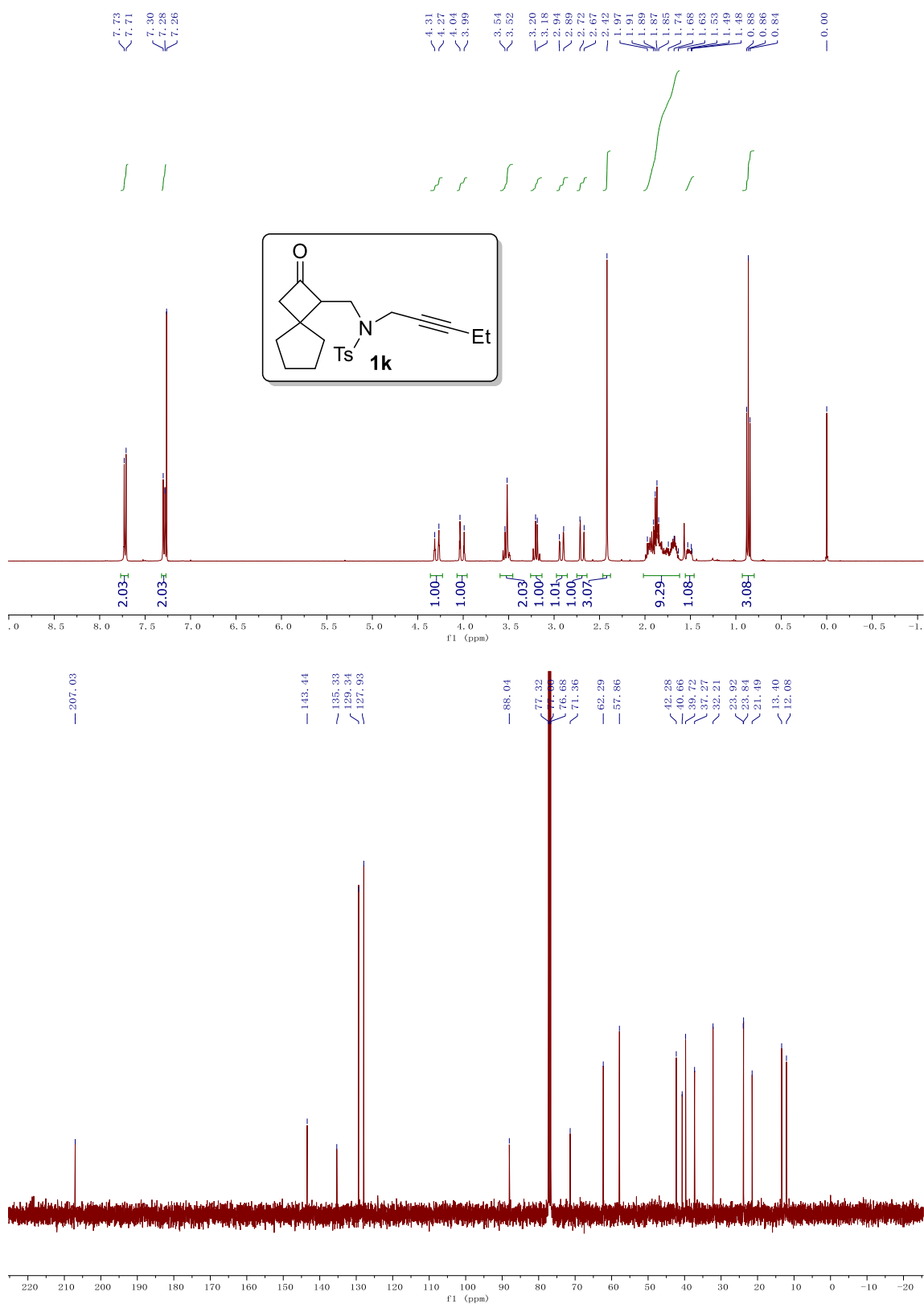


**Figure 5.11**  $^1\text{H}$  and  $^{13}\text{C}$  NMR spectrum of compound **2a**

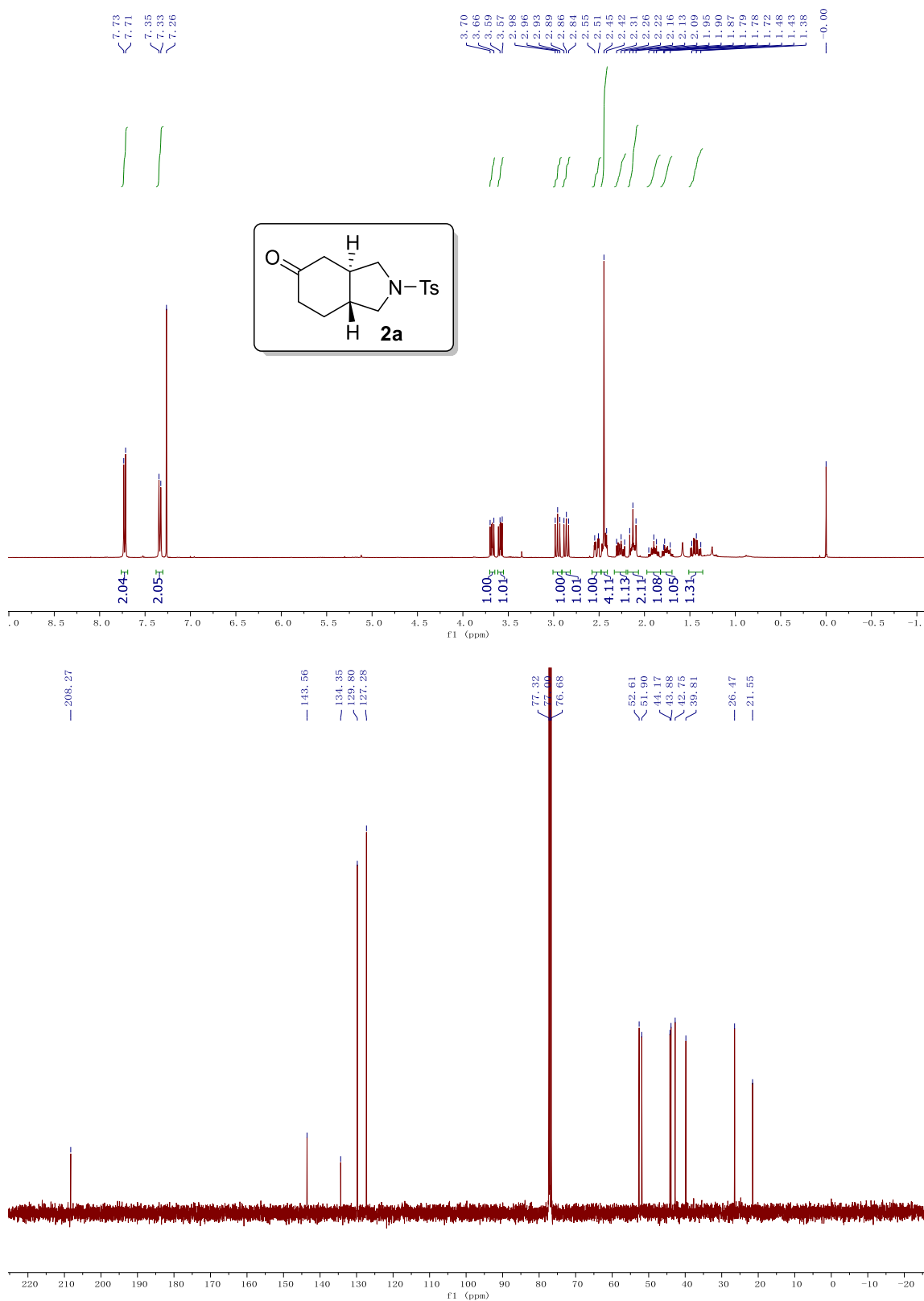


**Figure 5.12**  $^1\text{H}$  and  $^{13}\text{C}$  NMR spectrum of compound **2b**

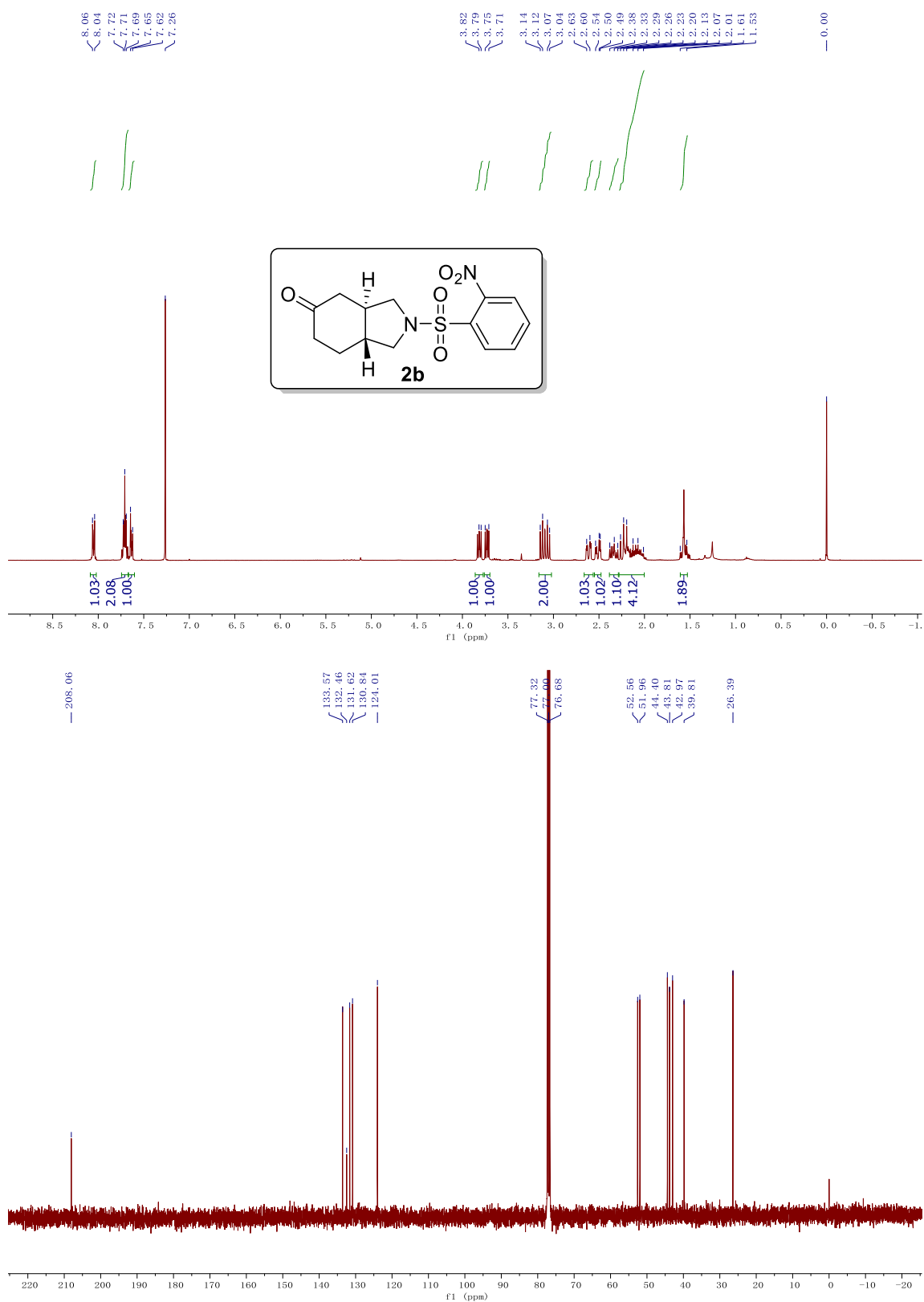


**Figure 5.13**  $^1\text{H}$  and  $^{13}\text{C}$  NMR spectrum of compound **2c**

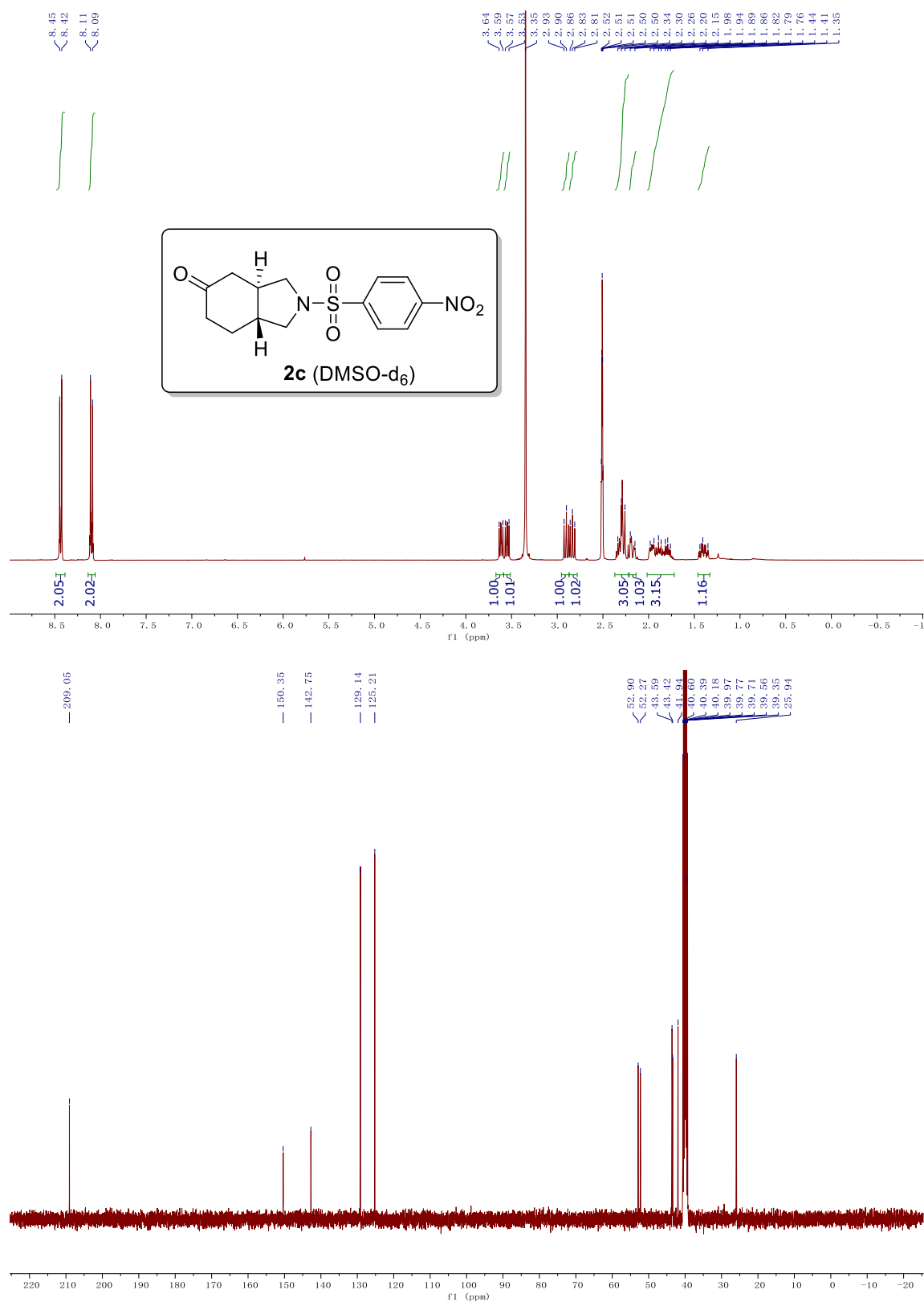




**Figure 5.14**  $^1\text{H}$  and  $^{13}\text{C}$  NMR spectrum of compound **2e**

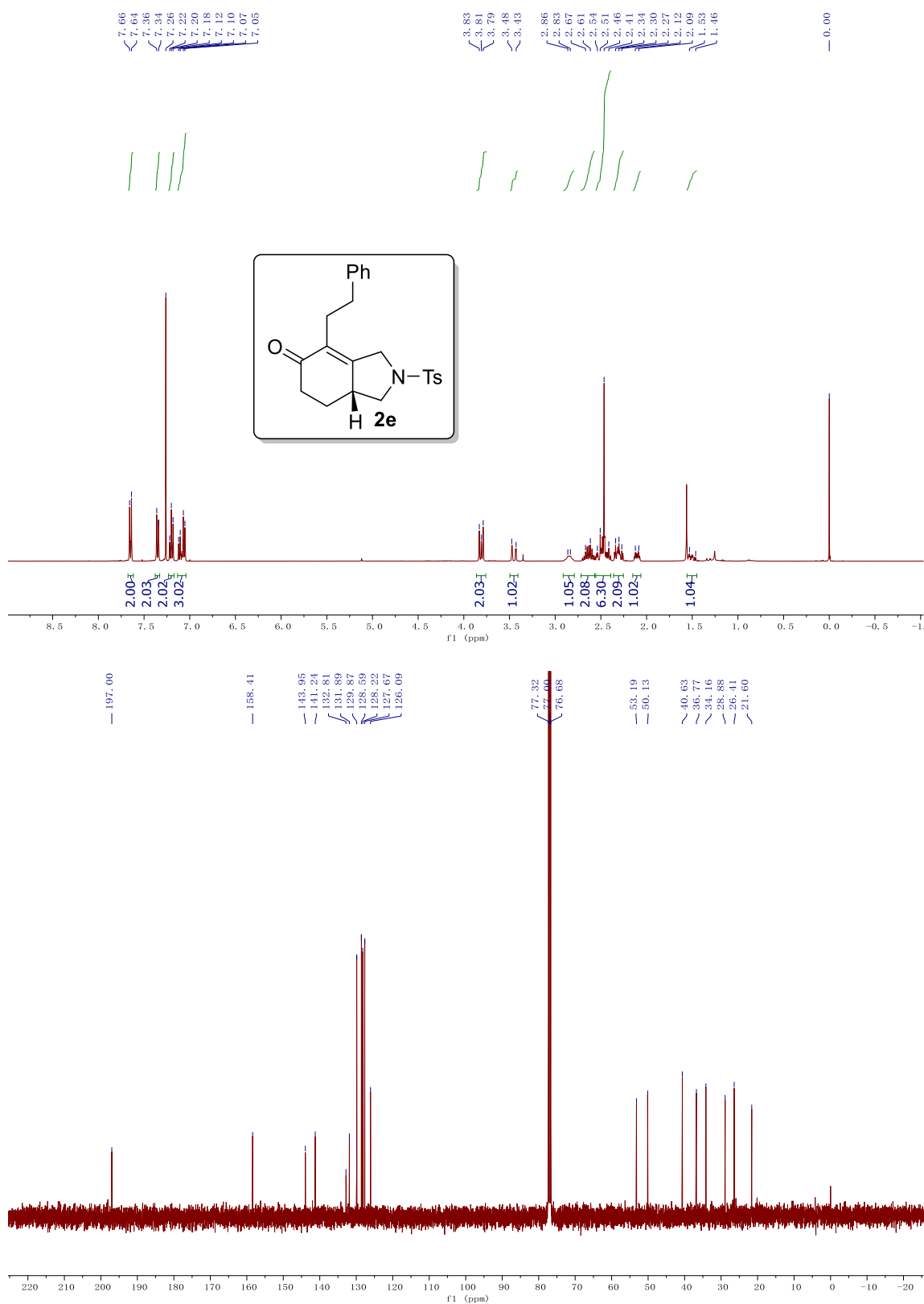


**Figure 5.15**  $^1\text{H}$  and  $^{13}\text{C}$  NMR spectrum of compound **2f**

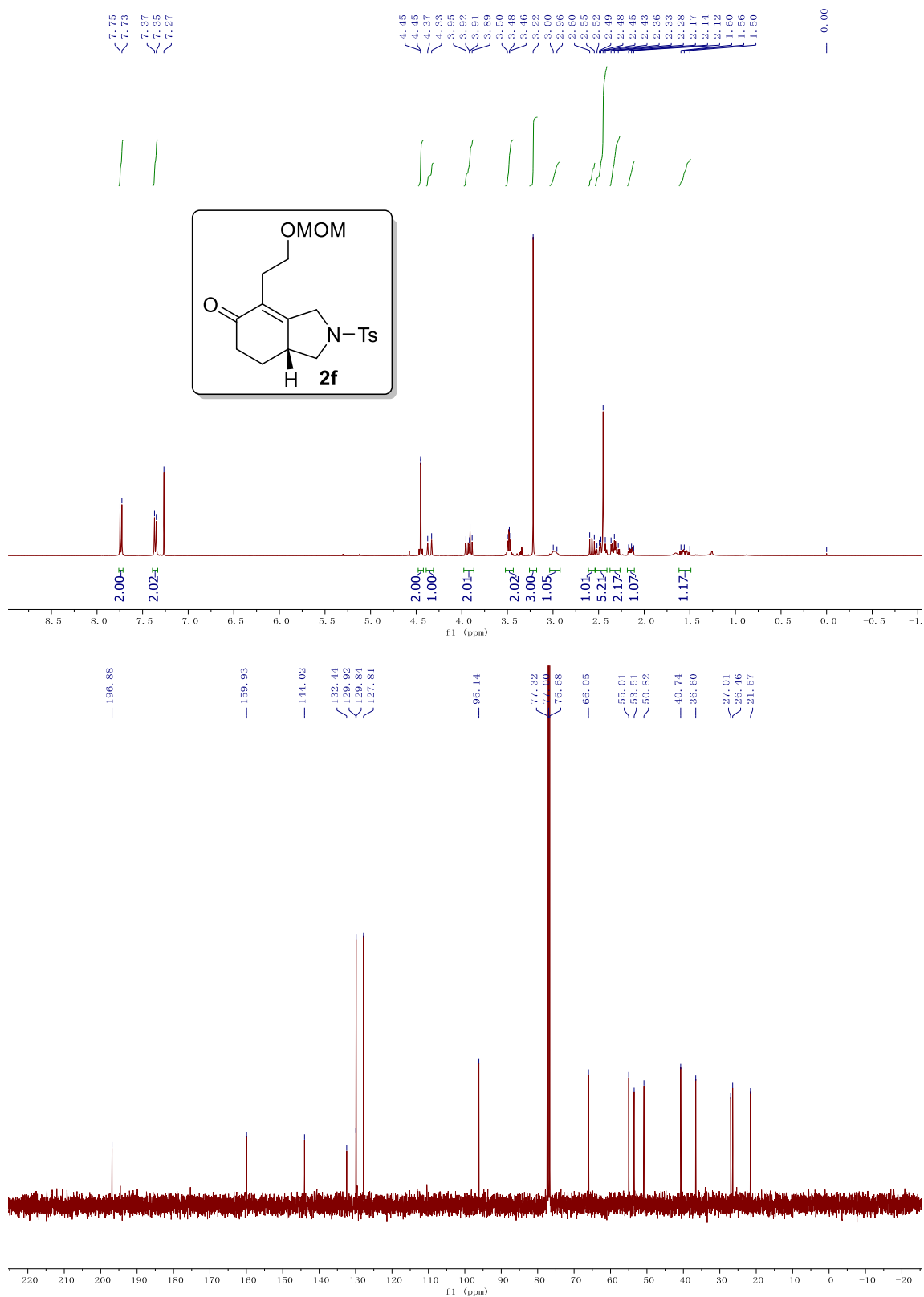


**Figure 5.16**  $^1\text{H}$  and  $^{13}\text{C}$  NMR spectrum of compound **2g**

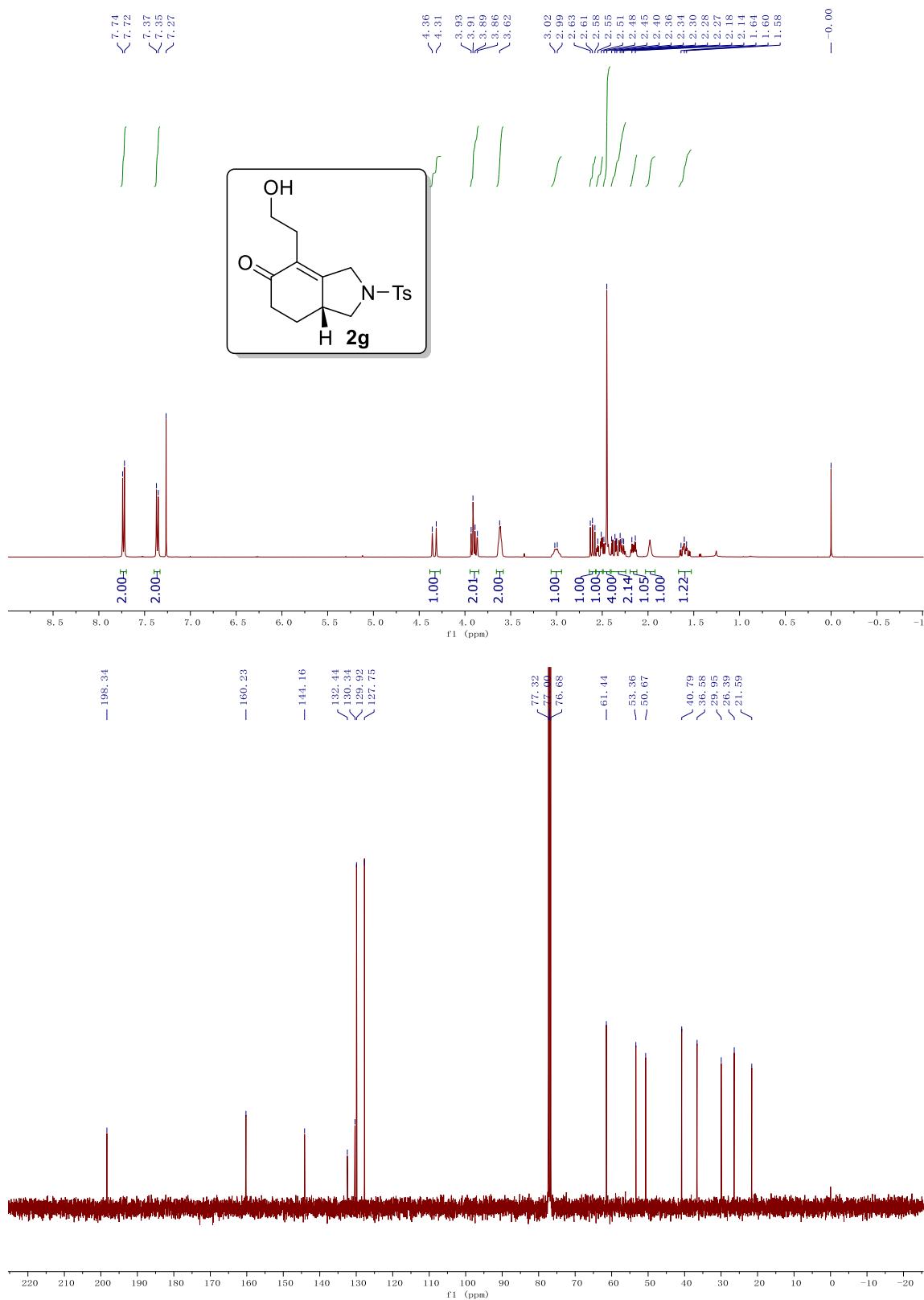


**Figure 5.17**  $^1\text{H}$  and  $^{13}\text{C}$  NMR spectrum of compound **2h**

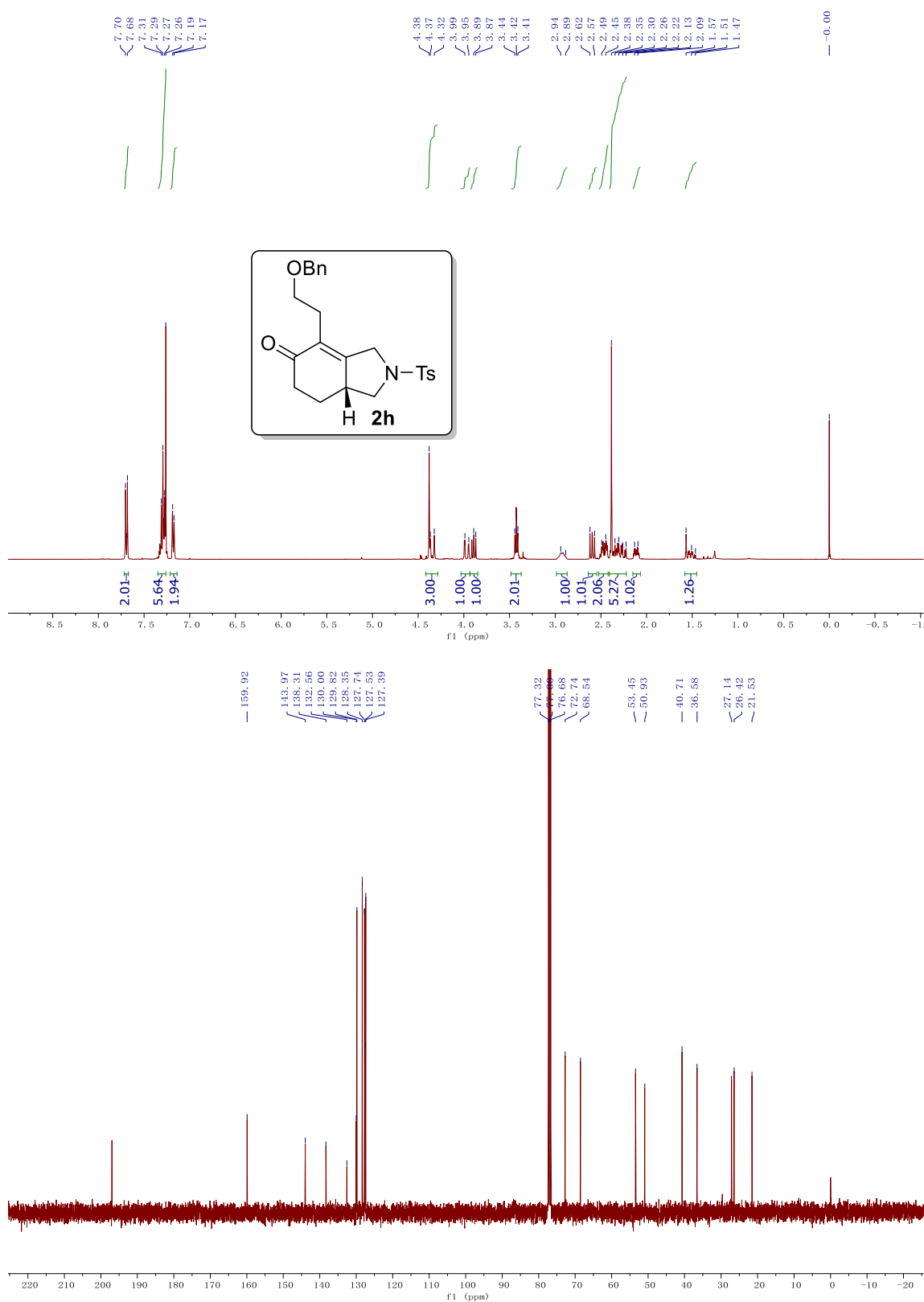


**Figure 5.18**  $^1\text{H}$  and  $^{13}\text{C}$  NMR spectrum of compound **2i**

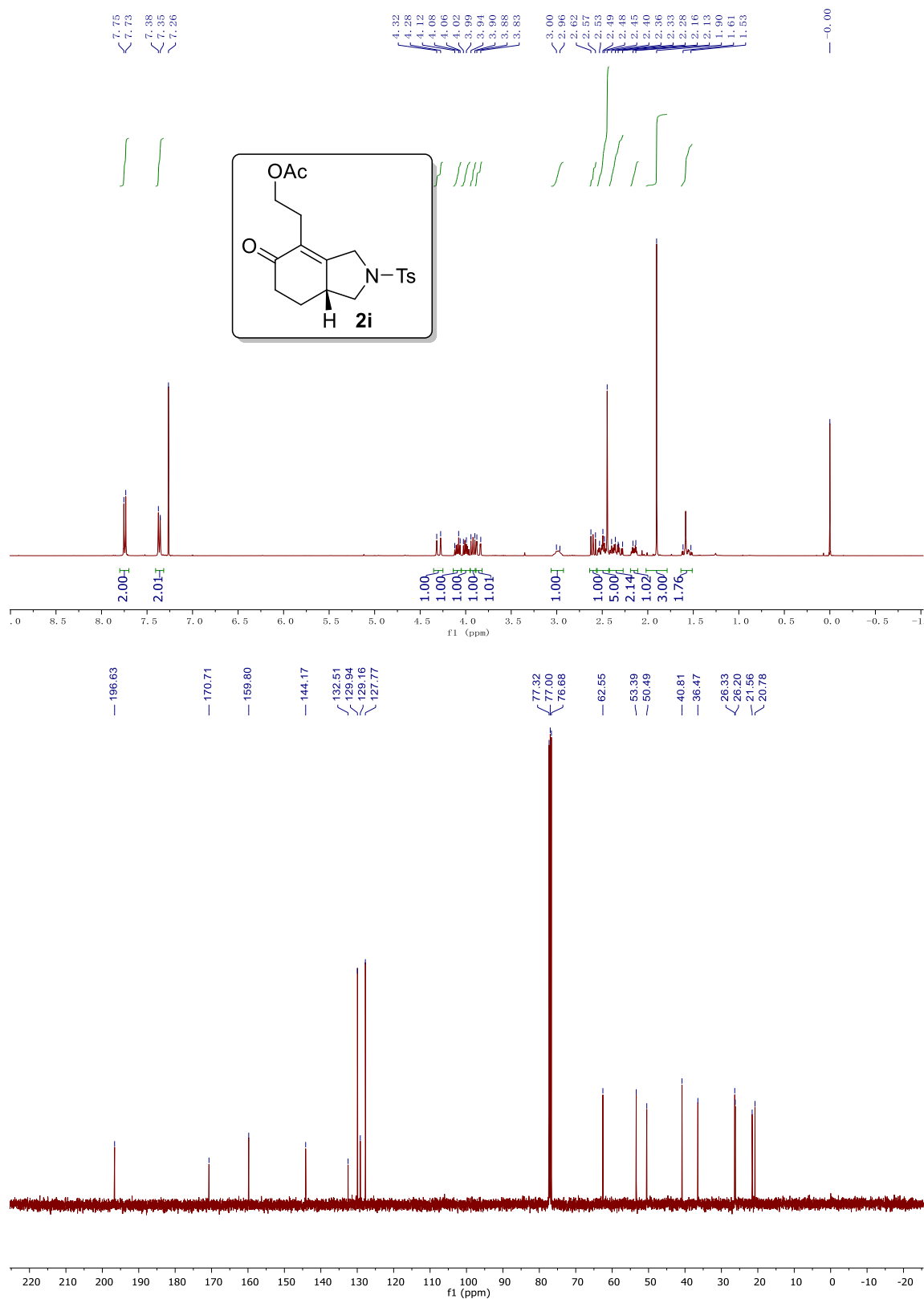


**Figure 5.19**  $^1\text{H}$  and  $^{13}\text{C}$  NMR spectrum of compound **2j**

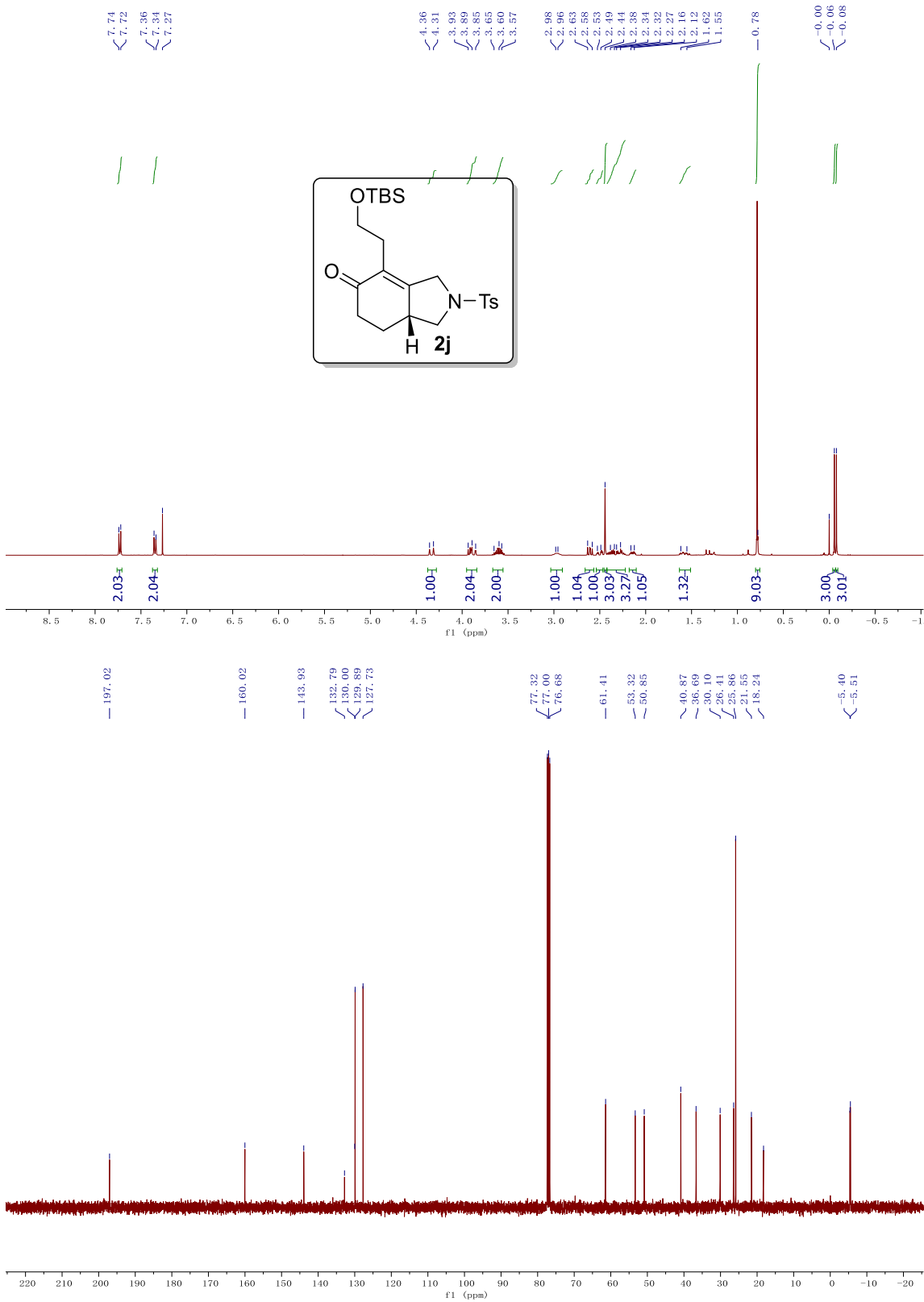


**Figure 5.20**  $^1\text{H}$  and  $^{13}\text{C}$  NMR spectrum of compound **2k**

